The Optimization of Combined Power–Power Generation Cycles

A. S. B. AL-ANFAJI

A thesis submitted in partial fulfilment
of the requirements of the University of Hertfordshire
for the degree of Doctor of Philosophy

The programme of research was carried out in the School of Engineering & Technology,
University of Hertfordshire, Hatfield, UK

November 2014

Abstract

An investigation into the performance of several combined gas-steam power generating plants' cycles was undertaken at the School of Engineering and Technology at the University of Hertfordshire and it is predominantly analytical in nature. The investigation covered in principle the aspect of the fundamentals and the performance parameters of the following cycles: gas turbine, steam turbine, ammonia-water, partial oxidation and the absorption chiller. Complete thermal analysis of the individual cycles was undertaken initially. Subsequently, these were linked to generate a comprehensive computer model which was employed to predict the performance and characteristics of the optimized combination.

The developed model was run using various input parameters to test the performance of the cycle's combination with respect to the combined cycle's efficiency, power output, specific fuel consumption and the temperature of the stack gases. In addition, the impact of the optimized cycles on the generation of CO2 and NOX was also investigated.

This research goes over the thermal power stations of which most of the world electrical energy is currently generated by. Through which, to meet the increase in the electricity consumption and the environmental pollution associated with its production as well as the limitation of the natural hydrocarbon resources necessitated. By making use of the progressive increase of high temperature gases in recent decades, the advent of high temperature material and the use of large compression ratios and generating electricity from high temperature of gas turbine discharge, which is otherwise lost to the environment, a better electrical power is generated by such plant, which depends on a variety of influencing factors. This thesis deals with an investigation undertaken to optimize the performance of the combined Brayton-Rankine power cycles' performance.

This work includes a comprehensive review of the previous work reported in the literature on the combined cycles is presented. An evaluation of the performance of combined cycle power plant and its enhancements is detailed to provide: A full understanding of the operational behaviour of the combined power plants, and demonstration of the relevance between power generations and environmental impact. A basic analytical model was constructed for the combined gas (Brayton) and the steam (Rankine) and used in a parametric study to reveal the optimization parameters, and its results were discussed. The role of the parameters of each cycle on the overall performance of the combined power cycle is revealed by assessing the

effect of the operating parameters in each individual cycle on the performance of the CCPP. P impacts on the environment were assessed through changes in the fuel consumption and the temperature of stack gases.

A comprehensive and detailed analytical model was created for the operation of hypothetical combined cycle power and power plant. Details of the operation of each component in the cycle was modelled and integrated in the overall all combined cycle/plant operation. The cycle/plant simulation and matching as well as the modelling results and their analysis were presented. Two advanced configurations of gas turbine cycle for the combined cycle power plants are selected, investigated, modelled and optimized as a part of combined cycle power plant. Both configurations work on fuel rich combustion, therefore, the combustor model for rich fuel atmosphere was established. Additionally, models were created for the other components of the turbine which work on the same gases.

Another model was created for the components of two configurations of ammonia water mixture (kalina) cycle. As integrated to the combined cycle power plant, the optimization strategy considered for these configurations is for them to be powered by the exhaust gases from either the gas turbine or the gases leaving the Rankine boiler (HRSG). This included ChGT regarding its performance and its environmental characteristics. The previously considered combined configuration is integrated by as single and double effect configurations of an ammonia water absorption cooling system (AWACS) for compressor inlet air cooling. Both were investigated and designed for optimizing the triple combination power cycle described above. During this research, tens of functions were constructed using VBA to look up tables linked to either estimating fluids' thermodynamic properties, or to determine a number of parameters regarding the performance of several components.

New and very interesting results were obtained, which show the impact of the input parameters of the individual cycles on the performance parameters of a certain combined plant’s cycle. The optimized parameters are of a great practical influence on the application and running condition of the real combined plants. Such influence manifested itself in higher rate of heat recovery, higher combined plant thermal efficiency from those of the individual plants, less harmful emission, better fuel economy and higher power output.

Lastly, it could be claimed that various concluding remarks drawn from the current study could help to improve the understanding of the behaviour of the combined cycle and help power plant designers to reduce the time, effort and cost of prototyping.

Acknowledgement

I would like to record my sincere aprretiation to my principal supervisor Dr. Sami H. Nasser, who continually & convincingly inspired my research journey until the accomplishment of this work. Without his guidance & persistence help, this dissertation would not have been achievable. His support strongly offered me the confidence through the hard times of research life. His help cannot be described in few words.

I also dedicate my gratefulness and thanks to my second supervisor Dr. Badi for his support throughout this research. I send my huge thanks to the staff of School of Engineering and information Sciences/Department of Aerospace, Automotive, and Design Engineering for their support throughout the main time of this report. In here, great thanks to Mrs. Lorraine Nichols and special one to Avis Cawley, Kathy Lee, Laura Jonse and many others.

Thanks appreciation to the Iraqi presidency (the office of Vice President) for the opportunity and the support during the first three years of research, in here, special thanks to Mr. Hayder Al obaydi for his help and patients. I also enclose my great appreciation to the Iraqi government employees for their support in reissuing my visa to return and continue my research.

My enormous appreciation for the unconceivable part of: My parents and sister in law who continuously provided the home and living requirements to me and my family after the cut of my income; My Parents and brothers who played a great part in removing the weight from my shoulders and always provided me with encouragement to finish my research; And my wife, my daughter Sara and my new baby son who were under great alert and bared the hard times.

However, above all, I thank my God Allah almighty for his mercy and compassionate upon me to know such individuals.

Contents

Abstract I
Acknowledgement III
Contents IV
List of Figures VIII
List of Tables XX
Nomenclature XXI
CHAPTER 1 1
1.1 An outlook on power generation 1
1.2 Elementary power cycle thermodynamics 4
1.3 Theory of the combined cycle power plants 5
1.4 Enhancements to the combined cycle power plant 11
1.5 An overview on the superiority of the present research 15
1.6 Expectations from applying advanced enhancements to CCPP 17
1.7 Aims and objectives of the current research 17
1.8 Important statements throughout the research 18
CHAPTER 2 19
2.1 Introduction 19
2.2 Theoretical considerations for the gas cycle power plant 19
2.2.1 Background and theory 20
2.2.2 Simple gas turbine cycle performance 26
2.2.3 Regenerated gas turbine cycle 29
2.2.4 Reheated gas turbine cycle 31
2.2.5 Intercooled gas turbine cycle 33
2.2.6 Intercooled reheated gas turbine cycle 35
2.3 The steam turbine cycle power plants 36
2.3.1 Background 36
2.3.2 Theory of the steam cycle power plant 38
2.4 Theory of the combined power cycles 49
2.5 Conclusions 52
CHAPTER 3 53
3.1 Introduction 53
3.2 Survey of relevant studies 54

3.2.1 Energy and exergy analysis for the gas turbine power cycle 54
3.2.2 Parametric studies and optimizations of the gas/steam combined cycle power and power plants. 64
3.2.3 Energy and exergy analysis and parametric studies on gas/ammonia-water combined cycle power plants. 76
3.2.4 Triple combination power generation cycles 82
3.2.5 Partial oxidation combustion enhancements for gas turbines and the chemical gas turbine for fewer emissions and better performance combined power cycles. 87
3.2.6 Gas turbine cycle enhancements by inlet-air-cooling system 93
3.3 The observations from the studies in literature review 101
3.3.1 Observations from combining two power cycles in a thermal power plant: 115
3.3.2 Observations regarding the performance of gas turbine cycles: 115
3.3.3 The observations over cooled gas turbine engines 116
3.3.4 The observations over gas turbine cycle effect on the performance of combined cycle power plant: 116
3.3.5 The observations about the effect of (HRSG) and steam cycle on the combined cycle performance 117
3.3.6 Observations on the performance of (gas turbine /ammonia-water turbine combined cycle power plant) 118
3.3.7 Observations over triple combination cycles power generation plants 119
3.3.8 Observations on upgrading partial oxidation to gas turbine cycle and combined cycle power plants 119
3.3.9 Observations over upgrading the gas turbine cycle and the combined cycle power plants by inlet-air-cooling systems 120
3.4 Recommendations from observations 121
CHAPTER 4 126
4.1 Introduction 126
4.2 Thermodynamic consideration of the parametric study 127
4.2.1 Combining two power plants in series with supplementary firing: 128
4.2.2 Gas/steam combined power cycle 129
4.3 Assumptions and the limitations for the parametric analysis 141
4.4 Discussion 143
4.4.1 Gas turbine cycle performance 144
4.4.2 The performance of gas /steam combined cycle power plant 158
4.4.3 Additional topics 195
4.5 Conclusions from the parametric study 224

CHAPTER 5 229
5.1 Introduction and general background 229
5.2 Combined cycle power plant program 231
5.2.1 Equations for combined cycle power plant performance characteristics, configurations and basic analysis 232
5.2.2 Components models 232
5.2.3 Specifications for conventional combined cycle's models 250
5.3 Components matching 253
5.3.1 Gas turbine engine components matching 253
5.3.2 Steam turbine components matching 258
5.4 Emissions 265
5.4.1 Emissions of carbon dioxide 265
5.4.2 Emission of nitrogen oxide 269
5.5 Optimization of conventional combined power cycles 269
5.6 Conclusions 275
CHAPTER 6 277
6.1 Introduction and background 277
6.2 Combustion of rich and lean fuel mixtures: 279
6.3 ChGT solution program model 281
6.3.1 Configurations and basic analysis 282
6.3.2 ChGT program for components' models 284
6.3.3 ChGT model specifications 300
6.4 Emissions from fuel rich fuel lean combustors in ChGT 306
6.5 Optimization of the ChGT cycle 306
6.5.1 Fuel rich combustor parameters effect 306
6.5.2 Fuel lean combustor parameters effects 313
6.5.3 Combining the effect from both combustors 317
6.5.4 Condenser and HRSG parameters effects 321
6.5.5 1st HRSG parameters effects 323
6.5.6 Ambient temperature effect 326
6.6 Results and discussion from optimization 328
6.7 Conclusions 332
CHAPTER 7 333
7.1 Introduction and background 333
7.2 Ammonia water mixture 336

7.2.1 Ammonia toxicity 336
7.2.2 Ammonia water mixture's thermodynamic properties 336
7.2.3 Material's prohibitions 337
7.3 AWT engine simulation model 340
7.3.1 Configurations 342
7.3.2 Ammonia water turbine engine model calculations 343
7.3.3 Ammonia water turbine engine components modelling 345
7.3.4 Ammonia water engine model specifications 356
7.4 Optimizing the ammonia water turbine engine 360
7.4.1 Ammonia water cycle parameters effect on Kalina cycle's performance 361
7.4.2 The results from optimization AWC 369
7.4.3 AWC parameters' effect on the performance of the gas/ ammonia water CCPP 370
7.4.4 Comparison on ChGT/AWC configurations 373
7.5 Conclusions 376
CHAPTER 8 378
8.1 Introduction 378
8.2 Strategies of inlet air cooling 379
8.3 Ammonia-water absorption chillers for gas turbine inlet air cooling 379
8.4 Absorption chiller system model program 381
8.4.1 The conducted configurations of absorption chiller systems and its basic analysis: 382
8.4.2 Calculations for AWACS model 384
8.4.3 Components models 386
8.4.4 AWAC model specifications 394
8.5 Optimization 400
8.6 Results and conclusions 401
CHAPTER 9 403
9.1 Overview on the work done 403
9.2 Research conclusions 404
9.3 Recent developments to the CCPP performance 406
9.4 Observations from the recent patents 408
9.5 Recommendations 408
REFERENCES 410

List of Figures

Figure 1.1 Total world power generation in the year 2010 data given by IEA [1] 3
Figure 1.2 Brayton /Rankine combined cycles on T-S diagram..... 6
Figure 1.3 Simple gas/steam turbines combined cycle power and power plant..... 7
Figure 1.4 The combination between a gas turbine and a steam turbine cycles..... 9
Figure 1.5 Combined cycle efficiency functioned to the efficiency of each cycle 11
Figure 1.6 The effect of the losses on the efficiency of the combined cycle 12
Figure 1.7 Triple combination power cycle enhanced by heat pump system..... 14
Figure 1.8 Different cycles performances effects on the efficiency of the triple and combined cycle..... 15
Figure 2.1 Closed circuit gas turbine power plant..... 21
Figure 2.2 Open circuit gas turbine power plant 22
Figure 2.3 Ideal air standard Brayton cycle on T-S diagram 23
Figure 2.4 Ideal and real Brayton cycles on T-S diagram..... 25
Figure 2.5 Real Brayton cycles on P-V diagram..... 28
Figure 2.6 Real Brayton cycles on T-S diagram 30
Figure 2.7 Increased pressure and normal Brayton cycles on T-S diagram..... 31
Figure 2.8 Main components of an ideal reheated gas turbine cycle 32
Figure 2.9 Simple and reheated Brayton standard cycles on T-S diagram 33
Figure 2.10 Simple and intercooled Brayton..... 34
Figure 2.11 Main components of an intercooled gas turbine cycle..... 34
Figure 2.12 Main components of an ideal intercooled reheated gas turbine cycle 35
Figure 2.13 Simple and intercooled reheated gas Brayton standard cycles on T- S diagram .. 36
Figure 2.14 Main components of a basic Rankine cycle steam turbine power plant 37
Figure 2.15 Ideal Rankine cycle on pressure-volume diagram 39
Figure 2.16 Ideal Rankine cycle on T-S diagram..... 39
Figure 2.17 Basic and increased boiler pressure Rankine cycles on T-S diagram..... 42
Figure 2.18 Basic and low condenser pressure Rankine cycles on T-S diagram 42
Figure 2.19 Basic and superheated Rankine cycle on T-S diagram 43
Figure 2.20 Main components of a basic reheated steam turbine power plant 44
Figure 2.21 Ideal reheated Rankine cycle on T-S diagram 45
Figure 2.22 Open and the closed feed water heaters 46
Figure 2.23 Ideal regenerated Rankine cycle using open feed water heater on T-S diagram .. 47
Figure 2.24 Regenerated steam turbine power plant with an open feed water heater..... 47

Figure 2.25 Ideal regenerated Rankine cycle with closed feed water heater on T-S diagram .48
Figure 2.26 Main components of a regenerated steam turbine power plant with closed feed water heater.....48
Figure 2.27 Flow diagram of a combined power plant 50
Figure 3.1 A brief classification on the subjects of the conducted studies in this literature review 55
Figure 3.2 Simple, reheated, and partial oxidation gas turbine cycles 89
Figure 4.1 The simple heat recovery steam generator (HRSG) 135
Figure 4.2 The efficiency of simple gas turbine cycle versus the specific work output 145
Figure 4.3 The relationship between pressure ratios and exhaust temperature for simple gas turbine cycle 145
Figure 4.4 The relationship between the specific power output and SFC of simple gas turbine cycle.....146
Figure 4.5 The efficiency of regenerated gas turbine cycle versus the specific work output 147
Figure 4.6 The exhaust gases temperature of regenerated gas turbine cycle versus the pressure ratios 147
Figure 4.7 The SFC of regenerated gas turbine cycle versus itd specific work output.....148
Figure 4.8 The specific power output of reheated gas turbine cycle versus the thermal efficiency 149
Figure 4.9 The exhaust gases temperature of reheated gas turbine cycle versus the pressure ratios 149
Figure 4.10 The SFC of a reheated gas turbine cycle versus the specific work output.....150
Figure 4.11 Intercooled gas turbine cycle's specific work output versus its thermal efficiency 151
Fig. 4.12 Exhaust gases' temperature of intercooled gas turbine cycle versus its pressure ratio 151
Figure 4.13 The relationship between specific work output and specific fuel consumption of intercooled gas turbine cycle 152
Figure 4.14 Intercooled reheated gas turbine cycle's thermal efficiency functioned to the specific work output 153
Figure 4.15 The SFC versus the specific work output of intercooled reheated gas turbine cycle 153
Figure 4.16 The thermal efficiency versus specific work output of intercooled regenerated reheated gas turbine cycle.....154

Figure 4.17 The exhaust temperature of the gases versus the pressure ratios of intercooled regenerated reheated gas turbine cycle 155
Figure 4.18 The SFC versus the specific work output of intercooled regenerated reheated gas turbine cycle 155
Figure 4.19 The thermal efficiency versus the specific work output for different gas turbine cycles 158
Figure 4.20 The effect of boiler pressure on the efficiency and specific work output of simple gas turbine/simple steam turbine combined power cycle 162
Figure 4.21 The effect of boiler pressure on the efficiency and specific work output of simple gas turbine/dual pressure reheated steam turbine combined cycle 162
Figure 4.22 The effect of boiler pressure on the efficiency and specific work output of simple gas turbine/triple pressure reheated steam turbine combined power cycle 163
Figure 4.23 The effect of boiler pressure on specific fuel consumption (SFC) and stack gases temperature of simple gas /simple steam combined cycle 164
Figure 4.24 The effect of boiler pressure on specific fuel consumption (SFC) and stack gases temperature of simple gas/dual pressure steam combined cycle 164
Figure 4.25 The effect of boiler pressure on specific fuel consumption (SFC) and stack gases temperature of simple gas/triple pressure reheated steam combined cycle 165
Figure 4.26 Boiler pressures' effect on the thermal efficiency of combined cycles of simple gas turbine and different steam turbines 166
Figure 4.27 Boiler pressures' impact on the specific work output of combined cycles of simple gas turbine and different steam turbines 167
Figure 4.28 The effect of boiler pressure on temperature of stack gases of combined cycles of simple gas turbine and different steam turbines 167
Figure 4.29 The effect of boiler pressure on the specific fuel consumption of combined cycles of simple gas turbine and different steam turbines 168
Figure 4.30 The effects of boiler pressure on the thermal efficiency of combined cycles with different gas turbines and simple steam turbine 168
Figure 4.31 Boiler pressures' effects on the specific work output of combined cycles with different gas turbines and simple steam turbine 169
Figure 4.32 Boiler pressures' effects on the temperature of stack gases of combined cycles with different gas turbines and simple steam turbine 169
Figure 4.33 The effect of boiler pressure on the specific fuel consumption of combined cycles with different gas turbines and simple steam turbine 170

Figure 4.34 The effect of condenser pressure on specific work output and thermal efficiency of simple gas turbine simple steam turbine combined cycle 171
Figure 4.35 The effect of condenser pressure on the specific work output and the thermal efficiency of simple gas turbine dual pressure steam turbine combined cycle 171
Figure 4.36 The effect of condenser pressure on the specific work output and the thermal efficiency of simple gas turbine triple pressure steam turbine combined cycle 172
Figure 4.37 The effect of condenser pressure on the temperature of stack gases and the specific fuel consumption of simple gas turbine reheated steam turbine combined cycle 173
Figure 4.38 The effect of condenser pressure on the temperature of stack gases and the specific fuel consumption of simple gas turbine dual pressure reheated steam turbine combined cycle 173
Figure 4.39 The effect of condenser pressure on the temperature of stack gases and the specific fuel consumption of simple gas turbine triple pressure reheated steam turbine combined cycle 174
Figure 4.40 The effect of condenser pressure on the thermal efficiency of combined cycles with simple gas turbine and different steam turbines combined cycles 174
Figure 4.41 The effect of condenser pressure on the specific work output from simple gas turbine cycle and different steam turbine combined cycles 175
Figure 4.42 The effect of condenser pressure on the temperature of stack gases in simple gas turbine combined with different steam turbines 175
Figure 4.43 The effect of condenser pressure on the specific fuel consumption of simple gas turbine cycle combined to different steam turbines 176
Figure 4.44 The effect of condenser pressure over thermal efficiency of combined cycles with different gas turbine cycles and simple steam cycle 177
Figure 4.45 The effect of condenser pressure over specific work output of combined cycles with different gas turbine cycles and simple steam cycle 178
Figure 4.46 The effect of condenser pressure over stack temperature of combined cycles with different gas turbine cycles and simple steam cycle 178
Figure 4.47 The effect of (ΔTppm) on the thermal efficiency of simple gas turbine / simple steam turbine combined cycle 181
Figure 4.48 The effect of (ΔTppm) on the specific work output of simple gas turbine simple steam turbine combined cycle 181
Figure 4.49 The temperature of stack gases versus (ΔTppm) of simple gas turbine/ simple steam turbine combined cycle 182

Figure 4.50 The specific fuel consumption versus (ΔTppm) of simple gas turbine simple steam combined cycle 182
Figure 4.51 The effect of (ΔTppm) on thermal efficiency of combined cycle with dual pressure steam generator 184
Figure 4.52 The effect of (ΔTppm) on specific work output of combined cycle with dual pressure steam generator 184
Figure 4.53 The effect of (ΔTppm) on stack temperature of combined cycle with dual pressure steam generator 185
Figure 4.54 The effect of (ΔTppm) on specific fuel consumption of combined cycle with dual pressure steam generator 185
Figure 4.55 The effect of (ΔTppm) on thermal efficiency of a combined cycle with triple pressure steam generator 187
Figure 4.56 The effect of (ΔTppm) on the specific work output of a combined cycle with triple pressure steam generator 187
Figure 4.57 The effect of (ΔTppm) on the temperature of stack gases out of a combined cycle with triple pressure steam generator 188
Figure 4.58 The effect of (ΔT_{PPM}) on specific fuel consumption of combined cycle with triple pressure steam generator 188
Figure 4.59 The effect of the ambient temperature on the performance simple gas turbine combined cycle 190
Figure 4.60 The effect of the ambient temperature the performance of regenerated gas turbine combined cycle 190
Figure 4.61 The effect of the ambient temperature on the performance of reheated gas turbine combined cycle 191
Figure 4.62 The effect of the ambient temperature on the performance of intercooled gas turbine combined cycle 191
Figure 4.63 The effect of the ambient temperature on the performance of the intercooled reheated gas turbine combined cycle 192
Figure 4.64 The effect of the ambient temperature on the performance of intercooled reheated regenerated gas turbine combined cycle 192
Figure 4.65 The effect of the ambient temperature on the thermal efficiency and the specific work output 193
Figure 4.66 The effect of the ambient temperature on the (SFC) and the temperature of stack gases 194

Figure 4.67 The effect of low pressure mass flow rate on the thermal efficiency and the specific work output of (SGDPSCC) 196
Figure 4.68 The effect of high pressure mass flow on the thermal efficiency and the specific work output of (SGDPSCC) 197
Figure 4.69 The effect of the low pressure mass flow on (SFC) and the temperature of stack gases of (SGDPSCC) 197
Figure 4.70 The effect of the high pressure mass flow on the (SFC) and the temperature of stack gases of (SGDPSCC) 198
Figure 4.71 Intermediate pressure mass fraction as function to high pressure mass flow on the thermal efficiency and the specific work output of (SGDPSCC) 198
Figure 4.72 The mass flow rate of low pressure as a function to that for high pressure on efficiency and specific work output of (SGTPSCC) 200
Figure 4.73 The effect of the intermediate and low pressure mass flows as a function to that for high pressure on thermal efficiency and specific work output of (SGTPSCC) 200
Figure 4.74 Low pressure mass flow as a function to intermediate pressure effect on thermal efficiency and specific work output of (SGTPSCC) 201
Figure 4.75 The effect of the mass flow rate of high pressure as a function to that for intermediate pressure on thermal efficiency and specific work output of (SGTPSCC) 201
Figure 4.76 The effect of changing the intermediate pressure on (SFC) and temperature of stack gases of (SGTPSCC) 202
Figure 4.77 The effect of changing the low pressure on (SFC) and temperature of stack gases of (SGTPSCC) 202
Figure 4.78 The effect of changing the intermediate and low pressure on (SFC) and temperature of stack gases of (SGTPSCC) 203
Figure 4.79 The effect of the low pressure mass flow as a function to intermediate pressure on (SFC) and temperature of stack gases of (SGTPSCC) 203
Figure 4.80 High pressures' effect on the specific fuel consumption (SFC) and the temperature of stack gases of (SGTPSCC) 204
Figure 4.81 Intercooling pressure effect on thermal efficiency and specific power output of intercooled gas turbine cycle 205
Figure 4.82 Intercooling pressure effect on thermal efficiency and specific power output of intercooled reheated gas turbine cycle 206
Figure 4.83 Intercooling pressure effect on thermal efficiency and specific power output of intercooled reheated regenerated gas turbine cycle 206

Figure 4.84 Intercooling pressure effect on thermal efficiency and specific power output of Intercooled gas turbine simple steam turbine combined cycle 207
Figure 4.85 Intercooling pressure effect on intercooled reheated gas turbine simple steam turbine combined cycle 207
Figure 4.86 Intercooling pressure effect on thermal efficiency and specific work output of intercooled gas turbine simple steam turbine combined cycle 208
Figure 4.87 Intercooling pressure effect on (SFC) and temperature of stack gases of intercooled gas turbine simple steam turbine combined cycles 209
Figure 4.88 Intercooling pressure effect on thermal efficiency and specific power output of intercooled gas turbine triple pressure reheated steam turbine combined cycle 209
Figure 4.89 Intercooling pressure ratio effect on (SFC) and the temperature of stack gases of intercooled gas turbine triple pressure reheated steam turbine combined cycle 210
Figure 4.90 Intercooling pressure ratio effect on thermal efficiency and specific power output of intercooled gas turbine and different steam turbine combined cycles 211
Figure 4.91 Intercooling pressure effect on thermal efficiency and specific power output of intercooled reheated regenerated gas turbine triple pressure steam turbine combined cycle. 213
Figure 4.92 Intercooling pressure effect on thermal efficiency and specific power output of intercooled reheated gas turbine triple pressure steam combined cycle 214
Figure 4.93 Reheat prssure ratio effect on the thermal effciency and the specific work output of reheated gas turbines 216
Figure 4.94 Pressure of reheat effect on the temperature of stack gases of a reheated gas turbine 216
Figure 4.95 Reheat pressure effect on the efficiency and the specific work output of combined cycle 217
Figure 4.96 Pressure of reheated gases effect on the stack gases temperature 218
Figure 4.97 Gases reheat pressure effect on the thermal efficiency and the specific power output of combined cycle 220
Figure 4.98 Gases reheat pressure effect on stack temperature and specific fuel consumption of combined cycle 220
Figure 4.99 Gases reheat pressure effect on thermal efficiency and specific power output of combined cycle for different pressure ratios 221
Figure 4.100 Gases reheat pressure effect on the temperature of stack gases and the (SFC) of combined cycle 221
Figure 4.101 Pressure of reheat effect on thermal efficacy of simple combined cycle 223

Figure 4.102 Pressure of reheat effect on stack gases temperature of simple combined cycle 223
Figure 5.1 Pressure ratio versus mass flow on normalized map for axial 233
Figure 5.2 Isentropic efficiency versus mass flow on normalized map for axial 234
Figure 5.3 Air compressor model 234
Figure 5.4 Combustion chamber model 236
Figure 5.5 The isentropic efficiency versus the pressure ratio on normalized map for axial gas turbine at various normalized rotational speed (N) 237
Figure 5.6 The mass flow versus the pressure ratio on normalized map for axial gas turbine at various normalized rotational speed (N) 238
Figure 5.7 Gas turbine model 238
Figure 5.8 Steam re-heater model 240
Figure 5.9 Steam super-heater model 241
Figure 5.10 Steam evaporator model 242
Figure 5.11 Steam economizer model 243
Figure 5.12 Steam turbine model 244
Figure 5.13 Steam condenser model 244
Figure 5.14 Water pump model 245
Figure 5.15 The heat recovery steam generator (HRSG) model 247
Figure 5.16 HRSG model performance prediction by Ganapathy [88] 249
Figure 5.17 Matching procedure for single shaft simple gas turbine based on Razak [8] 257
Figure 5.18 Overall model (solution program) flow chart for the SGSSCCPP 259
Figure 5.19 Flow chart of regenerative gas turbine cycle model in CCPP model 260
Figure 5.20 Flow chart of reheated gas turbine cycle in CCPP model 261
Figure 5.21 Flow chart of inter-cooled gas turbine cycle in CCPP model 262
Figure 5.22 Flow chart of intercooled reheated gas turbine cycle in CCPP model 263
Figure 5.23 Simple and regenerated Steam cycle HRSG model 264
Figure 5.24 Reheated HRSG model flow chart 264
Figure 5.25 The thermal efficiency nad CO_2 emissions versus the load power for one kg of air 268
Figure 5.26 The thermal efficiency and CO_2 emissions versus load power for one kg of air 268
Figure 5.27 Corrected pressure ratio versus corrected mass flow for air compressor running lines imposed on gas turbine running lines 270
Figure 6.1 Diagram of a combined cycle based on chemical gas turbine 283

Figure 6.2 Flow diagram of a combined cycle based on chemical gas turbine system, studied by Mohamed [66] 283
Figure 6.3 Fuel rich combustion chamber model 287
Figure 6.4 Fuel rich turbine model 288
Figure 6.5 Simple fuel rich HRSG model 289
Figure 6.6 Fuel lean combustion chamber model (design 2) 292
Figure 6.7 Fuel lean combustor model 292
Figure 6.8 Fuel lean turbine model 294
Figure 6.9 Fuel lean HRSG model 296
Figure 6.10 Steam turbine model 297
Figure 6.11 Steam condenser model 298
Figure 6.12 Water pump model 298
Figure 6.13 Compressed air heat exchanger model 299
Figure 6.14 Flow chart for the 1st design ChGT solution model 304
Figure 6.15 Flow chart representing 2nd design ChGT solution model 305
Figure 6.16 GC thermal efficiency versus specific work output affected by T_{g4} 307
Figure 6.17 ChGT design1 thermal efficiency versus specific work output affected by T_{g4} . 307
Figure 6.18 Emissions of NO_X versus emissions of CO_2 affected by T_{g4} 308
Figure 6.19 SC thermal efficiency versus specific work output affected by T_{g4} 308
Figure 6.20 Fuel rich combustor equivalence ratio effect on specific work output and the thermal efficiency of ChGT design 1 309
Figure 6.21 Fuel rich combustor equivalence ratio effect on specific work output and the thermal efficiency of GC design 1 309
Figure 6.22 The thermal efficiency versus the specific work output of the second design 310
Figure 6.23 The thermal efficiency versus specific work output affected by rich fuel combustion equivalence ratio 311
Figure 6.24 The SFC versus exhaust gases temperature affected by equivalence ration of the fuel rich combustor 312
Figure 6.25 The NOx emissions versus CO_2 emissions affected by rich fuel combustion equivalence ratio 313
Figure 6.26 The thermal efficiency versus specific work output affected by the equivalence ration of lean fuel combustion in first design 314
Figure 6.27 The steam quality at turbine outlet versus the specific fuel consumption affected by the lean combustion equivalence ration of the first design 314

Figure 6.28 Fuel lean combustion temperature effect on thermal efficiency and specific work output for the 2nd design 315
Figure 6.29 The specific fuel consumption versus turbine discharges temperature affected by lean fuel combustion temperature 316
Figure 6.30 The thermal efficiency versus specific work output affected by 316
Figure 6.31 Steam quality at turbine outlet versus SFC affected by gases temperature at lean combustion turbine inlet 317
Figure 6.32 GC thermal efficiency versus specific work output affected by the equivalence ratios 318
Figure 6.33 SC thermal efficiency versus specific work output affected by the equivalence ratios 318
Figure 6.34 CC thermal efficiency versus specific work output affected by the equivalence ratios 319
Figure 6.35 Air splits ratio versus steam to air mass flow rate ratio affected by the equivalence ratios 319
Figure 6.36 Specific fuel consumption versus CO_2 emissions affected by equivalence ratios 320
Figure 6.37 Specific fuel consumption versus NO_X emissions affected by equivalence ratios 320
Figure 6.38 The thermal efficiency versus specific work output 321
Figure 6.39 Steam quality at turbine outlet versus the specific work output 322
Figure 6.40 Steam quality at turbine outlet versus the thermal efficiency 322
Figure 6.41 Steam quality at turbine outlet versus the thermal efficiency 323
Figure 6.42 Specific work output from the ChGT affected by the P_{s2}, T_{g4} and r_{AC} for the 1^{st} design 324
Figure 6.43 Steam pressure effect on steam generation affected by T_{g4} 324
Figure 6.44 Rich fuel turbine gases temperure effect on specifc work output of the ChGT. 325
Figure 6.45 Rich fuel turbine gases temperure effect on specifc work output from the steam turbine 325
Figure 6.46 Ambient temperature effect on specific work output and the thermal effciiency of the ChGT design 1 326
Figure 6.47 Ambient temperature effect on specific work output and the thermal effciiency of the SC in design 1 327
Figure 6.48 Ambient temperature effect on specific work output and the thermal efficiency of the GC in design1 327

Figure 6.49 Ambient temperature effect on the specific fuel consumption and CO_2 emissions 328
Figure 7.1 Kalina cycle power system one distillation step 334
Figure 7.2 kalina cycle processes on temperature entropy diagram.....334
Figure 7.3 Gas turbine / ammonia water turbine combined cycle.....335
Figure 7.4 Heat transfer between the gas and steam and AWM of the same conditions 338
Figure 7.5 Heat extraction from exhaust gases difference between AWM and steam.....339
Figure 7.6 Temperature saturated lines distribution for constant pressure.....339
Figure 7.7 Saturation lines alternated by the change in the pressure of the AWM.....340
Figure 7.8 The first case of HRSG HRVG integrated to ChGT.....341
Figure 7.9 The second case of integrating HRSG and HRVG in ChGT.....341
Figure 7.10 The third case of integrating HRSG and HRVG into ChGT 341
Figure 7.11 The simplified Kalina cycle that studied by Marston [40].....342
Figure 7.12 Canoga park AWC flow diagram.....343
Figure 7.13 HRVG components based in a horizontal flow configuration.....346
Figure 7.14 Integrated HRVG in a conventional HRSG horizontal configuration 346
Figure 7.15 Flow diagram of AWC economizer model 348
Figure 7.16 Steam/ ammonia water evaporator.....348
Figure 7.17 Flow diagram of AWC evaporator control model 349
Figure 7.18 Flow control diagram of AWC super-heater model.....350
Figure 7.19 Flow chart of AWC turbine model 351
Figure 7.20 Flow chart of AWC condenser model.....351
Figure 7.21 Flow chart of AWC absorbers model 352
Figure 7.22 Flow chart of AWC distiller model.....353
Figure 7.23 Flow chart of AWC separator model 354
Figure 7.24 Processes of separator and the feed heater for a certain.....355
Figure 7.25 Flow chart of AWC simulation model.....358
Figure 7.26 Integrated steam\ ammonia HRVG model.....359
Figure 7.27 Simple AWC HRSG Model.....360
Figure 7.28 KC thermal efficiency versus ammonia basic concentration.....361
Figure 7.29 KC specific work output versus ammonia basic concentration 362
Figure 7.30 The thermal efficiency versus the specific work output for different turbine inlet pressure and ammonia basic concentrations.....363
Figure 7.31 The thermal efficiency versus the specific work output for different turbine inlet pressure and ammonia basic concentrations.....363

Figure 7.32 The thermal efficiency versus the specific work output affected by gas turbine discharges temperature and turbine inlet ammonia concentration 364
Figure 7.33 The thermal efficiency versus the separator temperature for different ammonia basic and working concentration 364
Figure 7.34 The thermal efficiency versus the specific work output affected by HRVG pressure for different gas turbine discharge temperature 365
Figure 7.35 Ammonia lean solution and rich vapour concentrations versus separator temperature affected by ammonia lean solution mass fraction 367
Figure 7.36 The thermal efficiency versus separator temperature affected by ammonia lean solution mass fraction 367
Figure 7.37 Separator temperature effect on specific work output for different Z ratios 368
Figure 7.38 Separator temperature effect on AWM mass flow rate for different Z ratios 368
Figure 7.39 The thermal efficiencies of CC, GC and AWC versus their specific work output 371
Figure 7.40 The thermal efficiency of AWC GC and CC versus the specific work output ... 372
Figure 7.41 The thermal efficiency versus the specific work output of AWC affected by P_E 372
Figure 7.42 The thermal efficiency of CCPP versus the specific work output affected by P_{Ev} 373
Figure 7.43 AWC and ChGT thermal efficiency functioned to the pressure of condenser ... 374
Figure 7.44 ChGT specific work output functioned to the pressure of condenser 374
Figure 7.45 ChGT specific work output functioned to the pressure of absorber 375
Figure 7.46 AWC and ChGT thermal efficiency functioned to the pressure of absorber 375
Figure 8.1 AAR for gas turbine inlet air cooling 381
Figure 8.2 Single effect ammonia water 382
Figure 8.3 Two- stage double effect AWAC 383
Figure 8.4 Evaporator model 386
Figure 8.5 Absorber model 388
Figure 8.6 Pump model 389
Figure 8.7 Rectification process on enthalpy concentration diagram 390
Figure 8.8 Rectification column model 390
Figure 8.9 Desrober model 391
Figure 8.10 Condenser model 392
Figure 8.11 Solution heat exchanger model 393
Figure 8.12 Pre-cooler model 394

Figure 8.13 Steam/ ammonia water evaporator or desorber 396
Figure 8.14 AWAC Simulation model program flow chart 398
Figure 8.15 AWAC Solution model design two flow chart 399

List of Tables

Table 3.1 The bibliography of the studies undertaken by this literature review 102
Table 4.1 The assumed values and the considered ranges in this parametric study 142
Table 4.2 A sample on the results regarding the performance of different gas turbine cycle 156
Table 5.1 Operating parameters used in the current study 251
Table 5.2 Gas turbine features in current CCPP 252
Table 5.3 Selected results from a number of the optimized CCPP configurations 274
Table 6.1 Parameters ranges for both configurations models 302
Table 6.2 GC, SC and ChGT performance characteristics results after optimizing turbine inlet temperatures, compression ratios and the equivalence ratios of both combustors 331
Table 7.1 Parameters ranges for the 1st and 2nd AWC configurations models 357
Table 8.1 The range of the parameters 397

Nomenclature

Symbol/s

C_p	Specific heat at constant pressure	kJ/kg.K
$\dot{m}$	Mass flow rate	kg/s
ΔT	Change in Temperature	°C
f	Fuel to air ratio	kg/kg
h	Specific enthalpy	kJ/kg
H	Enthalpy	kJ
I	Exergy losses	kJ/kg·s
LCV	Lower calorific value	kJ/kg
P	Pressure	bar
Q	Heat	kJ/kg·s
q	Specific heat	kJ/kg
S	Entropy	kJ/k
s	Specific entropy	kJ/kg·K
SFC	Specific fuel consumption	kg/kW·h
T	Temperature	°C
W	Power	kW
x	Steam dryness factor	-
Y	The ratio of steam mass fraction during regeneration	-
γ	Specific heat ratio	-
ε	Effectiveness of heat transfer	-
η	Thermal efficiency	-
θ	Maximum to minimum temperature ratio	-
λ	Pressure losses factor	-
ν	Specific volume, or unused heat to the total heat input ratio	m^3/kg , -
ζ	Cycle temperature parameter	-
τ	Torque	N·m
σ	Irreversibility parameter	-
ϕ	Equivalence ratio	-
ρ	Density	kg/m^3
w	Specific work	kJ/kg

Abbreviations

Abs	Absorber
a	Air (state)
AAR	Ammonia absorption refrigeration
AC	Air compressor
ACF1	Air compressor function 1
ACF2	Air compressor function 2
ACGS	Advanced Co-generation System
Ar	Argon
AW in	Heat or work added into ammonia water system
AW out	Heat or work subtracted from ammonia water system
awa	Ammonia water mixture to air
AWAC	Ammonia water absorption chillers
AWACS	Ammonia water absorption chillers system
AWM	Ammonia water mixture
AWMC	Ammonia water mixture cycle
AWMT	Ammonia water mixture turbine
B	Basic (for ammonia concentration)
Bwr	The ratio of the back work
B, 1B,2B,3B,4B	State points for Brayton cycle
c	Compression
C/C	Carbon reinforced carbon composites
C_2H_6	Ethane
C_3H_8	Propane
C_4H_{10}	Butane
CC	Combustion chamber
CCPP	Combined cycle power plant
CH_4	Methane
ChGT	Chemical gas turbine configuration
ChGT	Chemical gas turbine
CLTFXhP	Compressed liquid functioned to AWM concentration, enthalpy and pressure

CO	Carbon monoxide
CO_2	Carbon dioxide
Con	Condenser
COP	Coefficient of performance
Cor	Corrected
$CRCC_{life}$	Life factor
cw	Cooling water
D3	Kalian cycle sub system
Des	Desorber
DFT	Air density functioned to it temperature
Dis	Distiller (vaporizer)
DP	Design point
DPCC	Dual pressure combined cycle
DPRehS	Dual pressure reheated steam
DPSC	Dual pressure steam cycle
E	Evaporator
e	Emission rate
EC	Economizer
EV	Expansion valve
Ev	Evaporator
F	Rich ammonia vapour to basic solution ratio
f	Fuel to air ratio or fuel
fLFTEREFFLCV	Lean fuel to air ratio functioned to equivalence ratio, combustion chamber efficiency and LCV
fRFTEREFFLCV	Rich fuel to air ratio functioned to equivalence ratio, combustion chamber efficiency and LCV
fs	Water (state)
g	Gas or Air (state)
G in	Heat or work added into gas system
G out	Heat or work subtracted from gas system
g1Int	Gases Intercooler inlet(state)
g2Int	Gases Intercooler outlet(state)
g2Reg	Air at regenerator inlet (state)
g3Reh	Gases at reheater outlet (state)

g4Reg	Gases at regenerator inlet (state)
g4Reh	Gases at reheater inlet (state)
GCF1	Lean combustion gases enthalpy functioned to the equivalence ratio and the temperature
GCF2	Air enthalpy functioned to the temperature
GCF3	Rich combustion gases enthalpy functioned to the equivalence ratio and the temperature
GCF7	The temperature of the air functioned to the enthalpy of the air (function)
GCPP	Gas cycle power plant
GE	General electric company
gE	Gas (state) at exhaust
gEI	Gas at evaporator inlet
gEO	Gas at evaporator outlet
gRehO	Gas at reheater outlet
gStack	Gases at stack inlet
GT	Gas turbine
GTF1	Gas turbine function 1
GTF2	Gas turbine function 2
H_2	Hydrogen
H_2S	Hydrogen sulphide
hBFXP	Boiling point enthalpy of AWM
hDFXP	Due point enthalpy of AWM
HE	Heat exchanger
hfFP	Saturated water enthalpy functioned to the pressure function
hFPTx	AWM enthalpy functioned to the pressure, temperature and the concentration function
hFsP	Saturated water enthalpy functioned to the entropy and the pressure function
hFXPs	AWM enthalpy functioned to concentration, pressure and entropy function
hFXTP	AWM enthalpy functioned to the concentration, temperature, pressure function
hgFP	Saturated steam functioned to pressure function
HP	High pressure state

HRSG	Heat recovery steam generator
HRSGI	State points at Heat Recovery steam generator Inlet
HRSGO	State points at Heat Recovery steam generator outlet
HRVG	Heat recovery vapour generator
IEA	International energy agency
in	Input
in1, in2	State points at intercooler inlet and outlet respectively
IntG	Intercooled gas
IntRehGC	Intercooled reheated gas
IntRehGSSCC	Intercooled reheated regenerated gas simple steam combined cycle
IntRehRegGC	Intercooled reheated regenerated gas
IP	Intermediate pressure state
ISO	International Organization for Standardization
JANAF	Jadranski naftovod
KC	Kalina cycle
KC0	Kalina cycle system zero
KC1	Kalina cycle system 1
KC2	Kalina cycle system 2
KC3	Kalina cycle system 3
KCS1D2	Kalina cycle system 1 with distillation subsystem 2
KC34	Kalina cycle system 34
KC6	Kalina cycle system 6
KC8	Kalina cycle system 8
KSC6D2	Kalina cycle system 6 with distillation subsystem 2
KSC6D3	Kalina cycle system 6 with distillation subsystem 3
KSC8D3	Kalina cycle system 8 with distillation subsystem 3
L	Lower or bottoming cycle
l	Lean combustion
LCVLFTER	Lean combustion low calorific value functioned to temperature and the equivalence ratio function
LCVRFTER	Rich combustion low calorific value functioned to temperature and the equivalence ratio function
Lin	Input to the lower or bottoming
LL	Lean liquid (for ammonia concentration)

LP	Low pressures state
M	Methane
min	Minimum
max	Maximum
MF	Mass flow parameter
MR	Mass flow ratio
N	Rotational speed
N_2	Nitrogen
NASA	USA National Aeronautics and Space Administration
ND	Non dimensional
NH_3	Ammonia
NO_X	Nitrogen oxides
NTU	Number of transfer units method
out	Discharged for heat or generated for work
PC	Pre-cooler
PG	Power generator
P_{Int}	Pressure of inter-cooling
PmixbyCp	The pressure of gases after mixing with air in chgt using the specific heat at constant pressure (function)
POGT	Partial oxidation gas turbine
PP	Power plant
ppm	Minimum pinch point
PR	Pressure ratio parameter
P_{Reh}	Pressure of reheat
Ps3Reh	Pressure of the steam at reheater outlet
PSB	Pressure of the steam through boiler
Q	Heat
q	Specific heat
Q_{in}	Input heat
R	Rich ammonia mixture (for ammonia concentration)
r	Cycle pressure ratio
r	Rich fuel
r_c	Pressure ratio at the compressor
r_t	Pressure ratio at the turbine

R,R1,R2	
Rec	Rectifier Or recuperator
Reg	Regenerator
reg1, reg2	State points at regenerator inlet and outlet respectively
RegS	Regenerated steam
reh1, reh2	State points at re-heater inlet and outlet respectively
RehGC	Reheated gas cycle
RehP	Reheated pressure
RehR	Reheated pressure ratio for gas turbine
RehS	Reheated steam ratio for steam turbine
s	Steam, or water (state)
s in	Heat or work added into steam system
s out	Heat or work subtracted from steam system
s1reg	Steam at regenerator inlet (state)
s2f	Steam at economizer outlet (state)
s2g	Steam at evaporator outlet (state)
s2HP	Steam at high pressure evaporator (state)
s2IP	Steam at intermediate pressure evaporator (state)
s2LP	Steam at low pressure evaporator (state)
s2reg	Hot water at closed feed water outlet
s3reg	Steam at feed water heater inlet
s3Reh	Steam at reheater outlet (state)
s3Sup	Steam at superheater outlet (state)
s4reg	Low quality steam to the condenser inlet
s4Reh	Steam at reheater inlet (state)
s4s	Steam at after isentropic expansion (state)
s4Sup	Steam after isentropic expansion from superheated area
sa	Steam to air
SB	Steam boiler
SC	Steam cycle power plant
SCon	Steam condenser
SCR	Selective catalytic reduction
SEI	Steam at evaporator inlet (state)
Sf	Saturated water

SFC	Specific fuel consumption
SFHP	Steam entropy functioned to enthalpy and pressure (function)
SFXPh	Saturated AWM entropy functioned to concentration pressure and enthalpy (function)
sg	Saturated steam
SHE	Solution heat exchanger
SOx	Sulphur oxide
S_{Reh}	Reheated steam ratio
SS	Simple steam
ST, ST1,ST2	Steam turbine
Stack	Stack gases conditions (status)
STAG	General electric steam turbine system in combined cycle power plant
STideal	Ideal steam turbine (for work)
STreal	Real steam turbine (for work)
Sup	Super heater, heat supplied
t	Total
T′	Fluid real temperature at heat input or discharge
TBFXP	Boiling point temperature functioned to ammonia concentration and the pressure of AWM (function)
TDFXP	Due point temperature functioned to ammonia concentration and the pressure of AWM (function)
TFP	Steam evaporation temperature functioned to the pressure (function)
TFPhX	AWM temperature functioned to pressure, enthalpy and ammonia concentration (function)
TFPP	Compressed water temperature functioned to the pressures between condenser and evaporator (function)
th	Thermal for efficiency
TIT	Turbine inlet temperature
TmixbyCp	The temperature of gases after mixing with air in chgt using the specific heat at constant pressure (function)
TPRehS	Triple pressure reheated steam
TPS	Triple pressure steam
TPSC	Triple pressure steam cycle

$T_{Sg4,}$ h_{sg4}	Property of steam based on gases properties
U	Heat transfer coefficient
U	Upper or topping cycle
UHC	Unburned hydrocarbons
un, un1 , un2	Unused heat for specific heat
Uout	Output from the upper or topping
US NIST	USA national institute of standards and technology
v	Volume
VFP	Air volume functioned by the pressure (function)
W	Working solution (for ammonia concentration)
W-MTS	Waseda university AWM turbine system
W_{out}	Specific work output
WEO	World energy outlook
WP	Water pump
WPHP	High pressure water pump
WPideal	Water pump ideal (for work input)
WPIP	Intermediate pressure water pump
WPLP	Low pressure water pump
WPreal	Water pump real (for work input)
x	Carbon number of moles
X	Dryness factor
XFSP	Steam dryness fraction functioned to the entropy and the pressure (function)
XFSPX	AWM dryness fraction functioned to the entropy and the pressure (function)
y	The mass flow rate of the lean solution to that of the basic solution
y	Hydrogen number of moles
Y_s	Regenerated steam to total steam mass ratio
Z	Lean solution mass fraction
θ_{SHE}	Specific ratio between the temperature of the lean solution at the heat exchanger inlet and that for the basic solution stream from the other inlet end.

CHAPTER 1
INTRODUCTION INTO POWER GENERATION PRINCIPLES AND THERMODYNAMICS

1.1 An outlook on power generation

The satisfaction of human progressive lifestyle, accommodations and developments are the main goal behind many ideas throughout the history of mankind. Consequently, facilities such as transports, air-conditionings and many other modern life necessities are created. These were established to be powered by the energy released from different energy sources. Primarily, fossil fuel, nuclear reaction and renewables are the resources to generate such energy. In each case, the energy has its own form, requirements and the specific mechanism by which it usefully released and used by the individual facility.

In general, the demand for energy has progressively increased as a result of the rapid growth in the population and life style. On the other hand, the continuous inefficient utilization of some of energy resources like the fossil fuel (coal, oil and gas) in the past IEA, [1] has led to great disastrous consequences (pollution, change in weather pattern, global warming, etc.). Global energy needs are expected to grow over the next decades with the domination of fossil fuels as the energy source. As a result, emissions represented by CO_2 are expected to sharply increase, and thus, its dramatic consequences. The expectations of World Energy Outlook (WEO) scenario between 2011 and 2035 show a severe increase in world's energy needs (exceeding two-third). This will result in a significant increase in CO_2 emissions level (by 20%) in addition to a long-term temperature increase of about 3.6 °C [2].

Essentially, different paths of strategies are usually used to meet the two correlative demands above. Employing such strategies may guarantee the increase of energy conservation with acceptable levels of environmental impact. The first path focuses on employing different clean energy sources to power those facilities (i.e. nuclear reaction and renewables). The

technologies by which such energy sources are utilized are either already fully developed with low outputs, or featured by unstable operating availability. On the other hand, the high costs of construction and maintenance (particularly of nuclear stations) added more difficulties to the use of such technologies. The second path of solutions targeted establishing new and more efficient thermal power stations. This path also included improving the performance of the operating stations by increasing its thermal efficiency combined with considerable drop of its harmful discharges. This path is what this research is entirely based on.

Most of the world energy consumption related to CO_2 emissions was devoted for power generation. The energy released for such a cause was greater than that utilized in transports, industry, building, etc. In view of that, the current research focused on power generation facilities only. Fossil fuel-fired power plants are responsible for producing most of the currently generated electricity around the world with its correspondent environmental impact. Such power generation facilities consume 32% of the fossil fuel resources, and responsible for 41% of the energy release associated with CO_2 emissions [3]. A percentage of 67.4% of the total global public electricity produced in 2010 was generated from coal, oil and gas, as it was confirmed by IEA, [1] of such percentage the usage of coal, natural gas and oil were (60, 33 and 7%) respectively. More than 90% of the produced electricity was generated by thermal power stations. The average thermal efficiency of electricity production from a standalone fossil fuel mechanism commonly does not exceed 36% [4].

In general, two strategies were often proposed to control CO_2 emissions from such plants, the first was improving the efficiency of power generation. The second was employing CO_2 capture and permanent storage strategy for the operating plants. Improving the efficiency of power production is one of the most important procedures to reduce world's dependency on fossil fuels for power generation. Thus, the better the efficiency is, the less the environmental impact and the greater is the power generation. According to the great share of such power plants on generating CO_2 emissions, improving their efficiencies has the greatest influence on reducing such emissions worldwide. Combined cycle power plant represents one of the latest and most useful strategies to increase the efficiency of power generation. It also has further control on reducing global warming and plant emissions than regular configurations.

The combination between gas turbine cycle and the steam turbine cycle is one of the most promising technologies in power generation. The main concept of such cycles based on supplying the heat to gas cycle only. Therefore, it uses the same components of the above cycles to generate more efficient power output. The heat from gas turbine exhaust powers the

steam cycle. This cycle works between the high temperature of the gas turbine and the low temperature of steam turbine heat rejection. Therefore, the performance of the combined power plant is better than the performance of both plants individually. It is also suitable to run facilities similar to those run by the steam turbine or the gas turbine power plants. As an example, it is successful in providing a power output that suits the middle size peak facilities like a gas turbine and the large base load facilities like a steam turbine. Using natural gas to power combined cycle power plants improves its efficiency and consumes less time and costs than coal fired power plants. Therefore, this research undertakes to concentrate on the use of natural gas as power plant fuel rather than any other type of fossil fuel.

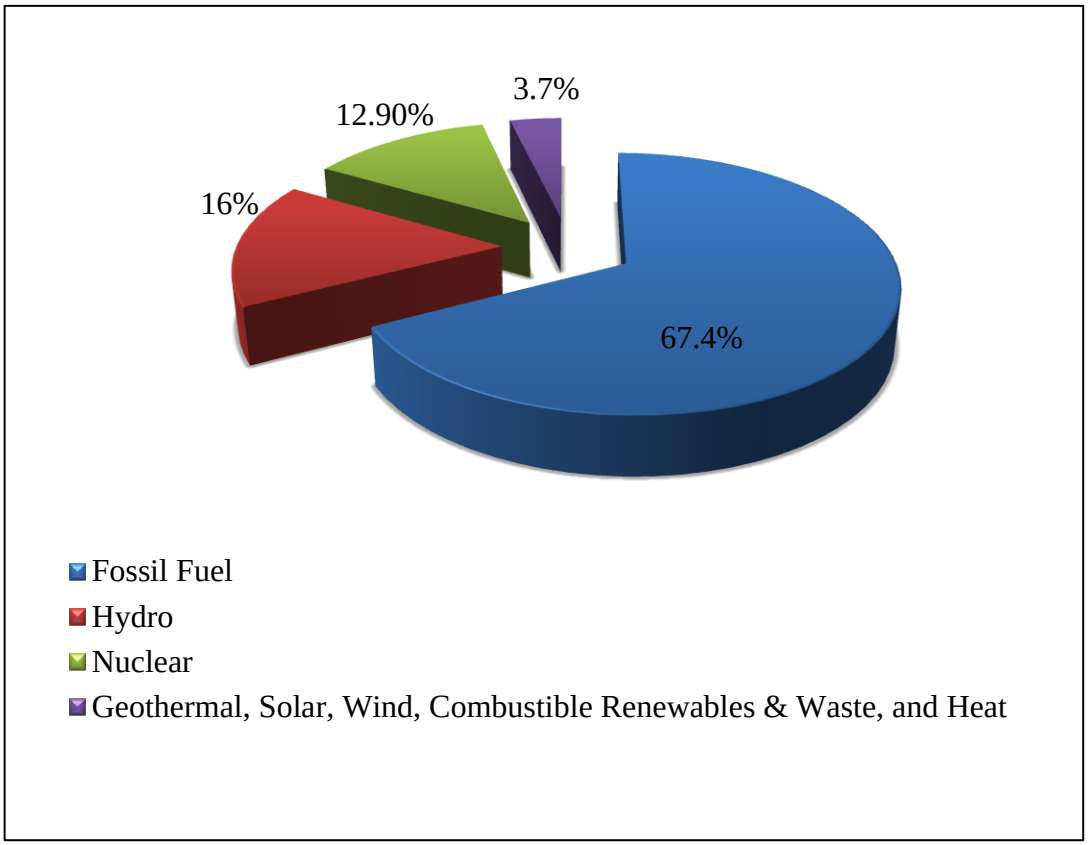

Figure 1.1 Total world power generation in the year 2010 data given by IEA [1]

Nowadays, combined cycle power plants reach a generation efficiency of approximately 60% with reduced emissions. Many extra modifications can be employed in such plant to improve its performance like supplementary firing, reheating, regeneration, etc. Although, a large number of combined cycle configurations were adopted by various studies, only few were developed. This research considers a variety of combined cycle power plant configurations.

1.2 Elementary power cycle thermodynamics

The ultimate aim of any study that considers the thermodynamic analysis of a power plant is to reach maximum plant efficiency. This is defined as the power generated from a certain amount of fuel consumed. The thermal efficiency of a power plant is given by equation 1.1. Here, Q_{in} represents the heat input from burned fuel, while W_{out} symbolizes the work output and η_{th} represents the thermal efficiency.

$$\eta_{th} = \frac{(W_{Out})_{net}}{(Q_{in})_{total}} \quad \ldots (1.1)$$

Furthermore, the performance of a power cycle that operates between two certain temperatures is provided by measuring how close its performance to the performance of the Carnot engine. The difference between the two performances is caused by the internal and external irreversibilities, and these were the reasons as to why a closed cycle can't reach the performance of the Carnot. In addition to the irreversibilities, two other parameters are referred by the previous studies to be responsible for such deficiency in performance. These are: the maximum and minimum temperature parameters (ζ_{in}) and (ζ_{out}), both parameters can be combined to produce a single cycle temperature parameter (ζ). The external irreversibilities can be classified into irreversibility during heat addition (σ_{in}) and irreversibility during heat rejection (σ_{out}). These two parameters can also be combined to produce the irreversibility parameter (σ) of the cycle. For Carnot cycle, the ζ and σ embrace unity, while for any other cycle, these values are less than one. The values of the temperature parameters ζ are given in Equations (1.2 – 1.4) and that of the irreversibility parameters σ in Equations (1.5 – 1.7), as shown hereafter.

$$\zeta \equiv \frac{\zeta_{in}}{\zeta_{out}} \quad \ldots (1.2)$$

$$\zeta_{in} = \frac{T'_{in}}{T_{in\,max}} \quad \ldots (1.3)$$

$$\zeta_{out} = \frac{T'_{out}}{T_{out\,min}} \quad \ldots (1.4)$$

$$\sigma \equiv \frac{\sigma_{in}}{\sigma_{out}} \quad \ldots (1.5)$$

$$\sigma_{in} = \frac{Q_{in}}{T'_{in}} \quad \text{... (1.6)}$$

$$\sigma_{out} = \frac{Q_{out}}{T'_{out}} \quad \text{... (1.7)}$$

According to the energy conservation and second law of thermodynamics principles, the total heat input cannot be entirely used to generate the power output. As a result, some heat must be rejected (usually to a sink of lower temperature). Hence, the thermal efficiency can be represented by equation (1.8). Using the above parameters; the efficiency equation can be generated as shown by equation (1.9). In this equation another parameter emerges is the ratio between the minimum to the maximum temperatures (τ).

$$\eta_{th} = \frac{Q_{in} - Q_{out}}{Q_{in}} \quad \text{... (1.8)}$$

$$\eta_{th} = 1 - \frac{\tau}{\sigma\zeta} \quad \text{... (1.9)}$$

$$\tau = \frac{T_{min}}{T_{max}} \quad \text{... (1.10)}$$

1.3 Theory of the combined cycle power plants

This section reviews the elementary theoretical concepts of the gas/steam combined power plant that performs on Brayton/Rankine power cycles. It identifies cycles' inputs, outputs, and the correspondent assumptions required for the theory of such cycle. The concept of a combined cycle power plant is based on increasing the heat recovery from the same heat input to generate extra power. The advantage from the combined cycles is guaranteed by using the appropriate working fluid and its physical states to attain the best heat transfer between cycles. Experimentally, the best successful configuration was proved to be between the gas turbine Brayton cycle and the steam turbine Rankine cycle. The processes involved in this combination are illustrated thermodynamically by Fig.1.2. The main components of the combined power plant are schematically shown in Fig.1.3.

The increase in the power output from a conventional combined cycle can be clearly seen in Fig.1.2, which illustrates the combination between Brayton and Rankine cycles on T-S diagram. With respect to equation of the specific work $w = C_P \times \Delta T$, the gas cycle operates

between certain turbine inlet and outlet temperatures Tg_3 and Tg_4 respectively. Therefore, the work generated by such cycle is governed by such temperature's difference. The working fluid directs the work output process in Rankine cycle to take place between points (s_3) and (s_4). The combined cycle works between the maximum temperature of the Brayton cycle and the minimum temperature of the Rankine cycle. Therefore, the work generated by the combined cycle is generated between point (g_3) and point (s_4). This work is clearly greater than the work generated by each cycle individually with respect to the working fluids and the losses between the points (g_4) and (s_3).

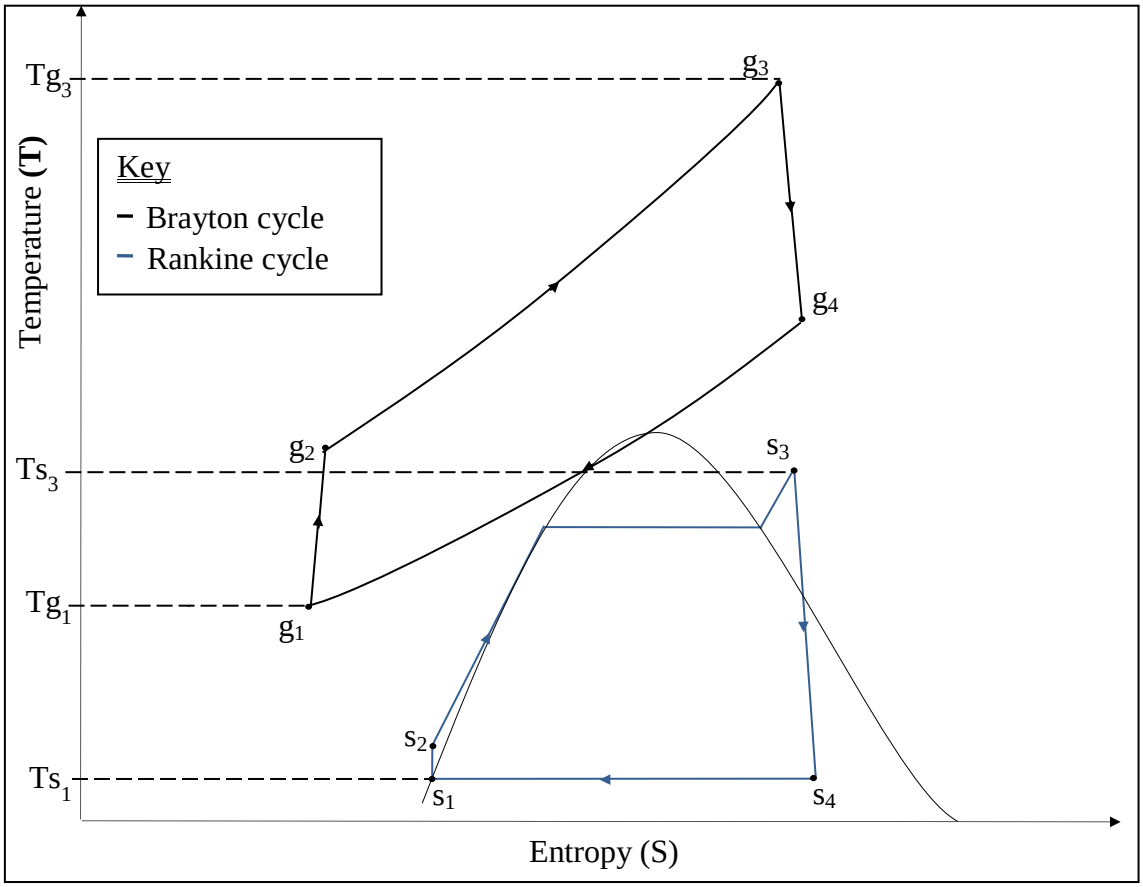

Figure 1.2 Brayton /Rankine combined cycles on T-S diagram

In practice, as in any power cycle, the combined cycle power plants' processes are affected by different operating parameters. Such processes occur in the plant's components and generate considerable energy losses. In the current work, the losses and the operating parameters of each individual cycle in combined cycle configurations as well as various processes are included when combined cycle power plants are investigated. Therefore, in order to investigate the performance of the combined cycle and its optimization it is vitally important to identify the parameters which govern cycle's efficiency and power output. From a thermodynamic point of view, the thermal efficiency of a combined cycle is essentially increased by the rise in the temperature of the fluids (gases or steam) at the turbine inlet of

each cycle and the drop in the heat losses at heat recovery steam generator (HRSG) shown schematically in Fig.1.3.

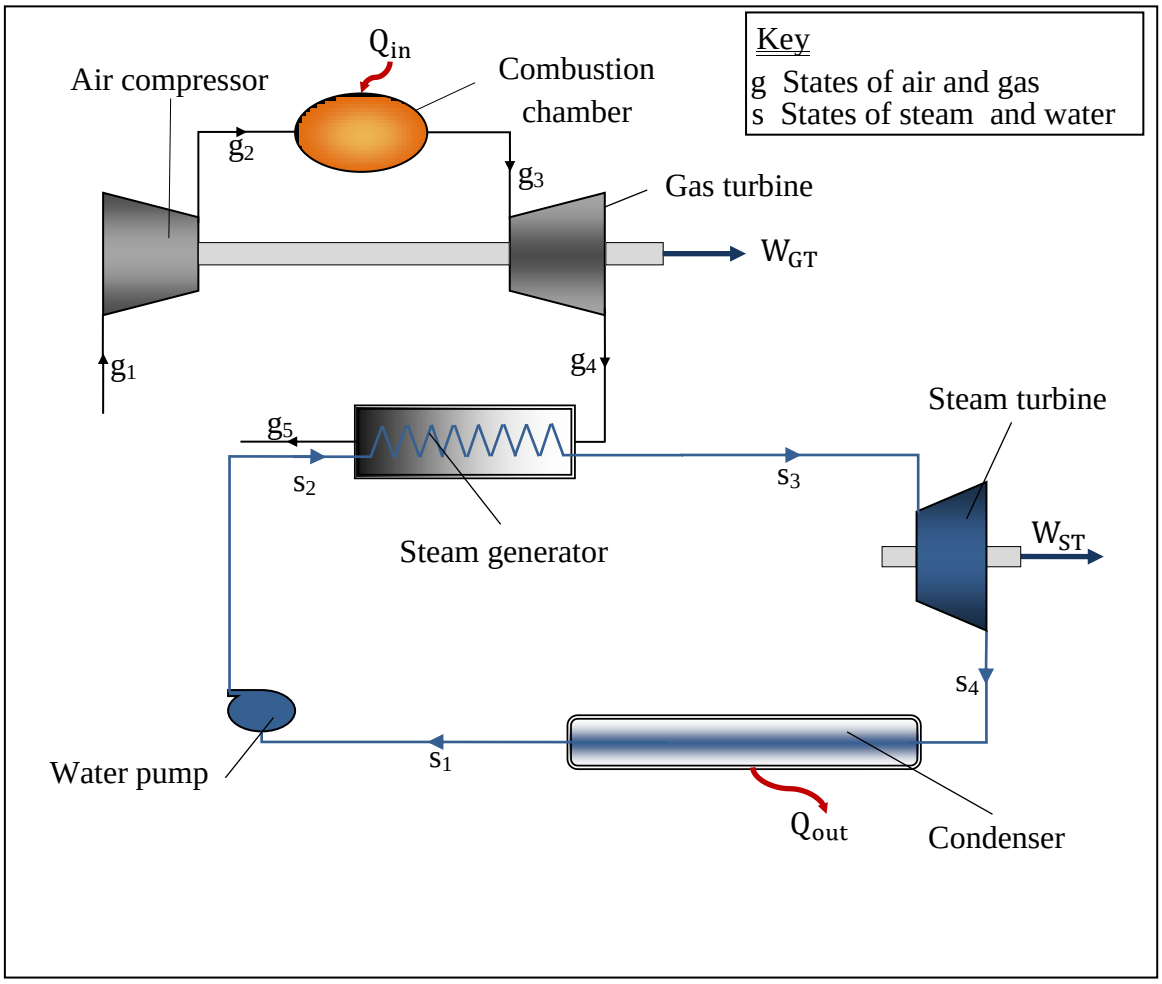

Figure 1.3 Simple gas/steam turbines combined cycle power and power plant

The work outputs from the gas turbine and the steam turbine plants/engines are represented by equations (1.11 and 1.12), respectively. The total heat input to the cycle is represented by equation (1.13). If the steam is totally generated from the waste heat recovered from the turbine exhaust gases, there is no need for additional heating. Otherwise, an additional heat input is required to generate the steam at the appropriate condition in order to run the steam turbine. Accordingly, the thermal efficiency and the work output of the CCPP are represented by equations (1.14 and 1.15), respectively

$$W_{GC} = W_{GT} - W_{AC} \quad \text{... (1.11)}$$

$$W_{SC} = W_{ST} - W_{WP} \quad \text{... (1.12)}$$

$$Q_{CCin} = Q_{CC} + Q_{HRSG} - Q_{Losses} \quad \text{... (1.13)}$$

$$\eta_{CC} = \frac{W_{CC}}{Q_{Gin}} \quad \text{... (1.14)}$$

$$W_{CC} = W_{GCout} + W_{SCout} \quad \text{... (1.15)}$$

$$W_{CC} = \eta_{GC} Q_{GCin} + \eta_{SC} Q_{SCin} \quad \text{... (1.16)}$$

Here the work generated by the gas and the steam plants/engines are expressed in terms of the efficiency and the heat input into each ($W_{GCout} = \eta_{GC} Q_{GCin}$), ($W_{SCout} = \eta_{SC} Q_{SCin}$) as shown in equation (1.16). The heat input into to the steam engine and that output from the gas turbine are represented by ($Q_{SCin} = Q_{GCout} - Q_{un1}$) and ($Q_{GCout} = Q_{GCin} - W_{GCout}$). The equations above utilize these relations and after simplification equations (1.17-1.20) are generated regarding the following term, ($\nu_{un1} = Q_{un1} / Q_{GCin}$).

$$W_{CC} = \eta_{GC} Q_{GCin} + \eta_{SC} Q_{GCin} - \eta_{SC} \eta_{GC} Q_{Gcin} - \eta_{SC} Q_{un1} \quad \text{... (1.17)}$$

$$W_{CC} = Q_{GCin} \left(\eta_{GC} + \eta_{SC} - \eta_{SC} \eta_{GC} - \eta_{SC} \nu_{un1} \right) \quad \text{... (1.18)}$$

$$\eta_{CC} = \eta_{GC} + \eta_{SC} - \eta_{SC} \eta_{GC} - \eta_{SC} \frac{Q_{un1}}{Q_{GCin}} \quad \text{... (1.19)}$$

$$\eta_{CC} = \eta_{GC} + \eta_{SC} - \eta_{SC} \eta_{GC} - \eta_{SC} \nu_{un1} \quad \text{... (1.20)}$$

Equation (1.19) can be re-written as in equation (1.21).

$$\eta_{CC} = \eta_{GC} + \eta_{SC} \left(1 - \eta_{GC} - \frac{Q_{un1}}{Q_{GCin}} \right) \quad \text{... (1.21)}$$

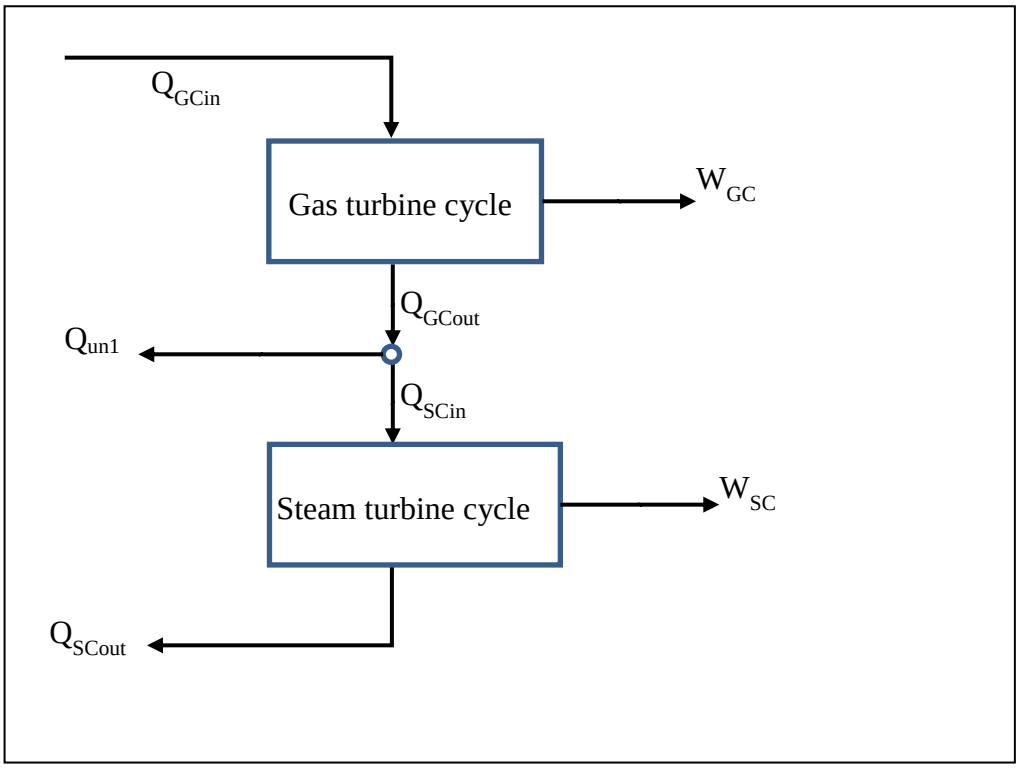

Figure 1.4 The combination between a gas turbine and a steam turbine cycles

By considering the heat losses for the simple individual power cycle and applying it to the gas turbine plant/engine, equation (1.22) is converted into (1.24).

$$\eta_{GC} = \frac{Q_{GCin} - Q_{GCout}}{Q_{GCin}} \quad \text{... (1.22)}$$

$$\eta_{GC} = 1 - \frac{Q_{GCout}}{Q_{GCin}} \quad \text{... (1.23)}$$

$$\eta_{GC} = 1 - \frac{\tau_{GC}}{\sigma_{GC}\zeta_{GC}} \quad \text{... (1.24)}$$

Where;

$$\zeta_{GCin} = \frac{T'_{GCin}}{T_{GC\,max}}, \zeta_{GCout} = \frac{T'_{GCout}}{T_{GC\,min}}, \sigma_{GCin} = \frac{Q_{GCin}}{T'_{GCin}}, \sigma_{GCout} = \frac{Q_{GCout}}{T'_{GCout}}, \zeta_{GC} \equiv \frac{\zeta_{GCin}}{\zeta_{GCout}},$$

$$\sigma_{GC} \equiv \frac{\sigma_{GCin}}{\sigma_{GCout}} \; \tau_{GC} = \frac{T_{GC\,min}}{T_{GC\,max}}$$

Now, consider the same losses for the steam turbine plant/engine in the following. Therefore, equation (1.25) is converted into (1.27).

$$\eta_{SC} = \frac{Q_{SCin} - Q_{SCout}}{Q_{SCin}} \quad \text{... (1.25)}$$

$$\eta_{SC} = 1 - \frac{Q_{SCout}}{Q_{SCin}} \quad \text{... (1.26)}$$

$$\eta_{SC} = 1 - \frac{\tau_{SC}}{\sigma_{SC}\zeta_{SC}} \quad \text{... (1.27)}$$

Where;

$$\zeta_{SCin} = \frac{T'_{SCin}}{T_{SC\,max}},\ \zeta_{SCout} = \frac{T'_{SCout}}{T_{SC\,min}},\ \zeta_{SC} \equiv \frac{\zeta_{SCin}}{\zeta_{SCout}},\ \sigma_{SCin} = \frac{Q_{SCin}}{T'_{SCin}},\ \sigma_{SCout} = \frac{Q_{SCout}}{T'_{SCout}}$$

$$\sigma_{SC} \equiv \frac{\sigma_{SCin}}{\sigma_{SCout}}, \text{ and } \tau_{SC} = \frac{T_{SC\,min}}{T_{SC\,max}}$$

Substituting equations (1.24) and (1.27) in equation (1.21) generates equation (1.28) and after simplifying equation (1.29) is generated, which represented in equation (1.30) by the main losses' factors (ν_{un1}, ν_G and ν_S).

$$\eta_{CC} = 1 - \frac{\tau_{GC}}{\sigma_{GC}\zeta_{GC}} + \left(1 - \frac{\tau_{SC}}{\sigma_{SC}\zeta_{SC}}\right)\left(1 - \left(1 - \frac{\tau_{GC}}{\sigma_{GC}\zeta_{GC}}\right) - \frac{Q_{un1}}{Q_{GCin}}\right) \quad \text{... (1.28)}$$

$$\eta_{CC} = 1 - \frac{\tau_{GC}}{\sigma_{GC}\zeta_{GC}}\frac{\tau_{SC}}{\sigma_{SC}\zeta_{SC}} + \frac{Q_{un1}}{Q_{GCin}}\left(\frac{\tau_{SC}}{\sigma_{SC}\zeta_{SC}} - 1\right) \quad \text{... (1.29)}$$

$$\eta_{CC} = 1 - \nu_{GC}\nu_{SC} + \nu_{un1}\left(\nu_{SC} - 1\right) \quad \text{... (1.30)}$$

Where;

$$\nu_{un1} = \frac{Q_{un1}}{Q_{GCin}},\ \nu_{SC} = \frac{\tau_{SC}}{\sigma_{SC}\zeta_{SC}}, \text{ and } \nu_{GC} = \frac{\tau_{GC}}{\sigma_{GC}\zeta_{GC}}$$

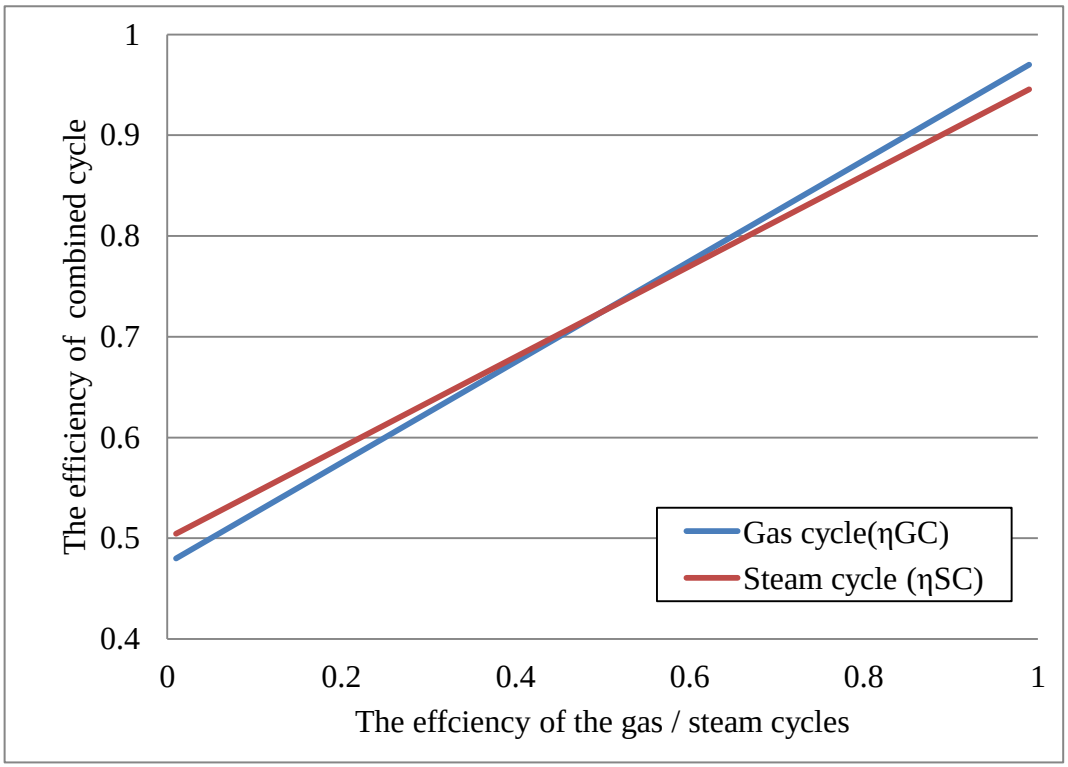

Figure 1.5 Combined cycle efficiency functioned to the efficiency of each cycle

The figure 1.5 shows the relationship between the efficiency of the combined cycle as compared to both the gas and steam cycles based on the developed equation above. The increase in the efficiency of the combined cycle is very evident in Fig.1.5. Here, it is useful to begin to investigate the effects of the losses of each part of a combined cycle power plant on efficiency of the whole combined cycle as indicated by equation (1.30). The figure 1.6 shows that the heat transfers losses between cycles have amplified effects on the efficiency of the combined cycle. It is also clear that the effect of the gas cycle efficiency on the combined cycle is much greater than that of the steam cycle.

1.4 Enhancements to the combined cycle power plant

This research investigates an optimum design for a configuration in which a combined cycle power plant is based on chemical gas turbine (ChGT) configurations and enhanced by ammonia-water Kalina cycle turbine and absorption chiller for gas turbine compressor's intake air cooling. It is worth as a starting point to use the basic thermodynamic analysis, those previously considered for the combined cycle to investigate the new combination. It identifies the most effective cycles by such combination.

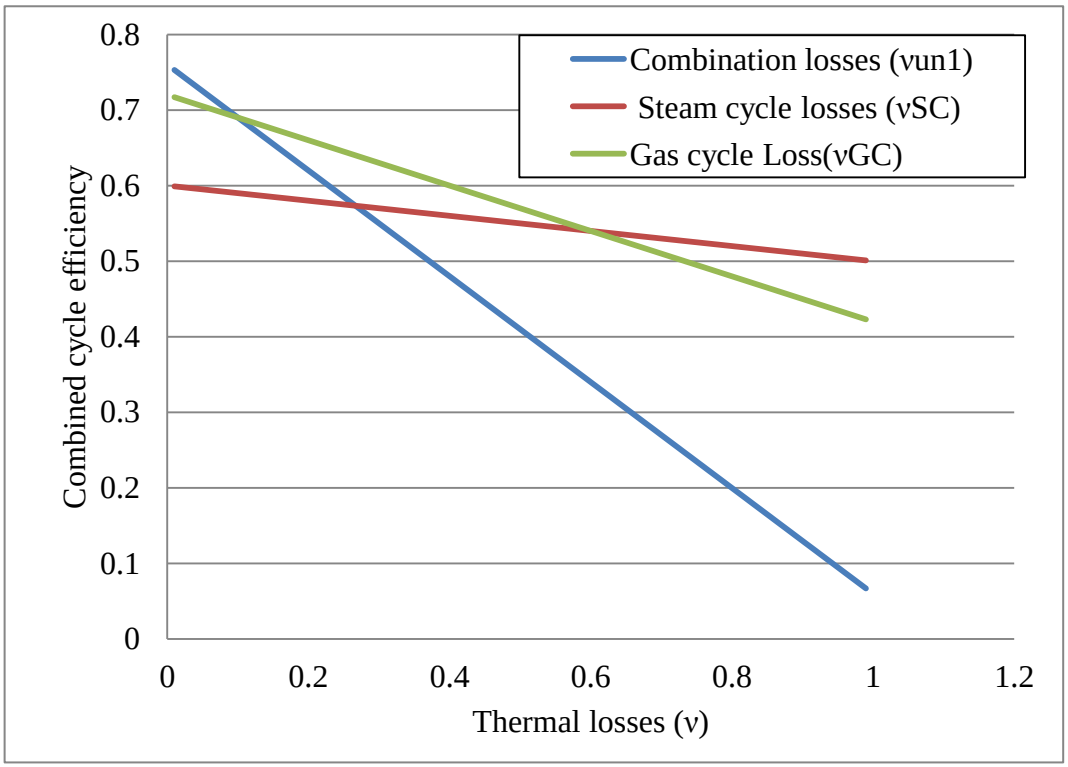

Figure 1.6 The effect of the losses on the efficiency of the combined cycle

The power generated from the triple cycle is represented by equation (1.31), where; (W_{TC}) is the net power output from the cycle, (W_{GC}) is the power generated from the gas turbine cycle, (W_{SC}) is the power generated by the steam turbine cycle, (W_{AWC}) is the power generated from the ammonia water mixture turbine cycle and (W_{ACC}) is the augmentation in the power generated from the gas turbine by the effect of the absorption chiller cooling. Regarding the same bases considered for the cycles above, equation (1.31) can be rewritten and expressed by equations (1.32 and 1.33). These equations are used to identify the efficiency of the TC in equation (1.34).

$$W_{TC} = W_{GCout} + W_{SCout} + W_{AWCout} + W_{ACCout} \quad \text{... (1.31)}$$

$$W_{TC} = Q_{GCin}\eta_{GC} + Q_{SCin}\eta_{SC} + Q_{AWCin}\eta_{AWC} + \frac{Q_{ACCin}}{COP_{ACC}} \quad \text{... (1.32)}$$

$$W_{TC} = Q_{GCin}\left[\begin{array}{l}\left(\eta_{GC} + \eta_{SC}\left(1-\eta_{GC} - \dfrac{Q_{Un1}}{Q_{GCin}} - \dfrac{Q_{AWCin}}{Q_{GCin}}\right) + \eta_{AWC}\dfrac{Q_{AWCin}}{Q_{GCin}}\right) \\ + \left(\dfrac{\left(\begin{array}{l}1-\eta_{GC} - \dfrac{Q_{Un1}}{Q_{GCin}} - \dfrac{Q_{AWCin}}{Q_{GCin}} \\ -\eta_{SC}\left(1-\eta_{GC} - \dfrac{Q_{Un1}}{Q_{GCin}} - \dfrac{Q_{AWCin}}{Q_{GCin}}\right) - \dfrac{Q_{Un2}}{Q_{GCin}}\end{array}\right)}{COP_{ACC}}\right)\end{array}\right] \quad \text{... (1.33)}$$

$$\eta_{TC} = \left(\begin{array}{l}\eta_{GC} + \eta_{AWC}\mu_{AWC} \\ +\eta_{SC}\left(1-\eta_{GC} - \nu_{Un1} - \mu_{AWC}\right)\end{array}\right) + \left(\dfrac{\left(\begin{array}{l}1-\eta_{GC} - \nu_{Un1} - \nu_{Un2} - \mu_{AWC} \\ -\eta_{SC}\left(1-\eta_{GC} - \nu_{Un1} - \mu_{AWC}\right)\end{array}\right)}{COP_{ACC}}\right) \quad \text{... (1.34)}$$

Where

$$\mu_{AWC} = \frac{Q_{AWCin}}{Q_{GCin}},\ \nu_{Un1} = \frac{Q_{Un1}}{Q_{GCin}} \text{ and } \nu_{Un2} = \frac{Q_{Un2}}{Q_{GCin}}.$$

Consider that the power given to the absorption chiller is regained from the gas turbine inlet air cooling strategy and assume the power gain is greater, accordingly it is considered that such gain is equal to that required by the absorption system. Therefore, such gain in power is related to the performance of this system.

The effect of the combined cycle's performance characteristics on the efficiency of the whole combined cycle as represented by equation (1.34) is illustrated by Fig.1.8. Initially, it is convenient to investigate such combination between the cycles above to clarify how efficient such cycle should be and to compare such performance with that of the conventional combination. As it can be seen from such figure, it is evident that:

(i) The efficiency of the conducted cycle is less affected by the performance of each cycle individually than the conventional combined cycle.

(ii) The range of such cycles' efficiency starts with values greater than that of the conventional and ends with a range smaller than that for the conventional. Accordingly, the effect of the conventional combined cycles on the combined cycle performance is greater.

(iii) Among the different cycles, the ammonia water cycle efficiency has the slightest effect on the performance of the triple combined cycle efficiency. The greatest effect among the cycles is the efficiency of the gas cycle. The other two cycles' have modest effects and the COP of the absorption chillers system has a slighter effect than the efficiency of the steam cycle.

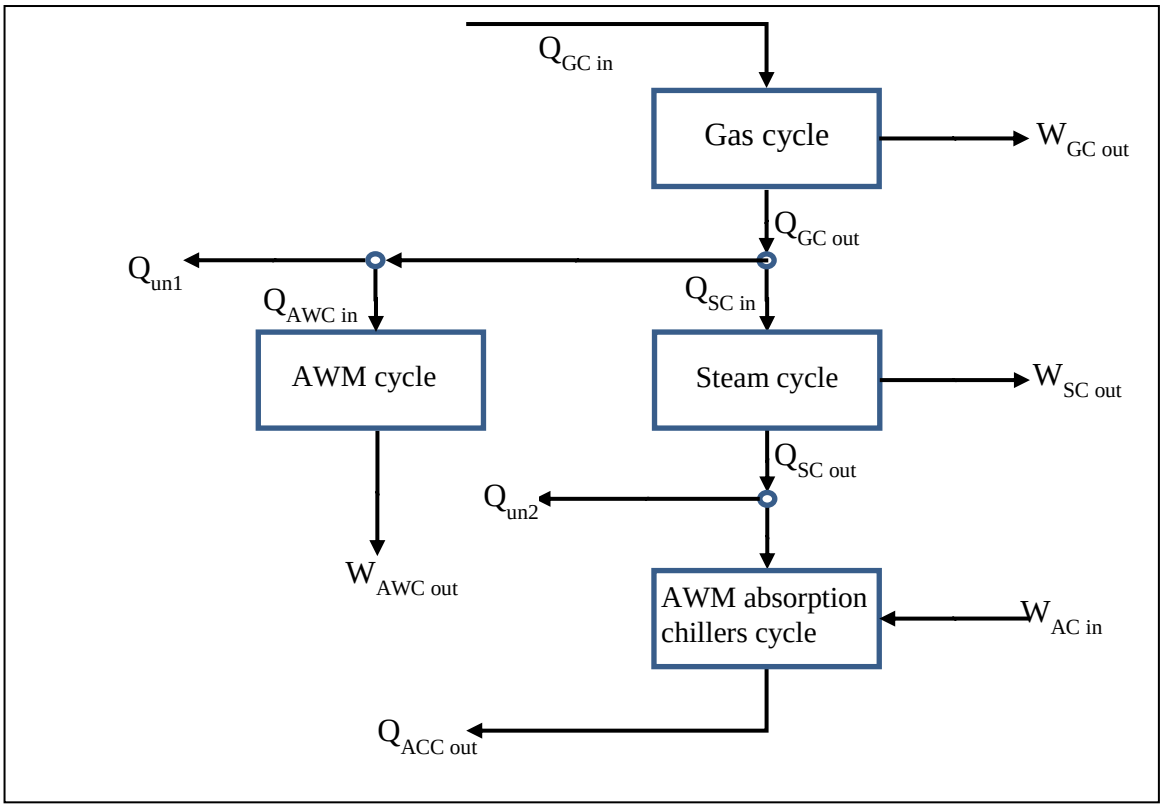

Figure 1.7 Triple combination power cycle enhanced by heat pump system

According to the points above, there are restrictions behind which this combination is going to operate successfully:

(i) The heat rejected from the gas cycle has to satisfy the required heat that operates the steam cycle and the ammonia water cycle.

(ii) The low steam quality rejected from the steam cycle has to satisfy the heat requirement to operate the absorption chiller system, or the cooling system will operate with an opposite effect.

(iii) The gain in the power from the gas turbine inlet air cooling has to recover the power required to operate the heat pump (the absorption chiller system).

(iv) The performance characteristics represented by the efficiency and the environmental impact represented by the SFC and the rejected heat (i.e. the temperature of the exhaust gases) should be better than those for the conventional combined cycle power plant.

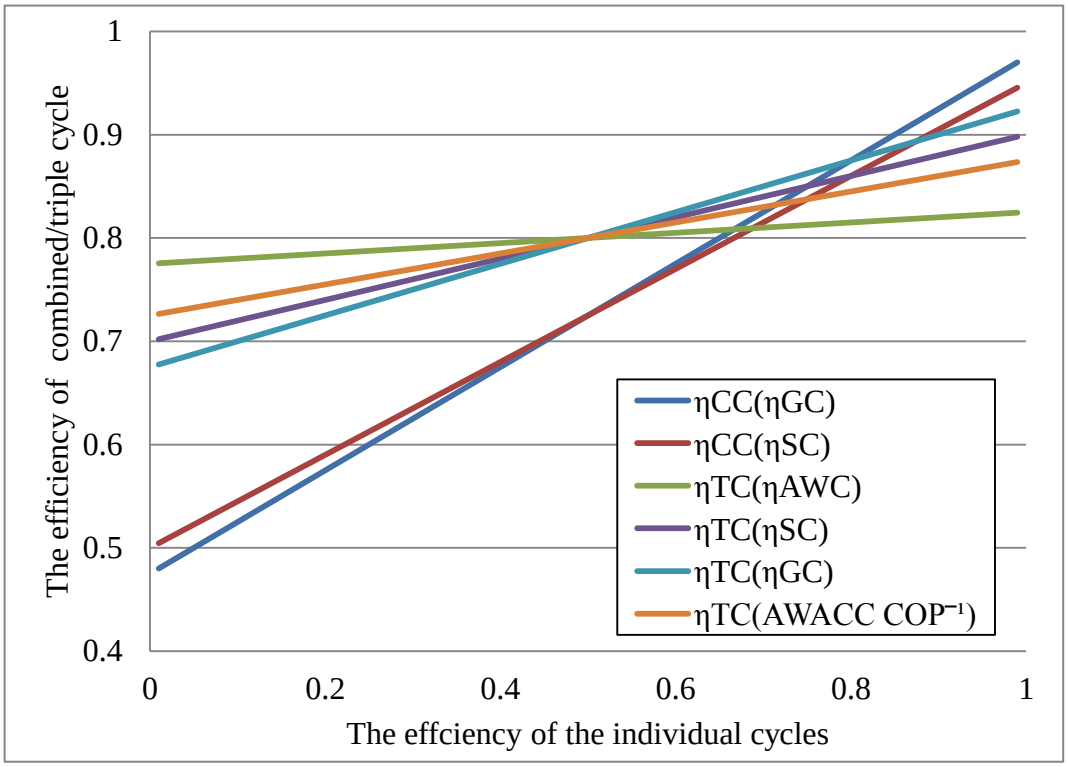

Figure 1.8 Different cycles performances effects on the efficiency of the triple and combined cycle

1.5 An overview on the superiority of the present research

(i) Usually the studies on the combined cycle power plants focus on one of the following elements: economics, environmental and performance characteristic. This research focuses on the performance of the combined cycle and its environmental impact. The economic considerations are important on constructing and operating of various combined cycle power plants for which many previous studies were undertaken. However, costs are usually dependent to the oil prices which are unstable and subjected to abrupt changes in recent years. Accordingly, to avoid inadequate conclusions and results, this research will not consider the economics and cost element.

(ii) The configurations conducted by this study do not consider steam or water injection into the gas turbine for cooling purposes as in some previous studies.

(iii) Unlike most of the previous studies on CCPP, which concentrate on the effects of the parameters of one of the cycles, which form the CCPP cycle, the current study focuses on the effects of the parameters of both cycles.

(iv) Most of the previous works investigates different optimized configurations of one of the cycles, which form the combined cycle. However, in the present research, both the gas and the steam cycles with various optimization configurations are studied.

(v) Many previous researches considered non-conventional methods to optimize the performance of the combined cycle through the HRSG. This study, also, consider such optimization but through the method of pinch point temperature difference.

(vi) A number of previous studies have investigated the deterioration effects of various components on the performance of the combined cycle. In the current study, however, the effects of various components' optimization on the performance of the combined cycle are undertaken rather than deteriorations.

(vii) Several researches utilized data from existing power plants. In this study, the data are generated from the parametric study but based on ranges similar to those exist in real power plants.

(viii) In this work, ammonia-water cycles are utilized to enhance the performance of the combined cycle power plant. This included AWM power cycles (Kalina cycle) and AWM absorption refrigeration cycles (AWAC system).

(ix) Unlike most of the previous studies (reported in the literature review), this study concentrates on investigating the performance of different power and absorption ammonia-water cycles on the combined cycle rather than each cycle individually.

(x) Instead of the partial oxidation gas turbine employed in the previous researches, this study undertakes ChGT configurations. It also investigates the validity of the ChGT by integrating ammonia water power cycles and absorption chillers.

1.6 Expectations from applying advanced enhancements to CCPP

The following points are anticipated to arise from introducing the above enhancements' methods into a conventional combined cycle power plant.

(i) Improving the power output and the efficiency of the gas turbine engine due to the use of the inlet air cooling system and the temperature difference through the gas turbine using the C/C composites.

(ii) A drop of the CO_2 and NO_X emissions through reducing the combustion emissions and performance improvements.

(iii) More heat is recovered if ammonia water mixture is utilized in the HRSG.

(iv) An increase of the efficiency of the bottoming cycle by the Kalina cycle with or without Rankine cycle.

(v) An increase of the power generated from the bottoming cycles.

(vi) A considerable drop down in the temperature of the exhaust gases than that released by the conventional combined cycle that works on the same conditions.

1.7 Aims and objectives of the current research

(i) Identify the operating and design parameters that affect the operation and performance of the combined power cycles and plants.

(ii) Provide a critical and comprehensive review of various research studies of conventional and novel combined power cycles and plants. Consequently, identify the gaps in the literature that warrant further research and investigation.

(iii) Develop an in-house computer model to simulate gas and steam turbine cycle performance to incorporate in the comprehensive model described in the next aim.

(iv) Develop and construct a comprehensive computer model to predict the influence of the previously identified parameters on the performance of combined power cycle plants.

(v) Undertake a parametric study, using the developed model, to identify the main operating parameters which control the optimization of various combined cycle power plants.

(vi) Explore various principles through which further optimization of the combined power cycles can be investigated. As a result, several strategies are to be examined and their effects on the performance of the combined-cycle power plant will be assessed parametrically.

(vii) Investigate the effect of enhancing the combined cycle power plant with non-conventional strategies. These may include using different operating cycles, working fluids and engine components.

(viii) Undertake a parametric study by which the performance of the combined cycle power plant is examined. This is achieved by making changes to the main operating parameters and assessing their impact on the environment and performance characteristics. The results of the parametric study are duly compared and discussed.

(ix) Identify the design point parameters of the gas and steam turbines which are necessary to optimize the combined cycle using the parametric study described above.

1.8 Important statements throughout the research

In the work described, hereafter, the following should be noted:

(i) The terms Brayton Rankine and Kalina are used to describe the gas, steam and ammonia-water cycles respectively. In some cases, these terms are followed by word "engine" for clarification.

(ii) The terms "specific power output" and the "specific work output" are synonymous.

(iii) The terms "exergy efficiency" and the "2nd law efficiency" are identical parameters.

CHAPTER 2
THEORETICAL CONSIDERATIONS

2.1 Introduction

The basic concept of a power cycle is the conversion of the fuel energy into power output, which is normally associated with a waste of energy. In such procedure, a series of thermodynamic processes operates on the working fluids, which circulate between the high temperature heat source and low temperature heat sink. This chapter considers the thermodynamic analysis of gas turbine and steam turbine power plants, which are based on Brayton and Rankine cycle, respectively. The main objective of this chapter is to identify the main operating parameters of such cycles theoretically. This chapter also discusses the conventional configurations of gas turbine power plant and steam turbine power plant and various ways of enhancing the designs of each plant. It also reviews the classic procedures to optimize the performances of Brayton and Rankine cycles and the combined cycle. Accordingly, this chapter gives an understanding on the main parameters affecting the performance of combined cycle power plant. Additionally, it analyses the performances of each configuration using power and efficiency equations. Finally, it sets a number of main operating parameters on both the steam turbine and gas turbine cycles; it also identifies the main operating parameters on the conventional combined cycle power plant.

2.2 Theoretical considerations for the gas cycle power plant

The theory of the gas turbine is of great importance to understand the way in which a gas turbine operates. The history of the gas turbine engine development runs through a long journey of slow but certain progress by utilizing many theories and efforts from various industries. Those theories depend largely on many fundamental design parameters that also control the performance of turbines. The influence of these parameters on the overall performance of the turbine based on these theories is detailed hereafter.

2.2.1 Background and theory

The concept of a gas power cycle dates back to 1791 when John Barber patented his idea on open and closed cycles as the basis to implement the gas turbine power plant. The first design of today's gas turbine was made in 1873 by Franz Stolze, which was operating on open circuit and using internal combustion. The Joule/Brayton cycle represents the thermodynamic principle of any gas turbine cycle power plant.

The gas turbine engine operates by circulating the air and the burned gases through its components. The mechanical power generated by the expansion of the gases rotates turbine which in turn operates the generator to produce the required power output. These gases results from burning the fuel with the compressed air in the combustion chamber. Many other components are required to maintain the operation of such system. However, the basic components of a closed system gas turbine cycle are shown schematically in Figure 2.1. While the components of an open system gas turbine cycle are illustrated in Figure 2.2.

During the latest five decades, the low initial costs of the gas turbine engine made it among the top choices to cover the operation of services under emergencies and peak load periods. The great success of the gas turbine industry was made when the low costs natural gas was used to fuel such engines. The exhaust gases from such configurations had higher proportions of hydrogen and lower proportions of carbon dioxide than the products of liquid fuel engines. In any operating conditions, the design point of a real gas turbine engine is to reach the performance of the ideal cycle. On the other hand, eliminating the losses of heat and pressure in its components gives another degree of performance, which is represented by improving the efficiency of the component. Principally, the performance of gas turbine cycle is evaluated by obtaining the value of the work output to the heat provided.

An open cycle gas turbine can not be considered thermodynamically unless it has been treated as a closed gas cycle. This means that an assumption has to be made to equalize the state of the gases at turbine exhaust and the state of the air at the compressor inlet. The performance of any conventional gas cycle is generally improved when the optimum operating parameters are employed to obtain the maximum efficiency. In order to attain such performance different strategies and enhancements can be used; therefore, a variety of materials and components are usually required. Those developments have been successfully applied on the first advanced gas turbine configuration which went into service in the nineteen nineties. Generally, advanced gas turbines may include: exhaust heat regeneration, inter-cooling between

compressors, and reheating. The advanced gas turbine engine has to use the appropriate values of the parameters in order get further optimization in power generation.

The efficiency of power generation from the gas turbine cycle is usually represented by the thermal efficiency which is illustrated by the equation (2.1):

$$\eta_{thGC} = \frac{W_{out}}{Q_{in}} \qquad \ldots (2.1)$$

Figure 2.3 shows the processes involved in an ideal gas turbine cycle, these are: (a) isentropic compression, (b) constant pressure heat addition, (c) isentropic expansion, and (d) constant pressure heat rejection to the atmosphere.

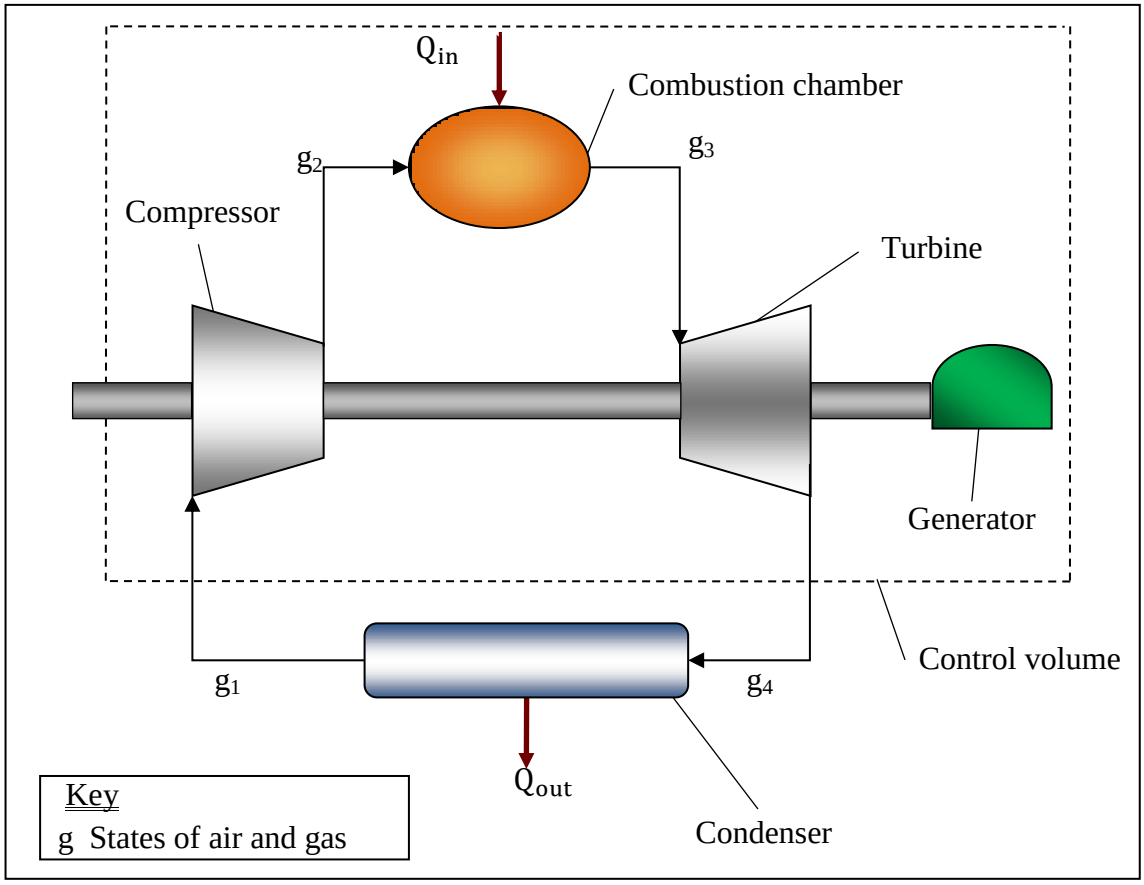

Figure 2.1 Closed circuit gas turbine power plant

Equation (2.1) can be transferred to equation (2.2), in which the work output from gases expansion in the turbine is (W_{GT}). The work required by the air compressor and the heat input from the fuel burning are represented by (W_{AC}) and (Q_{CC}) respectively. The heat waste to atmosphere and other losses equals the subtraction of the work output from the heat input.

$$\eta_{thGC} = \frac{W_{GT} - W_{AC}}{Q_{CC}} \qquad \ldots (2.2)$$

Equation (2.2) is in turn transferred to equation (2.3), in which the mass flow rate of the air and the burned gases are represented by $\dot{m}_a$ and $\dot{m}_g$ respectively and the specific heat of the air for constant pressure process is represented by Cp_a. The specific heat of the burned gases is represented by Cp_g and (T) represents the temperature of the air or gas in the cycle. For simplicity a steady flow perfect gas is considered as the working fluid in the cycle and the mass flow rate considered constant in the gas turbine components. Accordingly, the equation of thermal efficiency becomes the following, in which the mass flow rate is $\dot{m}_B$ and the specific heat at constant pressure of a perfect gas is Cp_B. This equation can be shortened to equation (2.5).

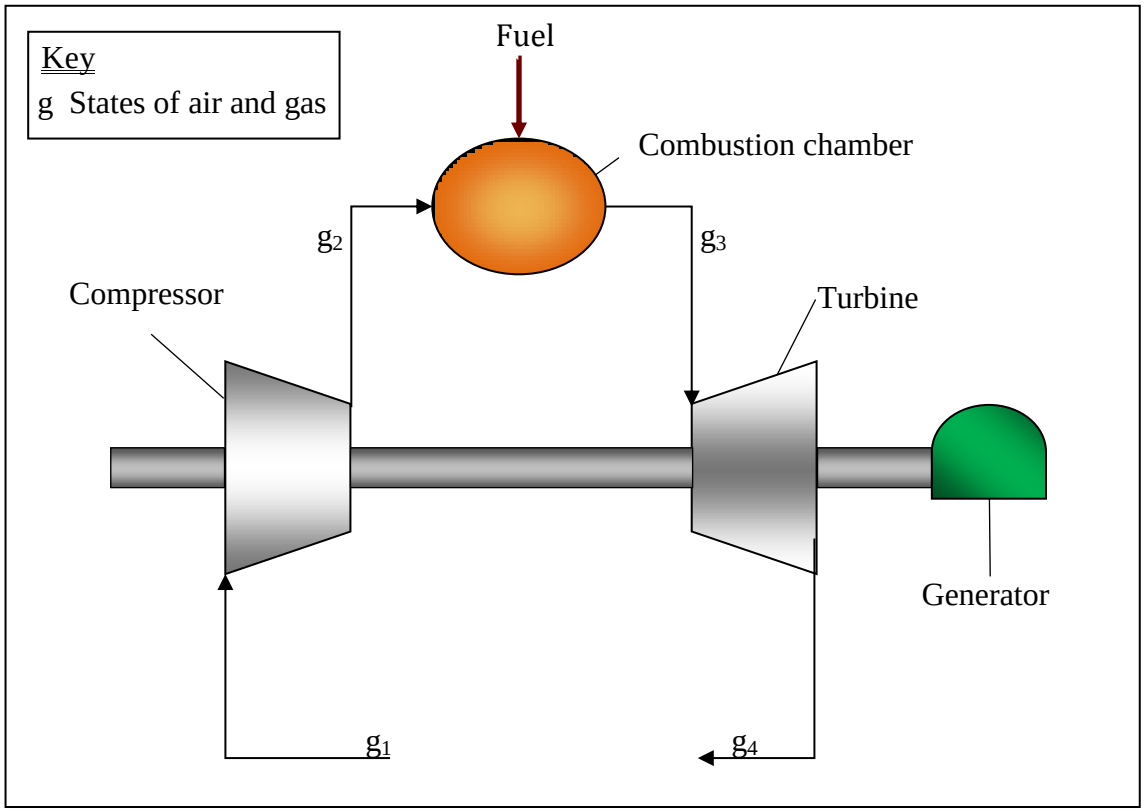

Figure 2.2 Open circuit gas turbine power plant

$$\eta_{thGC} = \frac{\dot{m}_g Cp_g \left(T_{g3} - T_{g4}\right) - \dot{m}_a Cp_a \left(T_{g2} - T_{g1}\right)}{\dot{m}_g Cp_g T_{g3} - \dot{m}_a Cp_a T_{g2}} \qquad \ldots (2.3)$$

$$\eta_{thGC} = \frac{\dot{m}_B Cp_B \left(T_{g3} - T_{g4}\right) - \dot{m}_B Cp_B \left(T_{g2} - T_{g1}\right)}{\dot{m}_B Cp_B \left(T_{g3} - T_{g2}\right)} \quad \ldots (2.4)$$

$$\eta_{thGC} = \frac{\left(T_{g3} - T_{g4}\right) - \left(T_{g2} - T_{g1}\right)}{\left(T_{g3} - T_{g2}\right)} \quad \ldots (2.5)$$

Hence, the relation between the temperatures and the pressure at the start and the end of each isentropic process is represented by equations (2.6) and (2.7) below. In which, the specific heat ratio of the perfect gas over the isentropic process is (γ). The pressure ratios of the compression and the expansion are r_c and r_e respectively. Also, for simplicity, the gas constant ratio is taken as $\left(k = \frac{\gamma - 1}{\gamma}\right)$.

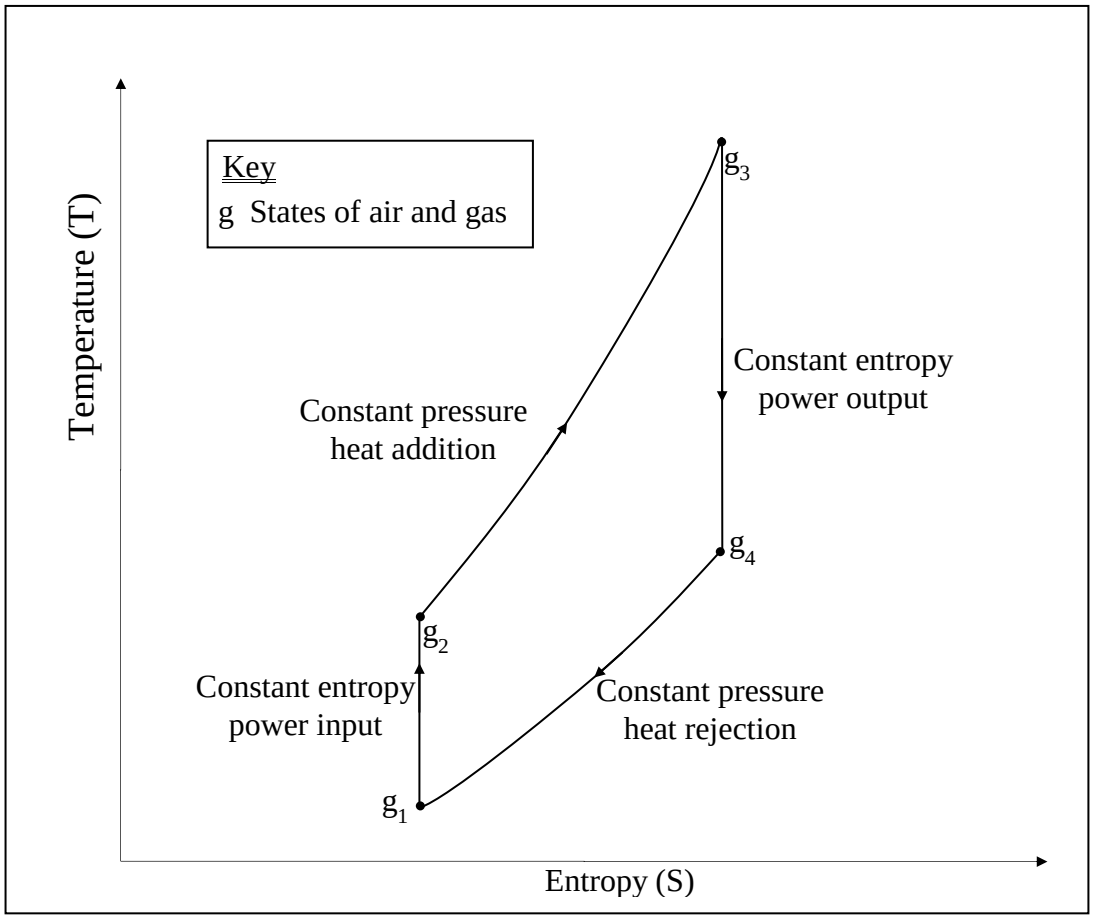

Figure 2.3 Ideal air standard Brayton cycle on T-S diagram

$$\frac{T_{g2s}}{T_{g1}} = \left(\frac{P_{g2}}{P_{g1}}\right)^{\frac{\gamma-1}{\gamma}} = \left(r_c\right)^k \quad \ldots (2.6)$$

$$\frac{T_{g4s}}{T_{g3}} = \left(\frac{P_{g4}}{P_{g3}}\right)^{\frac{\gamma-1}{\gamma}} = \left(\frac{1}{r_e}\right)^k \quad \ldots (2.7)$$

Neglecting the pressure losses generates the relations $P_{g3} = P_{g2}$, and $P_{g1} = P_{g4}$ as a result equation (2.8) comes into consideration. The heat losses by the friction change the cycle diagram of the Brayton cycle into the one in Figure 2.4. The efficiency of the turbine and the compressor are illustrated by equations (2.9), and (2.10).

$$\frac{P_{g4}}{P_{g3}} = \frac{P_{g1}}{P_{g2}} = r_c = r_e = r \quad \ldots (2.8)$$

$$\eta_{GT} = \frac{\text{Real work output}}{\text{Isentropic work output}} = \frac{T_{g3} - T_{g4}}{T_{g3} - T_{g4s}} \quad \ldots (2.9)$$

$$\eta_{AC} = \frac{\text{Isentropic work input}}{\text{Real work input}} = \frac{T_{g2s} - T_{g1}}{T_{g2} - T_{g1}} \quad \ldots (2.10)$$

Using equations (2.6) to (2.9) in equation (2.5) generates to the following equation, which can be summarized into equation (2.11).

$$\eta_{thGC} = \frac{\left(T_{g3} - T_{g3} - \eta_{GT}\left(T_{g3} - T_{g3}\left(\frac{1}{r_e}\right)^k\right)\right) - \left(\frac{T_{g1}\left(r_c\right)^k - T_{g1}}{\eta_{A.C.}} + T_{g1} - T_{g1}\right)}{\left(T_{g3} - \left(\frac{T_{g1}\left(r_c\right)^k - T_{g1}}{\eta_{AC}} + T_{g1}\right)\right)} \quad \ldots (2.11)$$

This equation can be more simplified into equation (2.13), where $\left(\theta = \frac{T_{g.3}}{T_{g.1}}\right)$

$$\eta_{thGC} = \left[\frac{\theta\eta_{GT}\left(1 - r^{-k}\right) - \left(\frac{\left(r\right)^k - 1}{\eta_{AC}}\right)}{\theta - 1 - \left(\frac{\left(r\right)^k - 1}{\eta_{AC}}\right)}\right] \quad \ldots (2.12)$$

$$\eta_{thGC} = \frac{\left(\eta_{AC} \times \eta_{GT} \times \theta - r^{k}\right)\left(\frac{r^{k}-1}{r^{k}}\right)}{\eta_{AC}\left(\theta - 1\right) - \left(r^{k} - 1\right)} \quad \ldots (2.13)$$

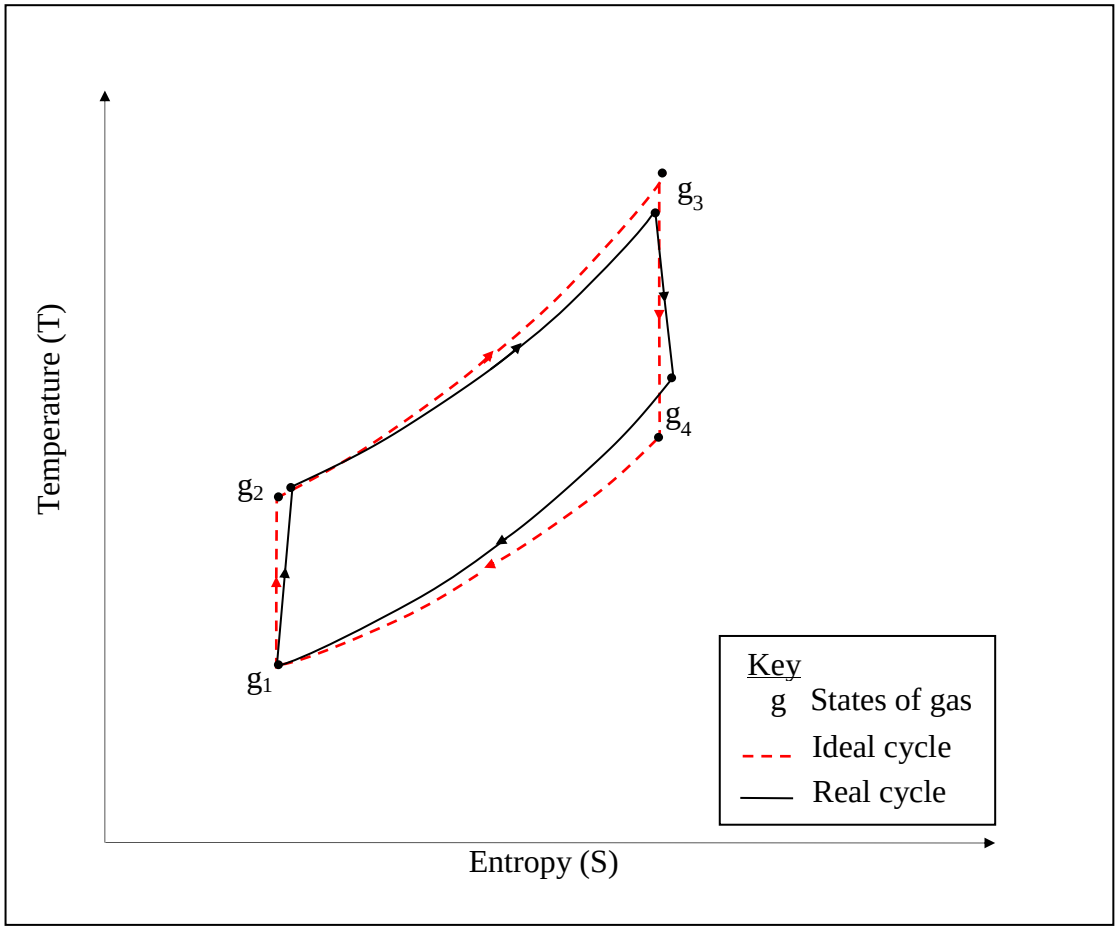

Figure 2.4 Ideal and real Brayton cycles on T-S diagram

The same assumptions are applied on specific network output of the gas cycle to generate the following equation. The power output from gas turbine cycle is one of the most important parameters on the performance of combined power plants. Employing the heat losses in equation (2.14) yields to the equation (2.15):

$$w = \frac{W}{\dot{m}_{B}} = Cp_{B}\left(T_{g3} - T_{g4}\right) - Cp_{B}\left(T_{g2} - T_{g1}\right) \quad \ldots (2.14)$$

$$w_{net} = \frac{Cp_{B}\left(\eta_{AC} \times \eta_{GT} \times \theta - \left(r\right)^{k}\right)\left(\left(r\right)^{k} - 1\right)}{\eta_{AC}\left(r\right)^{k}} \quad \ldots (2.15)$$

The equations above show the influence of the above parameters on the performance of the gas turbine cycle by their effect on its thermal efficiency and work output. The performance of the basic gas turbine power plant based on Brayton cycle is governed by many parameters. Initially, the thermal efficiency of this cycle depends on the parameters of the equation (2.16):

$$\eta_{thGC} = f(\eta_{AC}, \eta_{GT}, r, \theta, k) \quad \ldots (2.16)$$

$(\theta, r, \text{and } k)$ Are represented by their main factors, which generates new operating parameters (C_{pa}, Cp_g, T_{g3}, T_{g1}, r_{AC}, r_{GT} and γ). Additional parameters emerge when the losses in the combustion chamber and power generator are included, which represented by efficiencies (η_{CC}, η_{PG}). For the changes in the mass flow of the working fluid, two more parameters are introduced $(\dot{m}_a \text{ and } \dot{m}_g)$. From the considerations above it can be concluded that the thermal efficiency of a gas turbine is dependent on the parameters of the following equations:

$$\eta_{thGC} = f(\eta_{AC}, \eta_{GT}, Cp_a, Cp_g, T_{g1}, T_{g3}, r_{AC}, r_{GT}, \eta_{CC}, \eta_{PG}) \quad \ldots (2.17)$$

2.2.2 Simple gas turbine cycle performance

Equations (2.17) identify a number of parameters on which the gas turbine cycle performance depends. Therefore, it is appropriate to start analyzing how the gas turbine cycle performance can be improved through these parameters. The following are main observations gathered from analyzing the equations above:

(i) Any increase in the components efficiencies $(\eta_{AC}, \eta_{GT}, \eta_{CC}, \eta_{PG})$ increases the efficiency of the cycle.

(ii) The drop in the temperature T_{g1} at compressor inlet and the increase in temperature T_{g3} at the turbine inlet results in an increase in the thermal efficiency.

(iii) Any increase in the specific heat capacities Cp_a, Cp_g, and the heat capacity ratio γ increases the thermal efficiency and improves the work output for the gas cycle.

(iv) The increase in the pressure ratio of the compression (r_{GT}) and the decrease in the pressure ratio of the expansion (r_{AC}) increase the thermal efficiency and work output.

(v) The increase in the mass flow of the air and the mass flow burned gases ($\dot{m}_a$) and ($\dot{m}_g$) returns in an increase in the net power output only.

Principally, the considerations which guarantee the improvements in the performance of a gas turbine power plant cycle are: (a) the increase in the compression ratio (r_{AC}) and (b) the increase in the turbine inlet temperature $\left(T_{g3}\right)$.

The increase in the maximum temperature on which gas turbine cycle is to operate for the same pressure leads to more power generation from the gas cycle. This occurs due to the increase in the work made by gases expansion when there is no change in the work required for air compression. Graphically, Fig. 2.5 shows that the increase in the maximum temperature enlarges the area under the expansion curve. Therefore, the area under the curve (3B´4B´) gets greater than the area under the curve (3B4B) (as on P-V diagram the area under the curve represents the work input or output during such process, $W = \int PdV$). Consequentially the network output from the cycle $\left(W_{GC} = W_{GT} - W_{AC}\right)$ is clearly illustrated in such diagram. The increase in the temperature requires more heat addition and more heat rejection as illustrated in Fig.2.6. It shows that the area under the curve (2B B3') is greater than area under the curve (2B3B), and the area under the curve (4B´1B) is greater than the area under the curve (4B1B). These curves represent the heat addition, and heat rejection of the modified cycle and original cycle respectively (as the area under the curve of a T-S diagram represents the heat change during such process $\left(Q = \int Tds\right)$). As a result it is clear that the increase in heat rejection process is greater than the increase in the heat addition process which generates the increase in the thermal efficiency of the cycle.

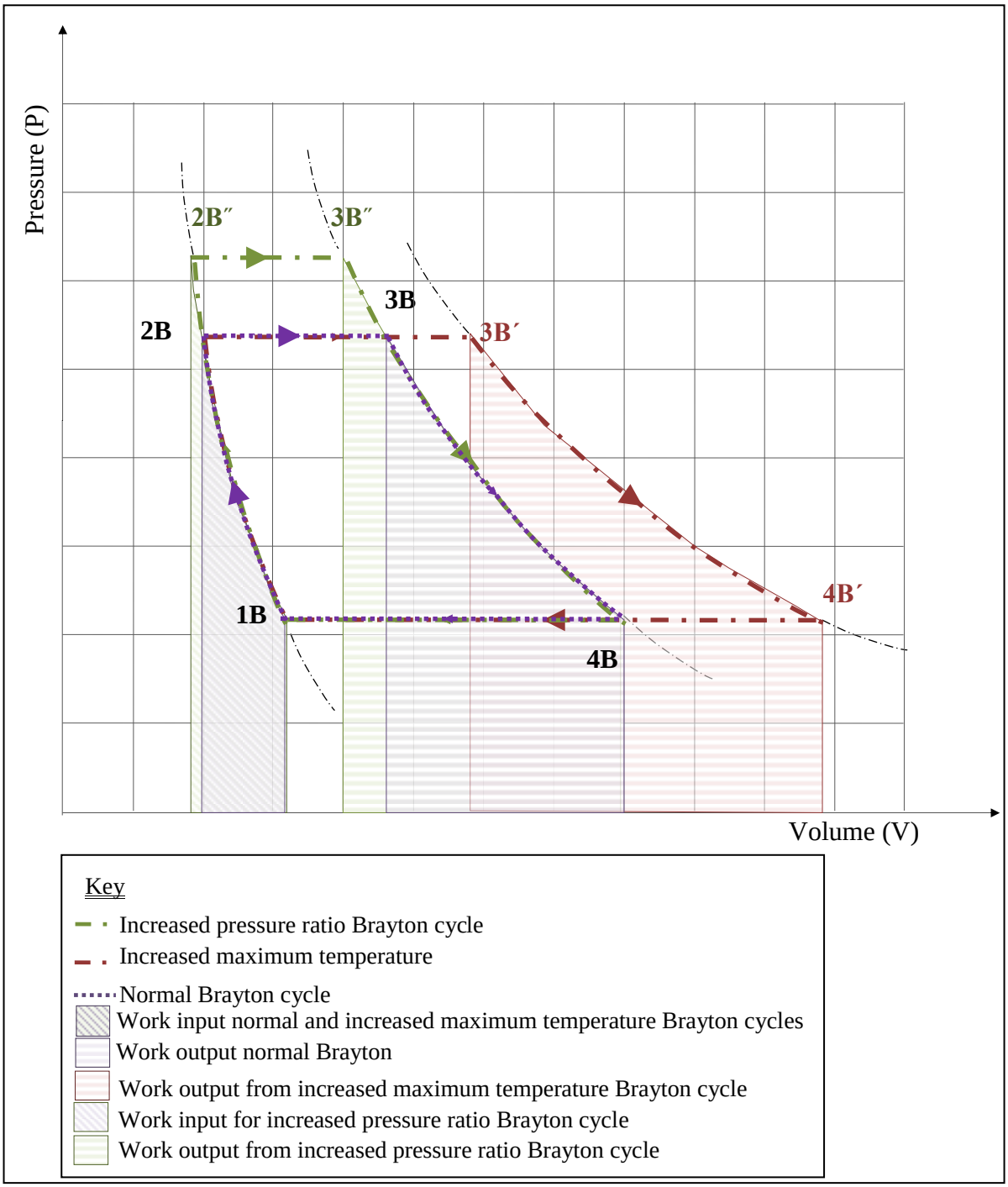

Figure 2.5 Real Brayton cycles on P-V diagram

In practice, the maximum temperature of the gas turbine cycle has been limited by the component's material. Therefore, another strategy has been used to improve the performance of simple gas cycle (i.e. the increase in the pressure ratio). Accordingly, the power generated from the expansion of the gases and that required for air compression have been increased. As illustrated in Fig. 2.5, the area under the curve (3B″4B) is greater than the area under the curve (3B4B).

Also the area under the curve (1B2B) is less than the area under the curve (1B2B”). Therefore, although there is an increase in work required for the compression, the increase in total work output is greater. While both the heat added, and the heat rejected are decreased as illustrated in Fig. 2.7. It shows that the area under the curve (2B″3B″) is smaller than the area under the curve (2B3B), and the area under the curve (4B″1B) is smaller than the area under the curve (4B1B).

Further optimization in the performance of the gas turbine cycle requires the utilization of additional components. It usually offered by employing extra strategies like: (1) regeneration, (2) reheating and (3) inter-cooling.

For single spool gas turbines engine, the turbine powers the compressor. The ratio of the back work (bwr) can be calculated by the Equation (2.18). Typically, this ratio takes a value in the range between 40 and 80%. It is interesting that in a steam power plant, this ratio has been rated in the range of 1 to 2%.

$$\text{bwr} = \frac{\dot{W}_{AC}}{\dot{W}_{GT}} \qquad \text{... (2.18)}$$

2.2.3 Regenerated gas turbine cycle

The temperature of the gas turbine exhaust gases is clearly higher than the ambient temperature. Therefore, some of the heat from the exhaust can be successfully recovered by employing the regeneration strategy. The regeneration employs extra heat exchangers, which use the heat of the exhaust gases to increase the temperature of the air prior to its entry to the combustion chamber. As in any heat exchanger, the heat recovery is affected by the irreversibility due to the heat loss to the atmosphere. Therefore, the temperature of the air at the heat exchanger outlet does not exceed the temperature of exhaust gases at its inlet.

The efficiency of regeneration represents the ratio between the real heat recovery by regenerator and the maximum heat that can be recovered as illustrated in equation (2.19). The irreversibly in the heat exchanger is represented by the difference between the enthalpy of exhaust gases and the enthalpy of the air at heat exchanger inlet. In practice, the efficiency of a regenerator is usually rated between 60 and 80%, whereas further increase necessitates for more fuel to be burned to attain the same turbine inlet temperature. If this does not happen, then the drop in the pressure shall guarantee degradations of the gas turbine cycle

performance. For such reason, the use of large heat transfer areas is the safest strategy to ensure high efficiency for the heat exchanger.

$$\eta_{Reg} = \frac{h_{g2\,Reg} - h_{g2}}{h_{g4} - h_{g2}} \qquad \ldots (2.19)$$

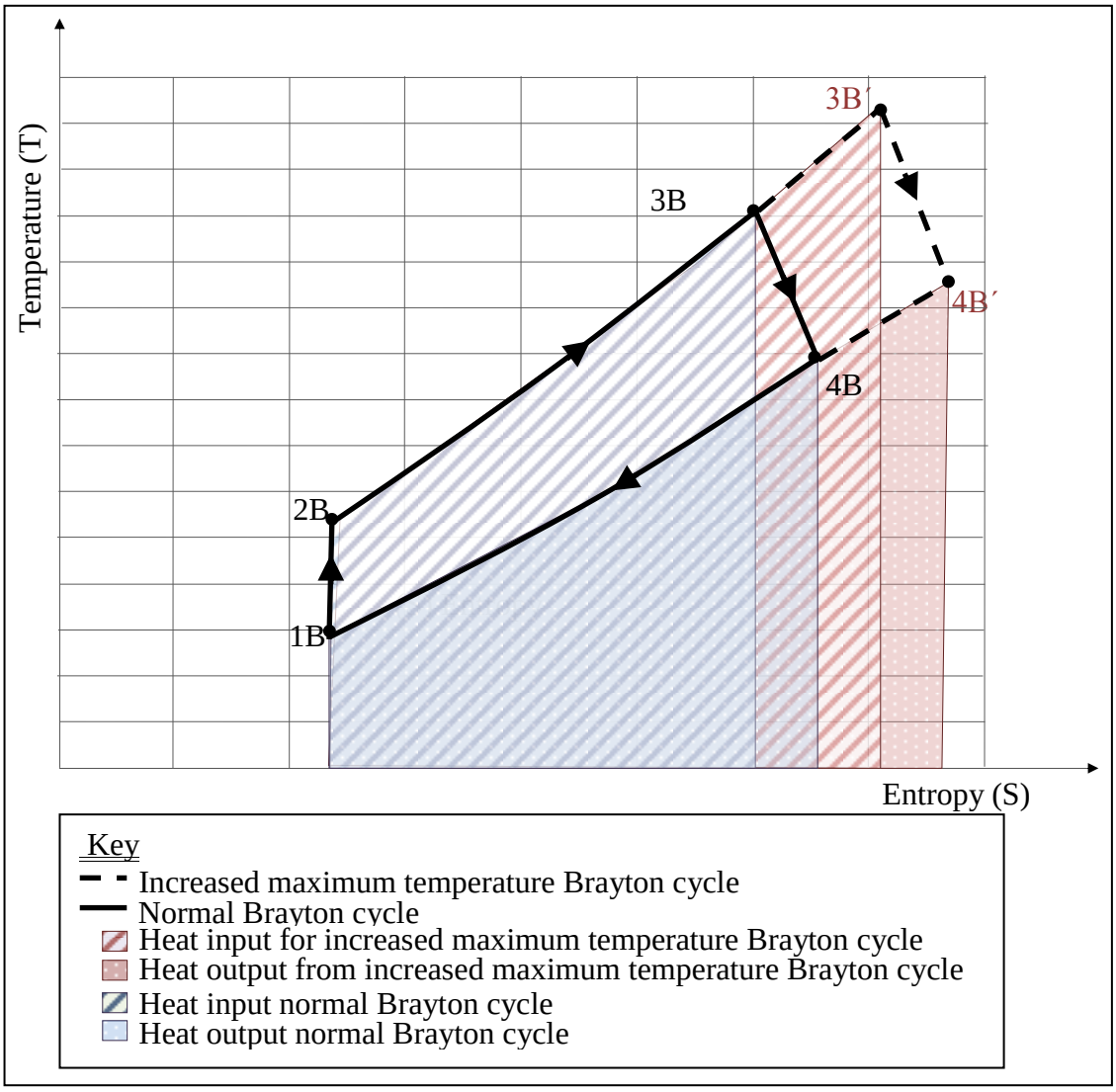

Figure 2.6 Real Brayton cycles on T-S diagram

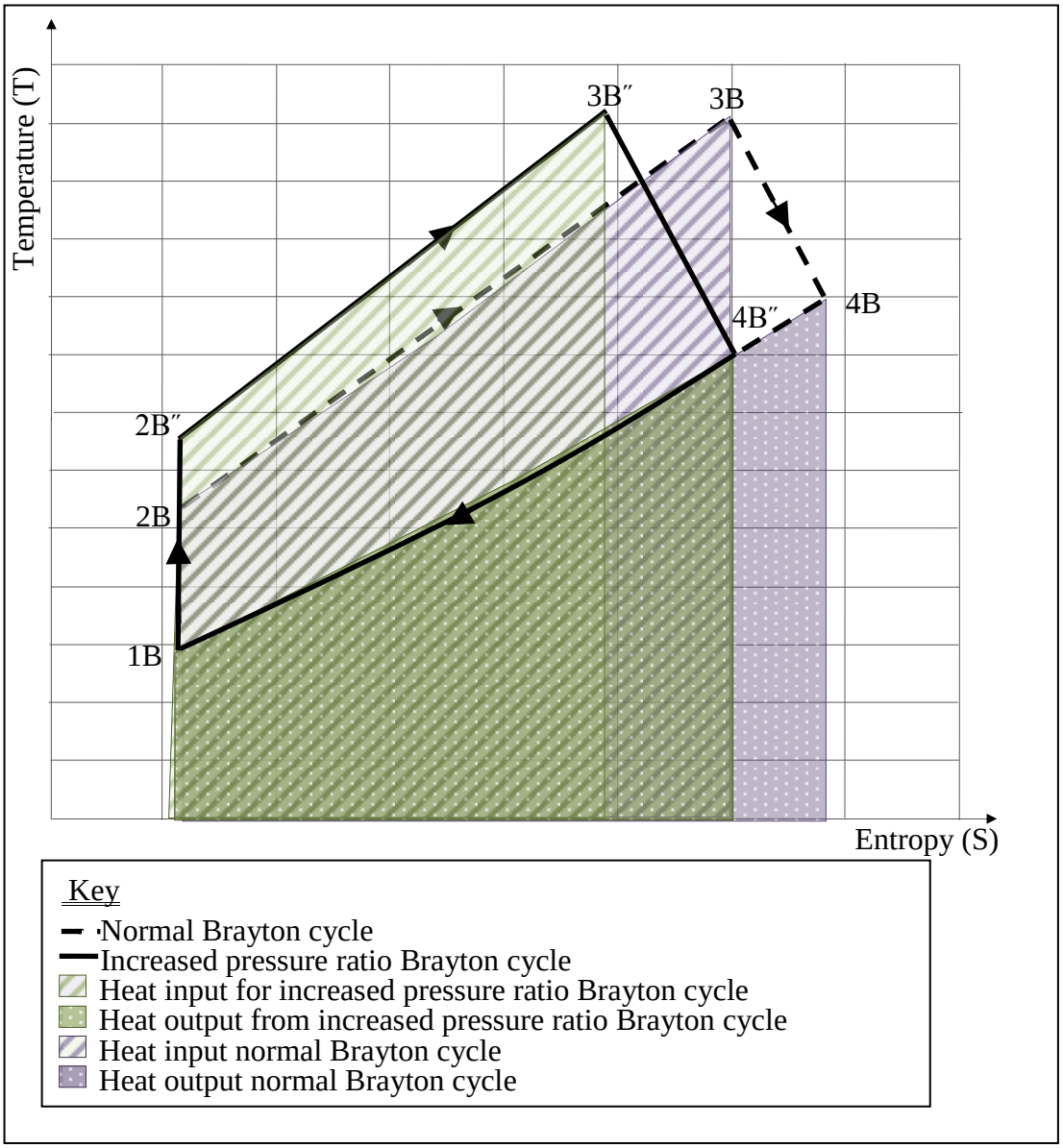

Figure 2.7 Increased pressure and normal Brayton cycles on T-S diagram

2.2.4 Reheated gas turbine cycle

The material of turbine blades restricts the maximum temperature of combustion gases entering the turbine. The main operating parameters which control the temperature of the combustion gases are the characteristics of fuel and air during combustion. Therefore, for a certain temperature of the gases the combustion gases have to be cooled before entering the turbine. This feature is utilized in multi stage combustors configurations in which the air from

the compressor is not used completely for combustion but utilized also combustion gases dilution and second combustion process. Gases in this multi stage combustion configuration are supplied with more heat by the second combustor before they expand through the second turbine. Therefore, the performance of gas turbine cycle is improved by the increase in the work output and thermal efficiency over the rates of conventional cycle power output and efficiency. Additionally, the increase in the maximum temperature of the cycle and the heat quality may ensure more increase in the efficiency by regeneration. The flow diagram of the basic components of the reheated gas turbine is illustrated in Figure 2.10. The processes of such cycle are shown on the temperature entropy diagram of Figure 2.11.

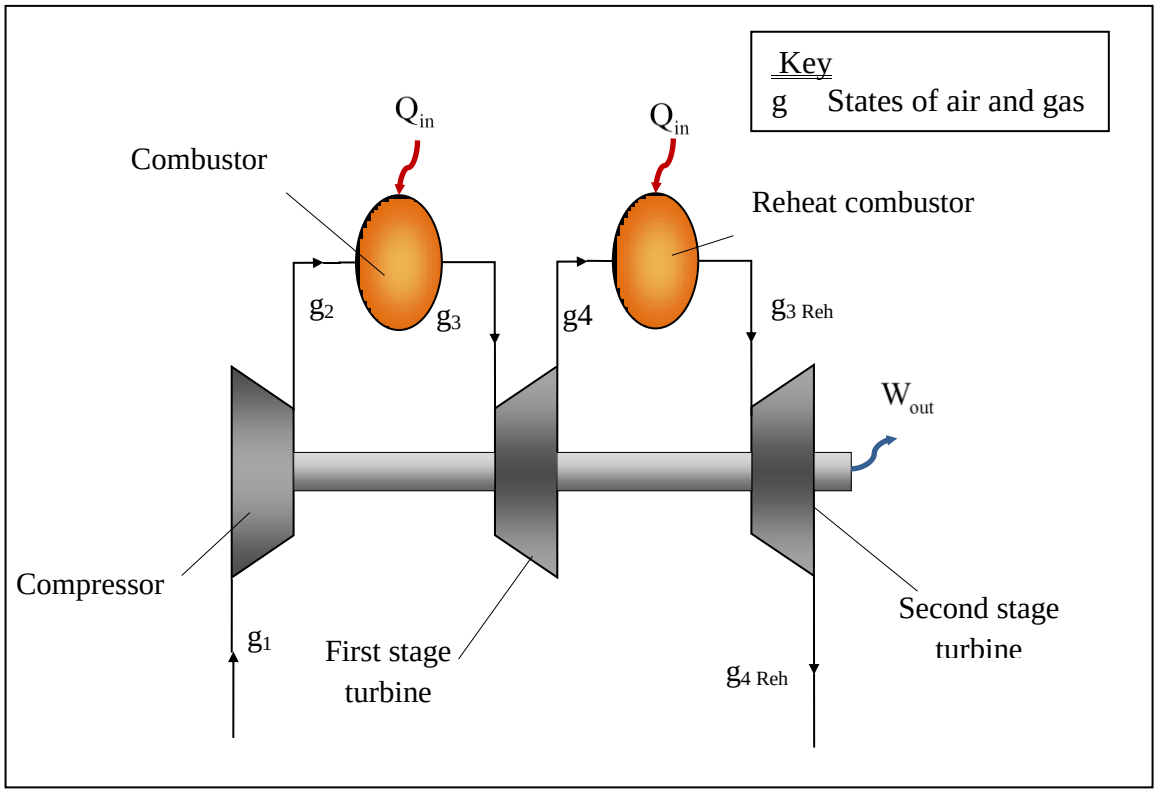

Figure 2.8 Main components of an ideal reheated gas turbine cycle

$$\eta_{th} = \frac{W_{GT1} + W_{GT2} - W_{AC}}{(Q_{CC1} + Q_{CC2})} \quad \ldots (2.20)$$

$$W_{out} = W_{GT1} + W_{GT2} - W_{AC} \quad \ldots (2.21)$$

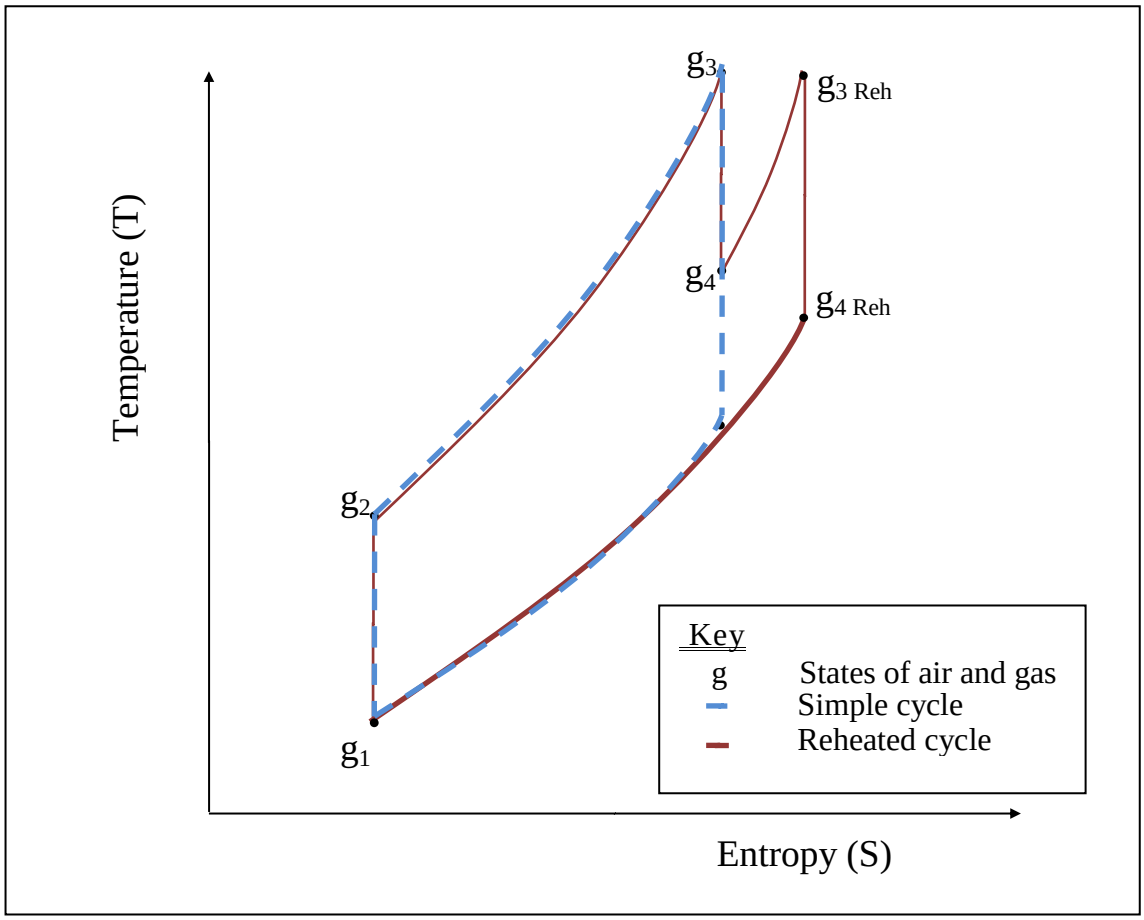

Figure 2.9 Simple and reheated Brayton standard cycles on T-S diagram

2.2.5 Intercooled gas turbine cycle

Another strategy which, can be employed, to improve the performance of simple gas turbine in which the net power output is increased by reducing the power required by the compressor. However, in such configurations, there is no increase in the thermal efficiency due to the drop in air temperature before combustion. Therefore, more fuel has to be used to attain the same temperature of the gases at the turbine inlet. The increase in the efficiency of the intercooled gas turbine over the efficiency of the conventional gas turbine is insured when regeneration is utilized. In this configuration multi (two) compressors are used. Hence, the equations of thermal efficiency and the work output are as following:

$$\eta_{th} = \frac{W_{GT1} - W_{AC1} - W_{AC2}}{Q_{CC1}} \quad \ldots (2.22)$$

$$W_{out} = W_{GT} - W_{AC1} - W_{AC2} \quad \ldots (2.23)$$

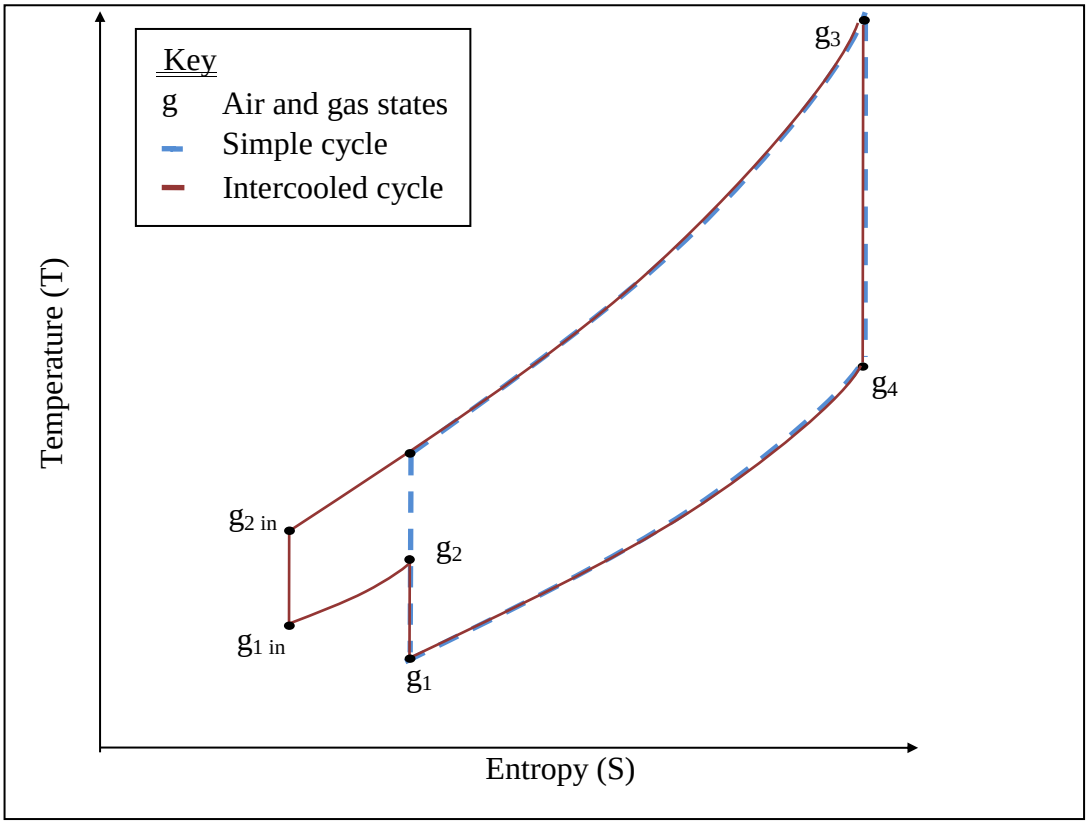

Figure 2.10 Simple and intercooled Brayton

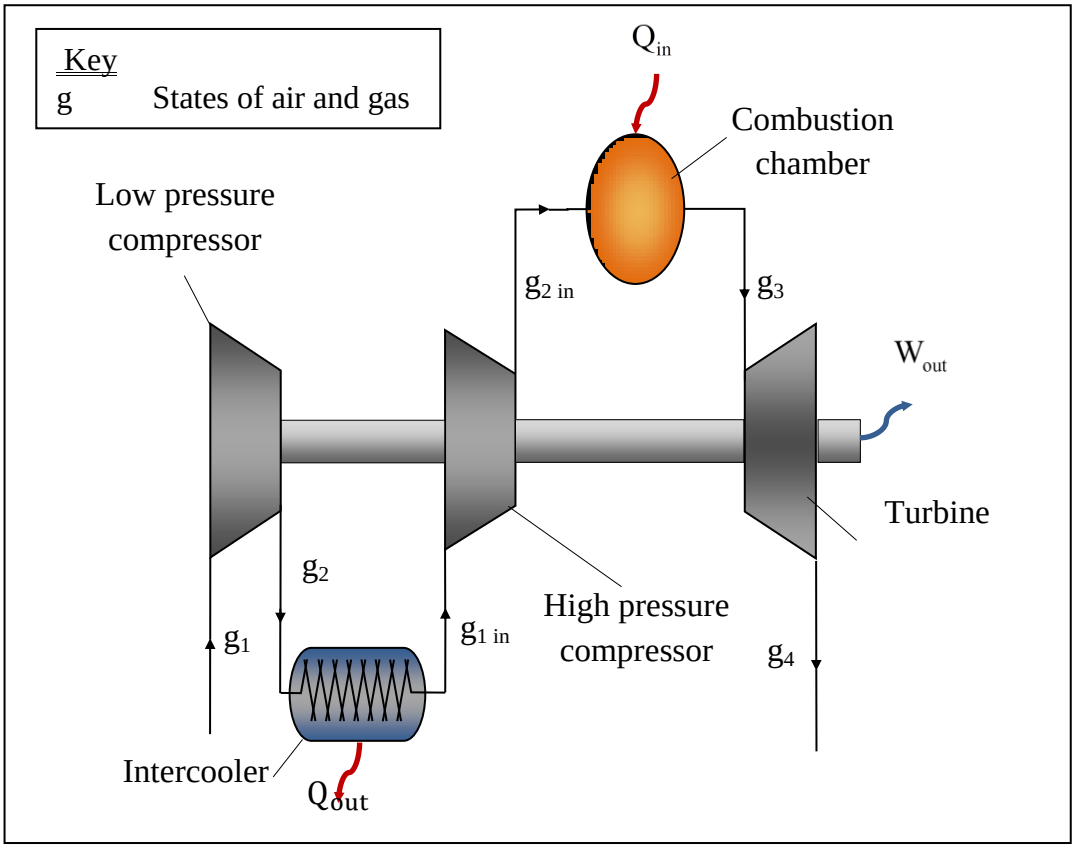

Figure 2.11 Main components of an intercooled gas turbine cycle

2.2.6 Intercooled reheated gas turbine cycle

The intercooled reheated gas turbine generates more power than the simple gas turbine. The improvement in the power output increases by the use of regeneration. Figures 2.14-2.15 illustrate the components and the process of such configurations. The thermal efficiency and the work output of the intercooled reheated regenerated gas turbine power cycle are given by the following equations:

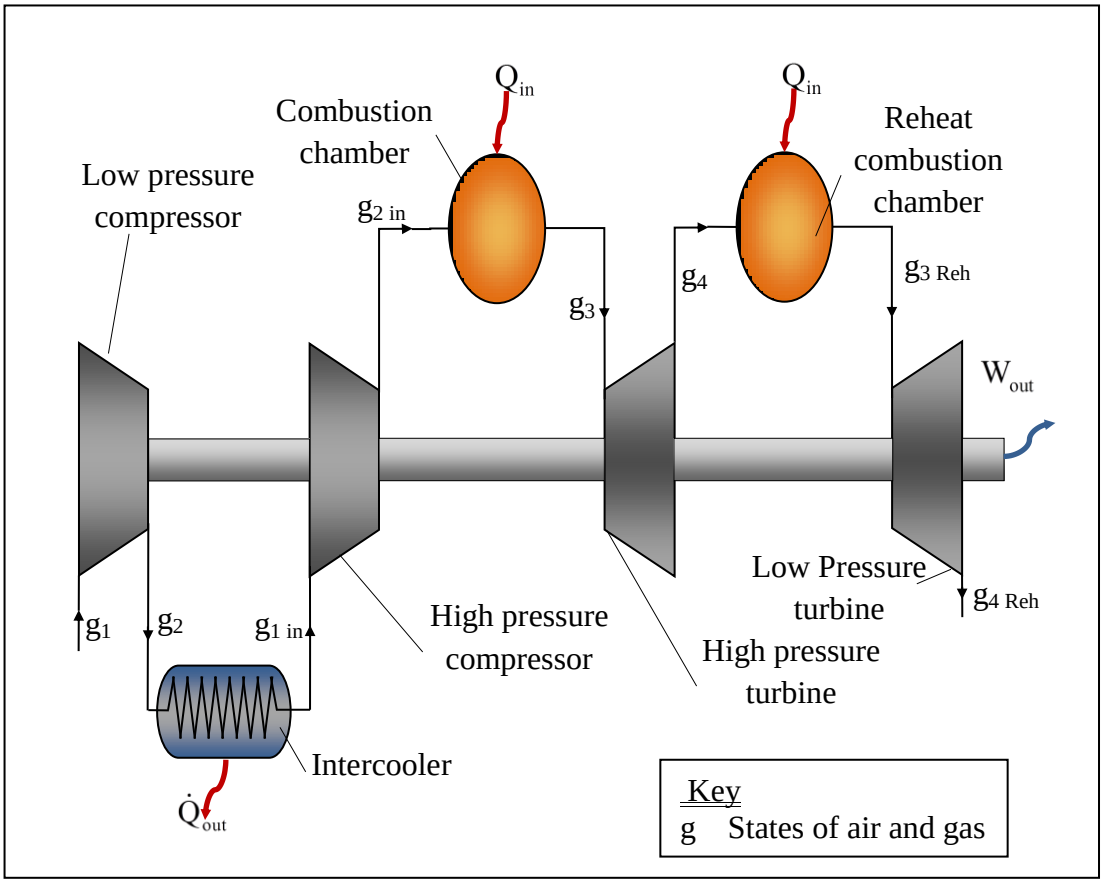

Figure 2.12 Main components of an ideal intercooled reheated gas turbine cycle

$$\eta_{th} = \frac{W_{GT1} + W_{GT2} - W_{AC1} - W_{AC2}}{\left(Q_{CC1} + Q_{CC2}\right)} \quad \ldots (2.24)$$

$$W_{out} = W_{GT1} + W_{GT2} - W_{AC1} - W_{AC2} \quad \ldots (2.25)$$

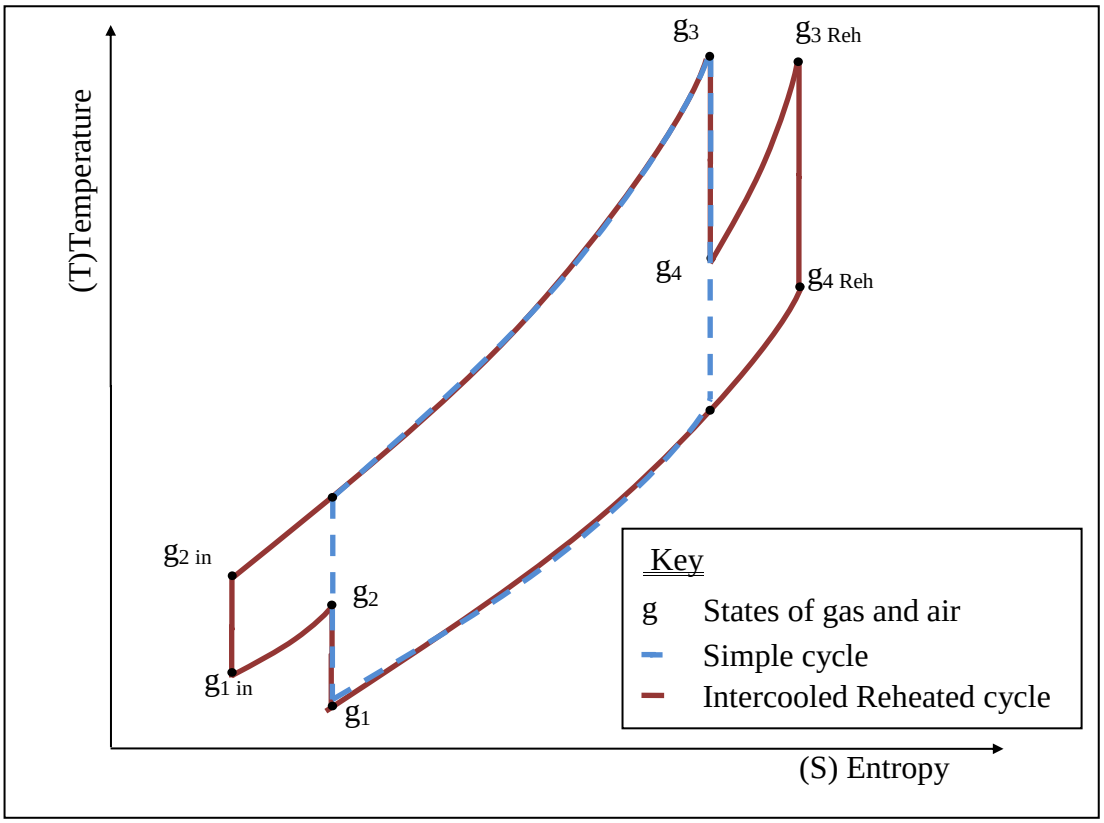

Figure 2.13 Simple and intercooled reheated gas Brayton standard cycles on T- S diagram

2.3 The steam turbine cycle power plants

In this section the theory, the history and the performance parameters of the steam power production cycle are reviewed. The classic parameters affecting the performance are identified for both the simple and the developed steam turbine cycles power plant.

2.3.1 Background

The journey of the steam turbine in power plant industry started in 1884 when a coal fired steam turbine generated an electrical power of 7.5 kW with a thermal efficiency of 1.6%. Year by year the improvements in the steam turbines were steady, but its applications were growing steadily in many industries other than power generation. Fossil fuel played a great part in improving the power outputs of the steam turbine engine. A peak power output from the steam turbines reached 100MW in the 1930s. This amount was boosted to 1000MW in the 1960s and to 1300 MW in the 1970s. In the 1960s, the gases from the gas turbine exhaust were used to power the steam turbine engine to generate the combined cycle power plant, which had higher performance.

The vast majority of the current thermal power plants are steam power plants which work on Rankine cycle and use water/steam as the working fluid. The main components of a simple steam turbine power plant are illustrated by Figure 2.14. Typically, the thermal efficiency of the steam turbine power plant that works on such cycle is expected to be about 39%. Many modifications are employed in such plants to improve their performance, each required undertaking different strategy.

The steam turbine engine may be enhanced by: (1) superheater, (2) reheater, (3) regenerator, (4) supercritical operation, (5) cogeneration, and (6) multi pressure (HRSG). Other approaches may be employed to cover the same objective in such plants like: (a) magneto-hydrodynamic systems, (b) Kalina cycle, and (c) ambient heat recovery using a substance of low boiling temperatures.

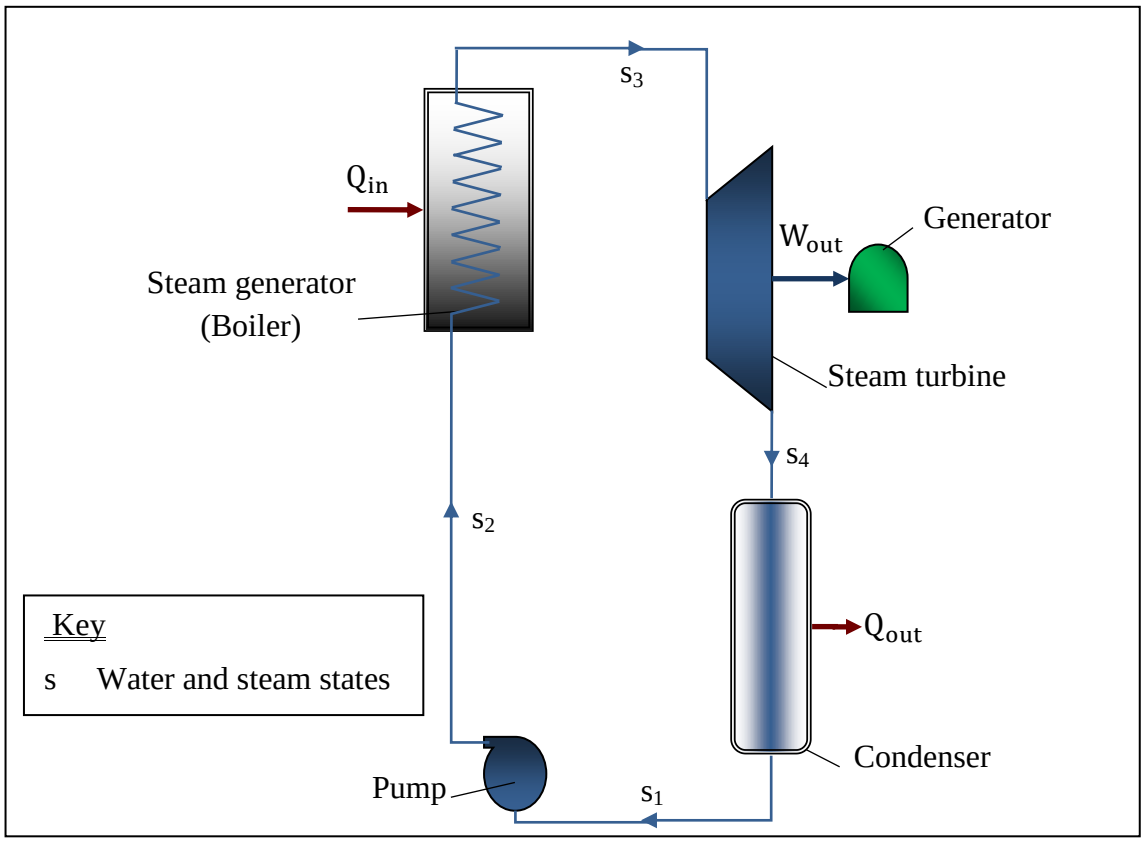

Figure 2.14 Main components of a basic Rankine cycle steam turbine power plant

2.3.2 Theory of the steam cycle power plant

The simple steam turbine power plant is usually based on four main components: (1) steam boiler, (2) steam turbine, (3) condenser, and (4) water pump as it is shown schematically in Fig. 2.14. The thermodynamic processes of the steam through such components are illustrated on the property diagrams of the ideal Rankine cycle of Fig. 2.15 and 2.16. The high pressure water is heated in the steam boiler to generate steam at high temperature. On the diagrams of properties, this process appears by the constant pressure heat addition between points (s2) and (s3). The steam turbine receives the boilers' outputs and uses the expansion of the high pressure and temperature steam to generate turbine power output. This process is illustrated in Fig.2.15, as an isentropic expansion changes the thermal properties of the steam from point (s3) to point (s4). Consequentially, the steam at low pressure and temperature needs to be cooled before it pumped again to the boiler. This is achieved in the condenser which appears on the property diagrams by the constant pressure heat rejection process between point (s4) and (s1). The work required by the water pump is represented by the thermodynamic properties of the isentropic compression process between point (s1) and (s2). Commonly, the efficiency of the steam cycle is obtained by using the following expression:

$$\text{Thermal efficiency of a steam cycle}(\eta_{thSC}) = \frac{\text{Work generated from the steam}(\dot{W}_{out})}{\text{Heat added to the steam}(\dot{Q}_{in})}$$

The expression that illustrates the thermal efficiency above is represented by equation (2.26). When the equations of mass and energy balance are applied on the components of the cycle for control volume considering steady state flow equations 2.27–2.30 are generated. In such equations, the changes in potential and kinetic energies are neglected. The work required by the water pump and that produced by steam turbine with no reference to the heat loss are given by equations (2.27) and (2.28), respectively.

The processes of heat addition and rejection in the boiler and the condenser with no regard to the pressure losses are illustrated by equations (2.29) and (2.30) respectively.

$$\eta_{thSC} = \frac{W_{ST} - W_{WP}}{Q_{SB}} \quad \ldots (2.26)$$

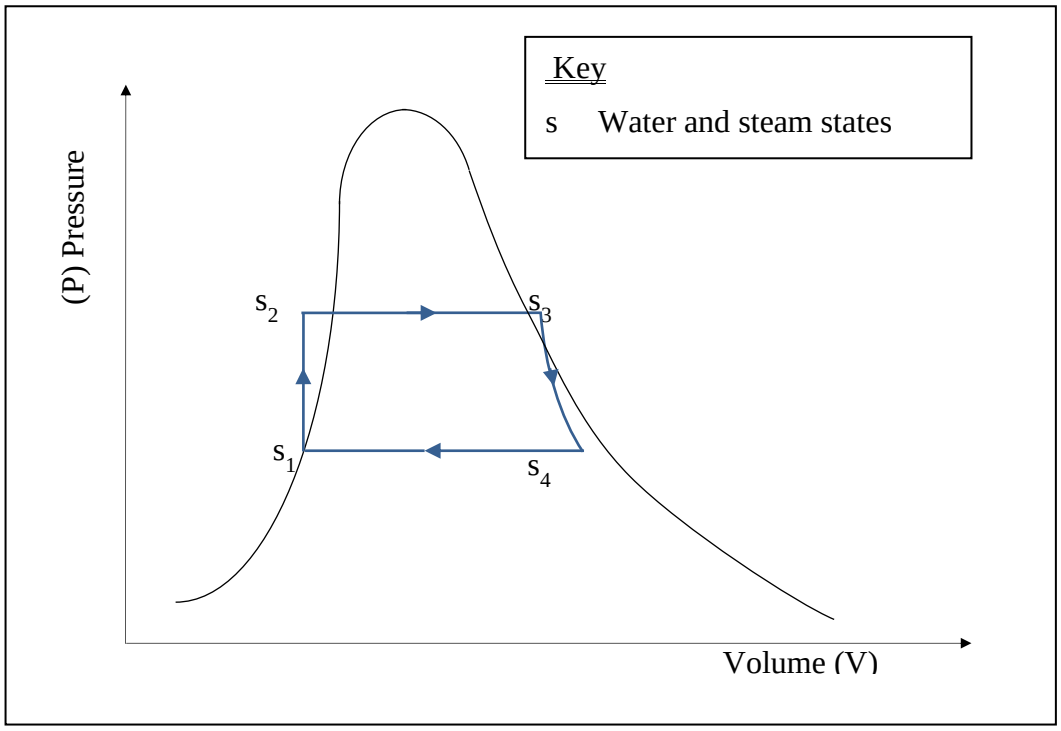

Figure 2.15 Ideal Rankine cycle on pressure-volume diagram

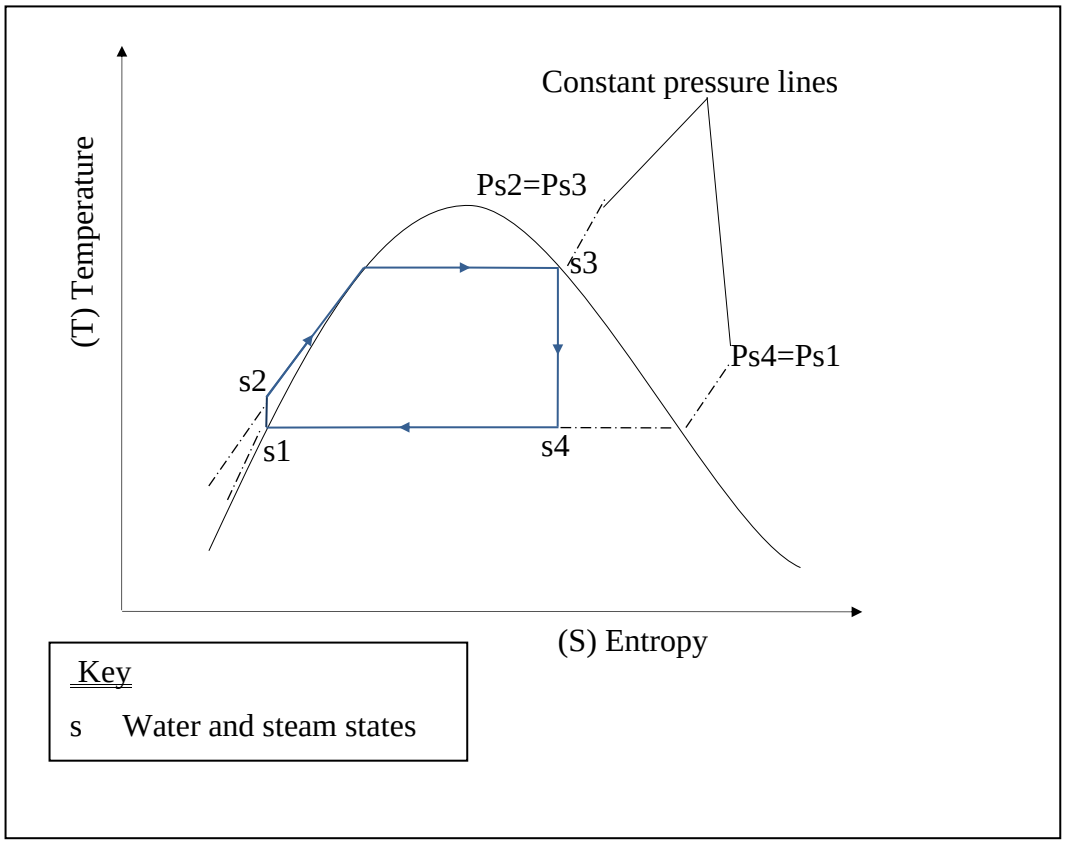

Figure 2.16 Ideal Rankine cycle on T-S diagram

$$\dot{W}_{ST} = \dot{m}\left(h_{s3} - h_{s4}\right) \quad \ldots (2.27)$$

$$\dot{W}_{WP} = \dot{m}\left(h_{s2} - h_{s1}\right) \quad \ldots (2.28)$$

$$\dot{Q}_{SB} = \dot{m}\left(h_{s3} - h_{s2}\right) \quad \ldots (2.29)$$

$$\dot{Q}_{SCon} = \dot{m}(h_{s4} - h_{s1}) \quad \ldots (2.30)$$

Equation (2.26) transfers to equation. (2.31) when equations. (2.27) – (2.30) are utilized.

$$\eta_{thSC} = \frac{\left(h_{s3} - h_{s4}\right) - \left(h_{s2} - h_{s1}\right)}{\left(h_{s3} - h_{s2}\right)} \quad \ldots (2.31)$$

Unlike the gas turbine cycle, the properties at any state in the steam cycle (enthalpy, entropy, etc.) are not analytically obtained. However, the steam/water table of properties is used. In real steam power plants (steam engines), the number of the considered parameters in the calculations is raised. Therefore, the heat losses in the steam turbine and the water pump are considered in calculations by regarding the isentropic efficiencies (η_{ST}, η_{WP}). The isentropic efficiency of the steam turbine and the water pump are represented by the equations (2.32) to (2.34). In these equations (W_{STreal}) and ($W_{STideal}$) represent the real and the ideal work generated by the steam turbine. While the real and the ideal works consumed by the water pump are represented by (W_{WPreal}) and ($W_{WPideal}$) respectively. Equation (2.31) is modifies into equation (2.34) after employing the isentropic efficiencies of the engine components.

$$\eta_{ST} = \frac{\dot{W}_{ST\ real}}{\dot{W}_{ST\ ideal}} \quad \ldots (2.32)$$

$$\eta_{WP} = \frac{\dot{W}_{WPideal}}{\dot{W}_{WPreal}} \quad \ldots (2.33)$$

$$\eta_{thSC} = \frac{\eta_{\ ST}\left(h_{s3} - h_{s4_s}\right) - \left(\frac{h_{s2_s} - h_{s1}}{\eta_{WP}}\right)}{\left(h_{s3} - h_{s2}\right)} \quad \ldots (2.34)$$

The work consumed by the water pump is usually very small in comparison to the work generated by the steam turbine. Analytically, this appears to be due to the slight change in specific volume of water along the water pump. Accordingly, the specific work of a water pump can be expressed by equation (2.35) which was used in equation (2.34) to obtain equation (2.36).

$$\frac{\dot{W}_{WP}}{\dot{m}} \approx v_{s4} \times \left(P_{s2} - P_{s2}\right) \quad \ldots (2.35)$$

$$\eta_{thSC} = \frac{\eta_{ST}\left(h_{s3} - h_{s4_s}\right) - \frac{v_{s4} \times \left(P_{s2} - P_{s1}\right)}{\eta_{WP}}}{\left(h_{s3} - h_{s1} - \frac{v_{s4} \times \left(P_{s2} - P_{s1}\right)}{\eta_{WP}}\right)} \quad \ldots (2.36)$$

From the above it can be concluded that the main important parameters which characterize the performance of any steam cycle through the thermal efficiency are represented by the following equation:

$$\eta_{thSC} = f\left(\eta_{ST}, \eta_{WP}, P_{s1}, \text{ and } P_{s2}\right) \quad \ldots (2.37)$$

The approach in designing any steam power plant (based on Rankine cycle) is to attain the performance of the ideal Rankine cycle. It implies the best utilization of the heat source into the power generation. Therefore, it is necessary to ensure the minimum losses in the heat and the pressure of the steam through steam power plant components.

Typically, the increase in the pressure of the steam through the boiler improves the performance of the simple steam engine. Similarly, the decrease in the pressure at which the steam is condensed affects the performance; however, it does not insure a substantial increase in the performance as boiler pressure does. Employing these strategies increases in the temperature of the heat addition process and drops in the temperature of the heat rejection process; therefore, the power generation is increased.

These strategies are governed by many restrictions, which decide the degree of optimization in the performance of the cycle of such engines (plants). Initially, turbines' blades materials restrict the pressure of the steam at the turbine inlet. Therefore, it has to be within a certain range. Secondly, the ambient saturation temperature limits the lowest steam pressure at which the condenser can operate. Beyond such limit, the operation of the condenser is useless in recirculation the purified water through the cycle to avoid turbine corrosion. In practice, the protective strategy that has been usually undertaken to avoid erosion in turbine blades is fixing the quality of the steam at the turbine outlet to not be less than 90%.

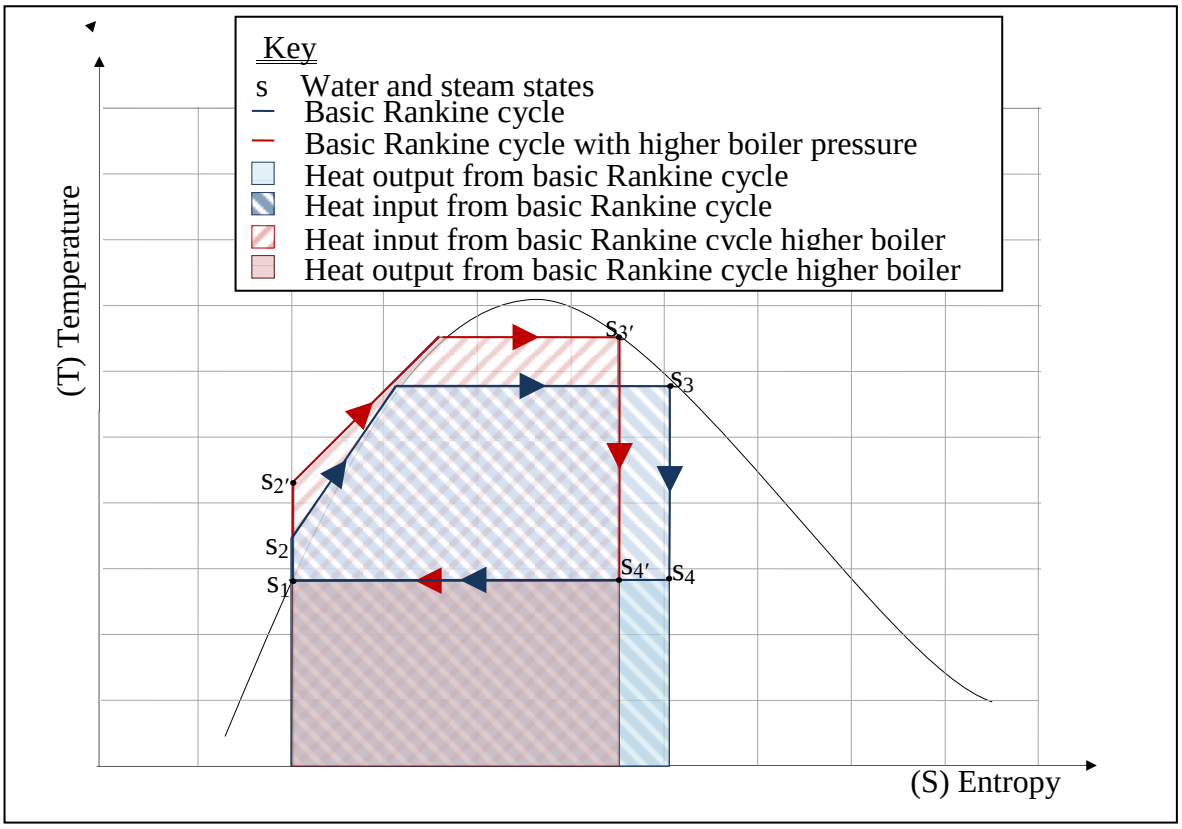

Figure 2.17 Basic and increased boiler pressure Rankine cycles on T-S diagram

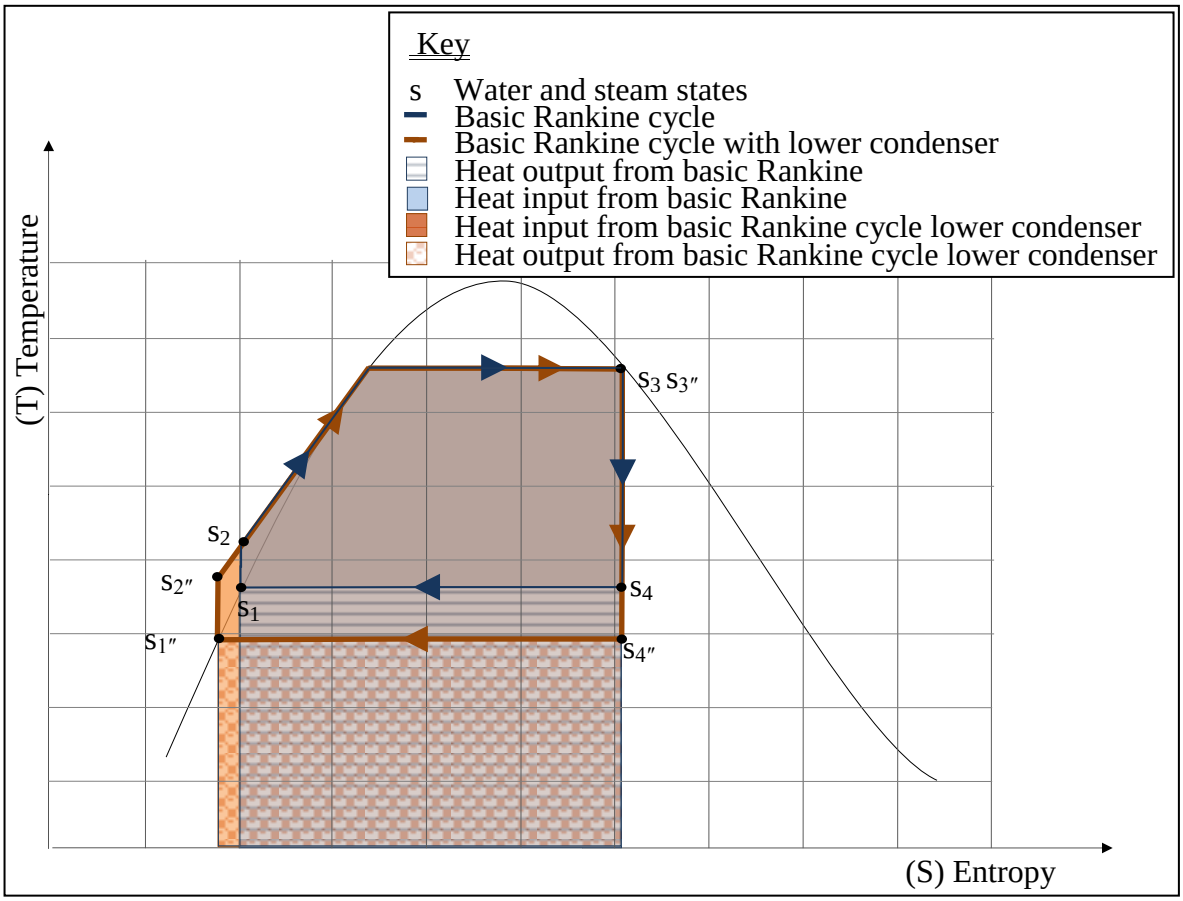

Figure 2.18 Basic and low condenser pressure Rankine cycles on T-S diagram

Further improvement in the performance of the steam power cycles requires one or more of the following strategies: (1) superheated steam, (2) reheated steam cycle, and (3) steam regeneration. The use of advanced blade materials enables higher steam temperatures by which more heat can be supplied to superheat the steam. The combination of super-heater and boiler forms the steam generator at which water is vaporized and superheated. The increase in the power output from the steam turbine permits using the steam with higher pressure at the turbine outlet to reduce the problems of low steam quality.

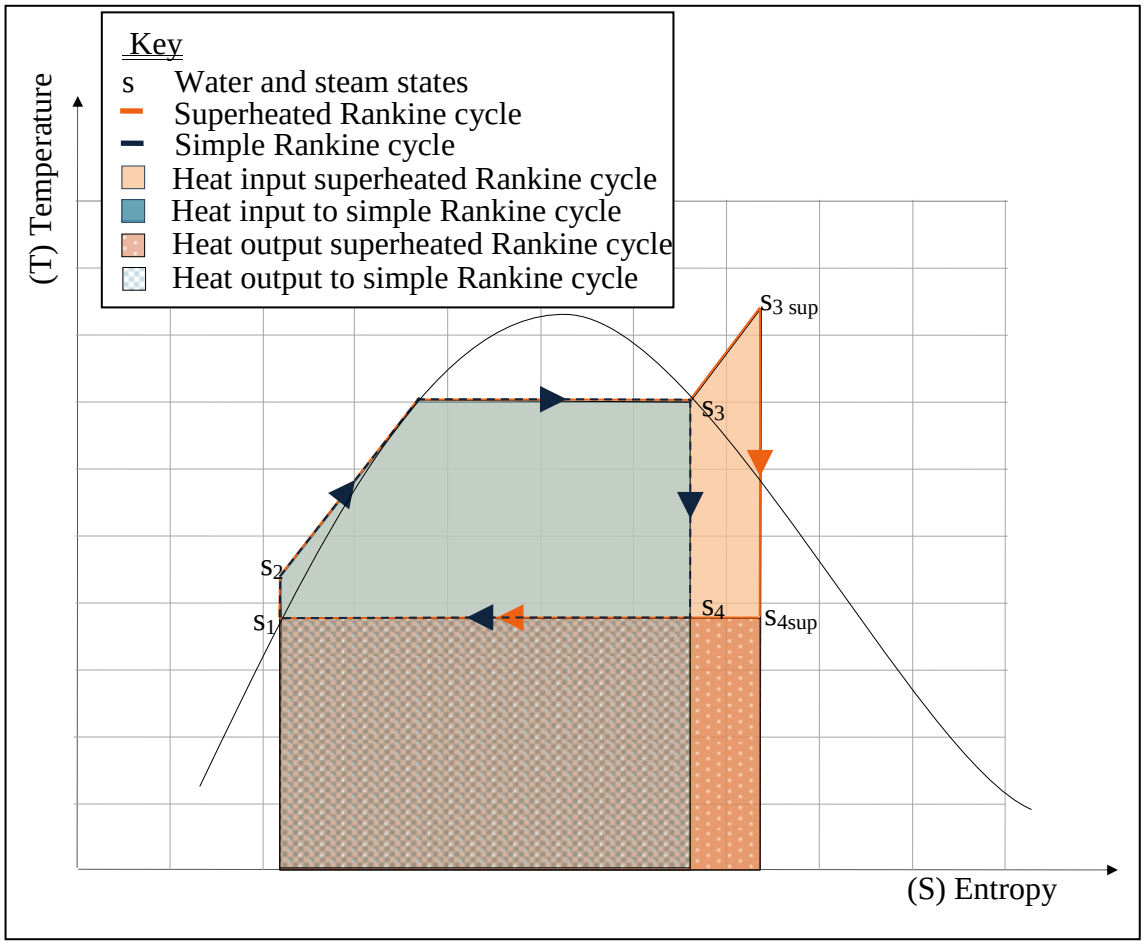

Figure 2.19 Basic and superheated Rankine cycle on T-S diagram

The reheated steam power engine employs more than one turbine. It also employs re-heaters by which an extra heat is supplied to generate additional power. In dual staged reheated steam turbine engines, the steam expands in the first turbine to a pressure greater than the pressure of the condenser. The low pressure steam from the first turbine is reheated to higher temperature in the re-heater and it is expanded in the second turbine to the condenser pressure. The pressure of the reheated steam has to be chosen carefully with regard to the pressure of the steam at the boiler to ensure the required augmentation in the power generated from each stage. Therefore, as higher as the pressure of the boiler as wider as the range of pressure of the reheated steam. The advantages from such configurations can be summarised

by the useful quality of steam at turbine outlet and the increase in thermal efficiency. The specific work output from reheated steam turbine engine is calculated by equation (2.38). While the main components of such engine and its processes on Rankine cycle are illustrated by Figs. 2.20 and 2.21.

$$\dot{W}_{SC} = \dot{W}_{ST1} + \dot{W}_{ST2} - \dot{W}_{WP} \quad \ldots (2.38)$$

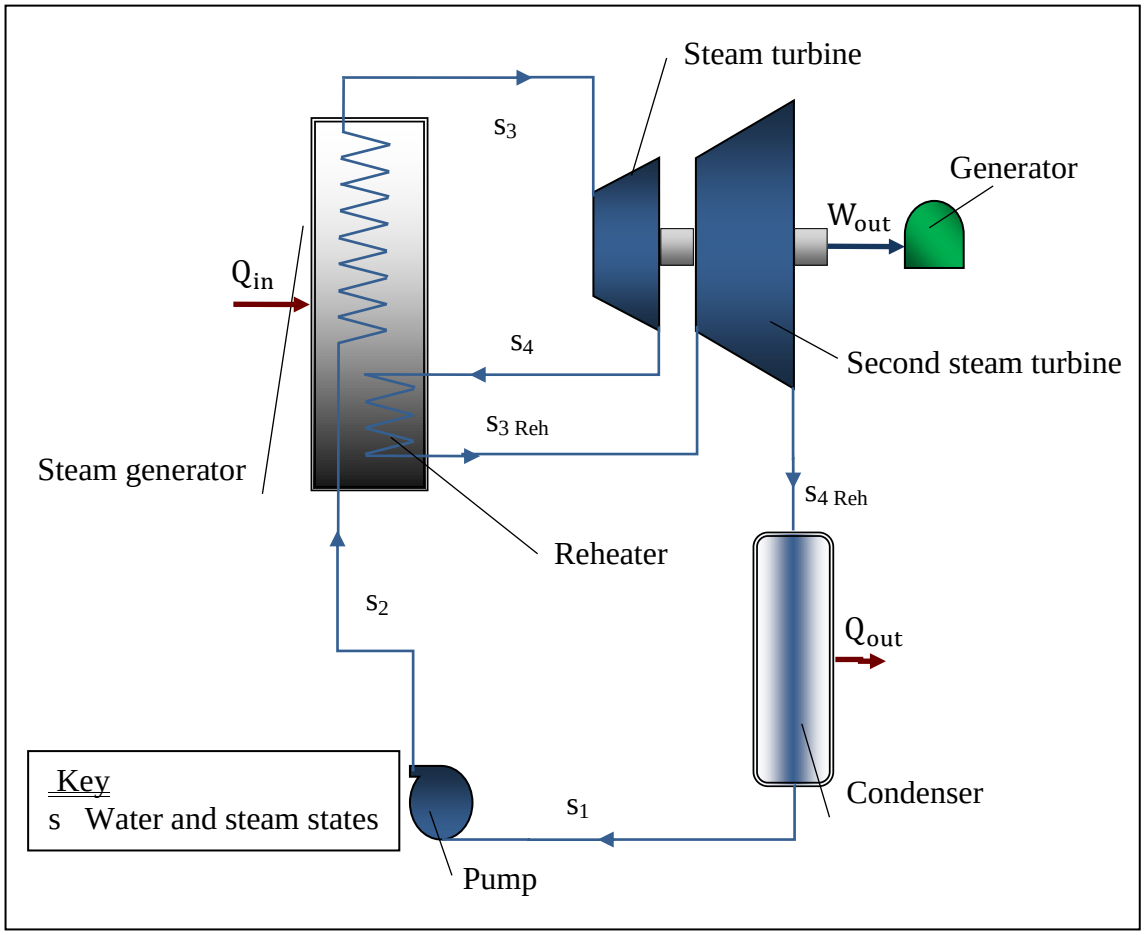

Figure 2.20 Main components of a basic reheated steam turbine power plant

The progressive developments in the materials of the steam engine components permit the using the steam at high pressure and temperature. Therefore, a steam quality exceeding super-critical conditions of approximately 221 bar and 600 °C can be utilized to improve performance of such plants. The feature of regeneration in steam cycles is based on the increase in the average temperature of the heat addition process to increase the thermal efficiency. It's usually applied by using either an open or closed as well as multiple feed water heaters.

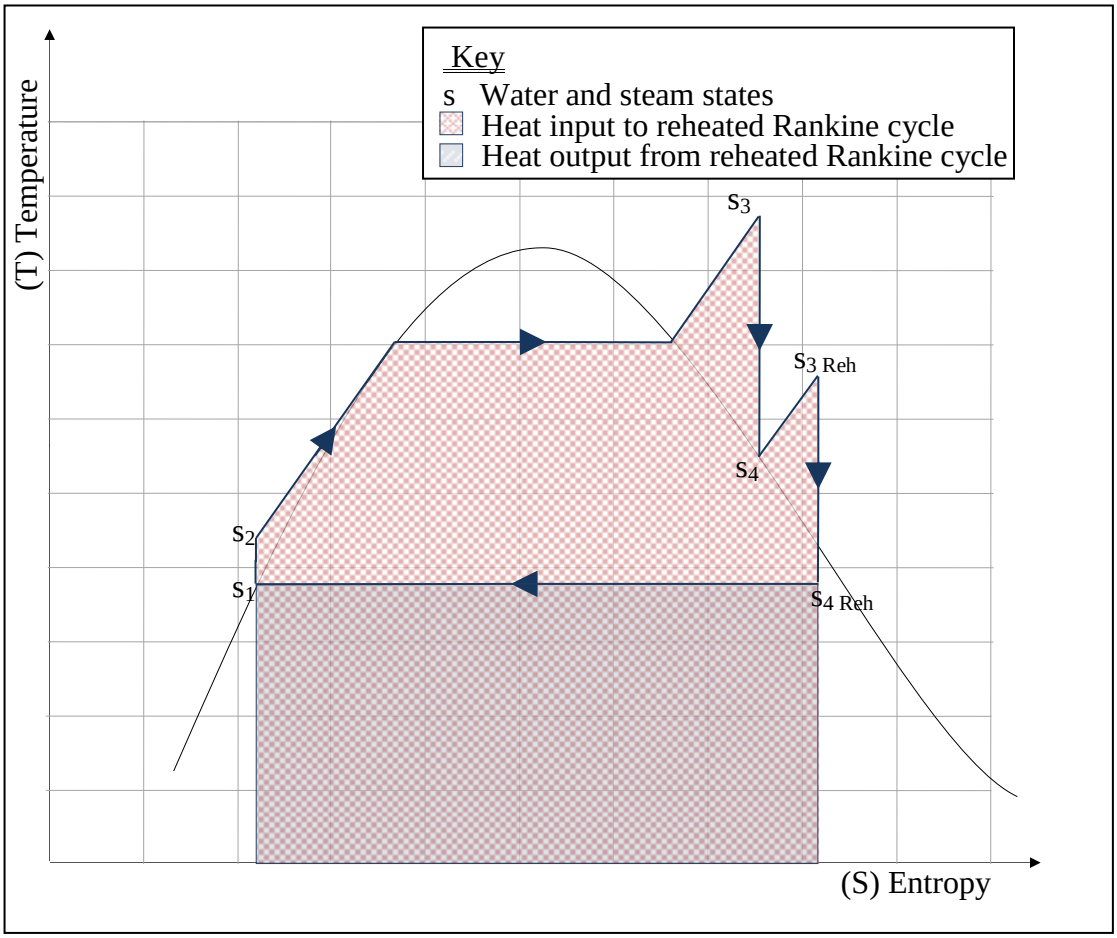

Figure 2.21 Ideal reheated Rankine cycle on T-S diagram

The flow diagrams of the open and closed type feed water heaters are illustrated in Fig. 2.22. The open configuration of such heaters uses a fraction of the steam which is discharged from turbine before a complete expansion to the condenser pressure. It mixes the high quality steam with the water. This technology insures an increase in the temperature of the water at the boiler inlet. Therefore, it reduces fuel required to heat the water to the same conditions, although. The reduction in the mass flow rate through the steam turbine drops the work output. Therefore, the mass flow of the extracted steam should be carefully chosen to attain the desired increase in the thermal efficiency. The advantage from utilizing closed type heaters is exchanging the heat between fluids without affecting the pressure in each stream. The steam turbine plant that uses multiple type heaters requires at least one open type heater which uses the steam at a pressure higher than pressure of the condenser. The mass flow rate that circulates through the steam turbine plant's components has to be calculated to obtain the accurate amount of the power generated from such plants as shown in equation (2.39). The total network output from such system is calculated using equation (2.40).

$$\dot{m}_t = \dot{m}_1 + \dot{m}_2 \quad \ldots (2.39)$$

$$\dot{W}_{SC} = \sum \dot{W}_{ST} - \sum \dot{W}_{WP} \quad \ldots (2.40)$$

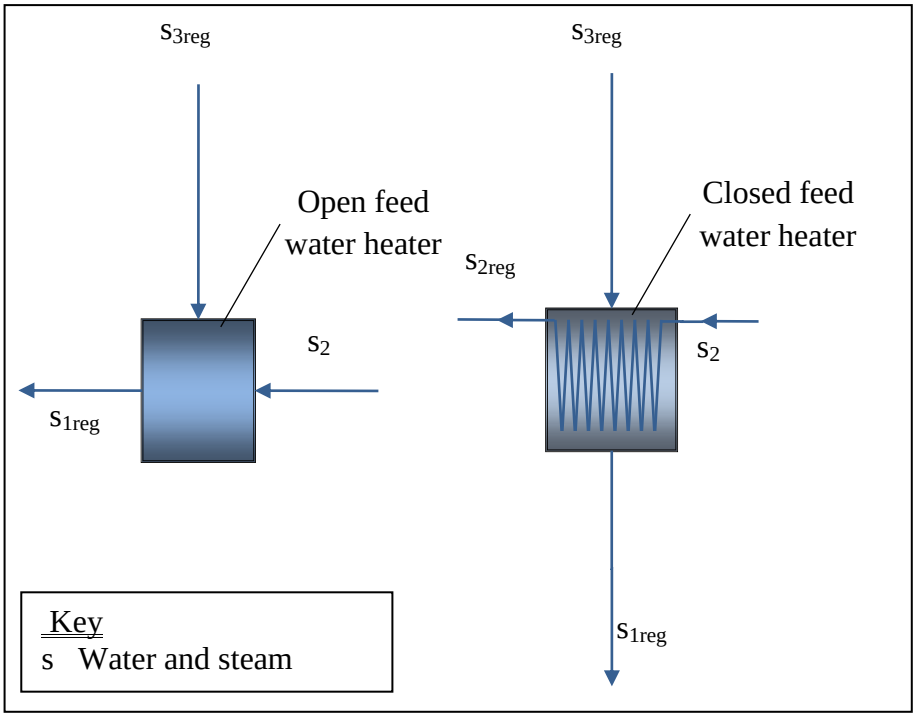

Figure 2.22 Open and the closed feed water heaters

The main components of a regenerated steam turbine plant that uses an open type and that uses closed type heaters are illustrated in the Fig. 2.23 and Fig. 2.24 respectively. The processes of the cycles of such engines are shown on the temperature entropy diagrams in Figs. 2.25 and 2.26. The ratio of the steam mass fraction (Y) from the main mass flow rate is illustrated by equation (2.41). Equation (2.42) calculates the steam mass fraction for an open type heater and equation (2.43) calculates the steam mass fraction for the closed type heater.

$$Y = \frac{\dot{m}_1}{\dot{m}_t} \quad \ldots (2.41)$$

$$Y = \frac{h_{s.1reg} - h_{s.2}}{h_{s.3reg} - h_{s.2}} \quad \ldots (2.42)$$

$$Y = \frac{h_{s2reg} - h_{s2}}{h_{s3reg} - h_{s1reg}} \quad \ldots (2.43)$$

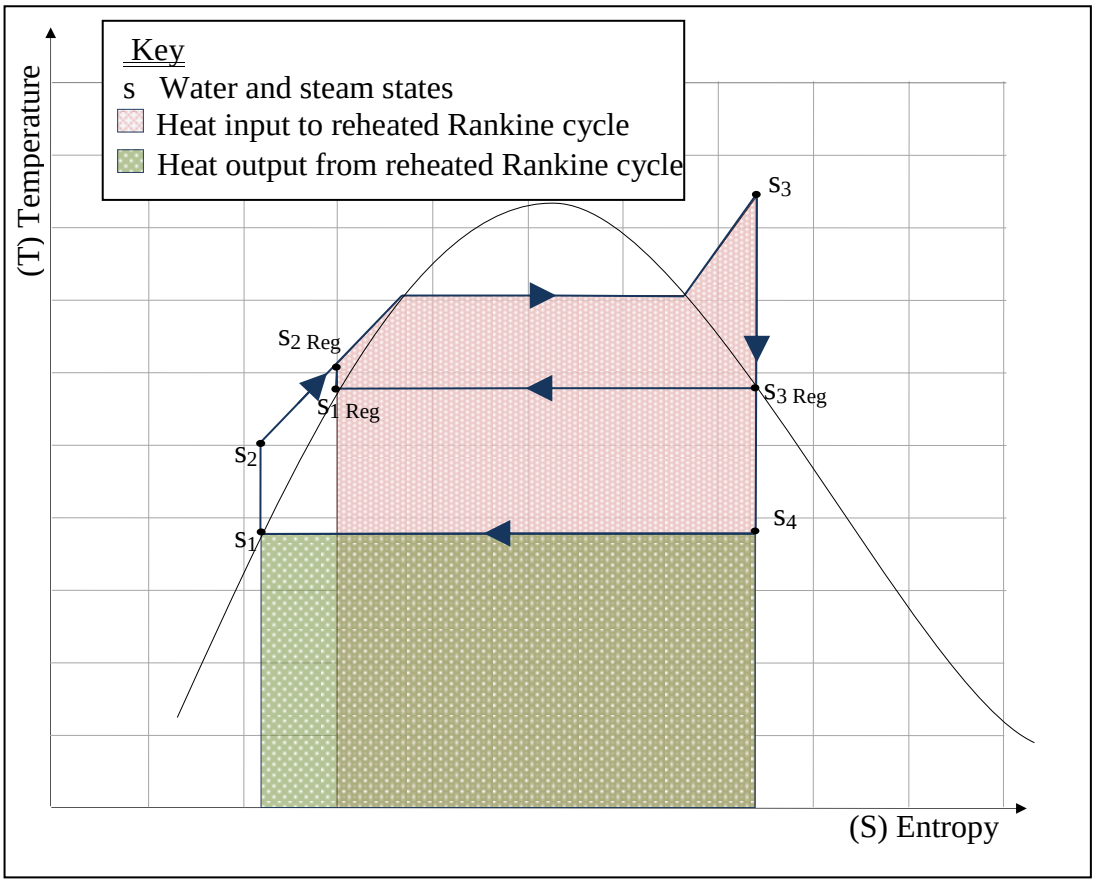

Figure 2.23 Ideal regenerated Rankine cycle using open feed water heater on T-S diagram

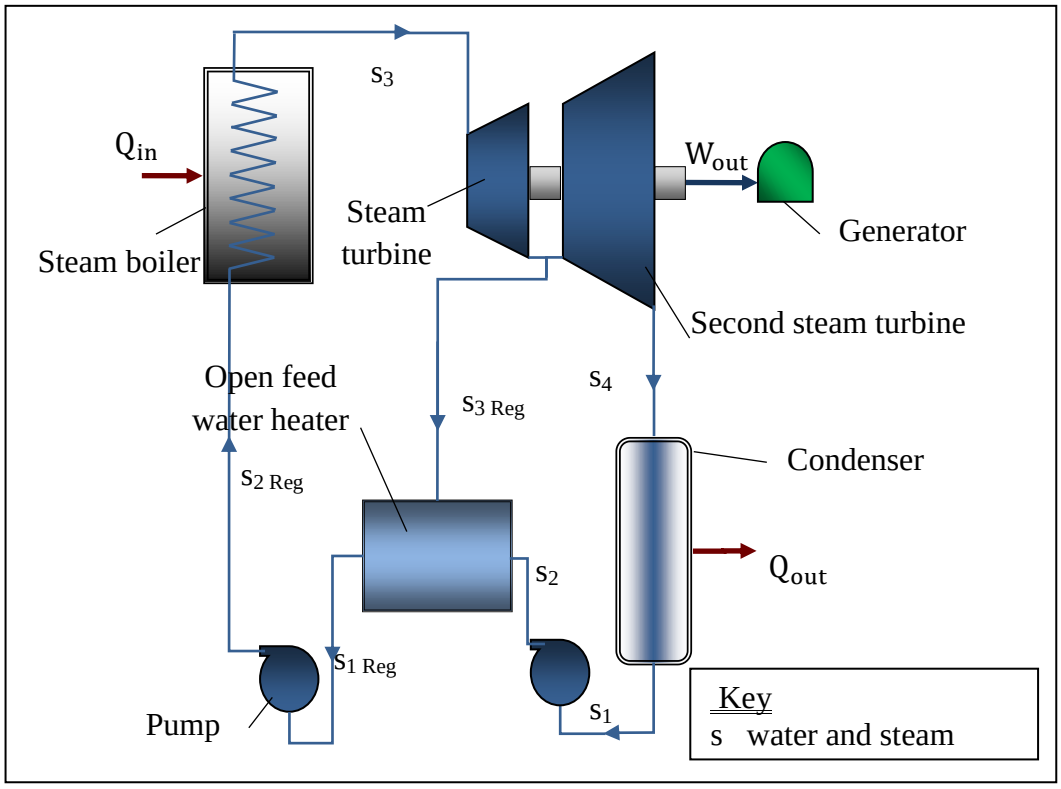

Figure 2.24 Regenerated steam turbine power plant with an open feed water heater

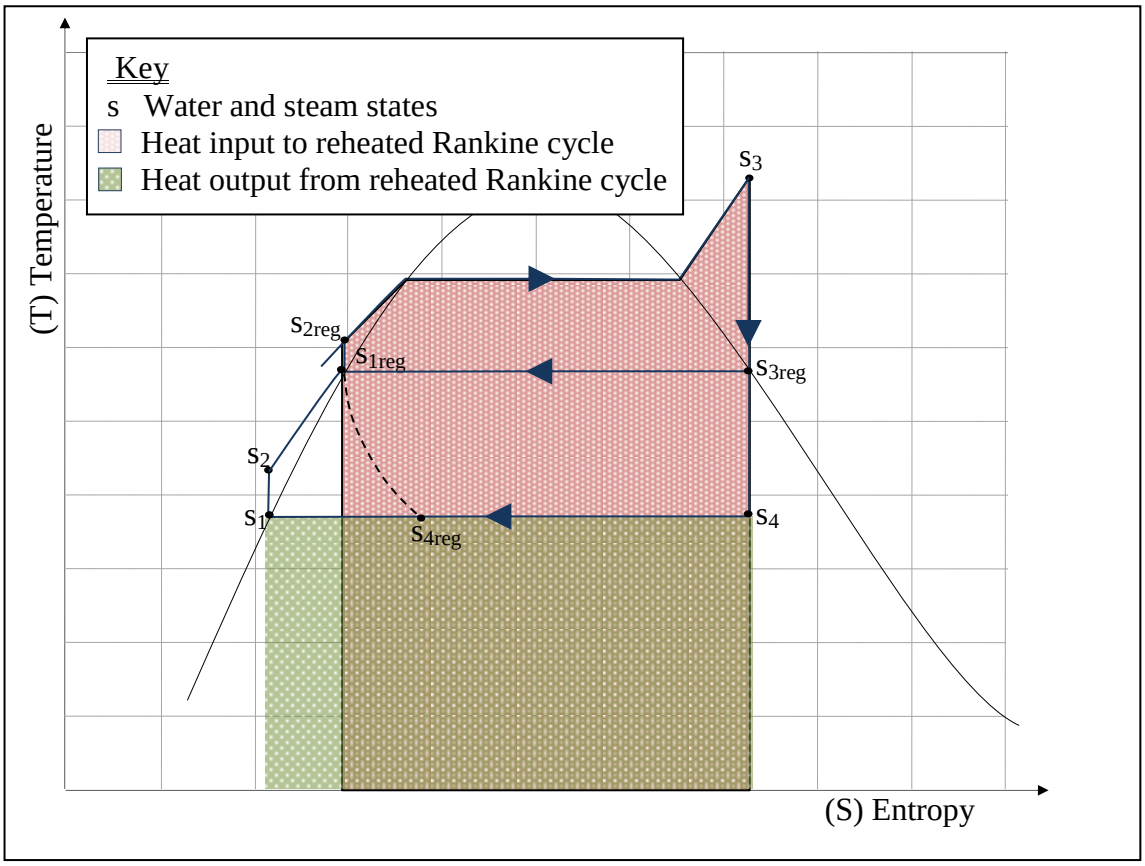

Figure 2.25 Ideal regenerated Rankine cycle with closed feed water heater on T-S diagram

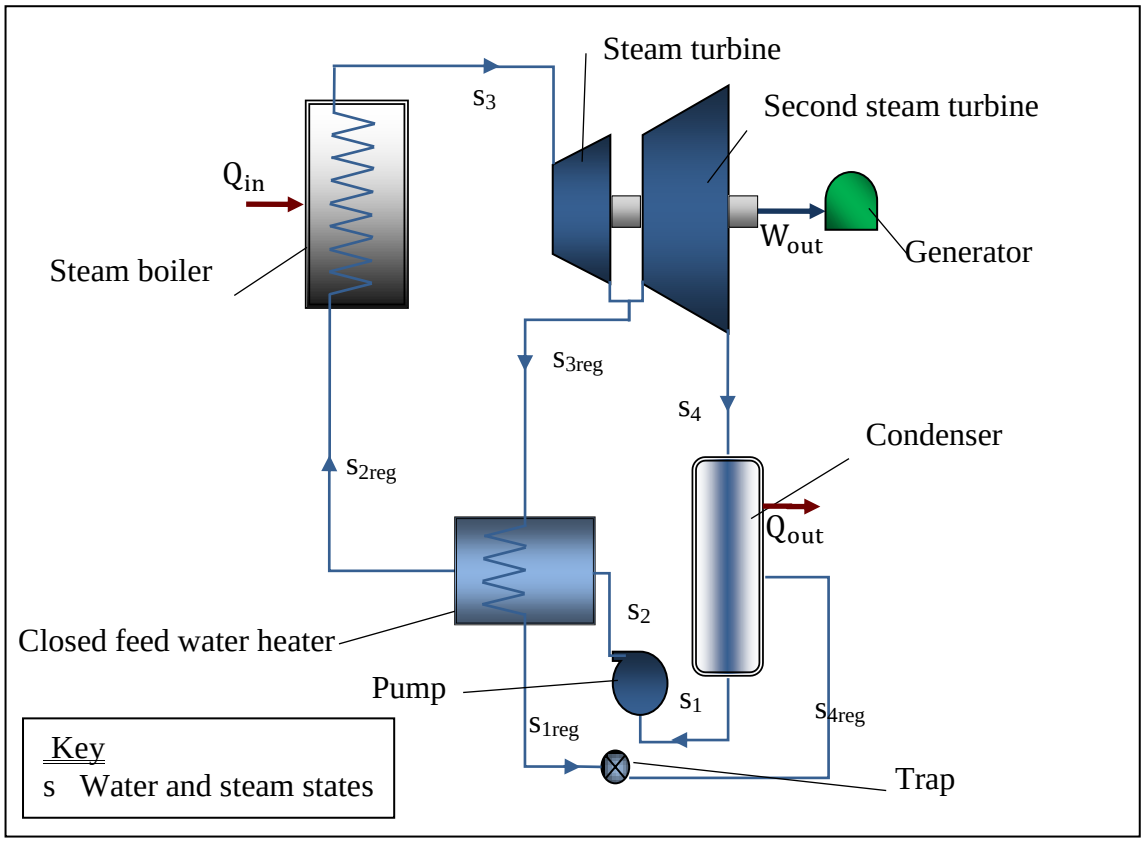

Figure 2.26 Main components of a regenerated steam turbine power plant with closed feed water heater

2.4 Theory of the combined power cycles

After a full optimization in the performance of the steam turbine plant, the only other solution for more improvements in the performance of the steam turbine power plant is the combined configurations. In such configurations, the heat is supplied to the topping cycle (Brayton cycle) only i.e. to the gas turbine plant. The bottoming cycle (the Rankine cycle) in the steam turbine plant uses all or part of the heat that has been taken from the exhaust of topping cycle of the Brayton plant. The efficiency of this configuration is higher than the efficiency of each cycle alone. In concept, this cycle uses the high temperature of heat addition process of the gas turbine cycle and the low temperature of the heat rejection process of the steam turbine cycle. Figure 2.29 shows the flow diagram of the heat transfer between the combined cycles. Applying the definition of the thermal efficiency on the cycle in Fig. 2.27 generates equation (2.44). The work output from this cycle is obtained from equation (2.45), in which the letter (U) represents the upper or topping cycle and the letter (L) represents the lower or bottoming cycle.

$$\eta_{thCC} = \frac{\dot{W}_U + \dot{W}_L}{\dot{Q}_{inU}} \quad \ldots (2.44)$$

$$\dot{W}_{CC} = \dot{W}_U + \dot{W}_L \quad \ldots (2.45)$$

$$\eta_U = \frac{\dot{W}_U}{\dot{Q}_{inU}} \quad \ldots (2.46)$$

$$\eta_U = \frac{\dot{Q}_{inU} - \dot{Q}_{outU}}{\dot{Q}_{inU}} \quad \ldots (2.47)$$

$$\eta_L = \frac{\dot{W}_L}{\dot{Q}_{inL}} \quad \ldots (2.48)$$

The efficiency of the upper cycle is represented by the equation (2.46), which has modified to equation (2.47) when the cycle works ideally. Equation (2.48) illustrates the efficiency of the lower cycle. In the combined cycle, the heat rejected by the upper cycle is totally recovered by the lower or bottoming cycle; therefore, therefore, ,cycle; therefore, Employing the above cons,mployingin equation (2.48) yielded equation (2.49). As a result, the equations by which

the work output and the thermal efficiency are obtained are modified to equations (2.50) and (2.51), respectively.

$$\dot{W}_L = \eta_L (1-\eta_U) \times \dot{Q}_{in.U} \quad \ldots (2.49)$$

$$\dot{W}_{CC} = \dot{Q}_{in.U} \left[\eta_U + \eta_L (1-\eta_U) \right] \quad \ldots (2.50)$$

$$\eta_{thCC} = \eta_U + \eta_L - \eta_L \eta_U \quad \ldots (2.51)$$

Analytically, equations (2.50) and (2.51) confirm the increase in the thermal efficiency and the work output of the combined cycle over the efficiency and the work output of the upper and the lower cycles individually. As (η_U, η_L) are less than 1, the efficiency of the lower cycle is increased by $(\eta_U - \eta_U \eta_L)$. On the other hand, the efficiency of the upper cycle is increased by $(\eta_L - \eta_U \eta_L)$. Employing the considerations above on the gas/steam combined cycle generates the following equation.

$$\eta_{thCC} = \eta_{GC} + \eta_{SC} - \eta_{GC} \eta_{SC} \quad \ldots (2.52)$$

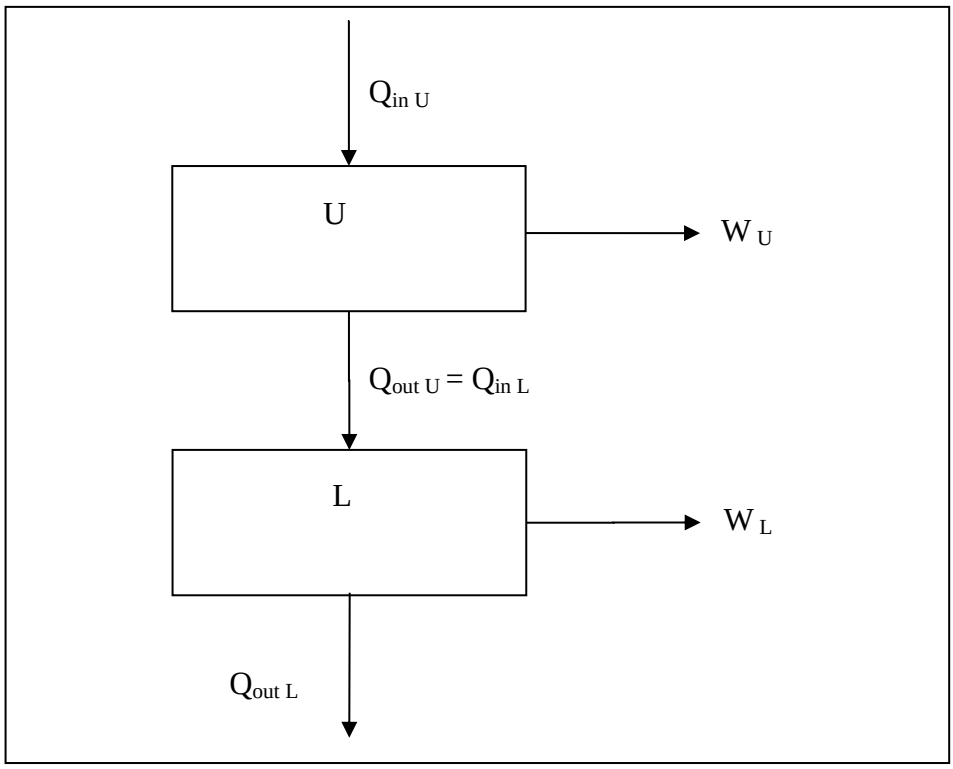

Figure 2.27 Flow diagram of a combined power plant

Practically, the heat recovery by the bottoming cycle is always less than the heat given by the topping cycle $(Q_{outU} \neq Q_{inL})$. Therefore, a new factor (ν_{Un}) is added to the equations of the efficiency and the power output. The relationship between characters of heat transfer in both cycles is obtained using the mass and energy balance as illustrated in equation (2.56).

$$\dot{W}_{CC} = \dot{Q}_{inU}\left[\eta_U + \eta_L\left(1 - \eta_U - \nu_{Un}\right)\right] \quad \ldots (2.53)$$

$$\eta_{thCC} = \eta_{GC} + \eta_{SC} - \eta_{GCSC} - \nu_{Un}\eta_{GC} \quad \ldots (2.54)$$

Here, (ν_{Un}) is the fraction of the unused (waste) heat from the heat added to the upper cycle.

$$\nu_{Un} = \frac{\dot{Q}_{Un}}{\dot{Q}_{inU}} \quad \ldots (2.55)$$

$$\dot{m}_{SC}\left(h_{outSC} - h_{inSC}\right) = \dot{m}_{GC}(h_{inGC} - h_{outGC}) \quad \ldots (2.56)$$

The operating parameters which rule the performance of the combined gas/steam cycle power plant through the power output and the thermal efficiency include:

(i) The operating parameters of the gas turbine cycle power plant.
(ii) The operating parameters of the steam turbine cycle power plant.
(iii) The operating parameters of the heat exchangers between cycles.

The operating parameters that control the thermal efficiency of combined power cycle regarding the first two points are illustrated by equation (2.57). It gives the minimum number of parameters, which influence the performance of simple combined cycle configuration. The number of such parameters increases when further modifications are employed. The efficiency of each unit in the heat exchanger and the states of the steam through such units are the parameters of the third point above.

$$\eta_{thCCPP} = f\left(\eta_{thGC}, \eta_{thSC}\right) = f(\eta_{AC}, \eta_{GT}, r, k, P_1, P_4, \eta_{ST}, \eta_{WP}) \quad \ldots (2.57)$$

2.5 Conclusions

1. Most of the operating parameters controlling the gas or steam power cycles performance also influence the combined cycles' performance. The degree of influence of these parameters is probably different in the combined cycle as compared to the individual cycles.

2. Additional parameters of the heat recovery steam generator (HRSG) are expected to have a great control on the performance of both the steam bottoming cycle and the combined cycle.

3. Improving the performance of individual cycles through its conventional parameters (the pressure change or the temperature change) is essential but limited to certain values governed by imposed restrictions.

4. Enhancing strategies can bring better performance than that for simple gas or steam cycles. While combining these optimized configurations will ensure better performance but within certain ranges for operating parameters.

CHAPTER 3
LITERATURE REVIEW

3.1 Introduction

This Chapter briefly reviews and discusses, in six individual sections, the previous practical and theoretical research on various types of combined power cycles. The first section covers features such as performance, input and operating parameters of the combined power cycles. It also deals with optimized cycles configurations and compares various cycle's configurations. The second section concentrates on researches over the optimization of the conventional combined power cycle via its operating parameters. A third section devoted to study gas/ammonia-water combined power cycles and its performance optimization. Also in this section, several types of combined cycles are compared and discussed. These include various gas/ammonia-water combined power cycles, ammonia-water cycle and steam cycle as bottoming cycles. The fourth section covers studies based on triple combination by gas/steam/ammonia-water power cycle plants, including the performances and operating parameters of such plants. It also discusses some works on the combination of power- power-heat/power and refrigeration cycles. The fifth section deals with the study that applies partial oxidation in the combustion chamber of the gas turbine cycle. It investigates the performance and the optimization of such configurations in gas turbine cycle and in the combined power cycle. Furthermore, shown in this section many comparisons between the performances of conventional combined cycle and the above cycles, which focused on their optimization, emissions and heat losses. The last section reviews the works, which compares the performance of different gas turbine cycles with inlet air cooling strategies. This section focuses on the use of ammonia-water absorption chillers in the gas turbine cycle inlet air-cooling to ensure power augmentation.

The conclusions from each section were formulated to form the main observation and to identify the shortfall in the research area which needs further consideration or research. Figure 3.1 summarize in flow chart style the main areas on which the previous studies concentrated as revealed by the current review.

3.2 Survey of relevant studies

The conclusions from each section in this chapter contribute to two major points; the first is introducing a full understanding on the behaviour of operating cycles and the optimizations in their performance. The second leads to identify the approach for future work, which was based on further optimizations in plants' performance and ensure more environmental protection. This section was divided into six parts each of them includes a comprehensive review on a number of studies that represents the most important researches in its subject. Briefly, the review starts with studies on thermodynamic analysis of different gas turbine cycles. The second and the third part of this section targeted the studies of enhancing the performance of different combined cycles. The first three parts together share the first aforesaid point, while the combination of the last three parts of this section covers the second point.

3.2.1 Energy and exergy analysis for the gas turbine power cycle

The aims from any study on the performance of the power cycle are to ensure the optimum performance the engine operating on such cycle. This goal is usually represented by reaching the maximum efficiency and satisfying the required demands (i.e. power generation). In addition to that, in the last few decades, these parameters were enclosed by meeting acceptable environmental aspects. The efficiency is defined as a measure of cycle's performance when it operates with respect to certain conditions. The maximum efficiency occurs during the time when the operating parameters are at certain values. Therefore, identifying these parameters is the reason behind analyzing any power cycle. The thermodynamic analysis of the gas turbine cycle and the combined cycle power plants were the subjected by many research as detailed hereafter.

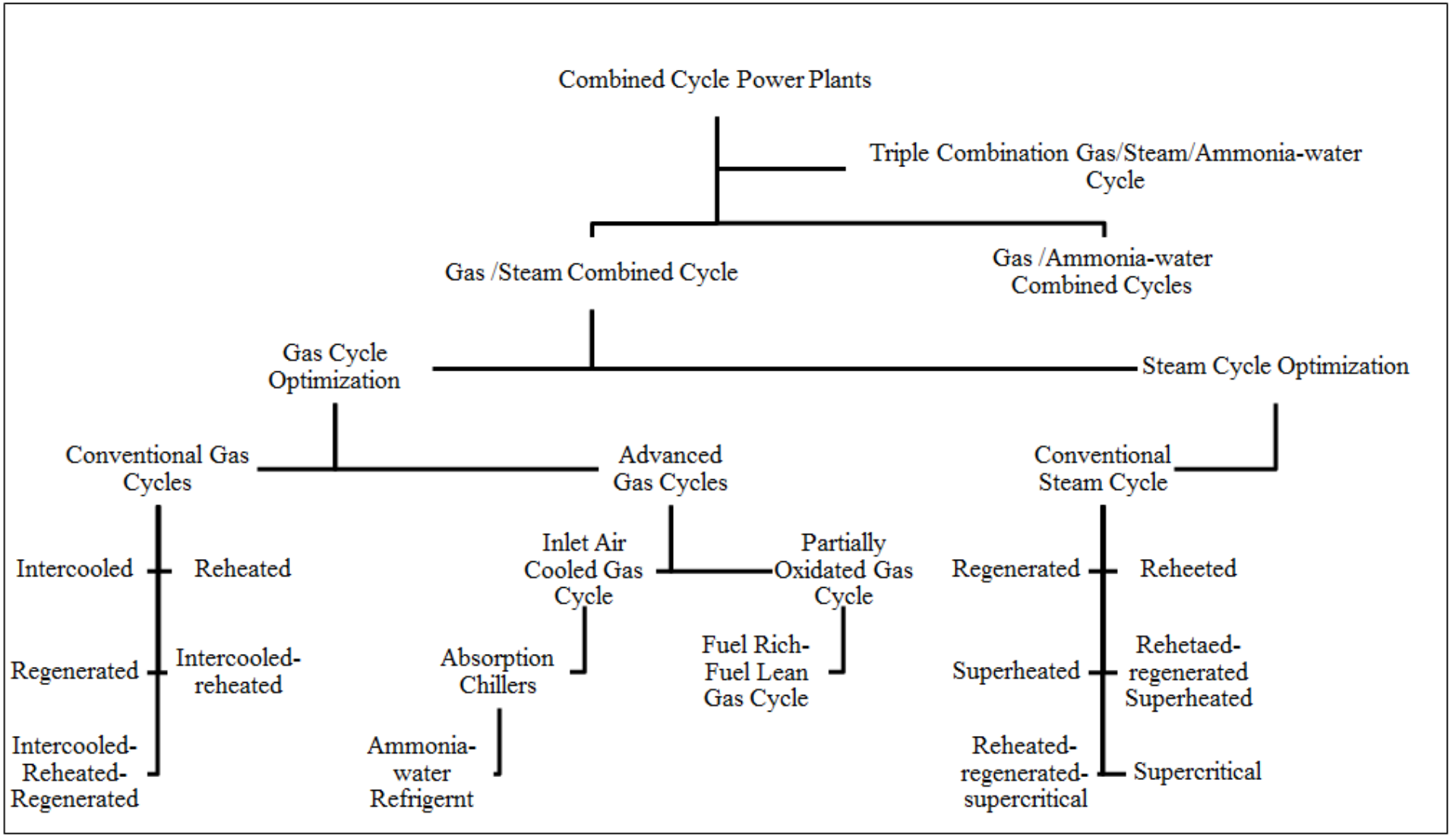

Figure 3.1 A brief classification on the subjects of the conducted studies in this literature review

Simplified thermodynamic considerations of different thermal cycles, including the power cycles were presented by Moran and Shapiro [[5]. The performances of the gas turbine cycles were studied by considering the thermodynamics aspects of the cycle with some basic and very simple approach. Other researchers EL-Hadik [6], Guha [7], Razak [8] and, et al. [9] also undertook analytical studies to investigate the performance of more realistic advanced gas turbine cycles. Many advanced gas turbine cycles were also described and investigated by other workers, including Horlock [10] and Korobitsyn [11]. In addition, the performance of the gas turbine cycle as an individual cycle within the combined power cycle was investigated by Horlock [12] and [13], Horlock [14], Khaliq and Kaushik [15] and Ameri, et al. [16] . An early graphical analysis method was developed by a number of workers to study the performance of power cycles like Horlock, et al., [13] who focused on the use of reheat and recuperated gas turbine cycles. Several authors investigated the performance of the already operating combined cycle power plants like Khaliq, and Kaushik [15] and Ameri, et al. [16]. Others including Briesch, et al. [17], Al-Hamdan [18] and Polyzakis, et al. [19] considered the optimization of the conventional gas turbine cycles. They all studied the influence of cycles' operating parameters on the plants' performance.

The influences of ambient conditions on the performance of power cycles were studied by EL-Hadik [6]. In his study, he regarded the effects of ambient temperature and pressure, and relative humidity. Hadik developed a computer program to obtain power cycles' performance characteristics for different turbine inlet temperatures and pressure ratios. He considered full load and part load operation modes in his study. His conclusions confirmed the great influence of ambient conditions on the gas turbine cycle performance. The ambient temperature was found to have the dominant influence on the performance among those parameters. Such effect became superior by the increase of the temperature of the gases at turbine inlet and the pressure ratio. The increase in the ambient temperatures reduced the thermal efficiency and increased the power output for a certain range of turbine inlet temperatures. On the other hand, the performance characteristics of the cycle were uninfluenced by the ambient pressure, while the changes of humidity had a negligible effect. Hadik study demonstrated in a very simple way the influence of the ambient parameters on the performance of the turbine. It is, however, falls short of realistically testing the findings on real gas turbine plant.

The performance of gas turbine was also examined by Guha [7]. His study dealt with the effects of the combustion of non-perfect gases on such performance. It considered the effects of the losses of the specific heat and the fuel pressure individually and together. He modelled

the gas turbine cycle starting from the air standard cycle and summarized the following conclusions:

(i) The optimum pressure ratio for the maximum efficiency increased by the increase of the specific heat of the air and the increase of the mass of the fuel. Although, the decrease of the maximum efficiency by the effect of the specific heat, it was increased to when more fuel was utilized. Relatively, when combining both parameters, the increase of the maximum efficiency by fuel addition effect takes over its reduction due to the specific heat effect.

(ii) The maximum efficiency had a great drop when the combustion pressure losses were considered. The optimum pressure ratio value was dropped slightly by such effect. Therefore, the main effective parameter on the optimum pressure ratio was the specific heat of the air. While the main effective parameter on the maximum thermal efficiency was the pressure losses. Combining both parameters had a significant effect on the optimum pressure ratio and modest effect on maximum thermal efficiency.

(iii) The greater the cycle temperature ratio, the greater was the rise of the real cycle efficiency over the air-standard cycle efficiency.

Again, Guha's work dealt with a simple gas turbine cycle and was untested in a real model despite the availability of data on such models. The gas turbine cycle was comprehensively investigated by Saravanamuttoo et al., [9] and Razak [8]. They identified the main affecting parameters and investigated many gas turbine configurations. Their works focused on single and twin spool gas turbine cycles performances. The study of Saravanamuttoo et.al, [tah [9] targeted the performance of each component in the gas cycle and how to meet the design conditions by utilizing experience and experimental tests. However, the investigations of Razak, [8] went further and considered the effect of ambient conditions as well as the performance of the individual components. A number of gas turbine cycle strategies were discussed by both workers these include water injection and inlet air-cooling. Razak, [8] observed the following points:

(i) Most of the power augmentation by water injection into the compressor was due to the drop of the ambient air temperature. The increase in power was limited by the amount of injected water, which depended on air humidity.

(ii) Power augmentation by water injection into the combustion chamber was due to the increase of the mass flow. Therefore, it was not restricted by the ambient conditions

rather than emissions. On the contrary, the thermal efficiency was decreased by such process and this decrease became greater by the drop of the ambient temperature.

(iii) The power output was increased by the increase of the ambient temperature.

(iv) The waste heat of the water injected gas turbines cannot be recovered by condensation. This was due to exhaust gases temperature, which was significantly greater than the temperature of boiling water. Although, the emissions of NO_x were reduced by water injection, the emissions of CO and CO_2 were consequently increased. The amount of such emissions increased more at a lower ambient temperature.

(v) The degree of power augmentation by inlet air-cooling was different from one technology to another. Technologies were classified with regard to their efficiency starting from wet-media-cooling, fogging, and ending by chilling systems. The choice for the best was restricted by the atmospheric conditions of the operation site which changed yearly. (This was comprehensively investigated by the last section of literature review).

Horlock [10], investigated the thermodynamics of high efficiency gas turbine cycles and presented different suggestions to develop its' simple configuration. He identified the parameters of such cycle that corresponded to low CO_2 emissions. Horlock study covered many aspects, including (1) cooled gas turbine, (2) wet gas turbine, (3) combined power cycle, (4) novel gas turbine cycles and (5) heat and power combined cycle. Horlocks study is summarized by the following points:

(i) Cooling the gas turbine made a little drop in the plant efficiency, which reduced the combustion temperatures. Therefore, the maximum thermal efficiency of a cooled cycle would not correspond to high temperature at turbine inlet. Simple gas turbine engine may be competed to advanced steam injected gas turbine engines in performance characteristics. The advanced configurations may employ regeneration or inter-cooling which increased the efficiency but requires greater pressure ratios over that for simple cycle. The efficiency increased more for more complex cooled combined cycle power plants. Although, these designs required greater pressure ratio.

(ii) Supplementary fired steam turbines didn't improve combined cycles' performance than the high temperature gas turbine. Furthermore, the efficiency of such configuration was increased when reheated configuration was utilized.

(iii) The HRSG exergy losses were dropped when dual pressure system was utilized, which increased the overall efficiency by 2-3%. While further increase in the thermal efficiency was guaranteed for the triple pressure HRSG system.

(iv) The limitations of the temperature of the water at the boiler inlet restrained corrosion in conventional combined cycle. The efficiency of the preheated loop configuration was greater than that for the bled feed heated configuration. The reason behind that was the heat of such configurations was extracted from the exhaust gases directly.

(v) The performance of novel plants may attain high thermal efficiency. Modified gas turbine power plant by thermo-chemical recuperation or partial oxidation weren't competitive to the conventional combined cycle power plant. Therefore, oxidation for power cycles was not sufficiently attractive except for multi partially oxidized combined cycle. These configurations were to be discussed by the last section in this chapter.

Steam injection within the combustion chamber of the gas turbine cycle was discussed by Korobitsyn [11], who described it as an economically competitive configuration to the combined cycle plant for power output within the range of 150 MW and 43% efficiency. This efficiency was less than that for the combined power cycle. But the utilization of inter-cooling and reheating guaranteed an efficiency of 55%. Steam injection with recuperation and water injection made this cycle competitive to the combined cycle power plant but only for power output of up to 30 MW. Further augmentation in the power gave the cycle poorer performance and involved additional requirements. Korobitsyn analyzed different power cycles and discussed combining different power generating systems into combined cycles. His study confirmed the following points:

(i) The use of the bottoming cycle usually compensated the insufficiencies (shortfalls) of a topping cycle. Thus, the performance of the combined cycle was more efficient than standalone individual cycles.

(ii) The input and the output parameters such as the power output and the fuel requirements limited the entire combination of the combined cycle.

(iii) Reheating for the gas turbine cycle was the closest form of combustion to the isothermal heat addition process.

Korobitsyns' analysis confirmed the general views on the combined cycle's efficiency superiority as compared to individual cycles. It also highlighted the impact of certain input and output parameters on the performance of the combined cycle.

The performance of gas turbine cycle, steam cycle, and combined cycle plants were comprehensively studied by Horlock [12]. Essentially, he analysed, studied, and discussed the operating parameters of combined cycle plants in two main paths. In the first, the effects of various components efficiencies on the overall combined cycle efficiency were considered. In the second, the conclusions from different parametric studies on the parallel and series modes of the gas turbine/steam turbine combined cycle and its advanced configurations were discussed. Horlock highlighted three important points regarding the plant combination: (1) minimizing the heat loss between cycles on series mode had a significant effect on cycle's performance, (2) the efficiency of the combined cycle was lowered by the parallel mode, and (3) supplementary firing reduced the thermal efficiency but increased the power output. His work can be summarized in the following points:

(i) The slight variation of the optimized combined cycle's efficiencies was due to the assumptions rather than the approach.

(ii) The performance characteristics of the combined cycle power plant were dominated by the parameters of the gas turbine cycle. Unless there was recuperation or feed heating in the steam bottoming cycle. .

(iii) The drop of the efficiency due to fuel addition in a supplementary fired combined cycle was eliminated by steam cycle efficiency raise due to firing. The magnitude of such increase was controlled by the firing temperature and the air excess percentage in the gases at the turbine outlet.

In a successive study Horlock [20] considered the heat losses between the individual cycles in a combined cycle and identified the main path to improve its performance. Three improvement elements were suggested: (1) the increase of combustion temperature, (2) the minimization of HRSG irreversibility and (3) the minimization of the heat losses between cycles. The lead of the combined cycle over different other systems was also confirmed in this study.

Horlock et al., ([13] and [14]) adopted a graphical method for gas turbine cycle to study the performance of combined cycle power plant. Particularly, he focused on the optimum pressure ratio for maximum thermal efficiency of the conventional and the reheated combined

cycle power plants. While he directed the second study in 2000 to investigate the effect of non perfect gases and pressure loses on the performance of simple and recuperated gas turbine cycles. In such study, the optimum pressure ratios for maximum specific work output and efficiency were considered. The following summarized the main observations from both studies:

(i) The optimum pressure ratio for the combined cycle appeared between the one corresponding to the maximum work output and that corresponding to the maximum efficiency. This value was greater than that for the Brayton air standard cycle and smaller than that for the reheated gas turbine combined cycles.

(ii) Although the mathematical predictions were inaccurate, it provided an elementary understanding. Accordingly, it provided a guidance to choose the optimum pressure ratio, which was useful in comparison to the complex design in practice.

(iii) The increase of the pressure losses reduced the specific work output and thermal efficiency. Consequently, the optimum pressure ratio for maximum specific work output was increased, while that for the maximum efficiency was slightly changed.

(iv) The mass flow rate of the fuel had a slight effect on the specific heat addition due to large mass of the air flow. While the optimum conditions were essentially influenced by steam injection into the flow.

(v) The increase of the specific heat after combustion dominates the maximum efficiency of a simple gas turbine cycle and the increase in its optimum pressure ratio. This effect was similar on specific work output of the combined cycle but not its optimum conditions.

Although Horlock et al., work produced some interesting details of the parameters which limit the performance of the combined cycle, its accuracy, however, is rightly questionable.

The second law thermodynamics were used by Khaliq, and Kaushik [15] to analyse the conventional and reheated gas turbine combined cycle power plants. They investigated these cycles' performances with reference to the effects of the following parameters on the cycle's performance: (1) pressure ratio, (2) cycle temperature ratio, (3) the number of reheating processes and (4) the pressure losses. They took into consideration the losses by exergy for all components of these cycles. Their conclusions confirmed two points. The first indicated that, the augmentation of the specific work output of the reheated cycles was great, but it reduced

by the successive reheating stages. The second was that, components' exergy losses were less effective on performance of reheated combined cycle power plants.

Utilizing the second law of thermodynamics was also undertaken by Ameri, et al., [16] to investigate the effects of irreversibility of each component on the performance of the combined cycle. The influence of external reheating on the steam bottoming cycle was considered. The steam turbine engine was combined with two air compressors and two gas turbine engine by two (HRSG). The following points summarize Ameri's study:

(i) The combustion chamber had losses by irreversibility. Therefore, its exergy efficiency was much lower than that for any other component in the gas turbine cycle.

(ii) The second major exergy loss was for the heat recovery steam generator (HRSG). Therefore, combined cycle's losses were significantly reduced by its optimization.

(iii) Combined cycle's power generation was improved by the externally fired HRSG, but the thermal and the exergy efficiencies were reduced.

Many technologies to increase the combined cycle's efficiency to around 60% were discussed by Briesch, et al., [17]. The operating parameters of both the gas and steam cycles were optimized, but the gases' temperature at the turbine inlet was kept constant at 1427 °C. The study also considered utilization of cooling processes and employing a higher degree of processes shared by the gas and the steam. The study strategies comprised: (1) utilizing the steam to cool the gas turbine, (2) utilizing closed steam cooling, (3) increasing the compression ratio, (4) intercooled gas turbine cycle, (4) regenerated gas turbine cycle, (5) intercooled regenerated gas turbine cycle, (6) reheated gas turbine cycle, (7) thermo-chemical recuperation and (8) steam injection for gas turbine cycle. Their study showed that, the efficiency of 60% was feasible by adopting these strategies.

A detailed parametric study was made by Al-Hamdan [18] who investigated the effect of operating parameters of the gas turbine cycle on the performance of the combined cycle power plant. A computer program was developed for such investigation, which went over different gas turbine cycle configurations each was combined to a simple steam turbine cycle. The results his study can be summarized in the following points:

(i) The operating parameters for maximum thermal efficiency and specific work output did not have the same values. While, the maximum efficiency and the maximum specific work output of the reheated gas turbine cycle had similar optimum parameters.

(ii) Supplementary firing wasn't feasible unless it gave a significant increase in the efficiency of steam bottoming cycle.

(iii) For a constant pressure ratio, the increased temperature of the gases at the turbine inlet increased the efficiency of the combined cycle. This effect was magnified by increasing the temperature of the gases at the turbine inlet.

(iv) Reheated gas turbine wasn't useful for of the combined cycle unless two conditions are met. The first when it was used to increase a low gases temperature at the turbine inlet. The second was when it was used to attain a great augmentation in the specific work output.

(v) Employing intercooled gas turbines for the combined cycle had no important increase on the thermal efficiency and the specific work output.

(vi) The values of the operating parameters of the combined cycle efficiency were different from those for the gas turbine cycle efficiency. These values were close to the parameters of the gas turbine specific work output.

Different gas turbine configurations investigated were described, optimized, and evaluated by Polyzakis, et al., [19]. These comprised: (1) simple gas cycle, (2) intercooled gas cycle, (3) reheated gas cycle, (4) intercooled reheated gas cycle and (5) intercooled reheated regenerated gas cycle. Each cycle was combined with a steam cycle by which it had to generate 2/3 of combined cycle power plant output (300 MW). They investigated the best combination between the two cycles within the previous condition. Such criteria was considered with respect to the highest overall efficiency and lowest maintenance and reliability during base load operation. The results were obtained by using a simulation program which regarded a maximum temperature and pressure for the steam at turbine inlet of 650 °C and 160 bar respectively. It was also restricted by a minimum condensation pressure of 0.03bar. They focused on the suitable pressure ratio for each gas turbine cycle and on the steam cycle design parameters. They also studied design and off design performance for each configuration. The study's results confirmed the following:

(i) Off design performance characteristics of simple gas turbine cycle, reheated gas turbine cycle and intercooled gas turbine cycle were identical. While those for the optimum thermal efficiency and the optimum specific work output were not the same.

(ii) The optimum values of the parameters for the maximum thermal efficiency and those for the maximum specific power output were not the same as those for gas turbine cycles.

(iii) The temperature of the gases at turbine exhaust was altered by the reduction of the temperature of the air at compressor inlet by inter-cooling.

(iv) The reheated gas combined cycle had the optimal design performance. It had an efficiency of 53.5% for a dryness fraction of 0.8.

3.2.2 Parametric studies and optimizations of the gas/steam combined cycle power and power plants.

The combined cycle power plant is studied by many researchers who concentrated mainly on improving the performance of the cycle through optimizing the performance of the gas turbine cycle of the combination. This section reviews the earlier works in which parametric studies were undertaken to optimize the combined cycle performance by improving the performance of both the (HRSG) and the steam cycle. It includes the studies which deal with unconventional HRSG optimization procedures. It also refers, mostly, to studies which consider the regular (HRSG) optimization method (choosing the Pinch Point Temperature difference). A number of such studies regarded improving the degree of heat usage between the combined cycles in the (HRSG) by employing the steam for gas turbine blade cooling to permit high turbine inlet temperature (TIT). While some studies combine the optimization of the HRSG, the steam turbine cycle and the gas turbine cycle. Most of the following studies employ simulation programmes to solve the analysis equations, while others used data from existed power plants. In addition, this section considers the studies which regard degradation in cycles' components as well.

The use of analytical method to optimize steam cycle was followed by Bolland, [21], Kehlhofer et al. [22], Dincer and AL-Muslim, [23], Topolski and Badur [24], Al-Qur'an [25], and Xiang and Cheng [26]. The optimization of steam cycle and HRSG by unconventional procedure is studied by Casarosa and Franco [27] and [28], Franco and Russo [29], and Casarosa et al. [30]. The use of steam for gas turbine blade cooling is noted in the studies of Bassily [31], [32]and [33]. The deterioration of the gas cycle and the steam cycle in the combined power plants was successfully presented by Zwebek, et al. [34], [35]and [36].

Different configurations of the combined cycle were evaluated by Bolland, [21] including the following steam cycles: (1) dual pressure reheated steam cycle, (2) triple pressure steam cycle, (3) triple pressure reheated steam cycle, (4) dual pressure supercritical reheated steam cycle and (5) triple pressure supercritical reheated steam cycles. Bolland compared the performance of dual pressure steam combined cycle with the performance of the other cycles with respect to the efficiency and the temperature of the stack gases. The exergy analysis is also used to estimate the improvement in the performance of each steam cycle configuration. The results confirmed a combined cycle thermal efficiency range between 54% and 55%. It also showed a rise in the thermal efficiency of the reheated cycle between 0.2% and 0.4%. While it reported an increase in the thermal efficiency of triple pressure steam cycle configurations of between 0.5% and 0.6% above that of the dual pressure steam cycle configurations efficiency. In additionally, the efficiency of supercritical reheated steam cycle configurations was shown to be approximately 0.5% greater than the efficiency of subcritical reheated steam cycle configurations.

The comparison also revealed that the optimum efficiency and power output was achieved by the triple pressure supercritical reheated combined cycle configuration. It also showed that dual pressure reheated steam combined cycle generates stack gases with the highest temperature. This temperature reached 94.9 °C, which was approximately 13% greater than the temperature of the exhaust gases from triple steam combined cycle. Bolland [21] recommended the use of a reasonable boiler pressure to ensure a full optimization in the efficiency of different cycles. The work of Bolland [21] reported very small increase in the thermal efficiency (0.1-0.2%) and these improvements should be treated with real caution.

A comprehensive study was made by Kehlhofer et al. [22]. They focused on the design parameters of the bottoming cycle and their effects on the performance of the combined cycle. For that reason, their study undertook different types of Heat Recovery Steam Generators (HRSG) including multi pressure's units. The use of reheat and supplementary firing was also considered in their study. The study covered the change in the performance due to: (1) live steam pressure and temperature, (2) (HRSG) design parameters and (3) adding feed-water reheating. The power cycles were compared with respect to their performance characteristics. The results confirmed that, the maximum efficiency for the gas turbine/dual pressure reheated combined cycle, reached 58.7%. While the greatest power output was generated by the simple gas turbine/supplementary fired steam turbine combined cycle. In general, their conclusions can be summarized as below:

(i) The heat source utilization in combined power cycles was more efficient than its utilization in increasing the maximum temperature or reducing the minimum temperature.

(ii) The power generation of the cogenerated combined cycle was more flexible than the combined power cycle as it was independent of the steam cycles. While, further flexibilities in power generation were attained by using supplementary fired for the steam bottoming cycle.

(iii) The combined cycle power plant had more advantages than the gas turbine cycle that was optimized by the pressure ratio, the turbine inlet temperature and reheating.

(iv) The efficiency of the combined cycle power plant had a wide range; therefore, within such range the criterion of the specific work output was selected.

The exergy and thermodynamics of reheated steam cycle, including 120 different cases were analysed by Dincer and AL-Muslim, [23]. They used mass, energy and exergy balance analysis to model and develop the reheated regenerated steam cycle. Cycle's operation considered live temperature range between 400 and 590 °C and live pressure range between 100 bar and 150 bar. The data for the parameters and the conditions of the power cycles were taken from an operating power plant. The performance of the combined cycle was studied with regard to the effect of gases temperature at the HRSG inlet combined with the effect of the compression ratio, the temperature of stack gases, superheated approach temperature, pinch points temperature difference and on cooling water. The following can be concluded from their study:

(i) For combined cycle power plant, the thermal and exergy efficiencies were increased by the increase in the temperature of the steam through the boiler. While the opposite occurred by when the amount of the regenerated steam increased.

(ii) The optimum design cycle was susceptible to more enhancements to ensure better performance. However, a minimum steam mass in reheat was recommended to attain such performance.

Dincer and AL-Muslim [23] study seems to be more realistic as it utilized data from existing combined power plant, which was combined with thorough analysis.

The thermodynamic analysis was also used by Topolski and Badur, [24] to investigate different gas/steam combined cycles. Their configuration comprised combining two gas

turbine engines with different types of heat recovery steam generators. The bottoming cycles were: simple steam cycle, dual pressure steam cycle and two different triple pressures cycle. They used an in-house developed code to obtain the results for optimal conditions, which confirmed the following conclusions:

(i) Further optimized and reliable heat exchanger arrangements were successfully managed by computer codes.

(ii) A state of performance near optimum conditions was attainable by optimizing the performance through heat exchangers arrangement.

(iii) There was a contradiction between the optimum performance of each HRSG component and the efficiency of the combined cycle. This paradox was greater when the HRSG units were further optimized.

There were no reasons given for such contradictions, which render such study very illusive.

Steam cycle's parameters were investigated by Al-Qur'an, [25], who concentrated on their effects on the performance of the combined cycle power plant. A computer program was developed to obtain some insight into these effects. Al-Qur'an work dealt with many combined cycles' configurations, including (1) Conventional Combined Cycle, (2) Simple Gas/ Dual Pressure Steam Combed Cycle, (3) Simple Gas/ Regenerative Steam Combed Cycle, (4) Reheated Gas/Single Pressure Steam Combined Cycle and (5) Reheated Gas /Duel Pressure Steam Combined Cycle. The following points can be summarized from his results:

(i) The increase of the pressure ratio for a certain gases temperature at turbine inlet reduced the temperature of the gases at exhaust.

(ii) The optimum operating conditions appeared in a range of live pressure between (30bar) and (60bar). Within this range, the increase of the live pressure increased the specific work of the steam turbine cycle. While further augmentation in the specific work was obtained from the recuperation of the gas cycle.

(iii) For a certain live pressure, the steam to air ratio was restricted by the temperature of gases at HRSG inlet. The increase of such temperature reduced the amounts of steam generation.

(iv) For a certain degree of gases temperature at the turbine inlet, the decrease of the steam pressure at which it condenses increased the efficiency. Such increase was restricted by the dryness of the steam at the turbine outlet.

(v) The thermal efficiency of the conventional combined cycle was increased by the increase of its specific work output. This increase went on for a particular range of pressure ratios over which the increase of the specific work combined with decrease in the efficiency. The simple gas turbine/ regenerative steam turbine combined cycle operated with efficiency lower than that for the conventional combined cycle.

(vi) The same tendencies were shown by the thermal efficiency and the specific work output of the reheated gas turbine/simple steam turbine combined cycle but with higher values. The increase of the thermal efficiency was greater than that for the conventional combined cycle only when the gases temperature at the turbine outlet was lower than (827ºC). Higher degrees of gases temperatures at turbine inlet reduced the thermal efficiency than the efficiency of the conventional cycle.

The minimization of exergy losses was used by Xiang and Cheng [26] to optimize the performance of (HRSG) of the conventional combined cycle power plant. The optimization considered utilizing supercritical conditions for the triple pressure reheated steam bottoming cycle. They also discussed the influence of gases temperature at the HRSG inlet on the efficiencies of the steam cycle thus the efficiencies of the combined cycle. Their conclusions confirmed the following points:

(i) The efficiency of the combined cycle power plant was increased by optimizing the (HRSG).

(ii) The optimization of the (HRSG) of the simple gas turbine/triple pressure reheated steam combined cycle guaranteed increasing the efficiency by 0.7%. Further increase in the efficiency was achieved when recuperation was utilized for the gas turbine.

(iii) The efficiency of the steam cycle was increased within a gases temperature of 590 °C at the HRSG inlet. The increase of the temperature beyond 590 ^{o}C decreased the thermal efficiency of the steam cycle.

Unlike the previous authors (Xiang and Cheng), Franco, Casarosa and Russo regarded non conventional procedure to optimize the performance of the steam bottoming cycle and HRSG. In their studies, they replaced the pinch point temperature difference method by

thermodynamic and thermo-economic considerations. Thermodynamically, by optimization for fewer exergy losses from HRSG by improving the coefficient of heat transfer for multi streams heat exchangers. The thermo-economic approach was employed by reducing the costs of such technology. They used such procedure on different configurations of combined power cycles as shown in what follows.

Initially, Casarosa, and Franco**,** [27] optimized the operating parameters of the (HRSG) thermodynamically. The minimization of exergy losses was relied on the effectiveness of gas-side sections of (HRSG). Their study regarded single and dual pressure steam bottoming cycles with a null pinch point temperature difference to obtain an initial condition selection for the main operating parameters of the (HRSG).

The above method was used by Franco and Casarosa [28] to check the possibility of optimizing the performance of the combined power cycle to attain a thermal efficiency over 60%. They undertook to design the combined cycle based on two strategies. The first employed super critical conditions and parallel heat exchangers to optimize the performance of (HRSG). The second utilized inter-cooling, reheating and regeneration for the gas turbine cycle/plant. They considered different combined cycle configurations. These were: (1) recuperated gas turbine/ triple pressure reheated superheated steam turbine combined cycle, (2) reheated, recuperated gas turbine/ triple pressure reheated superheated steam turbine combined cycle and (3) intercooled, reheated recuperated gas turbine/ triple pressure reheated superheated steam turbine combined cycle. They discussed the effects of following parameters on the performance of the combined cycle; (1) the temperature of gases at HRSG inlet, (2) the temperature of the gases at the regenerator inlet, (3) the total pressure ratio, (4) intermediate pressure ratio in expansion, (5) intermediate pressure ratio in compression and (6) the ratio between gas and steam engines power outputs. Their conclusions can be summarized to the following points:

(i) A thermal efficiency of 60% for combined cycle was attainable by the use of multi streams and critical conditions for the steam at the turbine inlet.

(ii) The heat required for steam generation was reduced by (HRSG) optimization, thus more heat was to be recovered in gas turbine.

(iii) An efficiency of 65% for combined power cycle was obtained by the use of reheated, regenerated gas turbine engine. While further increase of the efficiency of such configuration was achieved when inter-cooling was utilized.

(iv) Steam turbine cycle's power augmentation was restricted by the gas to steam ratio. Therefore, the heat recovered by the gas turbine cycle was always greater than that recovered by the steam cycle. This gas to steam ratio was increased by optimizing the performance of the combined cycle.

The same method was used again by Franco and Russo [29] but this time to investigate optimizing the performance of the combined cycle to attain an efficiency of 60%. The combined cycle configurations comprised simple gas turbine and various steam turbine cycles. Therefore, different kinds of heat recovery steam generators were utilized. These were: (1) Single pressure HRSG with super-heater, (2) Single pressure HRSG with super-heater and reheater, and the reheater inlet temperature higher than saturation, (3) Single pressure HRSG with super-heater and reheater, and the reheater inlet temperature lower than saturation, (4) Dual pressure HRSG with a single steam turbine, (5) Dual pressure HRSG with separated steam turbines, (6) Dual pressure HRSG with super-heater and high pressure reheater and (7) Triple pressure HRSG with super-heater and high pressure reheater. Their conclusions confirmed the following points:

(i) For a certain temperature of the gases at the inlet of the heat recovery steam generator (HRSG), the increase of the live pressure guaranteed generating the steam closer to critical conditions.

(ii) Combined cycle efficiency close to 60% was attainable by optimizing the steam cycle and the heat recovery even though there wasn't any modification to the gas turbine.

(iii) Utilizing the high temperature gases at turbine outlet by regeneration reduced the fuel consumption and increased the efficiency of gas turbine cycle. Therefore, an efficiency of greater than 60% was expected from the regenerated gas cycle/optimized (HRSG) steam turbine combined cycle.

Further optimization to the heat recovery steam generator was investigated using the same method by Casarosa et al. [30]. His optimization regarded: (1) the number of pressure levels, (2) the live pressures, (3) the mass flow ratio and (4) the temperatures of the gases at (HRSG) inlet. Different configurations for steam bottoming cycle were included single pressure HRSG and the configurations similar to those before. The conclusions were summarized into the following three points:

(i) The method of separating the thermo-economic and thermodynamic aspects of (HRSG) was successful in designing the HRSG instead off the conventional method.

(ii) Increasing the live pressure of the steam for a fixed gases temperature at the HRSG inlet assured critical steam states at turbine inlet.

(iii) An efficiency percentage close to 60% was attainable for the combined cycle by the optimization the parameters of the HRSG and steam cycle. Such efficiency was to increase by few percentages over 60% if the gas turbine optimization was included.

Dual and triple pressure steam cycle configurations of 350 cases were modelled and optimized for the combined power cycle by Bassily [31]. His study considered steam injection into the combustion chamber of the gas turbine to reduce the NO_x emissions. He investigated the effects of different parameters on the optimum performance characteristics of the combined cycle. These effects were undertaken with respect to specific ranges of: the pressure of the steam at the at the feed water heater, the minimum pinch point temperature differences, the approach temperature difference at the superheater, the temperature of the steam at the turbine inlet and the dryness of the steam at the turbine outlet. The investigated parameters were: (1) the temperature of the gases at the turbine inlet, (2) the temperature of the steam at the turbine inlet and (3) the minimum pinch point temperature difference for each unit. Bassily discussed previous parameters influences' on GTC and combined cycle characteristics. Which included the temperature of stack gases, the specific work output and the thermal efficiency of both the. The conclusions are summarized in the following points:

(i) Upgrading the dual pressure HRSG by the triple-pressure HRSG narrowed the range of pinch point's temperature differences for the intermediate pressure. Hence, the optimum efficiency of the combined cycle was dropped by such upgrade by about 3%.

(ii) The optimum performance of triple-pressure steam turbine combined cycle was correspondent to: (1) the maximum temperature of the gases at the turbine inlet, (2) the maximum steam pressure and temperature at the turbine inlet and (3) the minimum steam mass flow injected to the gas turbine.

(iii) The optimization was significantly affected by: (1) the dryness of the steam at turbine outlet, (2) the pressure of the steam at the feed water heater, (3) the approach temperature difference at the super-heater and (4) the number of pinch point temperature differences.

(iv) The dual-pressure steam turbine combined cycle had an efficiency of between 0.5 and 2 per cent greater than efficiency of the conventional combined cycle. The efficiency of the combined cycle had further increase by the utilization of the exhaust gases energy.

Therefore, more research was needed to reduce the work of compressor and for more efficient use of the waste heat.

In a successive study, Bassily [32] modelled eighty different cases of dual pressure reheated steam turbine combined cycles. He used direct research and variable metric to optimize the cycle and by reducing the irreversibility of the HRSG by reducing the pinch point temperature difference. The performance characteristics of the optimized combined cycle were compared with these for the regular dual pressure reheated combined cycle. His investigation considered effect of: (1) minimum pinch point's temperature difference, (2) the approach temperature difference at the super-heater, (3) the pressure and the temperature of the steam at turbine inlet, (4) the temperature of the stack gases and (5) steam dryness at turbine outlet. The main points concluded from his study was summarised below:

(i) More research was required to model and optimize the triple pressure reheated steam engine for the combined cycle power plant and on its reduced irreversibility HRSG.

(ii) The global optimum performance of the duel-pressure reheated combined cycle power plant was corresponding to: (1) the maximum temperature of the gases at the turbine inlet and minimum degree of minimum pinch point temperature difference.

(iii) The performance characteristics of combined cycles were improved by reducing the irreversibility of the HRSG, although, the optimized case had the most efficient performance. The effective parameters on the performance of such configuration were: (1) steam dryness at the turbine outlet, (2) steam approach temperature difference and (3) minimum pinch point temperatures differences.

(iv) For certain values of turbine inlet temperature and minimum pinch point temperature difference, the efficiency of an optimized case was greater than that for the reduced irreversibility case by 1%. This efficiency was greater than that for the regular cycle by about 3.5%. While the greatest network output was generated from the reduced irreversibility configuration. On the other hand, the optimized configuration combined cycle operation required greater compression ratio and minor values for the steam pressure and temperature.

The most common enhancements to improve combined power cycle performance were discussed by Bassily, [33]. His investigation included upgrading the simple gas turbine/triple pressure steam combined cycle by reheated regenerated gas turbine engine. Therefore, this configuration was modelled and optimized by reducing the irreversibility of (HRSG). The

performance of the combined cycle was compared with the performance of other configurations with different degree of optimization. The configurations were: (1) simple gas turbine/ triple pressure reheated steam turbine combined cycle (2) reheated regenerated gas turbine cycle/ triple pressure reheated steam turbine combined cycle and (3) reheated regenerated gas turbine cycle/ triple pressure optimized steam turbine combined cycle. As usual, Bassily used cooled gas turbine engine model in all configurations. He focused on the effect of gases temperature at turbine inlet on: (1) compression ratio, (2) the temperature of stack gases, (3) gas mass flow rate, (4) temperature of the gases at HRSG inlet, (5) the approach temperature difference at the super-heater, (6) the pinch point temperatures difference, (7) the irreversibility of heat recovery steam generator and (8) the mass flow rates of the fuel and the cooling water. The effect of these parameters on the performance characteristics of gas turbine cycle and the combined cycle were discussed. The results showed the following points:

(i) Reheated regenerated gas turbine/triple pressure reheat steam combined cycle was recommended as the most promising configurations. While more research was required for fully optimized gas cycle.

(ii) The efficiency and the specific work output of the combined cycle power plant were increased using reheated regenerated gas turbine. Further increase in such performance parameters was insured by reducing the irreversibility of (HRSG). Such cycle's augmentation was ranged between 1.9% and 5.75% for the efficiency and between 3.5% and 29.5% for the specific work output.

The impacts of the gas turbine cycle's components degradations on the performance of the conventional combined cycle were discussed by Zwebek and Pilidis [34]. They also discussed the effects of the performance of both the gas turbine and the steam turbine cycles. The study considered the degradations made by: (1) compressor fouling, (2) compressor erosion, (3) compressor isentropic efficiency, (4) turbine fouling, (5) turbine erosion, (6) turbine isentropic efficiency degradation, (7) compressor and turbine fouling, (8) compressor and turbine erosion, and (9) compressor and turbine isentropic efficiencies' degradations. The deteriorations in the combustion chamber were neglected. The effect of the efficiency of gas turbine and compressor and the mass flow rate in gas turbine were investigated for different parameters. Those were: (1) the temperature of the gases at HRSG inlet, (2) steam mass flow rate, (3) the specific work from gas turbine cycle, steam turbine cycle and total combined

cycle and (4) the thermal efficiency of gas, steam and combined cycles. The conclusions showed the following points:

(i) Gas cycle's efficiency, power output, and exhaust gases temperature were enormously affected by the degradation of compressor and turbine isentropic efficiencies together. It had a neglected effect on the mass flow rate of the exhaust.

(ii) Steam turbine output was severely affected by the joint influence of compressor and turbine isentropic efficacies. While steam cycle's efficiency, steam generation, and (HRSG) isentropic efficiency were heavily affected by the faults of the gas turbine over those for compressors.

(iii) Combined cycle performance was more sensitive to the deteriorations of the gas turbine cycle than those for the steam turbine cycle. The dominant effect on the performance of the combined cycle was made by the gas turbine isentropic efficiency.

Despite the fact that this study provided a very good insight into the effects of some important deterioration parameters on the performance of the combined cycles, it ignored a very important part and that is of the gas turbine plant combustion chamber. The shortfalls in the performance of the combustion chamber certainly affect the maximum temperature of the cycle as well as the combustion gases temperature at the inlet to the (HRSG). Both of these elements are important in the quantification of the combined cycle efficiency and power output.

In a subsequent study, Zwebek and Pilidis [35] investigated the effects of the steam turbine cycle degradations on the performance of combined cycle plant. Identical design conditions to those of the earlier study were considered for the gas turbine cycle. This investigation concentrated on the deterioration made by: (1) economizer, (2) evaporator, (3) super-heater, (4) steam turbine isentropic efficiency, (5) condenser, (6) steam turbine fouling, (7) steam turbine erosion, (8) the combination of all faults mentioned before and (9) (HRSG) foaling due to higher level of back pressure. The changes of steam temperature at turbine inlet, temperature of stack gases, thermal efficiency and power generated from steam and combined cycles were examined. The impact of these parameters on the changes in: (1) the effectiveness of economizer, evaporator, and super-heater, (2) steam mass flow rate and (3) the pressure and the temperature exhaust gases from gas turbine on the performance of the combined cycle were examined. Two major conclusions were drawn from this study. The first is that both the power output and the efficiency of the steam turbine cycle were heavily affected by steam

turbine isentropic efficiency. The second is that any degradation in the HRSG and condenser deteriorations had a lower impact on the performance of the steam turbine cycle and the combined cycle than that made by the steam turbine degradations.

Finally, Zwebek and Pilidis [36] investigated the effects of the degradation of the components of both gas turbine and the steam turbine cycles. These were: (1) compressor isentropic efficiency degradation, (2) turbine isentropic efficiency degradation, (3) compressor and turbine fouling, (4) compressor and turbine erosion, (5) economizer degradation, (6) evaporator degradation, (7) super-heater degradation, (8) steam turbine fouling, (9) steam turbine erosion, (10) steam turbine isentropic efficiency degradation, (11) condenser degradation, (12) the combination of all faults above, and (13) gas turbine back pressure increase due to heat exchanger of HRSG surfaces fouling. Their results confirmed:

(i) Combining the degradations of both cycles generated an almost linearly deterioration on the combined cycle.

(ii) The degradations made by gas turbine components and steam turbine isentropic efficiency degradation as a combined factor made the greatest deterioration on performance characteristics of the combined cycle power plant. Therefore, the efficiency and the power output of the combined cycle were significantly affected by gas turbine isentropic efficiencies, mass flow rate and steam turbine isentropic efficiency.

(iii) The lowest degree of the stack gases' temperature resulted from the degradations of both cycles. The degradation of the gas turbine cycle had the greatest impact on the temperature of the turbine exhaust gases. Thus such degradation was the dominant on the efficiency of heat recovery steam generator rather than steam cycle component degradation. Therefore, the temperature of stack gases was extremely changed by the gas turbine cycle compressor and turbine isentropic efficiencies and the mass flow rate over any other parameter.

It is rather surprizing that Zwebek and Pilidis [34], [35] and [36] did not consider the combustion chamber deterioration impact on the performance of the combined cycle. In particular, and as it was mentioned before, any changes to the combustion chamber characteristics bound to change the temperature of the combustion gases entering both the turbine and the HRSG. The behaviour of both components affects the entire cycle’s efficiency and output.

3.2.3 Energy and exergy analysis and parametric studies on gas/ammonia-water combined cycle power plants.

The reduction of the bottoming cycle's irreversibility is the only way to increase its efficiency if it operates between two fixed temperatures of the heat source and sink. Formerly, the optimization of steam cycle's operating parameters was employed for an increase in the performance. Multi pressure condensation was often used to improve the quality of heat transfer and compensate HRSG exergy losses due to the mismatch between streams. The absence of further technical developments to reduce such losses inspired plant's designers to utilize mixtures instead of single fluid. Hence, mixture's properties improved the thermodynamic match of the heat transfer between streams. Specifically, the production of variable boiling temperature of the mixture for a constant pressure heat supply process. However, replacing the steam by a mixture didn't insure enough augmentation for the bottoming cycle performance. The condenser's heat losses by the rapid heat exchange process caused an increase of the back pressure, thus a drop of the efficiency. Thus, lean ammonia concentrations were used through the condenser to ensure a drop in the back pressure and an increase in the power output. This method is used in the Kalina cycle.

In Kalina cycle, the temperature of the cooling fluid at condenser inlet governed the quality of the condensed mixture at the outlet. The temperature of the condensed mixture was lower than the temperature of the coolant at condenser's outlet. This was different from what happened in the steam cycle, in which steam quality at the condenser outlet was controlled by the temperature of the coolant at the exhaust. Thus, the temperature of the steam was higher than the temperature of the coolant at condenser exhaust.

The studies, reviewed hereafter in this section, focused on the performance of the Kalina cycle as a bottoming cycle in the combined cycle power plant. In these studies, the influences of different parameters on the performance of the combined cycle were reviewed as well as the gas turbine cycle operating parameters. Researchers compared different configurations of Kalina cycle with steam cycles considering their performances as well as the performance of the Kalina cycle individually.

The operating parameters of the Kalina cycle were identified by Micak, [37] and Zhang et al [38] in order to evaluate its performance thermodynamically. Various configurations of such cycle were studied by Marston [39] and [40], who made a comparison based on the cycle's performance characteristics. In his study, He used results from a computer model to optimize

the performance of the Kalina cycle. A variety of Kalina cycle configurations were also modeled by Ibrahim, and Klein, [41], who compared its performances to that of Maloney and Robertson cycle. The influence of Kalina cycle's parameters on the performance of the combined cycle power plant attracted the attention of many researchers, including Marston and Hyre [42] and Srinivas et al., [43], who compared the performance of the Brayton/Kalina combined cycle with the conventional power cycle. While Kalina and Tribus [44] added further heat exchanging processes to the conventional Kalina cycle's configuration to improve its performance. Srinivas et al. [43], Kalina and Tribus [44] and [45]) used exergy and energy analysis together to investigate the performance of the Kalina cycle. While others like Hanliang et al. [46] considered the exergy analysis only.

Hanliang et al., [46], used exergy analyses to optimize the performance of Kalina cycle through its operating parameters. They focused on single distillation Kalina cycle powered by low temperature heat sources. Their discussion focused on the effect of the recycling ratio on the back pressure of the cycle. Accordingly, their work did not influence the pump's work. They obtained many equations to calculate the suitable back pressure for any mixture's concentrations, which regarded no pressure losses. Their results are summarized by the points below:

(i) The determination of the back pressure was significantly controlled by the temperature of condensation and the ammonia's basic solution.

(ii) The basic concentration of the ammonia is restricted by: (1) the recycling ratio, (2) the conditions of distillation subsystem and (3) the heat recovered.

(iii) Mixture's conditions at the turbine inlet were the dominant on the optimum performance rather than other parameters.

Micak [37] used the first and second laws of thermodynamics to evaluate the performance of Kalina and steam cycles comprehensively. They analysed the losses and identified the main effective parameters affecting the Kalina cycle's performance. They highlighted the lack of experience about the ammonia-water mixture operation in the Kalina cycle.

The first law of thermodynamics was also utilized to analyze Kalina cycle by Zhang et al. [38], who focused on single distillation configurations. They developed a program to identify the main affecting parameters on the performance of Kalina cycle. These parameters included: (1) gases pressure and temperature at turbine inlet, (2) gases pressure at turbine outlet, (3)

mixture concentrations and the basic solution and (4) the multiplication ratio. They concluded that the performance of the Kalina cycle was influenced by such parameters.

Marston and Hyre [42], compared the performance of different bottoming (steam) cycle configurations, including: (1) triple pressure reheated steam cycle and (2) single and triple stage Kalina cycles. They utilized a software program to optimize the performance of such cycles through their operating parameters. Their conclusions confirmed that, the power output of both Kalina cycles individually was greater than the power generated by steam cycle. Conventional Brayton cycle was about 2% less than the single Kalina cycle and 11.6% less than the triple Kalina cycle. Accordingly, the thermal efficiency of the combined Brayton/Kalina cycles was greater than the thermal efficiency of the combined Brayton/Rankine cycle. The gain of the efficiency was about 0.36% for single stage Kalina cycle configuration and 1.95% for the triple stage Kalina cycle configuration. This represents a moderate theoretical gain in the thermal efficiency of the combined cycles gained through computer model, which is subjected to too many approximations.

The analysis of Kalina cycle for the use in combined cycle power plant was also carried out by Srinivas et al. [43]. They examined the effect of many parameters on the performance characteristics of the Kalina cycle and combined power cycle. These parameters included: (1) the pressure, temperature and ammonia concentration of the mixture at turbine inlet, (2) Mixture's temperature at separator inlet, (3) the compression ratio, (4) the ambient temperature and (5) the temperature of the gases at turbine inlet. They compared the performance characteristics Brayton/Kalina combined cycle with the conventional Brayton/Rankine combined cycle. They also included the triple pressure steam combined cycle in the comparison. The operating conditions were the same for the gas turbine in both configurations. Their investigation assumed an ammonia concentration of 0.6 at the turbine inlet and considered different pressure ratios and a heat source temperature ranged between 200 and 400 °C. Their results confirmed the following:

(i) A great increase of the combined cycle's exergy efficiency was guaranteed when an ammonia concentration of up to 0.7 was utilized at the turbine inlet.

(ii) The ambient conditions and the mixture's concentrations at turbine inlet had the greatest effect on the exergy efficiency of the Kalina and the combined cycle.

(iii) The exergy efficiency of the Kalina cycle was increased by the increase of the mixture pressure at turbine inlet. The same efficiency was decreased by the increase of ambient

temperature and both the ammonia concentration and the temperature of the mixture at the turbine inlet.

(iv) The exergy efficiency of the combined cycle wasn't affected by the variation of mixture's temperature in the separator.

The optimization of Kalina cycle through its sub-systems was comprehensively discussed by Kalina and Tribus [44]. They considered optimizing the performance of the power generation and the distillation/condensation of the sub-system. Their investigation included twelve different configurations of Kalina cycle. They comprehensively discussed Kalina cycle system KC1D2 and compared its performance with the performance of steam cycle. Their results showed an exergy efficiency of 70% for the Kalina cycle. Such result was owed to the drop of the exergy losses and the gain of power due to the drop of the back pressure. This performance would not be attainable unless the right choice of ammonia concentrations through each process. Their comparisons showed that, the thermal efficiency of Brayton/Kalina was greater than the efficiency of the Brayton /dual pressure Rankine combined cycles.

In a successive study Kalina and Tribus [45] described a specific method in optimizing the performance of Kalina cycle. In this method, they improved the performance of one sub-system by making changes in another. They also evaluated the optimization in the performance of the whole combined cycle. They discussed different optimized configurations, including various sub-systems like KC6D2, KC6D3, and KC8D3. In order to achieve optimization of the power sub-system, they divided the main stream of such sub-system into more streams at different pressures. As a result, the heat recuperation was improved; more turbines were employed and more heat was added between turbine stages. The performance of the distillation sub-system was improved by adding further regenerated streams. Hence, the exergy losses from distillation and condensation processes were reduced and the thermodynamic match between the regenerated streams was increased. The following points showed the main observations from their results:

(i) An exergy efficiency of 78.7% resulted from utilizing the D3 sub-system with the KC6 sub-system. This efficiency was about 1% greater than the efficiency of the D2 sub-system's cycles. A thermal efficiency of 39.08% for the bottoming cycle was achieved by utilizing the KC8 subsystem with D3 sub system. This result corresponded to a thermal efficiency of 58.1%, and an exergy efficiency of up to 80.7% for the combined cycle.

(ii) The performance characteristics of the above Kalina cycles were greater than those for steam cycle. In details, using Kalina cycle instead of Rankine cycle guaranteed: (1) The power output was greater by a range between 11% and 27.6%, (2) The exergy efficiency was greater by a range between 8% and 26% and (3) The thermal efficiency of the combined cycle was greater by a range between 3.7% and 8.8%.

The interesting work of Kalina and Tribus revealed the possibility of extending further the energy efficiency of the combined Brayton/Rankine cycle. It would be interesting to see if the extra complication introduced into the cycle, as a result extra components and sub-systems, work in practice (real plants). An increase in the heat recovery and high efficiency cycles in real combined cycle plants is highly desirable in utilizing wisely the limited energy resources.

Four different Kalina cycle's configurations of various degrees of complexity (KC0, KC1, KC2, and KC3) were studied and compared by Marston [39]. The effects of many operating parameters on the performance of each cycle were discussed. Marston considered certain optimum mixture's temperature in the separator for each corresponding specific mass fraction at the turbine inlet of each cycle. His work tested: (1) ammonia mass fraction at separator inlet, (2) the thermal efficiency of the cycle, (3) the exergy fraction and (4) gases temperature at turbine exhaust. The tested cycles revealed the following:

(i) The performances of the combined cycle that used the configurations described above were superior over Brayton/simple Kalina combined cycle.

(ii) For a certain ammonia concentration at turbine inlet (0.7), the performance of KC3 configuration was the superior over KC2, KC1 and KC0 configurations. Such performance showed high thermal efficiency and low stack gases temperature.

(iii) The mass flow rate through the intermediate loop and the volatile fraction of the ammonia made a significantly efficient energy generation. Such performance was due to the efficient heat transfer between the low pressure high temperature side and the high pressure low temperature side. Accordingly, cycle's performance was to be further optimized if multi stream heat exchangers were to be employed.

In a successive study Marston [40] utilized and improved a computer model to optimize the Kalina cycle in order to compare the results with those generated by EL-Sayed and Tribus [47]and [48]. He identified the effective parameters and developed a method for balancing the heat transfer in Kalina cycle. His method based on getting the advantage from the volatile ammonia compositions. In such system, the high ammonia concentration's mixture was

directed to the heat source and the low ammonia concentration's mixture was directed to the heat sink. The investigation covered the effects of: (1) the mixture's mass flow rate at separator inlet, (2) the mixture's temperature at separator inlet and (3) the concentration of the ammonia in the mixture at the turbine inlet. Marston discussed the effects of such parameters on the thermal and exergy efficiency of the Kalina cycle. He also considered the influence of the ammonia concentration at turbine inlet on the temperature of stack gases and recommended more investigation into the actual performance and detailed viable economic analysis. The conclusions from his study can be identified in the following points:

(i) Mixture's mass flow at the turbine inlet and mixture's temperature in the separator were the main affecting parameters on optimizing the Kalina cycle. However, in practice, these parameters were controlled by adjusting the mass flow rate of the mixture.

(ii) Comprehensive parametric studies were needed, if further optimizations in Kalina cycle's performance were required. In such studies, the simplicity of the components and the superiority of the performance were to be considered to guarantee the advantages over the steam cycle.

Marston work and recommendations revealed two important facts. The first is the importance and influence of various mass flow rates in the Kalina cycle on the cycle's performance optimization. The second is the necessity to undertake further comprehensive studies on a Kalina cycle of simple but high performance components to assess its advantages over the steam cycle.

The theoretical study of Ibrahim and Klein [41] compared between Maloney and Robertson cycle with Kalina cycle performances. They identified each cycle's maximum power output, which was generated from low temperature heat source for a certain ambient pressure. They used a specific methodology to evaluate the performance of each cycle. In such study, they considered a heat source temperature of 182 °C, a heat sink temperature of 13 °C and a thermal capacitance of 10 kW/K (here the capacitance is the product of multiplying the mass flow rate by the specific heat). They compared the performance of each cycle with the performance of the maximum power cycle. This cycle was internally reversible and formed by combining a group of Carnot cycles. They also discussed the effects of the thermal capacitance and the size of the heat exchangers on maximum power output. Their results and conclusions are summarized by the following pints:

(i) Maloney and Robertson cycle's performance was better than the performance of the Kalina cycle when the thermal capacitance ratio was up to 5. However, a thermal capacitance ratio of over 5 confirmed the performance superiority of the Kalina cycle.

(ii) Ninety per cent of the maximum power was generated by Kalina cycle. While only seventy per cent of the maximum power was generated by Maloney and Robertson cycle when both powered by the same heat quality. Therefore, Kalina cycle was preferred for large heat transfer sections, while Maloney and Robertson cycle was the choice for small heat transfer surfaces.

(iii) The power output from both cycles was increased when the size of the heat exchanger's hot side was enlarged.

(iv) The use of mixture in heat addition and heat rejection gave more flexibility in designing such power cycles. It also reduced the thermodynamic irreversibility and pinch point temperature difference.

The comparison of power output of both Maloney and Robertson and Kalina cycles with the maximum power generated from a zero internal irreversibility cycle (generated from combined Carnot cycles) in Ibrahim and Klein studies seems to be highly inappropriate for real applications. Internal irreversibility is impossible to eliminate in real life applications. Furthermore, the use of single temperature value for both the energy source and sink make the above conclusions highly questionable. It would have been interesting if Ibrahim and Klein supported their conclusions by studies on a wide range of source and sink temperatures.

3.2.4 Triple combination power generation cycles

As it was previously cited, the performance of the combined cycle power plant was improved through different strategies. The following studies discuss improving the performance of combined cycle through the use of waste heat. In these studies, ammonia was used for more heat recovery by power and/or refrigeration systems.

Ammonia water power generation system working on Kalina cycles were instigated by most of the following studies. Other configurations were undertaken by a number of researchers like Marrero, et al [49]. Some studies regarded the use of waste heat to optimize topping cycles. However, a number of studies regarded advanced designs, in which additional units were utilized like the refrigeration systems for turbine inlet air cooling. The influence of power augmentation on the performance of gas turbine and combined power cycles were

investigated by Amano [50], [51] and [52], Tomizawa et al., [53] and Takeshita et al. [54] and [55]. Their main objective was boosting the power output with a considerable reduction of the emissions. Some studies considered classic triple combination cycles as in the research of Murugan and Subbarao [56].

Waste heat was used to power ammonia-water power cycle by Amano, et al., [50]. He integrated two Kalina cycles KC1 and KC34 to form a system powered by low temperature heat source. The range of the heat source temperatures was between 200-400°C for the earlier and between 100-200°C for the later. Amano, et al. modelled both cycles and evaluated their performances. He investigated the systems' influence on the performance of the combined power cycle and considered the effects of vapour characteristics in the generator and the distillation/condensation sub-systems. The results confirmed the augmentation of work output by such cycle (W-MTS), but such performance required a heat source temperature of approximately 160°C higher than that required for each cycle individually.

The use of ammonia-water mixture for low temperature steam heat recovery was investigated by Murugan and Subbarao [56]. They integrated this system with the power cycle to increase its power output and reduce its thermal pollution. The quality of the steam was over the minimum prohibited limit. Therefore, the turbine was more secured from corrosion and blades' damage. The ammonia-water cycle used an inlet steam pressure which ranged between (2 and 10 bars). This corresponded to a steam temperature range of approximately (120-180°C). Murugan and Subbarao optimized the steam cycle by improving the performance of condensation. They optimized the ammonia-water cycle by fitting four variables into their optimum conditions. These variables were (1) ammonia fraction at evaporator inlet, (2) mixture pressure at turbine inlet and (3) the temperature of heat source at the inlet and outlet. They used a simulation program to investigate the effect of such parameters on the thermal efficiency of the combined cycle and investigated the network output as a function to the concentrations of the ammonia at turbine inlet as well as the pressure of the steam at evaporator inlet. Their study revealed the following points:

(i) The heat usage from low temperature steam was more considerable in improving the performance of the combined cycle by Kalina rather than the steam cycle.

(ii) The efficiency was increased with the increase in ammonia mass fraction at evaporator inlet. This increase was up to 0.8455 whereas any further increase resulted in an efficiency drop, although the increase in the power output. The power output of the optimized steam combined cycle was 14.7% lower than power output of the ammonia-

water combined cycle. Correspondently, the thermal efficiency for the earlier was less by 2.1% than the efficiency of the latter for the same heat source. They attributed these losses to the fluids' mismatch through condensing process.

(iii) A saturated steam pressure of just above the atmospheric pressure is suitable for heat recovery by ammonia-water mixture.

The above configuration was more optimized earlier by Amano et al. [50] and [51] by using ammonia-water in a hybrid power and refrigeration combined cycle. The refrigeration cycle was a single stage ammonia absorption system powered by a steam at a pressure of 5.9 bar (gauge). This cycle was fit to provide an evaporation temperature of 10°C and a cooling water temperature of 32°C. They developed a simulation model to obtain the properties of the ammonia water mixture and to investigate the performance of each cycle. The use of a wider range of hot steam temperature (100-200°C) was considered during the investigation. The focus was on the effect of ammonia-water mixture pressure at turbine inlet, the coefficient of performance and the heat required by ammonia absorption refrigeration system. They also focused on the effect of mixture's temperature and fraction at evaporator outlet on the ammonia water turbines output. Their results showed the ability of such modified design to generate a work output of about 9-13.3% greater than the work output from both systems individually. Such performance was generated when: (1) the ammonia mass fraction was (0.45) at evaporator outlet and (2) the mixture temperature at separator inlet was between (53°C) and (63°C) with a pressure of 28 bars at turbine inlet.

Amano et al. [52] also investigated the steady state characteristics of the bottoming stage in the turbine system of the advanced cogeneration system ACGS. This time they experimentally investigated the use of a hot steam temperature between (165-180°C) and evaluated the performance of the ammonia water turbine system. They also considered the effects of the distillation/condensation and vapour generator sub-systems on the performance of combined cycle and focused on the effects of: (1) the mixture temperature at second separator inlet (2) the reflux loop, (3) the pressure of evaporation and (4) the changes in temperature of the heat source. Their study revealed the following:

(i) The mixtures' temperature at the second separator inlet had an essential role on the performance of the distillation/condensation distillation/condensation sub-system such that the power generation was increased by 0.97 kW per 1^{o}C.

(ii) Heat transfer in the distillation/condensation sub-system was magnificently improved by the influence of the reflux loop.

(iii) The wise use of ammonia-water basic compositions and the sensible variation in steam heat boosted the power output over that generated from constant composition cycles.

The performance of the advanced cogeneration system ACGSs' third stage was studied by Tomizawa et al., [53], who developed a mathematical model for such investigation. Their design modified the bottoming cycle to include an ammonia-water turbine and an ammonia-water refrigerator with an ice storage system. Experimental data were used to investigate the performance of this cycle after optimization during three different nightly operation periods. It was concluded that, each interval during the night had its own plan of operation, which governs the characteristics of the heat transfer in an ice storage system. As a result, the area and the mass of the ice storage were governed by such plan.

Marrero, et al. [49] investigated the triple combination cycle by combined cycle design, which included Gas/Steam/Ammonia combined plant working on Brayton/Rnakine/Rnakine cycle. The performance of the gas turbine cycle was improved using steam cooling, intercooling, and gas to air heat recuperation. While two feed water heaters were utilized to improve the performance of the steam cycle. In their design, the ammonia water cycle recovered the heat from the (HRSG) to ensure further augmentation in the performance. They used energy and exergy analysis to analyze the combined cycles. The cycle was optimized with reference to: (1) the pressure ratio, (2) gases temperature at turbine inlet, (3) compressors and turbines efficiencies, (4) the pinch point temperature difference, (5) the mass flow of the steam injected into the combustion chamber and (6) the effectiveness of heat exchangers. The following points summarize the main conclusions:

(i) The irreversibility of the combustion chamber was the greatest among the cycles' heat addition in various cycle's components. This was governed by the temperature of the gases at turbine inlet and the mass flow of the injected steam in the combustion chamber.

(ii) The degree of the thermal match between streams in the HRSG was increased by employing the ammonia bottoming cycle.

(iii) Cycle efficiency was slightly altered by the effect of the pinch point temperature difference.

(iv) A triple combination cycle was likely to operate on a thermal efficiency of 60% when modern gas turbines were used. While, if more optimizations were employed further increase in the efficiency was expected.

Further experimental investigations on Advanced Co-generation System (ACGS) were made by Takeshita et al. [54]. They focused on the efficient utilization of low temperature waste heat to increase the efficiency of the combined cycle. For that reason, an experimental facility was constructed and used to investigate the possible technologies for energy savings. This facility was used to study the effect of the ammonia mass fraction at evaporator on the performance of the ammonia-water mixture turbine system (i.e. Kalina cycle). The experimental conditions of the ammonia at evaporator inlet comprised: (1) a mixture temperature between (180-190°C), (2) an absolute pressure of (6.4 bar) and (3) a range of mass fractions between (0.4-0.7 kg/kg NH_3). The influence of these parameters on the performance of the combined cycle was represented by: (1) the power output, (2) heat transfer at low pressure condenser and (3) the transferred heat though evaporation. Their results were summarized by:

(i) When the basic composition of ammonia-water was degraded, the volumetric flow rate of the mixture at turbine outlet was the main affecting parameter on the performance of the turbine.

(ii) The work output was improved by the reduction in mixtures' basic composition as a result to the increase of the pressure ratio.

(iii) The basic composition of 0.6 kg/kg for the mixture returned in a good agreement between the simulation and the experimental data results.

(iv) The overall heat transfer coefficient at the evaporator was improved by the reduction of the basic composition and the increase of the steam velocity. While, the heat transfer coefficient of the low pressure condenser was linearly increased by the increase of the mixture velocity and the reduction of the basic composition.

The results of Takeshita et al. studies produced much reliable details due to its reliance on the data from experimental facility, which was constructed for the sole purpose of these studies. In this way, assumptions on the efficiencies of various components as well as the effects of the internal and external irreversibility were eliminated. Here, it must be stressed that the effects of any component's irreversibility rely totally on the scale of the constructed

experimental facility. As such a small scale plant prototype may produce different from a full scale and in use power plant.

The performance the ACGS in different combined power cycles was also studied by Takeshita, et al., [55]. They investigated and compared the performances of: (1) conventional gas/steam combined cycle, (2) gas/steam/ammonia-water–AAR (Ammonia Absorption Refrigeration) combined power cycle and (3) gas/steam/ammonia-water combined power cycle. They utilized a system to switch between different modes to direct the heat for more power demands during the periods of unstable heat and unsteady power demand.

The combined cycle comprised a (ST-6L-81) gas turbine, which generated the power from gases at a temperature of 1004°C and discharged it at temperature of (853°C). It also used a single pressure (HRSG) to generate a steam at 230°C and pressure of 19.6bar. Urea spray was used as a catalyst to reduce the amount of the exhaust gases when there were no further bottoming cycles. For advanced configurations, the ammonia-water mixture at turbine inlet required a temperature of (164°C) and a pressure of (15bar). Their results confirmed that the ACGS combined cycle had better performance than the conventional combined cycle performance. This performance was due to the increase of the power output and the use of Kalina cycle. It was also found that these advantages were more to occur during Spring/Autumn mode rather than other modes, i.e. when no heat load was required for the steam cycle. Hence, for such mode, only 46% heat was required from the steam to power the Kalina cycle.

Takeshita et al studies, in general, resulted in more reliable conclusions as these studies depended on real and practical data taken from full experimental facilities.

3.2.5 Partial oxidation combustion enhancements for gas turbines and the chemical gas turbine for fewer emissions and better performance combined power cycles.

The essential advantage from using chemical gas turbine is the utilization of chemical energy during rich fuel combustion in lean fuel combustion chamber Lior et.al [57]. This feature is effectively used by introducing two advanced technologies to conventional gas turbine. These technologies are: (1) partial oxidation combustion process and (2) Carbon-fibre-reinforced-Carbon (C/C) composites for rich combustion turbine blades, Yamamoto, et al. [58].

Partial oxidation is defined as the burn of the fuel with less oxygen than is required for the complete combustion. Historically, the concept of partial oxidation was described by Ribesse [59] and Maslennikov [60] but wasn't defined until 1991 by Nurse [61]. This concept was successfully implemented to improve the performance of conventional gas turbine engines and to reduce its impact on the environment. Bearing in mind that, conventional gas turbine combustion is usually a lean fuel combustion process. Accordingly, in practice, conventional gas turbine was upgraded by a fuel rich combustion chamber to feed rich fuel gases to an additional stage gas turbine. As a result, NO_X emissions were reduced and combustion performance was increased beyond conventional gas turbines levels Korobitsyn, [11].

Partial oxidation was utilized in chemical gas turbines' configurations by Arai in 1995 where Carbon-fibre-reinforced-Carbon (C/C) composites were used in the material of gas turbine blades Korobitsyn [11]. A high gases temperature at the turbine inlet was permitted by using such material (generally above 1500 °C). Therefore, the efficiency fuel-rich and fuel-lean combustion was increased Yamamoto et al., [62]. The use of C/C composites in gas turbine engines was developed by Kobayashi, et al., [63]. In 1998 Lior et al, showed the high performance of the chemical gas turbine power cycle by a thermal efficiency of 61% [57]. With the advancement of C/C material science in such cycle configurations, further increase in the temperatures of the gases at turbine inlet approached (1800 °C). This allowed an increase in the efficiency of the partial oxidation gas turbine combined power cycle (Chemical Gas Turbine) to 68% Korobitsyn, [11].

A review, presented in this section, represents a summary of the studies on partial oxidation in gas turbine cycle which focused on investigating either fuel-rich or fuel-lean combustion. Particularly, the majority of these studies considered investigating the performance of fuel-rich and reheated fuel-lean combustion processes together (shown schematically in Fig. 3.2). Chemical gas turbine was discussed by a number of these studies, in which its performance was compared with other power cycles, including: conventional gas turbine, conventional combined cycle and their optimized configurations. In addition, the emissions and exergy losses from chemical gas turbine cycles were also considered in some of these studies.

The performance of fuel-rich combustor in chemical gas turbine was investigated experimentally by Kobayashi, et al., [63]. They regarded the influence of different parameters on the performance of such power cycle configurations, including flammability limits. They also evaluated combustion gases components of and temperature. Their tested range regarded

a combustion pressure between (11 bar) and (41 bar) and an equivalence ratio between (0.7) and (1.75). The results from the tests confirmed:

(i) Combustion gases were slightly influenced by pressure change. In details, the increase of gases pressure widened the range of flammability of rich combustion. While it kept constant flammability for lean combustion and led to a drop in NO_X emissions.

(ii) A combined cycle efficiency of 66% was attained with an equivalence ratio of 2 for the rich combustion chamber.

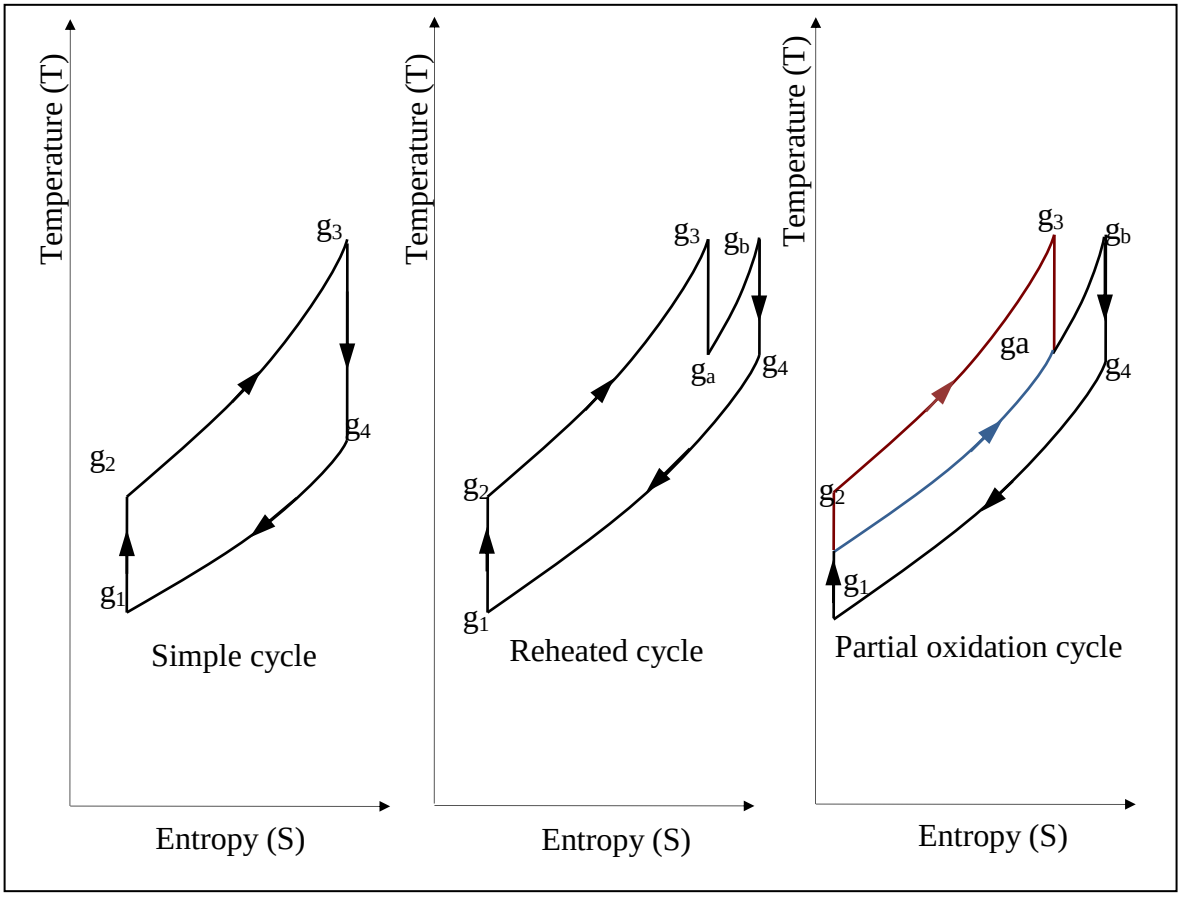

Figure 3.2 Simple, reheated, and partial oxidation gas turbine cycles

Similar analysis was undertaken by Lior et al. [57], who modelled the chemical gas turbine and investigated its NO_x emissions. They, also, used a simulation program to obtain the results which revealed the following points:

(i) For low equivalence ratio, the NO_x emissions in stack gases were increased by the increase of the gases temperature at lean turbine inlet.

(ii) For identical gases temperature at turbine inlet, the optimum efficiency appeared for low equivalence ratio lean combustor. Further increase of such efficiency required more increase of turbine inlet temperature.

(iii) The heat input and exergy losses were increased when the same temperature of gases at lean and rich turbines inlet is employed and the equivalence ratios are reduced. However, the opposite occurred when the equivalence ratio is reduced below a certain value.

(iv) The decrease in the equivalence ratios of lean combustion increased the power output from lean gas turbine. At the same time, the power generated by the rich fuel gas turbine was reduced due to the increase of compressor's mass flow rate.

(v) The highest value of the NO_x emissions was from a cycle of a thermal efficiency of (67.6%) and an isentropic efficiency of (95%). Such outputs were the results from a gases temperature of 1700 °C at turbine inlet and equivalence ratio of (0.5).

Partial oxidation combustion in gas turbine was studied, analyzed and, discussed by Korobitsyn [11]. He compared such power cycle performance with those including simple and reheat gas turbine configurations with and without recuperation. The results from his study showed the following:

(i) Among the different configurations, the simple gas turbine cycle had the maximum efficiency but not the maximum specific work output. While, the reheated gas turbine cycle had the greatest specific power output and the highest exhaust temperature. The same results were indicated for the recuperated configurations, but the efficiencies were greater. The specific power output was slightly lower and the temperature of exhaust gases was higher.

(ii) The reheated combined cycle had the best efficiency and the lowest amount of the exergy losses among other cycles. While, the power output from the simple combined cycle was the greatest.

(iii) Compared with the other cycles, the partial oxidation combined cycle had the best efficiency when recuperation is utilized. According to that, the minimum exergy losses were for the reheated combined cycle and the maximum power output was for simple cycles.

(iv) The power output of the partial oxidation gas turbine dropped when the access air was reduced. Although, at the same time the efficiency was increased and the NO_x emissions was reduced. This was caused by the increase of gases temperature at the turbine inlet.

Energy and exergy analyses were considered, again, by Korobitsyn et al. [64] in an investigation of the chemical gas turbine performance. He used two simulation packages to model the configuration and to obtain the results which showed that a thermal efficiency of (64%) is attainable. The results also confirmed that a thermal efficiency of (65%) was achievable from an increase in the lean gases temperature at turbine inlet. Similarly, the thermal efficiency was increased; the NO_x emissions and the exergy losses were decreased as the rich gases temperature at turbine inlet was increased.

Similar research work was undertaken by Yamamoto et al. [62] but he regarded the optimization through pressure ratio and the (HRSG) size. They compared the performance of a simple gas turbine and the conventional combined cycle. Their results showed the chemical gas turbine cycle's advantages over the conventional combined power cycle in thermal efficiency and exergy efficiency. This corresponded to only 75% the size of the conventional configuration's (HRSG) to maintain the same performance. This (HRSG) size was enlarged by the increase of the gases' temperature at turbine inlet. The domination of compressor on the performance characteristics of chemical gas turbine made it close to the simple gas turbine cycle in performance. He urged for further research on the use C/C composites.

The performance of partial oxidation gas turbine was tested by Abdel-Rahim and Mohamed, [65]. They studied cycle's optimum performance and compared the results with those for the reheated gas turbine cycle. Their conclusions identified three major points:

(i) For a constant temperature ratio of the cycle, the isentropic temperature ratio significantly affected the thermal and exergy efficiencies and slightly affected the heat addition. This effect was greater on the performance parameters of the reheated gas turbine cycle.

(ii) The effect of mass fraction through the rich fuel combustors was different on the thermal efficiency, the exergy efficiency and the power output.

(iii) The reheated gas turbine cycle was the dominant on the maximum thermal efficiency when the isentropic temperature ratio was low. Beyond a certain point, the maximum efficiency was for the partial oxidation gas turbine cycle.

The thermodynamic analysis was used by Yamamoto, et al., [58] to study the performance of another configuration based on chemical gas turbine. They used a simulation program to model cycle's components. Their investigation considered the effect of: (1) the thermal efficiency, (2) the exhaust emissions, (3) the exergy analysis and (4) the HRSG size. They compared the performance of conventional combined cycle with that for the chemical gas turbine. They recommended more research to be carried on C/C composites. Their results showed the following points:

(i) The performance of chemical gas turbine was better than the performance of the conventional combined cycle, which was due to: (1) the drop of the exergy losses (up to 40%), (2) the drop of NO_x emissions and (3) the smaller HRSG size (75%) for the same output.

(ii) A thermal efficiency of over (65%) was predictable when the temperature of the gases at the fuel-rich turbine inlet was (1800 °C). This performance also corresponded to an equivalence ratio of (0.9) at fuel-lean combustion.

Yamamoto, et al. work highlighted the importance of the chemical gas turbine cycle and prompted further investigation by Mohamed [66], who in turn optimized the cycle and evaluated its best performance through its controlling parameters. Mohamed, also compared his results with those form partial oxidation power cycle of Abdel-Rahim and Mohamed [65] and confirmed the following:

(i) The optimum thermal efficiency, exergy efficiency and power output were correspondent to an isentropic temperature ratio of (1.8). If this value was increased over such point, the above parameters were therefore decreased. This point corresponded to a pressure ratio of 7.8, which resulted in a thermal efficiency of 57%. The augmentation of the power output was (28.76%) over the power generated by the partial oxidation gas turbine.

(ii) The main effective parameters were identified to be; (1) the air mass fraction (effects linearly), (2) the fuel to air ratio, (3) the turbine efficiency, (4) the compressor efficiency and (5) the HRSG efficiency.

The performances of two cogeneration systems based on the chemical gas turbine were also investigated by Yamamatoo, et al., [67]. He focused on the combustion two systems and compared their effects on the cycle's performance. The first system was fuel-rich/fuel-lean combustion, while the second was fuel-lean/fuel lean combustion system. A simulation

program was used to analyze the model of each system and to investigate their influence on combined cogeneration cycle. They recommended more investigations on practical rich-fuel combustion. The following can be concluded from their study:

(i) The power generation from the fuel-rich/fuel-lean combustion cycle was greater than that generated by the conventional cogeneration cycle. In such configuration, the air excess of the lean combustor was dropped, nevertheless, the power augmentation continued.

(ii) The combustion exergy losses and the NO_x emissions were also dropped than their values for the conventional configuration. A drop of 36% in the NO_x emissions was generated by utilizing such combined cycle configuration. While more drop in the NO_x emissions was insured by the increase of the temperature and the pressure of gases at the turbine inlet.

(iii) Thermal efficiency of 53% was attained by using gases of a temperature higher than (1800 °C) and pressure greater than (40 bar) at the turbine inlet.

3.2.6 Gas turbine cycle enhancements by inlet-air-cooling system

An enhancement into the performance of power cycles by inlet air cooling systems was undertaken by many studies. This section focuses on enhancing the performance of gas turbine cycle by ammonia-water absorption chillers inlet air cooling system. It is categorized into three parts each represents a specific area of investigation. Firstly, the performance of absorption chillers refrigeration systems was evaluated by the studies of Horuz, [68], Goodheart, [69], Fernandez-Seara, and Vazquez, [70], Chua, et al., [71] and Adewusi and Zubair, [72]. Secondly, the performance of gas turbine inlet-air-cooling by ammonia-water absorption chillers was individually investigated by Yang, et al., [73], Ondryas, et al., [74], Najjar [75], Sigler, et al., [76] and Khaledi, et al., [77]. Finally, the performance of different ammonia-water absorption chillers strategy was compared by Brown, et al., [78], Lucia, et al., [79], Erickson, et al., [80], Dawoud, et al., [81].

The study of Horuz, [68] investigated the performance of ammonia-water and water-lithium bromide absorption refrigeration systems. It compared the effect of using these systems individually on the inlet air cooled gas turbine. It considered many parameters, including: (1) the coefficient of performance, (2) cooling capacity, and (3) the maximum and minimum pressures in the system. Horuz conclusions revealed that the ammonia-water systems can be

used in large industrial applications to ensure very low air temperatures. His conclusions assigned lithium bromide-water system for air conditioning applications. Hence, the acceptable performance of the latter was less complex although, it was more limited by crystallization and the need for a higher temperature to operate than the earlier (ammonia-water) system.

The lithium bromide single stage absorption chillers system was comprehensively studied by Goodheart [69]. He examined its performance for different designs, including half-effect absorption cycle, which was used to recover heat from low-temperature hot water. In his study, he investigated the suitable change in these designs in order to operate at low temperature chillers. He modelled systems components with regard to the inside and the outside heat transfer coefficients. He optimized systems for a certain heat source temperature and regarded the effect of many parameters on systems performances. These included: (1) hot water flow rate, (2) cooling water temperature, and (3) the flow arrangements in cooling and heating. His conclusions revealed the following:

(i) For a certain range of firing temperatures, the single absorption system provided cheaper refrigeration capacity than the half-effect cycle. On the other hand, a temperature below such range transmits the lead of performance to the half-effect units.

(ii) The size of the chillers was affected by firing temperature because of the rapid change in the area of heat transfer to ensure the same refrigeration capacity.

(iii) The best way to design the single absorption system powered by low temperature heat sources was by investigating the heat-exchanging areas of all its components.

(iv) The great effects of mixture's desorption at the states of low pressure and concentration of the half-effect cycle insured the requirement for smaller generators than those for single cycle.

(v) The optimum mass flow rate for the cooling water wasn’t affected by the temperature of the heat sources.

(vi) More research is required to study the effect of tubes' arrangements in each component of an absorption chillers system.

The optimal generator’s temperature for single stage ammonia-water absorption refrigeration systems was studied by Fernandez-Seara, and Vazquez [70]. They regarded its effect on the thermal operating conditions and the design parameters of such system. They implemented

simple model on a computer program to investigate the influence of such temperature on system performance, and revealed the following points:

(i) The optimum generation temperature was increased by the reduction of the efficiency of solution heat exchanger. The same appeared by the increase in pressure drop between evaporator and absorber. It was also increased by the increase of the absorption or condensation temperatures and the reduction of the evaporation temperature.

(ii) The optimum generation temperature was slightly affected by the variation in: (1) the solution heat exchanger efficiency, (2) the efficiency of pre-cooler heat exchangers, (3) the efficiency of the pump and (4) the refrigerant concentration. The optimum temperature was independent of the reflux of distillation column and temperature difference between the inlet and the outlet ends of evaporators. While it was dependent on the amount of cooling water and the temperature of the evaporation process.

The classic single-stage ammonia–water absorption chillers system was thermodynamically modelled and developed to design point by Chua, et al., [71]. In their study, natural gas was directly fired in the generator to power the system. They used multi-stream non-isothermal heat-and-mass transfer analysis to model the generator, rectifier, and absorber. The remaining components followed the conventional modelling approach. Their conclusions showed that the internal losses in the vapour phase of the rectifier and in regenerative heat transfer units were the dominant over that in other components. The losses of these components represented about 30% of thermal energy input. Therefore, these units controlled the main losses of the entire system and its performance. Chua, et.al [71], recommended for further developments in cycles' components modelling which included the pressure losses.

The study of Adewusi, and Zubair, [72] used second law analysis to investigate the performance of single-stage and two-stage ammonia–water absorption refrigeration systems. They studied the changes in the values of entropy and coefficient of performance. They used software termed "Engineering Equation Solver" to calculate the thermodynamic properties of the working fluids. Their results showed the following points:

(i) Among both systems components, entropy change of the two-stage absorption chillers' generator was the dominant on the total entropy change. As a result, the total entropy generated by two-stage absorption chillers was greater than that generated by single absorption chillers. This was due to the increase of irreversibility in the generator when more than one stage was used. Conversely, the COP of the two-stage absorption chillers

was greater than that for single absorption chillers. Therefore, the two-stage absorption chillers system was less efficient exergetically but more efficient thermodynamically.

(ii) Consequentially, further investigation was required to understand the contradiction between the values of thermal and exergitical observations.

Single stage ammonia absorption system for gas turbine was investigated by the study of Yang, et al., [73]. In such configuration, the waste heat from the gas turbine engine was used to power the chillers which in turn augment the power output from gas turbine. Yang, et al., [73] considered different values and ranges for the operating parameters including: (1) ambient temperatures between (0 and 45 °C), (2) gases temperature at turbine inlet (TIT) of (750 °C), (3) a minimum difference between the temperature of the gases at stack and at gas turbine exhaust of (5°C). They confirmed the increase of the gas turbine performance characteristics by the drop of the air temperature at compressor inlet. Such increase in either the efficiency or the power output was reduced by the escalation of ambient temperature, which required larger pressure ratio. The maximum thermal efficiency and the maximum specific power output was greater than those for conventional regenerative gas cycle. Such performance was guaranteed by increasing in the effectiveness of the regenerator and selecting the right temperature of evaporation with respect to the ambient temperature.

Gas turbine power augmentation by inlet air cooling was developed by Ondryas, et al., [74]. He showed the superiority of such process during summer peak hours. As in the previous studies, absorption chillers were used to generate low air temperature at the compressor inlet. The heat from the gas turbine exhaust was used to operate the absorption chillers system. While the electrical chillers system was used for further drop in the temperature of the air at compressor inlet. He investigated the effect of such gas turbine configuration on the performance of the cogeneration cycle and concluded that, during the periods of high ambient temperature, the inlet air cooling was an effective method to boost the power output of such configuration.

The work of Najjar [75] focused on the performance of inlet-air-cooled gas turbine. An aqua-ammonia absorption chillers system was used to cool the air at compressor inlet. The heat from the gas turbine exhaust gases was used to drive such system. Najjar studied such system's effect on the performance of both the gas turbine cycle and the combined cycle. He evaluated each cycle regarding its performance characteristics, which involved the power output, the thermal efficiency, and the specific fuel consumption. He compared the results with the results for the simple gas turbine cycle for various compression ratios and ambient

temperatures. The temperature of the gases at turbine inlet was kept (1027 °C). Najjar's study showed that, the inlet-air-cooled combined cycle was a viable configuration. The following points can also be concluded from his work:

(i) The power output of the cooled gas turbine was significantly increased due to the rise of the density which increased the mass flow. The thermal efficiency and the fuel consumption were increased slightly. Accordingly, the amount of the combustion gases was increased, while the NO_x emissions were reduced. Although, the increase of the ambient temperature was slight on the thermal efficiency and the specific fuel consumption, it increased the augmentation of the power output.

(ii) The inlet-air-cooled combined cycle had a better performance than the simple gas turbine cycle. The power output and thermal efficiency were greater by 21% and 38%, respectively. While the drop of specific fuel consumption was by 28%. The configuration performance was less sensitive to the operating parameters than the gas turbine.

Inlet-air-cooling for combined cogeneration cycle was investigated by Sigler, et al., [76]. They used commercial software to obtain the results, which considered gases temperature at turbine outlet and exhaust of (105 °C) and (75 °C), respectively. The cooling system was a single absorption chillers system, which was powered by the heat of the waste gases from the H.R.S.G. They compared the performance of the simple gas turbine/triple pressure steam turbine combined cycle and the inlet-air-cooled gas turbine/dual pressure steam turbine combined cycle. They perceive the need for further optimizations for inlet-air-cooled gas turbine/triple pressure steam turbine combined cycle that use inlet absorption chillers system. Their results confirmed the following points:

(i) Inlet-air cooled combined cycle was superior in power generation during the periods of high ambient temperatures. However, it did not increase the thermal efficiency due to the increase of the fuel consumption.

(ii) Absorption chillers system was more superior to improve the performance of the power cycles by inlet-air-cooling than evaporative and fogging systems. It was more viable and did not require equipment's upgrades as for the other technologies.

(iii) The performance of the absorption system was not affected by the change of the wet bulb temperature. However, it was affected by the increase of the ambient air temperature over 35 °C, which was difficult to be dropped to 5 °C.

The performances of simple gas turbine and combined cycle power plants were studied by Khaledi, et al., [77]. They focused on the impact of the atmospheric conditions on the inlet-air-cooled gas turbine/dual pressure steam turbine combined cycle. An absorption chillers system was used for air cooling at the compressor inlet. They developed in-house computer codes to model the performance of power cycles and absorption chillers. Their investigation included using two kinds of heat sources for the absorption system: (1) an internal source, which reduced the power output and (2) an external, which had no effect on thermal efficiency but improved the power output. Their results showed a good degree of agreement between the computed data and the data from manufacturers. The main conclusions were summarized by the following points:

(i) The performance of the gas turbine cycle depended on the temperature of the air at the compressor's inlet. The power output from this configuration was more affected than the thermal efficiency by such parameter.

(ii) Although the performance of gas turbine was augmented by fogging, such systems cannot be used in humid and hot climates. The absorption refrigeration system fully controlled the temperature of the air at the compressor inlet, thus it efficiently governed gas turbine's power generation.

(iii) Gas turbine inlet air cooling decreased the power output of the steam turbine. This reduction occurred, mainly, because of the increase in the steam pressure in the condenser.

(iv) The power output and the efficiency of the gas turbine were increased by inlet air cooling. The external system configuration performance had a greater increase than the internal configuration.

(v) When the internal system was used for the combined cycle, the efficiency was decreased and the power output was increased. However, when the external system was utilized for the combined cycle, the power output was increased, but the thermal efficiency remained unchanged.

Various types of inlet-air-cooling technologies were investigated by Brown, et al. [78]. These include (1) evaporative cooling, (2) refrigeration chillers with cooling storage units for various types of storage systems and (3) refrigeration chillers without cooling storage units. They identified the potentials of these technologies in dropping the air temperature from a range between (4 and 7 °C) to a temperature of (-18 °C). They also investigated the impact of

such reduction on the performance of different power cycles for various operating schedules and climates. Their comprehensive study evaluated and discussed 3500 different cases with respect to cycle's performances and concluded the following:

(i) Inlet-air-cooled power cycles were competitive to conventional cycles in performance.

(ii) The performance of ammonia compression chillers with weakly ice storage was the best choice. The combined cooling configurations were viable, but not over the ammonia compression systems for 24 hours operating periods. However, the performances of both systems were more desirable than the lithium bromide absorption chillers.

(iii) Power augmentation by cooling the air to a temperature below freezing was more valuable than cooling the air to a temperature above freezing.

(iv) Further investigation was required to cool the air to a temperature close to -17 °C. More work was also needed to investigate the possibilities in preventing or minimizing the icing. While more developments were required on: (1) computer modelling of the compressor inlet air cooling, (2) the use of multiple evaporation temperatures and (3) the viable requirements of cooling during peak load periods.

The work of Lucia, et al., [79] compared four kinds of inlet-air-cooling systems. Each system was employed for a cogeneration power plant, which comprised of a simple gas cycle and a simple steam cycle. Their study was carried out with regard to the conditions of two different sites. The cooling systems were: (1) one stage absorption chillers, (2) two stage absorption chillers, (3) evaporative cooling system and (4) an integrated system of evaporative cooling and two stages absorption chillers. The results considered yearly operation intervals and concluded:

(i) The yearly results confirmed the advantages from utilizing inlet air cooling system for gas turbine power augmentation.

(ii) The power output from the two staged absorption chillers' inlet-air cooled gas turbines was increased by range from (5%) to (10%). This was increased to (18%) during hot months of the year. While relatively, there was a slighter augmentation in the power output for the one stage absorption configuration.

(iii) The one stage absorption chillers system was powered by a steam at a pressure of 2.5 bars. This pressure was lower by 5.5 bars than the pressure required for the two stages

system. The single stage system also required 67% of the cooling water that was required by the two stage system for condensation.

(iv) The absorption systems were more suitable to operate with wider range of ambient temperature and higher temperatures than the evaporative cooling system.

(v) The integrated system used the two stage absorption system during high ambient temperature period and the evaporative cooling system with low ambient temperature. Therefore, the power output from the integrated inlet air-cooled gas turbine had the best performance.

The inlet-air-cooled for small to medium size gas turbines were tested by Erickson, et al., [80], who considered: (1) evaporative cooling, (2) mechanical vapour compression refrigeration, (3) Lithium Bromide waste heat absorption refrigeration system and (4) Aqua ammonia waste heat absorption refrigeration system. Their study discussed each system and compared system's performances, benefits and operation limits for warm climates operation. Each system was used to cool the air from a temperature of (35 to 5 °C), except the Lithium Bromide system. In such system the temperature was to be dropped to (10 °C) to avoid an essential increase in the costs. The comparison considered the effect of the operating parameters on the power output, the usage of heat source and the fuel requirement. They focused on the advantages from utilizing the fourth option for six different operating sites. The results for the sites were compared with reference to the level of CO_2 emissions, the fuel savings, the fuel increase, and the marginal efficiency. Their results showed the following:

(i) Ammonia absorption system had the maximum increase of the power output which was 19% of the total generated power. This was greater than the power generated by Lithium Bromide absorption system configuration by 20%, greater than the power generated the mechanical compression refrigeration system configuration by 25% and 60%-300% greater than the power generated by the evaporative cooling systems.

(ii) The heat recovery by aqua ammonia absorption system was increased by 9.9%. This amount was greater than the increase of the heat recovered by Lithium Bromide absorption system by approximately 27%. It was also twice the increase of the heat recovered by the mechanical compression refrigeration systems. Similarly, it was greater by 65%-400% than the heat recovery by evaporative cooling systems.

(iii) Ammonia refrigeration systems was managed to drop the temperature of the air at compressor inlet from 35°C to 5°C. This was correspondent to an increase of the power

output and the efficiency by 22% and 9% respectively. In addition, the drop of the combustion temperature reduced the NO_x emissions. Hence, better performance was guaranteed at warmer climates in addition to the increase of the fuel savings which also caused the drop of the CO_2 emissions.

A typical meteorological year (TMY) data was used by Dawoud, et al. [81] to evaluate several inlet air cooling techniques for the gas-turbine power plants. Their study considered: (1) evaporative cooling, (2) fogging cooling, (3) chilling systems with lithium bromide –water and aqua-ammonia absorption cooling and (4) vapour-compression refrigerated cooling system. They also compared their effects on the power augmentation of small-size gas-turbine power plants. In his study they considered: (1) monthly power augmentation, (2) monthly maximum peak power and (3) annual progression in power generation. They concluded the following:

(i) The annual augmentation of the power was increased progressively starting by the evaporative cooling and ending by the refrigerated cooling.

(ii) According to annual results, the ammonia-water absorption refrigeration was superior to other systems such that its power augmentation was ranged from 39% to 46% greater than the lithium bromide absorption chillers configuration. This amount was greater than fogging cooling configurations by 95%-126%. While it was greater than the augmentation that was made by evaporative cooling configurations by a range between 117% -152%.

3.3 The observations from the studies in literature review

This section comprises a summary of the main observations and conclusions from literature review detailed above. These observations motivated the current work which is detailed in the following chapters. They are divided to nine sections each represented a specific region of research in review and detailed in Sections 3.3.1-3.3.9. A very brief summary of the review is also provided in Table 3.1.

General Field	Study details	Authors/Reference	The main detected findings
3.2.1 Energy and exergy analysis for gas turbine power cycle	Employed thermodynamic analyses to investigate the performance of the gas turbine cycle individually	EL-Hadik [6], Guha [7], Razak [8], and Saravanamuttoo, et al. [9]	• The ambient temperature made a great influence on GTC performance. • The optimum pressure ratio for the maximum efficiency increased by the increase of the specific heat of the air and the increase of the fuel mass flow but dropped slightly by combustion pressure losses. • Water injection increased the power and CO and CO2 emissions and reduced the thermal efficiency and NOx emissions. Such impacts are greater by the drop of the ambient temperature. • Among different inlet air-cooling technology, the greatest power augmentation is by chilling systems. This is restricted by the atmospheric conditions of the operation site.
	Detailed study of promoted gas turbine cycles	Horlock, [13], Korobitsyn [11], Razak [8], and Saravanamuttoo, et al. [9]	• The performance of CCPP was more efficient than standalone individual cycles. It was improved by (1) the increase of combustion temperature, (2) the minimization of HRSG irreversibility and (3) the minimization of the heat losses between cycles. But it was limited by input and the output parameters. • The bottoming cycle usually compensated the insufficiencies of a topping cycle.

Table 3.1 The bibliography of the studies undertaken by this literature review

	Considered gas turbine cycle as a part of combined cycle power plants as	Horlock [12], [13]and [14]	• The mathematical predictions provided a guidance to choose the optimum parameters to compare it with complex designs in practice. The variations of predicted CCPP characteristics are due to the assumptions rather than the approach. These characteristics are dominated by the GT parameters, except for recuperation or feed heated ST. • The efficiency of a CCPP is increased by series mode not by parallel mode. • Supplementary firing increased CCPP power output but not probably the thermal efficiency which is controlled by the firing temperature and the percentage of air excess in turbine discharge gases. • The optimum rAC for the CCPP is between rAC corresponded to the maximum work output and the maximum efficiency. It also dominated by the CPg dominates the SG cycle maximum efficiency. The optimum conditions were essentially influenced by steam injection into the air flow.
	Investigated the performance of combined cycles over operating power plants.	Khaliq, and Kaushik, [15], and Ameri et al., [16]	• The CC has the lowest exergy efficiency among GT main components. The HRSG has second major exergy loss is for the HRSG. Externally fired HRSG improved CCPP power generation but reduced its thermal and the exergy efficiencies.

Table 3.1 The bibliography of the studies undertaken by this literature review-(cont.)

	The influence of different operating parameters of optimized Gas cycle on gas cycle individually and under combined cycle configurations	Briesch, et al., [17], Al-Hamdan, [18], and Polyzakis, et al. [19]	• The Enhancing CCPP to an efficiency of 60% was feasible by: improving the operating process parameters for GT and ST, increasing TIT to 1427°C, employing advanced cooled GT, providing further integration between the GT and ST. • The CCPP optimum parameters for the maximum thermal efficiency and specific power output are not the same as those for GTC. • The operating parameters for maximum thermal efficiency and specific work output are different. These were closer to GTC specific work output parameters. • RehGT is viable for CCPP if it had a great augmentation in specific work output.
3.2.2 Parametric studies and optimizations of combined cycle over gas/steam power plants	Optimized steam bottoming cycles were tested analytically under the consideration of the combined cycle power plant	Bolland, [21], Kehlhofer et al. [22], Dincer, and AL-Muslim, [23], Topolski, and Badur, [24], Al-Qur'an, [25], Xiang, and Cheng, [26]	• A CCPP is more efficient than a GC and RehGC with optimized pressure ratio and turbine inlet and outlet temperatures. It also operates on wider efficiency range for a certain power output. Its performance was improved by (1) increasing steam evaporation temperature, (2) reducing of the steam condensation pressure (3) within the right pressure ratio. Such performance was restricted by steam dryness fraction and pressure ratio. • The CCPP performance was also improved by optimizing the HRSG through an optimized heat exchangers arrangement with the reasonable boiler pressure. While a further increase in the efficiency was achieved by recuperation in GC.

Table 3.1 The bibliography of the studies undertaken by this literature review-(cont.)

			• For a certain gases temperature at turbine inlet, the pressure ratio controlled GT exhaust gases temperature. The increase in such temperature for a certain live steam pressure reduced steam generation. Such temperature increased the SC efficiency beyond 590 °C. • The RehGSSCC had the similar tendencies to conventional CCPP in thermal efficiency and specific work output but of higher values. Among different SC configurations, the supercritical TPRehSCC achieved the optimum efficiency and power output. While a TPSCC had a lower exhaust gases temperature than DPRehSCC.
	The optimization of steam bottoming cycle and HRSG through non-conventional procedure	Casarosa, and Franco, [27]& [28], Franco, and Russo [29], and Casarosa, et al. [30]	• A thermal Efficiency close to 60% for the CCPP was attained by the optimizing HRSG and steam cycle parameters. This became 60% by multi streams and critical steam conditions at turbine inlet and over 60% by when GT was optimized. This appeared for RegGTCC with optimized HRSG and with RehRegGT, which was about 65%, While further increase in the efficiency was provided by inter-cooling. • The heat required for steam generation was reduced by (HRSG) optimization, thus more heat was available for GT recuperation. • Power augmentation in SC was restricted by the gas to steam ratio, which was increased by optimizing CCPP performance.

Table 3.1 The bibliography of the studies undertaken by this literature review-(cont.)

			• Increasing the live pressure of the steam for a fixed gases temperature at the HRSG inlet assured closer steam conditions to critical at turbine inlet. • Separating the thermo-economic aspects from thermodynamic aspects of (HRSG) was successful.
	Several studies contain the use of steam in gas turbine system for cooling the blade under higher operating temperatures.	Bassily [31], [32], and [33]	• Although it improved the performance, upgrading the DP HRSG to TP HRSG narrowed the range of pinch point's temperature differences for the intermediate pressure, hence, the optimum efficiency. The DPST in a CC had a maximum 2% greater efficiency than the conventional CCPP, which increased more by exhaust gases recuperation. • The optimized CCPP operated on greater compression ratio and minor values of steam pressure and temperature. The optimum performance of multi pressure SC in a CC was correspondent to: (1) the maximum temperature of the gases at the turbine inlet, (2) the maximum steam pressure and temperature at the turbine inlet and (3) the minimum steam mass flow injected to the GT. • The performance characteristics of CCPP were improved by reducing HRSG irreversibility, although, an optimized HRSG provided more efficient performance. The effective parameters on its performance were: (1) steam dryness at the turbine outlet, (2) steam approach temperature difference and (3) minimum pinch point temperatures differences.

Table 3.1 The bibliography of the studies undertaken by this literature review-(cont.)

			• RehRegG/TPRehSCC was the most promising configurations, while more research was required to: reduce the AC work, for efficient use of the waste heat, for fully optimized GC and to model and to optimize the TPRehST engine for the CCPP and on its reduced irreversibility HRSG.
	Used degradation of gas and steam cycle to obtain their influence on the performance of combined cycle	Zwebek, et al. [34], [35]and [36]	• The performance of CCPP was more sensitive to GC deteriorations than SC, while combining the degradations of both cycles had almost linearly deteriorated CCPP. It was affected dominantly by the GT isentropic efficiency and significantly by the GC isentropic efficiencies combined with mass flow rate and ST isentropic efficiency. • The efficiency, the power output and the exhaust gases' temperature from GC were enormously affected by the degradation of AC and GT isentropic efficiencies as a combined parameter. The GC components' degradation dominated HRSG efficiency rather than other SC components. The temperature of stack gases was extremely depended on the AC and GT isentropic efficiencies and the mass flow rate over any other parameter. • ST output was severely affected by AC and GT isentropic efficacies. While SC efficiency, steam generation and HRSG isentropic efficiencies were heavily affected by GT faults than AC. The power output and the efficiency of the SC were heavily affected by ST deterioration followed by HRSG degradation. Condenser deteriorations had the minimum impact on SC and CCPP performance.

Table 3.1 The bibliography of the studies undertaken by this literature review-(cont.)

3.2.3 Energy and exergy analysis, and parametric studies of gas/ammonia-water combined cycle power plants	Identified the main operating parameters for Kalina cycle. Different types of Kalina cycles studied and compared computer model optimization.	Marston, [39], [40], Micak, [37], and Zhang et al. [38]	• The CC of a complex Kalina had a superiorly better performance than the simple Kalina CCPP. • Manipulating the mass flow rate an ammonia fraction cycle's performance can further be optimized for more efficient energy generation by multi stream heat exchangers. • lack of experience about the ammonia-water mixture • Kalina cycles' performance was influenced by: (1) gases pressure and temperature at turbine inlet; (2) gases pressure at turbine outlet; (3) mixture concentrations and the basic solution and; (4) the multiplication ratio.
	Included second law of thermodynamics in their investigations.	Hanliang et al. [46], Kalina and Tribus [44]& [45], Srinivas et al. [43]	• Mixtures' conditions at turbine inlet dominate the optimum performance than other parameters. • The KCS8D3 Kalina cycle had better performance characteristics than steam cycle and its CCPP had also better performances Conventional CCPP. While the thermal efficiency of Brayton/Kalina is greater than the efficiency of the Brayton /dual pressure Rankine CCPP. • An exergy efficiency of 70% is attainable regular KC which turned into 78.7% and 80.7% by KCS6- D3 and KCS8D3 respectively.

Table 3.1 The bibliography of the studies undertaken by this literature review-(cont.)

	Compared the results with the conventional combined cycle.	Marston and Hyre, [42], and Srinivas, et al., [43]	• Kalina cycles generated more power output than steam cycle. Kalina CCPP had greater power output than conventional CC by about 2% in single cycle and 11.6% in triple cycle. • The thermal efficiency of the combined Brayton/Kalina cycles was greater the thermal efficiency of the combined Brayton/Rankine cycle by about 0.36% in single stage KC and 1.95% in triple KC. • The CCPP's exergy efficiency was increased significantly by utilizing ammonia concentration of up to 0.7 at turbine inlet and was not affected by separators' AWM temperature. It was also increased by the increase AWM pressure at turbine inlet. However, it decreased by the increase of ambient temperature and both the ammonia concentration and AWM temperature at the turbine inlet. • The ambient conditions and the mixture's concentrations at turbine inlet had the greatest effect on the exergy efficiency of the Kalina and the CCPP.
	Compared Maloney and Robertson and Kalina cycles.	Ibrahim, and Klein, [41]	• Maloney and Robertson cycle's performance was not better than the performance of the KC when the thermal capacitance ratio is over 5. • Mixture's utilization in heat addition and heat rejection gave more flexibility to power cycle design and reduced the thermodynamic irreversibility and pinch point temperature difference.

Table 3.1 The bibliography of the studies undertaken by this literature review-(cont.)

3.2.4 Cycles with triple combination for power generation	Classical triple combination cycles.	Murugan and Subbarao [56]	• A saturated steam temperature with a pressure just above the atmosphere was adequate for heat recovery by AWM. Therefore, it is more useful in KC CCPP than RC. • The efficiency was increased with the increase of the ammonia mass fractions at evaporator inlet to up to 0.8455. The thermal efficiency was dropped with further increase although the increase in the power output. • The power output and the thermal efficiency of KC in a CCPP are better than both of optimized Rankine CCPP.
	Advanced designs triple combination cycles.	Amano, et al. [50], [51], and [52], Tomizawa, et al. [53], and Takeshita et al., [54] and [55]	• The wise AWM basic composition and the sensible variation in steam heat boosted the power output over that generated from a constant composition cycle. A composition of 0.6 kg/kg matches both the simulation and the experimental data. While only 46% from the steam heat was required to power the KC. • The ACGS CCPP had better performance than the conventional CCPP performance, which more likely during Spring/Autumn mode. In which the proper AWM temperature at the second separator with reflux loop was combined with the right steam and AWM velocities and AWM basic composition at evaporator and LP condenser respectively.

Table 3.1 The bibliography of the studies undertaken by this literature review-(cont.)

			• The augmentation of work output by (W-MTS) cycle, required higher heat source temperature and generated more work output than both its systems individually. • Each interval during the night had its own characteristics of the heat transfer in an ice storage system and governs the area and the mass of the ice storage.
	Triple combination with Rnakine ammonia-water bottoming cycle.	Marrero, et al. [49]	• Combustion chamber irreversibility was the greatest among cycles' components. It was governed by the temperature of the gases at turbine inlet and the mass flow of steam injected into the combustion chamber. • The thermal match between HRSG streams was increased by employing the ammonia bottoming cycle. A triple combination cycle was likely to operate on 60% thermal efficiency in modern GTC, and improved by optimization.
3.2.5 Partial oxidation combustion to enhance the performance of gas cycle and the chemical gas turbine configurations	Partial oxidation in gas turbines, and different configurations of chemical gas turbine.	Yamamoto, et al., [67], [62], [58], Kobayashi, et al. [63], Korobitsyn, et, al. [11] and [64], Lior, et al., [57], Abdel-Rahim and Mohamed, [65] and [66]	• The POGC had minor efficiency than SGC and RecGC, but better than RehGC. It's recuperated configuration had the best efficiency. Its specific work output was greater than SGC and below RehGC and RecGC. Its exhaust temperature is below RehGC and higher than RecGC. • The performance of ChGT had better performance than conventional CCPP by better thermal and exergy efficiencies and power output, lower NOx emissions and smaller HRSG size.

Table 3.1 The bibliography of the studies undertaken by this literature review-(cont.)

			• The ChGT main affecting parameters on its performance were; (1) the air mass fraction, (2) the fuel to air ratio, (3) compressor, turbine and HRSG efficiencies, (4) isentropic temperature ratio, (5) the equivalence ratios of lean combustion, (6) the equivalence ratios of rich combustion and (7) turbine's inlet temperature.
3.2.6 Enhancing the performance of gas cycle by compressor inlet air cooling using ammonia-water absorption chillers	Absorption chillers as a refrigeration system	Horuz, [68], Goodheart, [69], Fernandez-Seara, and Vazquez [70], Chua, et al., [71], and Adewusi, and Zubair, [72]	• Ammonia-water systems were not limited by crystallization and used in large industrial applications. It insured much lower air temperatures using lower temperature source than lithium bromide-water system. • Single absorption system provided cheaper refrigeration capacity than the half-effect cycle from the same firing temperature. The half-effect performance is better for a temperature below such range. The two-stage absorption chillers was less efficient exergetically but more efficient thermodynamically. • The best way to design low temperature heat sources single absorption system was by investigating the heat-exchanging areas of all its components. Further developments in cycles' components modelling included pressure losses. • The optimum generation temperature was dependent on the amount of cooling water and the temperature of the evaporation process. • The rectifier and in regenerative heat transfer units controlled the main losses of the entire system and its performance.

Table 3.1 The bibliography of the studies undertaken by this literature review-(cont.)

	The performance of ammonia-water absorption chillers as an inlet air cooling system.	Yang, et al., [73], Ondryas, et al., [74], Najjar [75], Sigler, et al., [76] , and Khaledi, et al., [77]	• The power output of a cooled GTC was significantly increased, the thermal efficiency and the fuel consumption were slightly increased and NOx emissions were reduced. Its performance was less sensitive to GC operating parameters. It had greater maximum characteristics than RegGC. • Absorption chillers systems were better for GTC inlet-air-cooling than evaporative and fogging systems. It fully controlled AC inlet air temperature, thus efficiently governed GT power output. It was independent of wet bulb temperature, but affected by an ambient temperature over 35 °C. • For CCPP, inlet air cooling decreased ST power output but was superior for power generation during high ambient temperatures. The efficiency did not increase by AWAC of an external source and decreased by an internal source.
	Comparisons between AWAC and other gas turbine inlet air cooling strategies.	Brown, et al., [78], Lucia, et al., [79], Erickson, et al., [80], Dawoud, et al., [81]	• The yearly results confirmed inlet air cooling system advantages for GTC power augmentation, which was greater by the AWACS and required lower heat source than other systems. It operates on a wider range of ambient temperature than other systems and of better performance at warmer climates. It was responsible for the drop of the combustion temperature, NO_X and CO_2 emissions and fuel savings. It was capable for GT power augmentation by cooling the air below freezing temperature.

Table 3.1 The bibliography of the studies undertaken by this literature review-(cont.)

			• The two staged absorption chillers provide more augmentation than single stage, but operate on a higher pressure and require fewer amounts of cooling water in condensation. • The integrated system of the two stage absorption - evaporative cooling system had the best performance in the power output from inlet air-cooled GTC. • The performance of ammonia compression chillers with weakly ice storage was viable, but not over 24 hours operating periods.

Table 3.1 The bibliography of the studies undertaken by this literature review-(cont.)

3.3.1 Observations from combining two power cycles in a thermal power plant:

The deteriorations in the performance of the upper (Brayton) cycle were usually turned into the advantage of the bottoming (Rankine) cycle. Therefore, the combined cycle power plant is more efficient than a single cycle power plant. This prospect was significantly utilized in series combination configurations rather than parallel in which it regularly had an efficiency drop. However, the combination between different cycles is, in its entirely governed by the operation requirements and the anticipated outputs of the power plant. These parameters like the performance characteristics of an optimized combined cycle are often to have different values in different studies. Such variations are in general due to the assumptions rather than the approach.

3.3.2 Observations regarding the performance of gas turbine cycles:

Ambient conditions have a great effect on the performance of gas turbine cycle, among which the ambient temperature has most of such effect. Such influence increases with the increase of engines' turbine inlet temperature and pressure ratio. For a gas turbine of high turbine inlet temperature, the increase of the ambient temperature decreases its thermal efficiency and specific work output.

The optimum pressure ratio for maximum specific work output and that for maximum thermal efficiency are always greater than the pressure ratios of the air standard cycle. Pressure losses reduce these characteristics, thus in order to attain the maximum specific work output, the optimum pressure ratio has to increase. In order to attain the maximum efficiency, the optimum pressure ratio needs to change slightly. For a constant gases temperature at turbine inlet, the increase of the pressure ratio reduces the temperature of the gases at the gas turbine exhaust. The heat losses from combustion chamber are greater than the losses of any other component of the gas turbine engine. The specific heat of the combusted gases controls the maximum thermal efficiency and the optimum pressure ratio of simple gas turbine cycle. It has the same great effect on the specific work output of combined cycle, but such effect is smaller on the optimum parameters. The isentropic efficiencies of the compressor and the turbine as an individual parameter had an enormous effect on the temperature of the exhaust gases, the thermal efficiency and the power output of the gas turbine cycle.

3.3.3 The observations over cooled gas turbine engines

Cooling the gas turbine drops its thermal efficiency slightly, which appears to be minor for high combustion temperature gas turbine engines. Thus, the maximum efficiency such gas turbine cycle certainly does not correspond to an engine of a high temperature gases at its turbine inlet. Although, several promoted steam injected gas turbine engines are competitive in performance to the conventional designs. Furthermore, applying regeneration and inter-cooling to such configuration increases its thermal efficiency over that for the conventional design but operates with larger pressure ratio. While it requires an essentially greater pressure ratio to attain further increase of thermal efficiency for more complex designs of cooled gas turbine combined cycle. In addition, injecting the steam into combustor makes a great change to the optimum parameters of the gas turbine engine due to the increase in the mass flow rate.

3.3.4 The observations over gas turbine cycle effect on the performance of combined cycle power plant:

The overall efficiency of CCPP is greater than that for GTPP if it operates with the same optimum pressure ratio. While its optimum pressure ratio corresponded between that indicates the maximum work output and that indicates the maximum thermal efficiency. The thermal efficiency of the combined cycle does not affect by the same parameters that affect the thermal efficiency of gas turbine cycle. Usually these parameters are closer to those affecting specific work output parameters. The operating parameters of gas turbine cycle significantly controlled the performance characteristics of the combined power cycle if there was no gas recuperation in the gas turbine engine or steam feed heating in the steam turbine engine. Among different operating parameters, the specific work output of the gas turbine engine makes had a superior effect on the performance of the combined cycle power plant.

The increase of the specific work output of the simple combined cycle does not probably correspond to an increase of the thermal efficiency. It is restricted by a certain pressure ratio beyond which any increase in the specific work was combined with an efficiency drop. For a certain pressure ratio, increasing the temperature of the gases at the turbine inlet increases the thermal efficiency of the combined cycle power plant. The magnitude of such increase corresponds to how great is such difference between the temperatures of the gases at the turbine inlet. In regenerated gas turbine cycles, increasing the air temperature before combustion reduces the fuel mass required to attain the desired temperature of the gases at

turbine inlet. This process increases the efficiency of gas turbine cycle and the efficiency of the combined cycle.

The heat addition of the reheated gas turbine cycle is very close to the isothermal process. Thus, it improves the performance of gas turbine cycle. The values of the operating parameters for maximum performance characteristics are different from those for simple gas turbine cycle. Reheated gas turbine engine does not meet its design point unless it discharges low temperature gases or it had a great augmentation in the specific work output. For combined cycles, the high temperature gases at turbine output increased the thermal efficiency of the steam cycle. Therefore, in both situations, the performance of the combined power cycle was optimized.

The optimum pressure ratio for maximum efficiency of the reheated gas cycle was greater than that for simple gas turbine cycle. Inter-cooling the gas turbine engine increased the efficiency of combined cycle and had a slight effect on its specific work output. Novel gas turbine power plants may operate on a clean and high performance over the simple gas turbine cycle power plant but its thermal efficiency cannot reach that for conventional combined cycle power plant.

3.3.5 The observations about the effect of (HRSG) and steam cycle on the combined cycle performance

The isentropic efficiencies of the compressor and turbine as a single (combined) parameter had the greatest effect on specific work output of the steam turbine. The deficiencies of compressor had the greatest effect on: (1) the efficiency of the steam cycle, (2) the isentropic efficiency of (HRSG) and (3) the steam generation in the (HRSG).

The thermal and exergy efficiencies of conventional combined cycle increase by the increase of the temperature at which the boiler operates. This temperature may restrict the viability of the conventional combined cycle with no feed heating. Therefore, for some cases, enhancing the combined cycle power plant by a regenerated steam system decreased its thermal efficiency. If so, a preheat loop using the exhaust gases to heat the water to ensure a performance of an efficiency better than that for regenerated steam turbine combined cycles. Such efficiency also increases by the decrease of the pressure of condensation, but the quality of steam at turbine outlet roles such increase. While it decreases if the steam mass flow is greater than a certain amount thatsregenerated.

Feed heating and a preheating loop systems may be substantially required to improve the performance for the dual pressure steam combined cycle power plant that used sulphur fuel. The efficiency of combined cycle was increased by utilizing multi pressure steam turbine bottoming cycles. Such increase wasn't feasible for systems of more than three pressure levels. Further increase in the performance characteristics of such combined cycle power plants was attained by utilizing supercritical steam and reheat strategies.

The losses from the (HRSG) represent the second major exergy losses among the other combined cycle components' losses. Therefore, its optimization makes a magnificent impact on raising the exergy efficiency of the combined cycle. Accordingly, by doing so, the heat required for steam generation is reduced. Therefore, more heat is engaged to power the gas turbine cycle. As a result, the combined cycle can operate with an efficiency of about 60% by optimizing the HRSG and steam turbine cycle parameters. While, further increase in the performance parameters of the combined cycle power plants requires upgrading the gas turbine engine. Gases of a temperature beyond (827 ºC) at the reheated turbine inlet show no valuable increase of the thermal efficiency over conventional combined cycle.

The feasibility of supplementary firing in the combined cycle appears only with a significant increase in thermal efficiency of steam bottoming cycle. Otherwise, the use of supplementary firing results in lower efficiency, although the increase in the work output of combined power cycle. The amount of supplemented fuel restricts the performance of the combined power cycle because the increase in fuel addition does not join higher efficiency due to the constant rate of air excess in gas exhaust. The advantages from supplementary firing in steam bottoming cycles are not manifested at high degrees of turbine inlet temperature.

3.3.6 Observations on the performance of (gas turbine /ammonia-water turbine combined cycle power plant)

The performance of the bottoming cycle improves by utilizing ammonia-water turbine cycle rather than the steam turbine cycle. Its performance is superior in performance than power cycles with other mixtures and even than multi pressure steam turbine engines. The optimization in the performance of subsystems of the ammonia-water bottoming cycle increases its exergy and thermal efficiencies. It's caused by the reduction in the exergy losses of distillation/condensation processes and the improvements in the match between streams through regeneration.

The efficiencies of the ammonia-water cycle and the combined cycle are significantly affected by many parameters. Any increase in mixture's pressure at the turbine inlet raises the exergy efficiency. The increase of the ambient temperature and the temperature of the mixture at turbine inlet drops such efficiency. This also decreases by the increase of concentration of the ammonia at turbine inlet. The temperature of the separator has no effects on such efficiency in a combined cycle. To maintain a high efficiency, the kalina cycle is correspondent to an ammonia concentration beyond 70% of the mixture at the turbine inlet.

3.3.7 Observations over triple combination cycles power generation plants

Steam turbine bottoming cycles can not efficiently utilize the low heat quality steam. In contrast, ammonia-water turbine based on Kalina cycle is successfully powered by the heat from such steam. This configuration may require a steam only at saturation with a pressure just above atmosphere. This advantage is used effectively to optimize the performance of combined cycle using the waste heat from steam bottoming cycle. Usually, in such configurations the ammonia water systems recover the steam heat into power or refrigeration.

As a bottoming cycle, the performance characteristics of an ammonia-water turbine cycle are greater than the values for optimized condenser steam turbine cycles. This superiority in performance is due to the low exergy losses of ammonia-water cycles. Further increase in the power output observed when more harmony between ammonia-water compositions and the wise variation in steam heat rates. The interval and the site at which the plant operates affect these characteristics. In case of integrating both power and refrigeration as bottoming cycles, their output as a combined system is greater than that for both individually even with the same heat source.

3.3.8 Observations on upgrading partial oxidation to gas turbine cycle and combined cycle power plants

The use C/C composites allow utilizing high gases temperature at the turbine inlet of the partial oxidation gas turbine engines. Therefore, the increase of the thermal efficiency due to such temperature increase compensates its decrease due to the reduction in air the mass flow. It also decreases the exergy losses and NO_X emissions generated by such configuration. The increase of the temperature and the pressure of the gases at turbine inlet embraces further drop of such emission. However, partial oxidation gas turbine cycle generates less power than the reheated gas turbine cycle but with slightly greater efficiency. Such advantage occurs only if the turbine works with low rates of isentropic temperature ratio (T_{g3}/T_{g4}).

The chemical gas turbine cycle has better thermal and exergy efficiencies than the conventional combined cycle. It also has greater overall generated power, although, the reduction in its exhaust flow rates. Compressors' domination on its performance puts its characteristics closer to those of simple gas turbine cycle. In general, the performance of a chemical gas turbine cycle is controlled by: (1) the air fraction, (2) the fuel to air ratios, (3) the equivalence ratios (4) the pressure of rich fuel combustion, (5) the temperatures of the gases at turbines' inlets, (6) compressors and turbines' efficiencies, (7) HRSGs' efficiencies, (8) steam cycle's degree of optimization and (9) the pressure losses. These parameters differ in effects from a configuration to another.

The amount of NO_X emissions generated by chemical gas turbine exhaust is governed by the chemical composition and the temperature of combusted gases. These emissions reduce by the decrease in the air excess rather than drop of the combustion's temperatures. A drop in NO_X emissions is also obtained by the increase of the pressure at rich fuel combustion. These emissions rise by the increase in the temperature of the gases at turbine inlet for low equivalence ratio at lean fuel combustion. For a certain amount of heat recovery, the combined cycles based on chemical gas turbine requires smaller size of (HRSG) than the conventional combined cycle. Such size enlarges with the increase of the temperature of the gases at turbine inlet.

3.3.9 Observations over upgrading the gas turbine cycle and the combined cycle power plants by inlet-air-cooling systems

The decrease of the temperature of the air at compressor inlet increases the thermal efficiency and the specific work output of a gas turbine cycle power plant. Therefore, inlet air cooling strategy is a competitive approach to improve the performance and to reduce NO_X emissions of such power plant. It implies a great augmentation in the power output, but a small increase in the efficiency due to the increase of the fuel consumption. The competitive performance characteristics of an inlet air cooled gas turbine cycle improves with the increase of the ambient temperature. Therefore,it is usually synchronous is usually synchronousit is usually synchronousit is usually synchronouswith the periods of peak power demands. During such periods, the maximum performance characteristics are expected to be greater than what it is for conventional regenerative gas cycle. On the other hand,it requires the gas turbine to work on larger pressure ratios.

Waste heat inlet air cooling systems for combined power cycle increase its power output and thermal efficiency and drop its fuel consumption. This strategy is usually employed by one of the following systems: (1) evaporative cooling, (2) fogging, (3) mechanical vapour compression refrigeration and (4) absorption refrigeration by Ammonia or Lithium Bromide. Each system has its own method, requirements and operating medium and conditions at which it operates. Utilizing ammonia absorption systems provides more augmentation in the power output of the gas turbine engine than any other system. Its heat recovery is also greater than that of any other system. Therefore, it requires low temperature heat sources and works on a wide range of acceptable performance. Such performance isn't affected by wet bulb temperature and successfully operates over a wide range of atmospheric territorial conditions than fogging systems and with an approximate cost to evaporative cooling systems. Ammonia-water absorption refrigeration system enlarges the range of air temperature drop than other systems. Moreover, it provides more fuel savings. Therefore, it insures less of NO_X and CO_2 emissions. These advantages are greater at the times and places of warm climates.

Ammonia-water absorption refrigeration chillers system has different effects on the performance of each cycle of the combined power cycles. The type of heat sources has the greatest role on these effects. Using an external heat source increases the specific work output from both the steam and the gas turbines. The efficiency of gas cycle increases similarly, but combined cycle efficiency remains the same. Utilizing an internal heat source reduces the efficiency of the combined cycle. It also decreases the augmentation of the power output, which is governed by the number of the stages of such absorption system.

3.4 Recommendations from observations

1. During the periods of insufficient operation of the gas turbine cycles bottoming cycle's performance has a great effect on combined cycles' efficiency. This is the point of operation where more attention is required on optimizing the bottoming cycle parameters to improve the performance of the combined cycle power plant.

2. Any enhancement of a power cycle into the combination with another should meet operating requirements and fulfilling the desired outputs.

3. The difference in the values of the combined cycles' performance characteristics from one author to another is not a big deal when optimization, unless it comes up from an identical optimization process/approach.

4. The utilization of water or steam for gas turbine cooling is not appropriate to optimize its performance. In contrast, it can dramatically reduce turbine's efficiency.

5. The performance characteristics of a power plant improve by combining a bottoming cycle into the gas turbine cycle engine.

6. For a combined cycle power plant with no gas regeneration or steam feed heating, the attention should turn into gas turbine engine during optimization.

7. The maximum output parameters do not probably come with the optimum value of the same operating parameter.

8. Enhancing the gas turbines by using different systems changes the optimum values of the operating parameters. Although these enhancements usually involve further restriction in the parameters, it does not probably insure better performance characteristics.

9. As in reheated gas turbines, the design point of a combined power cycles is restricted by reaching the lowest turbine outlet temperature and by generating the greatest power output.

10. The optimization of the HRSG plays a great rule on optimizing the performance of the combined cycle, as its heat losses considered as cycles' second major losses. Accordingly advanced configurations assure a feasible improvement in performance. The viability of such optimization process by using multi pressure HRSG is limited by three pressure levels. For further optimization, the focus should turn to utilizing supercritical or reheated systems.

11. The temperature of stack gases does not probably drop by the optimization of the combined cycle power plant performance. Optimization is more related to the quality of the exhaust gases. Gas turbine parameters' optimization is the most controlling on the exhaust gases' temperature. Steam cycle parameters are not effective unless the steam cycle efficiency is considerably high.

12. Utilizing supplementary firing to improve the performance of the combined cycle power plant requires checking it feasibility by changing the parameters such as gas turbine inlet temperature (TIT) and the steam turbine isentropic efficiency (η_{st}).

13. Optimization for non-supercritical steam turbines as a bottoming cycle by the pressure of the steam at turbine inlet is restricted by the temperature of the gases at HRSG inlet.

14. The optimization processes on boiler's pressure range to improve CCPP performance is governed by the GT discharge gases at HRSG inlet. The increase of such temperature permits a suitable increase of steam live pressure, thus the steam turbine efficiency. Such increment is not valid for a certain temperature at the HRSG inlet.

15. The performance characteristics of a gas/ammonia combined cycle are greater than those of gas/multi pressure steam combined cycles.

16. A successful tool to optimize the performance of a gas\ammonia water combined cycle is by optimizing ammonia water cycles' sub systems. Therefore, the operating parameters of such cycle are more effective on the performance of the combined cycle.

17. The combined cycle power plant could be optimized by upgrading its conventional configuration with a third low heat powered system (for power generation or for cooling). In these systems, ammonia water is the most appropriate working fluid to recover the low heat from HRSG outlet gases. While some of these systems are capable of recover heat from the steam at the turbine outlet. It is better to optimize the performance characteristics of the combined cycle by such systems than optimizing the condenser of the steam cycle. Meeting the harmonic relation between the steam mass flow rate and ammonia concentrations can optimize such triple generation cycle configurations.

18. It is better for the performance of the triple power generation cycle with refrigeration to combine the bottoming systems in one configuration, were both are using the same working fluid.

19. It is important to bear in mind the effect of the sites and the operation intervals on the performance characteristics of the triple generation power cycle.

20. The smaller HRSG size of the ChGT than that for the conventional gas turbine opens the way forward further optimization in the HRSG to optimize the combined cycle that based on ChGT configuration.

21. Optimizing the ChGT towards less NO_x emission requires maintaining: (1) low air excess rather than low combustion temperature; (2) high pressure for the air at the rich combustor; (3) not a high combustion temperature for a very low equivalence ratio in

lean combustor; (4) controlled values of compositions and temperatures at the combustion.

22. The performance of the combined cycle is optimized by upgrading the conventional configuration into the chemical gas turbine (ChGT). Such upgrade insures an increase of the thermal efficiency and the exergitic efficiency and a reduction in the NO_x emissions.

23. Optimizing the combined cycle by upgrading reheated gas turbine cycle into POGT for better efficiency is restricted by the specific range of the isentropic temperature ratio.

24. The power of the reheated cycle is degraded if such upgrade is to be made.

25. The performance of the conventional combined cycle can be optimized by upgrading it with an inlet air cooling system to the gas turbine engine, unless such upgrade requires utilizing more fuel.

26. Improving the performance of the combined cycle by upgrading the inlet air cooling system into the gas turbine is better by utilizing ammonia water absorption chillers rather than any other systems. Such system is featured by: (1) Powered by a wide range of heat sources; (2) Functional over a wide range of atmospheric conditions with acceptable performance; (3) Does not require advanced equipment for construction; (4) Drops the exhaust gases temperature ; (5) Reduces the amount of the fuel required to power the system by supplementary fuel firing; (6) Reduces the amounts of the CO_2 and NO_x emissions by minimizing the fuel required to power the system.

27. A compromise between the waste heat usage between the bottoming cycles is required when inlet air cooling systems are used in gas turbines to maintain better performance characteristics. As an example, a steam turbine performance drops by using such system, which causes a drop in the efficiency and the power output of the entire combined cycle.

28. Optimizing CCPP by improving the performance of the steam cycle by optimizing the temperature of the steam at the boiler is restricted by the need for supplementary firing.

29. Optimizing the performance of the combined cycle by improving steam cycle performance characteristics by reducing the pressure of condensations is restricted by the quality of the steam at the turbine outlet.

30. Practically optimizing the combined cycle by improving its performance through increasing the pressure of the steam boiler requires controlling the temperature of the steam in the boiler.

31. The performance of the CCPP does not probably improve by optimizing the performance of the steam plant through regeneration configurations. Such optimization is governed by the temperature of the steam through the boiler.

CHAPTER 4
PARAMETRIC STUDY AND OPTIMIZATION

4.1 Introduction

An abundant number of researches on the design of gas and steam power plants were performed in the past two decades. In those studies, the performances of the power cycles were investigated focusing on the harmony between the performances of cycles' engine components. The performance of each component and that for the whole power cycle is affected by many parameters having varied degrees of influences. The studies confirmed the increase in the efficiency of gas cycle by the increase in the pressure ratios and turbine inlet temperature. It guaranties the increase in the power output and the thermal efficiency of a steam cycle by the increase in the temperature and the pressure of the steam at turbine inlet. Studying the operation of a power cycle starts from covering the effect of the above and many other parameters. The results recommend the points at which the cycles operate on design art performance. Investigating the effects of the operating parameters is usually made by employing a parametric study, which undertakes the impact of one parameter or more.

The design of gas and steam cycles as a part of combined cycle power plant differs from their design to work by their own. This is due to the changes in the mechanism and the amounts of the inputs of each cycle to maintain the desired performance. This chapter undertakes a parametric study to predict the change in performance characteristics of a combined power cycle and its design performance. Although the study calculates the thermal efficiencies for the gas and steam cycles, but those aren't considered as a criterion rather than the efficiency of the combined cycle. The operating parameters of a steam cycle as a part of the combined cycle are governed by the outputs from the gas cycle (i.e. the quality of the exhaust). Consequentially, the performance of the steam cycle and the combined cycle are significantly affected by the design of the heat recovery system between cycles.

The work in this chapter comprises three sections all are dedicated to study the performance different combined power cycle configurations. The thermodynamic considerations of the gas and steam cycles as a part of the combined cycle are illustrated in the first section. Microsoft Office Excel is used to accomplish the calculations and draw the results from the input data. The performance of 42 combined power cycle configurations is predicted including different gas turbines combined to different steam turbines in a varying degree of optimization. Specifically, it contains six gas turbines' configurations and seven steam turbines configurations.

The second section investigates the change in the performance of each configuration by the effect of following parameters: (a) the pressure ratio and the ratio of splits in pressure ratios when reheat and intercooled cycles, (b) compressor intake inlet temperature. (c) turbine inlet temperature, (d) steam to air ratio, and the fraction in steam mass flow rate multi pressure steam cycles, (e) the pressure of the steam at (HRSG), (f) the pressure of the steam during condensation, (g) the pressure of reheat in reheated steam cycles and (h) the minimum pinch point temperature difference. The results from the parametric study are discussed and the performances of the power cycles are evaluated in this section. It plots the effect of many parameters on the performance diagram of each cycle and discusses the relationships between those parameters. Conclusively, it indicates the optimum point of combined cycle performance for each configuration. It also studies the impact of such configurations on environment and gives the industrial recommendations to maintain best performance. Finally, it identifies the configurations with best performance and less impact on environment. The third section of this chapter associates the results and the conclusions from the parametric study. This section discovers the areas that have not optimized and that require further optimization. Therefore, the paths to conduct the future work are specified and the main approach for the next stage of study is established. This requires achieving a combined power cycle with better performance and generates less harm to the environment.

4.2 Thermodynamic consideration of the parametric study

This parametric study is undertaken by using the thermodynamic equations of both the gas turbine cycle and the steam turbine but firstly let's start with the supplementary fired steam turbine combination with the gas turbine.

4.2.1 Combining two power plants in series with supplementary firing:

The series combination between two power cycles the same heat input was employed to generate power from all cycles. Theoretically, the thermodynamic considerations of any two power plants combined in series were discussed in chapter two. In which the thermal efficiency of such cycle can be obtained by the equation (2.43). In reality, the heat transfer process can not be fully isolated from surroundings, thus, the heat loss appears as unused heat energy (Q_{un}). In order to compensate this loss more heat (Q_{sup}) may be added to the lower cycle via supplementary firing. Consequentially, the equation of efficiency of a combined cycle was modified to the following equation (4.1). Employing equations (2.46) in equation (4.1) generates equation (4.2). Using equation (2.48), the work generated by low cycle can be represented by equation (4.3).

$$\eta_{CCPP} = \frac{W_U + W_L}{Q_{inU} + Q_{sup}} \quad \ldots (4.1)$$

$$\eta_{CCPP} = \frac{\eta_U + \dfrac{W_L}{Q_{inU}}}{1 + \dfrac{Q_{sup}}{Q_{inU}}} \quad \ldots (4.2)$$

$$W_L = \eta_L Q_{inL} = \eta_L \left(Q_{sup} + Q_{outU} - Q_{un} \right) \quad \ldots (4.3)$$

Employing the equation above in equation (4.2) generates a new equation for the efficiency of combined power cycle equation (4.4).

$$\eta_{CCPP} = \frac{\eta_U + \eta_L \left(\dfrac{Q_{sup}}{Q_{inU}} + 1 - \eta_U - \dfrac{Q_{un}}{Q_{inU}} \right)}{\left(1 + \dfrac{Q_{sup}}{Q_{inU}} \right)} \quad \ldots (4.4)$$

In general, there are three main observations that summarize the performance of combined power cycles in series combination:

I. The use of supplementary firing in the combined power cycle results in an efficiency drop, unless there is a significant increase in the efficiency of the lower cycle. Accordingly, in this parametric study the steam turbine will not be supplementary fired. Therefore, in this chapter and the latter only the heat from the exhaust gases will be responsible on generating the steam for the steam turbine.

II. Choosing the right combination between cycles' efficiencies results in an increase in the efficiency of the combined cycle. Therefore, the gas turbine exhaust gases should be chosen to fit for powering the steam turbine cycle.

III. The heat loss during the heat exchange process does not affect the performance of the upper cycle, thus the upper cycle dominants the efficiency of the combined cycle. Although it has a great effects on the steam generation, therefore, on the performance of the steam bottoming cycle.

4.2.2 Gas/steam combined power cycle

The fundamentals of conventional simple gas/steam combined power cycle were conducted by the first chapter in this research. Where, the processes in such cycle were illustrated on the diagrams of properties and the main components were plotted on a flow diagram. As it has been illustrated in the second chapter, the performance of gas turbine cycle or steam turbine cycle individually was improved by employing different procedures. The performance of gas cycle configurations were improved by: reheating, inter-cooling, regeneration, or altogether. In steam cycle those procedures were represented by the use of multi pressure expansion, reheating, and regenerating systems.

In this section, various configurations of combined cycle were thermodynamically analysed, and their performance was optimized starting from simple example of combined power cycle. The considerations in this section were used in the parametric study to obtain the results which draw the performance of each combine cycle.

4.2.2.1 The calculations for gas turbine cycle

This section demonstrates different equations all together form a procedure to calculate the performance of gas cycles' components as a part of the combined power cycle. In this section, the procedure involves a higher realistic degree than that in chapter two. However, to simplify the thermodynamic analysis of gas turbine cycle the following assumptions were considered:

1. The air and gases in gas turbine cycle were perfect gases.

2. The specific heat capacities during cycles' processes were constant.

3. The drop in the pressure during combustion is constant and it represents a percentage of the pressure at the inlet of the combustion chamber.

Now, cycles' components will be analysed gradually to obtain the performance of the cycle, i.e. thermal efficiency and power output:

(A) Air Compression

The work required by an air compressor is represented by the following equation. Employing the relationships between the temperature and the pressure before and after compression generates equation (4.6). The compressed air equation (2.6) is used to simplify equation (4.6) to equation (4.7).

$$W_{AC} = \dot{m}_a C_{p\,a} \left(T_{g2} - T_{g1} \right) \quad \ldots (4.5)$$

$$W_{AC} = \dot{m}_a C_{p\,a} \frac{T_{g1}}{\eta_{AC}} \left[\left(\frac{P_{g2}}{P_{g1}} \right)^{\frac{\gamma_a - 1}{\gamma_a}} - 1 \right] \quad \ldots (4.6)$$

$$\dot{W}_{AC} = \dot{m}_a C_{p\,a} \frac{T_{g1}}{\eta_{AC}} \left[r_c^{\,K_a} - 1 \right] \quad \ldots (4.7)$$

The temperature of the air at the end of compression was obtained by the following equation. This equation was similarly summarized to equation (4.9) after employing equation (2.6).

$$T_{g2} = T_{g1} + \frac{T_{g1}}{\eta_{AC}} \left[\left(\frac{P_{g2}}{P_{g1}} \right)^{\frac{\gamma - 1}{\gamma}} - 1 \right] \quad \ldots (4.8)$$

$$T_{g2} = T_{g1} + \frac{T_{g1}}{\eta_{AC}} \left[r_c^{\,K_a} - 1 \right] \quad \ldots (4.9)$$

(B) Combustion

The fuel burns in a compressed air atmosphere in the combustion chamber to generate gases with much higher temperature. While equation (4.10) calculates the heat energy (q_{CC}) that air collects during combustion. In which, the fuel to air ratio is represented by f and the LCV is the low calorific value of the fuel, while equation (4.11) represents the energy that is captured by the working fluid. Modifying this equation generates equation (4.12) which calculates the fuel to air ratio for such combustion. As it has been assumed above, the drop in the pressure of the working fluid after combustion is a percentage of that before combustion as represented by equation (4.13).

$$q_{CC} = f\left(LCV\right) \quad \ldots (4.10)$$

$$\eta_{CC} f\left(LCV\right) = \left(1+f\right) C_{pg}\left(T_{g3} - T_{g2}\right) \quad \ldots (4.11)$$

$$f = \frac{1}{\left[\frac{\eta_{CC}\left(LCV\right)}{\left(C_{pg}T_{g3} - C_{pa}T_{g2}\right)} - 1\right]} \quad \ldots (4.12)$$

$$\lambda_{CC} = 1 - \frac{P_{g3}}{P_{g2}} \quad \ldots (4.13)$$

(C) Gas Expansion

The work output from gas turbine is expressed by the following equation. Employing the isentropic relations between the temperatures and pressures of the gases at turbine generates equation (4.15). Employing equation (2.7) for the combusted gases in the above equation yields in equation (4-16).

$$\dot{W}_{GT} = \left(1+f\right)\dot{m}_a C_{p\,g}\left(T_{g3} - T_{g4}\right) \quad \ldots (4.14)$$

$$\dot{W}_{GT} = \left(1+f\right)\dot{m}_a C_{p\,g} T_{g3}\eta_{GT}\left(1 - \left(\frac{P_{g4}}{P_{g3}}\right)^{\frac{\gamma_g - 1}{\gamma_g}}\right) \quad \ldots (4.15)$$

$$\dot{W}_{GT} = \dot{m}_a(1+f) \times C_{p\,g} \times T_{g3} \times \eta_{GT}\left(1 - \frac{1}{r_t^{K_g}}\right) \quad \ldots (4.16)$$

The temperature of the gases at gas turbine outlet can be obtained by using the equation (4.17). This equation can be simplified into equation (4.18). The use of the fuel in power generation was appointed by specific fuel consumption, which was obtained from equation (4.19).

$$T_{g4} = T_{g3} - \eta_{GT} T_{g3}\left(1 - \left(\frac{P_{g4}}{P_{g3}}\right)^{\frac{\gamma_g - 1}{\gamma_g}}\right) \quad \ldots (4.17)$$

$$T_{g4} = T_{g3} - \eta_{GT} T_{g3} \left(1 - \frac{1}{r_t^{K_g}} \right) \quad \ldots (4.18)$$

$$SFC = \frac{3600 \times f}{\dot{W}_{GC}} \quad \ldots (4.19)$$

(D) The performance of gas turbine topping cycle

The following equations represent the efficiency and specific work output from gas turbine cycle respectively:

$$\eta_{GC} = \frac{w_{GT} - w_{AC}}{f(LCV)} \quad \ldots (4.20)$$

$$w_{GC} = w_{GT} - w_{AC} \quad \ldots (4.21)$$

(E) Optimization Notes

The use of intercooler between compressor stages requires the use of (r_{c1}) and (r_{c2}) for first and second compressors. The temperature of the air at the second stage inlet (T_{g1Int}) was assumed to be restored to the same temperature at first compressor inlet (T_{g1}). Therefore, the temperature of the air at the second turbine outlet (T_{g2Int}) was changed by (r_{c2}) only. The relationships between the pressure's ratios in the two stages were illustrated by equation (4.22). The relationship between the pressures at the ends of each compressor was illustrated by equation (4.23), and (4.24). Pressure after inter-cooling process was obtained by the equation (4.25) below.

$$r_c = r_{c1} \times r_{c2} \quad \ldots (4.22)$$

$$r_{c1} = \frac{P_{g2}}{P_{g1}} \quad \ldots (4.23)$$

$$r_{c2} = \frac{P_{g2Int}}{P_{g1Int}} \quad \ldots (4.24)$$

$$P_{g1Int} = P_{g2} \times (1 - \lambda_{Int}) \quad \ldots (4.25)$$

The use of regeneration employs the temperature of the air at regeneration outlet (T_{g2Reg}) at combustion chamber inlet instead of T_{g2}. This change was employed in the equation (4.9)

above as well. The effectiveness can be assumed similar to the change in air side enthalpy to the maximum enthalpy change in this process. For a certain value of regenerator effectiveness, the temperature of the air at combustion inlet can be obtained via equation (4.27). For a certain pressure losses' ratio, the pressure at the inlet of the combustion chamber is calculated using equation (4.28).

$$\varepsilon_{reg} \cong \frac{\left(h_{g2Reg} - h_{g2}\right)}{\left(h_{g4} - h_{g2}\right)} \quad \ldots (4.26)$$

$$T_{g2Reg} = T_{g2} + \varepsilon_{reg}\left(T_{g4}\left(\frac{C_{pg}}{C_{pa}}\right) - T_{g2}\right) \quad \ldots (4.27)$$

$$P_{g2Reg} = P_{g2} \times (1 - \lambda_{Reg}) \quad \ldots (4.28)$$

The temperature of the gases at regenerator outlet (T_{g4Reg}) can be determined by applying energy balance equation on regenerator to obtain equation (4.29). While for a certain ratio of the pressure drop, the pressure of the gases at regenerator exit was calculated by equation (4.30).

$$T_{g4Reg} = T_{g4} - \frac{C_{p\,a}\left(T_{g2Reg} - T_{g2}\right)}{\left(1 + f\right) \times C_{p\,gReg}} \quad \ldots (4.29)$$

$$P_{g4Reg} = P_{g4} \times (1 - \lambda_{Reg}) \quad \ldots (4.30)$$

By integrating regeneration into intercooled gas turbine, the temperature of the air at regenerator inlet is assumed similar to that at intercooler outlet. Therefore, (T_{g2}) was replaced by (T_{g2Int}) in equation (4.27) and the (P_{g2Int}) replaced (P_{g2}) in equation (4.28). While by applying reheat, the temperature of the gases after second expansion (Tg4Reh) is utilized instead of (T_{g4}).

For reheated gas turbine, the temperature at pressure turbine inlet is assumed similar to that of high pressure turbine. The value of rt is replaced by (r_{t1}) for the high pressure turbine and (r_{t2}) for the low pressure turbine. The equation below calculates the total pressure ratio from pressure ratio splits. The temperature of the gases at turbine inlet is replaced by (T_{g3Reh}) in low pressure turbine calculations. The expansion ratio in for each turbine and the total expansion ratio were computed from the value of the pressures by the following equations. For a certain

pressure drop ratio, the pressure of the gases at low pressure turbine inlet was obtained by equation (4.35).

$$r_{t1} \times r_{t2} = r_t \quad \ldots (4.31)$$

$$r_t = \frac{P_{g3}}{P_{g4Reh}} \quad \ldots (4.32)$$

$$r_{t1} = \frac{P_{g3}}{P_{g4}} \quad \ldots (4.33)$$

$$r_{t2} = \frac{P_{g3Reh}}{P_{g4Reh}} \quad \ldots (4.34)$$

$$P_{g3Reh} = P_{g4} \times (1 - \lambda_{Reh}) \quad \ldots (4.35)$$

In a reheated gas turbine cycle, the fuel to air ratio includes the one for the first combustion process and that for the second. In this case, the fuel was consumed using the same air mass flow rate but with more fuel (f). The following equation illustrates the total fuel mass f_t for reheated gas turbine cycle. The work output from the second turbine can be obtained from equation (4.16) above with respect to its new gases status.

$$f_t = f_{CC1} + f_{CC2} \quad \ldots (4.36)$$

Employing inter-cooling reheating and regeneration together requires the all above changes. Additionally, the temperature of the gases at regenerator inlet T_{g4} should be replaced by that from the second gas turbine T_{g4Reh} .in equation (4.29).

4.2.2.2 The calculations for heat recovery steam generator (HRSG)

The following equation represents the energy balance in a heat recovery steam generator. In which, the left side represents the change in the heat contain of exhaust gases. While the right side is the change in the heat contain of the steam cycle.

$$(1 + f)\dot{m}_a Cp_g \times \eta_{HRSG} \left(T_{g4} - T_{g\,stack}\right) = \dot{m}_s (h_{s3} - h_{s2}) \quad \ldots (4.37)$$

The increase in the temperature of the gases at stack means low heat recovery by steam, thus low performance for the (HRSG). This temperature was restricted by the lowest degree by

which condensation has to be avoided. The type of the fuel in use limits this temperature; more precisely, it depends on fuels sulphuric content. Figure 4.1 shows simple (HRSG) configuration in which the heat exchanged between the exhaust gases and the water or the steam in three stages.

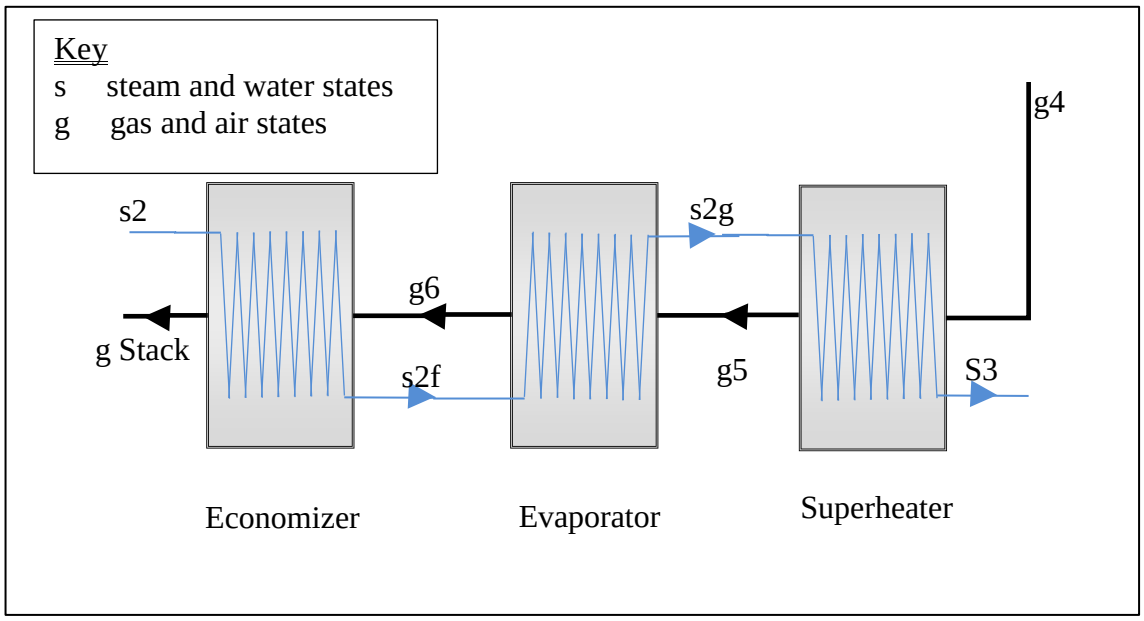

Figure 4.1 The simple heat recovery steam generator (HRSG)

The first is economizing: where the heat was recovered by high pressure low temperature water T_{s2} to generate sub saturated steam or water with high temperature. The second is evaporation: in which the water was converted into steam at the same temperature but with more heat content. The third is superheating where steam temperature increases over saturation zone to generate steam at the maximum temperature of the steam cycle (T_{s3}).

(A) Superheating:

The effectiveness of a superheater can be represented by the temperatures of steam and gas by equation (4.38) below. Therefore, for certain effectiveness, the temperature of the steam at turbine inlet can be obtained by equation (4.39). The temperature of the saturated steam can be obtained from the tables of the steam for a specific pressure. The temperature of the gases at turbine outlet was calculated similarly as in previous section. The efficiency of a superheater was demonstrated by equation (4.40). The enthalpy of the steam at turbine inlet is a function to temperature and pressure at this point i.e. $h_{s3} = f(P_{s3}, T_{s3})$.

$$\varepsilon_{sup} \cong \frac{\left(T_{s3} - T_{s2_g}\right)}{\left(T_{g4} - T_{s2_g}\right)} \quad \ldots (4.38)$$

$$T_{s3} = \varepsilon_{sup}\left(T_{g4} - T_{s2_g}\right) + T_{s2_g} \quad \ldots (4.39)$$

$$\eta_{Sup} = \frac{\dot{m}_s (h_{s3} - h_{s2_g})}{(1+f)\dot{m}_a C_{p\,g}\left(T_{g4} - T_{g5}\right)} \quad \ldots (4.40)$$

(B) Evaporating

Throughout evaporation, the temperature of the steam was assumed to be unchanged, but the steam changes its phase from liquid to gas only. Therefore, $T_{s2g} = T_{s2f} = T_{s2}$ and the equation (4.39) was modified into equation (4.41). In this equation, the temperature of the steam during evaporation (T_{s2}) was obtained from the steam tables at the pressure (P_{s3}). The temperature of the gases at the evaporator outlet was calculated by equation (4.42) using the assumed value of pinch point temperature difference (ΔT_{ppm}).

$$T_{s3} = \varepsilon_{sup}\left(T_{g4} - T_{s2}\right) + T_{s2} \quad \ldots (4.41)$$

$$T_{g6} = \Delta T_{ppm} + T_{s2} \quad \ldots (4.42)$$

The efficiency of an evaporator is represented by steam and gas status at evaporator inlet and outlet in equation (4.43). The energy balance between evaporator and superheater as one heat exchanger is illustrated in equation (4.44). This equation is used to obtain the steam to air flow rate in equation (4.45). Where, the enthalpy of the saturated water (h_{s2f}) is obtained using steam tables at the pressure (P_{s3}).

$$\eta_E = \frac{\dot{m}_s\left(h_{s2_g} - h_{s2_f}\right)}{(1+f)\dot{m}_a C_{p\,g}(T_{g6} - T_{g5})} \quad \ldots (4.43)$$

$$\eta_E \eta_{Sup}(1+f)\dot{m}_a C_{p\,g}(T_{g.4} - T_{g6}) = \dot{m}_s\left(h_{s3} - h_{s2_f}\right) \quad \ldots (4.44)$$

$$\frac{\dot{m}_s}{\dot{m}_a} = \frac{\eta_E \times \eta_{Sup} \times C_{p\,g}(1+f) \times (T_{g4} - T_{g6})}{\left(h_{s3} - h_{s2_f}\right)} \quad \ldots (4.45)$$

(C) Economising

Applying energy balance equation on the economizer yields equation (4.46). By which the temperature of the stack gases can be obtained by equation (4.47). Where (h_{s2}) is the enthalpy of saturated water at the HRSG inlet and can be computed by equation (4.45). In this equation (P_{s2}) is the pressure of the water at the water pump outlet in sub-cooled region. The table of water properties was used to obtain the specific volume of the saturated water (υ_{s1f}) at the pump inlet pressure.

$$\eta_{EC} = \frac{\dot{m}_s (h_{s2} - h_{s2_f})}{\dot{m}_a \times C_{p\,g} (1+f) \times (T_{g4} - T_{g6})} \quad \ldots (4.46)$$

$$T_{g\ Stack} = T_{g6} - \frac{\dot{m}_s (h_{s2_f} - h_{s2})}{(1+f)\dot{m}_a C_{p\,g} \eta_{EC}} \quad \ldots (4.47)$$

$$h_{s2} = h_{s1} + \frac{\upsilon_{s1}(P_{s2} - P_{s1})}{\eta_{WP}} \quad \ldots (4.48)$$

The heat exchange in heat recovery steam generator is restricted by the following points:

I. The temperature of the gases at gas turbine exhaust (T_{g4}) has to be higher than that for superheated steam (T_{s3}).

II. The temperature of the gases at evaporator outlet (T_{g6}) has to be greater than that of the water saturation temperature (T_{s2g}) by the value of the minimum temperature difference (ΔT_{PPM}).

III. The temperature of the gases at stack (T_{gstack}) must be higher than that for the water at steam generator inlet (T_{s2}).

IV. Choosing the right value of pinch point temperature difference is required to compromise between thermal efficiency and the size of heat recovery steam generator.

4.2.2.3 The calculations for steam power cycle:

As in above the components of steam cycles were analysed gradually to obtain the performance of the cycle. The considerations for the calculations in steam cycle were carried out via six sections as follows.

(A) The Heat Addition:

The heat addition processes were well demonstrated above by HRSG components. The heat addition process in a steam boiler or (HRSG) was illustrated by equation (4.49). The heat added to the steam in the boiler or (HRSG) per unit mass flow is obtained by equation (4.44). The enthalpy of the steam at turbine inlet (h_{s3}) was obtained from the table of properties at boiler pressure and turbine inlet temperature. And the enthalpy of the water at (HRSG) inlet (h_{s2}) was obtained using equation (4.48).

$$q_{SB} = h_{s3} - h_{s2} = (1+f) \times C_{Pg} \times \eta_{SB} \times (T_{g4} - T_{g\,stack}) \quad \ldots (4.49)$$

(B) Steam Expansion:

The specific work output generated by the steam turbine is obtained by equation (4.50). The quality of the steam at turbine outlet (x_{s4}) is calculated by equation (4.51). Where, if steam dryness factor (X_{s4}) at turbine outlet is less than unity, the enthalpy is calculated by equation (4.52). And if the calculated value of dryness factor is equal or greater than one, the enthalpy is obtained using superheated steam tables in corresponding to the entropy and pressure (s_{s4}, P_{s4}) where $(s_{s4} = s_{s3})$.

$$w_{ST} = \eta_{ST}(h_{s3} - h_{s4s}) \quad \ldots (4.50)$$

$$x_{s4} = \frac{(s_{s4} - s_{s4f})}{(s_{s4_g} - s_{s4_f})} \quad \ldots (4.51)$$

$$h_{s4s} = h_{s4_f} + x_{s4}(h_{s4_g} - h_{s4_f}) \quad \ldots (4.52)$$

(C) Steam Condensation:

The heat rejected per unit mass flow rate is calculated by equation (4.53). Where, the enthalpy of the steam at turbine outlet is calculated by equation (4.54).

$$q_{SCon} = h_{s4} - h_{s4_f} \quad \ldots (4.53)$$

$$h_{s4} = h_{s3} - \eta_{ST}(h_{s3} - h_{s4s}) \quad \ldots (4.54)$$

(D) Water Pumping:

The equation (4.55) below was used to calculate the specific work of the water pump. In this equation, the specific volume of water during pumping process was assumed constant. This was due to the very small change in this character after pumping. Therefore, the specific volume of saturated water (υ_{s1}) was used, which was obtained from properties table at condenser pressure (P_{s1}).

$$w_{WP} = \frac{\upsilon_{s1}(P_{s2} - P_{s1})}{\eta_{WP}} \quad \ldots (4.55)$$

(E) The performance of steam turbine cycle:

The total specific work output is calculated by equation (4.56) using the values obtained from equations (4.50), and (4.55). The thermal efficiency of a steam cycle is calculated by equation (4.57) using the results from equations (4.56), and (4.49).

$$w_{SC} = w_{ST} - w_{WP} \quad \ldots (4.56)$$

$$\eta_{thSC} = \frac{\dot{w}_{SC}}{\dot{q}_{SB}} \quad \ldots (4.57)$$

(F) Optimization Notes:

When steam cycle was optimized by reheat new sections were added to (HRSG) unit. The essential advantage in reheat was governed by the pressure of reheat (P_{s3reh}). The above strategies were similarly used to calculate the enthalpy of the reheated steam (h_{s3reh}). Equations (4.49), (4.50) were used to obtain the specific work and the heat addition in reheated turbine. A new parameter was added to equation (4. 56) to generate equation (2.38). The use of regeneration in steam cycle employed equations (2.39 – 43) to obtain specific steam work and the mass flow rate for each sub-cycle. In which, the kind of feed water heater decides which of the above equation to use. The considerations of both points above were required for the calculations in reheated regenerated steam cycles. The use of dual pressure or

triple pressure cycles adds more sections to the (HRSG) unit. The calculation considered additional water pumping, heat addition, and steam expansion processes. The specific work in duel and triple steam cycles were computed by the equations below:

$$w_{STDPSC} = w_{ST1} + \left(1 - \frac{\dot{m}_{s\,LP}}{\dot{m}_{s\,HP}}\right) w_{ST2} \quad \ldots (4.58)$$

$$w_{WPDPSC} = w_{WP1} + \left(1 - \frac{\dot{m}_{sLP}}{\dot{m}_{s\,HP}}\right) w_{WP2} \quad \ldots (4.59)$$

$$w_{ST\,TPSC} = w_{ST1} + \left(1 - \frac{\dot{m}_{s\,IP}}{\dot{m}_{s\,HP}}\right) w_{ST2} + \left(1 - \frac{\dot{m}_{s\,IP}}{\dot{m}_{s\,HP}} - \frac{\dot{m}_{s\,LP}}{\dot{m}_{s\,HP}}\right) w_{ST3} \quad \ldots (4.60)$$

$$w_{WP\,TPSC} = w_{WP1} + \left(1 - \frac{\dot{m}_{s\,IP}}{\dot{m}_{s\,HP}}\right) w_{WP2} + \left(1 - \frac{\dot{m}_{s\,IP}}{\dot{m}_{s\,HP}} - \frac{\dot{m}_{s\,LP}}{\dot{m}_{s\,HP}}\right) w_{WP3} \quad \ldots (4.61)$$

In general, the processes of heat addition in multi pressure steam turbine cycle were illustrated below. In those equations, the components of each process were considered as one unit. All considerations in the calculations of simple (HRSG) components were applied on those with multi live pressure.

$$q_{SB\,DPSC} = q_{SB1} + \left(1 - \frac{\dot{m}_{s\,IP}}{\dot{m}_{s\,HP}}\right) q_{SB2} \quad \ldots (4.62)$$

$$q_{SB\,TPSC} = q_{SB1} + \left(1 - \frac{\dot{m}_{s\,IP}}{\dot{m}_{s\,HP}}\right) q_{SB2} + \left(1 - \frac{\dot{m}_{s\,IP}}{\dot{m}_{s\,HP}} - \frac{\dot{m}_{s\,LP}}{\dot{m}_{s\,HP}}\right) q_{SB3} \quad \ldots (4.63)$$

4.2.2.4 The calculations for combined cycle performance

The thermal efficiency of a combined gas/steam power cycle is computed by using the results from equations, (4.21), (4. 56) and (4.12) in equation (4.64). While its specific work output is calculated by submitting the results obtained from equations (4.21) and (4. 56) in equation (4.65).

$$\eta_{th\,CCPP} = \frac{w_{Total}}{q_{CC}} = \frac{w_{GC} + w_{SC}}{(1+f)(LCV)} \quad \ldots (4.64)$$

$$W_{CCPP} = W_{GC} + W_{SC} \quad \ldots (4.65)$$

$$\eta_{CC} = f\left(T_{g1}, T_{g3}, \left(\frac{\dot{m}_s}{\dot{m}_a}\right), C_{pa}, C_{pg}, r_a, r_g, k_a, k_g, \eta_{AC}, \eta_{GT}, \eta_{CC}, \eta_{HRSG}, \eta_{ST}, \eta_{WP}, P_{s2}, P_{s4} \right) \quad \ldots (4.66)$$

$$W_{CC} = f\left(T_{g1}, T_{g3}, \frac{\dot{m}_s}{\dot{m}_s}, C_{pa}, C_{pg}, r_a, r_g, k_a, k_g, \eta_{AC}, \eta_{GT}, \eta_{CC}, \eta_{HRSG}, \eta_{ST}, \eta_{WP}, P_{s2}, P_{s4} \right) \quad \ldots (4.67)$$

4.3 Assumptions and the limitations for the parametric analysis

I. The range of the temperature ratio (T_{g3}/T_{g1}) was assumed to start from the compression temperature ratio (T_{g2}/T_{g1}) to that with cycles' maximum temperature.

II. The range of the pressure started from one where zero specific work output from gas turbine to its maximum value, which was governed by technological characteristic.

III. The ranges of steam temperature at turbine inlet considered the values from saturation to the maximum value for a certain pressure. Those values were restricted by technological factors and illustrated in the table of properties.

IV. The temperature of gas turbine exhaust has to stay higher than steam temperature by the minimum pinch point temperature difference. In general, the range of this value was assumed regarding economic and design parameters.

V. The quality of steam at turbine outlet must not be less than 90% to avoid blades' corrosion in steam turbine.

VI. The temperature of the stack gases should be higher than the minimum value for corrosive condensation and greater than 139 °C to avoid the corrosions by sulphuric acid.

VII. The parameters in this study were realistically chosen and further development in those ranges may be considered in the future.

VIII. Some of the parameters were constants during the calculations to observe the changes in performance by the effect of others.

The following table summarizes the assumed values in this parametric study:

Parameters	**Values/ranges**
T_{g1}	0 -60 °C
P_{g1}	1.013bar
T_{g3}	800-1800 °C
r_c, r_t	4-36
P_{s2}	20-140 bar
P_{s4}	0.55 -0.05 bar
ΔT_{MPP}	10-25 ºC
x_{s4}	0.9
η_{CC}	0.80
η_{AC}	0.98
η_{GT}	0.88
η_{ST}	0.87
$\eta_{WP}, \eta_{SB}(\eta_{HRSG})$	0.85
$\eta_{Sup}, \eta_{E}, \eta_{EC}$	0.9
η_{PG}	0.98
λ_{CC}	0.3
$\varepsilon_{EC}, \varepsilon_{Sup}, \varepsilon_{E}$	0.9
LCV	42400 kJ/kg
$C_{p\,a}$	1.005 kJ/kg
$C_{p\,a}$	1.155 kJ/kg
γ_a	1.4
γ_g	1.333

Table 4.1 The assumed values and the considered ranges in this parametric study

4.4 Discussion

This section graphically reviews and comprehensively discusses the results achieved by the equations above with regard to the specified limitations. It studies the effect of the main operating parameters on the characteristics that indicate the performance of different power cycles. It also demonstrates the advantages and the disadvantages of these cycles and identifies cycles' required and prohibited processes. As a result, it reveals the points at which the performance of a combined power cycle is fully optimized. This discussion goes over three sub partitions the first is interested in the effect of the main operating parameters on the performance of gas turbine engine cycles. The effects of such parameters on the combined power cycle are studied in the second. The third considers some of the parameters, which appear on specific configurations only.

Different configurations are considered for the gas turbine engine: (a) simple gas turbine, (b) regenerated gas turbine, (c) reheated gas turbine, (d) intercooled gas turbine, (e) regenerated-reheated gas cycle and (f) intercooled-regenerated-reheated gas turbine. This parametric study considers investigating the use of gas turbine inlet temperatures range between 800°C and 1800°C. It also considers an overall pressure ratio range between 4 and 36. The expansion ratio of reheated turbines and the compression ratios of intercooled compressors are assumed identical. The exhaust gases from the gas turbine engine are used to power the steam turbine engine.

The following configurations are the cycles considered in this work, under which the steam turbine engine is used to work on: (a) simple steam cycle, (b) reheated steam cycle, (c) regenerated steam cycle, (d) reheated regenerated and (e) multi pressure steam cycles (dual or triple pressure steam cycles). The calculation of combined power cycle performance requires investigating steam turbine parameters. The live pressure value in such cycles is ranged between 20bar to 180bar, while the back pressure values are ranged between 0.05bar and 0. 55bar. The pressure of reheated steam is restricted by specific operating limits. Therefore, its value is considered with respect to the live pressure and it's ranged between 10bar and 70bar. The pressure of the feed heating in regenerated steam turbines is measured with regard to the back pressure and ranged between 0.5 bars and 6 bars.

4.4.1 Gas turbine cycle performance

This section discusses the relationships between the design parameters of the gas turbine cycles and both the performance and the environmental impact of such cycles. The performance of the gas cycles is represented by change the thermal efficiency and the specific work output. On the other hand, the impact on the environment is represented by the change in the specific fuel consumption and the temperature of gases at turbine exhaust. For that reason, different figures are revealed to illustrate such relationships for a wide range of (r) and (TIT). This section takes into account different configurations of gas turbine cycles to enlarge the range of the results by including more cases. The configurations are: simple gas turbine cycle, regenerated gas turbine, reheated gas turbine, intercooled gas turbine, intercooled reheated gas turbine and intercooled reheated regenerated gas turbine.

4.4.1.1 Simple gas turbine cycle (SGC)

The relationship between specific work output and thermal efficiency for different (TIT) and (r) is illustrated in Fig. 4.2. It shows an increase in the thermal efficiency and the specific work by the increase of the compression ratio (r) for each curve of a (TIT). The increase in (r) over a certain value reduces the thermal efficiency and the specific work output. The increase of TIT shifted (r) at which the deflection happens to higher values. The function between thermal efficiency and specific work output tends linear with the increase in (TIT) for a given (r). The maximum thermal efficiency and the maximum specific work output appears when the gas turbine is working on the highest (TIT). For a constant (TIT) the (r) at which maximum efficiency is not the same to that for the maximum specific power output. But it tends the same by the increase in (TIT). The relationship between stack gases temperature and (r) for different (TIT) is illustrated in Fig. 4.3. It shows an increase in the temperature of the exhaust gases when the temperature of the gases at the turbine inlet is increased and (r) is kept constant. For any (TIT), the temperature of exhaust gases drops by the increase in (r).

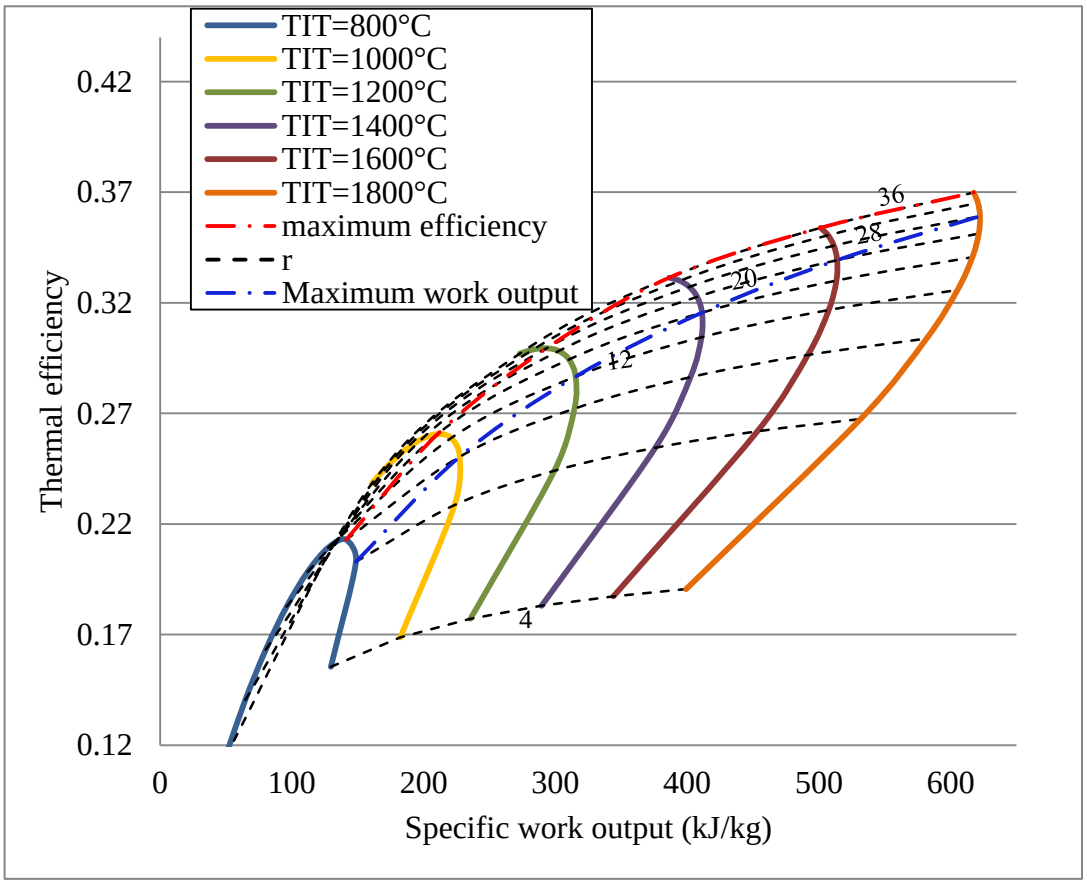

Figure 4.2 The efficiency of simple gas turbine cycle versus the specific work output

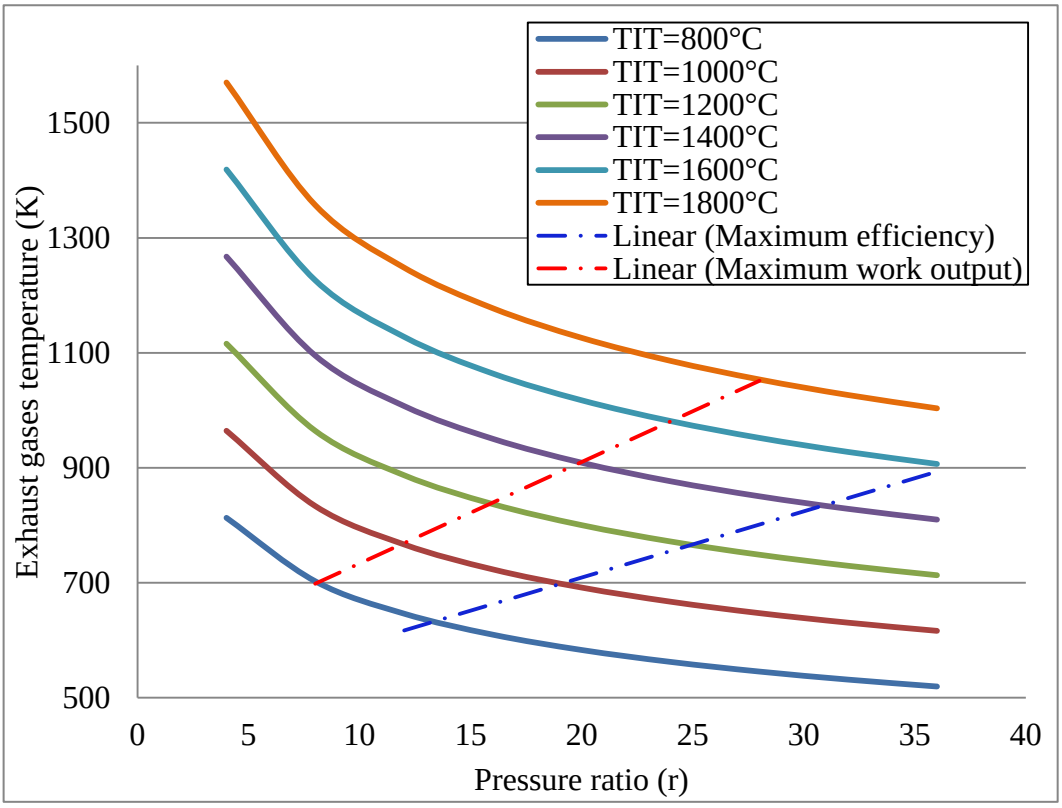

Figure 4.3 The relationship between pressure ratios and exhaust temperature for simple gas turbine cycle

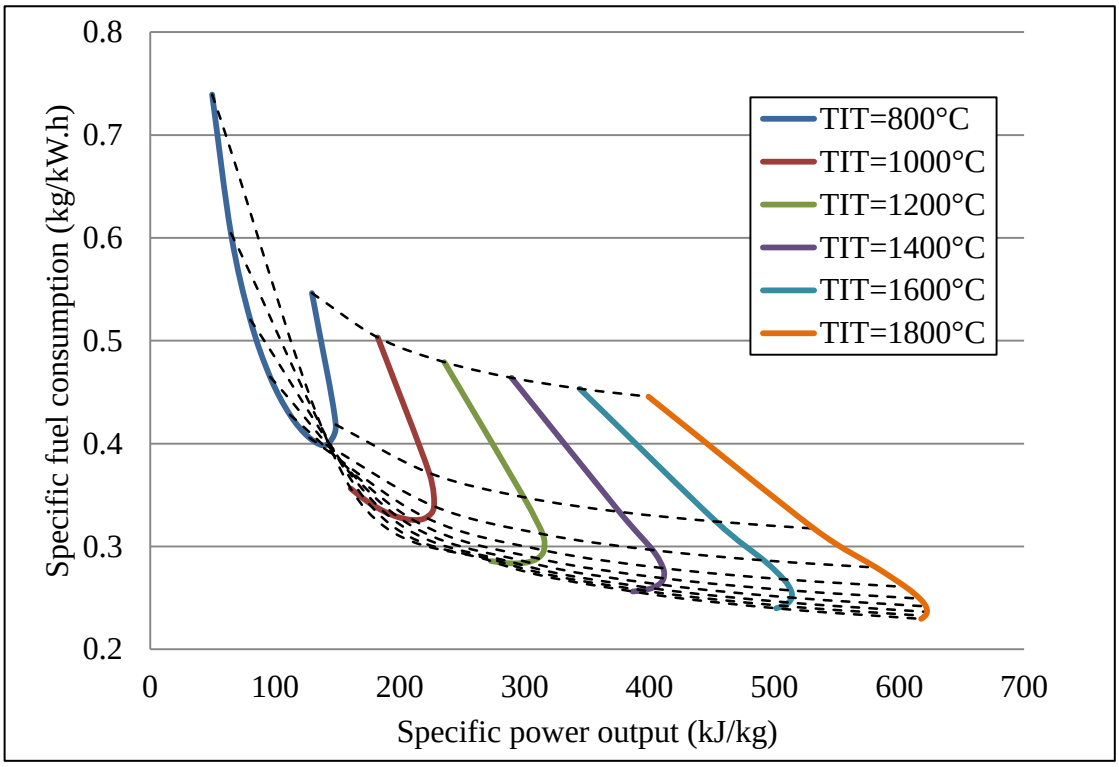

Figure 4.4 The relationship between the specific power output and SFC of simple gas turbine cycle

The relationship between the specific fuel consumption and the specific work output is illustrated by Fig. 4.4. It shows a drop in the specific fuel consumption by any increase in the (TIT). The minimum specific fuel consumption does not appear when the specific work output is the maximum. The optimum values for specific fuel consumption and specific work output are governed by the (r), which differs by the change in the (TIT). The optimum (r) appears with larger values by the increase in the (TIT). For a fixed (TIT), the increase in the (r) over the optimum value increases the (SFC) and decreases the specific work output.

4.4.1.2 Regenerated gas turbine cycle (RegGC)

The relationships above are similarly presented by the figures below to investigate the performance of the regenerated gas turbine cycle. The operating range of such cycle appears narrower than the simple cycle, because gases' insufficiency for regeneration limits such range. The difference between the heat contents of the streams is very small at low degrees of (TIT) with high (r). As a result, the temperature of the gases at turbine outlet drops while the temperature of the air at the compressor outlet increases.

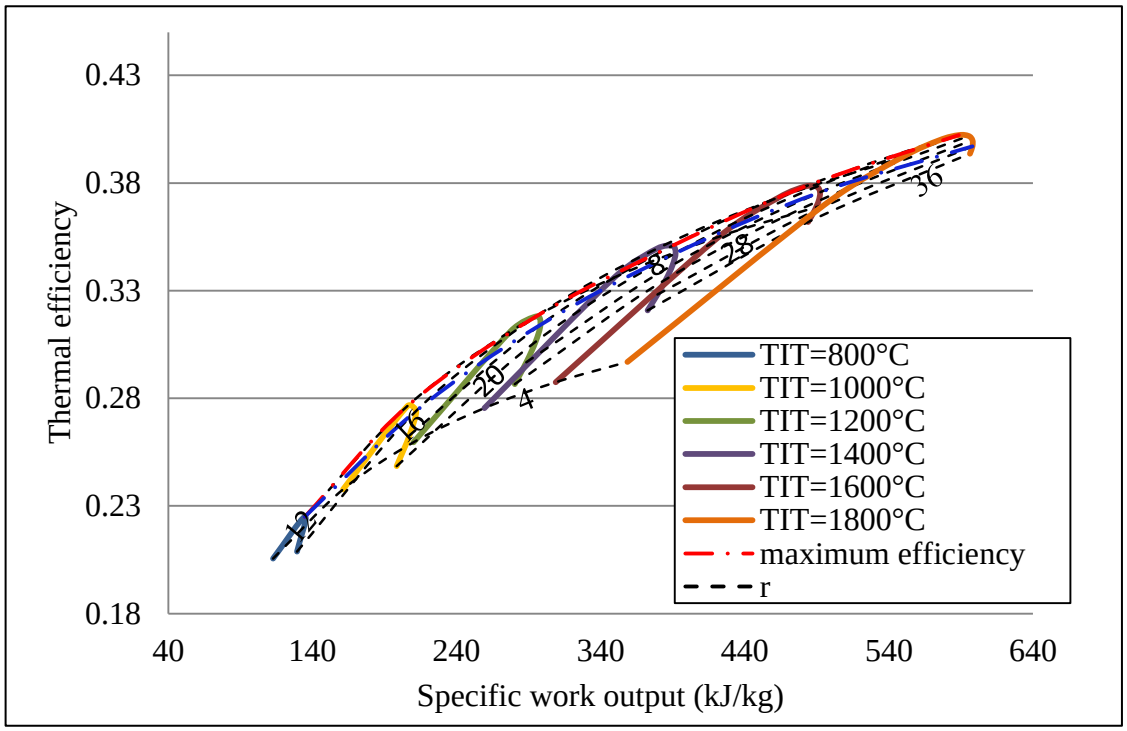

Figure 4.5 The efficiency of regenerated gas turbine cycle versus the specific work output

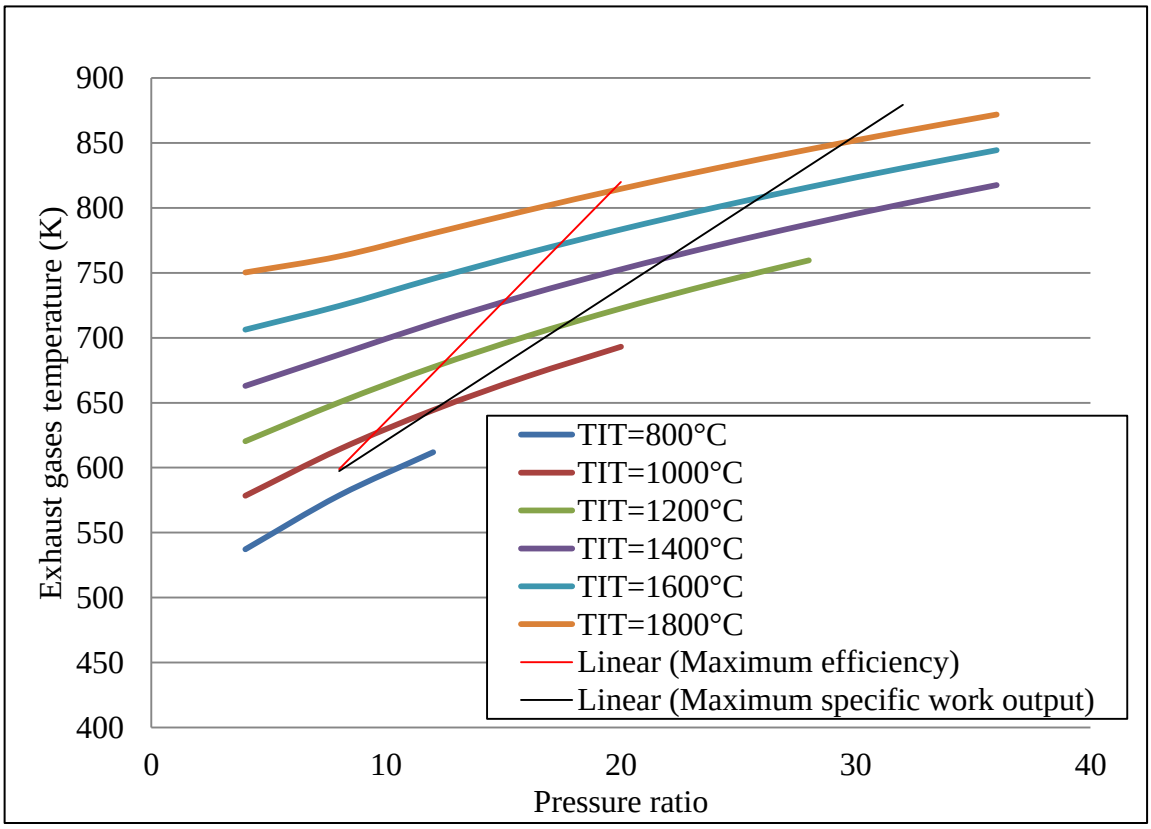

Figure 4.6 The exhaust gases temperature of regenerated gas turbine cycle versus the pressure ratios

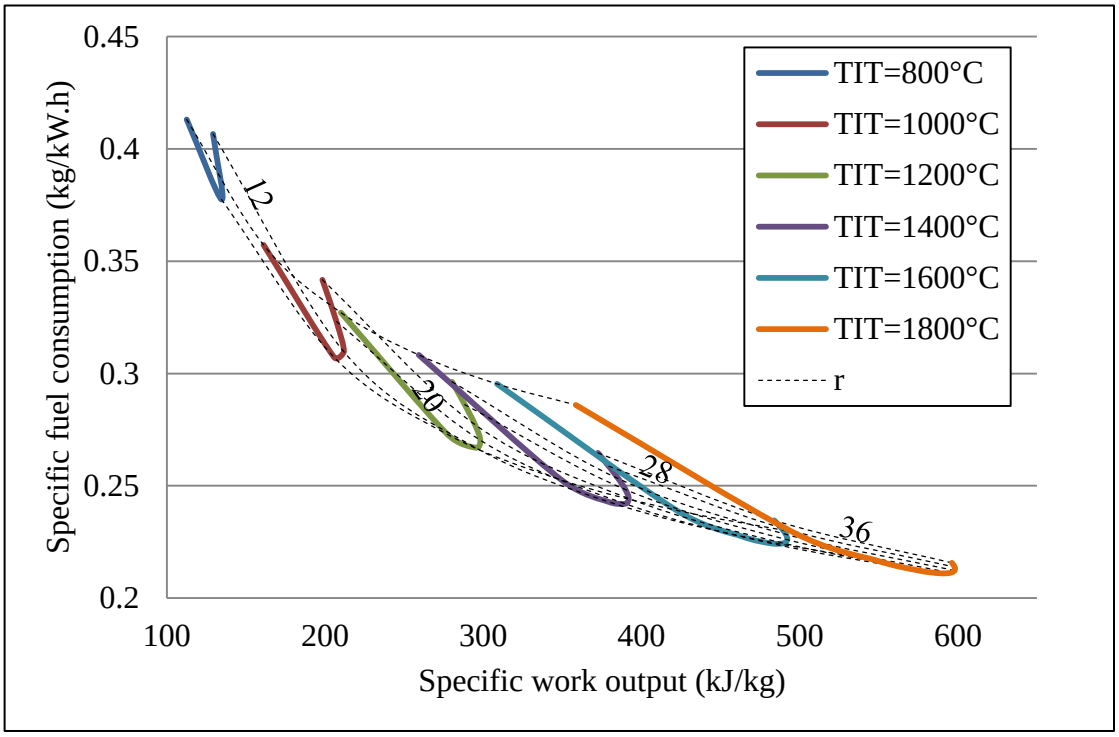

Figure 4.7 The SFC of regenerated gas turbine cycle versus itd specific work output

The relationship between the thermal efficiency and the specific work output is similar to that for (SGC). However, the increase in the (r) over the optimum value always results in a drop in the thermal efficiency. The temperature of stack gases increases linearly with the increases of the (r) as shown in Fig. 4.6. The increase in such temperature drops by the increase in (TIT). This appears due to the increase in air temperature before regeneration. The relationship between the specific work output and the (SFC) is similar to the simple gas turbine as shown by Fig. 4.7. Above a certain (r), the specific work output drops, although the increase in the (SFC).

4.4.1.3 Reheated gas turbine cycle (RehGC)

The relationship between the thermal efficiency and the specific work output of the reheated gas turbine appears similar to that for simple cycle but more liners as shown in Fig. 4.8. It demonstrates the deflection points at which the relation modified for cycles that works on low (TIT) only. The maximum efficiency of such cycle is lower than that for simple gas turbine cycle, although the same (TIT), but the specific work output is always greater. This comes in agreement to Al- Hamdan [18] on superiority of W_{GC} for RehGC to be viable. However, the

(RehGC)s that operates on low (TIT)s has a better efficiency and generates more specific work output.

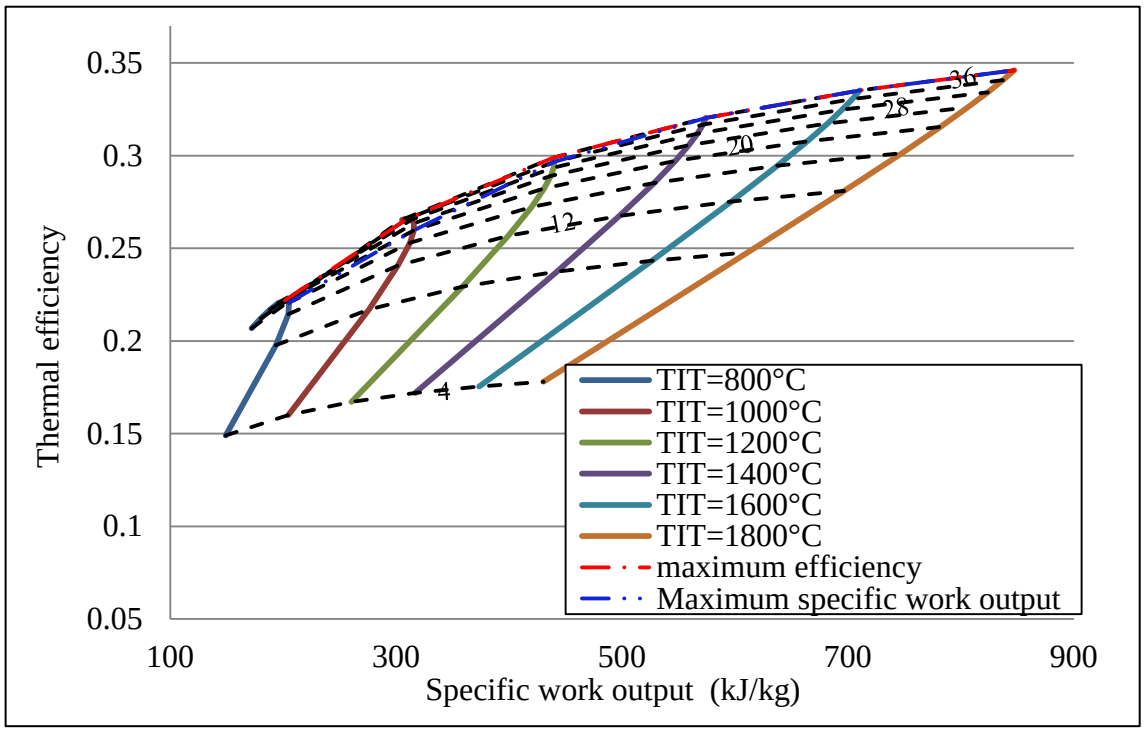

Figure 4.8 The specific power output of reheated gas turbine cycle versus the thermal efficiency

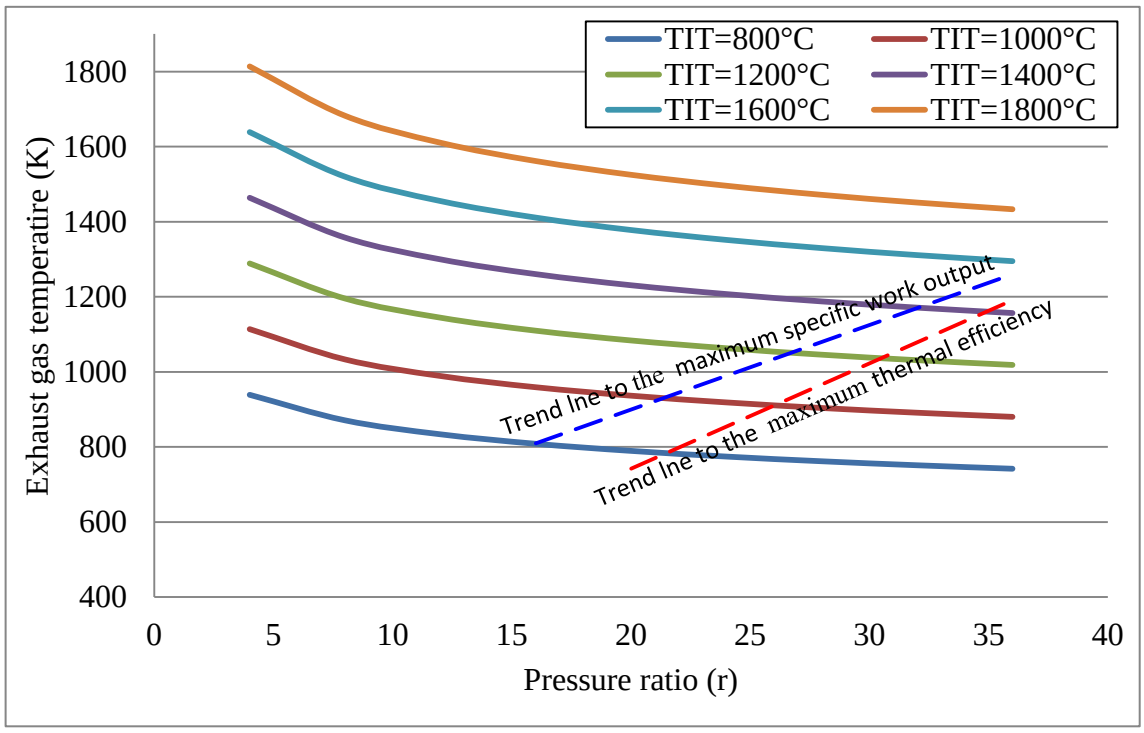

Figure 4.9 The exhaust gases temperature of reheated gas turbine cycle versus the pressure ratios

The change in the temperature of exhaust gases by the effect of (r) appears slighter than that for simple gas turbine cycle Fig. 4.9. This temperature is always higher than that for (SGC) even when the same (TIT) is utilized. The relationship between specific fuel consumption and specific work output is illustrated in Fig. 4.10. It shows that the specific fuel consumption is affected similarly as the simple gas by the change in the (r) and (TIT). Except for the cycle that works on low (TITs) and high (r), the specific fuel consumption in reheated gas turbine is greater than that for simple cycle. There is an agreement between the results here and the results of al-hamdan [18] which confirmed that maximum efficiency and specific work output have the same optimum parameters.

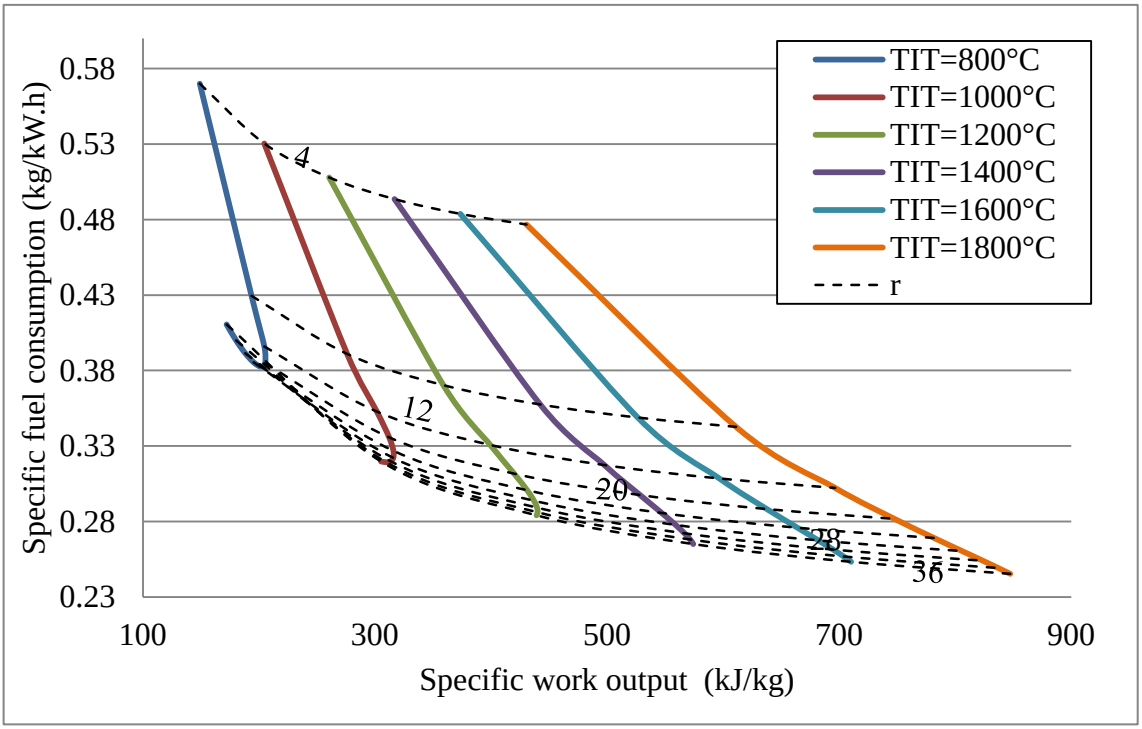

Figure 4.10 The SFC of a reheated gas turbine cycle versus the specific work output

4.4.1.4 Intercooled gas turbine cycle (IntGC)

The above relationships are similarly employed to investigate the performance of intercooled gas turbine. Figure 4.11 shows a linear relationship between the thermal efficiency and the specific work output linear for most of the performance curves. In such figure, the maximum efficiency appears when the gas turbines operate on large (r) except those with low (TIT)s. The maximum efficiency of the (IntGC) is always higher than that for (SGC) and (RehGC) if the same (TIT) has been utilized. If high (TIT) is utilized in such configuration, the maximum efficiency goes to the (SGC). Nevertheless, the increase in the maximum efficiency of such

cycle is still minor than the maximum efficiency of regenerated configuration. The (IntGC) generates less specific work output than that for (RehGC) even if they operate using the same conditions. This specific work output is greater than that generated by simple and regenerated gas turbine cycles when they operate on large (r).

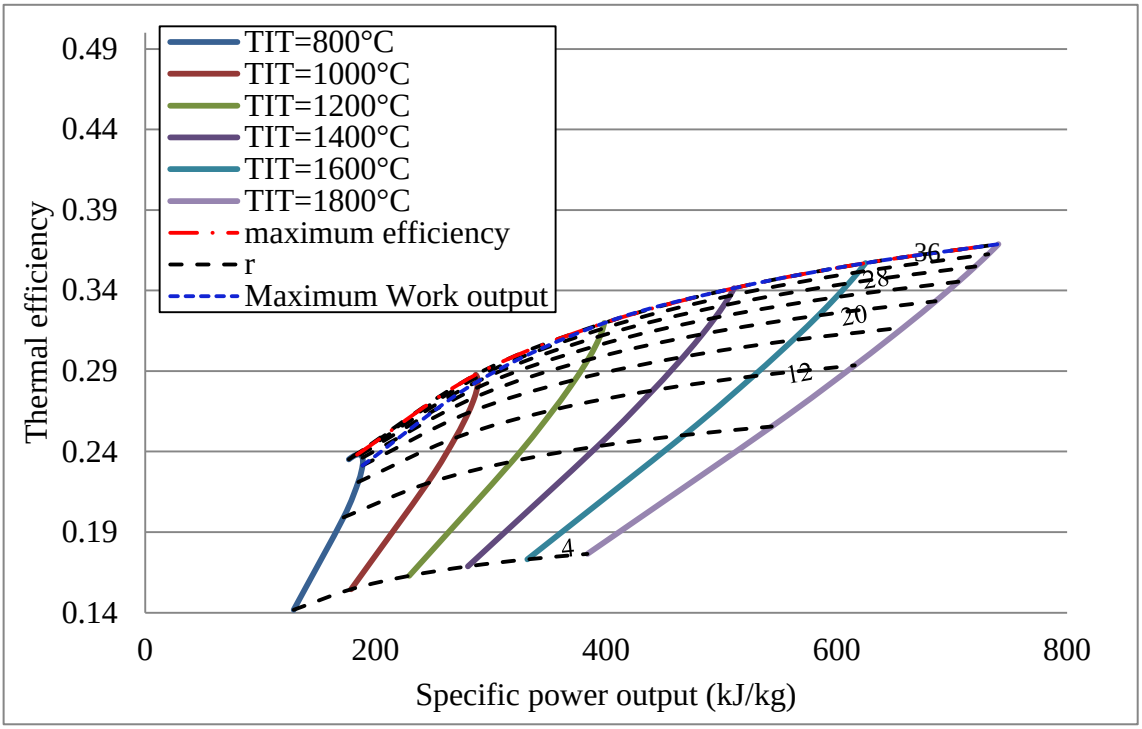

Figure 4.11 Intercooled gas turbine cycle's specific work output versus its thermal efficiency

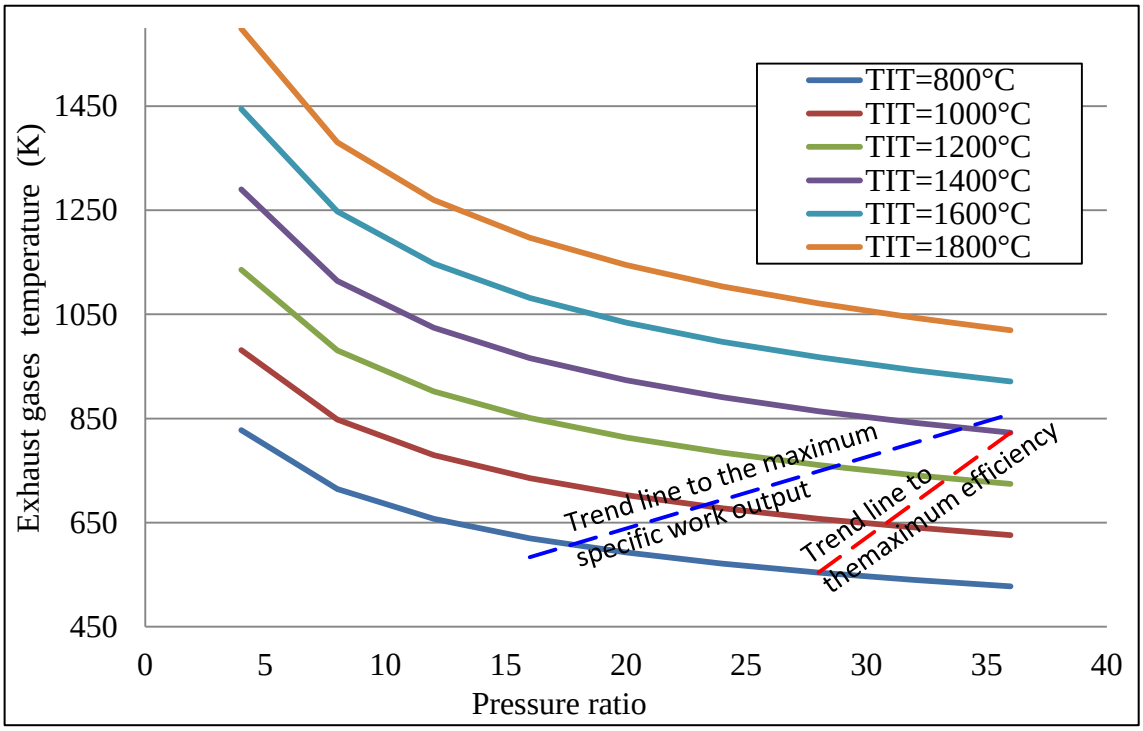

Fig. 4.12 Exhaust gases' temperature of intercooled gas turbine cycle versus its pressure ratio

The difference between the specific work output of this cycle and other cycles reduces by the use of small (r). Such specific work output gets less than specific work generated by (SGC). This tendency appears more by the increase in (TIT). Figure 4.12 illustrates the changes in the temperature of exhaust gases by the effect of the (r) and (TIT). The temperature of exhaust gases appears to change similarly as the simple cycle but with slightly lower values. It's much lower than the temperature of stack gases of (RehGC). The relationship between the (SFC) and the specific work output of this cycle appears similar to that simple and (RehGC)s as shown in Fig. 4.13. It shows that the (SFC) of such cycle is less than that for reheated and (SGC)s when large (r) and low (TIT).

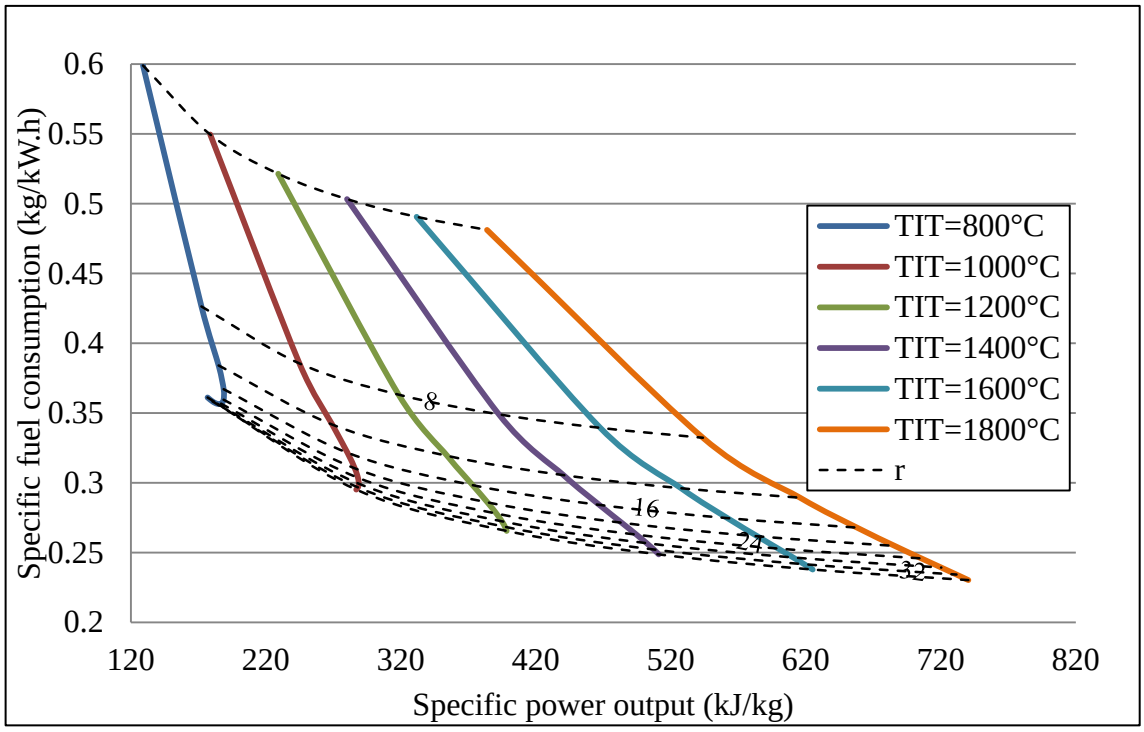

Figure 4.13 The relationship between specific work output and specific fuel consumption of intercooled gas turbine cycle

4.4.1.5 Intercooled reheated gas turbine cycle (IntRehGC)

The effect of the (TIT) and the (r) on the performance of intercooled (RehGC) is similar to that in the configurations above. The Fig. 4.14 shows the relationship between the specific work output and the thermal efficiency for different (TIT)s. It shows the maximum efficiency with the maximum (TIT) and (r). The maximum efficiency of such configuration is greater than that for the cycles above except the engines those to operate with low (TIT)s. The intercooled reheated gas turbine generates the largest work output over other cycles. The change in the temperature of exhaust gases of the (IntRehGC) is identical to that for (RehGC).

Figure 4.15 illustrates (SFC) as a function to the specific work output for a range of (r)s and (TIT)s. The (SFC) is lowest among that for the configurations above except (RegGC). This advantage turns the opposite when low (TIT) and high (r) are used for such engines.

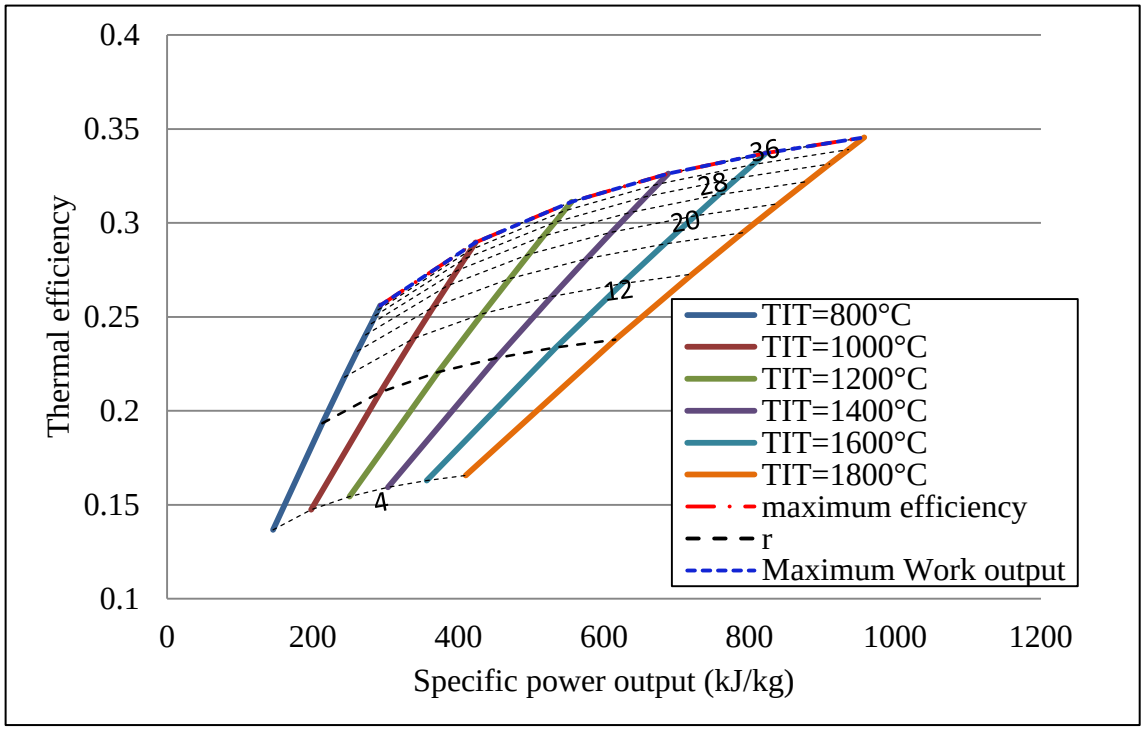

Figure 4.14 Intercooled reheated gas turbine cycle's thermal efficiency functioned to the specific work output

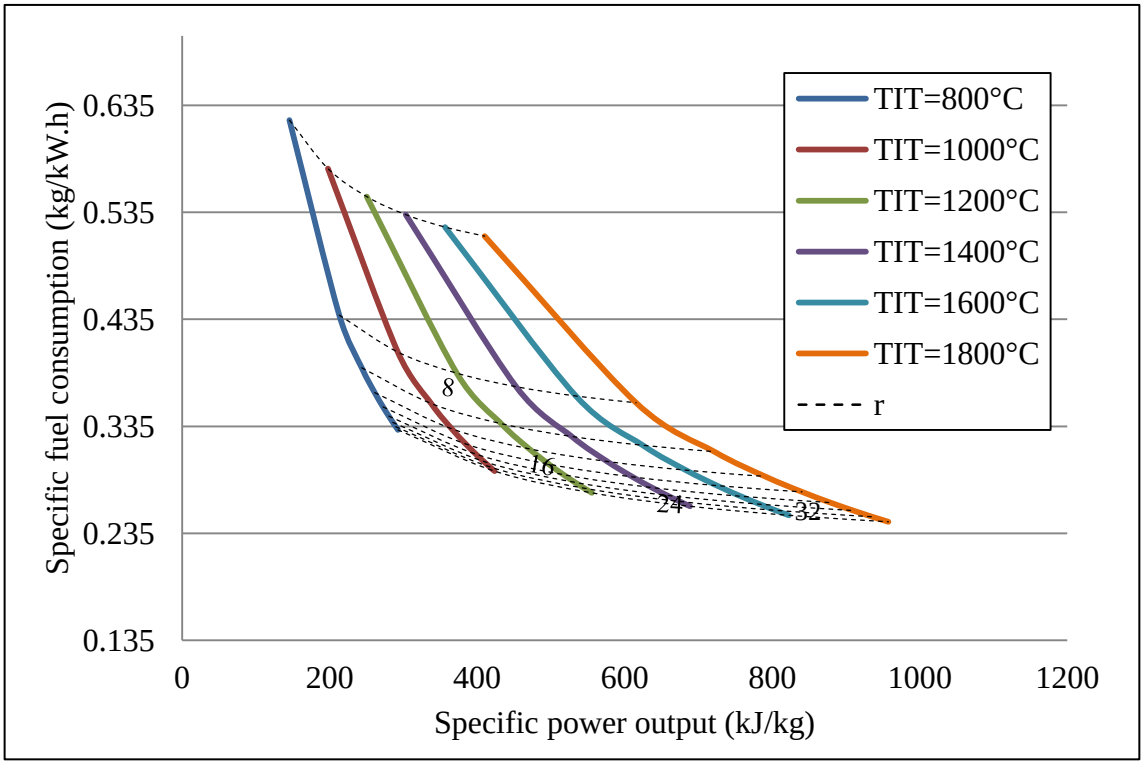

Figure 4.15 The SFC versus the specific work output of intercooled reheated gas turbine cycle

4.4.1.6 Intercooled reheated regenerated gas turbine cycle (IntRehRegGC)

The changes in the performance characteristics of (IntRehRegGC) by the effect of (TIT) and (r) are shown in Fig. 4.16. The results demonstrate a higher efficiency than that for other cycles for the same (TIT) and (r). Therefore, the maximum efficiency of this cycle remains the highest over the efficiency of other configurations. This configuration generates the second largest specific work output following (IntRehGC). The effect of changing (r) on the temperature of exhaust gases is illustrated by Fig. 4.17 including various (TIT)s. It shows that the temperature of exhaust gases had a similar impact to that of (SGC).

This configuration emits exhaust gases with a lower temperature than that for the configurations above even if it uses the same (TIT). The deference between such temperatures increases for low (TIT) and high (r) as in simple, regenerated, and intercooled gas turbines. The relationship between the specific work output and the (SFC) appears similar to that for the cycles above although, the (SFC) of this configuration is the lowest (Fig. 4.18).

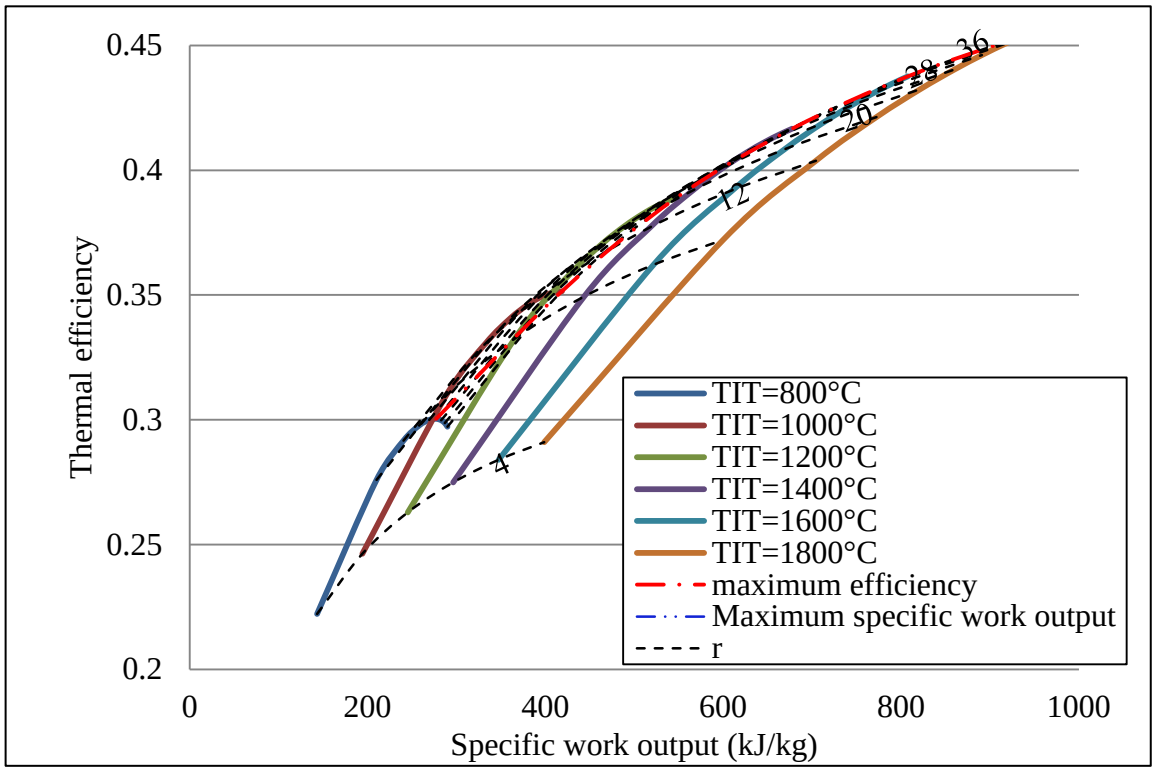

Figure 4.16 The thermal efficiency versus specific work output of intercooled regenerated reheated gas turbine cycle

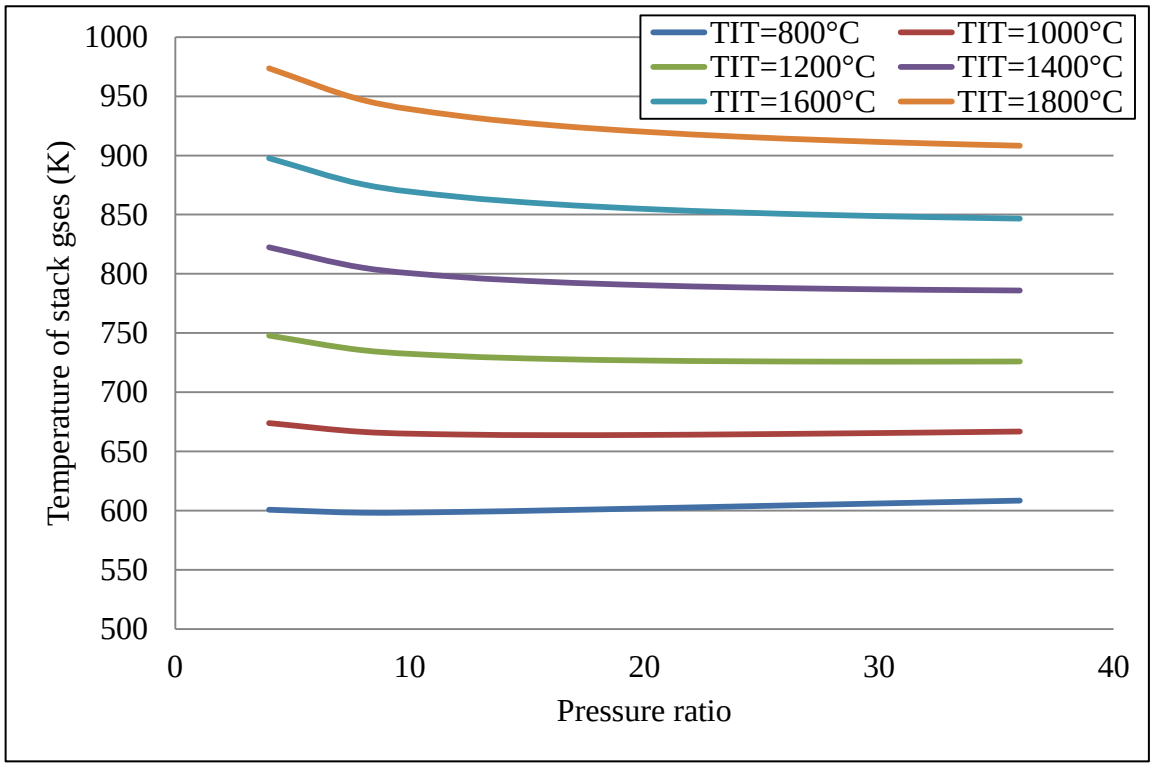

Figure 4.17 The exhaust temperature of the gases versus the pressure ratios of intercooled regenerated reheated gas turbine cycle

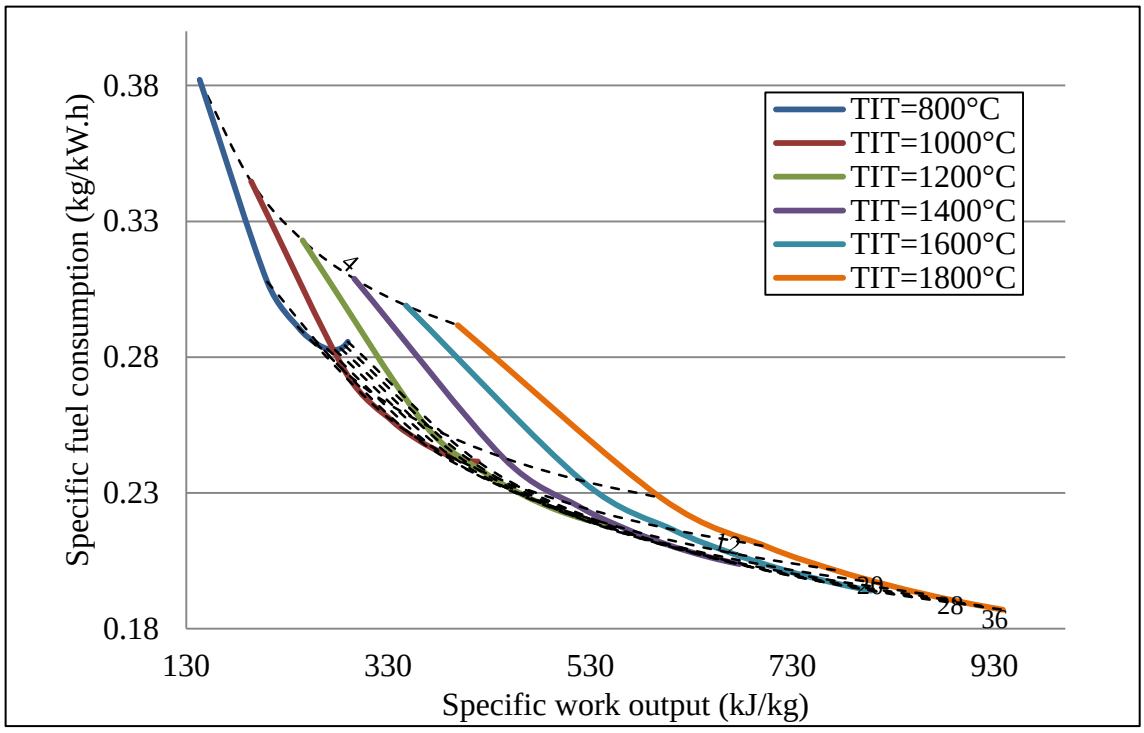

Figure 4.18 The SFC versus the specific work output of intercooled regenerated reheated gas turbine cycle

4.4.1.7 Comparisons amongst gas turbine cycles

This section compares the inputs, the operating and the output parameters for the above cycles to evaluate their performance. It also determines and discusses the conditions for the optimum performance points for different gas cycles. And it gives the technical recommendations for such configurations when operating at optimum performance. The following table represents the results for maximum thermal efficiency in the above gas turbine cycles.

All cycles above share the maximum thermal efficiency and the lowest specific fuel consumption with the highest turbine inlet temperature and pressure ratio. However, the maximum efficiency and the minimum specific fuel consumption of a regenerated gas turbine cycle do not correspond to the largest (r). The maximal performance attained by each of the above cycles requires advanced materials and requirements to reach and maintain the high temperature and pressure.

Gas Cycle	η_{GC}	w_{GC} **(kJ/kg)**	**SFC(kg/kW.h)**	T_{gE}**(°C)**	**r**	**TIT(°C)**
SGC	0.369	618	0.0393	730	36	1800
RegGC	0.402	588	0.0345	542	24	1800
RehGC	0.346	847	0.0577	1160	36	1800
IntGC	0.368	740	0.0473	747	36	1800
IntRehGC	0.345	957	0.0653	1163	36	1800
IntRehRegGC	0.454	938	0.0487	635	36	1800

Table 4.2 A sample on the results regarding the performance of different gas turbine cycle

From the table above it is clear that employing each of the strategies above improves the specific work output from the simple cycle except the one with regeneration. The configuration that generates the maximum specific work output is not probably similar to that for the maximum thermal efficiency. The maximum specific work output is generated by intercooled reheated gas turbine cycle. The amount of the specific work difference verifies how beneficial the addition of another strategy is. The intercooled reheated gas turbine operates with a maximum efficiency less than that for the intercooled reheated regenerated turbine by 34.7%, but the specific work output is greater by only 2%.

The table above shows a small variation in the specific fuel consumption in different gas turbine cycles. The specific fuel consumption reduces than that for simple gas cycle by employing regeneration alone but increases with the other strategies. The lowest amount of fuel is burned in the regenerated gas turbine cycle, while the major amount appears in the intercooled reheated gas cycle. Although the intercooled reheated regenerated gas cycle represents the most efficient use of heat to generate power it does not burn the lowest amount of fuel. The configuration with the maximum efficiency burns (24%) more fuel than that in simple cycle and (41%) fuel more than the regenerated gas cycle. As a result, the risks of raising the unfavorable emissions are more emerged. The values of those emissions must be taken in mind due to their serious impact on environmental pollution. Therefore, employing an intercooled reheated regenerated gas cycle (for example) requires more control on emissions over the simple cycle.

The temperature of the exhaust gases is very high in simple gas cycle and falls with regeneration but rises with other gas cycles. The table above shows the highest temperature of exhaust gases for intercooled reheated gas cycle (1163 °C). The lowest temperature is for regenerated gas cycle (542 °C). Consequentially, more procedures are required to treat the gases with high temperature in reheated and intercooled configurations. The ignorance of such high temperature is a great loss of the energy by which an important share of the power output may be generated. This heat loss plays an essential rule on power plants' impact to increase the global warming. The high temperature from gas cycle can be efficiently utilized to generate more power from less fuel consumption in combined cycles. This configuration generates exhaust gases with a temperature of much lower than that of the regenerated gas cycle. The use of regeneration reduces the range of exhaust gases temperatures to meet a beneficial power production via steam cycle.

The results confirm that, the intercooled reheated regenerated gas turbine cycle does not make the lowest impact on the environment, although it's high performance. The minimum impact on environment appears using the regenerated gas turbine cycle. However, it generates a specific work output of (37%) less than the intercooled reheated regenerated cycle with a drop in the efficiency by (11.5%). While the intercooled reheated regenerated gas cycle generates exhaust gases of (17%) higher temperature and burns (41%) more fuel. Environmentally, the high temperature from intercooled regenerated reheated gas turbine can be considered as an advantage in combined configurations. However, the emissions from fuel burning can't be under further control. The figure below shows the superiority of intercooled reheated regenerated gas turbine in achieving high thermal efficiency over other gas turbine cycles.

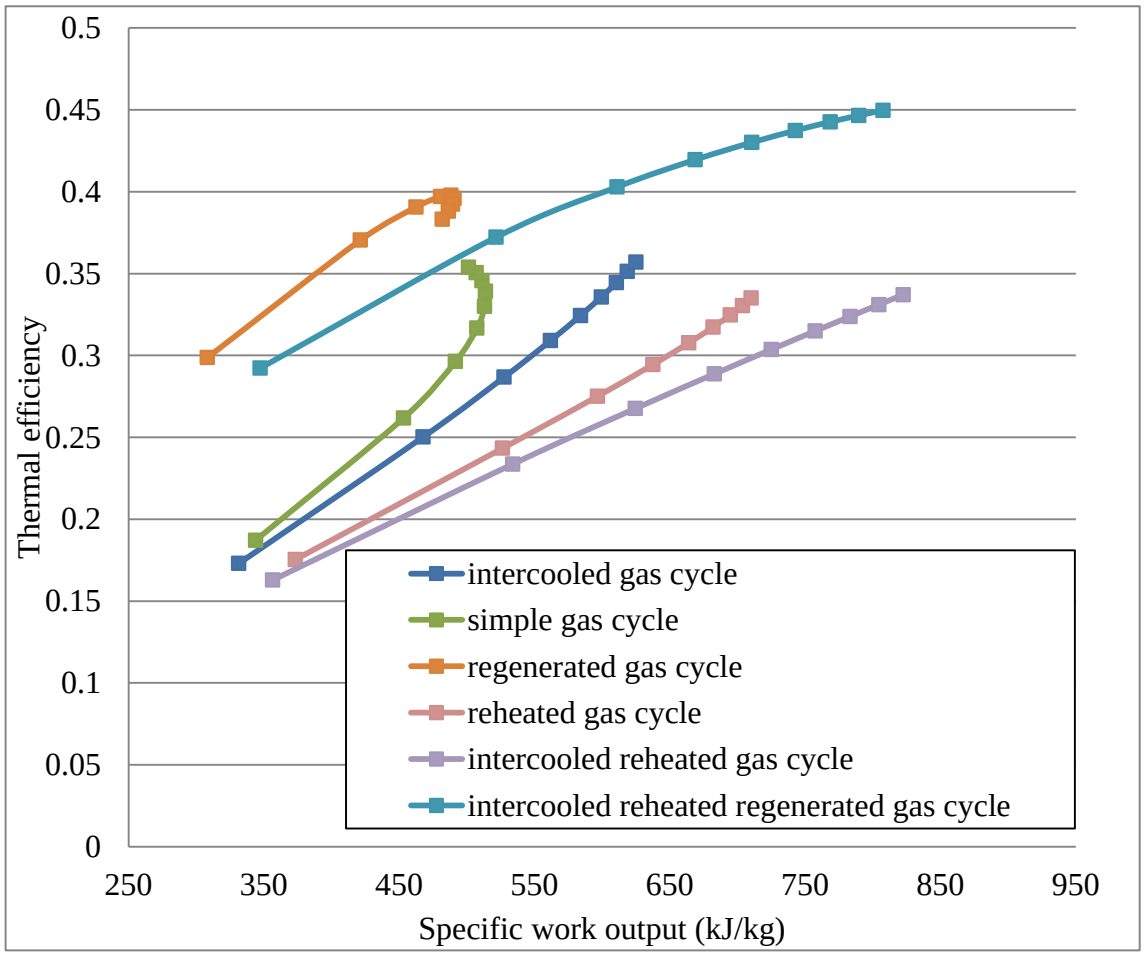

Figure 4.19 The thermal efficiency versus the specific work output for different gas turbine cycles

4.4.2 The performance of gas /steam combined cycle power plant

This section investigates the influence of different parameters on the performance of a number of combined power cycles. Each of the pervious gas turbine configurations is used to power seven different steam turbine engines. Such combination generates 42 new configurations of a combined cycle power plant. The steam engine configurations covered simple, reheated, regenerated, dual pressure, dual pressure reheated, triple pressure reheated and triple pressure reheated steam cycles.

Simple thermodynamics is used to optimize a number of cycles operating parameters and consequently, the cycles' performance. Currently, the parameters from the gas turbine cycle are combined with those for steam turbine. The thermodynamic considerations of the gas turbines and steam turbine cycles components are used to obtain the results. Microsoft Excel Desktop program has been used to calculate the results and illustrate the diagrams. The

performance parameters represented by the thermal efficiency and the specific work output, and the environmental parameters represented by the specific fuel consumption and the temperature of stack gases are investigated with respect to the changes in the following parameters:

a. The pressure ratio (r)

b. The pressure of reheat ($P_{Reh.}$).

c. The pressure of inter-cooling ($P_{Int.}$).

d. The temperature of the air at compressor intake (T_a).

e. The turbine inlet temperature (TIT).

f. The steam to air mass flow ratio (m_s/m_a)

g. The fraction of steam mass flow rate in multi pressure steam cycles (Y).

h. The pressure of the live steam (P_{s3}).

i. The pressure of the back steam (P_{s4}).

j. The Pressure of reheated steam ($P_{sReh.}$).

k. The minimum pinch point temperature difference (ΔT_{mpp}).

This section undertakes many comparisons between the tested cycles to evaluate their performance. Primarily, this appoints the best performance energetically and environmentally. Therefore, it shall meet an efficient operation with acceptable limits of exhaust gas temperatures and specific fuel consumption. The optimization is carried out with respect to the permitted limits and the practical acceptable choices for different parameters. This section identifies the area for further research and gives the recommendations for further optimization over typical combined power cycles. The permitted limits (steam quality, turbine inlet temperature, etc.) and the common ranges (the pressure ratio, efficiencies, losses, etc.) are considered with respect to the previous knowledge.

The former section considers the affecting parameters of the gas turbine only. Now the operating parameters of steam turbine are included. Steam generation in the (HRSG) is dependent on the temperature of the gases at the turbine outlet, the pressure of live steam and the mass flow in HRSG components.

In this discussion, the temperature of the gases from GT discharge is a result for the changes in the compression ratio and the TIT of the gas turbine cycle. Thus, both are discussed combined to other parameters. However, the results confirmed that, the increase in TIT increases the efficiency and the specific work output which is reported by [18]. It also confirmed that the increase in the compression ratio increased efficiency or more specific work output beyond its optimum value as in [25]. This value is different by cycle configuration for certain set of other operating and design parameters.

The results from the gas turbine cycle calculations showed a reduction in the temperature of the gases at GC exhaust by the increase in the compression ratio, which came similar to the results by [25], except for the RergGC, in which the temperature increase.

The results discussed below also confirmed that for a certain set of parameters, optimizing GC operating and design parameters is useless it attain better performance from the same GT combined to any ST cycle as confirmed by [22]. By such utilization, the optimum parameters for GC corrected to suit the CCPP as well, which is similar to the results from [18] and [19] .

4.4.2.1 The pressure of the steam through boiler and (HRSG) (P_{s3} or PSB)

This section investigates boiler pressures' effect on the performance of different combined power cycles. It discusses the changes in the thermal efficiency, power output, specific fuel consumption and the temperature of stack gases by the effect of such parameter. Firstly, this parameter is studied regarding its effect on the performance of simple gas turbine combined to different steam turbine power cycles. While its impact on the performance of combined cycles which employ different gas turbine cycle is discussed later in this section. The changes in the pressure of the boiler included five values (20, 50, 80,110, and 140) as shown by the following figures. The previous ranges for gas turbine parameters are considered here as well.

The results confirm a direct increase in the temperature of evaporation with the increase in boiler pressure if the temperature of gases at turbine outlet is constant. Consequentially, the steam is supplied to the turbine with temperature and enthalpy higher than before. But the increase in boiler pressure beyond certain value generates steam with an enthalpy lower than that before. The results from database showed that the increase in boiler pressure yields in:

a) An increase the enthalpy of steam at turbine inlet and outlet,

b) Higher temperature of gases at evaporator outlet,

c) Slight decrease in mass flow rate of steam,

d) The work generated by steam turbine and that required by the water pump were increased and

e) An increase in the total work and the efficiency of the steam cycle.

The efficiency and the power output of the combined power cycle were also increased by the increase in boiler pressure. The temperature of the gases at the turbine outlet was low with high pressure ratio for gas turbine cycle. The decrease in the mass flow rate was the best procedure to increase the effect of low temperatures and the boiler pressure effect on cycles' performances. This behaviour appears only in high pressure section of multi pressure (HRSG) due to the previous assumptions.

The figures below show the relationship between the efficiency and the specific work output in combined power cycles with different steam turbines. Each illustrates the increase in the efficiency and specific work output by the increase in boiler pressure. This behaviour was the dominant on all pressure ratios for high turbine inlet temperatures. The opposite appears for low turbine inlet temperatures but only for low pressure ratios. The pressure ratio of modification appears lowers with higher turbine inlet temperatures. This was due to the drop in the temperature of the steam at turbine inlet.

For multi pressure steam turbines combined cycles, the drop in the efficiency and specific work output appears with very low turbine inlet temperature only. The following figures illustrate the effect of changing the boiler pressure on the performances of simple gas turbine combined to simple, reheated, dual pressure reheated and triple pressure reheated steam turbines. The results confirmed the increase in the efficiency of CCPP by the increase in T_{s2} similarly to [23], but such increase in T_{s2} is limited by the P_{S2}. The results also confirmed generating higher quality steam by [29] the increase of P_{S3} which is limited critical steam generation to restricted area of operation.

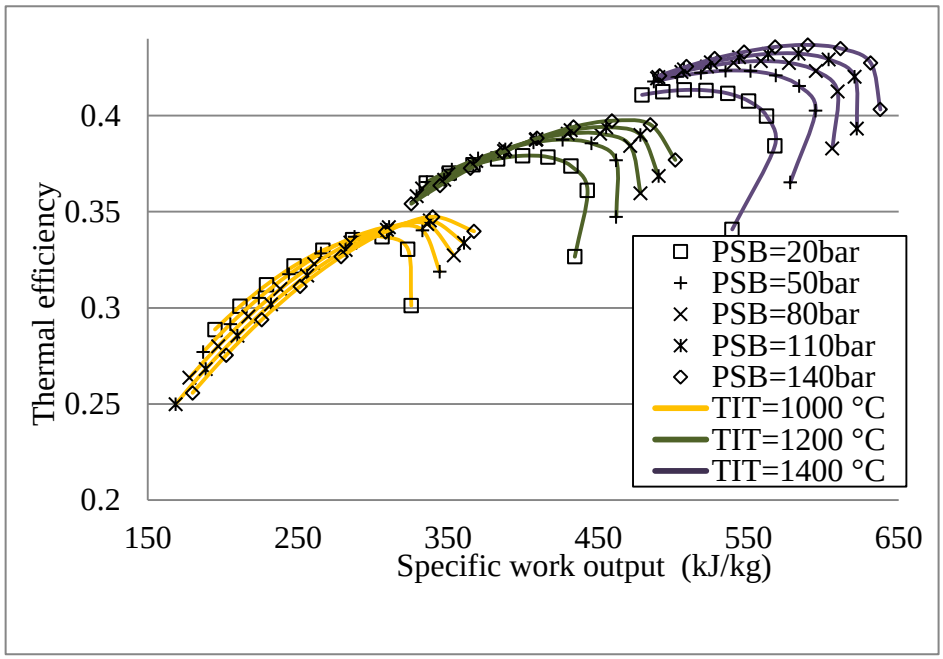

Figure 4.20 The effect of boiler pressure on the efficiency and specific work output of simple gas turbine/simple steam turbine combined power cycle

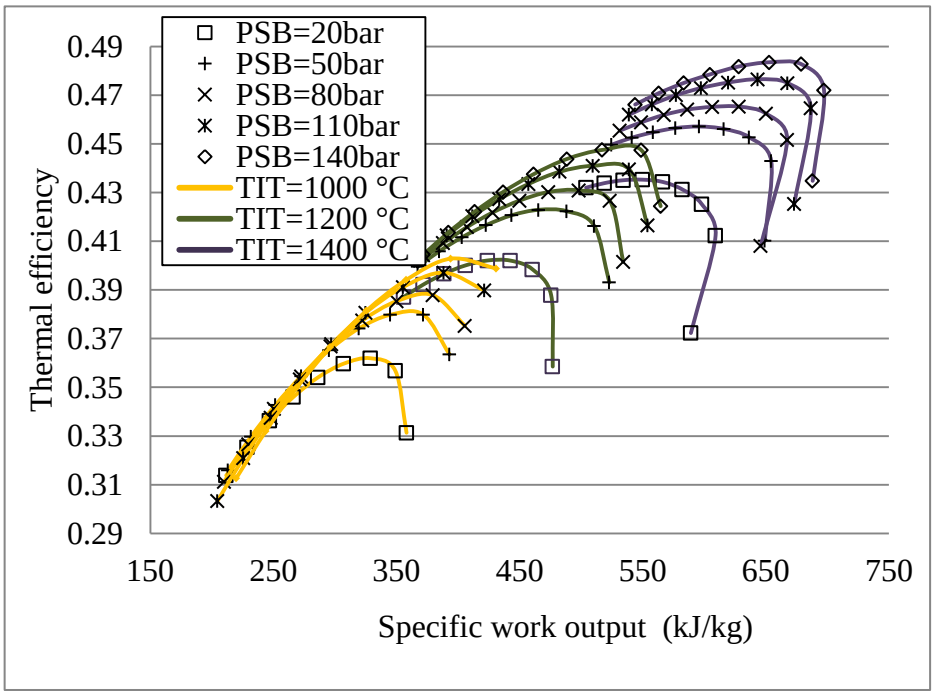

Figure 4.21 The effect of boiler pressure on the efficiency and specific work output of simple gas turbine/dual pressure reheated steam turbine combined cycle

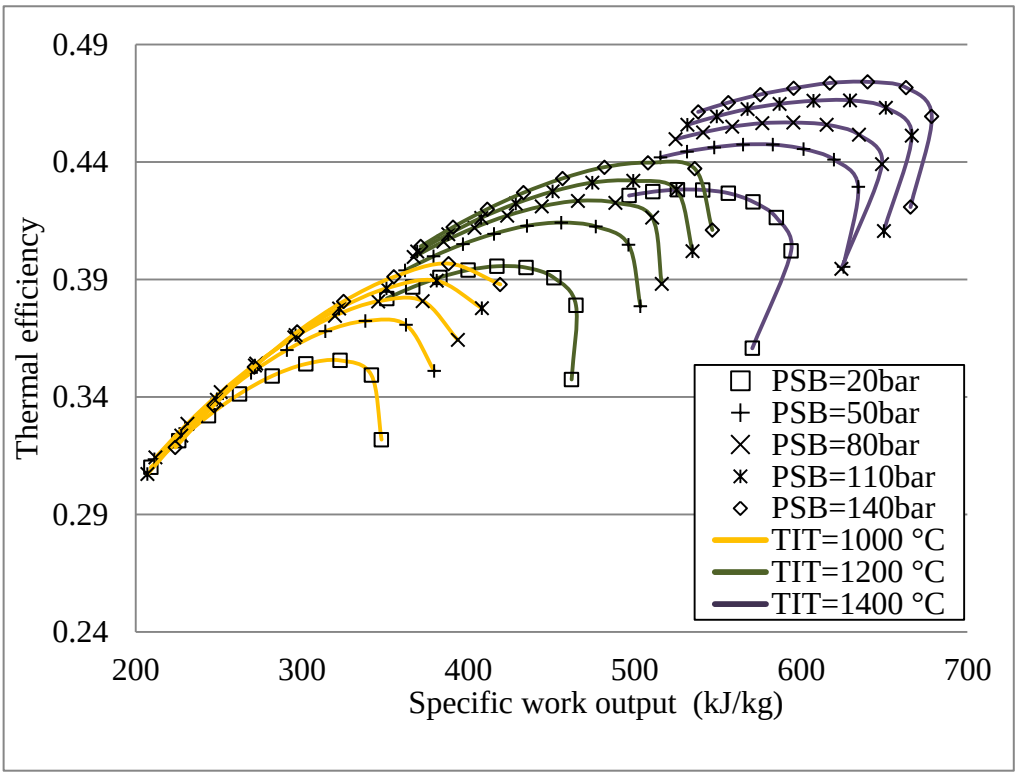

Figure 4.22 The effect of boiler pressure on the efficiency and specific work output of simple gas turbine/triple pressure reheated steam turbine combined power cycle

The impact of boiler pressure on the temperature of stack gases and specific fuel consumption in some of the studied configurations were illustrated by the following figures. This impact differs by the change of the gases at turbine inlet temperature and pressure ratio. The increase of the steam pressure at the boiler results in an increase in the temperature of stack gases for most of the considered (r)s. This increase is joined with a clear increase in the (SFC) when high pressure ratios and low (TIT). With the increase in (TIT) the increase in (SFC) becomes slighter and tends to decrease with high (TIT). Employing low pressure ratio in gas turbine led to a decrease in (SFC) by the increase in boiler pressure. This decrease was joined with an increase in the temperature of stack gases for low (TIT). But through the increase in (TIT) the increase in stack gases temperature was reduced and tends to decrease with high (TIT). The boiler pressure at which the modification takes place drops by the increase in (TIT). This behaviour was observed clearly in the figures of multi pressure steam turbines combined cycles. The quality of the steam at turbine falls down by the increase in boiler pressure. Consequently, the right value for boiler pressure is under further restrictions, therefore, it has to be chosen carefully.

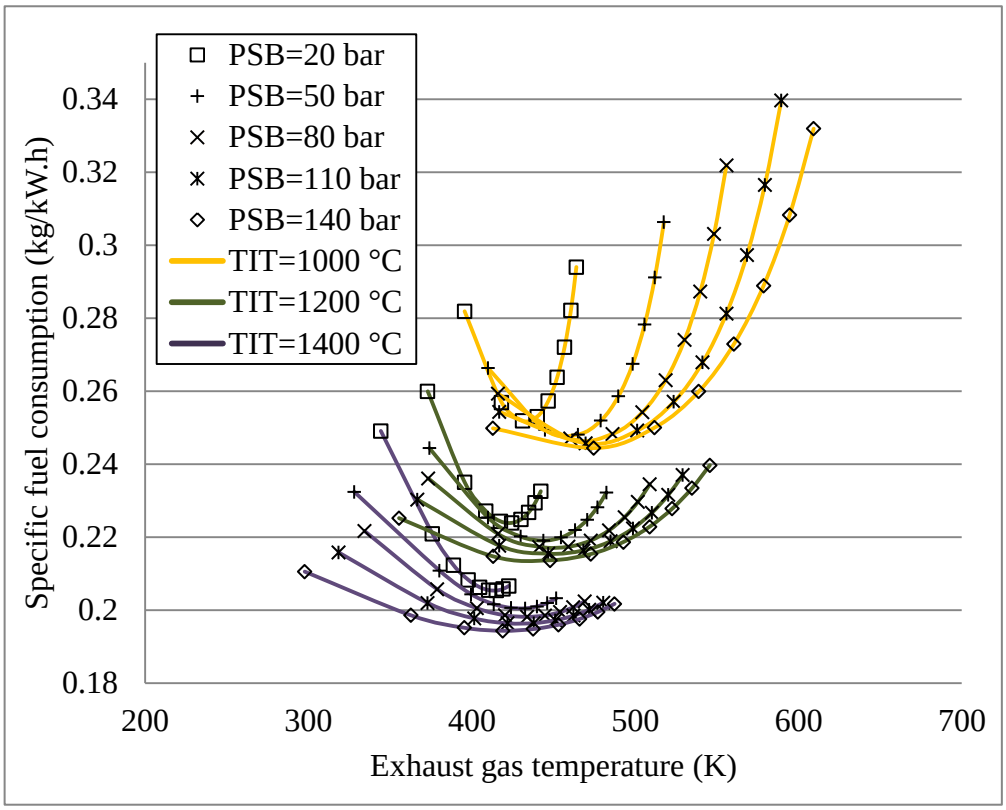

Figure 4.23 The effect of boiler pressure on specific fuel consumption (SFC) and stack gases temperature of simple gas /simple steam combined cycle

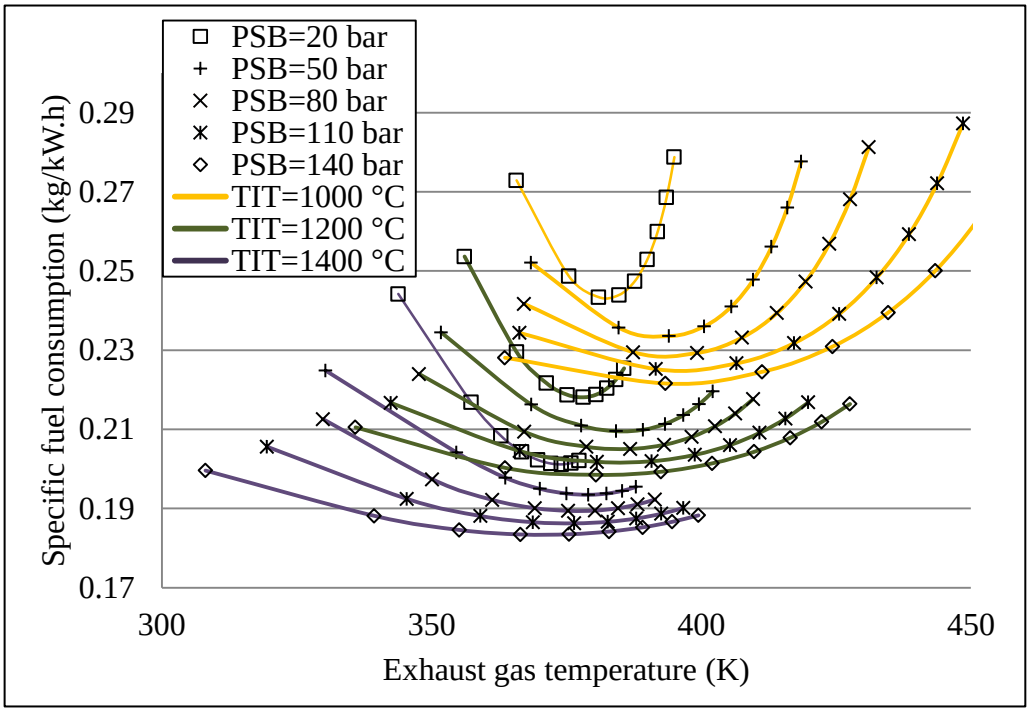

Figure 4.24 The effect of boiler pressure on specific fuel consumption (SFC) and stack gases temperature of simple gas/dual pressure steam combined cycle

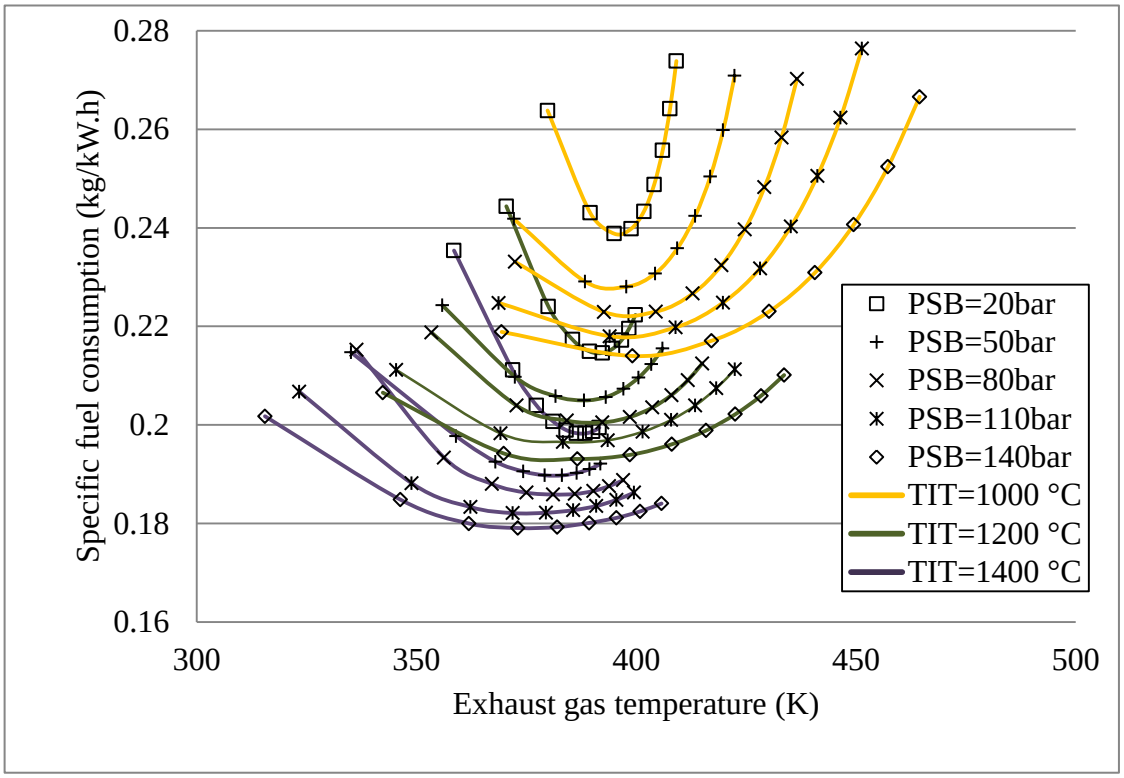

Figure 4.25 The effect of boiler pressure on specific fuel consumption (SFC) and stack gases temperature of simple gas/triple pressure reheated steam combined cycle

The effects of boiler pressure on the performance of simple gas turbine in combination with different steam turbines were illustrated in Figs. 4.26 -29. The results confirmed that the heaviest effect of boiler pressure on thermal efficiency and specific work output was for dual pressure steam turbines combined cycle. This increase was by about 5% and 9.9% for the efficiency and the specific work output respectively by the increase in boiler pressure from (20 bar) to (140 bar). The impacts of the change in boilers pressure on specific fuel consumption and on the temperature of stack gases were the largest in combined cycle that uses triple pressure reheated steam turbine. The increase in boiler pressure from (20 bar) to (140 bar) made a decrease in the stack temperature by (3 %) and specific fuel consumption by (10.6%).

The impact of boiler pressure on the performance of combined power cycles that employ different gas turbines and simple steam turbine is illustrated by Figs. 4.30-33. The first two figures confirmed boiler pressures' major effect on the thermal efficiency and specific fuel consumption of reheated gas turbine simple steam turbine combined cycle (RehGSSCC). For such cycle, an increase in thermal efficiency by 5.5% and a reduction in specific fuel

consumption by 12.3% were assigned by the increase of boiler pressure from (20bar) to (40bar). The specific work output from the combined cycle and the temperature of its stack gases were mainly affected by the change in boiler pressure in intercooled reheated gas turbine simple steam combined cycle (IntRehGSSCC). The above increase in boiler pressure modifies the specific work output by 11.5 % and changes the temperature of stack gases by 28.7%.

From the above it is clear that the major effect of boiler pressures on the thermal efficiency is made by using reheated gas turbine dual pressure steam turbine combined cycle (RehGDPSCC). The change in the specific work output appeared more by intercooled reheated gas turbine dual pressure steam combined cycle (IntRehGDPSCC). The temperature of stack gases is greatly affected by such parameter in intercooled reheated gas turbine triple pressure reheated steam combined cycle (IntRehGTPRehSCC). The maximum reduction in the specific fuel consumption by the effect of boiler pressure is for reheated gas turbine triple pressure reheated steam turbine combined cycle (RehGTPRehSCC).

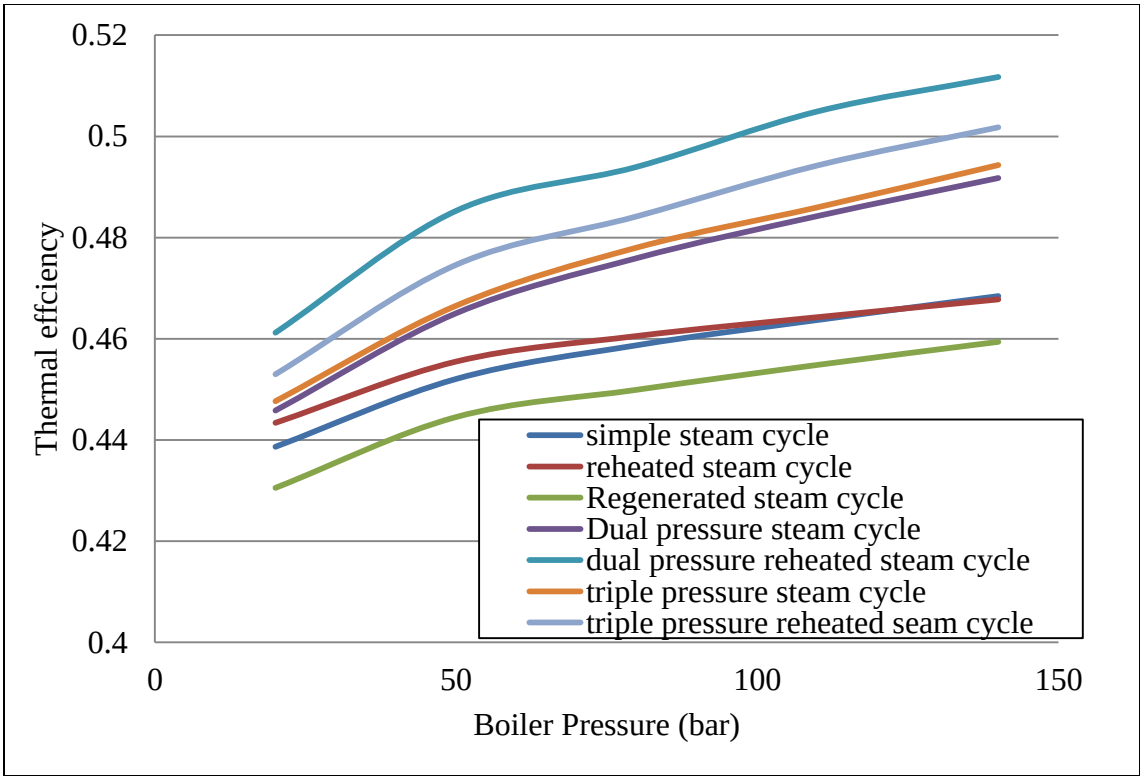

Figure 4.26 Boiler pressures' effect on the thermal efficiency of combined cycles of simple gas turbine and different steam turbines

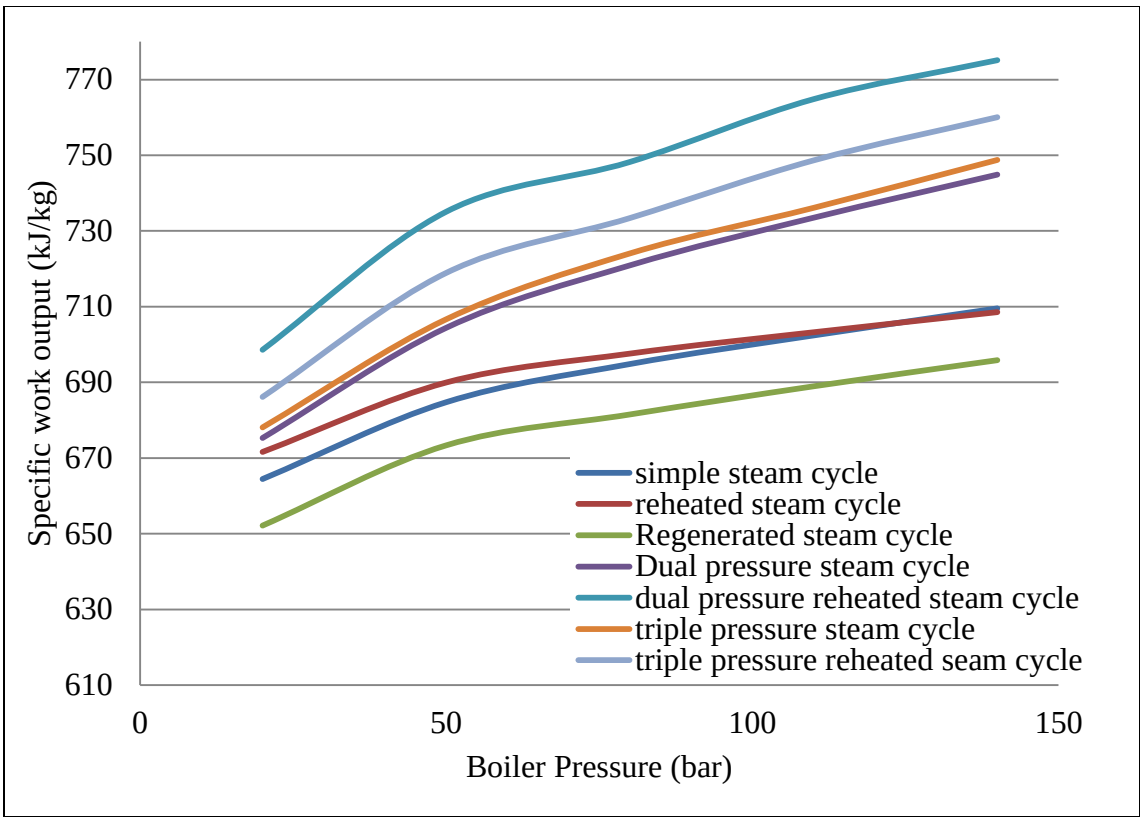

Figure 4.27 Boiler pressures' impact on the specific work output of combined cycles of simple gas turbine and different steam turbines

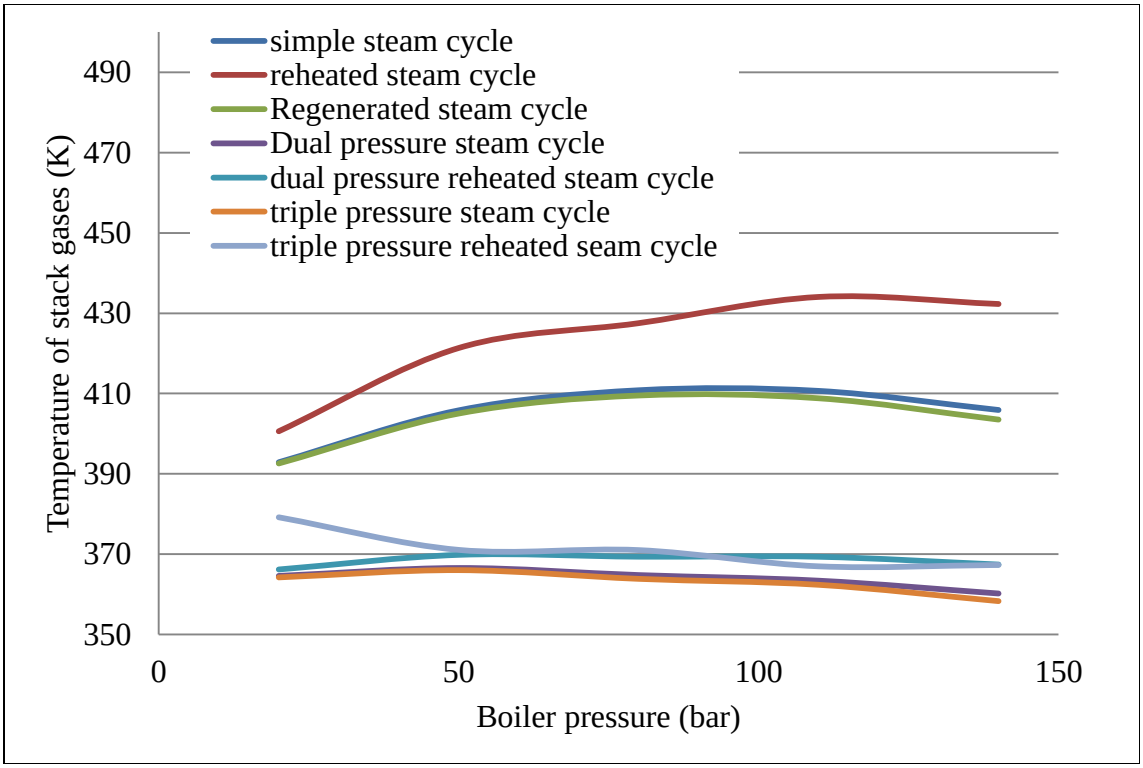

Figure 4.28 The effect of boiler pressure on temperature of stack gases of combined cycles of simple gas turbine and different steam turbines

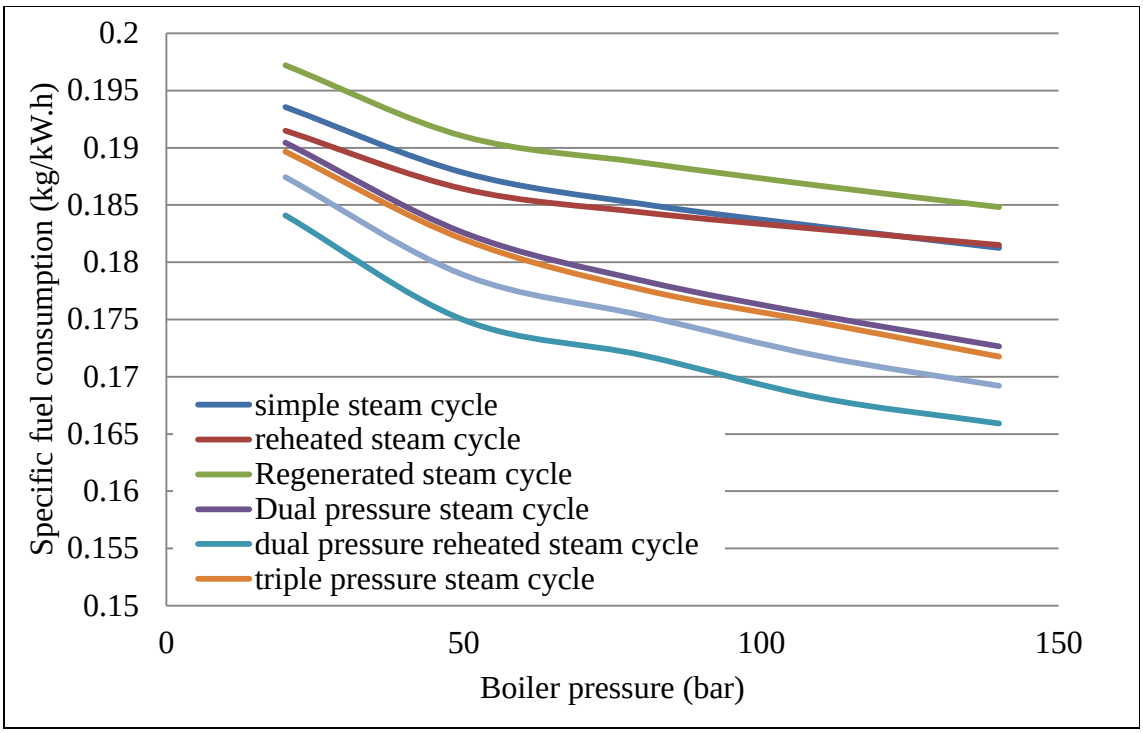

Figure 4.29 The effect of boiler pressure on the specific fuel consumption of combined cycles of simple gas turbine and different steam turbines

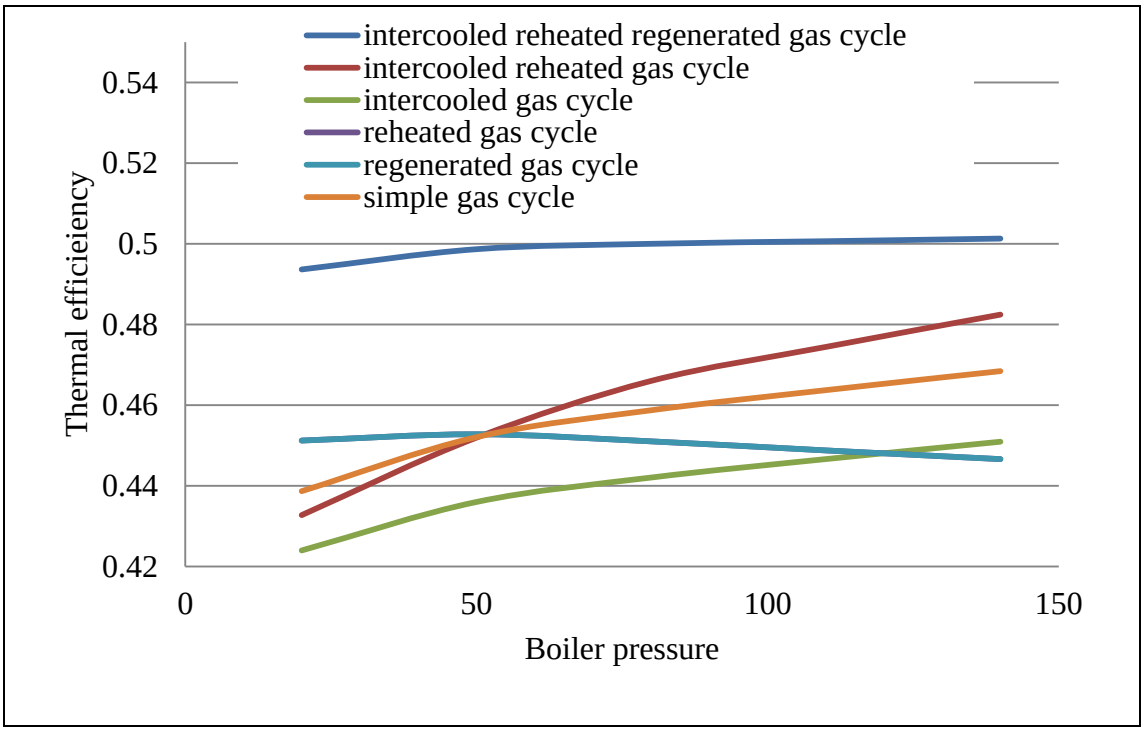

Figure 4.30 The effects of boiler pressure on the thermal efficiency of combined cycles with different gas turbines and simple steam turbine

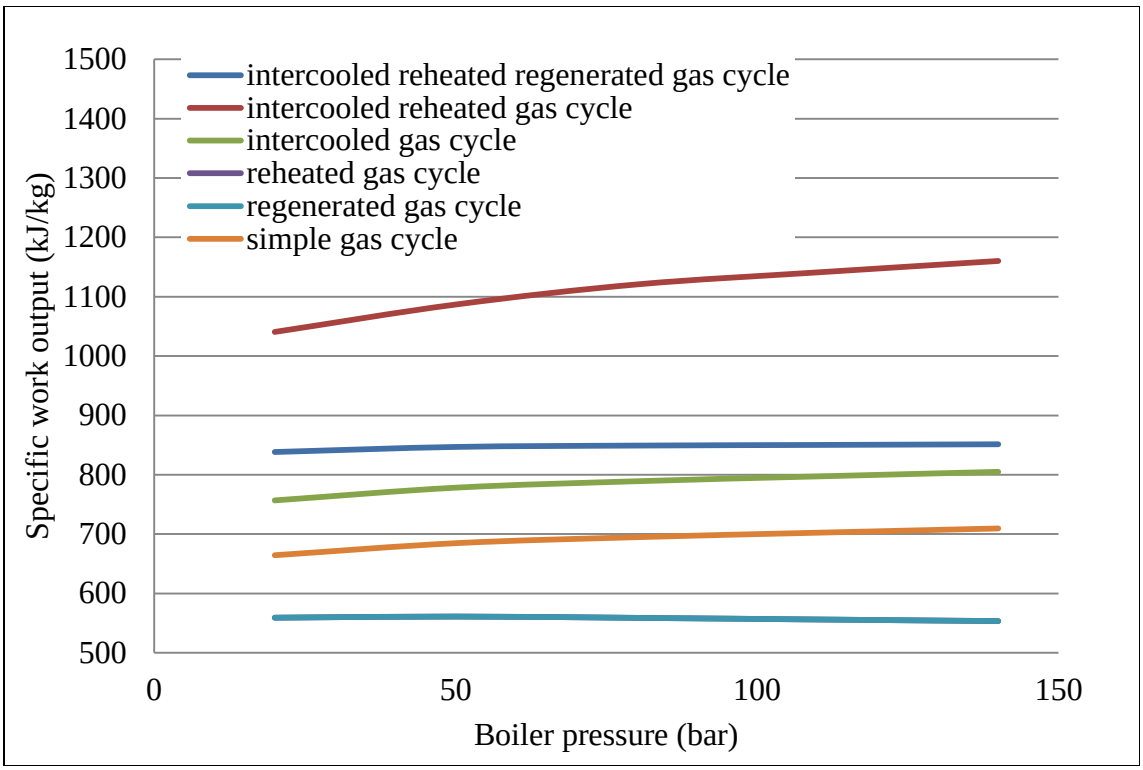

Figure 4.31 Boiler pressures' effects on the specific work output of combined cycles with different gas turbines and simple steam turbine

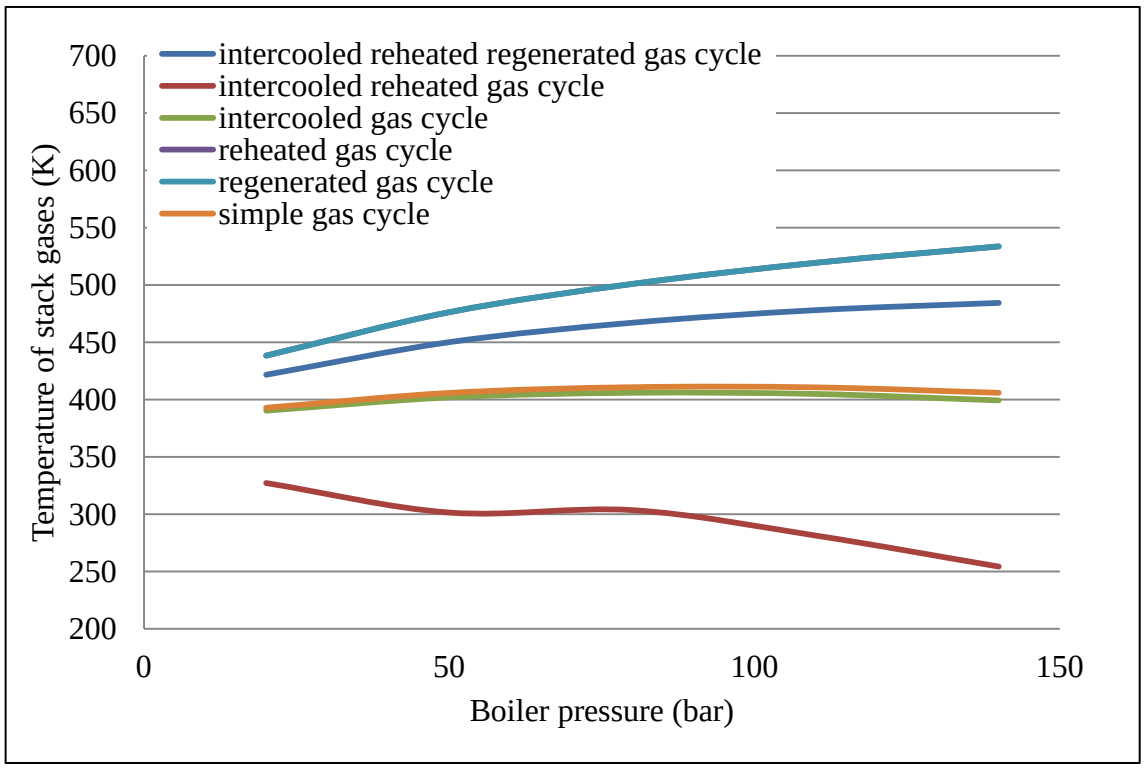

Figure 4.32 Boiler pressures' effects on the temperature of stack gases of combined cycles with different gas turbines and simple steam turbine

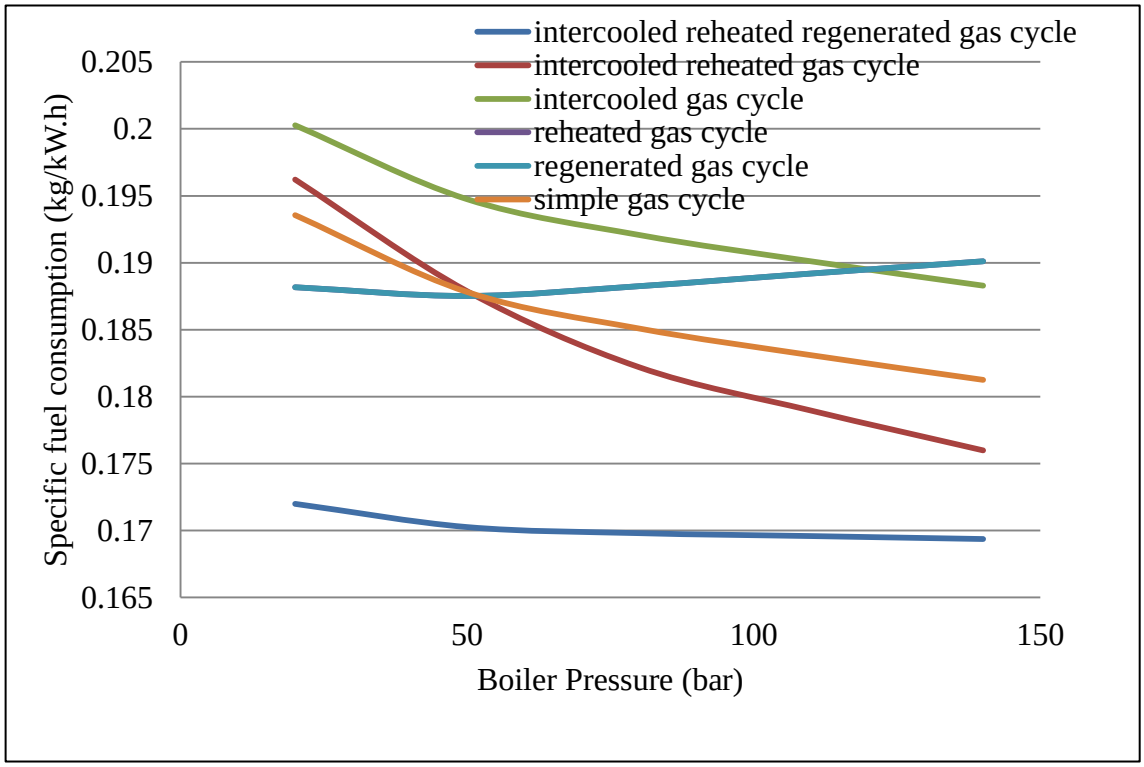

Figure 4.33 The effect of boiler pressure on the specific fuel consumption of combined cycles with different gas turbines and simple steam turbine

4.4.2.2 The pressure of steam condensation (P_{s4} or P_c)

This section investigates the impact of the steam pressure through the condenser (P_c) on the performance of different combined power cycles. The pressure of the steam at boiler inlet (P_b) or the high pressure in multi pressure steam cycles is kept constant. Initially, it studies condenser pressure effect on the performance of the combined cycle configurations that use simple gas turbine and different steam turbines. Later, it discusses such effect on the performance of combined cycle configurations that uses different gas turbines and simple steam turbine. The impact of steam pressure at condenser on the thermal efficiency and the specific work output is shown by the following figures. Generally, the reduction in (P_c) of any steam cycle increases its efficiency and its specific work output for constant temperature and pressure of steam at turbine inlet. In such case, the change in (Pc) affects the pressure of the water at boiler inlet only. For a certain (Pc) keeping the desired quality of the steam at turbine outlet may require changing the pressure or the temperature of steam at turbine inlet. The following figures show similar effects of (Pc) on the thermal efficiency and the specific work output of all cycles.

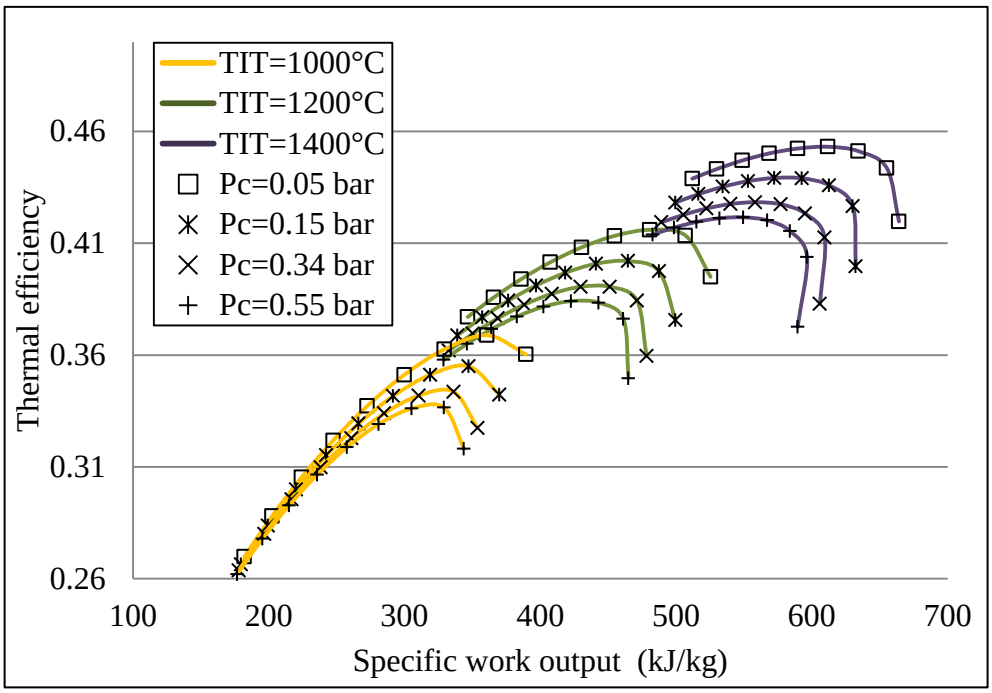

Figure 4.34 The effect of condenser pressure on specific work output and thermal efficiency of simple gas turbine simple steam turbine combined cycle

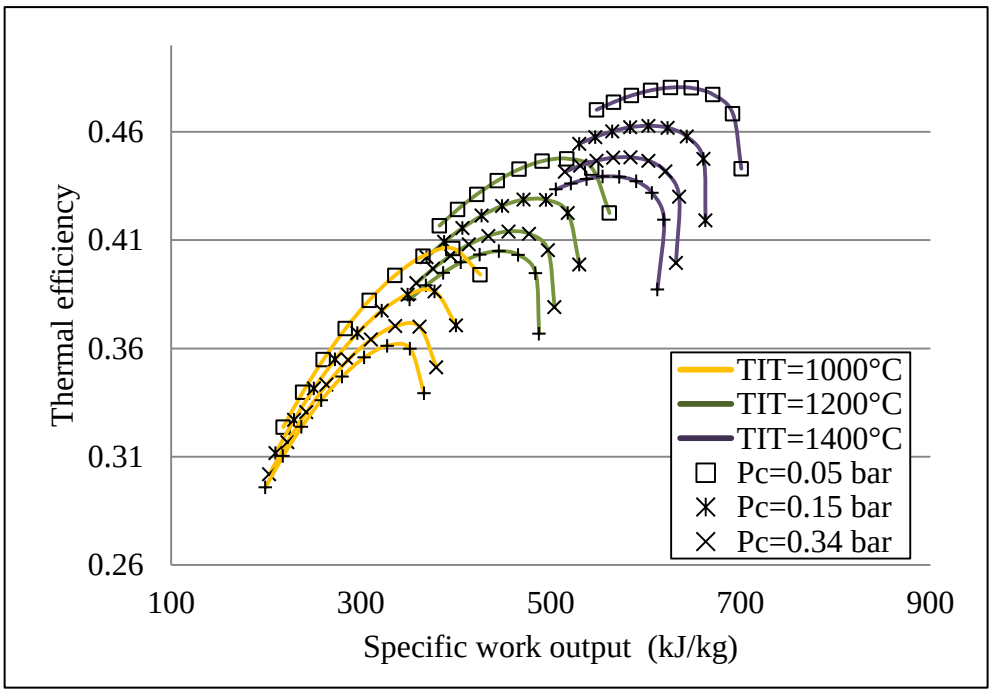

Figure 4.35 The effect of condenser pressure on the specific work output and the thermal efficiency of simple gas turbine dual pressure steam turbine combined cycle

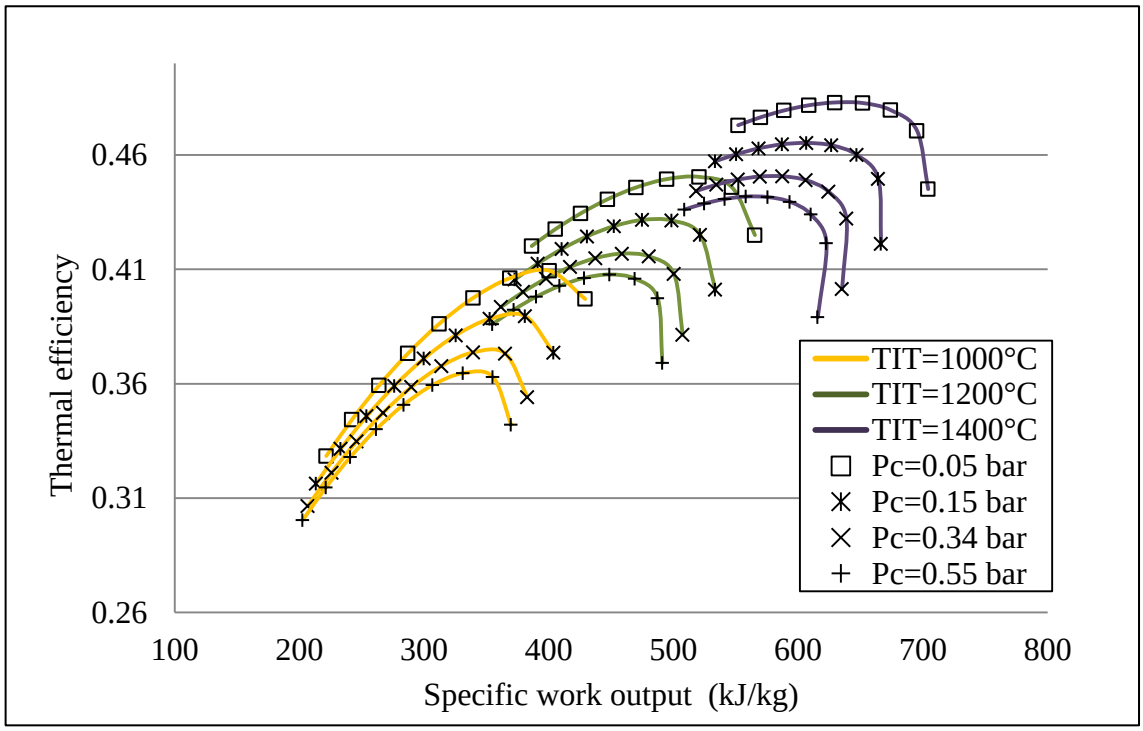

Figure 4.36 The effect of condenser pressure on the specific work output and the thermal efficiency of simple gas turbine triple pressure steam turbine combined cycle

These figures show that the reduction in (Pc) increases the efficiency and the specific work output for fixed (r) and (TIT). This increase reduces for the engine that uses high pressure ratio and low turbine inlet temperature. Over a certain range of (TIT)s such increase in the thermal efficiency and the specific work output becomes greater for the engine that uses low pressure ratio.

The impact of (P_c) on the temperature of stack gases and the (SFC) is shown by the following figures. It considered the combined cycle that uses simple gas turbine and different steam turbines. The effect of (P_c) is similar for all combined cycle configurations, but the value of the change differs from a configuration to another. The reduction in (P_c) always leads to a drop in (SFC) and the temperature of stack gases. This drop is influenced by the change of the (r) and (TIT). The effect of (P_c) is the smallest for the combined cycles that uses high pressure ratio gas turbine engines and it became less effective by the increase in (TIT)s.

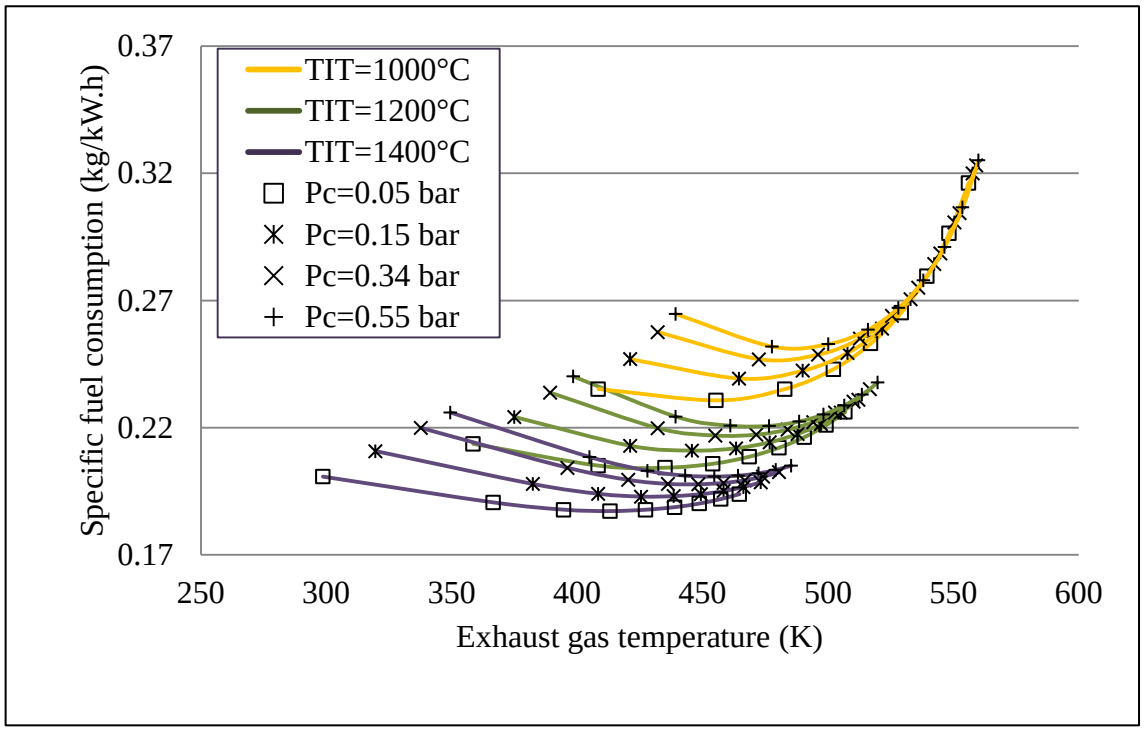

Figure 4.37 The effect of condenser pressure on the temperature of stack gases and the specific fuel consumption of simple gas turbine reheated steam turbine combined cycle

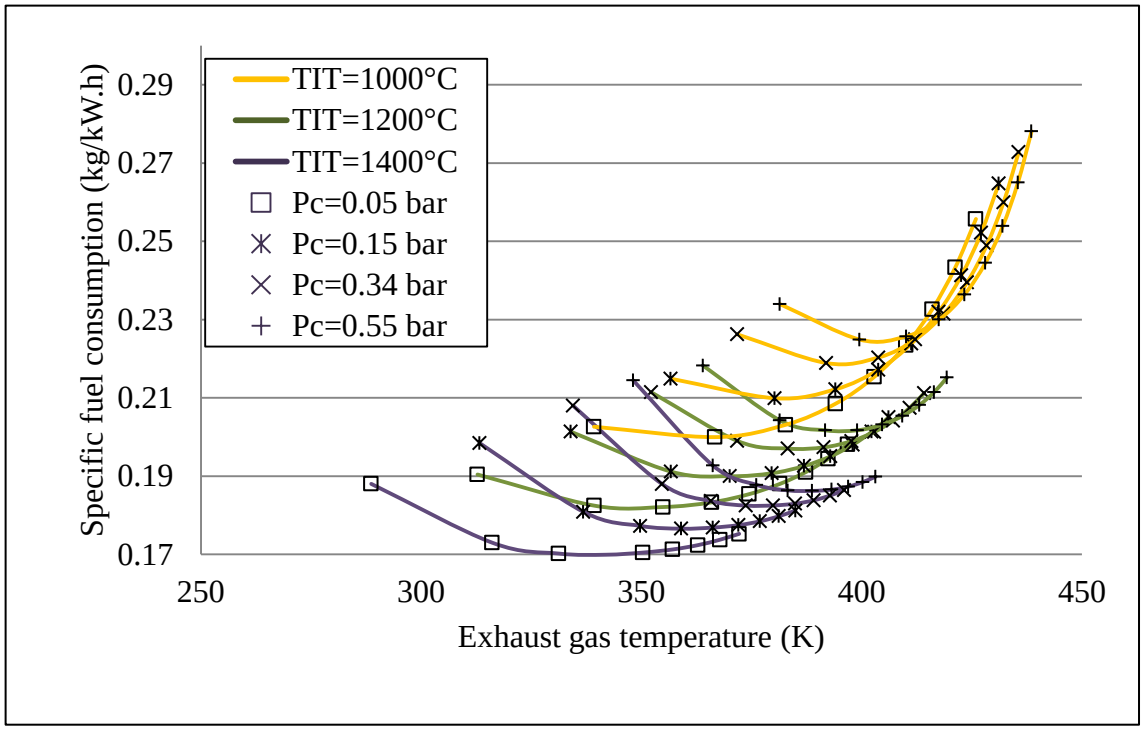

Figure 4.38 The effect of condenser pressure on the temperature of stack gases and the specific fuel consumption of simple gas turbine dual pressure reheated steam turbine combined cycle

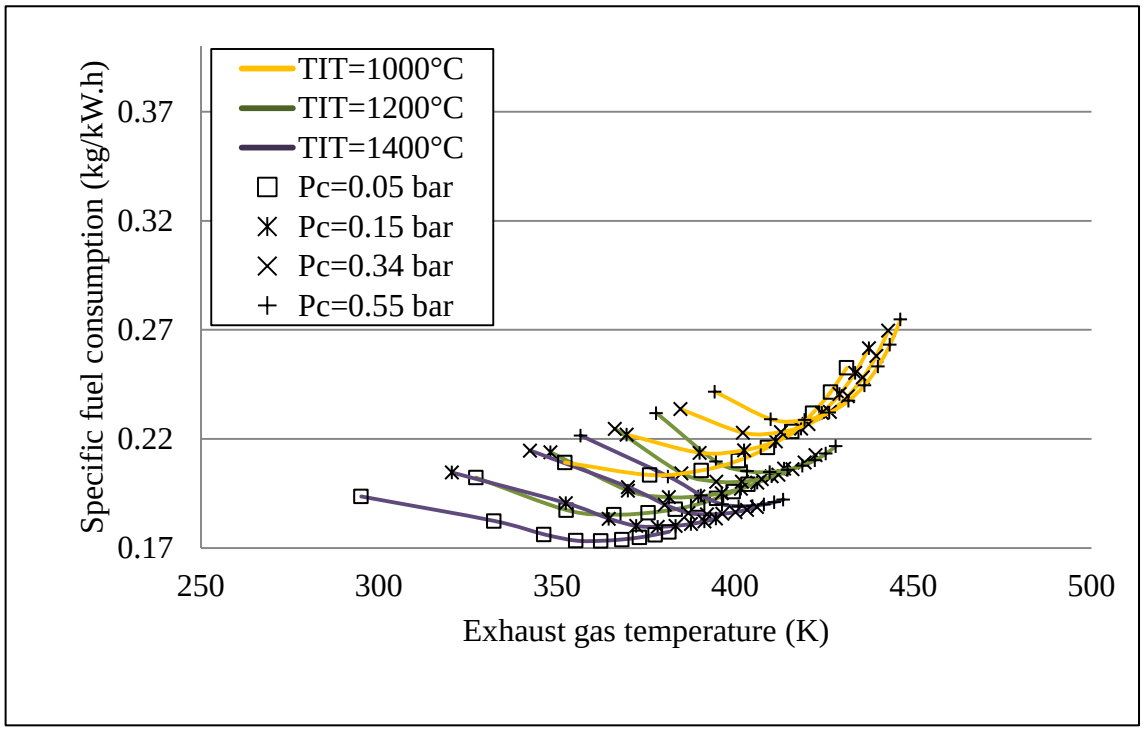

Figure 4.39 The effect of condenser pressure on the temperature of stack gases and the specific fuel consumption of simple gas turbine triple pressure reheated steam turbine combined cycle

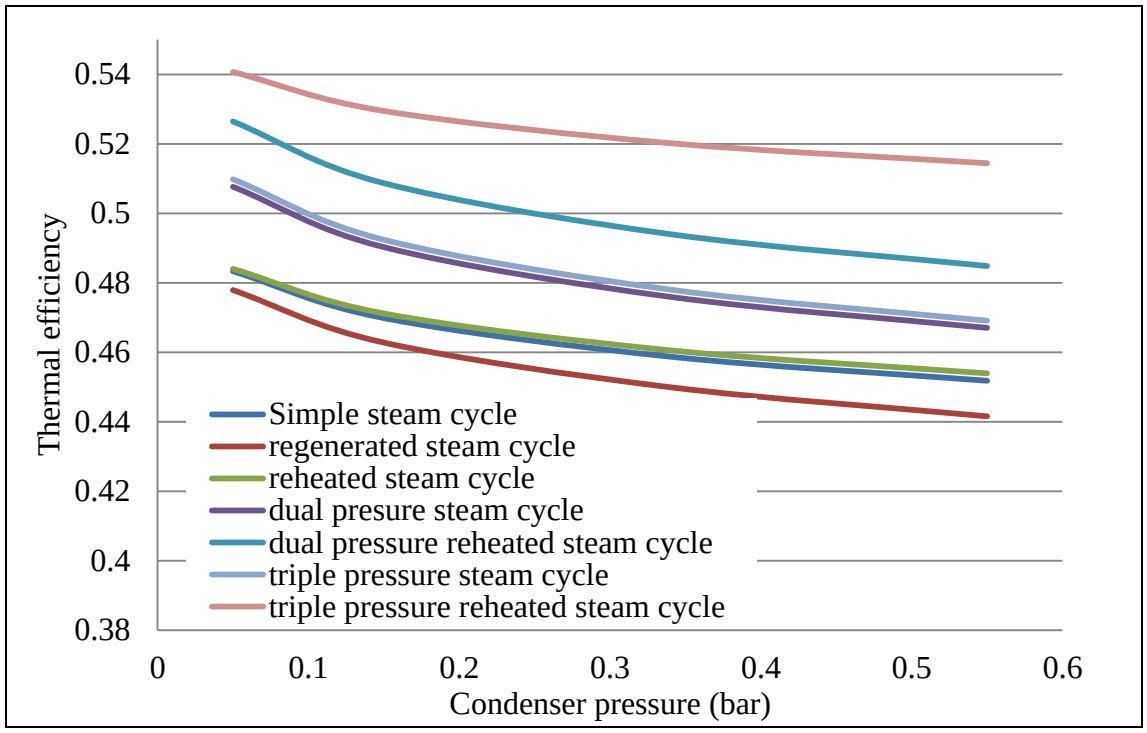

Figure 4.40 The effect of condenser pressure on the thermal efficiency of combined cycles with simple gas turbine and different steam turbines combined cycles

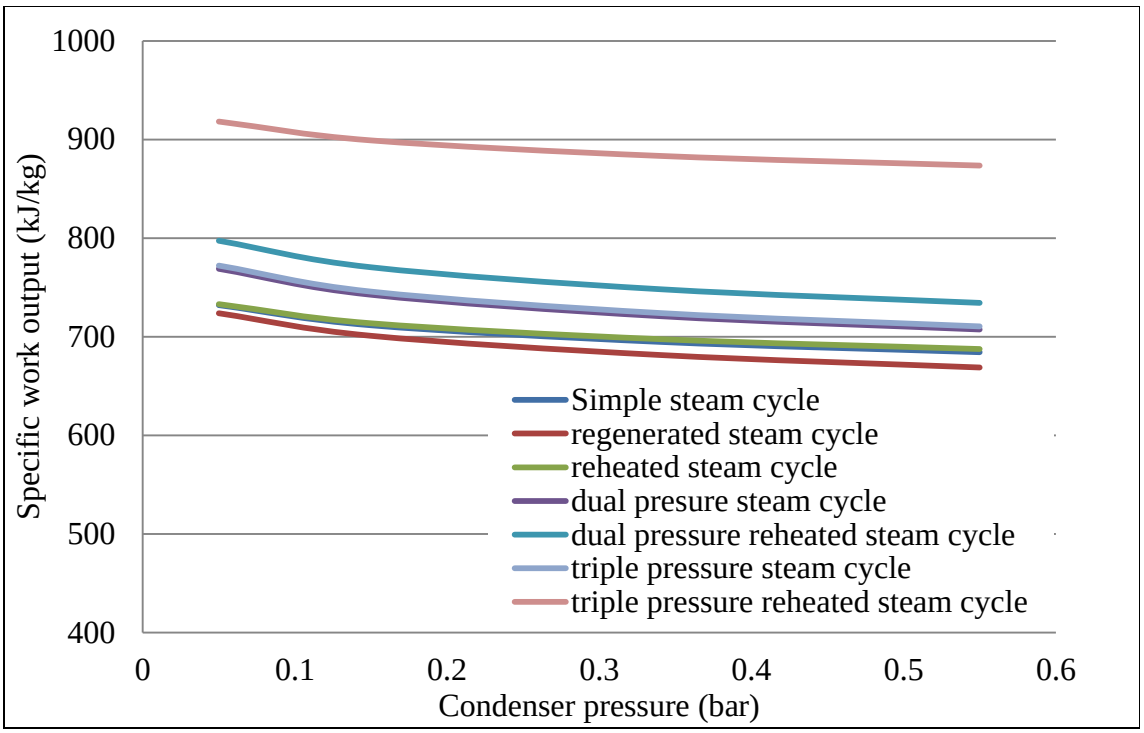

Figure 4.41 The effect of condenser pressure on the specific work output from simple gas turbine cycle and different steam turbine combined cycles

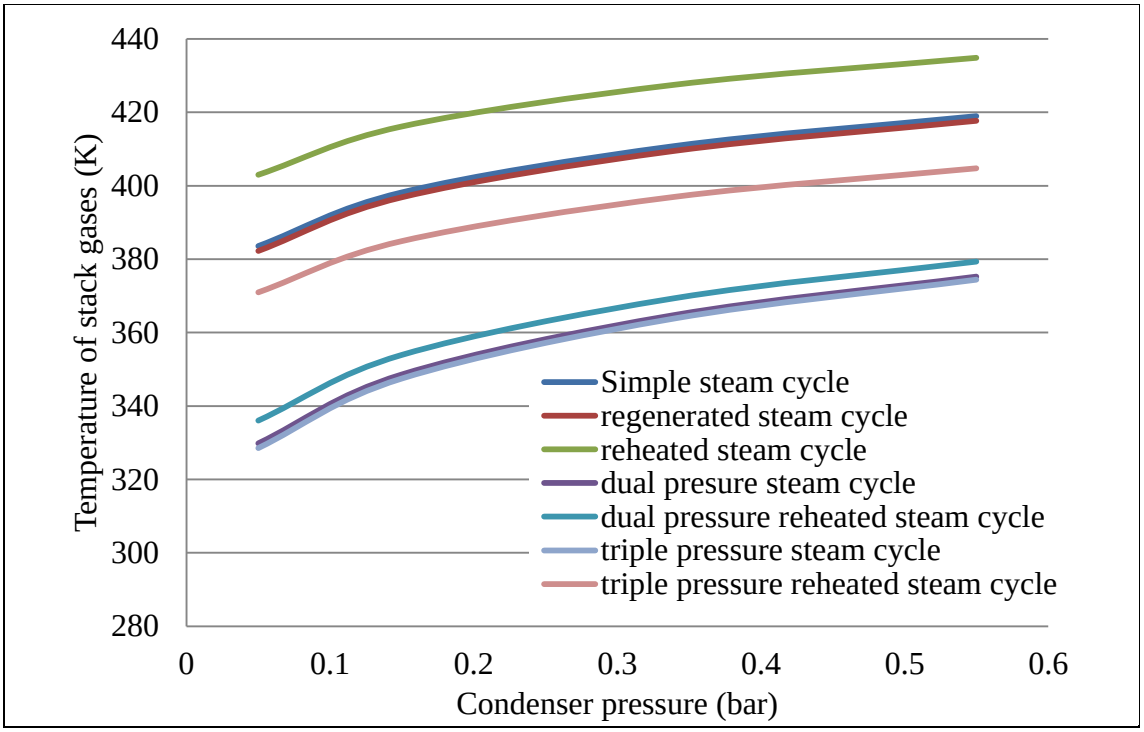

Figure 4.42 The effect of condenser pressure on the temperature of stack gases in simple gas turbine combined with different steam turbines

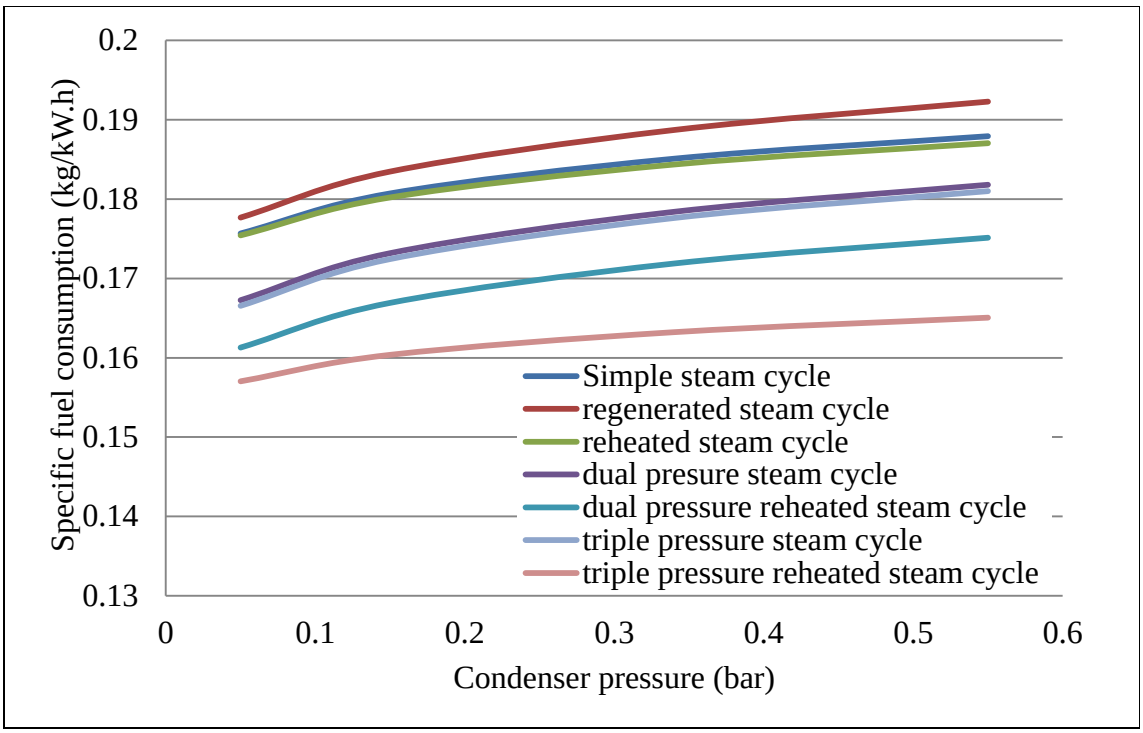

Figure 4.43 The effect of condenser pressure on the specific fuel consumption of simple gas turbine cycle combined to different steam turbines

The effect of (P_c) on the performances of the combined cycle of a simple gas turbine and different steam turbines are illustrated in Figs.4.40 – 4.43. The simple gas turbine engine was assumed to be designed to work on (TIT) of 1600ºC and (r) of 24. The figures show a very close effect on combined cycles with different steam cycles. The major effect (increase) in the thermal efficiency and specific work output was for dual pressure reheated steam turbine combined cycle. By which the reduction of (P_c) from (0.55bar) to (0.05bar) increased the thermal efficiency and the specific work output by (4%) and (8.6%) respectively. The heaviest effect (reduction) on the temperature of stack gases appears was pressure steam turbines combined cycle by 14%. The main effect (reduction) on specific fuel consumption was regenerated steam turbine cycle which droped by 7.6%. The minimum effect on the efficiency, the specific work output and the temperature of stack gases by (P_c) was for regenerated steam turbine combined cycle. The slightest effect on specific fuel consumption was for triple pressure reheated steam turbine combined cycle.

The same comparison was employed on different gas turbine turbines combined to simple steam turbine as illustrated by the following figures. The major effect of the (P_c) on the efficiency, the specific work output and the temperature of stack gases was for reheated gas turbines combined. In which, of condensation pressure from (0.55bar) to (0.05bar) increased

the thermal efficiency and the specific work output of the combined cycle by 4% and 8.4% respectively. The temperature of stack gases was decreased by about 25.5% due to such change. The major reduction in the specific fuel consumption was for reheated gas turbine combined cycle. A reduction of 7.2% was recorded by the drop of (P_c) from (0.55bar) to (0.05bar). The slightest effect of the (P_c) on the efficiency, the specific work output and the temperature of stack gases was for triple pressure steam turbine combined cycle. The slightest effect on the temperature of stack gases was made by reheated steam turbine combined cycle.

The results show that the major effect of (P_c) on the efficiency and specific work output of reheated gas turbine dual pressure steam turbine combined cycle. But the major effect on the temperature of stack gases appears on reheated gas turbine triple pressure steam turbine combined cycle. The greatest effect of (P_c) on (SFC) is made by intercooled reheated gas turbine regenerated steam turbine combined cycle.

The results here match the results of Al- Qur'an [25], in which the impact of P_C on the previous characteristics is restricted by the quality of the steam at turbine outlet.

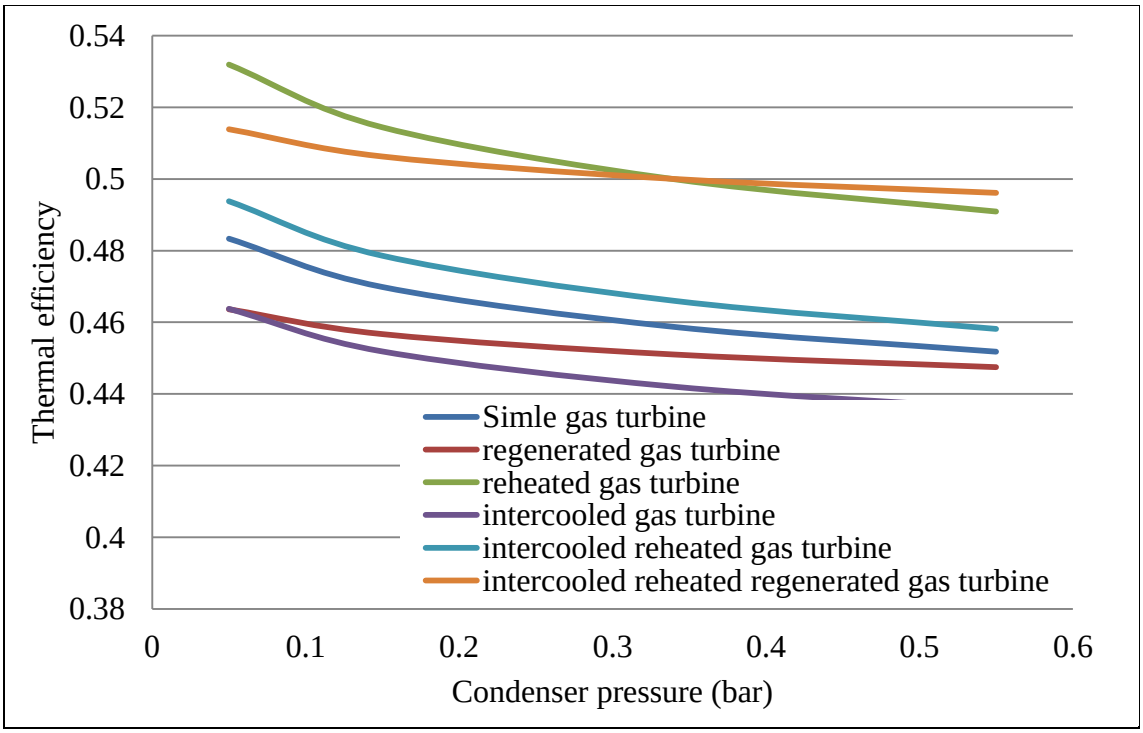

Figure 4.44 The effect of condenser pressure over thermal efficiency of combined cycles with different gas turbine cycles and simple steam cycle

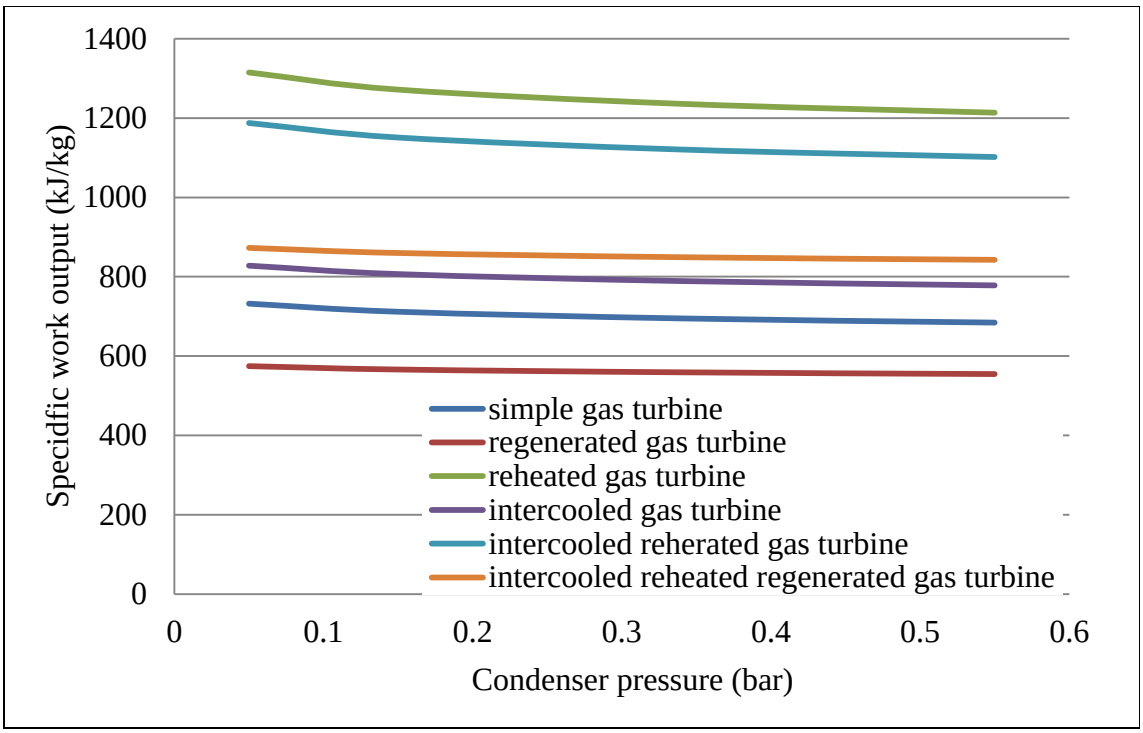

Figure 4.45 The effect of condenser pressure over specific work output of combined cycles with different gas turbine cycles and simple steam cycle

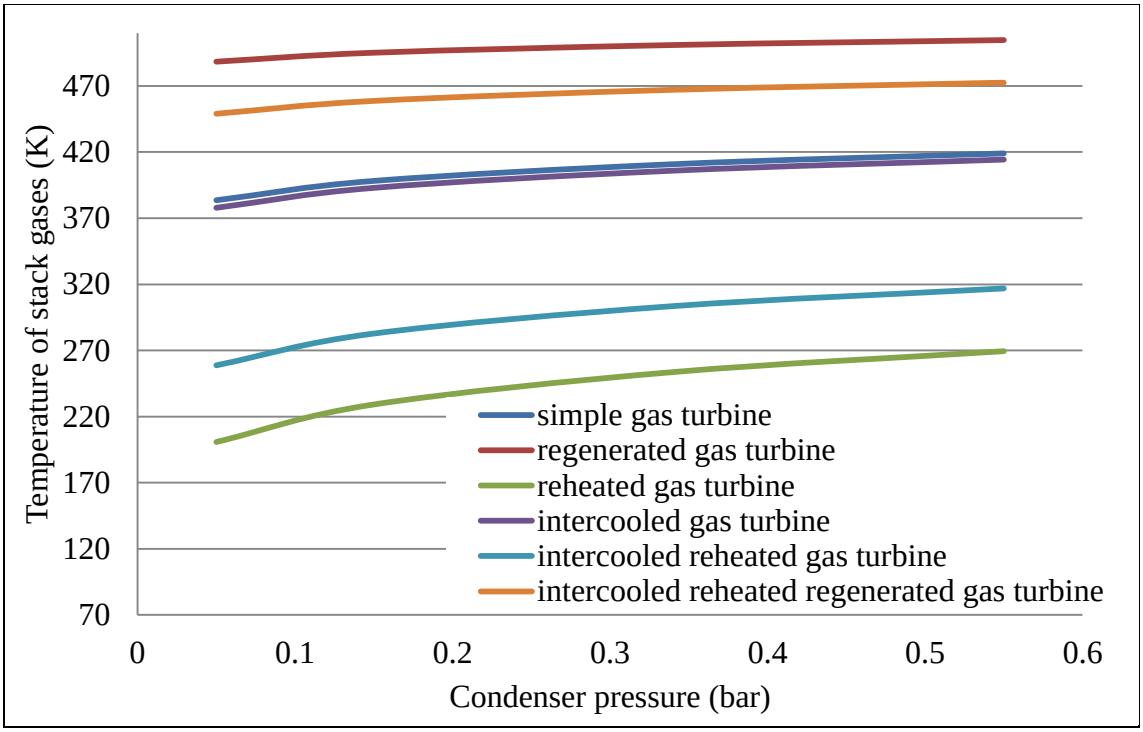

Figure 4.46 The effect of condenser pressure over stack temperature of combined cycles with different gas turbine cycles and simple steam cycle

4.4.2.3 Steam quality at steam turbine outlet (X_{s4})

Analytically, the quality of steam at steam turbine outlet was affected by several operating parameters of steam and gas cycles. The most effective parameters on steam quality were: the boiler pressure, the condenser pressure and the steam temperature at turbine inlet.

The steam quality was deteriorated by the increase of boiler pressure for certain condenser pressure and steam turbine inlet temperature. A similar result was generated by the reduction of condenser pressure for a constant boiler pressure and steam turbine inlet temperature. While a better steam quality was generated by fixing the pressure of condenser and boiler and the increase of the steam temperature at turbine inlet. This increase was governed by many parameters, including: gases temperature at HRSG inlet, the effectiveness of HRSG components and the mass flow rates of each stream and its fractions to the main stream in multi pressure steam cycles.

The increase of temperature of the gases from the turbine outlet was accomplished by employing different gas turbine cycle parameters. Furthermore, the increase of such temperature was differnt from a configuration to another (as discussed before).

Generally, the temperature of gases at turbine outlet was increased by the rise of gas inlet temperature and decreased by applying large pressure ratios. There was an exception to such a role by regenerated gas turbine cycle. According to that, gases' temperature was dropped to a specified pressure ratio over which the temperature was increased continuously.

Under a certain turbine inlet temperature, the heaviest effect on turbine outlet temperature by the increase in pressure ratio has been manifested by reheated gas turbine cycle. Therefore, it had the heaviest effect on the change in steam quality. Applying reheated gas cycles improved steam quality over wider range. Introducing intercooling made no changes to gases temperature at turbine outlet, thus it had no effect on steam quality. This was because the effect of intercooling occurs on air before combustion only. On the other hand, the pressure drops made a very small change.

The slightest effect on gases temperature at gas turbine outlet and steam quality was for intercooled reheated regenerated gas turbine cycle. However, the effect of the above parameters on the temperature of the gases at turbine outlet was always governed by resure of the steam at boiler and condenser.

4.4.2.4 Minimum pinch point temperature difference(ΔT_{ppm})

This section discusses the effect of changing the pinch point temperature difference on the performance of different combined power cycles. It analyses such effect for each unit of the HRSG and evaluates the impact on the boiler for several boiler configurations.

This investigation covered a range of ΔT_{ppm} chosen with respect to thermodynamic and economic considerations. This impact was similar on the performance of classic boiler units combined power cycles. In such units, steam quality required for turbine inlet was not affected.

In general, the increase of the minimum pinch point temperature difference (ΔT_{ppm}) decreased the thermal efficiency of the steam cycle. The thermal efficiency of combined power cycles was affected similarly by such parameter, which increased by the drop in turbine inlet temperature.

The effect of (ΔT_{ppm}) on the performance of simple steam turbine combined cycle is illustrated by Figs. 4.47 - 50. Such figures confirmed (ΔT_{ppm}) slight effect on the performance combined power cycle. This was clear on the slight change of the thermal efficiency, and the slighter changes in the specific work output and the specific fuel consumption. On the other hand, such increase in the minimum pinch point temperature difference led to a moderate increase in the temperature of stack gases. The rise in the temperature of the stack gases was dropped by the increase in (TIT). The change of (ΔT_{ppm}) from 10 to 25 °C was very slight on the performance simple steam generator combined cycle.

The maximum decrease in the efficiency by such effect was 1 percentage point, while the maximum decrease in the specific work output was over 0.7 %. On the other hand, the largest increase in the specific fuel consumption and the temperature of stack gases were less than 5.5%.

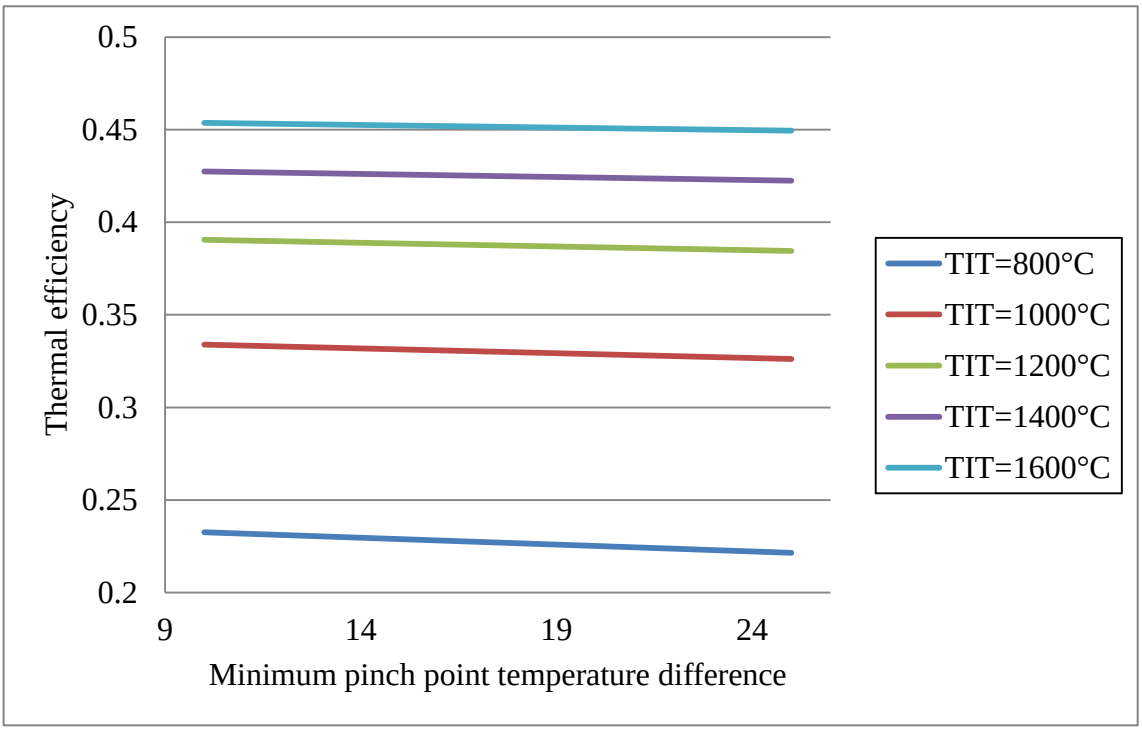

Figure 4.47 The effect of (ΔT_{ppm}) on the thermal efficiency of simple gas turbine / simple steam turbine combined cycle

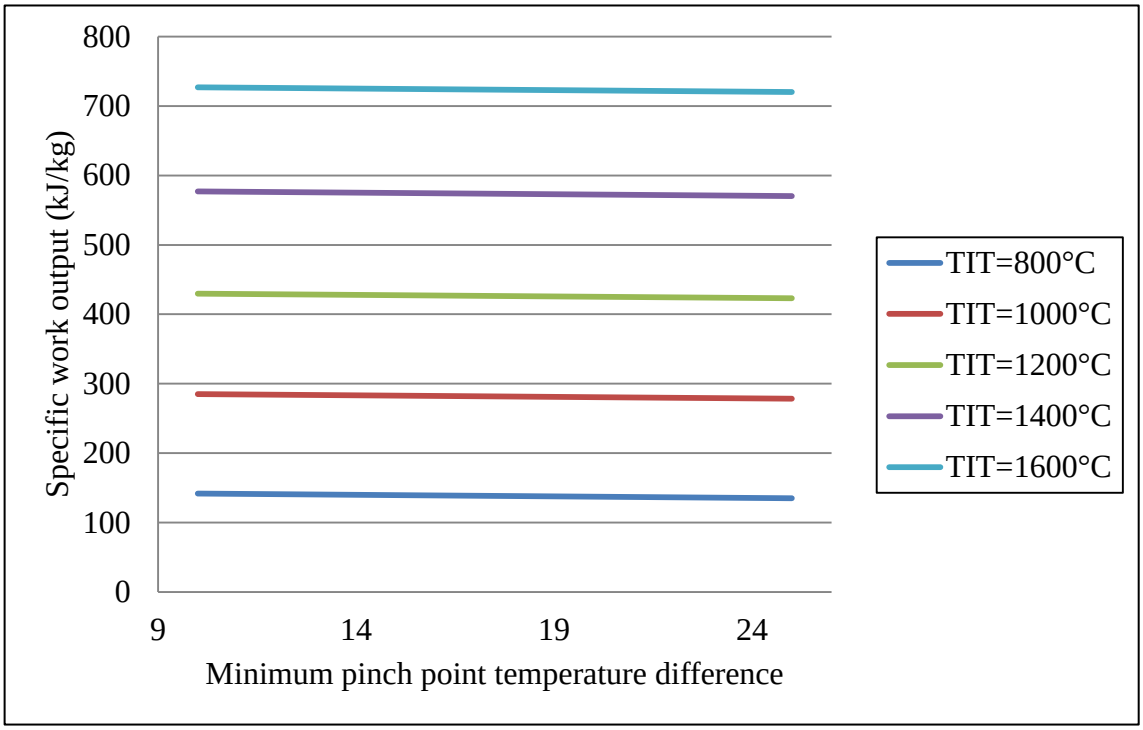

Figure 4.48 The effect of (ΔT_{ppm}) on the specific work output of simple gas turbine simple steam turbine combined cycle

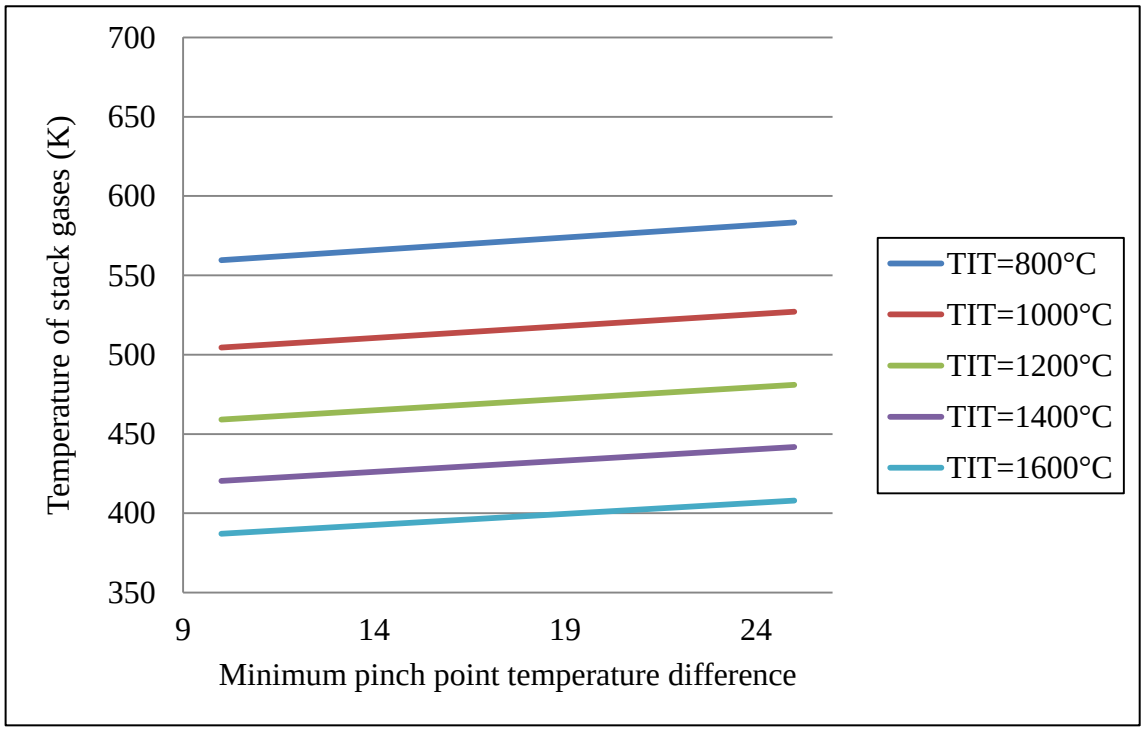

Figure 4.49 The temperature of stack gases versus (ΔT_{ppm}) of simple gas turbine/ simple steam turbine combined cycle

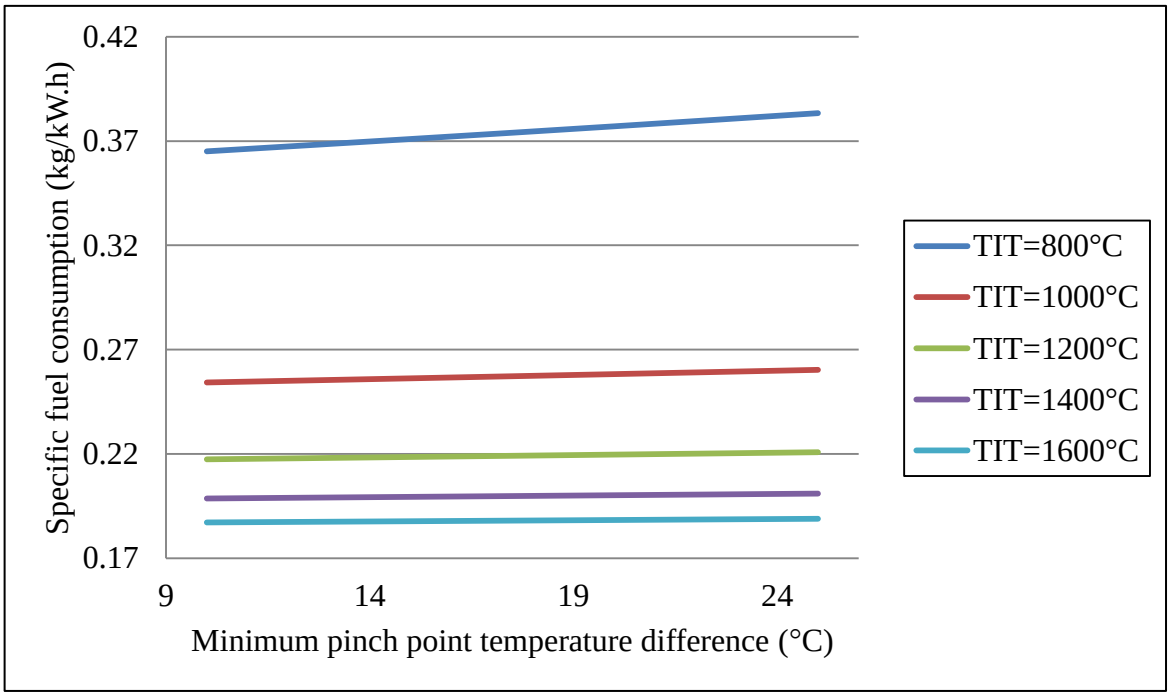

Figure 4.50 The specific fuel consumption versus (ΔT_{ppm}) of simple gas turbine simple steam combined cycle

The following discusses the impact of (ΔT_{ppm}) on the performance of combined cycle that uses multi pressure heat recovery steam generator. It draws the changes in the performance of the power cycles by such effect on each unit separately and all together.

The steam at high pressure and low pressure units were affected by such parameter in dual pressure heat recovery steam generator. The effect on the performance of simple gas turbine dual pressure steam turbine (SGDPSCC) by such parameter is observed by the figures below. The effect of (ΔT_{ppm}) on the performance of combined cycle that uses dual pressure reheated steam generator was similar but of different values. Therefore, it will be enough to discuss the performance of (SGDPSCC) only.

The effects of (ΔTppm) for high and low pressure units were identical on the thermal efficiency. Consequently, the largest change in thermal efficiency was for the (ΔTppm) of both units, Fig. 4.51. This effect was larger at low pressure unit than high pressure unit of reheat HRSG.

The effect of (ΔT_{ppm}) on the specific work output from such cycles was slighter than that on the thermal efficiency as illustrated by Fig. 4.52. This effect was nearly the same for the three previous cases. The change in the temperature of stack gases by the effect of (ΔT_{ppm}) was illustrated by Fig. 4.53. It shows that the temperature of stack gases was more affected by the change in (ΔT_{ppm}) of low pressure unit than the high pressure unit. The maximum effect of (ΔT_{ppm}) was made by changing the (ΔT_{ppm}) of both units. The specific fuel consumption was decreased slightly by the increase of (ΔT_{ppm}), as shown by Fig. 4.54. The specific fuel consumption in such figure was identically changed and the effect of both units was the maximum.

The results from the parametric study reviled that, the thermal efficiency of such cycles was maximally decreased by about 1% when the (ΔTppm) was increased from 10°C to 25°C. The temperature of stack gases and the specific fuel consumption were increased by 4.5% approximately, due to such increase in (ΔTppm). The maximum change in the specific work output was less than 1% due to the similar rise in (ΔTppm).

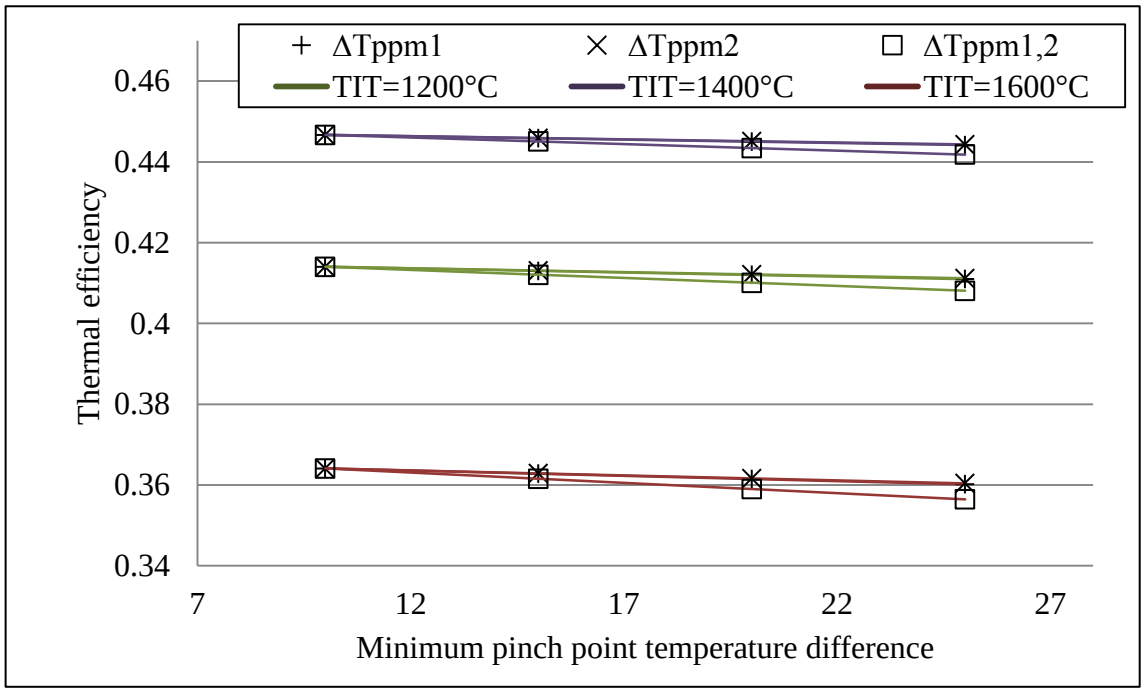

Figure 4.51 The effect of (ΔT_{ppm}) on thermal efficiency of combined cycle with dual pressure steam generator

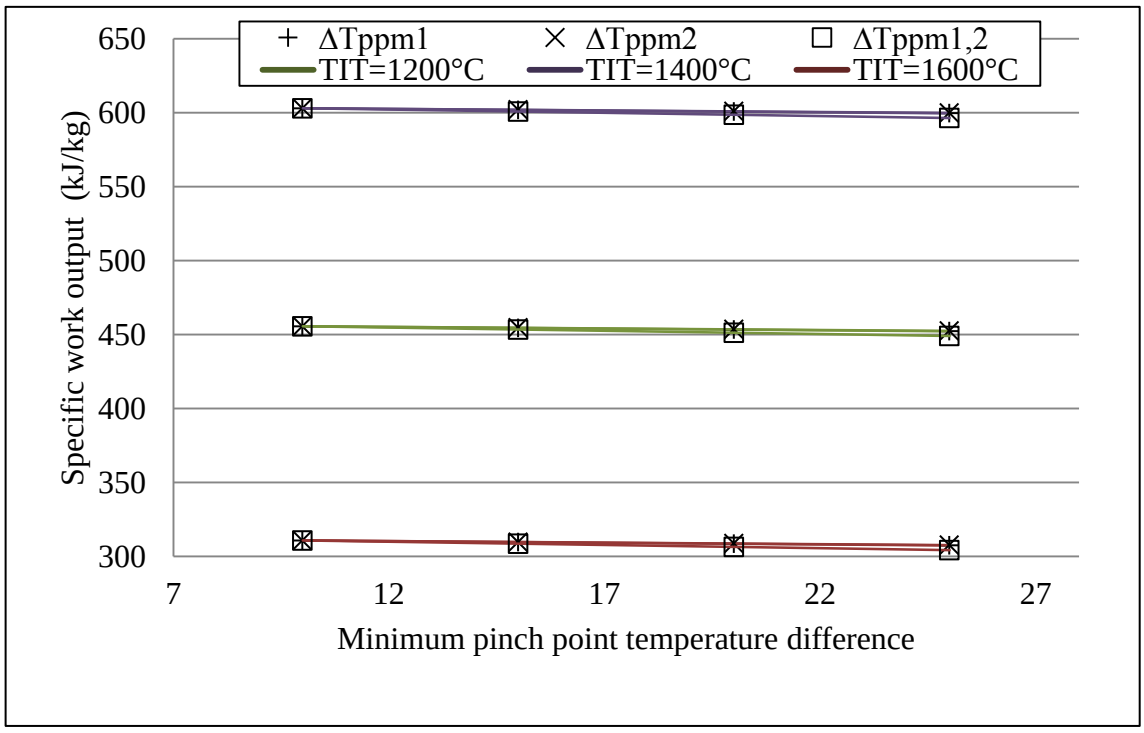

Figure 4.52 The effect of (ΔT_{ppm}) on specific work output of combined cycle with dual pressure steam generator

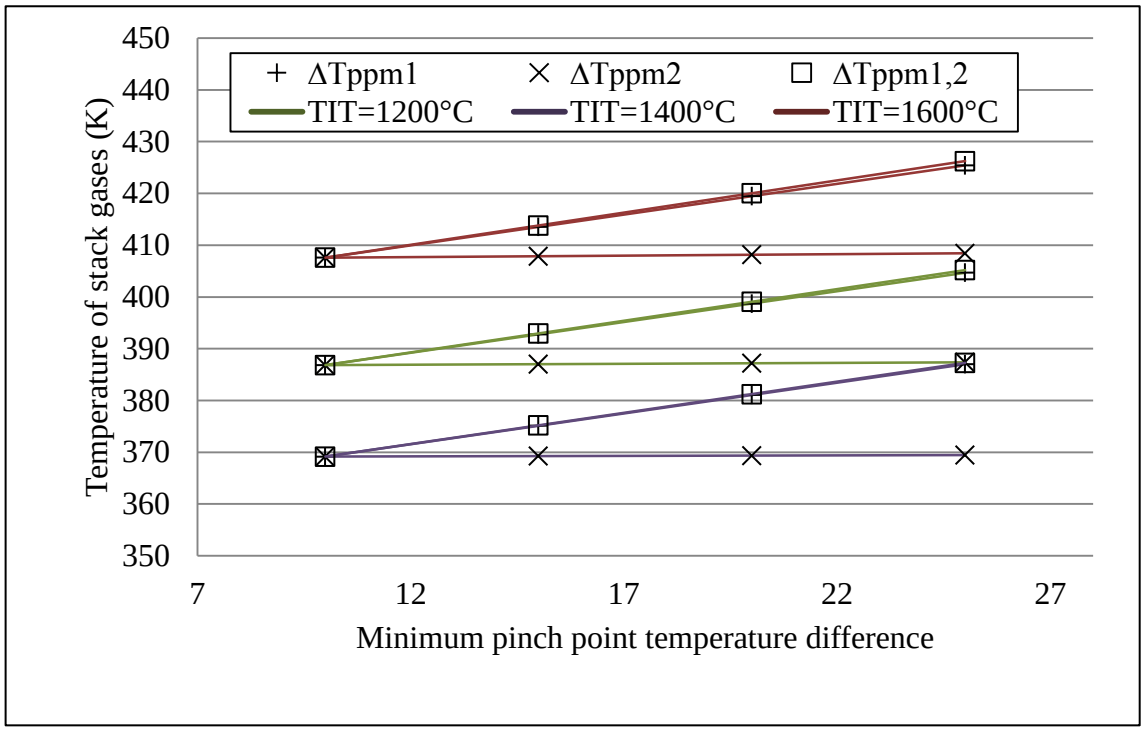

Figure 4.53 The effect of (ΔT_{ppm}) on stack temperature of combined cycle with dual pressure steam generator

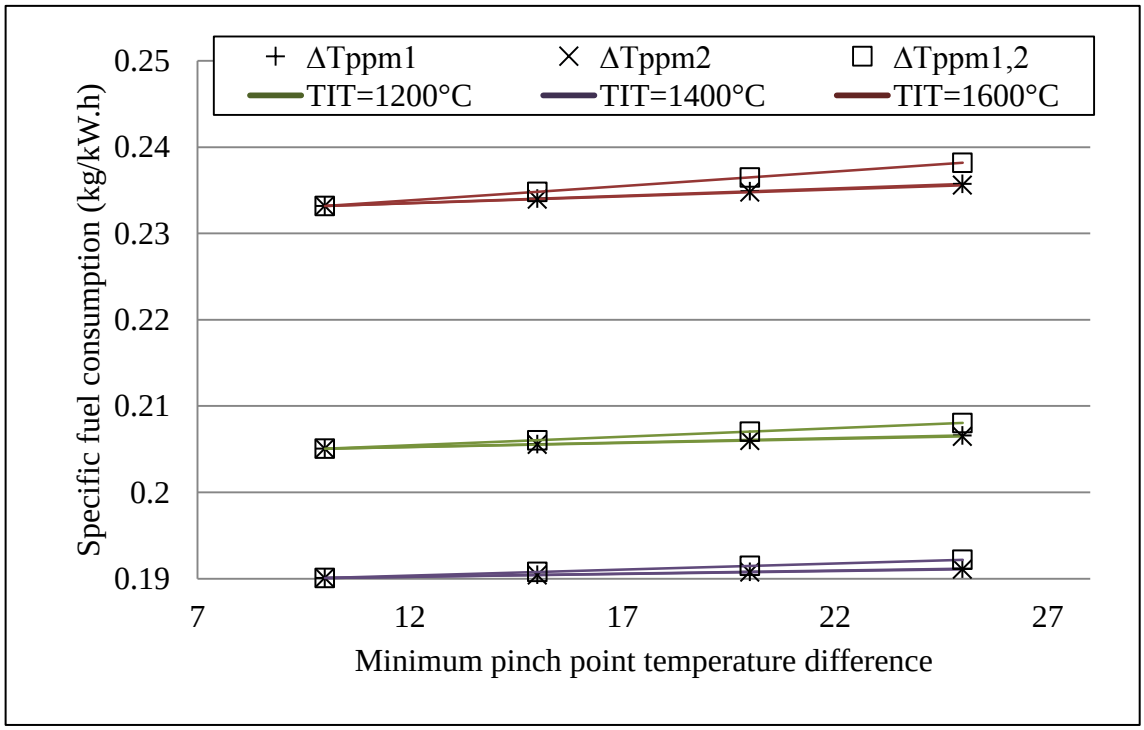

Figure 4.54 The effect of (ΔT_{ppm}) on specific fuel consumption of combined cycle with dual pressure steam generator

The following figures illustrate the impact of the minimum pinch point temperature difference on the performance of triple pressure (HRSG) combined cycle. The influence of ΔT_{ppm} on the efficiency of simple gas turbine triple pressure steam turbine combined cycle (SGTPSCC) is illustrated on Fig. 4.55. It shows that, the variation in the ΔT_{ppm} of all units had the largest change on cycle's thermal efficiency. The ΔT_{ppm} of the intermediate pressure unit had the slightest effect on the thermal efficiency. The ΔT_{ppm} of the low pressure unit had the greatest effect. The specific work output had a very slight effect by such change as illustrated by Fig. 4.56. In here, the slight effect of ΔTppm on performance characteristics resulted from [49] is confirmed by this results.

The change in the ΔT_{ppm} of all (HRSG) units had the maximum effect on the temperature of stack gases, as shown in Fig. 4.57. The ΔT_{ppm} of the intermediate pressure unit had the slightest effect on such temperature. The low pressure unit had the maximum change on such temperature. The specific fuel consumption was increased slightly by the increase of the ΔT_{ppm} as shown in Fig. 4.58. The change in the ΔT_{ppm} of all (HRSG) units made the maximum effect on the specific fuel consumption. The change in the ΔT_{ppm} of the low pressure unit made the greatest effect on the specific fuel consumption. The ΔT_{ppm} of the intermediate pressure unit made the slightest effect on the specific fuel consumption.

The maximum drop in the thermal efficiency by the increase in ΔT_{ppm} from 10°C to 25°C was about 1 percentage point for (SGTPSCC) and (SGTPRehSCC). Similarly, the decrease in the specific work output was less than 1%. While the increases in the specific fuel consumption and the temperature of stack gases was less than 5%. From the above it was concluded that, the temperature of stack gases is the most affect parameter by the influence of ΔT_{ppm} in all configurations. Therefore, it has a very clear impact on the environmental considerations. The effect of ΔT_{ppm} was improved by the increase in (TIT) in different rates for a certain (HRSG) design. This parameter is unimportant for power generation unless there is a significant development gas turbine design. By which, if gases of much higher temperature than nowadays is permitted to pass through the turbine.

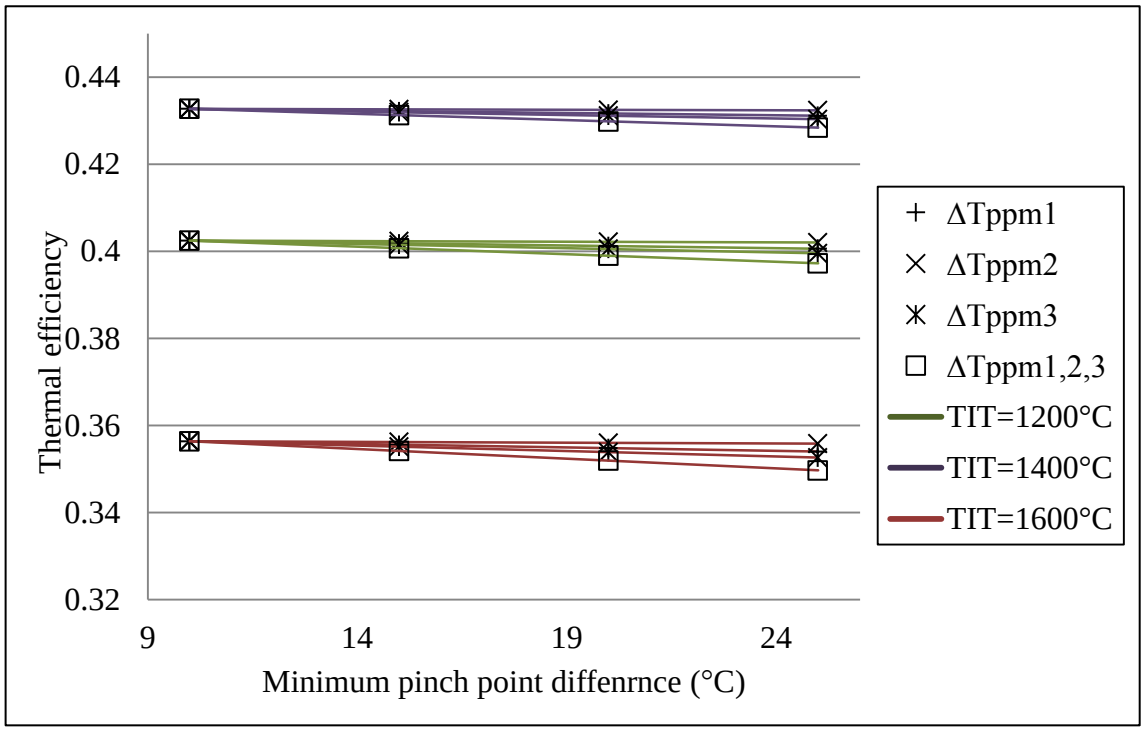

Figure 4.55 The effect of (ΔT_{ppm}) on thermal efficiency of a combined cycle with triple pressure steam generator

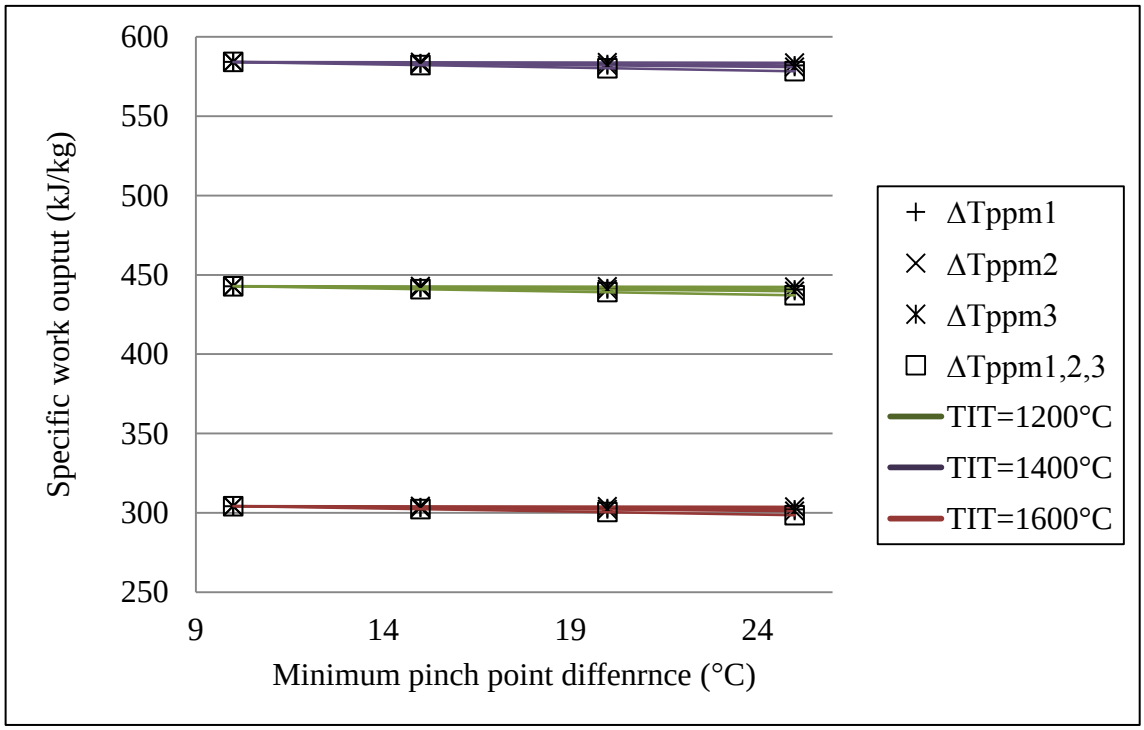

Figure 4.56 The effect of (ΔT_{ppm}) on the specific work output of a combined cycle with triple pressure steam generator

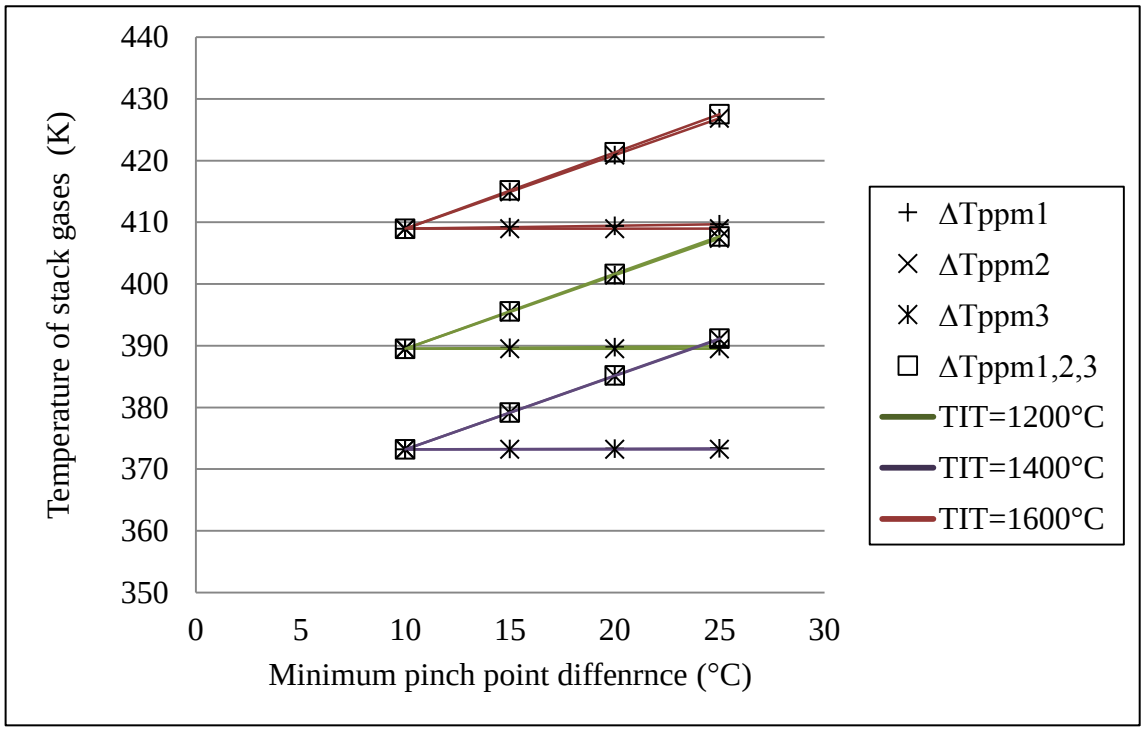

Figure 4.57 The effect of (ΔT_{ppm}) on the temperature of stack gases out of a combined cycle with triple pressure steam generator

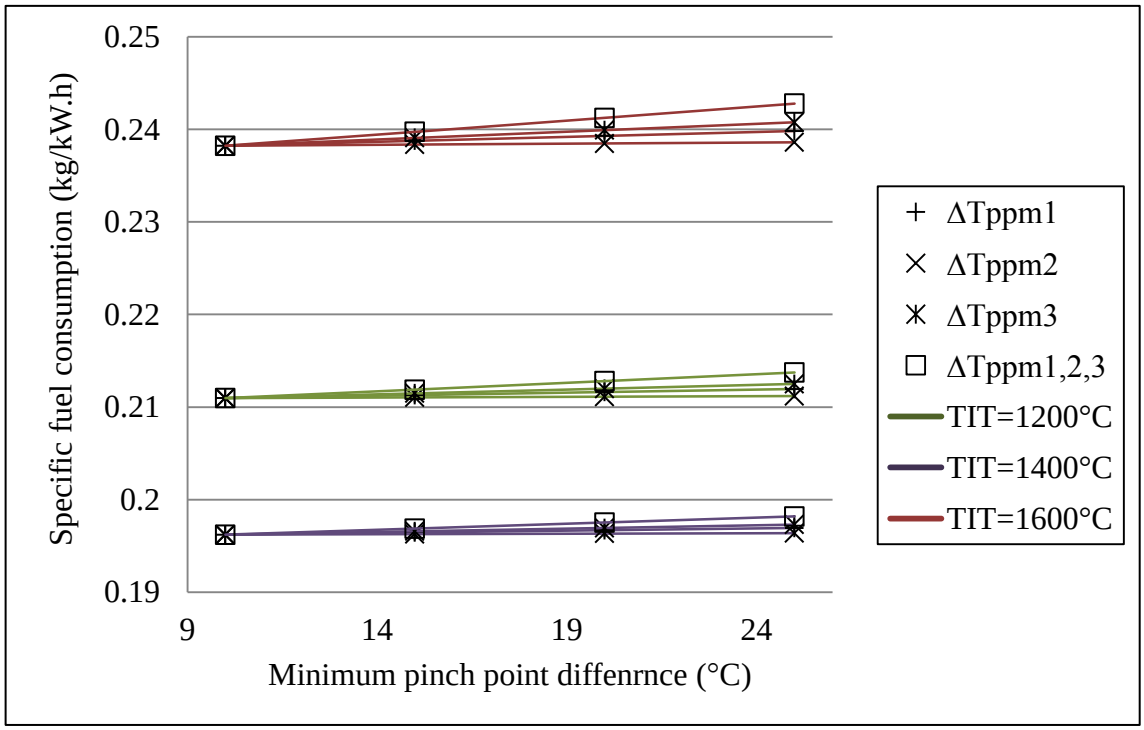

Figure 4.58 The effect of (ΔT_{PPM}) on specific fuel consumption of combined cycle with triple pressure steam generator

4.4.2.5 Ambient temperature

This section investigates the effect of air temperature at compressor intake on the performance of different power cycle configurations. This temperature is assumed to be identical to the ambient temperature for simplicity. The change in the performance of gas cycles and combined power cycles are studied with respect to four ambient temperature values (0° C, 20° C, 40° C, and 60° C). The results show that the ambient temperature has a moderate impact on the performance of gas turbine cycle which turns slighter on the performance of combined power cycles. The change in such temperature affects the compressors' work and the fuel to air ratio to attain the required (TIT). Therefore it has no impact on the performance of steam turbine engine of the combined cycle. As a result, thermal efficiency and the specific work output of the combined cycle are changes by the influence of gas turbine engine alone.

The effect of the ambient temperature on combined cycle performance differs with the with the pressure ratio of gas turbine engine. The range of change itself varies from configuration to another. The increase in the pressure ratio improves the decrease in the thermal efficiency and the increase of the specific work output. The drop of ambient temperature increases the efficiency and the specific work output of low pressure ratio gas turbine engines. This tendency becomes slighter for the gas turbine of lower pressure ratio. For the gas turbines that operate on low pressure ratios, the increase in specific work by the previous effect is combined with a drop in thermal efficiency.

The effect of ambient temperature on specific work output of the combined cycle decreases when most of the power is generated from the steam turbine. For the steam turbine engine that works between fixed pressures, the change in the steam mass fraction at turbine inlet is the governing parameter. Therefore, the greater is the power generated from steam cycle; the lower is the effect of ambient temperature on the performance of combined cycles. The (SFC) is slightly affected by the changes of the ambient temperature. The temperature of stack gases is independent of such parameter. This happens because (TIT) is fixed by the approach that considered in the calculations.

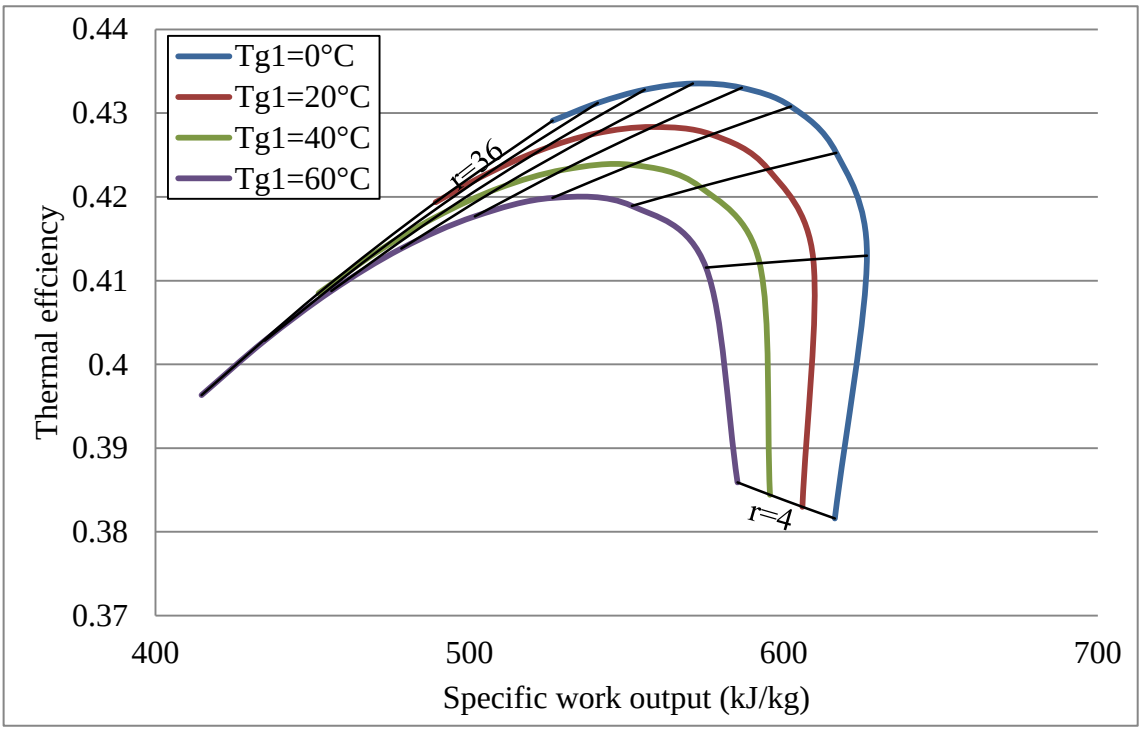

Figure 4.59 The effect of the ambient temperature on the performance simple gas turbine combined cycle

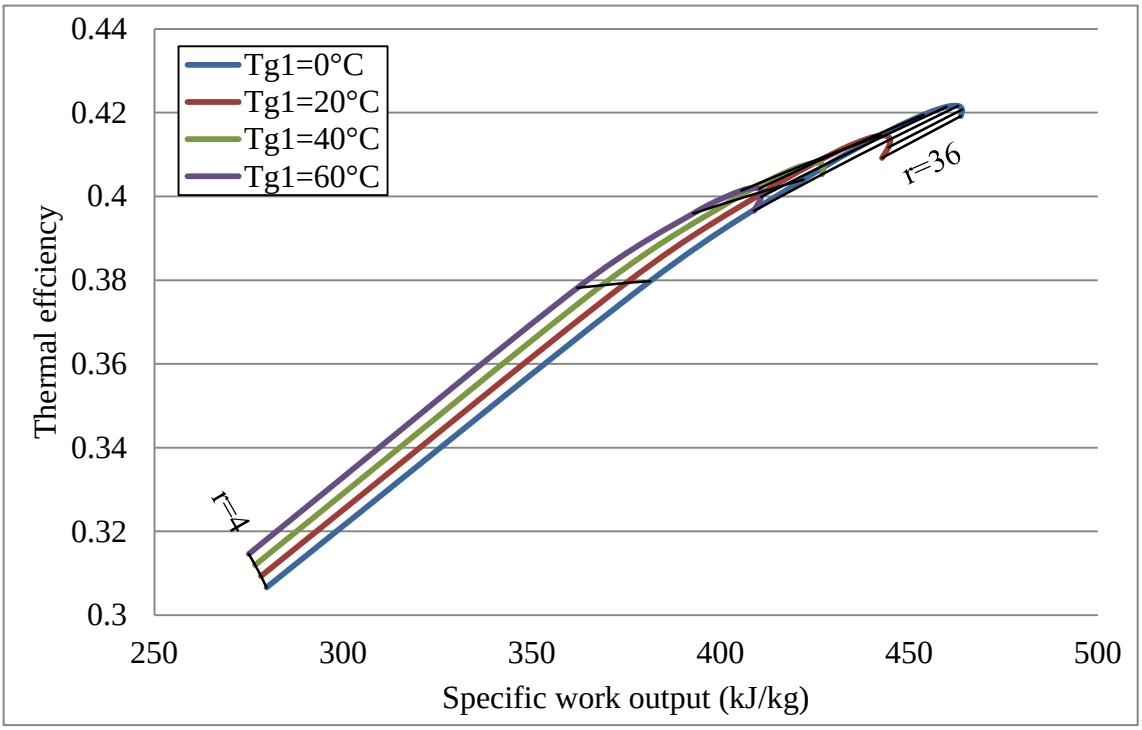

Figure 4.60 The effect of the ambient temperature the performance of regenerated gas turbine combined cycle

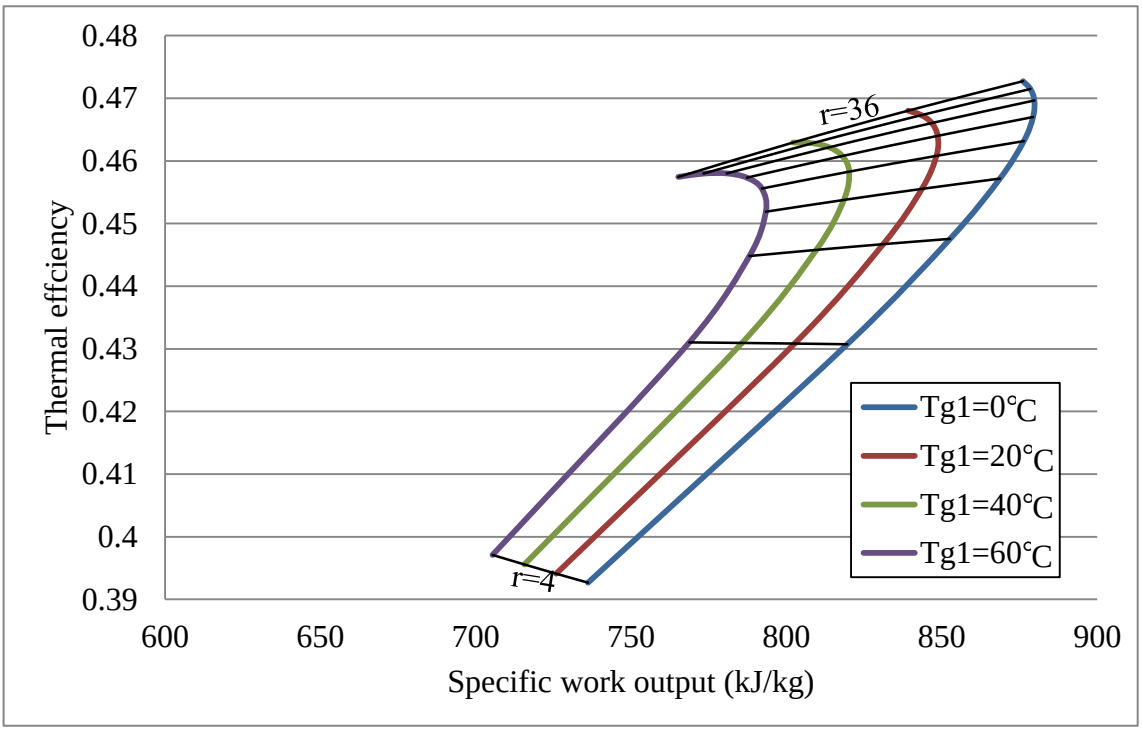

Figure 4.61 The effect of the ambient temperature on the performance of reheated gas turbine combined cycle

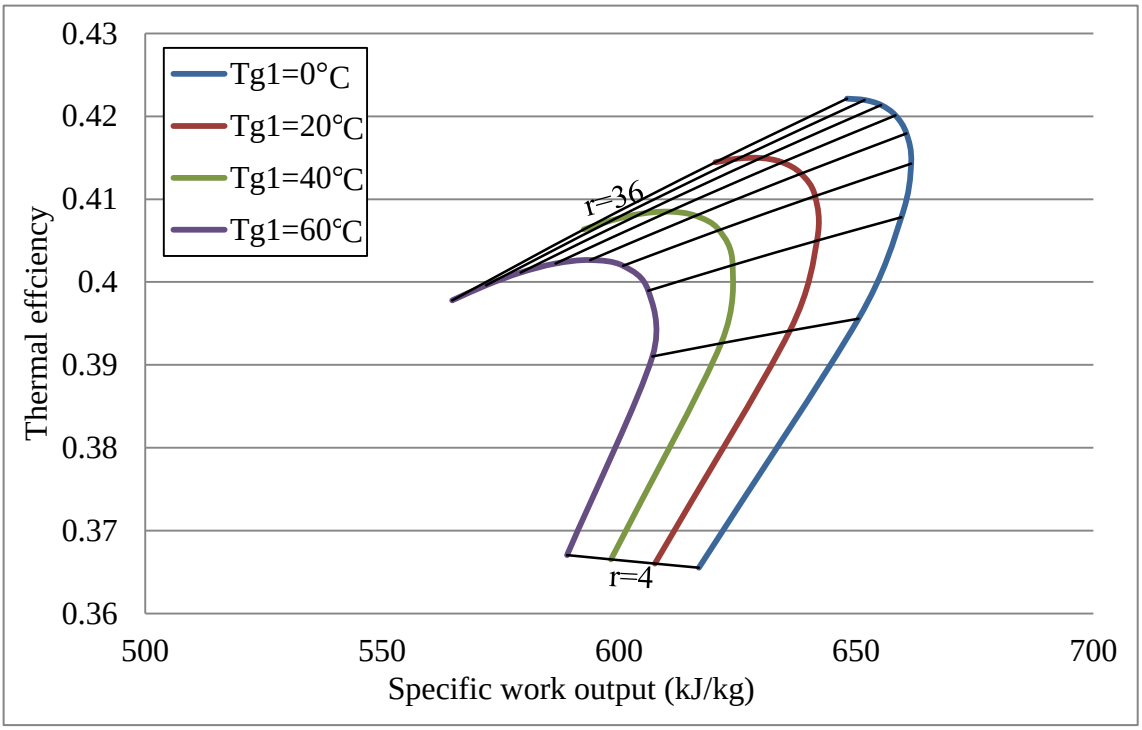

Figure 4.62 The effect of the ambient temperature on the performance of intercooled gas turbine combined cycle

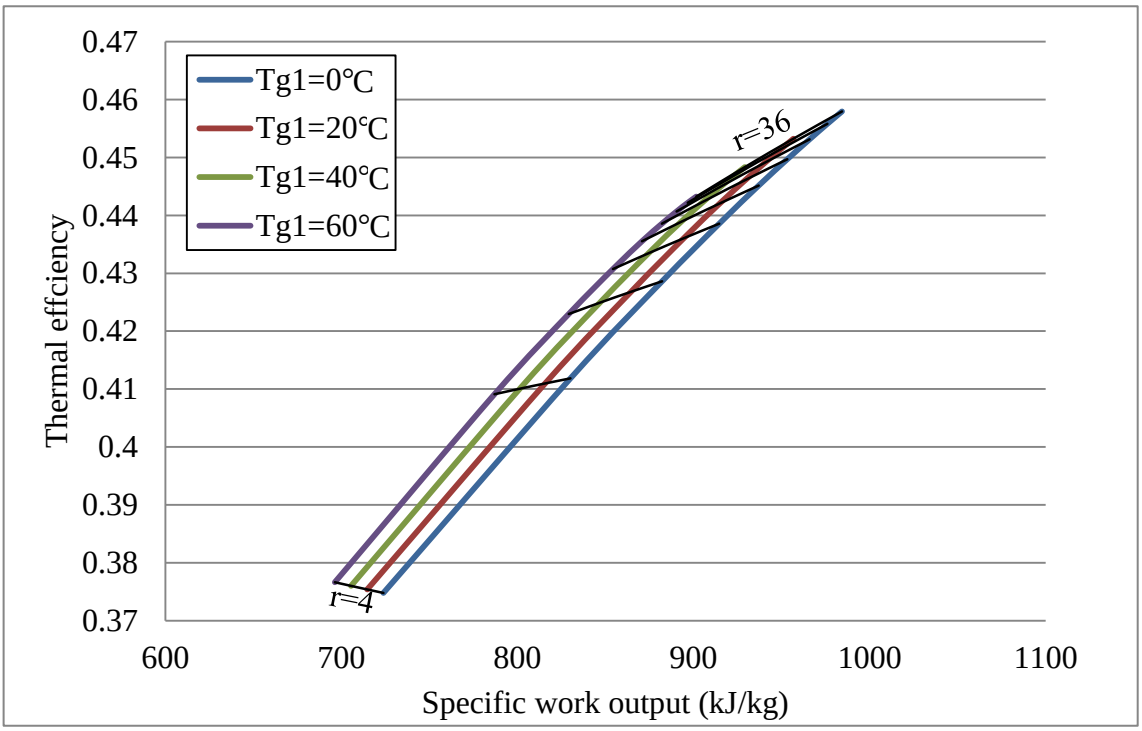

Figure 4.63 The effect of the ambient temperature on the performance of the intercooled reheated gas turbine combined cycle

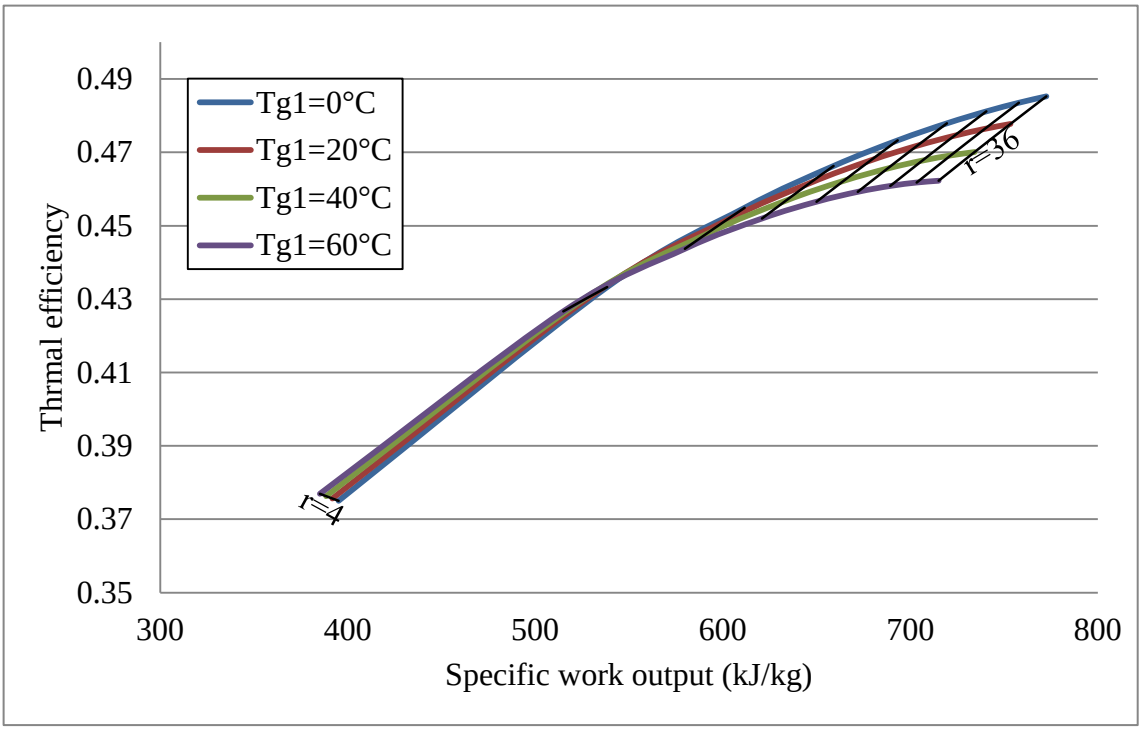

Figure 4.64 The effect of the ambient temperature on the performance of intercooled reheated regenerated gas turbine combined cycle

The variation in the performance of combined cycle by the change in ambient temperature differs from a gas turbine configuration to another. The thermal efficiency of the intercooled reheated regenerated gas turbine combined cycle configurations have the major effect by such parameter.

The increase of the ambient temperature from 0 to 60 °C reduces the thermal efficiency of such configuration by 1.5%. The major effect of such increase reduces the specific work output of simple gas turbine combined cycle by 12%. The greatest variation of (SFC) happens for the regenerated gas turbine combined cycle configurations. It increases by about 3% when ambient temperature is increased from 0 to 60 °C.

The effect of the ambient temperature on the thermal efficiency and the specific work output for different (TIT)s is illustrated by the Fig. 4.65. As it's shown the increase in thermal efficiency by the effect of the reduction in the ambient temperature reduces with the increase of the (TIT) of the gas turbine. The effect of ambient temperature on the (SFC) reduces with the increase of (TIT) Fig. 4.66. The reduction of the (SFC) by the drop of the ambient temperature gets larger with low (TIT).

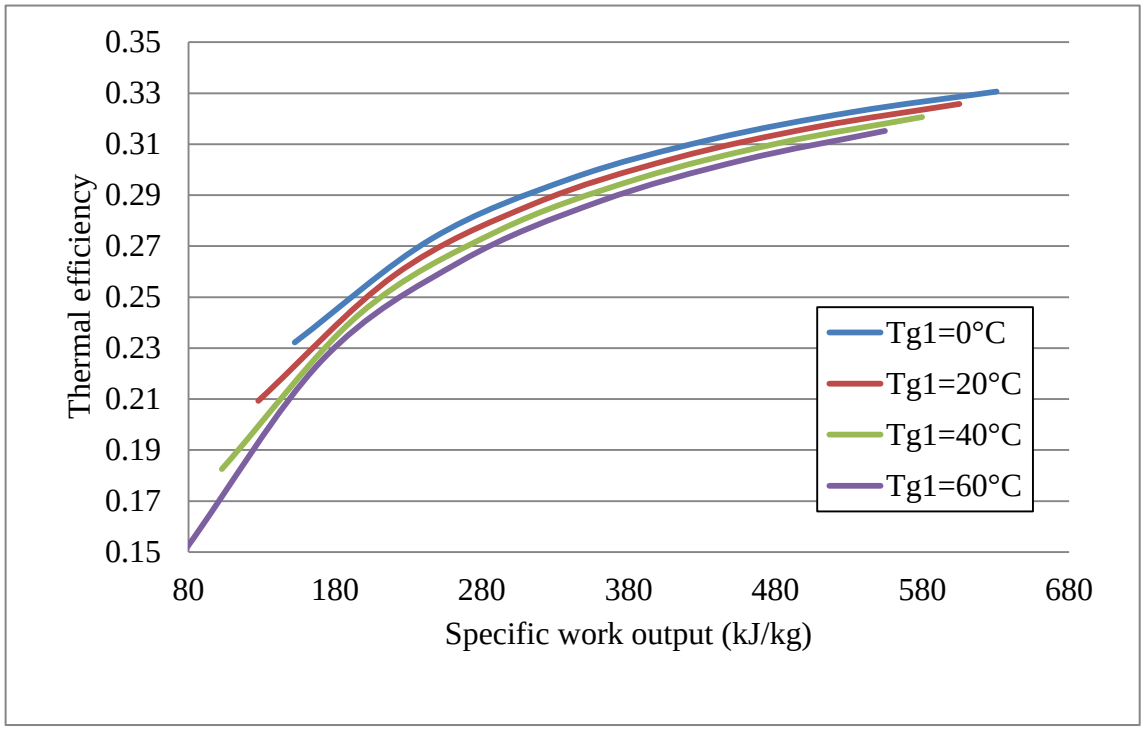

Figure 4.65 The effect of the ambient temperature on the thermal efficiency and the specific work output

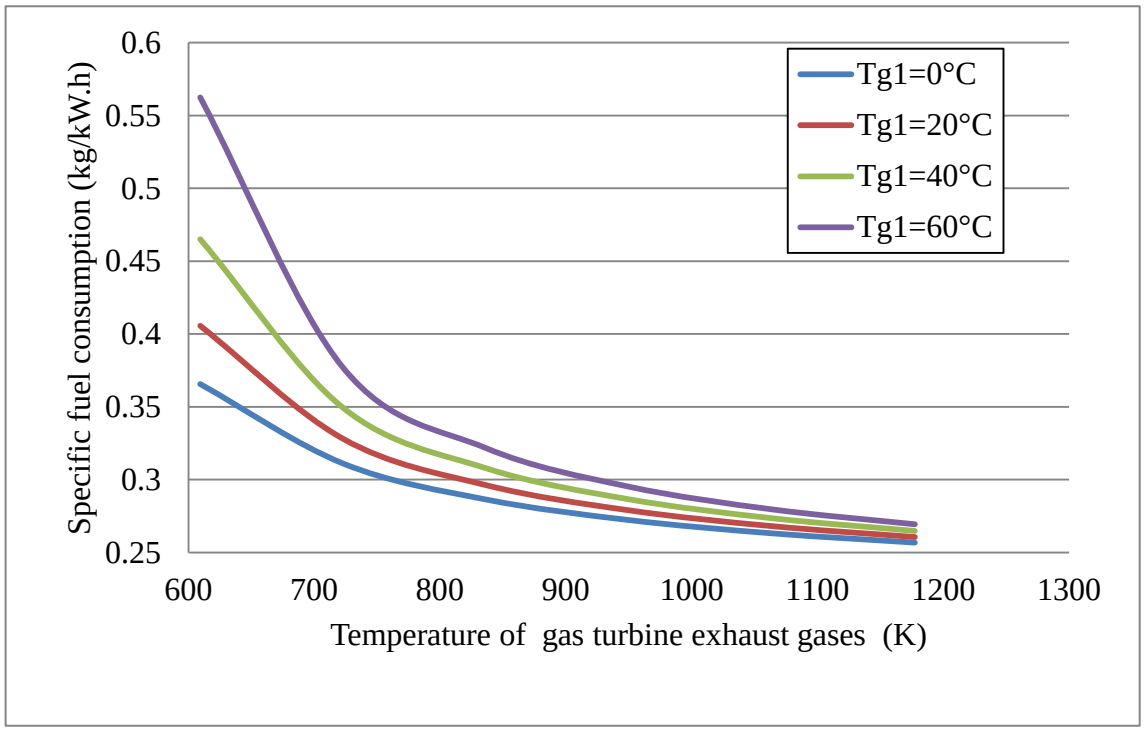

Figure 4.66 The effect of the ambient temperature on the (SFC) and the temperature of stack gases

The result from the parametric study confirms that the increase in the specific work output and the thermal efficiency of simple gas turbine combined cycle configurations are different but slight. The major effect of the ambient temperature on thermal efficiency and (SFC) with regard to different steam turbine combined cycles is on regenerated steam turbine combined cycle configurations. For such configuration, the thermal efficiency increases by (0.6%) and the (SFC) decreases by (14%) when ambient temperature is reduced from 60 to 0°C. The maximum effect of the ambient temperature on the specific work output is observed by triple pressure steam turbine combined cycle configurations. From the above it can be concluded that the efficiency of the intercooled reheated regenerated gas turbine regenerated steam turbine combined cycle is the configuration that most influenced by the changes in the ambient temperature. While the specific work outputs of simple gas turbine triple pressure steam turbine combined cycle configuration is the mostly influenced by the change of the ambient temperature.

4.4.3 Additional topics

This section investigates the change in the performance of the combined cycle power plants by the effect of alternative parameters. It considers the main parameters those appear when the engines are equipped by additional systems to increase its performance. Therefore, this section goes over the promoted combined cycle configurations rather than the conventional configuration. The followings are the important parameters those are covered in this discussion:

1. The discharged water mass flow in the multi pressure steam configurations.
2. The compression ratio of intercooled compressors.
3. The expansion ratio of reheated gas turbines.
4. The pressure of the reheat steam of the reheated steam turbines.

4.4.3.1 Steam mass flow rate

This section investigates the effect of the mass flow rate of the water discharged from the water pump before it enters the multi pressure heat recovery steam generators. Accordingly, the performance of the combined cycle power plant is evaluated regarding the mass flow rate in each unit of each (HRSG) system. Therefore, this section considers the multi pressure steam engine combined cycle configurations only. The mass flow rate fractions are represented with respect to the mass flow of the main stream and so the fractions are illustrated by the mass flow ratios between 0.25 and 4. The change of the ratio between the pair is considered to ensure a brief and complete cover of the effect of each fraction in the steam mass flow. For the dual pressure steam engines, the mass flow of the low pressure steam turbine is initially considered as a function to the mass flow of high pressure steam turbine. The increase in low pressure mass flow stream increases the power generation. Therefore, it increases the efficiency of the steam turbine engine and hence combined cycle plant performance characteristics. The slope of such linear increase decreases by the increase in the gas (TIT).

The increase in the high pressure mass flow stream as a fraction to the low pressure stream gives the same results. The effect of high pressure mass flow stream on the thermal efficiency is greater than the effect of low pressure stream. The effect of the high pressure mass flow on

the specific work output increases by the increase in the temperature of the gases at the turbine inlet. While the same effect decreases the thermal efficiency of such plant. The maximum effect of high pressure mass flow stream on the specific work output and the thermal efficiency appears when the turbine inlet temperature is the lowest. The same above tendency appears for the combined cycle power plant that uses triple pressure steam engine. The effect of the mass flow in such configurations is observed by considering the changing the mass flow rate of the low pressure, intermediate pressure and both together when high-pressure mass flow rate is a constant. The change of the high pressure mass flow stream as a function to that for low and intermediate pressure show the same tendency as well. Combining the change in the mass flow rates of intermediate and the low pressure makes a significant effect on the thermal efficiency and specific work output. Among all, the mass flow of the low pressure stream makes the slightest effects on the thermal efficiency and the specific work output of the combined cycle power plant. However, this effect decreases with the increase in (TIT). The effect of intermediate pressure steam mass flow on the thermal efficiency and the specific work output is greater than the effect of low pressure mass flow. The same tendency is manifested by the effect of the previous mass flow streams on the performance of triple pressure reheated steam combined cycle configurations. Generally the (SFC) and temperature of stack gases decreases with the increase of the mass flow rates in each stream.

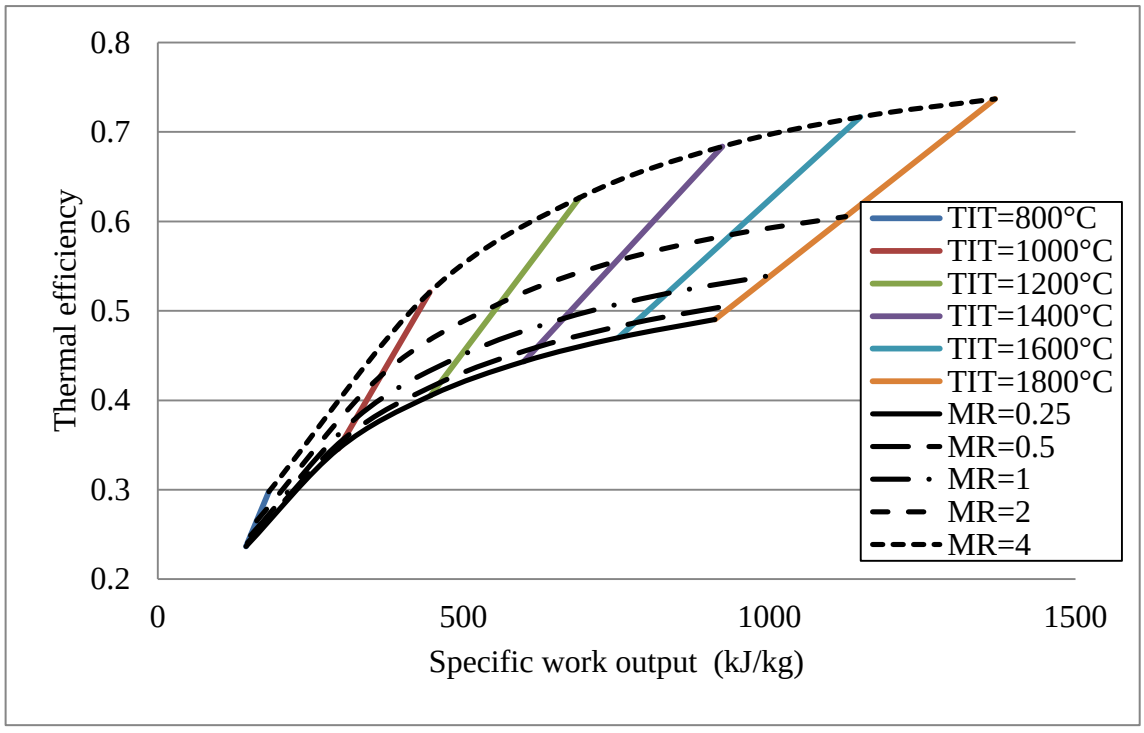

Figure 4.67 The effect of low pressure mass flow rate on the thermal efficiency and the specific work output of (SGDPSCC)

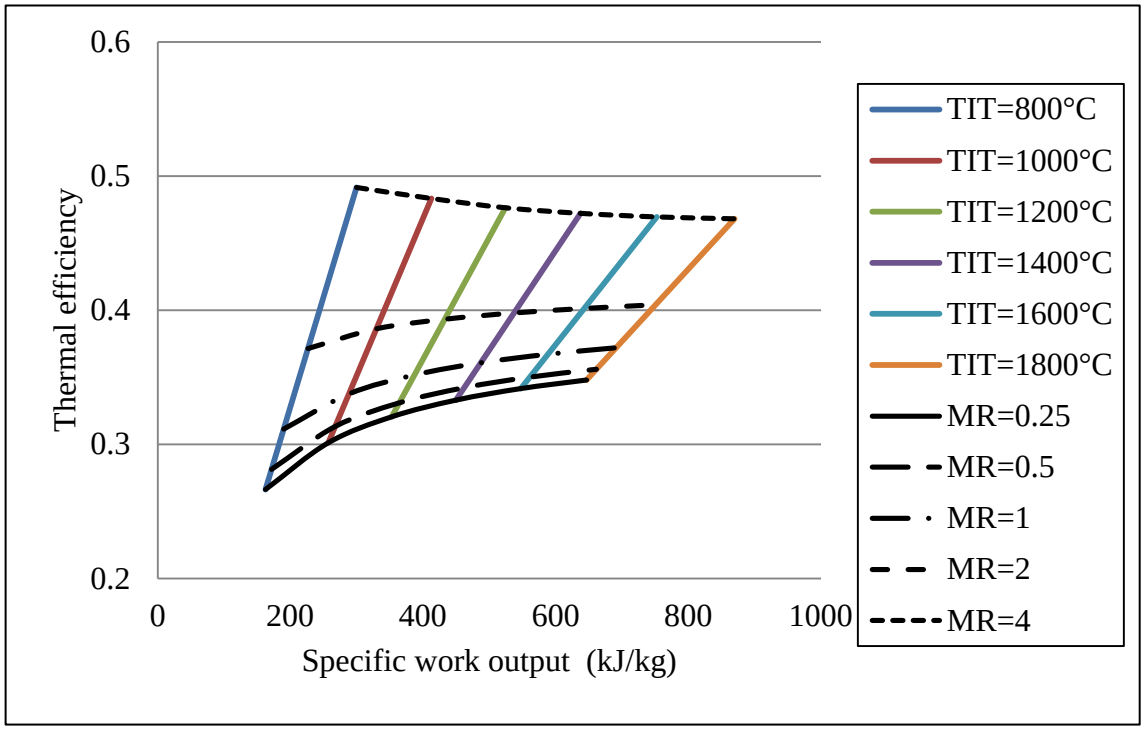

Figure 4.68 The effect of high pressure mass flow on the thermal efficiency and the specific work output of (SGDPSCC)

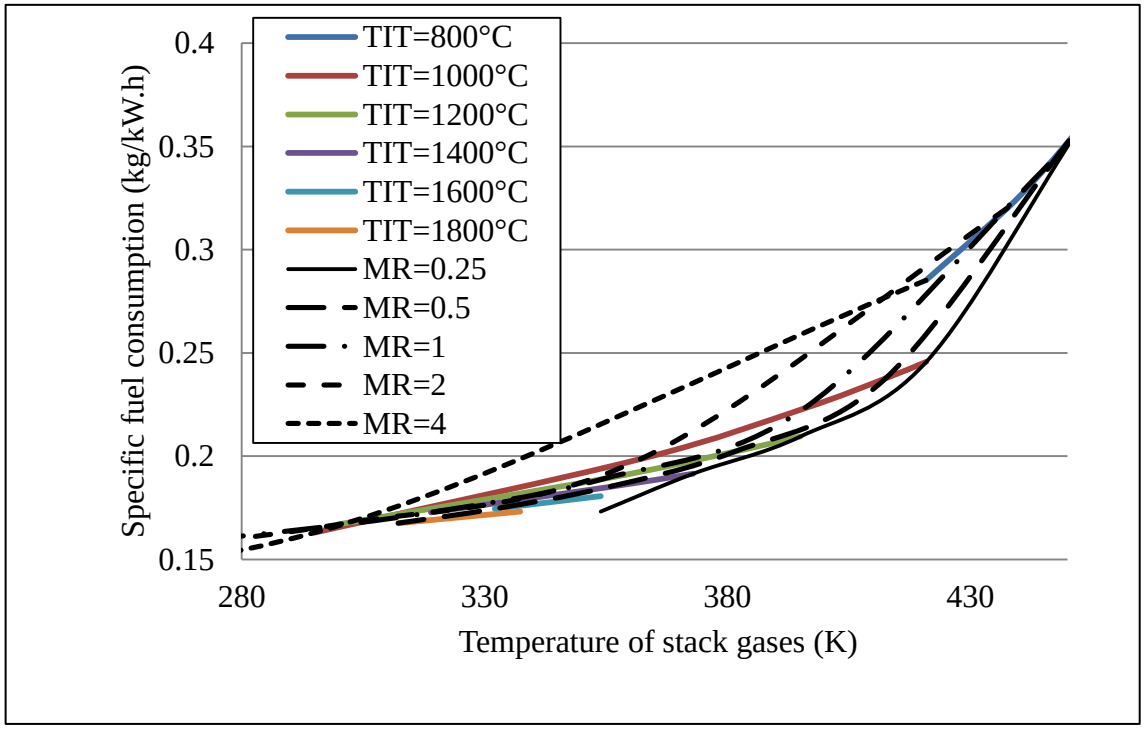

Figure 4.69 The effect of the low pressure mass flow on (SFC) and the temperature of stack gases of (SGDPSCC)

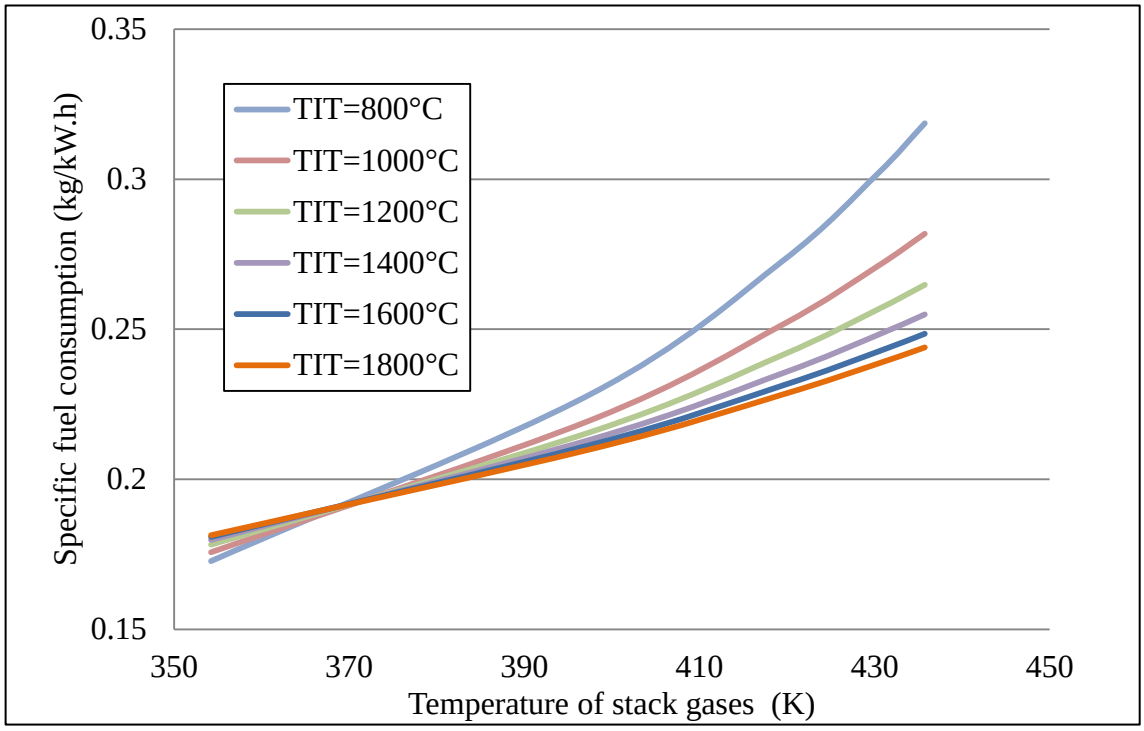

Figure 4.70 The effect of the high pressure mass flow on the (SFC) and the temperature of stack gases of (SGDPSCC)

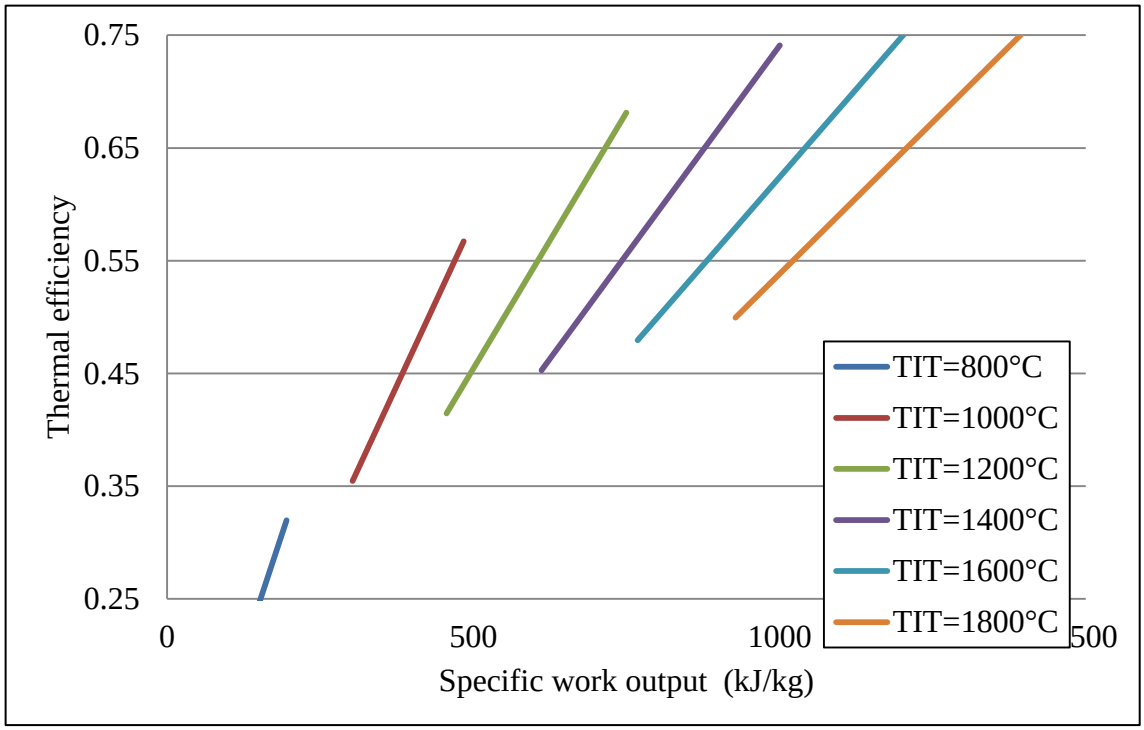

Figure 4.71 Intermediate pressure mass fraction as function to high pressure mass flow on the thermal efficiency and the specific work output of (SGDPSCC)

The degree of slop of such reduction drops when (TIT) of the gas turbine is increased. In dual pressure and dual pressure reheated steam turbine cycles, the increase in each mass flow rate reduces the (SFC) and the temperature of stack gases. The reduction in (SFC) by such effect drops when the gas turbine engine uses higher (TIT). The effect on stack temperature by low pressure mass flow rate increases with the increase of (TIT). The change in high pressure mass flow rate generates similar reduction in the temperatures of stack gases for all (TIT)s. The change in high pressure mass flow rate makes the greatest effect on the temperature of stack gases and (SFC). The effect of changing the mass flow rate fractions in triple pressure (HRSG) is illustrated by the Figs. 4.72 – 80. For triple pressure steam cycle and triple pressure reheated steam turbine combined cycles the maximum reduction in the temperature of stack gases and (SFC) is made by the effect of the mass flow rate of intermediate and low pressure together. The effect of the intermediate pressure mass flow is higher than that for low pressure. This happens due to the higher effect of intermediate pressure enthalpy over that for low pressure even when both masses are symmetrically increases.

The results here do not agree with [18] that the optimum design RehSC is corresponding to the minimum m_{sa} is required. The reheated steam is assumed to be the same of the High pressure. The increase of such steam mass flow rate increases both the efficiency and the work output of any configuration. The results agree with the [29] in which the augmentation in the W_{SC} is restricted by the m_{sa}. The results also agree with that the optimization in HRSG increases the msa. The results also agree with [25] in which the temperature of the GT discharge governs the msa for a certain P_{s3}, The results also confirmed the reduction in m_{sa} by reducing steam generation in evaporator by the increase in the temperature of the GT discharges for the same P_{s3}.

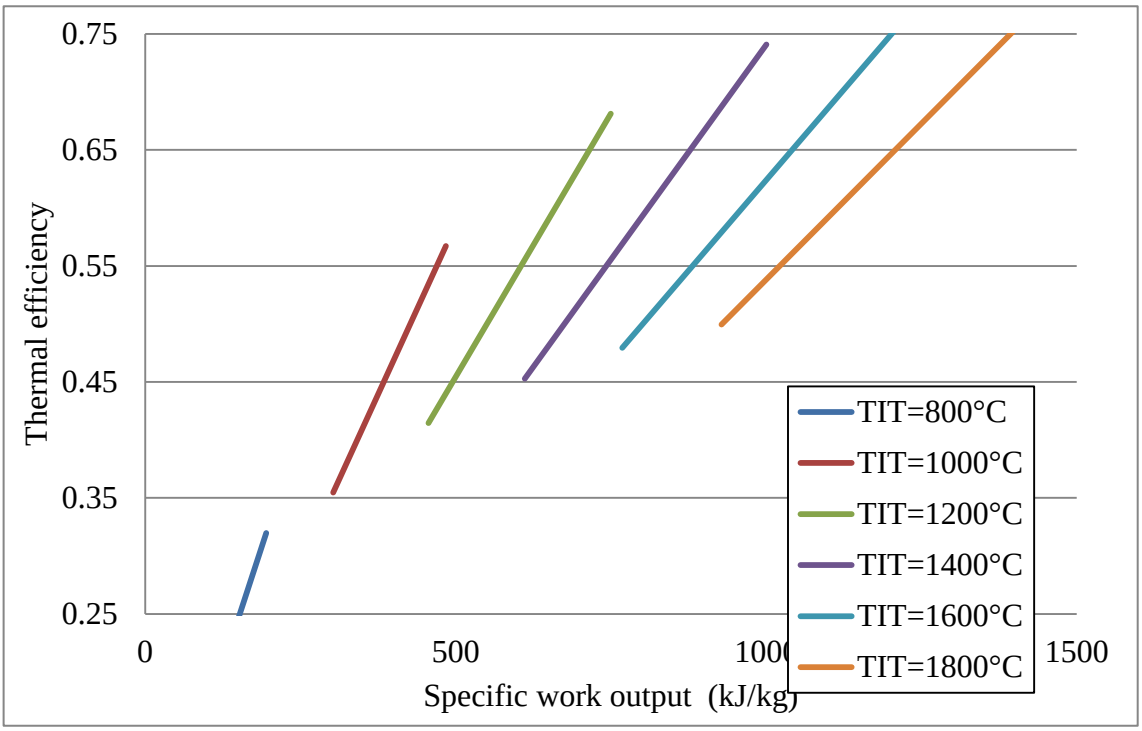

Figure 4.72 The mass flow rate of low pressure as a function to that for high pressure on efficiency and specific work output of (SGTPSCC)

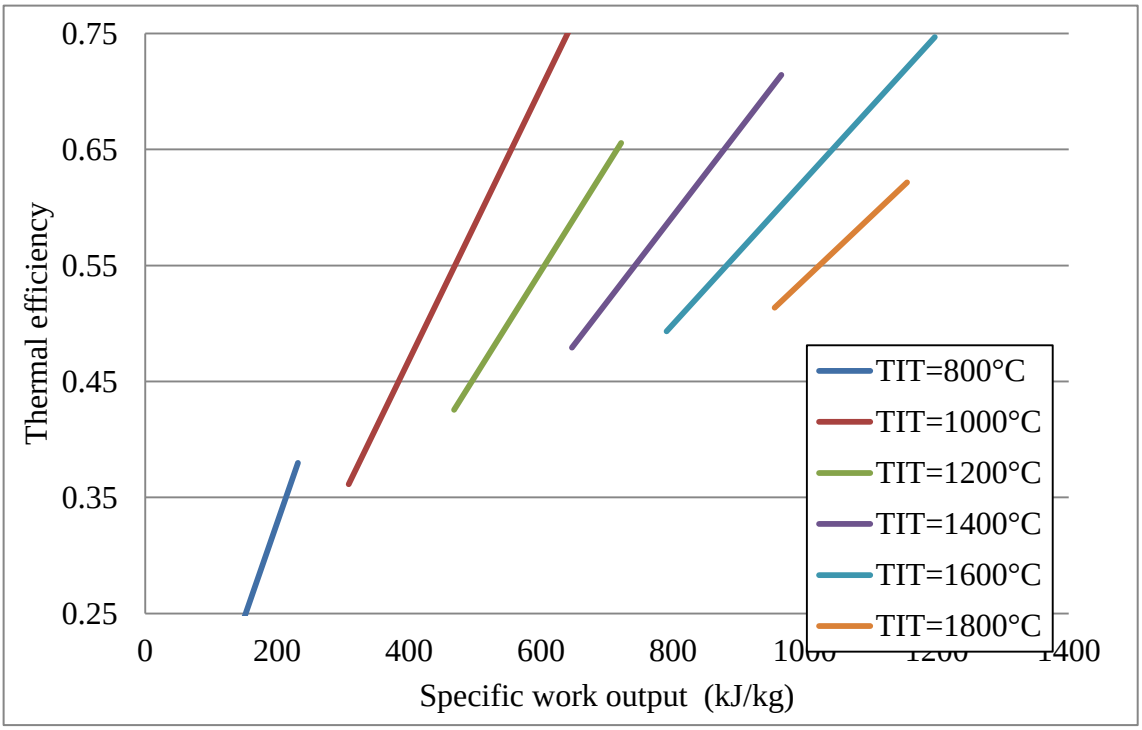

Figure 4.73 The effect of the intermediate and low pressure mass flows as a function to that for high pressure on thermal efficiency and specific work output of (SGTPSCC)

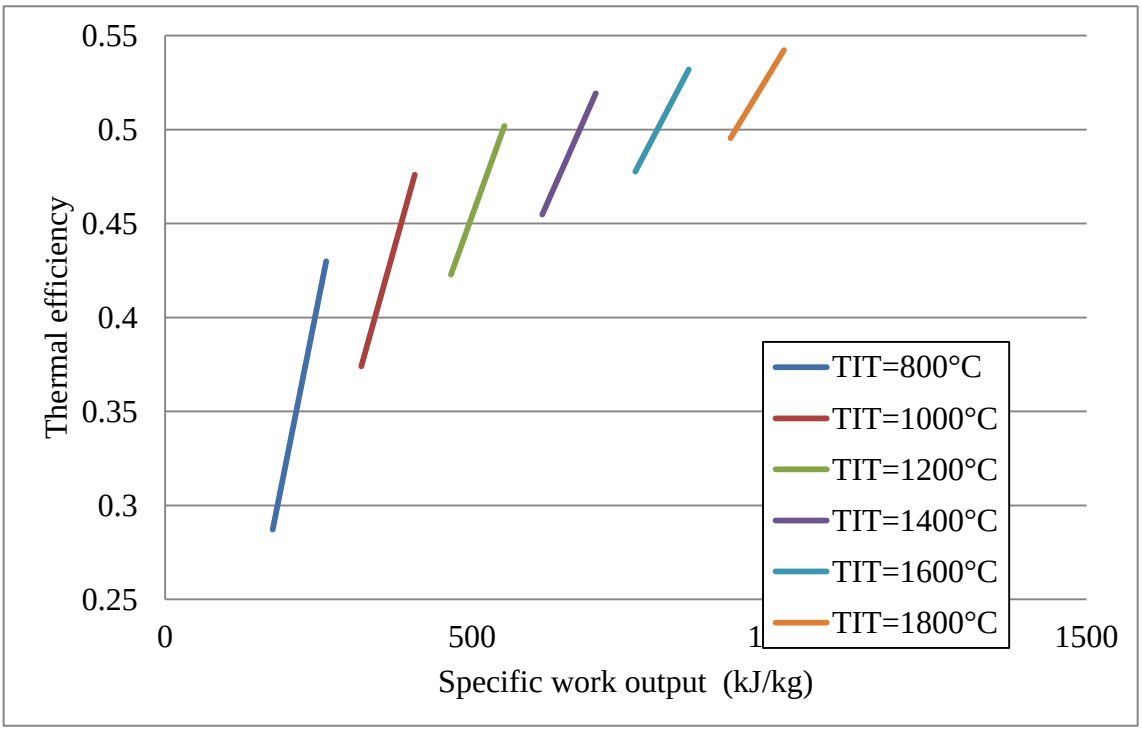

Figure 4.74 Low pressure mass flow as a function to intermediate pressure effect on thermal efficiency and specific work output of (SGTPSCC)

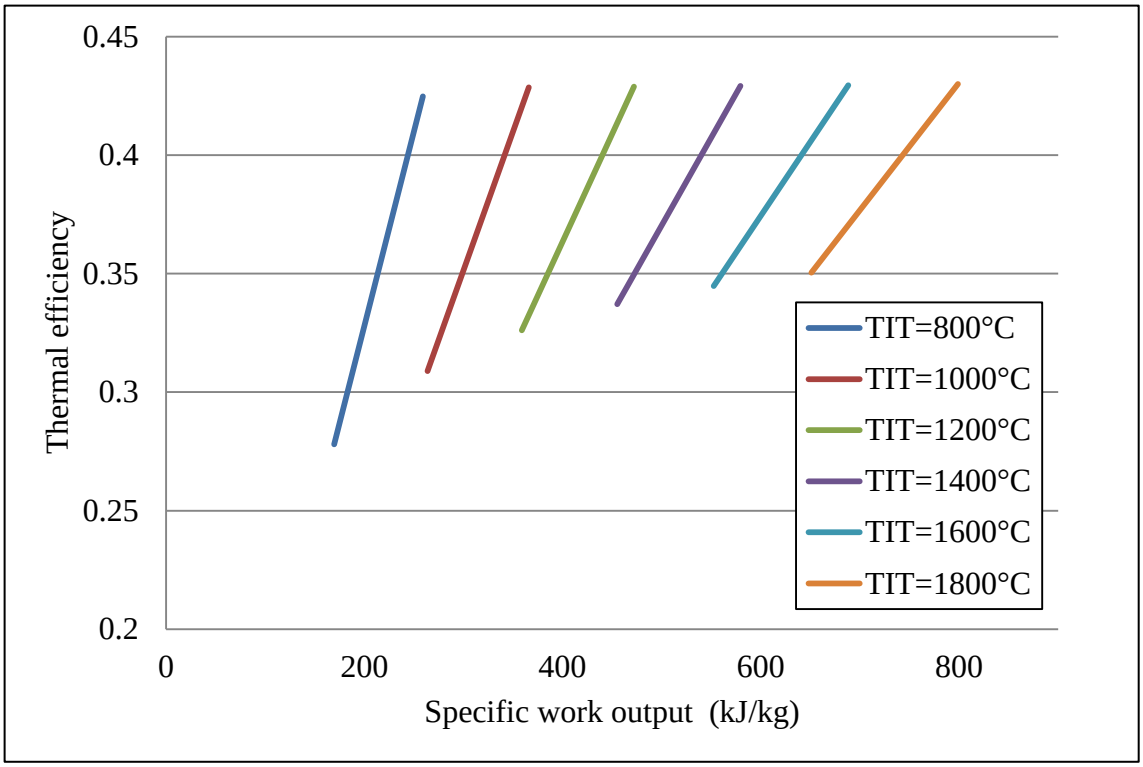

Figure 4.75 The effect of the mass flow rate of high pressure as a function to that for intermediate pressure on thermal efficiency and specific work output of (SGTPSCC)

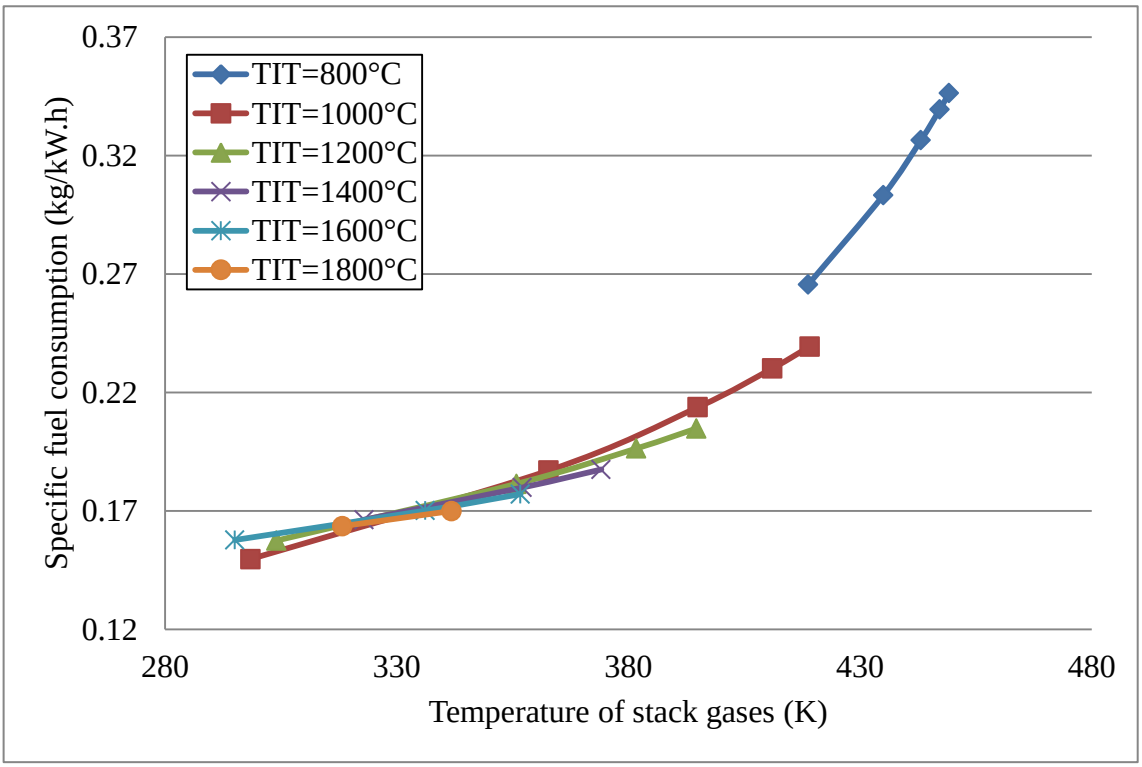

Figure 4.76 The effect of changing the intermediate pressure on (SFC) and temperature of stack gases of (SGTPSCC)

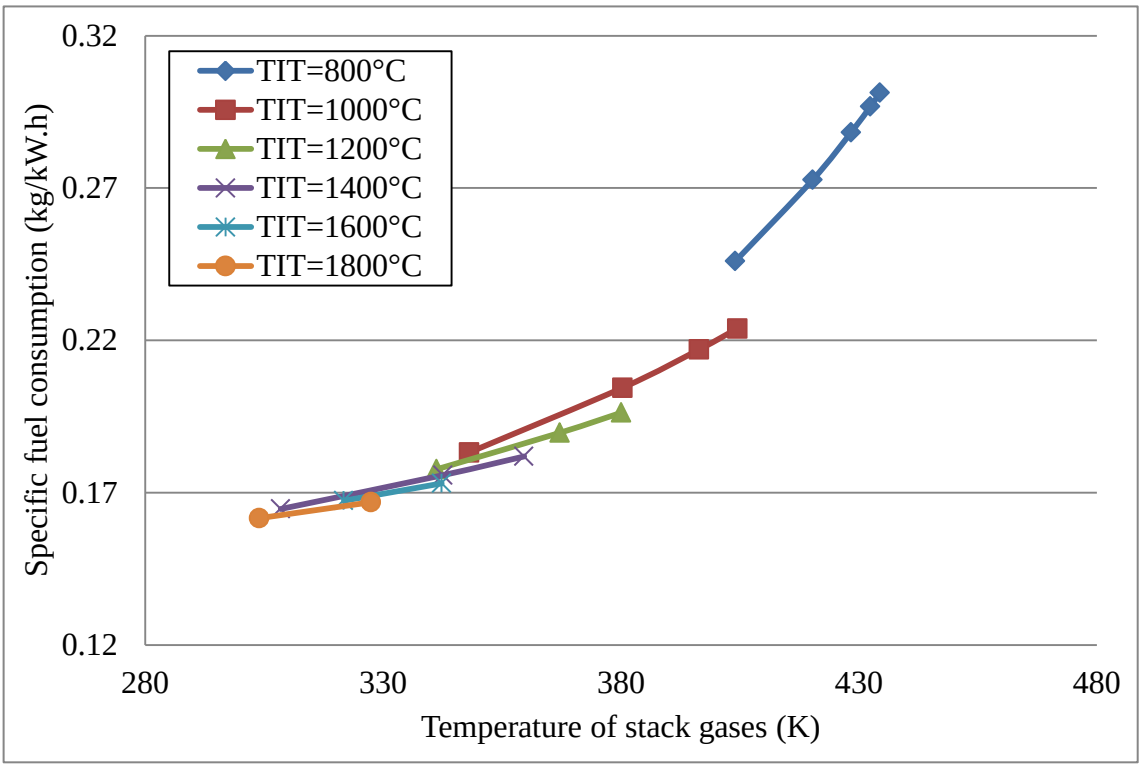

Figure 4.77 The effect of changing the low pressure on (SFC) and temperature of stack gases of (SGTPSCC)

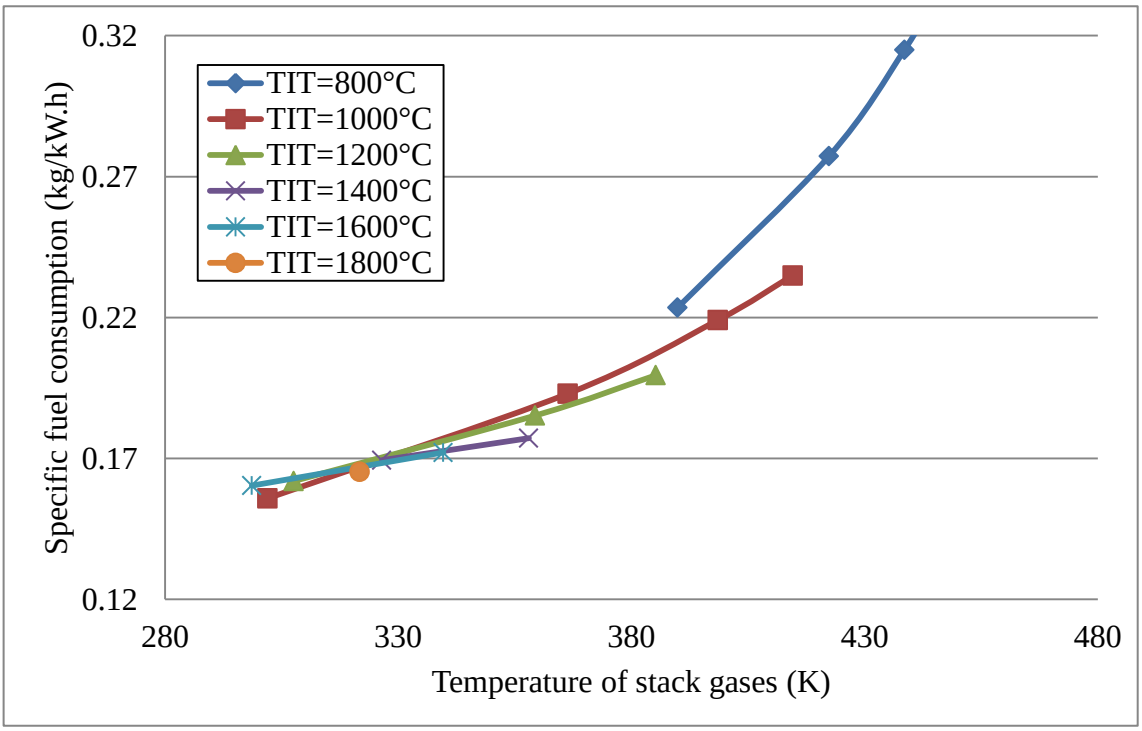

Figure 4.78 The effect of changing the intermediate and low pressure on (SFC) and temperature of stack gases of (SGTPSCC)

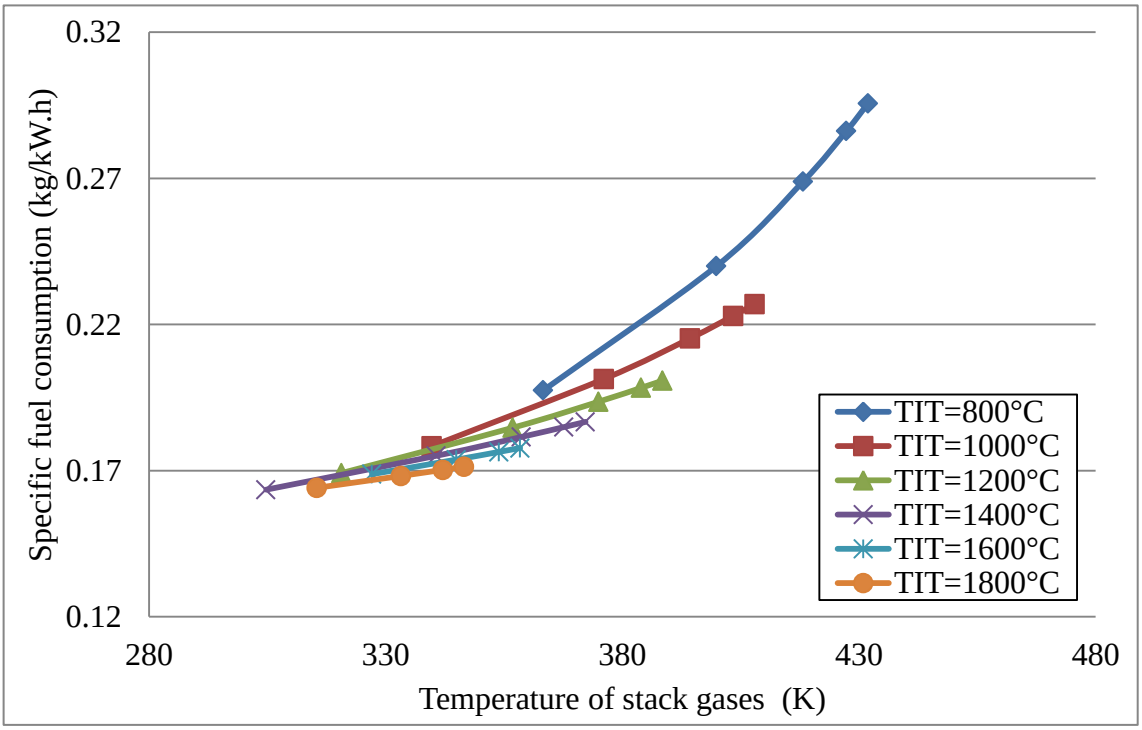

Figure 4.79 The effect of the low pressure mass flow as a function to intermediate pressure on (SFC) and temperature of stack gases of (SGTPSCC)

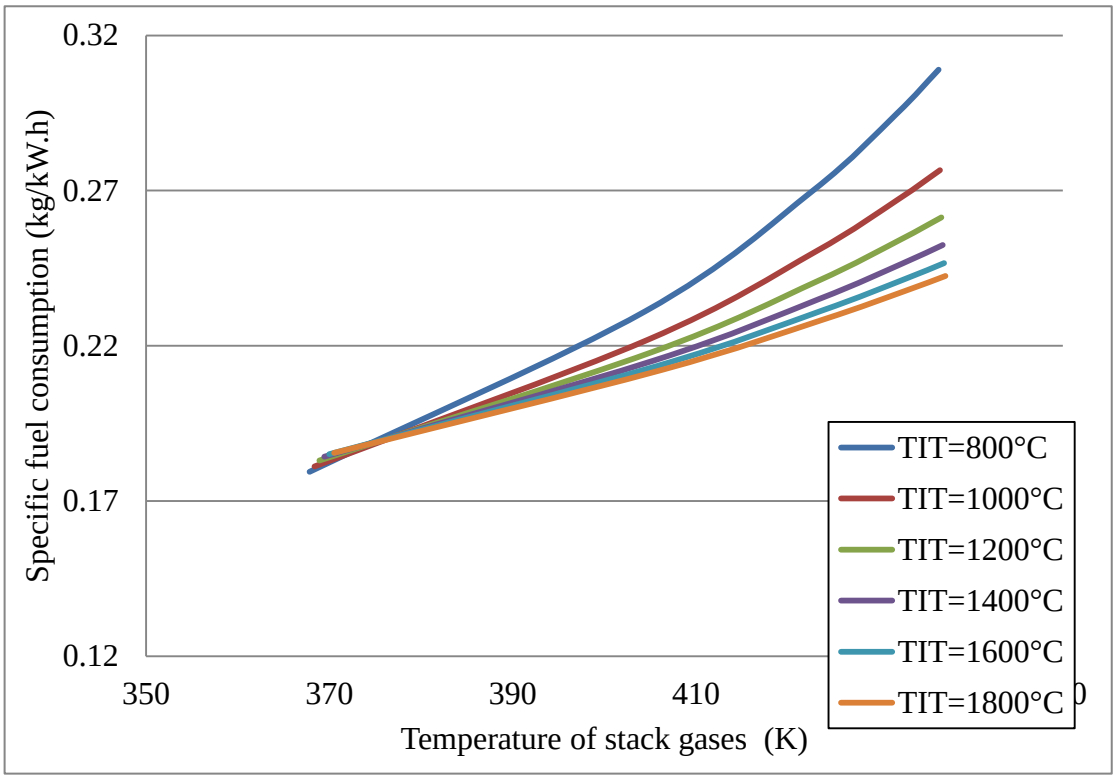

Figure 4.80 High pressures' effect on the specific fuel consumption (SFC) and the temperature of stack gases of (SGTPSCC)

4.4.3.2 Intercooling pressure (IntP)

This section investigates the effect of changing the pressure at which the air is cooled for intercooled gas turbine configurations. Therefore, it covers intercooled, intercooled reheated and intercooled reheated regenerated gas turbine combined cycle configurations only. As in the previous sections the thermal efficiency, the specific work output, the specific fuel consumption and the temperature of stack gases are investigated. A turbine inlet temperature of 1400 °C and a range of compression ratio (8-36) are considered in calculation. The pressure of boiler and condenser are fixed to 80bar and 0.34bar respectively. A range of compression pressure ratio splits ratio (r_{c1}/r_{c2}) is undertaken including (0.25, 0.5,1,2 and 4).

For intercooled gas turbine cycle, the thermal efficiency and the specific work output are decreased by any increase in the ratio of pressure ratio split. The performance characteristics of intercooled reheated and intercooled reheated regenerated gas turbine cycles are the same. For the entire splits' range, the increase in the pressure ratio increases the thermal efficiency and the specific work output. This tendency does appear reheated regenerated gas turbines for the range (rc2 ≥ rc1). In such a case, the specific work output increases with a drop in the

thermal efficiency. The same happens when such configurations are designed to work on high pressure ratio for the range (rc2 < rc1). In this section due to the considered approach, gases temperature at turbine inlet is fixed and gases temperature at turbine outlet is not affected by this parameter.

The performance characteristics of intercooled gas turbine simple steam turbine combined cycle configurations are affected similarly by such parameter as shown in Fig. 4.84. The ranges of such effects are enlarged by the increase of GTC pressure ratio. The increase in low pressure ratio GTC increases the thermal efficiency and the specific work output for split ratio range $r_{c2} < r_{c1}$. For high pressure ratios GTC, the increase in the thermal efficiency is combined with a drop in the specific work output. This modification appears on low pressure ratios GTC by the increase in r_{c1} over r_{c2}.

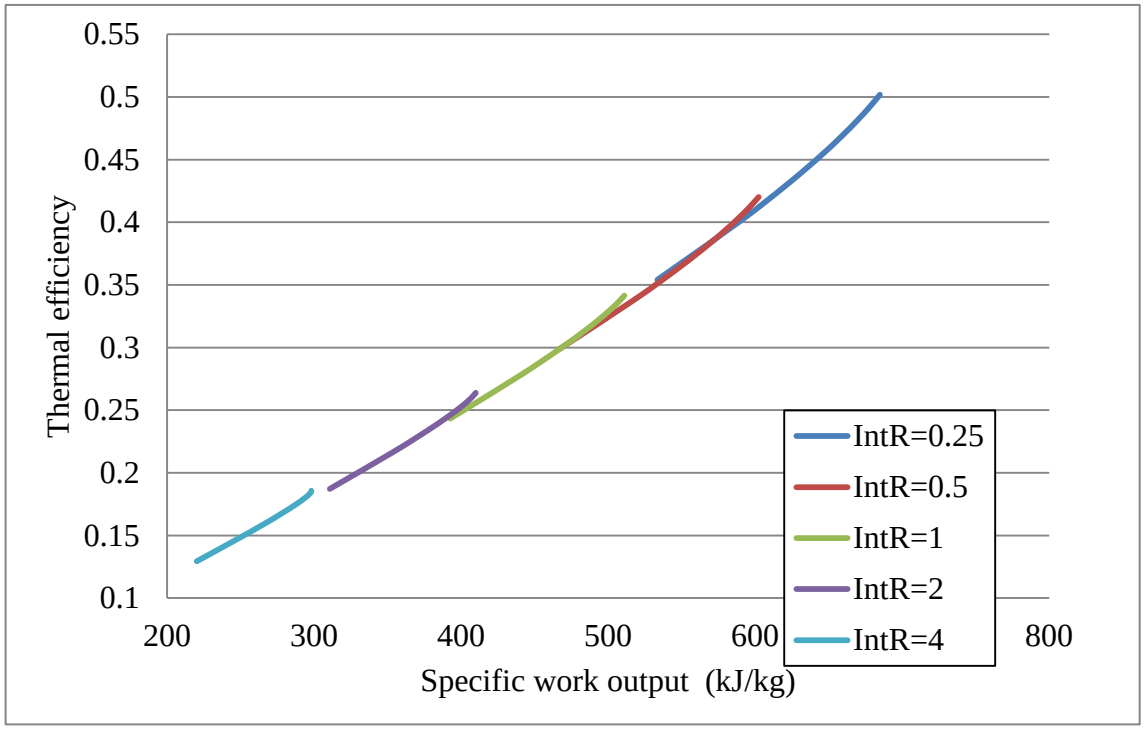

Figure 4.81 Intercooling pressure effect on thermal efficiency and specific power output of intercooled gas turbine cycle

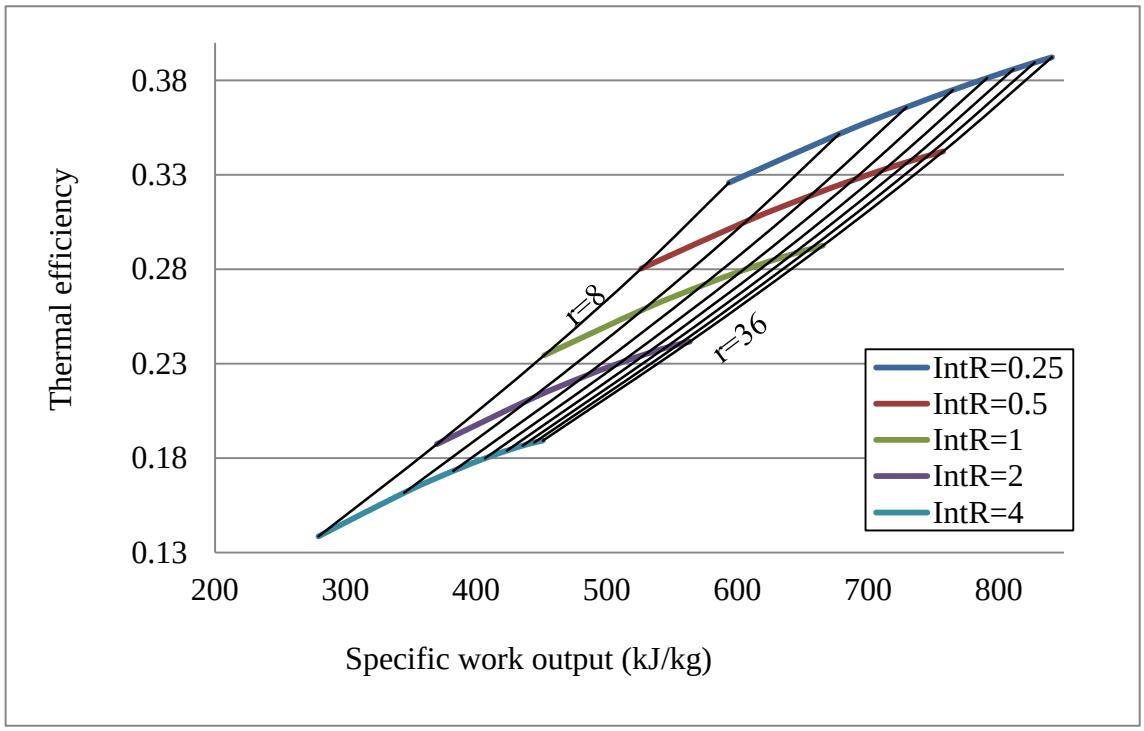

Figure 4.82 Intercooling pressure effect on thermal efficiency and specific power output of intercooled reheated gas turbine cycle

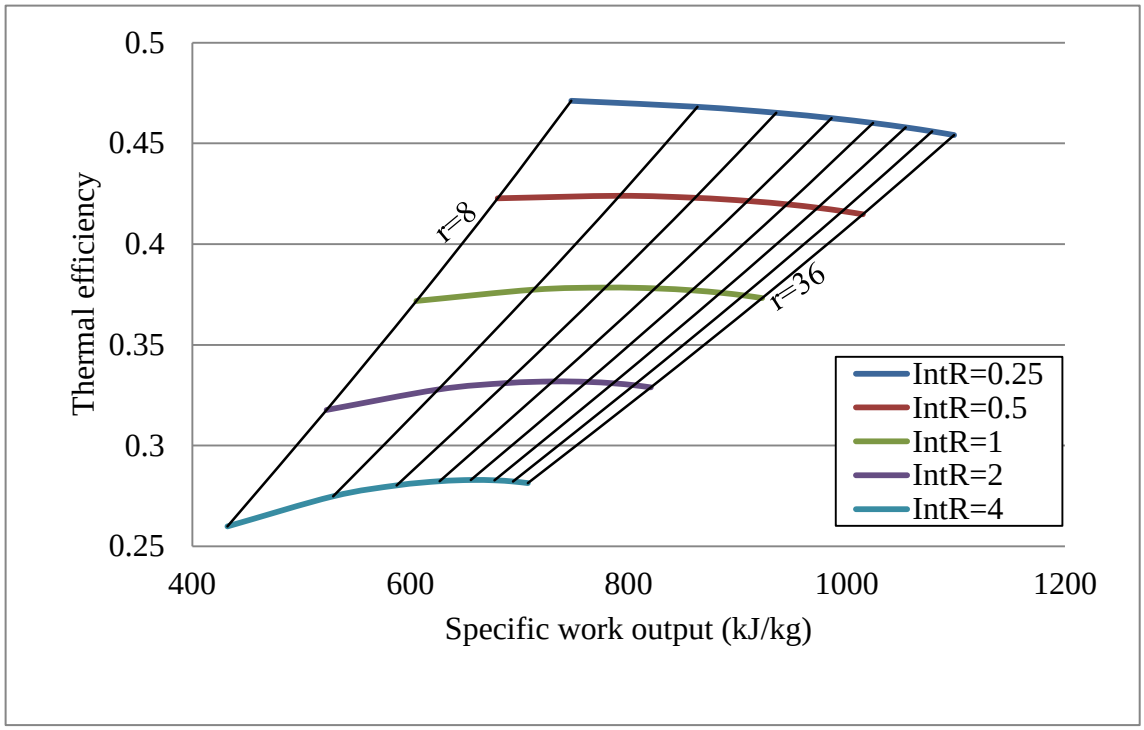

Figure 4.83 Intercooling pressure effect on thermal efficiency and specific power output of intercooled reheated regenerated gas turbine cycle

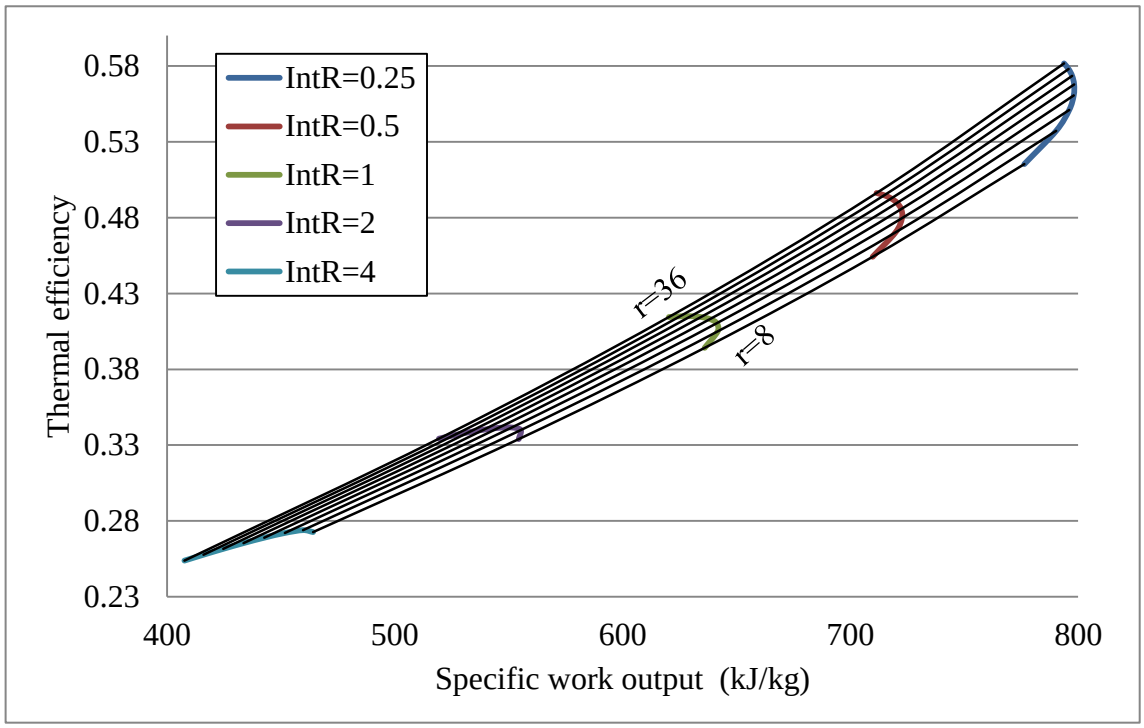

Figure 4.84 Intercooling pressure effect on thermal efficiency and specific power output of Intercooled gas turbine simple steam turbine combined cycle

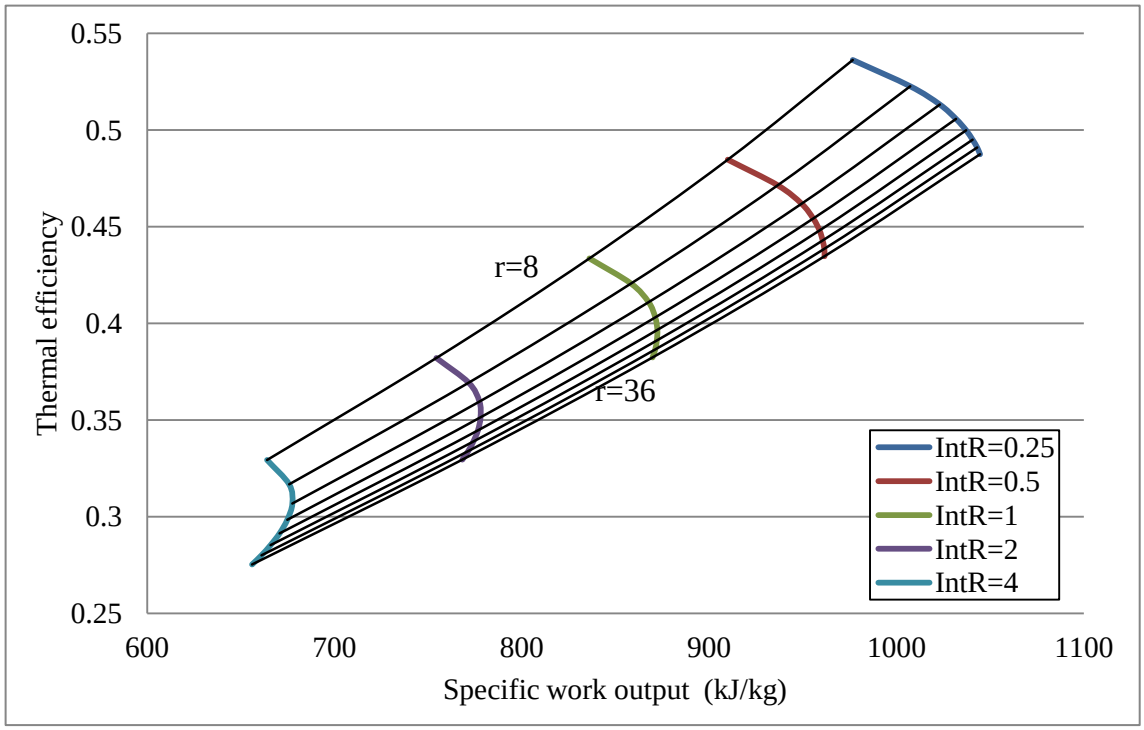

Figure 4.85 Intercooling pressure effect on intercooled reheated gas turbine simple steam turbine combined cycle

A split ratio of a range ($r_{c2} < r_{c1}$) decreases the specific work output and thermal efficiency by the increase of the pressure ratio. This tendency does not differ by using another steam turbine configuration if ($r_{c1} = r_{c2}$). The rest employs a slight decrease in thermal efficiency and heavy degredation in the power output, the reduction in thermal efficiency becomes sharper with much higher values of r_{c1} over r_{c2}.

The same behaviour appears for combined cycles with reheated and regenerated steam cycle. The temperature of stack gases increases when ($r_{c2} > r_{c1}$) with the increase in pressure ratio. The specific fuel consumption (SFC) decreases with low pressure ratios and increase with the rest of the investigated range. This tendency weakens with great values of r_{c2}. For ($r_{c2} \geq r_{c1}$), the temperature of stack gases increases but the (SFC) drops.

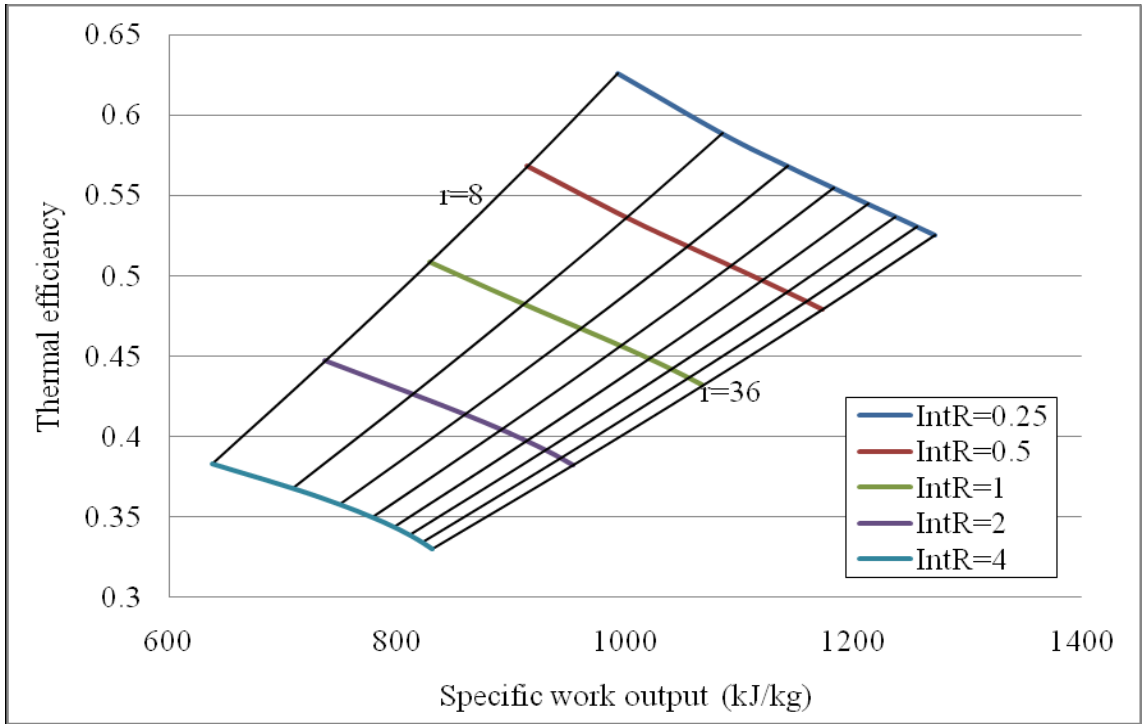

Figure 4.86 Intercooling pressure effect on thermal efficiency and specific work output of intercooled gas turbine simple steam turbine combined cycle

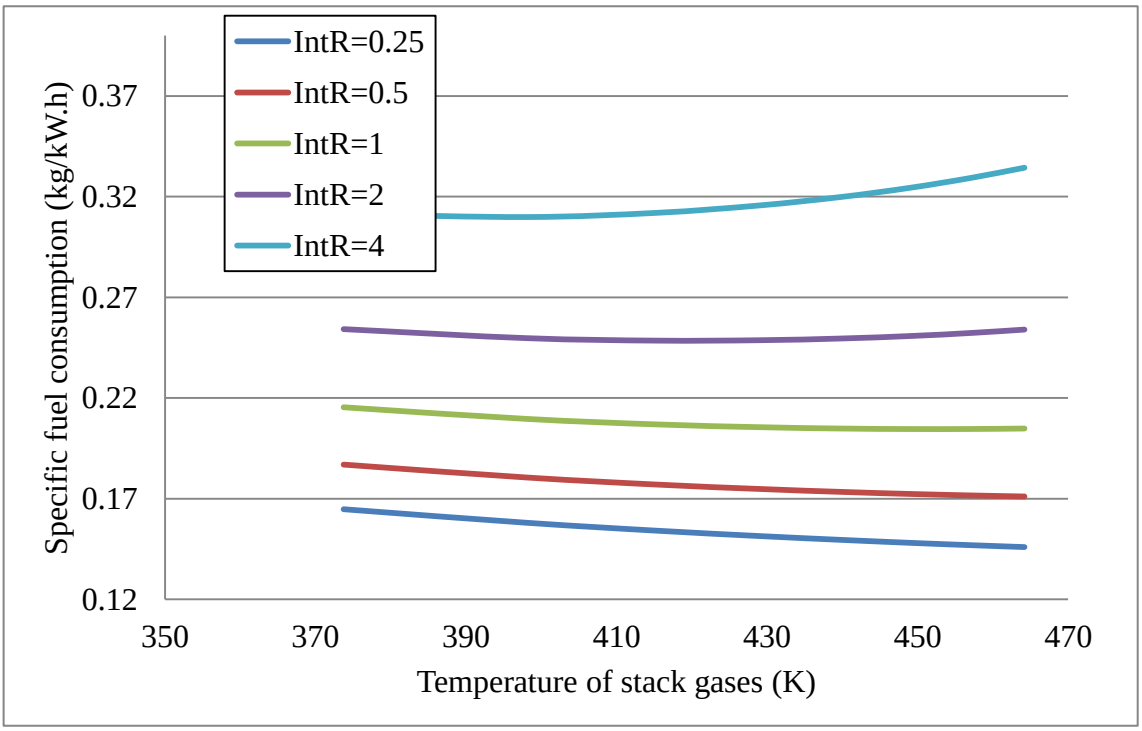

Figure 4.87 Intercooling pressure effect on (SFC) and temperature of stack gases of intercooled gas turbine simple steam turbine combined cycles

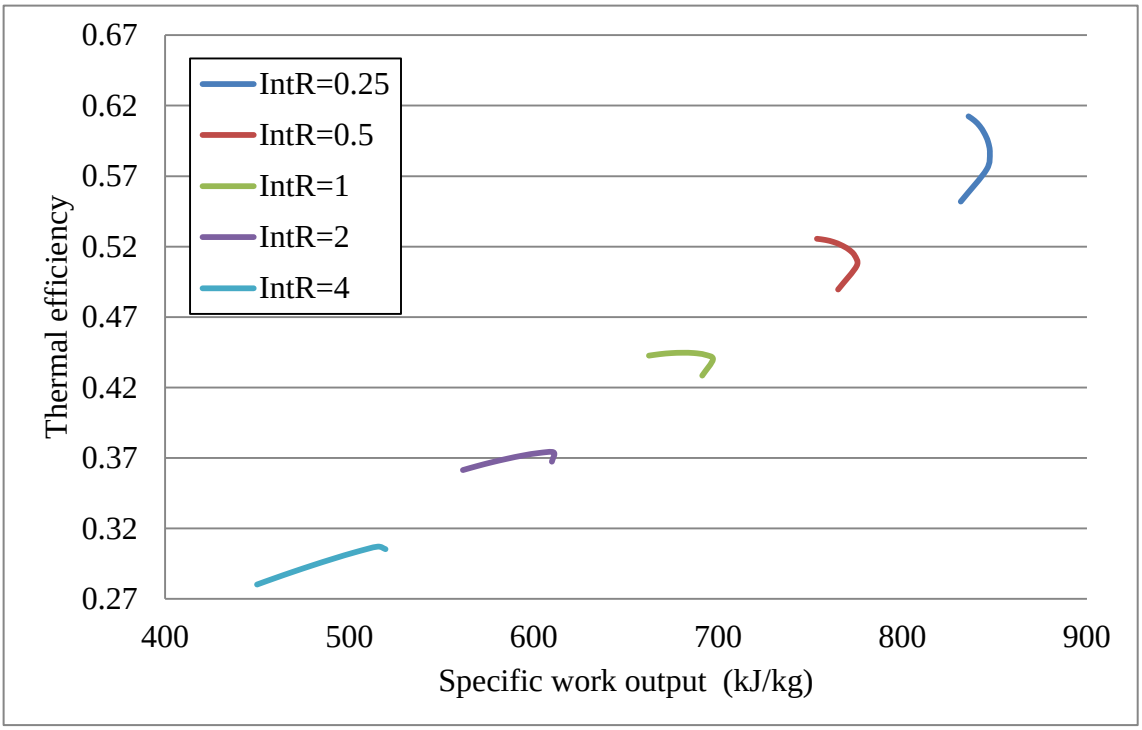

Figure 4.88 Intercooling pressure effect on thermal efficiency and specific power output of intercooled gas turbine triple pressure reheated steam turbine combined cycle

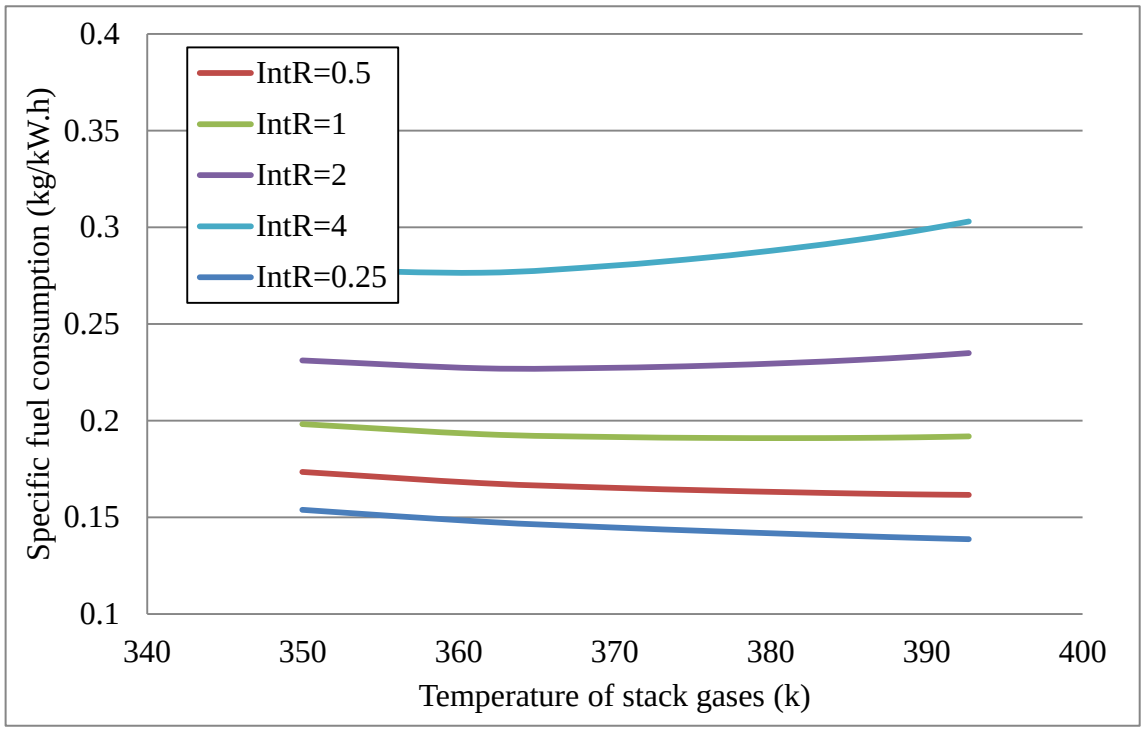

Figure 4.89 Intercooling pressure ratio effect on (SFC) and the temperature of stack gases of intercooled gas turbine triple pressure reheated steam turbine combined cycle

Introducing multi pressure steam cycles to combined cycles show an increase in thermal efficiency and power output with the increase in pressure ratios when ($r_{c2} \geq r_{c1}$). This behaviour tends the opposite with higher pressure ratios for the range ($r_{c1} < r_{c2}$). It involves all pressure ratio range with much higher values of r_{c1} over r_{c2}.

The maximum efficiency always corresponds to larger r_{c2} than r_{c1}, this appears with the lowest (SFC) and temperature of stack gases but not the maximum power output. The greatest power output is always corresponds to a greater r_{c1} than r_{c2}, which appears with different pressure ratio in each steam cycle. It comes with the minimum pressure ratio in simple, Reheated, and Regenerated steam cycles. But with the maximum pressure ratio in multi pressure steam cycles. The low temperature from turbine outlet due to the increase in the ratio limits steam quality. Therefore, the increase in second compressor pressure ratio widens the acceptable range of steam quality at steam turbine outlet.

For a pressure ratio of 20 and gases turbine inlet temperature of 1400°C, the maximum effect of the splits between compressors on thermal efficiency appears for dual pressure reheated steam turbine combined cycle. While splits minimum effect is for regenerated steam turbine combined cycles. The opposite is the effect of switching the pressure ratios between the both

compressors. The heaviest effect over temperature of stack gases is for simple steam turbie combined cycles. The lowest among these CCPP is the dual pressure steam turbine, dual pressure reheated steam turbine, triple pressure steam turbine and triple pressure reheated steam turbine combined cycles. The heaviest effect on (SFC) belongs to: dual pressure steam turbine, dual pressure reheated steam turbine and triple pressure steam turbine combined cycles.

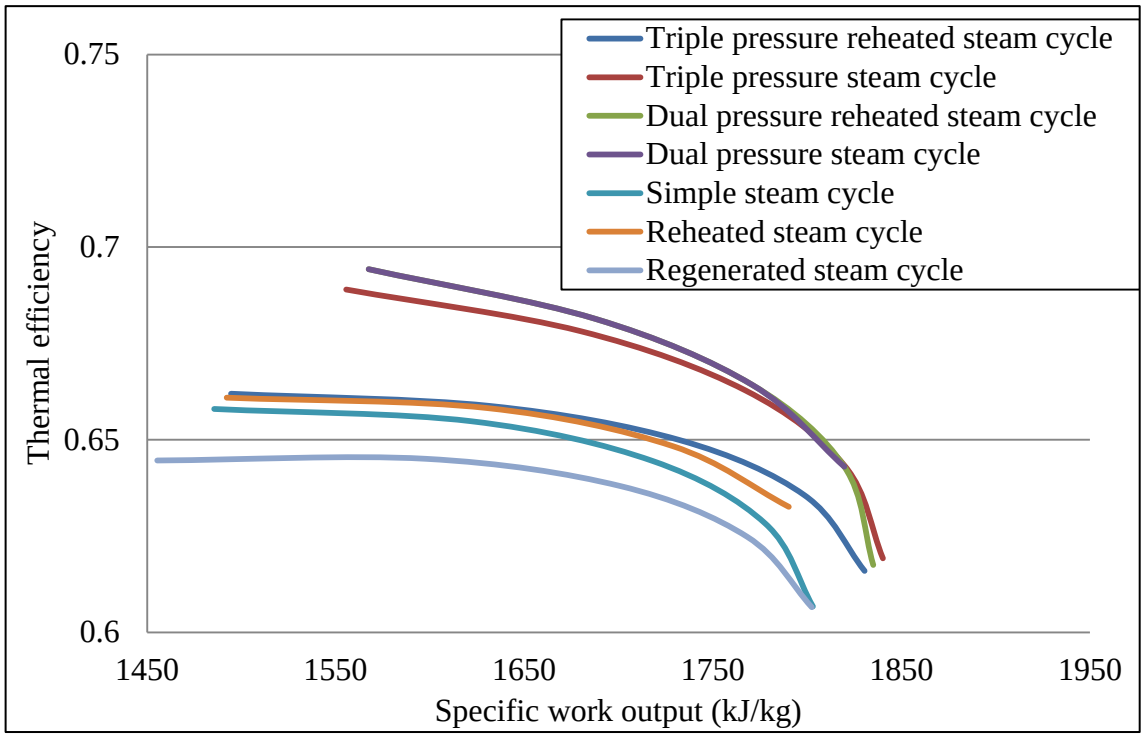

Figure 4.90 Intercooling pressure ratio effect on thermal efficiency and specific power output of intercooled gas turbine and different steam turbine combined cycles

The intercooled reheated gas turbines show the same relationships as in the intercooled gas turbine but with less impact on the thermal efficiency and greater impact on the specific work output. The intercooled reheated regenerated gas turbine cycle has lower effect on the thermal efficiency and the greater effect on the specific work output than the previous case. The effect on turbine exhaust temperature is slighter than intercooled reheated gas turbine configuration. In such configurations, the effect of splits ratio on the thermal efficiency and the specific work output is similar. The increase in the pressure ratio for the range ($r_{c2} > r_{c1}$) increases the thermal efficiency and specific power output. The opposite happens for the range ($r_{c2} < r_{c1}$). As

a result, the increase in split ratio always drops the thermal efficiency and increases the specific work output.

The Specific Fuel Consumption and the temperatures of stack gases appear with two tendencies. The first appears for low pressure ratios and a range of intercooling ratio ($r_{c2} > r_{c1}$). In such case the increase in intercooling ratio decreases the (SFC) and increases the temperature of stack gases. The opposite tends to appear by the increase of the pressure ratio for the range ($r_{c2} < r_{c1}$). The second relationship appears with high pressure ratios in which the increase in the split ratio always results in a rise of (SFC) and temperature of stack gases. By the increase of pressure ratio for each split the effect is similar to that for intercooled gas turbine simple reheated and regenerated steam combined cycle configurations.

For multi pressure steam turbine combined cycle configurations, the intercooled reheated gas turbines effect is similarly as intercooled cycles except that, the double behaviour appears more with the first. The effect of splits values on the performance of intercooled reheated regenerated gas turbine combined cycle configurations seem to be different than previous cases. The increase in splits ratio drops the thermal efficiency and the specific work output. For the same split ratio and range of pressure ratios when ($r_{c2}>r_{c1}$) the increase in pressure ratio increases the efficiency although the reduction in the specific work output. For the triple pressure and triple pressure reheated steam turbine combined cycles configurations, the specific work output tends to increase rather than decrease. The increase in pressure ratio always decreases the thermal efficiency and specific work output.

The increase in split ratio always increases the stack temperature and (SFC), the same happen with each split ratio for a range of pressure ratios when ($r_{c2} < r_{c1}$). The opposite leads to higher stack temperatures with a drop in (SFC) in all combined cycles

The temperature of stack gases isn't affected by intercooling because of the constant temperature at turbine inlet. Therefore it does not change by the change in intercooling pressure. As so, the changes in temperature of stack gases are the result from the changes in other sections in each configuration. The increase of TIT always increases the work output, thus it reduces the effect of intercooling on cycle's performance of intercooled reheated gas turbine CCPP. Applying this test over combined cycles equipped with different steam cycles decrease their specific work outputs and thermal efficiencies. This is observed on the combined cycles of each of the above GTC. But the change over a range of pressure ratios is different from GTC to another.

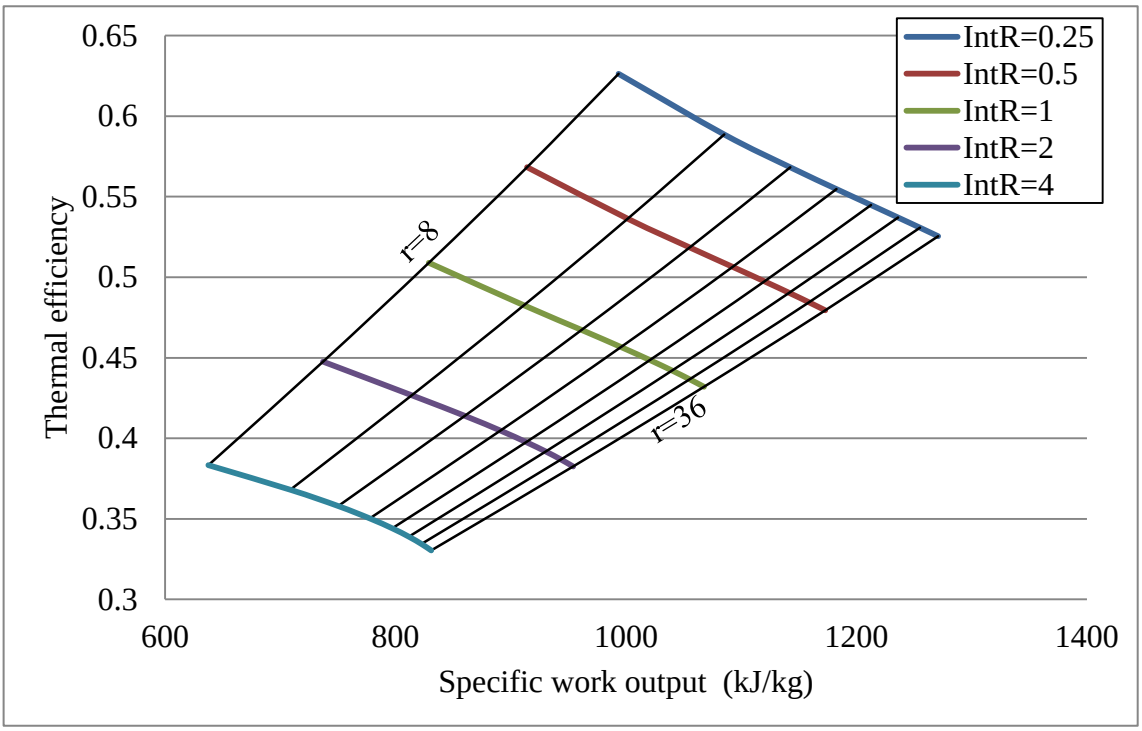

Figure 4.91 Intercooling pressure effect on thermal efficiency and specific power output of intercooled reheated regenerated gas turbine triple pressure steam turbine combined cycle

For intercooled reheated gas turbine combined cycle configurations, the increase in split ratio decreases the thermal efficiency and specific work output. The effect of pressure ratio appears different on the performance for each spit ratio. For low split ratio ($r_{c2} > r_{c1}$), the increase in pressure ratios increases the thermal efficiency and the specific power output. The opposite happens by futher increase in the pressure ratio. The same appear when ($r_{c2}=r_{c1}$) for low pressure ratios. After such point the increase in pressure ratio leads to lower specific power output and thermal efficiency. Such behaviour appears in most of pressure ratios when ($r_{c2}<r_{c1}$). Greater specific work output and lower thermal efficiency is observed by intercooled reheated gas turbine cycles at low split ratio ($r_{c2} > r_{c1}$). This appears with most of the pressure ratio range when ($r_{c2} = r_{c1}$). While the drop in thermal efficiency and a deterioration of power output results at a very high pressure ratio when ($r_{c2} > r_{c1}$). The thermal efficiency decreases and the specific work output increases for all pressure ratios of any split ratio for intercooled reheated regenerated gas turbine combined cycle configurations.

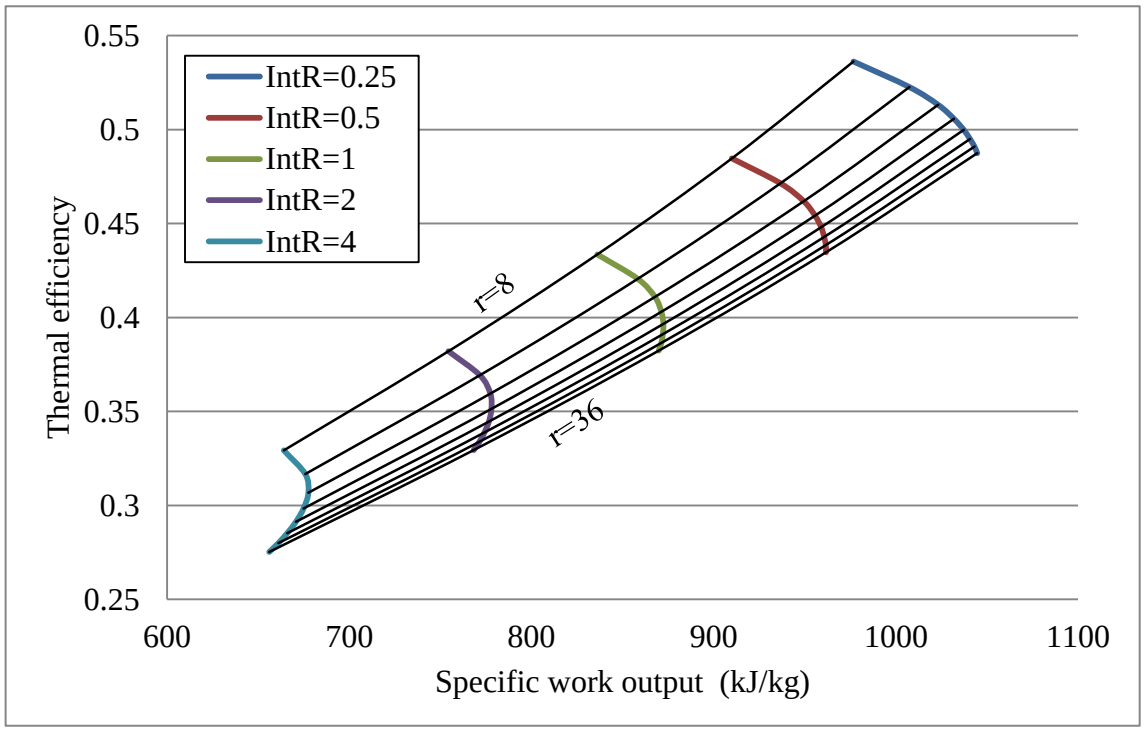

Figure 4.92 Intercooling pressure effect on thermal efficiency and specific power output of intercooled reheated gas turbine triple pressure steam combined cycle

4.4.3.3 Pressure of reheated gases (RehR) or (r_{t1}/r_{t2})

This section reviews the effect the pressure of reheat gases' on the performance of different gas turbine and combined power cycles. The change in the ratio of splits between the pressure ratio of the high pressure turbine and that for the low pressure turbine (r_{t1}/r_{t2}) is employed to represent the change of the pressure of reheat. The change in the performance of the power cycle goes over five values for a split ratio (0.25, 0.5, 1, 2 and 4). It starts from the value at which the gases expand in the first turbine the quarter pressure ratio of the second turbine and ends with the opposite. The change in the performance of the power cycles by the effect of reheat pressure is examined over two paths. The first employs the change in reheat pressure with the used range of turbine inlet temperature (800 - 1800 °C) and a pressure ratio of 16. The second undertakes the effect of reheat pressure with the usual range of the pressure ratio (8-36) and a turbine inlet temperature of 1400. This is applied on gas turbine and combined power cycles with reheated gas turbine. Therefore, it involves the power cycles with reheated, intercooled reheated and intercooled reheated regenerated gas turbine only.

a. The effect of the pressure of reheat and the change in turbine inlet temperatures

The impact of the pressure of reheat is very similar on the performance of different reheated gas turbine configurations. The increase in the pressure of reheat from shows a continuance decline in the efficiency of such cycles except the intercooled reheated regenerated cycle. In such configuration, the efficiency increases when the split ratio increases between 0.25 and 0.5. However, it tends to behave similar to the former cycles when the split ratio increases over 0.5. The specific work output increases by the increase in a split ratio between 0.25 and 1, while the increase over this range shows the opposite. The advantage behind the increase in the pressure of reheat is expected when the gases expand in the first turbine the half or less than half pressure ratio of second turbine. Therefore, to ensure an efficient specific work output the gases must expand to a pressure of 1/3 or less the turbine inlet pressure.

The increase in the pressure of reheat always leads to a drop in the thermal efficiency of reheated gas turbines. On the other hand, the specific work output increases for ($r_{t2} > r_{t1}$) and decreases for ($r_{t2} > r_{t1}$). This tendency appears for all turbine inlet temperature as illustrated in Fig. 4.93. It happens due to the increase in the fuel addition to maintain reheating the gases to the same previous temperature at the first turbine inlet. The temperature of the gases at the turbine outlet is severely influenced by such effect as shown by Fig. 4.94. Which shows the increase in the split ratio increase gases temperatures at turbine exhaust, although the same turbine inlet temperature. This increase in the GT discharge gets greater with the increase in the turbine inlet temperature. As a result, the drop in the pressure of reheat is the cause for such rise in the temperature of exhaust gases. Employing intercooled reheated gas turbines configurations come up with the same relations but slighter on the thermal efficiency and the specific work output. While for Intercooled reheated regenerated gas turbine configurations, this effect is greater on thermal efficiency and minor on specific power output. The increase in the efficiency appears for low turbine inlet temperature when ($r_{t2} > r_{t1}$).

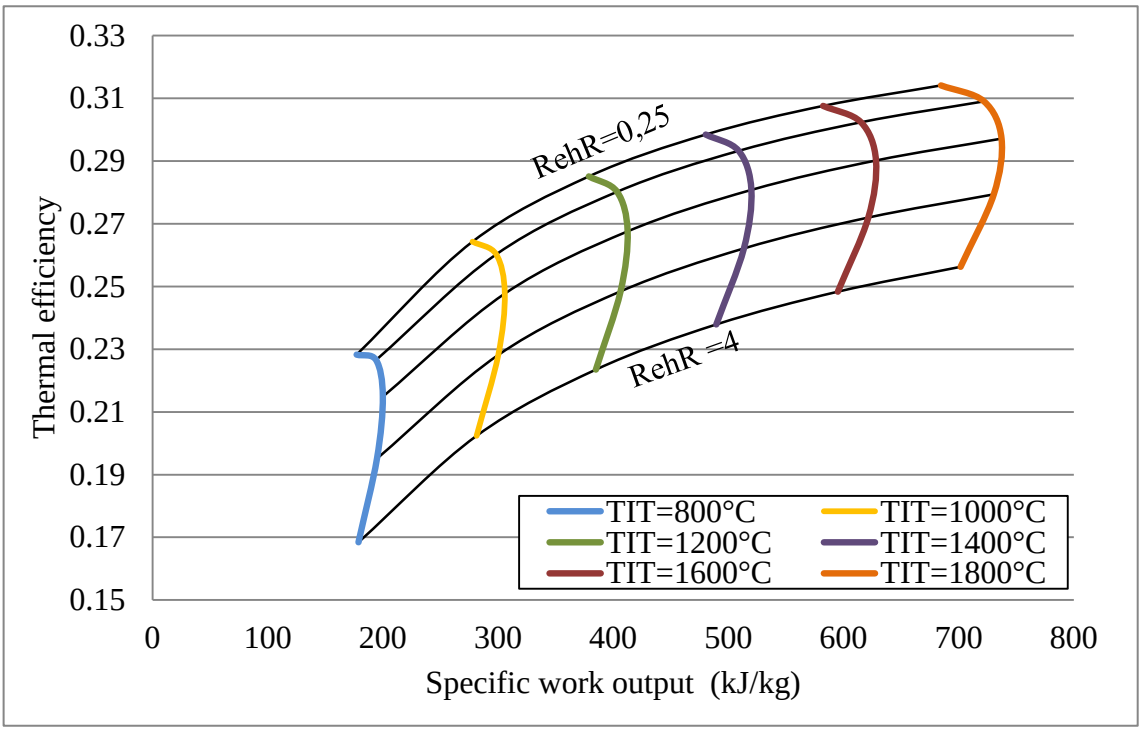

Figure 4.93 Reheat prssure ratio effect on the thermal effciency and the specific work output of reheated gas turbines

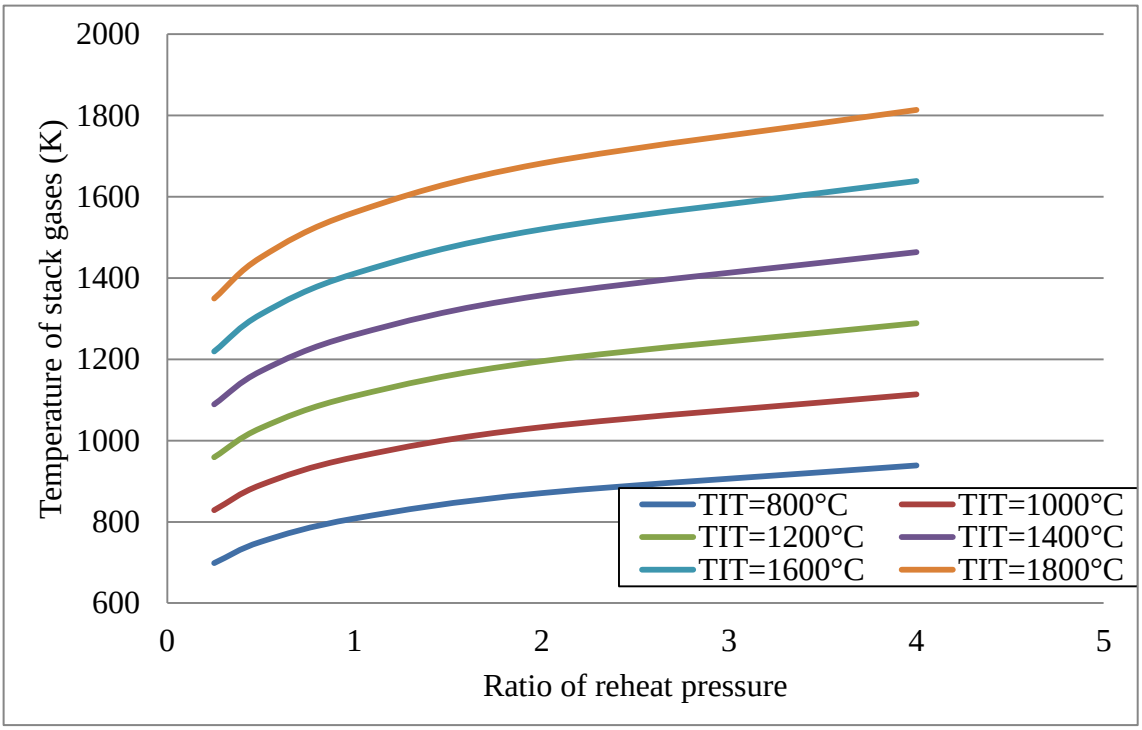

Figure 4.94 Pressure of reheat effect on the temperature of stack gases of a reheated gas turbine

b. The effect over different pressure ratios

This section confirms the results given by the previous section by investigating the effect of the pressure of reheat for a range of pressure ratios and constant turbine inlet temperature as shown by Fig. 4.95. It shows that, the reduction of the thermal efficiency is the slightest with the low pressure ratio for the range ($r_{t2} > r_{t1}$). The drop of the reheat pressure, the reheated gases expand from the same temperature over a smaller pressure ratio. Therefore, higher exhaust gases temperature is generated. This effect is greater in reheated and intercooled gas turbines over intercooled reheated regenerated gas turbine configurations.

The following figures illustrate the effect of the pressure of reheated gases on the performance of combined power cycles. The drop in the pressure of reheated gases increases the temperature of the gases at the turbine outlet. Therefore, more energy is available to generate steam of better quality by the same unit.

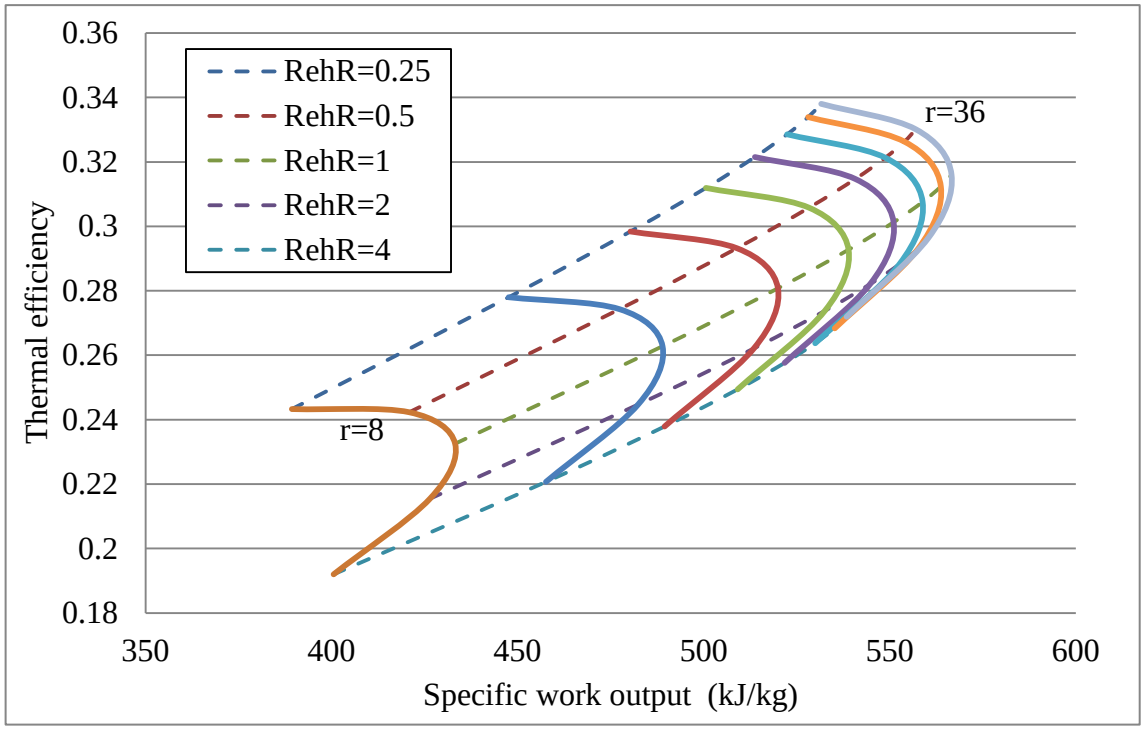

Figure 4.95 Reheat pressure effect on the efficiency and the specific work output of combined cycle

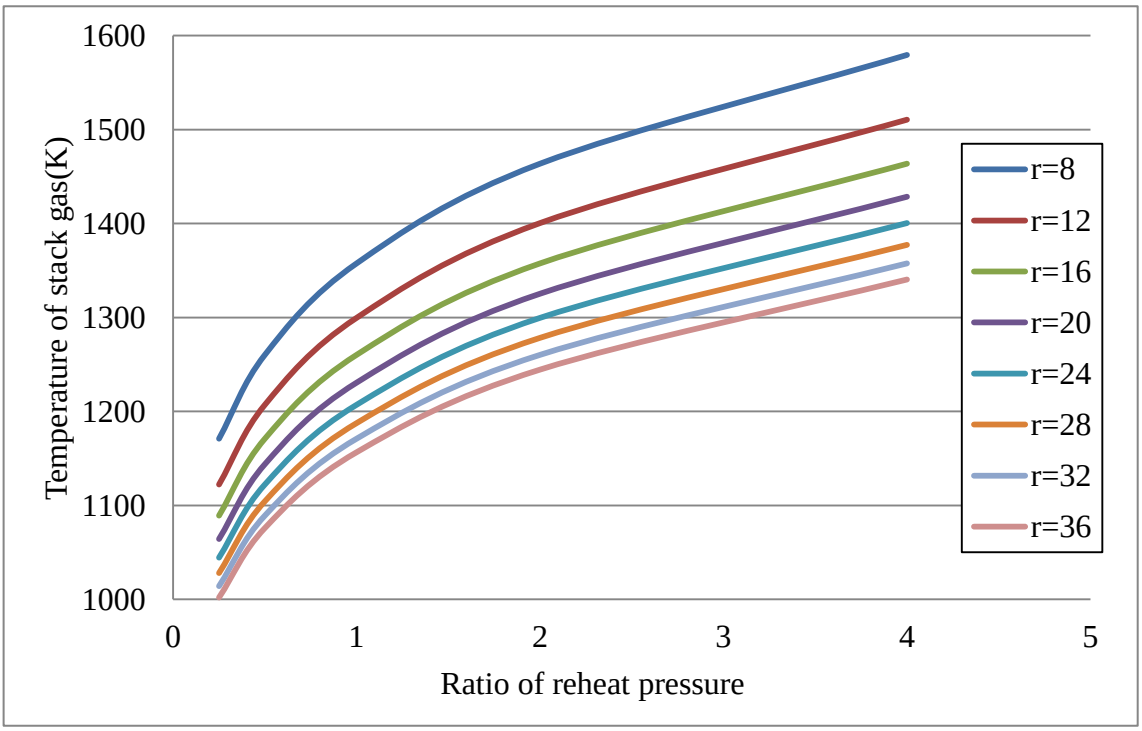

Figure 4.96 Pressure of reheated gases effect on the stack gases temperature

In general, the increase in pressure over rt2 leads to an increase in the efficiency, which reaches its maximum when ($r_{t2} = r_{t1}$). The thermal efficiency decreases when rt2 > rt1. While the specific work output continuously increases by the same effect. This tendency appears in all reheated gas turbines combined cycles. The maximum efficiency appears on the range ($r_{t2} > r_{t1}$), which drops the temperature of GT discharge gases. The thermal efficiency of a combined cycle power plant is heavily affected by the reheat pressure of intercooled reheated regenerated gas turbine combined cycle than CCPP of other gas turbine configurations. The effect of pressure of reheat on intercooled reheated gas turbine and reheated gas turbine is similar on the performance of all steam turbine cycles. This appears because gas turbine exhaust gases temperature is uninfluenced by inter-cooling. Therefore, the change in its performance away from reheated gas turbine combined cycle is only due to inter-cooling. The effect of reheat pressure of such gas turbine configurations is the heaviest on the performance of triple pressure steam combined cycle over other configurations. The maximum thermal efficiency differs by the kind of combined cycle configurations. This appears for ($r_{t2} = r_{t1}$) for all cycles in most of the investigated range of TIT. The reheated gas turbine combined cycle has the highest thermal efficiency. The increase in TIT over low degrees range transfers the lead of Maximum thermal efficiency to the intercooled reheated regenerated gas turbine

combined cycle. The maximum specific work output is always made by intercooled reheated gas turbine combined cycles.

For a constant steam pressure, the quality of the steam at the turbine inlet is affected by the TIT only. It increases by the rise of the temperature of gases at GT discharge due to the drop in the pressure of reheat. Accordingly, a steam of better quality is generated at the same boiler pressure. Therefore, a steam of better quality is rejected to the condenser. The effect of gases' reheat pressure on multi pressure steam turbine combined cycles appears only on the high pressure section of HRSG. The high value of the steam fractions at ST outlet can be suitably utilized to boost SC performance.

The effect of reheat pressure increases the thermal efficiency and the specific work output with a split ratio lower than 1 i.e. ($r_{t2} > r_{t1}$). The increase in split ratio over 1 drops the thermal efficiency, although the increase in specific work output in low pressure ratio gas turbine combined cycle configurations. Designing the gas turbines to work on high pressure ratios makes the decrease in thermal efficiency to appear earlier except for reheated steam turbine combined cycle configurations. In such configurations the tendency appears later (after a split ratio of 1). This effect is happened due to the changes in thermal efficiency and specific work output of the gas turbine engine. The temperature of stack gases decreases by the drop of the reheat pressure. It has various effects on the performance of different steam turbine engines. The highest stack gases' temperature is emitted by simple and reheated steam turbine combined cycle configurations. The heaviest effect of the change in the pressure of reheat on the temperature of stack gases occurs for the primary designed steam turbine combined cycle configurations. The figures below show the reduction in the temperature stack gases drown with a concaved line represents its effect on SFC. The specific fuel consumption slightly changes by such effect for the gas turbines designed to work with high turbine inlet temperature. On the other hand, the minimum SFC is shifted to a lower split ratio.

The effect of reheat pressure for a range of pressure ratios on the temperature of stack gases is the major for reheated steam turbine combined cycles. This effect is the slightest for intercooled reheated regenerated gas turbine combined cycle configurations. And finally, the increase in the pressure ratio shifts the minimum SFC points to a lower split ratio.

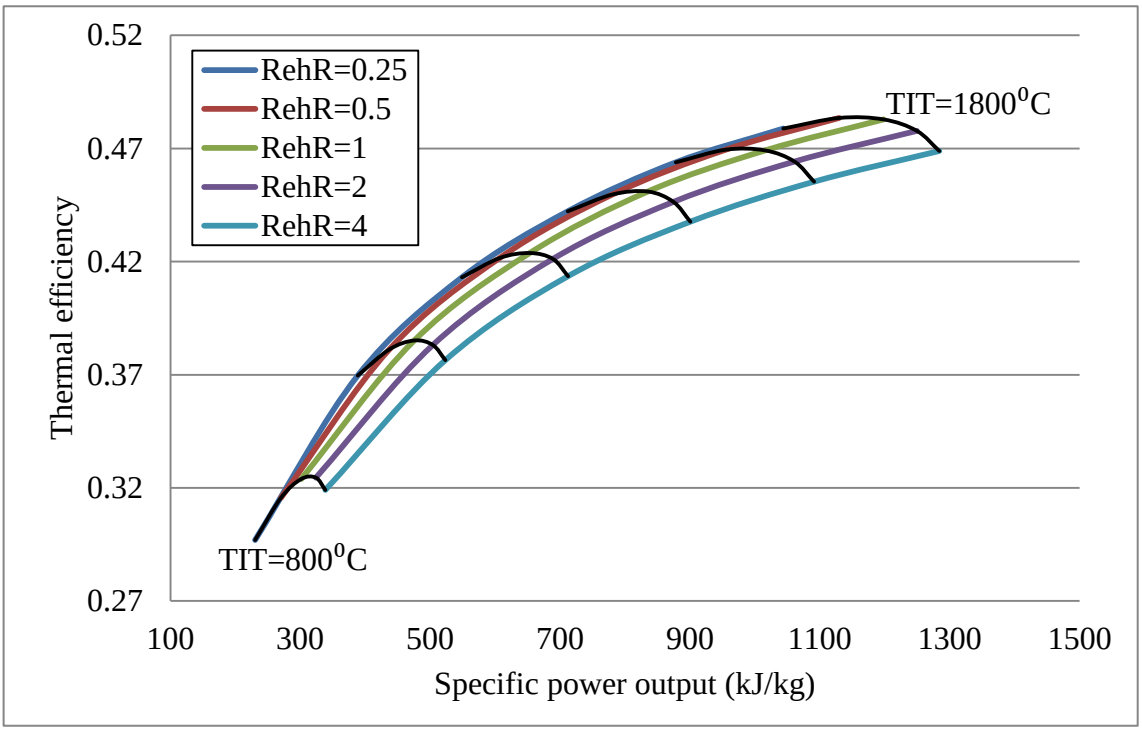

Figure 4.97 Gases reheat pressure effect on the thermal efficiency and the specific power output of combined cycle

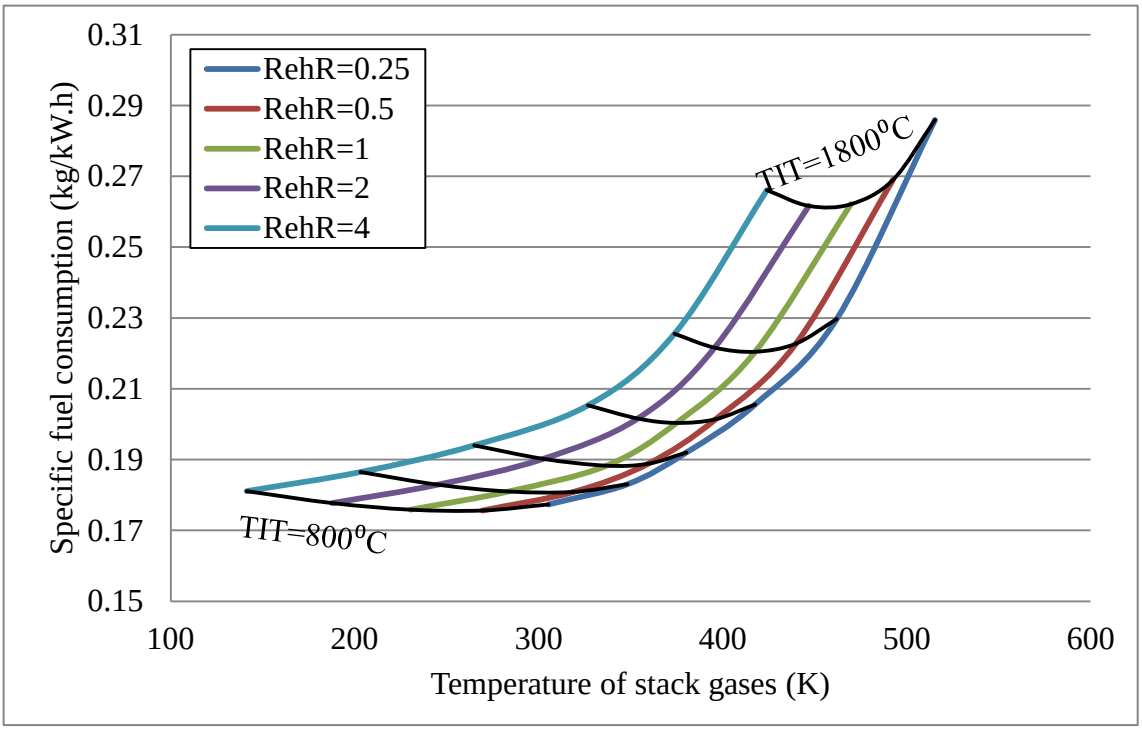

Figure 4.98 Gases reheat pressure effect on stack temperature and specific fuel consumption of combined cycle

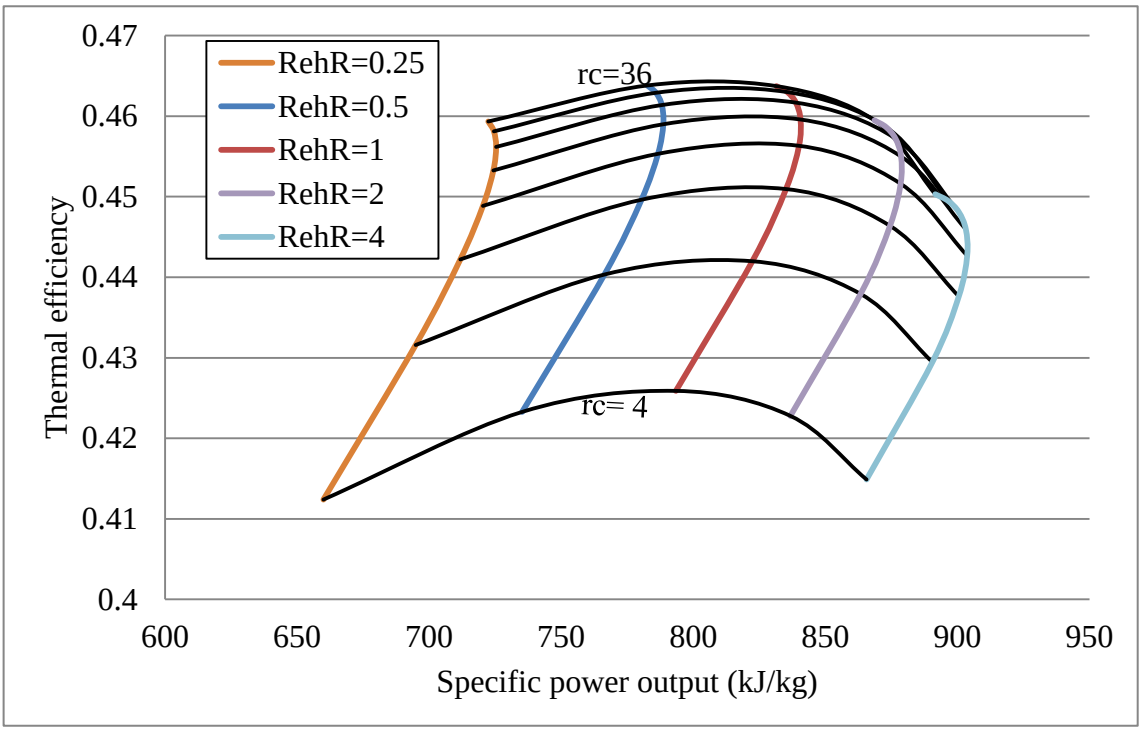

Figure 4.99 Gases reheat pressure effect on thermal efficiency and specific power output of combined cycle for different pressure ratios

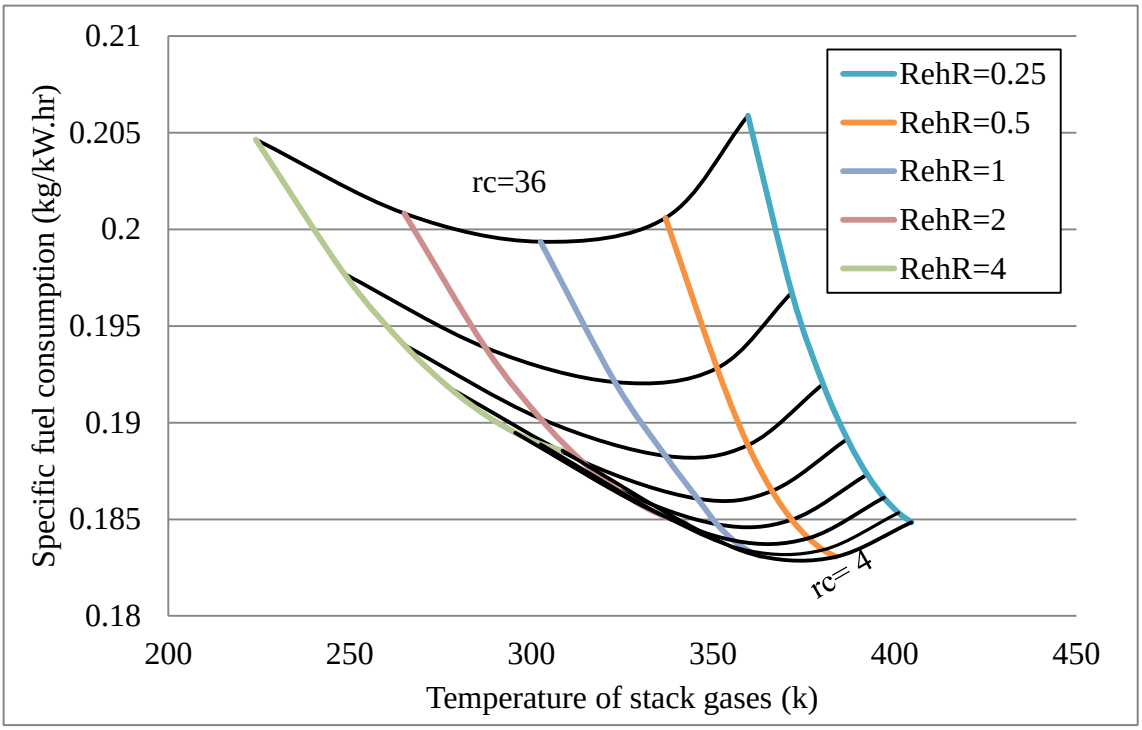

Figure 4.100 Gases reheat pressure effect on the temperature of stack gases and the (SFC) of combined cycle

4.4.3.4 The pressure of reheated steam (P_{s3Reh})

This section studies the effect of the SCs' pressure reheat on the performance characteristics of the combined power cycle. It considers all the above GTC configurations combined to any of the reheated SCs (reheated steam cycle, dual pressure reheated steam cycle and triple pressure reheated steam cycle). The increase of such pressure improves the quality of the reheated steam at turbine inlet when it reaches the temperature of the steam at the main turbine inlet. For a certain condenser pressure, the same tendency appears for the of the steam turbine outlet.

Reheating a low pressure steam increases the power slightly, and increase reheat expenses. Therefore, it is the parameter which decides the use of such process. Consequently, reheating high pressure steam must be chosen carefully, or it may restrict the reheat process. In general, the increase of the reheated steam pressure increases the work generated by the reheated turbine and reduces the work output from the main turbine. The effect of the pressure of the reheated steam on the performance characteristics of RehSC is greater than its effect on multi pressure SCs' configurations. The performance characteristics of these configurations deteriorate because its poweris generated from a greater number of steam turbines. The effect of the pressure of reheated steam on the performance and the environmental characteristics of different combined cycle configurations is depected by (Figs. 5.101 and 5.102). This pressure is restricted by steam pressure at boiler and condenser, but greatly depended on the first. Accordingly, in these figures, the pressure of reheated steam is a fraction of boiler pressure.

The results from the parametric study show that, the reduction in the pressure of the reheated steam increases cycle's thermal efficiency. This increase drops slightly by the increase in the pressure of the steam at high pressure. The influence of such increase on the specific work output is similar to that of the thermal efficiency of Fig. 4.101. The increase in the pressure of the reheated steam reduces the temperature of the stack gases. Such drop in the temperature of the stack gases rises by the increase of the pressure of the steam at the main turbine inlet. The pressure of the reheated steam had a converse effect on the steam turbine engine turbines.

The increase in the pressure of the reheated steam decreases the specific work generated by the reheated steam turbine and increases the specific work generated from the main turbine. The first is caused by the decrease in the enthalpy of the steam at the main turbine outlet. The second is caused due to the increase in the enthalpy of the steam at reheated turbine inlet and outlet.

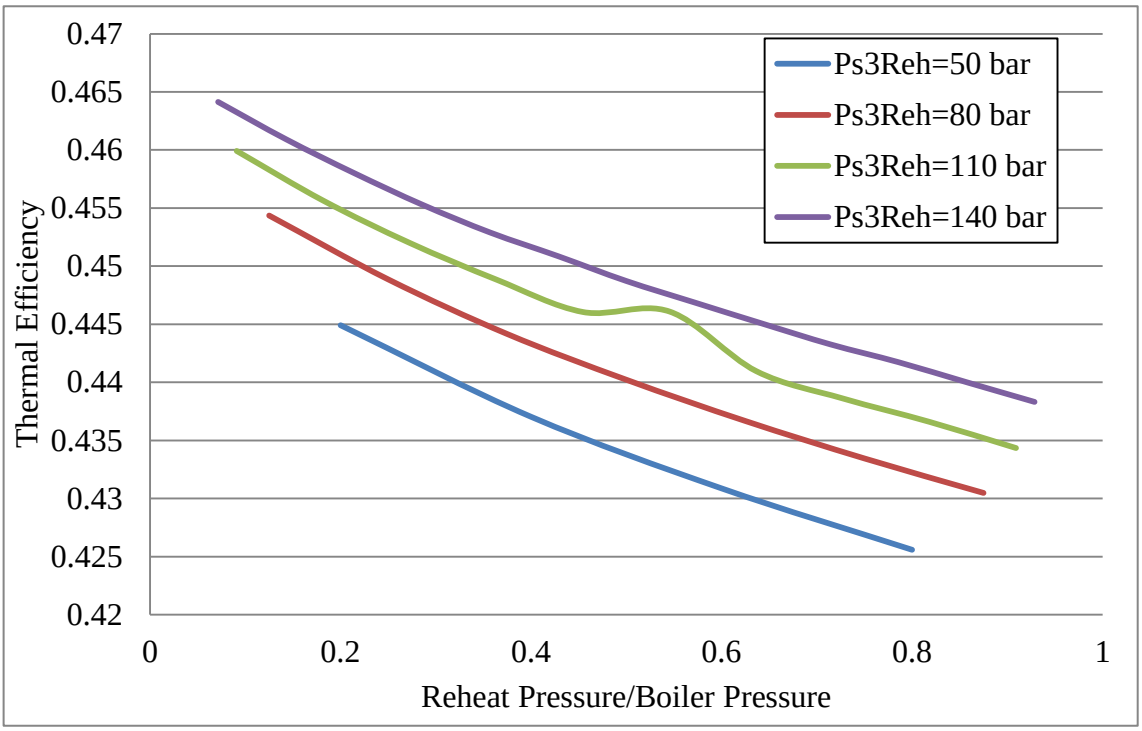

Figure 4.101 Pressure of reheat effect on thermal efficacy of simple combined cycle

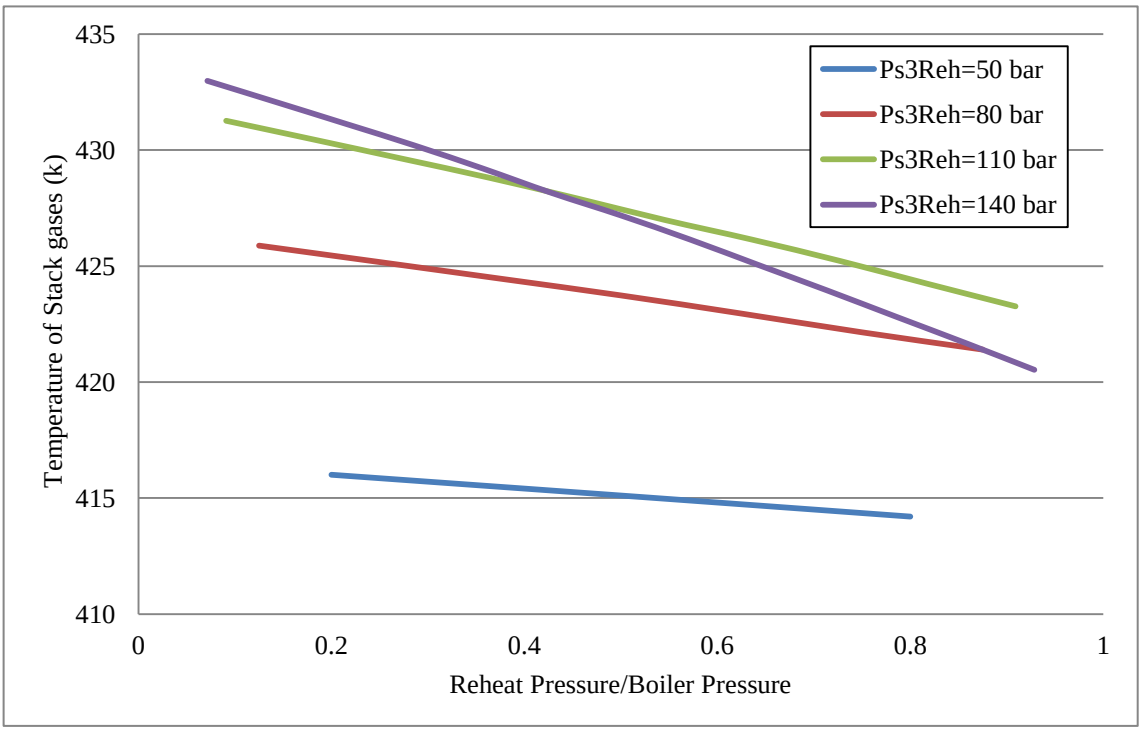

Figure 4.102 Pressure of reheat effect on stack gases temperature of simple combined cycle

4.5 Conclusions from the parametric study

1. The rise in turbine inlet temperature increases the efficiency and specific work output for the same pressure ratio. For fixed turbine inlet temperature, the increase in the pressure ratio does not ensure the increase in the specific work output and the thermal efficacy. Such increase is governed by a certain pressure ratio for each turbine inlet temperature, over which any increase in the pressure ratio decreases both. This point sweep to higher pressure ratios by the increase in turbine inlet temperature.

2. Specific fuel consumption and the temperature of stack gases were decreased with the increase in turbine inlet temperature. For a range of turbine inlet temperatures, the drop in specific fuel consumption was greater with the increase in pressure ratios. While the opposite appears for the temperature of stack gases.

3. The maximum efficiency for gas turbine cycle increases with turbine inlet temperature. The optimum parameters for maximum thermal efficiency and specific work output were not identical. The match between the pressure ratios and turbine inlet temperatures for maximum thermal efficiency and specific work output was governed by the pressure ratio. The optimum thermal efficiency always appears with highest turbine inlet temperature but not the largest pressure ratio.

4. The increase in boiler pressure increased the thermal efficiency and the specific work output for high turbine inlet temperatures and most of the pressure ratios. This change in the behaviour appears with high pressure ratios and swipe to lower pressure ratios with the decrease in turbine inlet temperature.

5. The specific fuel consumption and the temperature of stack gases were volatile with the change in boiler pressure. This tendency was governed by the temperature of the gases at turbine inlet and the pressure ratios. For low turbine inlet temperature and high pressure ratios, t increase in boiler pressure increased the specific fuel consumption and the stack gases temperature. By the increase in turbine inlet temperature, these tendencies were changed the opposite. The increase in boiler pressure with low pressure ratios dropped the specific fuel consumption and the temperature of stack gases.

6. Boiler pressure's heaviest effect on the thermal efficiency was observed by reheated gas turbine / dual pressure steam turbine combined cycle. The greatest effect on the temperature of stack gases was made by intercooled reheated gas turbine/ triple pressure reheated steam turbine combined cycle. While its greatest effect on the specific work

output was for intercooled reheated gas turbine/dual pressure steam turbine combined cycle. The maximum effect of boiler pressure on the specific fuel consumption was for reheated gas turbine/triple pressure reheated steam turbine combined cycle.

7. The decrease in condenser pressure always increased the thermal efficiency and the specific work output for fixed turbine inlet temperature and pressure ratio. Such increase in thermal efficiency and specific work output was augmented by the increase of TIT for the same pressure ratio. The effect of boiler pressure on thermal efficiency and specific work output was reduces with the increase in the pressure ratio.

8. The reduction of the condenser pressure decreased the specific fuel consumption and the temperature of stack gases. This decrease was varied with turbine inlet temperature and pressure ratio. However, such decrease was minimized for both with the increase of the ratio.

9. The effect of condenser pressure on the efficiency and the specific work output was the heaviest for reheated gas turbine/ dual pressure steam turbine combined cycle. The largest effect on the temperature of stack gases was for reheated gas turbine/ triple pressure steam turbine combined cycle. The heaviest effect on the fuel consumption was for intercooled reheated gas turbine/ regenerated steam turbine combined cycle.

10. The effect of minimum pinch point temperature difference was very close on conventional HRSG combined cycles. This included simple, regenerated and reheated steam turbines.

11. The effect of the minimum pinch point temperature diffrence on cycle's performance was different with the pressure of the heat units. However, in a multi pressure steam turbine, the heaviest effect was made by changing the pinch point temperature difference of all HRSG units together.

12. The minimum pinch point temperature differnce heavily affected the temperature of stack gases. However, it had a slight effect on thermal efficiency and a very slight one on specific work output.

13. The effect of the steam mass fractions varied with different steam turbine's configurations. The increase of each stream mass flow rate reduces SFC and stack gases temperature. The high pressure mass flow rate had the heaviest effect on temperature of stack gases and SFC. The mass flow rate of intermediate and low pressure together

made the greatest effect on SFC and the temperature of stack gases of triple pressure and triple pressure reheated steam turbines combined cycles. The effect of the intermediate pressure stream mass flow rate had more influence than the low pressure stream.

14. The increase in the ratio of low to high pressure steam streams increased the thermal efficiency and the specific work output. The slope of this linear relation was decreased with higher GT inlet temperature, which means that, the increase of the specific work output tends to be greater than that for thermal efficiency by the increase in the turbine inlet temperature.

15. Any increase in the steam mass flow rate increased the thermal efficiency and the specific work output. This increase was enlarged with the higher turbine inlet temperature. The increase in specific work output was enlarged over that for thermal efficiency with the increase in turbine inlet temperature.

16. The increase of the steam mass flow rate drops the specific fuel consumption and temperature of stack gases for any section in HRSG except for high pressure in which the increase in mass flow rate yields to a fixed drop in gases temperature.

17. By the increase in turbine inlet temperature, the influence of steam mass flow rate was greater on stack temperature and smaller on specific fuel consumption.

18. The increase in the split ratio of compression ratio for intercooled gas turbine cycle always led to leaner increase in thermal efficiency and specific work output. This was different with combined cycles.

19. For intercooled gas turbine combined cycle, the increase of inter-cooling pressure dropped the thermal efficiency and the specific work output by the increase in the pressure ratio of high pressure splits. With low pressure splits, this tendency was the opposite with the increase in the pressure ratio. But this tendency did not continue for high pressure ratios. It decreased the specific work output, although it increased the thermal efficiency.

20. Intercooled reheated gas turbine combined cycle had similar behaviour of intercooling pressure, to that of intercooled gas turbine combined cycle. In which the increase in the pressure ratio always droped the thermal efficiency and increased the specific work output.

21. The increase in the pressure of reheat always increased the thermal efficiency. It also increased the specific work output for a range of ($r_{t2} > r_{t1}$), but this behaviour dominates most of the investigated range for low turbine inlet temperature. Thermal efficiency was increased with a drop in specific work output with the rest of the range.

22. The temperature of stack gases increases with the increase of the split ratio. For the tested range of pressure ratios, the increase in thermal efficiency is combined with the increase of the specific work output for ($r_{t2} > r_{t1}$). The rest of the range confirms an increase in the thermal efficiency with a drop in the specific work output.

23. The increase in the pressure ratio of the GTC improves its power generation and thermal efficiency. These improvements are different from a configuration to another. The increase in the efficiency is restricted by an optimum pressure ratio, while the increase in the power output is boosted with the increase in the pressure ratio. Therefore, designing the GTC to work on a pressure ratio over the optimum decrease its efficacy, although it increases the power output.

24. The increase of the gases' temperature at turbine inlet improves the increase of the specific work output of the GTC even if it's designed to work on the same compression ratio. It also increases the optimum pressure ratio. A change in such behaviour appears by increasing the pressure ratio for a certain turbine inlet temperature. This tendency usually appeares for turbine inlet temperatures below 1400 ^{0}C.

25. The maximum increase in the thermal efficiency of all configurations is linear with the specific work output. However, this increase does not continue to high pressure ratios except for intercooled reheated gas turbines or if it operates on a very high TIT.

26. The specific fuel consumption decreases with the increase of the specific work output by the effect of the increase in the pressure ratio. This opposite tendency appears by setting the gas turbine engine to a pressure ratio greater than the optimum value. The drop in specific fuel consumption continues with the increase of the specific work output for the intercooled and intercooled reheated gas cycles. While it increases with the increase of the specific work output for low turbine inlet temperatures of intercooled reheated regenerated gas turbine cycle. This increase is combined with a reduction in the specific work output for regenerated cycle or if it operates on low TITs in simple and reheated gas turbines.

27. The ambient temperature has a slighter effect on the performance of combined cycle power plant than the gas turbine engines. The drop in the ambient temperature always serves in optimizing gas turbine's specific work output. The ambient temperature has a volatile effect on the thermal efficiency. Such influence is governed by the pressure ratio on which the gas turbine engine has been set on. The utilization of high pressure ratio slightly increases the thermal efficiency of the combined cycle plants. While the utilization of a very small pressure ratio gives the opposite effect.

28. The ambient temperature does not affect the temperature of the stack gases or the quality of the steam at any turbine exit. Although it has a slight effect on the performance of combined cycle configurations, it can ensure a degree of power augmentation with no impacts to the environment.

29. The increase in the split ratio from 0.25 to 4 reduces the thermal efficiency of intercooled reheated gas turbine but increases its specific work output.

30. The increase of TIT improves the effect of the pressure of reheat on the specific work output and degrades that on the thermal efficiency. T increase in the pressure ratio reduces the effect of the reheat pressure on the specific work output and the thermal efficiency. The maximum efficiency of such configuration is always correspondent to the highest (TIT) and (r) and a split ratio of 0.25. Therefore, employing a greater expansion ratio for the second turbine than the first (increasing the pressure of reheat), guaranties better performance than other configurations.

31. The increase in the split ratio increases the (SFC) and the temperature of stack gases. The effect of pressure of reheat on the (SFC) reduces by the increase of (TIT) and (r). The change in the temperature of stack gases by the effect of reheat pressure does not change by the increase in the (TIT), but drops with the increase in the pressure ratio(r). The increase in the pressure of reheat by which the gases expand from 1/3 or less of the high pressure is required to ensure an efficient increase in the specific work output. Therefore, the gases expand from greater pressure than before. Consequentially, the impact of the gases on the second turbine materials' increases. Accordingly, enhancing the materials of the second turbine is required.

CHAPTER 5
OPTIMIZATION OF COMBINED POWER CYCLES

5.1 Introduction and general background

This chapter deals with the details of the modelling and optimization of the gas and steam turbine components and its operation within the combined power and power cycles. Full description of the simulation process of the combined power and power cycles is also dealt with in this chapter.

The design point of the combined cycle power and power plant was proven to be difficult to obtain by the procedures of the previous chapter. This was caused by the complexity of the thermodynamic analysis as it is extremely difficult to define a mathematical solution for the gas turbine optimization equations. The control strategy of any plant changes with the change of the work load required. Therefore, it is important to analyse and determine the range of the operating parameters when the plant is operating on such variable loads.

The results of the preliminary calculations reported in chapter 4 provided the design data that suits any particular application. Accounting on such data any of the components in the gas turbine engine can be designed so the whole plant can provide the design point performance. The design point of a gas turbine engine is represented by the values of the following parameters: the specific speed, the pressure ratio and the mass flow rate on which the individual component is designed. Combining suitable operating range of gas turbine engine components reduces the level of possible operating points of each component. The said points on the characteristics map of each of the components running with steady speed operation are termed as "the equilibrium running points". The equilibrium running points for different speeds together forms the engine equilibrium running line employing both the turbine and compressor equilibrium running diagram. This diagram shows the operating zone proximity to compressor surge line. The strategy to optimize the performance during part load operation periods can be determined from such map. Therefore, there will be no need for prototype or

experimental tests to investigate variables' effects when a simulation program can give acceptable and accurate results.

The performance of the combined cycle power and power plant is described by the changes in its efficiency (ηcc) and power output (Wcc) taking into consideration the major practical limits such as: The metallurgical limit of the maximum turbine inlet temperature of (1500°C) for conventional combustor of a lean combustion process. The dryness fraction of the steam discharged from the turbine outlet not exceeding 90%. Although there is a very small percentage of sulphur in the content of the natural gas, the temperature of the stack gases must not be reduced to lower than 150°C .This is necessary to prevent the formation of Sulphuric acid at the exit of the HRSG. Determining the performance of the combined cycle power and power plant during the off-design operating periods is more difficult than determining its performance at the design point. Because in such operation periods the efficiency of each component changes, however, it can be obtained from the characteristics curves. The variation in the performance over the complete range of speed and power output refers to the off-design performance. The off-design performance characteristics are calculated by satisfying the compatibility (matching) of (ṁ, W and N) between the different components on which a specific software is required to operate on. The off-design performance is the states of the combined cycle power plant on the running line when it operates on the available loads Al-Quran et al., [25].

The off-design performance of a gas turbine is determined by the interaction of various engine components, i.e. components matching. The matching between the gas turbine components will restrict the suitable operating range of each component. Different procedures are modelled to predict and evaluate the performance of gas turbine as an integrated machine and its individual components. Employing these procedures requires some tools to manage the readings for the performance characteristics. Prototype on such mechanisms has been largely used in the past decade for the reason above, obviously they were costly and time consuming. The developments in the mathematical computation techniques in the recent years made computations and predictions the first choice for the designers. Hence, the approach of mathematical modelling for predicting the performance of gas turbine is the best solution economically.

A simulating program can be used to predict the map of performance during part load operation. Therefore, developing a model to simulate steam turbines as a part of the CCPP is important. Simulators were used extensively by Razak [8] and many authors to illustrate the

changes in the performance of gas turbine due to various parameters. As a result, the emissions and the estimated life of such engines were calculated. The change in different conditions is investigated by such simulators, as well as their effect on the emissions, life time and performance. Gas turbine components are complicated in both the design and during operation periods. This chapter is devoted for (1) Modelling the approach, (2) Matching the components and (3) Simulating in a computer program the combined cycle power and power plant performance.

The evaluation (ranking) of a fossil fuel power plant is identified by: (1) power plant arrangement, (2) turbine engine configurations and (3) the available alternatives for cycle design. It is a difficult job to categorize a plant arrangements and turbine configurations for CCPP. This is caused by the variant: (1) cycles' main parameters, (2) processes required for steam and (3) modes on which the plant operates. Accordingly, a substantial thermodynamic optimization is required in most plants [82]. Optimization can be simplified by understanding:

(i) The optimized component design alternatives.
(ii) The main boundaries of match between the component and other components of the cycle.

The model developed and described in this chapter the model established here is based on the limitations and the operation conditions and operating parameters required for the combined cycle of power plants rather than other applications. Therefore, practical values are used for exist application. It is clear from the work undertaken in the previous chapter that combined cycles' optimized parameters haven't been under full discussion. The previous chapter was inadequate in obtaining the points of the art design on which every single combination is operated.

5.2 Combined cycle power plant program

The previous chapters confirmed that although CCPP parameters have similar influence to its effect on each of the combined plants individually, however, there are some differences from their effects on CCPP. The performance map of each component in the CCPP will have a narrower operation view to satisfy the condition of components' acceptable performance. Accordingly, evaluating each component in the CCPP to satisfy its performance is the goal here. In which this will demonstrate these limitations on the performance map. However, this imposes limitation on the performance map as will be demonstrated hereafter.

5.2.1 Equations for combined cycle power plant performance characteristics, configurations and basic analysis

The general sets of equations which characterize the performance of the combined power plant are listed below. All symbols used refer to their usual meaning.

$$w_{GCPP} = (w_{GT} - w_{AC}) \times \eta_{PG} \quad \ldots (5.1)$$

$$\eta_{GCPP} = \frac{w_{GC}}{LCV \times f_{CC} \times 1000} \quad \ldots (5.2)$$

$$w_{SCPP} = (w_{ST} - w_{WP}) \quad \ldots (5.3)$$

$$\eta_{SCPP} = \frac{m_{sa}\ (w_{ST} - w_{WP})}{(1 + f_{CC})\ (h_{g4} - h_{gStack})} \quad \ldots (5.4)$$

$$\eta_{SCPP} = \frac{m_{sa}\ (w_{ST} - w_{WP})}{(1 + f_{CC})\ (h_{g4} - h_{gStack})} \quad \ldots (5.5)$$

$$\eta_{CCPP} = \frac{w_{CCPP}}{(f_{CC} \times LCV \times 1000)} \quad \ldots (5.6)$$

$$W_{CCPP} = \frac{m_{g1} \times w_{CCPP}}{1000} \quad \ldots (5.7)$$

$$SFC_{CCPP} = \frac{3600 \times f_{CC}}{w_{CCPP}} \quad \ldots (5.8)$$

5.2.2 Components models

In order to help on optimizing the system with regard to the current technologies' limitations the following restrains for each component are considered. The main components of combined cycle power plants considered here are as follows:

5.2.2.1 Air compressor model

The compressor is modelled here using the equations (5.9-5.12) in addition to many other functions. The performance characteristic's map indicates if the compressor is operating within acceptable working line. Its design and off design Non-dimensional tables given by

[83], [82] are used here to identify the characteristics of the axial compressor. These tables are corrected to the certain design point for any different compressor. Accordingly, Walsh and Flitcher [83] stated to multiply these values with the corresponding design point values. These tables are tabulated by Lazzaretto and Toffolo [82] using compressor maps given by Mirandola and Macor, [84]. These tables are graphically illustrated by Figs. 5.1-5.2. In the current work, these tables are used in two functions (ACF1 and ACF2), which were established to generate the non-dimensional speed and the non-dimensional isentropic efficiency for any given mass flow and pressure ratio. Instead of correcting the whole compressor map for an input value of design point, the input values to these functions were corrected for the non-dimensional characteristics map. The output from the function is turned back with regard to the given design point of such compressor. Equations 5.9-5.12 were employed in the air compressor model as shown in Fig. 5.3.

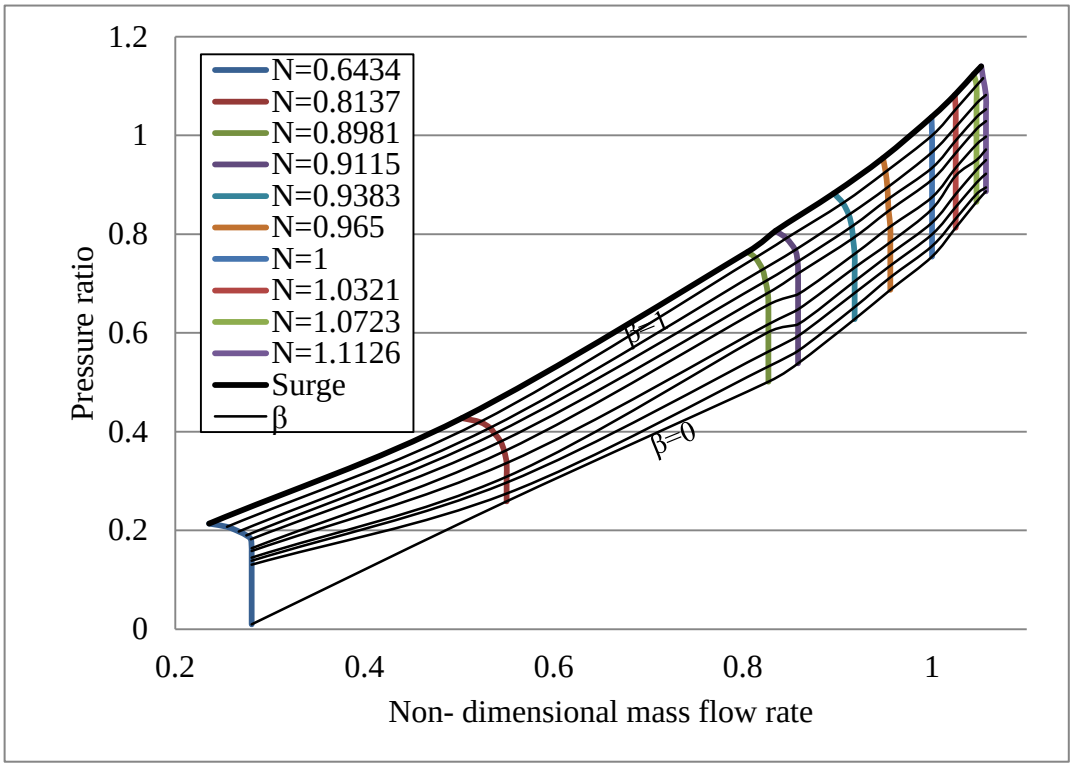

Figure 5.1 Pressure ratio versus mass flow on normalized map for axial

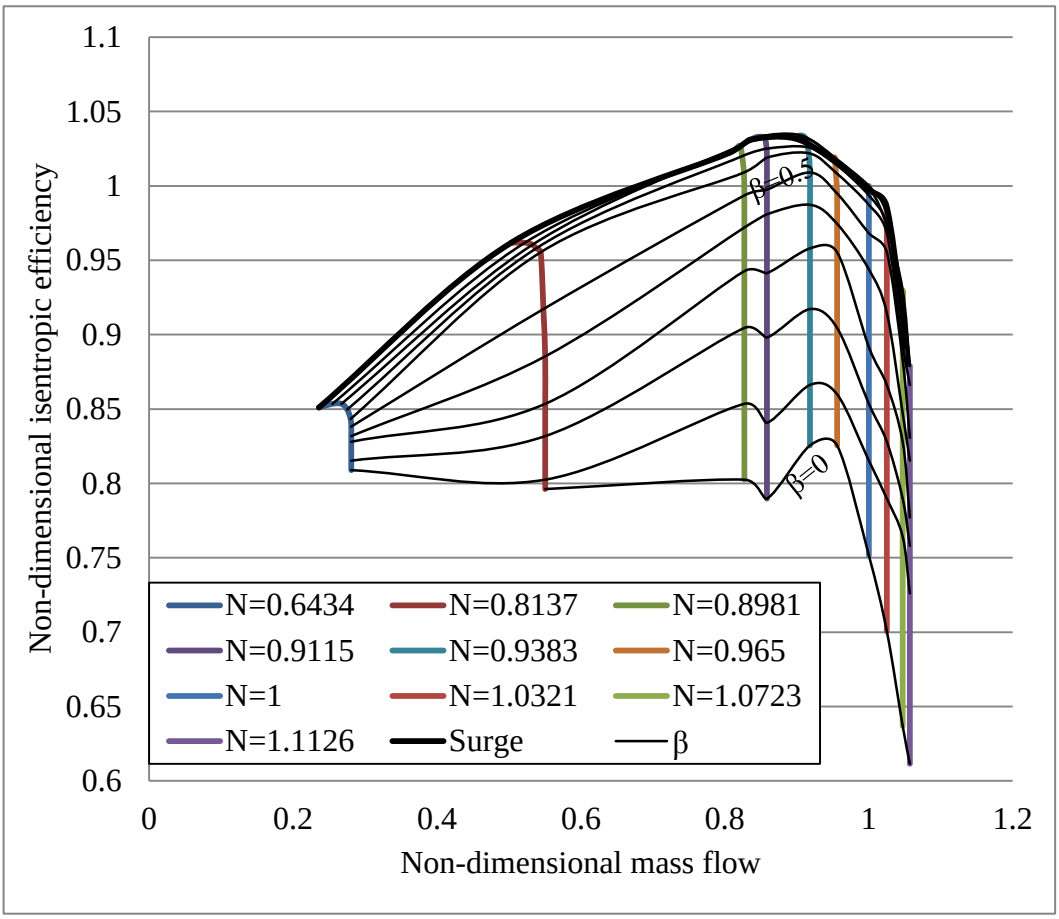

Figure 5.2 Isentropic efficiency versus mass flow on normalized map for axial

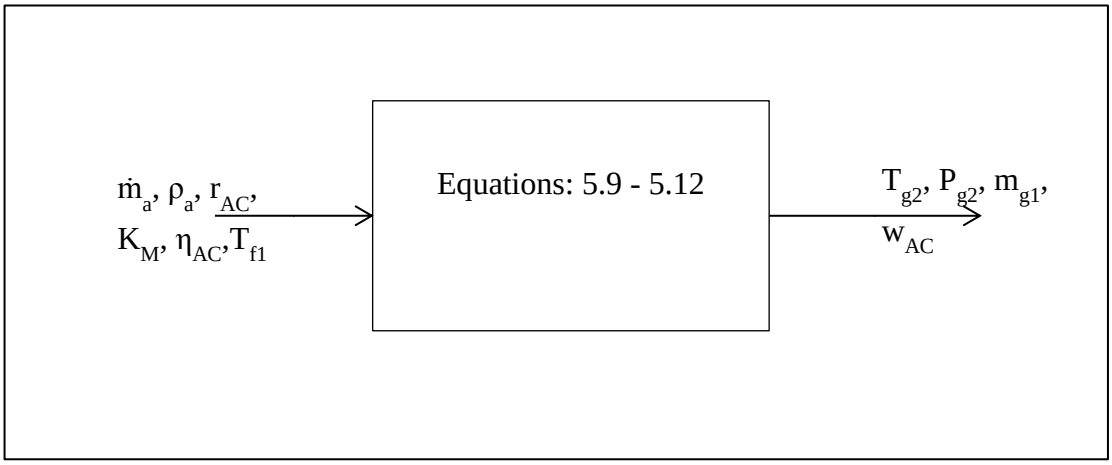

Figure 5.3 Air compressor model

$$m_{g1} = m_a \times \left(\frac{\rho_a}{\rho_{iso}} \right) \quad \ldots (5.9)$$

$$P_{g2} = P_{g1} \times r_{AC} \quad \ldots (5.10)$$

$$T_{g2} = T_{g1} \times \left[1 + \left(\frac{\left(r_{AC}\right)^{K_a} - 1}{\eta_{AC}} \right) \right] \quad \ldots (5.11)$$

$$w_{AC} = \frac{h_{g2} - h_{g1}}{\eta_{AC}} \quad \ldots (5.12)$$

5.2.2.2 Combustor model

Kobayashi, et.al [63] showed that increasing the pressure of lean combustor kept the flammability limit constant. They also reported for a stable lean combustion and for pressure between 11 bar and 41 bar a low value of ϕ_L= 0.7. In this model, the function fFTERLCVEFF is created to estimate the fuel to air ratio required for conventional combustion process. The function f2FTEREFFLCV was used to estimate the same ratio for reheat combustors. In both the temperature of the combustion were assumed to be given

The flame of any particular combustion chamber is unstable beyond the limit of rich and weak air to fuel ratio. The increase in the air velocity reduces the range of the air to fuel ratio between the rich and the weak limits. If the air mass flow is to increase beyond a certain value, it is impossible to initiate the flame at all. This is due to the failure of ignition and the establishment of a viable flame kernel which can propagate successfully. A suitable combustion chamber must cover the required range of the air to fuel ratio and the mass flow of the gas turbine engine on which it is intended to operate. This is defined by the stability loop which is the air to fuel ratio plotted against the air mass flow. The maximum air flow rate that corresponded to flame blowout was derived by Ballal and Lefebvre using the global reaction rate consideration [85].

$$\dot{m}_{max} = 1.93 V_C \left(P_C\right)^{1.25} \exp\left(\frac{T_o}{150}\right) \times \left(\phi_C\right)^{6.25} \quad \ldots (5.13)$$

Where (T_o) is initial temperature, V_C is the volume of combustion zone and P_C is its pressure. For the lean combustion, the effect of the pressure of combustion is almost constant for a range of the flammability limit. Fuel lean combustion is well known of its low NO_X emissions Kobayashi et al., [63]. For a certain ϕ_R the difference between the LHV of the Methane and that for syngas generated from the fuel rich combustion can get as high as 37%. The maximum air flow rate, air temperature and combustion gases pressure are given in Equations (5.13-5.15), these used in the model of Fig. 5.4 to generate the combustion chamber model.

$$T_{f2} = T_{f1} \times \left[1 + \left(\frac{\left(r_{AC}\right)^{K_M} - 1}{\eta_{AC}} \right) \right] \quad \ldots (5.14)$$

$$P_{g3} = P_{g2} \times (1 - \lambda_{CC1}) \quad \ldots (5.15)$$

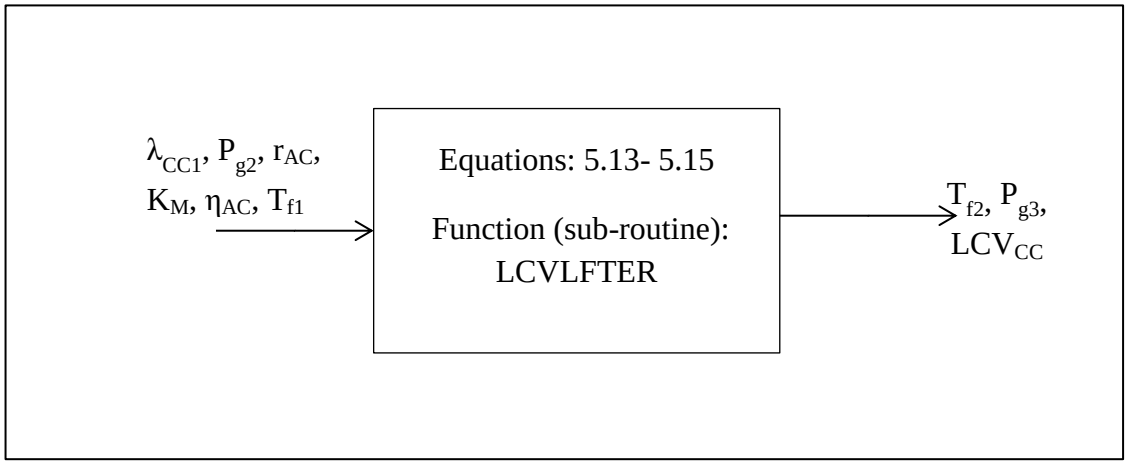

Figure 5.4 Combustion chamber model

5.2.2.3 Gas turbine model

The performance characteristics of the turbine are adopted from turbine map for NASA CR174646 taken from Kurzke [86] given by Srivastava [87]. These characteristics are illustrated in Figs. 5.5-5.6 in which the pressure ratio for such turbine is functioned to the isentropic efficiency in the first and to the mass flow rate in the second. While two functions (GTF1 and GTF2) were established using tabulated values of these figures to estimate the corrected values of isentropic efficiency and mass flow rate. In these functions, the same conditions were applied with regard to the corrected values of the inputs and outputs. As it has been reported from the previous studies, the gases at turbine exhaust was set to be not less than 150°C to avoid acidity of the stack gases. Equations (5.16 - 5.18) were employed to generate the gas turbine model shown in Fig. 5.7, which also show the model input parameters.

$$r_{GT} = \frac{P_{g4}}{P_{g3}} \quad \ldots (5.16)$$

$$T_{g4} = T_{g3} \times \left(1 - \eta_{GT} \times \left(1 - \left(r_{GT}\right)^{-K_g}\right)\right) \quad \ldots (5.17)$$

$$w_{GT} = (1 + f)\,(h_{g3} - h_{g4}) \times \eta_{GT} \quad \ldots (5.18)$$

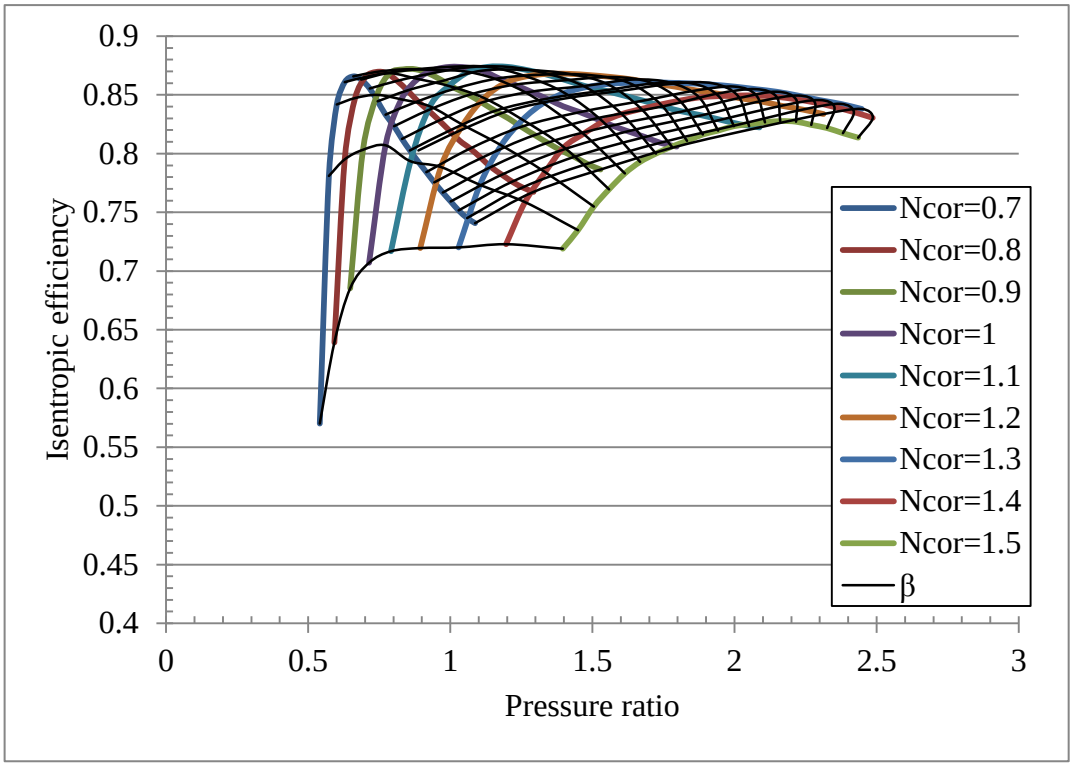

Figure 5.5 The isentropic efficiency versus the pressure ratio on normalized map for axial gas turbine at various normalized rotational speed (N)

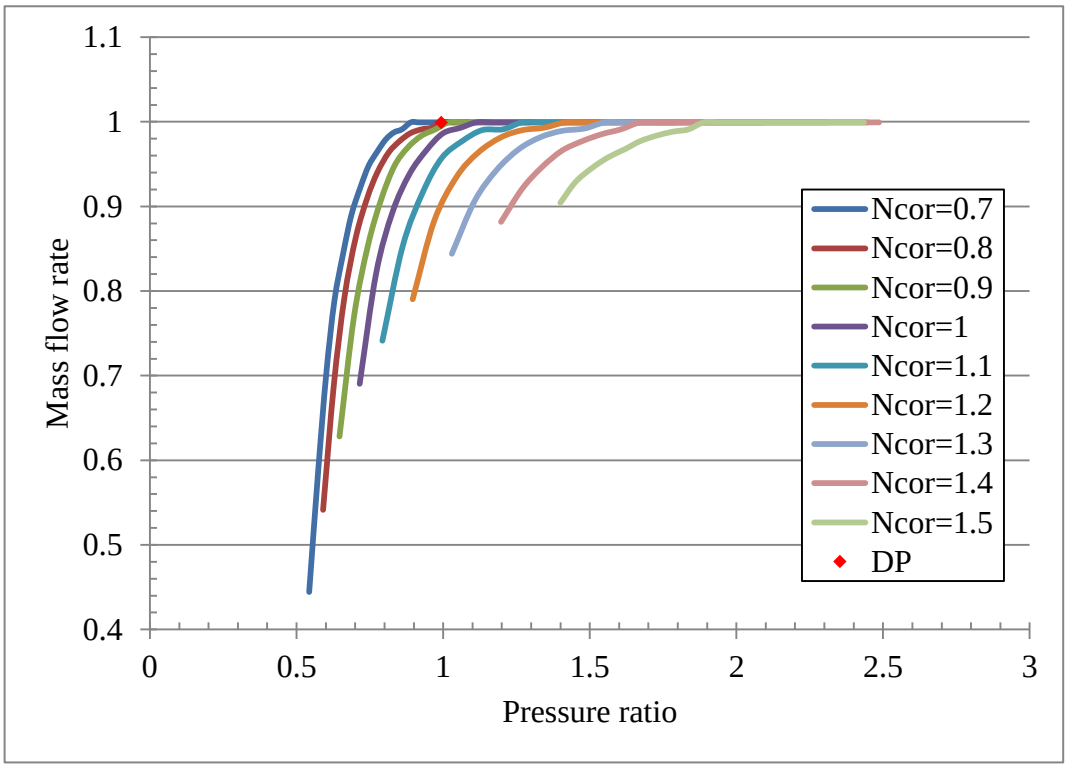

Figure 5.6 The mass flow versus the pressure ratio on normalized map for axial gas turbine at various normalized rotational speed (N)

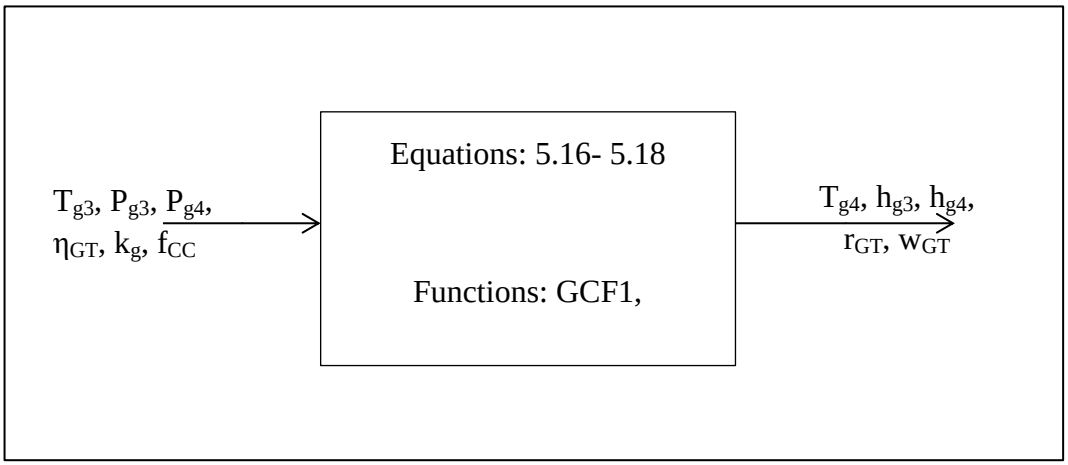

Figure 5.7 Gas turbine model

5.2.2.4 Steam re-heater model:

The pressure at the reheater is made to be equal to that for the intermediate pressure of the steam boiler. This pressure should be in compromise when the high pressure steam is reduced. Otherwise, the high pressure turbine enthalpy change is reduced. These two pressures shouldn't be close in value. On the other hand, if there was an increase in the high pressure, an increase in the Reheater pressure is similarly required. The temperatures of the gases at the

reheater outlet for single and multi-pressure HRSGs are determined using the typical effectiveness equations of 5.19-5.20.

$$T_{gRehO} = \frac{\left(T_{gEI} - T_{sEI}\varepsilon_{Reh}\right)}{\left(1 - \varepsilon_{Reh}\right)} \quad \ldots (5.19)$$

$$T_{gRehO} = \frac{\left(T_{gEI}^{HP} - T_{sEIHP}\ \varepsilon_{Reh}^{HP}\right)}{\left(1 - \varepsilon_{Reh}^{HP}\right)} \quad \ldots (5.20)$$

The pressure at which reheating is expected to occur is governed by the value (S_{Reh}) as shown by equations (5.21-5.23). This parameter has a different definition for different HRSG system.

$$P_{sReh} = S_{Reh} \times P_{s3}^{IP} \quad \ldots (5.21)$$

$$P_{sReh} = S_{Reh} \times P_{s3}^{LP} \quad \ldots (5.22)$$

$$P_{sReh} = S_{Reh} P_{s4} \quad \ldots (5.23)$$

The enthalpies of the reheated steam are calculated using the effectiveness equation as well for multi pressure and single pressure HRSG by equations (5.24 – 5.25) respectively:

$$h_{s3}^{RehP} = h_{s4} + \varepsilon_{Reh}\left(h_{sg4}^{RehP} - h_{s4}\right) \quad \ldots (5.24)$$

$$h_{s3}^{RehP} = h_{s4}^{HP} + \varepsilon_{Reh}\left(h_{sg4}^{HP} - h_{s4}^{HP}\right) \quad \ldots (5.25)$$

Where h_{sg4}^{RehP} and h_{sg4}^{HP} is estimated using the functions (hFTP) using T_{Sg4} and P_{s3}^{RehP} and T_{gRehO} and $Ps3^{HP}$. h_{s4s}^{HP} is estimated using the function (hFsP) as functioned to S_{s3}^{HP}, P_{sReh}, while h_{s4s}^{RehP} is also estimated using this function using S_{s3}^{RehP}, P_{s4}. S_{s3}^{RehP} is functioned to h_{s3}^{RehP}, P_{sReh} using the function (SFhP). Where h_{gRehO} is functioned to T_{gRehO} and ϕ_{CC1} using the function (GCF1). An assumption was regarded by such model, that the pressure losses of steam through re-heater are neglected. The steam re-heater model depicted in Fig. 5.8 was generated using equations (5.19 - 5.25). It should be noted that the re-heater effectiveness, steam pressure, steam temperature ...etc. were used as input to the model shown in Fig. 5.8.

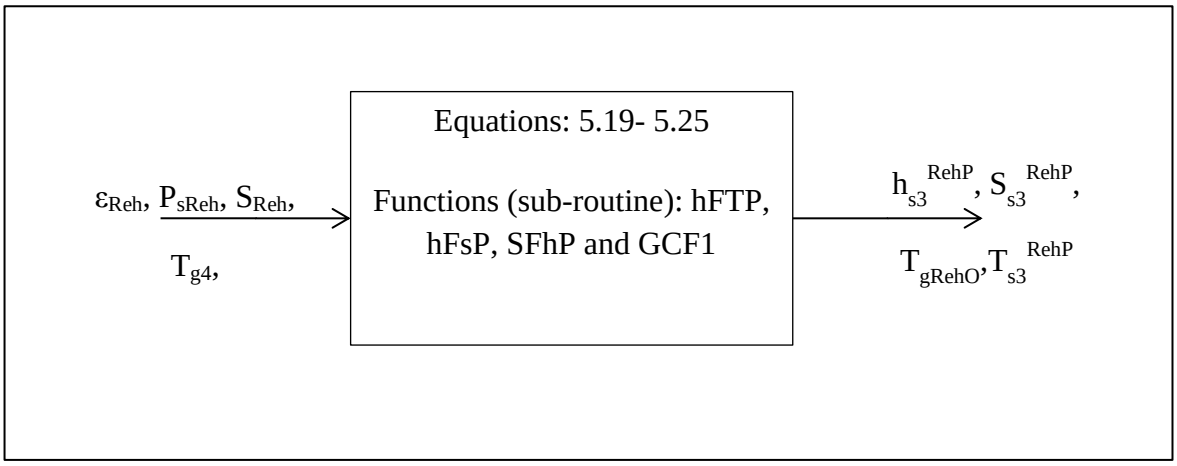

Figure 5.8 Steam re-heater model

5.2.2.5 Steam super-heater model

As it has been reported by Saravanamotto et al., [9], the terminal temperature difference and the pinch point temperature difference cannot be less than 20 °C for economically wise boiler size. The maximum high temperature of 1000 °C is considered although many other researchers took a maximum value of 560 °C like Sigler et al., [76]. Such temperature was reported to be achievable with supplementary heating in the HRSG. Many of those suggested a minimum temperature difference between the superheated streams and the exhaust of about 20 °C with respect to basis similar to those of the ΔT_{PPm}. The maximum pressure considered by others is within 1050 bar confirming of exciting plants of a pressure of 1700 bar.

The enthalpy of the steam discharged to the turbine super-heater outlet is determined by equation (5.26).In this equation h_{sg4} is estimated by function (GCF1) using T_{g4} and P_{s3}. S_{s3} for the steam at super-heater outlet is estimated using the function (SFhP) using h_{s3} and P_{s3}. Where the pressure of the steam through the super-heater is calculated using the equation (5.27).

$$h_{s3} = h_{gs2} + \varepsilon_{SH} \times \left(h_{sg4} - h_{gs2} \right) \quad \ldots (5.26)$$

$$P_{s3} = P_{s2} \times \left(1 - \lambda_{HRSG}\right) \quad \ldots (5.27)$$

Both equations (5.26 - 5.27) as well as the super-heater input parameters including steam pressure, steam temperature and the gas temperature were used to generate the steam super-heater model depicted by Fig. 5.9.

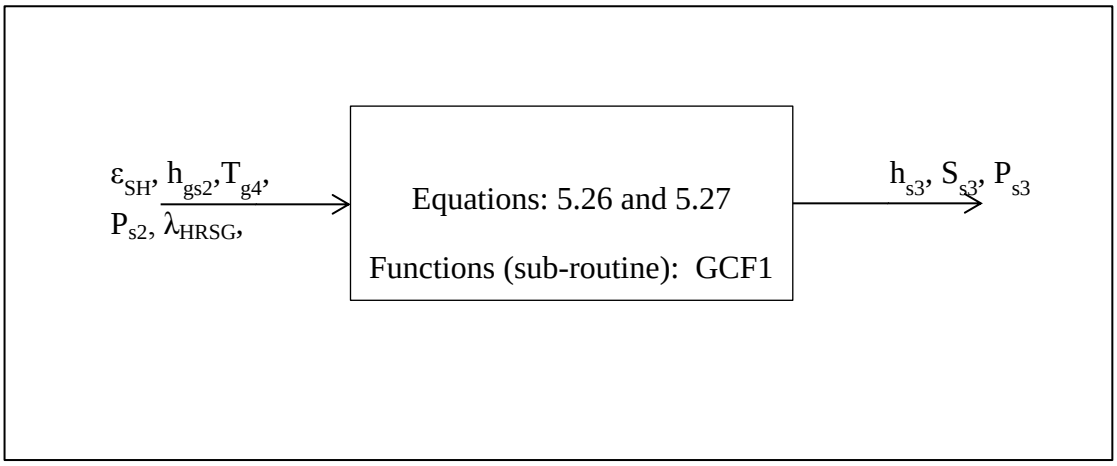

Figure 5.9 Steam super-heater model

5.2.2.6 Evaporator model

It is usual to consider the value of the pinch point temperature (ΔT_{PPm}) to be approximately 10^{o}C, which is a compromise of cost effective boiler to the plant overall performance. However, some researchers suggest a ΔT_{PPm} value of 8°C. In the current work, the range of this value is considered to be between 5 and 25 °C. The enthalpy of the steam generated by the evaporator (h_{gs2}) is estimated using the function (subroutine) (hgFP) as a function to the pressure of the evaporator regarding the losses at economizer and evaporator, which is given by equation (5.28). The temperature of the discharged gases from the evaporator is determined by equation (5.29). Both equations (5.28-5.29) are used to model the evaporator as shown in Fig. 5.10.

$$P_{s2E} = P_{s2}\left(1 - \lambda_{Ec} - \lambda_{E}\right) \quad \ldots (5.28)$$

$$T_{gEO} = T_{sE} + \Delta T_{ppm} \quad \ldots (5.29)$$

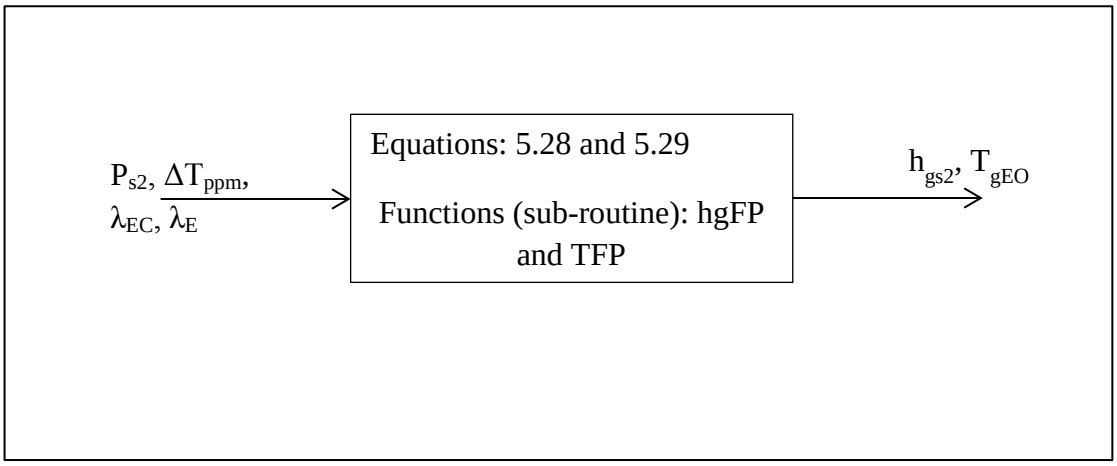

Figure 5.10 Steam evaporator model

5.2.2.7 Economizer model

The economizer duty is to heat the water coming from the pump using the heat from the gases discharged from evaporator's outlet. Environmentally, and from energy efficient approaches, it is preferable that the temperature of the gases to be as lowest as possible but with no other effects on components' materials. In this model, the economizer is expected to take the sup-cooled water and discharge it as saturated water. In the present work, the function (hfFP) is used to estimate the enthalpy of the steam at economizer outlet as a function to the pressure of the economizer (PsEC). This pressure is determined using the equation (5.30). It is also used to estimate the temperature of the steam at saturation using the function (TFP). The temperature of the gases at economizers' outlet to the stack is calculated using the equation (5.31). And the enthalpy of gases is calculated by the function GCF1 using TgStack and ϕCC. The steam evaporator model using the input parameters and equations 5.30 - 3.31 is shown in Fig. 5.11.

$$P_{s2EC} = P_{s2}\left(1 - \lambda_{Ec}\right) \quad \ldots (5.30)$$

$$T_{gStack} = T_{gEO} - \left[\varepsilon_{EC}\left(T_{gEO} - T_{s2}\right)\right] \quad \ldots (5.31)$$

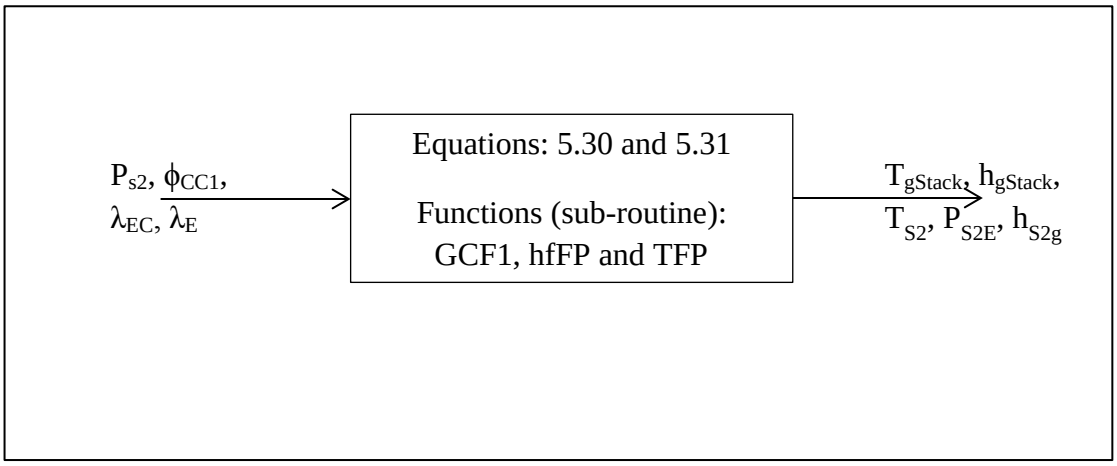

Figure 5.11 Steam economizer model

5.2.2.8 Steam turbine model

The steam turbine model is considered in a similar way as detailed in previous chapters. The enthalpy at the end of the isentropic expansion (h_{s4s}) is estimated first from the entropy (S_{s3}) and the pressure of the steam at turbine outlet (P_{s4}). The function (hFsP) is used to estimate such enthalpy, while the entropy (S_{s3}) is estimated using the function (SFhP) in which S_{s3}=f (h_{s3}, P_{s3}). Subsequently, the isentropic efficiency is assumed in order to calculate the generated specific work by the turbine. The quality of the steam at the turbine outlet is limited in this model, as before, to a vapour content of at least 90%. The function (XFSP) is used to estimate X_{s4} using S_{s3} and Ps4. The specific work generated from the steam turbine and the reheated steam turbine are given by equation (5. 32) and (5. 33) respectively. For the reheated steam turbine, the function (hFsP) is used to estimate h_{s4s} as a function to S_{s3} and P_{s3}^{RehP}.

$$w_{ST} = \eta_{ST} (h_{s3} - h_{s4s}) \times 1000 \quad \ldots (5.32)$$

$$w_{STReh} = \eta_{ST}^{RehP} \times \left(h_{s3}^{RehP} - h_{s4s}^{RehP} \right) \times 1000 \quad \ldots (5.33)$$

In these equations, the enthalpy of the steam at the reheated steam turbine inlet (h_{s4s}^{RehP}) is estimated by the function (hFsP) with respect to S_{s3}^{RehP} and P_{s4}. Where the entropy of the steam at S_{s3}^{RehP} is functioned to h_{s3RehP} and P_{sReh} and estimated using the function (SFhP). The specific work of the steam turbines (1-3) can then be calculated from equations 5.34-5.36 and as shown below.

$$w_{ST1} = \eta_{STLP} \times (h_{s3HP} - h_{s4sHP}) \times 1000 \quad \ldots (5.34)$$

$$w_{ST2} = \eta_{STLP} \times (h_{s3IP} - h_{s4sIP}) \times 1000 \quad \ldots (5.35)$$

$$w_{ST3} = \eta_{STLP} \times (h_{s3LP} - h_{s4sLP}) \times 1000 \quad \ldots (5.36)$$

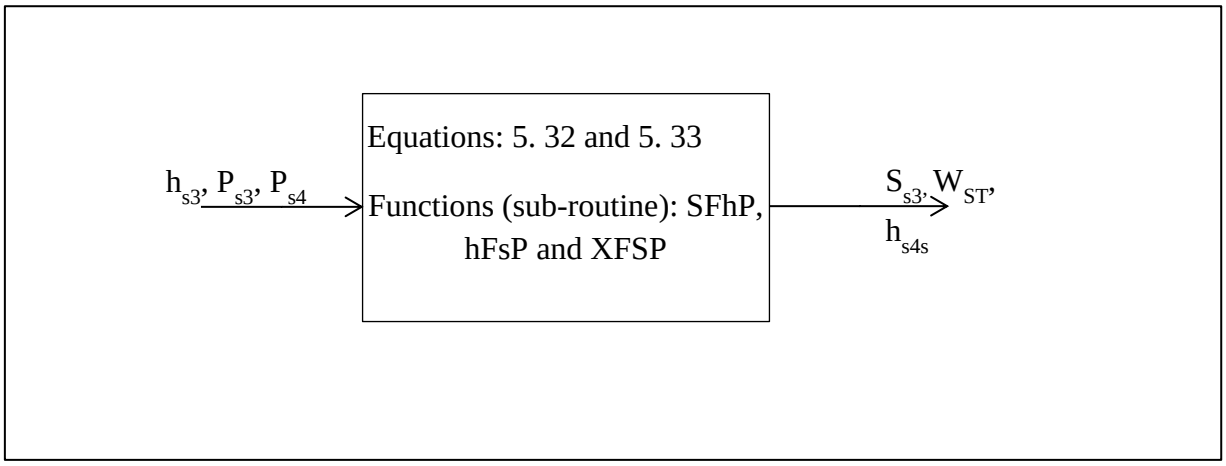

Figure 5.12 Steam turbine model

5.2.2.9 Steam condenser model

The condenser is considered as heat exchanger in which a hot fluid is cooled at an almost constant pressure and temperature. Accordingly, the status of the water at condensers' outlet is saturated water and the function (hfFP) is used to estimate the enthalpy at this point which is a functioned of the pressure of the water at the lower pressure (P_{s1}). In this model, no pressure losses are considered here for the condenser. Therefore, the condenser pressure to be identical to that for the turbine outlet. The function (VFP) is used to estimate the specific volume of the saturated water at condenser outlet using P_{s1} as shown by condenser model by Fig. 5.13.

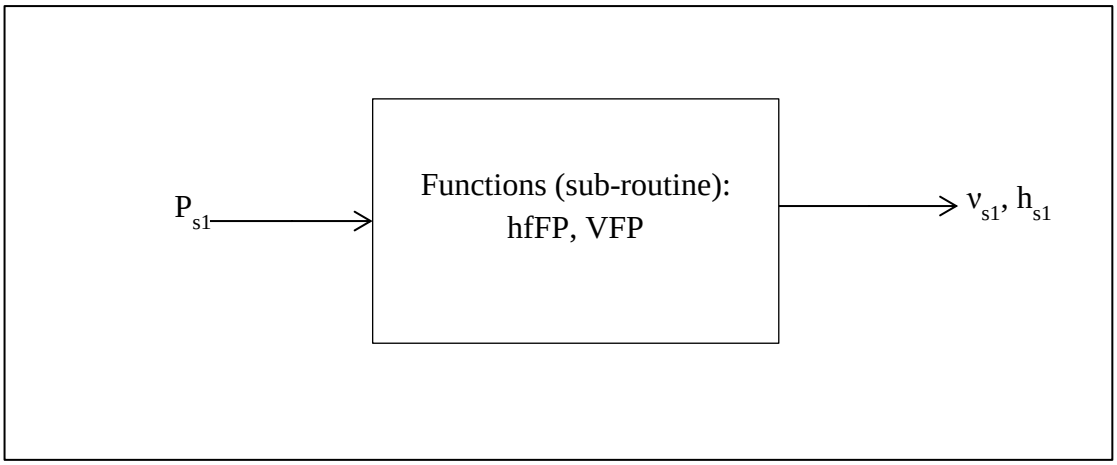

Figure 5.13 Steam condenser model

5.2.2.10 Water pumps model

The water pump is assumed to operate on the assumptions considered for the combined cycle configurations. The temperature of the water at the pump outlet is calculated using the same function (TFPP) as the $T_{s2LP} = f(P_{s2LP}, P_{s1})$ which considers an isentropic compression process. The work consumed by the water pump is calculated from equation (5. 37). The enthalpy of the water discharged by pumps is determined using equation (5.38). For multi pressure steam turbine configurations; the work consumed and the enthalpies of the water for the integrated pumps are determined using the same equations but with some changes to the inputs.

$$w_{WP} = \frac{(v_{s1} \times (P_{s2} - P_{s1}) \times 10^5)}{\eta_{WP}} \quad \ldots (5.37)$$

$$h_{s2} = h_{s1} + \left(\frac{v_{s1} \times (P_{s2} - P_{s1}) \times 10^5}{1000 \times \eta_{WP}} \right) \quad \ldots (5.38)$$

The power consumed by the pumps in multi pressure systems is similarly calculated as in equation (5.39) and (5.41).

$$w_{WP1} = \frac{(v_{s1} \times (P_{s2LP} - P_{s1}) \times 10^5)}{\eta_{WPLP}} \quad \ldots (5.39)$$

$$w_{WP2} = \frac{(v_{s2LP} \times (P_{s2LP} - P_{s2IP}) \times 10^5)}{\eta_{WPIP}} \quad \ldots (5.40)$$

$$w_{WP3} = \frac{(v_{s2IP} \times (P_{s2IP} - P_{s2HP}) \times 10^5)}{\eta_{WPHP}} \quad \ldots (5.41)$$

The water pump's model is shown in Fig. 5.14 with the input and output parameters.

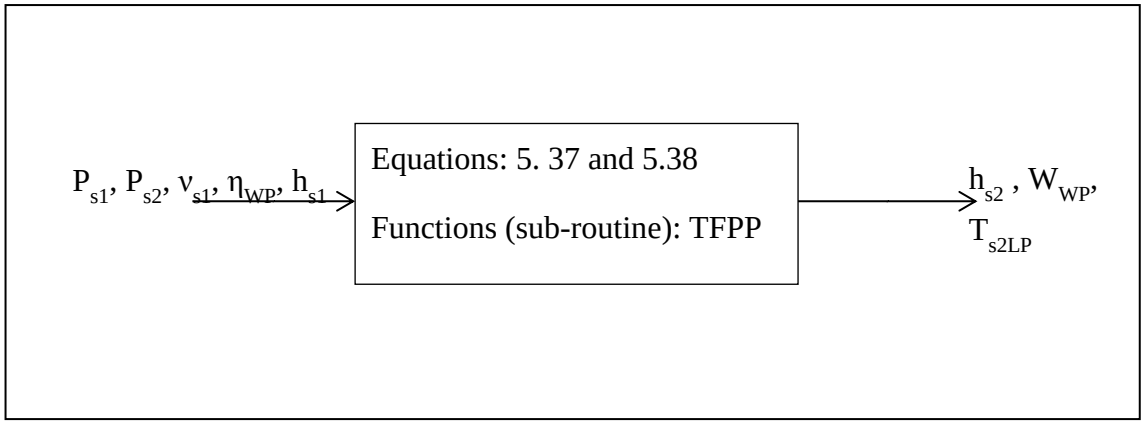

Figure 5.14 Water pump model

5.2.2.11 HRSG model

The main function of the heat recovery steam generator (HRSG) is to recover heat from the gases issuing from the gas turbine, which is otherwise wasted to the atmosphere, by generating steam for the steam turbine/plant. Supplementary fired HRSGs provide more power generation, although, it is related to higher fuel consumption, lower CCPP efficiency and related more emissions amounts. HRSG with no supplementary firing is of a low cost and related to the most efficient combined power generation cycles. Therefore, these are commonly used for combined cycle power plant. HRSG of two or three pressure levels are the most common these days. Most of the plants today are equipped with the natural-circulation Horizontal HRSGs Kehlhofer, et al.[22].

This study modelled horizontal unfired HRSGs only for the seven previous HRSG design cases are considered again in this chapter: Simple, Reheated, Regnerated, Dual pressure, Dual pressure reheated, triple pressure and Triple pressure reheated HRSGs. According to the manufacturers' records, this type of heat recovery steam generator operates on turbine outlet gas temperature (T_{g4}). Therefore, this model is limited by a temperature of gas turbine discharges of not less than 500°C. A temperature of less than that is considered impractical for large combined power plant installations where high steam pressure and temperature are required. This limitation is of a great importance when HRSG is integrated by additional components (this will be under further discussion later in this thesis).

In designing an appropriate/efficient HRSG the temperature difference between the outlet streams (gas and steam) must be kept the minimum. This is achieved by increasing the heat exchange surface area and increasing the heat transfer rate from the gas to the steam. Equations 5.42-5.45 govern the HRSG model which is shown in Fig. 5.15.

$$P_{g4} = \frac{P_{gE}}{1 - \lambda_{HRSG}} \quad \ldots (5.42)$$

$$\lambda_{HRSG} = \lambda_{Ec} + \lambda_{E} + \lambda_{SH} \quad \ldots (5.43)$$

$$\eta_{HRSG2} = \eta_{SH} \times \eta_{E} \times \eta_{EC} \quad \ldots (5.44)$$

$$m_{sa} = \frac{\eta_{HRSG}\,(1 + f_{CC})\,(h_{g4} - h_{gStack})}{(1000)(h_{s3} - h_{s2})} \quad \ldots (5.45)$$

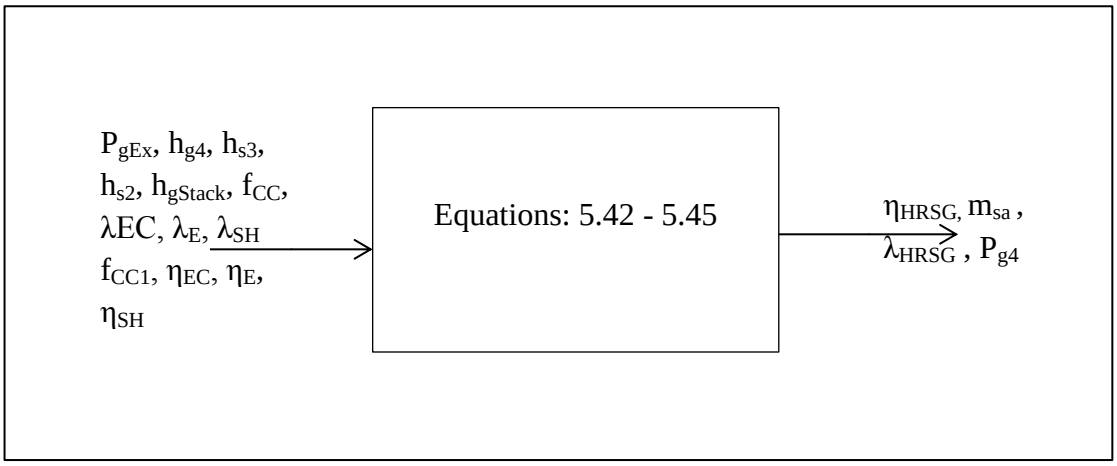

Figure 5.15 The heat recovery steam generator (HRSG) model

HRSG performance is restricted by three main effects. Each effect is linked to a number of parameters producing it, Ganapathy [88]. These were:

(i) The ambient temperature and this govern the performance through (a) the temperature of exhaust and (b) the mass flow rate of the exhaust, i.e. through the heat transfer rate.

(ii) The gas turbine load (it also controls the performance through both the temperature and the mass flow of the gas turbine exhaust gases). The mass flow generated by the evaporator, which implies to low steam mass flow generated

(iii) Steam turbine live pressure

These conditions usually shift HRSG performance from the design point when:

(i) The temperature and the mass flow of the exhaust do not satisfy the HRSG requirements for its design performance, also when there is a significant deterioration in the power generated from the gas turbine, and these are combined with an increase in the ambient temperature.

(ii) The economizer starts to generate steam or when the temperature of the exhaust is very high compared to the normal case.

(iii) The steam generated by the HRSG is less than the amount required to DP output, i.e. steam turbine power output decreases over the required range due to increase of the steam pressure at the turbine inlet. These margins are estimated when the mass flow generated by the evaporator is less than required to generate the power required from the steam turbine.

Forbidding steam extraction in economizer is important, which is usually caused by the low steam extraction in the evaporator. This is due to the low heat available to generate the minimum required mass flow rate of the steam at evaporator. Therefore, it decreases the mass flow through the economizer which makes it easier for the gases from evaporator outlet to extract steam here.

By collecting the gas temperature pressure flow and UA of the entire HRSG components can indicate the design point performance. Based on such performance data one can study predict off design performance. Iteration method or NTU method are used to evaluate the performance HRSG parts. The performance of HRSG as a whole component is based on the performance characteristics of its parts. Basically, the design mode term of UA is estimated and then corrected by the effect of the temperature and the flow of exhaust gases.

In this study, it is assumed that, HRSG parts are heat exchangers in series in which each has its own overall (Heat transfer coefficient U).

Practically heat exchangers' heat transfer coefficient is variable along each of these parts. The heat transfer coefficient (U) is significantly affected by:

(i) Low Reynolds number
(ii) Heat transfer surface geometry
(iii) Fluid physical properties.

Regardless to the start -up mode, Khelhofer et al., [22] identified the basics on which the optimum HRSG unit is to accomplish:

(i) High heat recovery rate or high efficiency

(ii) Low pressure losses at the GTC exhaust to minimize the losses in its power and efficiency, the pressure drops are in range between 25 and 35 millibar for today's HRSG.

(iii) Eliminate corrosion related to low temperature (this happens due to the presents of sulphuric acids, in this model natural gas is the fuel, accordingly the dew point temperature of the water governs such limit)

(iv) Today's HRSGs are designed for a minimum pinch point temperature between 5 and 15°C for high efficiency, and between 15 and 25 °C for valued efficiency

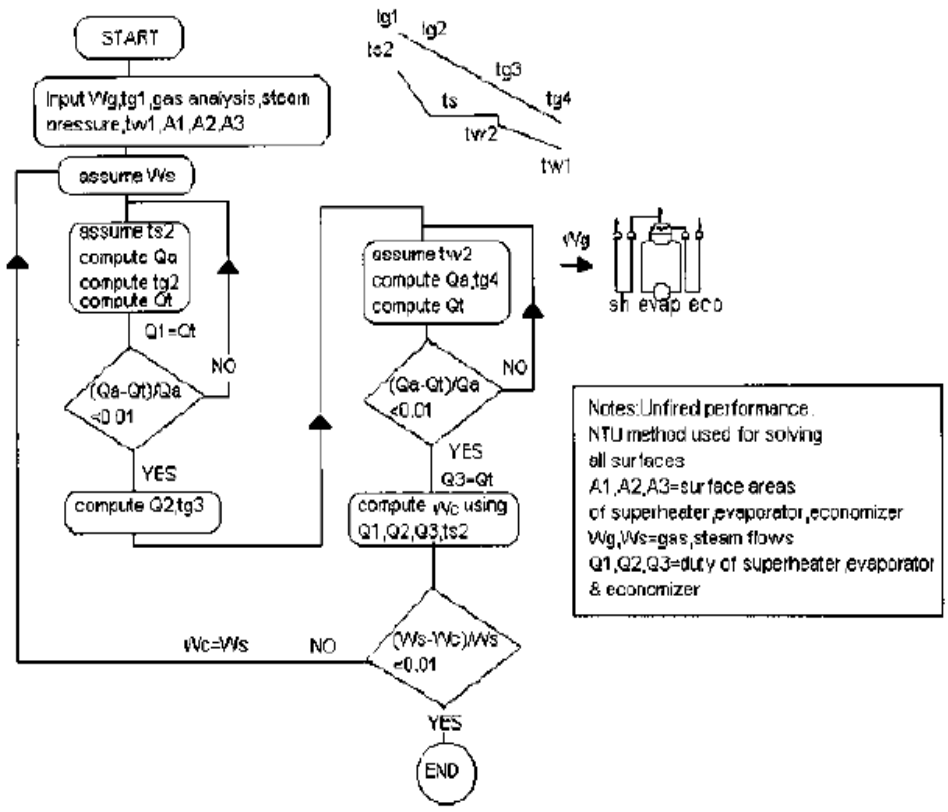

FIGURE 2.17 Logic used for evaluating HRSG performance.

Figure 5.16 HRSG model performance prediction by Ganapathy [88]

In addition to the simple and reheated HRSG configurations, this study considers dual pressure and Dual Pressure reheated HRSGs. For the dual pressure configuration, this model determines the steam to air mass flow ratio using equation (5.46) for the high pressure stream and (5.47) for the low pressure stream. The value of (m_R) is considered with respect to the streams' ratios of today's multi pressure HRSG. While for the triple pressure and triple pressure reheated HRSG, steam mass flow to air mass flow ratio is calculated using equations (5.48-5.50).

$$m_{sa}^{HP} = \frac{\eta_{HRSG}^{HP}\left(1 + f_{CC}\right)\left(\frac{\left(h_{gRehO} - h_{gEI}^{LP}\right)}{1000}\right)}{\left(h_{s3}^{HP} - h_{s2}^{HP}\right) + m_R\left(h_{s3}^{LP} - h_{gs2}^{LP}\right)} \quad \ldots (5.46)$$

$$m_{sa}^{LP} = m_{sa}^{HP} \times m_R \quad \ldots (5.47)$$

$$m_{sa}^{HP} = \frac{\eta_{HRSG}^{HP}\ (1 + f_{CC}) \left(\frac{\left(h_{gRehO} - h_{gEI}^{IP}\right)}{1000} \right)}{\left(h_{s3}^{HP} - h_{s2}^{HP}\right) + m_{R1}\left(h_{s3}^{IP} - h_{gs2}^{IP}\right)} \quad \ldots (5.48)$$

$$m_{sa}^{IP} = m_{sa}^{HP} \times m_{R1} \quad \ldots (5.49)$$

$$m_{sa}^{LP} = m_{sa}^{HP} \times m_{R2} \quad \ldots (5.50)$$

5.2.3 Specifications for conventional combined cycle's models

Certain details and operation parameters' restrictions are imposed on the overall model of the combined power cycle. These details and restrictions are summarized in this section where all symbols refer to their usual meanings.

5.2.3.1 Restrictions to the model from industrial applications

(i) Gases temperature restrictions through the HRSG: The temperature of the gases must satisfy the duty of each of HRSG components, which operate progressively. This is applied on multi pressure HRSG systems as well. Therefore, the following conditions are prevented: ($T_{gEO}^{HP} > T_{g4}$) , ($T_{gEI}^{HP} > T_{g4}$) , ($T_{gRehO} > T_{g4}$), ($T_{gEO}^{IP} > T_{gEO}^{HP}$), ($T_{gEI}^{IP} > T_{gEO}^{HP}$), ($T_{gEO}^{LP} > T_{gEO}^{IP}$), ($T_{gEI}^{LP} > T_{gEO}^{IP}$), ($T_{gEO}^{LP} > T_{gEO}^{HP}$), ($T_{gEI}^{LP} > T_{gEO}^{HP}$) and ($T_{gEO} > T_{g4}$), ($T_{gEI} > T_{g4}$) and ($T_{gRehO} > T_{g4}$). Where ($T_{g4}$) is the temperature of gases discharged from the gas turbine, (T_{gEO}) is the temperature of the gases at the evaporator outlet and (T_{gEI}) is the temperature of the gases at evaporator inlet.

(ii) Stream quality restrictions: The vapour content in the steam at turbine discharges must be at least 90% or corrosions are more likely to target steam turbine components. Therefore, in the current model such restriction is considered, which limits the calculation procedure.

5.2.3.2 Model limitations

(i) A maximum temperature at the steam turbine inlet of not greater than 700 °C.
(ii) A maximum temperature for the gas turbine inlet of not greater than 1500 °C.
(iii) A steam quality (X_{s4}) for the steam at the turbine outlet of not less than 90%.
(iv) It is assumed that there is no uncalculated bleeding through the components of the CCPP.
(v) The losses at the inlet and the exhaust of the components are not considered here.

5.2.3.3 Model parameters ranges

Ranges for the operating parameters those undertaken in this study are tabulated in table 5.1.

Parameter	Range
ϕ_{CC}	0.4 – 1
η_{WP} , η_{ST} , η_{AC}, η_{CC}, η_{GT}, η_{PG}	0.6 – 0.92
η_{SH}, η_{EC}, η_{E}	0.6 – 0.8
r_{AC}	4 – 36
T_{g3}	800 – 1500 °C
T_{g3Reh}	800 – 1500 °C
P_{Reh}	20 – 40 bar
P_{Int}	1.1 – 14.2 bar
λ_r,λ_l,λ_{SH},λ_E,λ_{EC}	0.03 – 0.06
ε_{Rec}, ε_{SH}, ε_{Rec}, ε_{Rec}	0.6 – 0.9
T_{g1}	-10 – 40 °C
P_{g1}	1.01300 bar
P_{g5}	1.1 – 2.1 bar
ΔT_{Pmm}	10 – 25 °C
P_{s2}	15 – 350 bar
P_{s1}	0.05 – 0.55 bar
$S_{Reh\ (SP)}$	1.1 – (P_{s3}/P_{s4})-0.1
$S_{Reh\ (DP)}$	1.1 – (P_{s3HP} / P_{s3LP}) - 0.1
$S_{Reh\ (TP)}$	1.1 – (P_{s3HP} / P_{s3IP}) - 0.1

Table 5.1 Operating parameters used in the current study

5.2.3.4 Model performance criteria

At the current stage of the model, the main requirement for the criteria is to investigate accomplishing the following points:

(i) The temperature of the gas at the HRSG exhaust of not less than 340 °C, (the maximum temperature for the thermodynamic properties of the (AWM) considered by this model).

(ii) The temperature of the steam at the turbine outlet of not less than 200°C, (the minimum required temperature for the absorption chillers to operate).

(iii) For reheated configurations (S_{Reh}) ranged from 1.1 to $\left[\frac{P_{s2}\ (1\ -\ \lambda_{HRSG})}{P_{s4}}\ -\ 0.1\right]$

(iv) The Temperature of gases from turbine exhaust is limited by the practical data given for GE HRSG of less than 538 °C for non-reheated HRSGs and 566 for reheated HRSGs. in this model the lower temperature of 500°C are the limitation here. These criteria can be applied to different combined cycle power plants configurations as documented by the following practical data:

Gas turbine (Company)	r_{AC}	N (rpm)	W (MW)	Q (kJ/kWh)	Gross efficiency (%)	Exhaust mass flow (kg/s)	Exhaust temperature (°C)
SGT6-5000F (Siemens)	18.9	3600	232	9278	38.8	551	593
SGT5-8000H (Siemens)	19.2	3000	375	8999	40	829	627
SGT5-4000F (Siemens)	18.8	3000	295	9053	40	692	586
GT13E2 (Alstom)	18.2	3000	202.7	9474	38	624	501
GT26 (Alstom)	35	3000	326	8933	40.3	692	603
6FA (General Electric)	15.6	5231	77	10295	35.3	212	597
9FA (General Electric)	17	3000	265	9757	37.3	602	641
9FB (General Electric)	18.1		279	9510	38.3	203	

Table 5.2 Gas turbine features in current CCPP

5.3 Components matching

It is the harmony in action between the components of each of combined cycles' components, which determines if the gas turbine plant performance is according to the designed performance map. The designed operation map indicates whether the engine (gas turbine plant) is working on design running conditions (line) or off design conditions. Matching between gas turbine plant components will restrict the performance characteristics' ranges of each component. Normally, the gas turbine plant (engine) is not required to work on design conditions; for this reason, components' matching is required to attain a satisfied operation even when the engine is operating of performance at off design conditions. Accomplishing such process between combined cycle power plant components leads to:

(i) Establish a power plant design of a better performance (towards the minimum costs for cycles' life).

(ii) When better performance is attained means better use of fuel consumption (towards the minimum pollution penalties from CO_2 and NO_X emissions).

5.3.1 Gas turbine engine components matching

Single shaft gas turbine is the arrangement usually utilized for power generation application, which is considered by this mode. The procedure of matching used in this model, described hereafter, is based on Razak [[8].

5.3.1.1 Gas turbine non dimensional groups

(i) Non-dimensional flow

The non-dimensional flow MF^{ND} is represented by:

$$MF^{ND} = \frac{m_{a1}\sqrt{\frac{R_{a1}T_{a1}}{\gamma_{a1}}}}{D^2 P_{a1}} \quad \ldots (5.51)$$

The flow area is constant for a given compressor. For a given compressor or turbine, the reference diameter of compressor and turbine is omitted as it is unchanged in such compressor or turbine. Using the definitions of R and γ changes the equation to the following:

$$MF^{ND} = \frac{m_{a1}\sqrt{Cp_{a1}T_{a1}(\gamma_{a1}-1)}}{\gamma_{a1}P_{a1}} \quad \ldots (5.52)$$

In terms of enthalpy, it is transferred to:

$$MF_{g1}^{ND} = \frac{m_{a1}\sqrt{h_{g1}(\gamma_a - 1)}}{\gamma_a P_{g1}} \quad \ldots (5.53)$$

For the turbine, the non-dimensional mass flow parameters group is represented by:

$$MF_{g3}^{ND} = \frac{m_{g3}\sqrt{h_{g3}(\gamma_g - 1)}}{\gamma_g P_{g3}} \quad \ldots (5.54)$$

(ii) Non-dimensional speed

$$N_{g1}^{ND} = \frac{N_{g1}}{\sqrt{\gamma_a R_a T_{g1}}} \quad \ldots (5.55)$$

Replacing R by Cp

$$N_{g1}^{ND} = \frac{N_{g1}}{\sqrt{Cp_a(\gamma_a - 1)T_{g1}}} \quad \ldots (5.56)$$

Similar to the mass flow parameter, the non-dimensional speed can be expressed in terms of the enthalpy as in the following equation:

$$N_{g1}^{ND} = \frac{N_{g1}}{\sqrt{h_{g1}(\gamma_a - 1)}} \quad \ldots (5.57)$$

For the turbine, similar analysis produces the following parameter for the turbine.

$$N_{g3}^{ND} = \frac{N_{g3}}{\sqrt{h_{g3}(\gamma_g - 1)}} \quad \ldots (5.58)$$

(iii) Pressure ratio

For the compressor, the pressure ratio can be expressed as follows:

$$PR_{AC}^{ND} = \frac{P_{g2}}{P_{g1}} \quad \ldots (5.59)$$

Where $(\frac{P_{g2}}{P_{g1}} = r_{AC})$

For the turbine, the pressure ratio is given in Equations 5.60-5.61.

$$PR_{GT}^{ND} = \frac{P_{g3}}{P_{g4}} \quad \ldots (5.60)$$

Or

$$PR_{GT}^{ND} = \frac{P_{g1} \times r_{AC}\left(1-\lambda_{CC}\right)}{P_{g4}} = r_{GT} \quad \ldots (5.61)$$

The above equations were implemented in a computer model for matching the gas turbine part of the combined plant. The flow chart of the developed, which is depicted in Fig. 5.16, is similar in some features to that of Razak [8].

Now in order to apply these groups on the compressor or the turbine map, it needs to be corrected by the design point groups. Therefore, the design point operating parameters for the specified compressor or turbine must be available or assumed. The equations above are similarly applied for compressor and turbine design point operation groups as follows:

$$MF_{DPg1}^{ND} = \frac{m_{DPg1}\sqrt{h_{DPg1}\left(\gamma_a - 1\right)}}{\gamma_a P_{DPg1}} \quad \ldots (5.62)$$

$$MF_{DPg3}^{ND} = \frac{m_{DPg3}\sqrt{h_{DPg3}\left(\gamma_g - 1\right)}}{\gamma_g P_{DPg3}} \quad \ldots (5.63)$$

$$N_{DPg1}^{ND} = \frac{N_{DPg1}}{\sqrt{h_{DPg1}\left(\gamma_a - 1\right)}} \quad \ldots (5.64)$$

$$N_{DPg3}^{ND} = \frac{N_{DPg3}}{\sqrt{h_{DPg3}\left(\gamma_g - 1\right)}} \quad \ldots (5.65)$$

In these equations, the following can be pointed out:

$$N_{DPg1} = N_{DPg3}, \qquad h_{DPg1} = f\left(T_{g1}\right), \qquad h_{DPg3} = f\left(T_{g3}, \phi_{CC}\right), \qquad m_{DPg1} = f\left(\rho_a, \rho_{g1}, \dot{m}_{DPa}\right),$$

$$P_{DPg1} = 1.013(\text{bar}), \qquad P_{DPg3} = f\left(P_{DPg1}, r_{DPAC}, \lambda_{DPCC}\right), \qquad \gamma_a = 1.4, \qquad \gamma_g = 1.33,$$

$m_{DPg3} = f\left(m_{DPg1}, T_{DPg3}, \phi_{DPCC}\right)$, $h_{DPg3} = f\left(T_{DPg3}, \phi_{DPCC}\right)$, $r_{DPAC} = f\left(P_{DPg1}, r_{DPAC}\right)$,

$r_{DPGT} = f\left(P_{DPg1}, r_{DPAC}, \lambda_{DPCC}, P_{DPg4}\right)$.

The functions and the equations considered for component's modelling are utilized to estimate these groups. The corrected groups are generated using equations (5.66 -71):

$$PR_{AC}^{Cor} = \frac{r_{AC}^{ND}}{r_{DPAC}^{ND}} \quad \ldots (5.66)$$

$$PR_{GT}^{Cor} = \frac{r_{GT}^{ND}}{r_{DPGT}^{ND}} \quad \ldots (5.67)$$

$$MF_{g3}^{Cor} = \frac{MF_{g3}^{ND}}{MF_{DPg3}^{ND}} \quad \ldots (5.68)$$

$$MF_{g1}^{Cor} = \frac{MF_{g1}^{ND}}{MF_{DPg1}^{ND}} \quad \ldots (5.69)$$

$$N_{AC}^{Cor} = \frac{N_{g1}^{ND}}{N_{DPg1}^{ND}} \quad \ldots (5.70)$$

$$N_{GT}^{Cor} = \frac{N_{g3}^{ND}}{N_{DPg3}^{ND}} \quad \ldots (5.71)$$

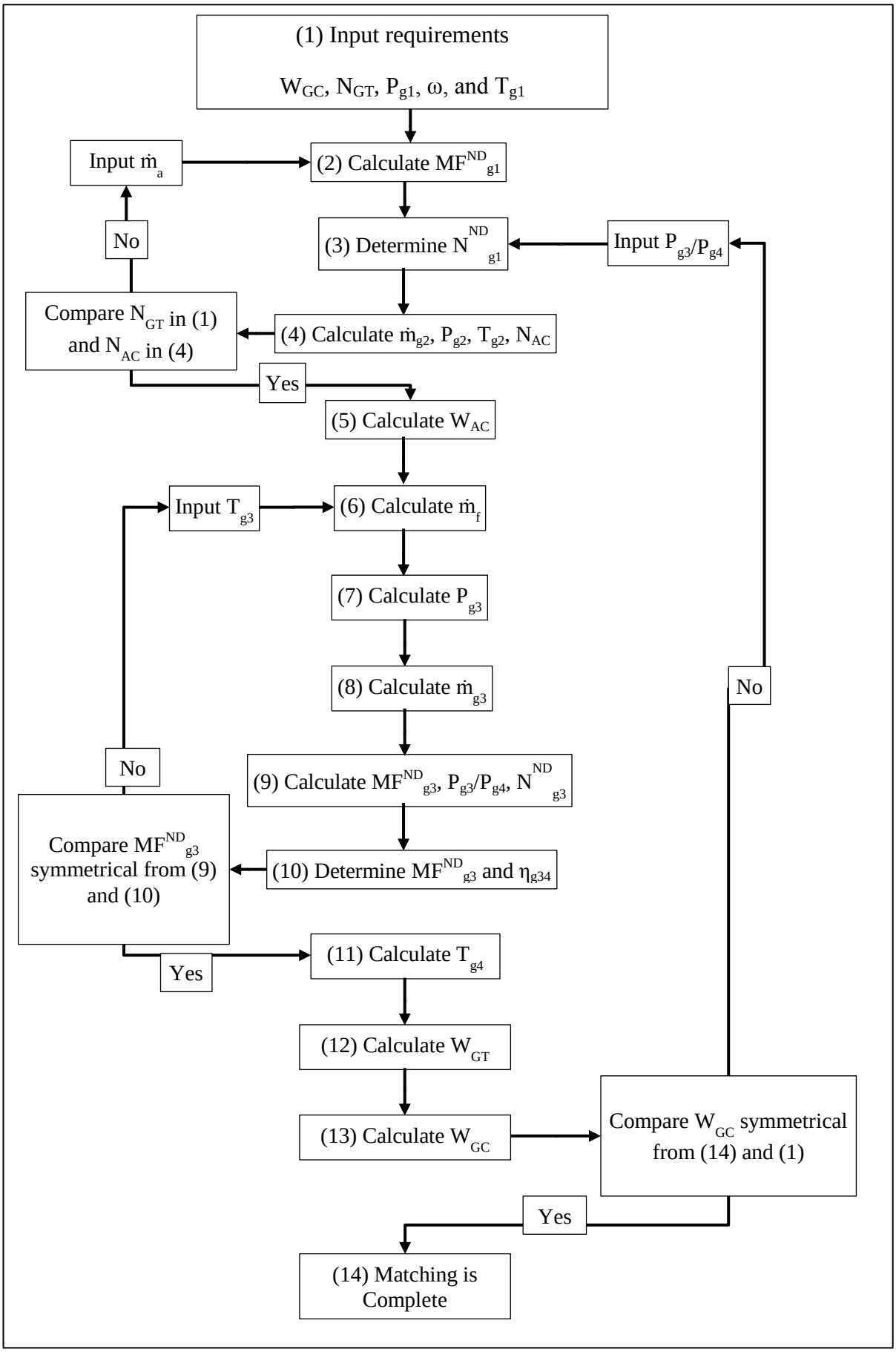

Figure 5.17 Matching procedure for single shaft simple gas turbine based on Razak [8]

5.3.2 Steam turbine components matching

The matching procedure of the steam turbine components, which is detailed hereafter, was undertaken to construct the CCPP model; depicted in Fig. 5.17.

(i) Matching between HRSG and ST

For a certain steam mass flow rate, the increase of the load increases the pressure of the steam at turbine inlet. For unfired HRSG, the elevation of steam pressure decreases the power generated from the turbine. This is because of the decrease in the amount of the steam generated. Accordingly, a compromise between turbine output load and the pressure is expected to attain an acceptable performance. In such matching the characteristics of the HRSG and steam turbine is required to reach to an operating point of various loads on which the previous compromise is considered Ganapathy [88]. The effects of the increase of steam generation pressure on various parameters are as follows:

a. The mass flow of the steam (m_{sa}) decreases, because the temperature profile is limited by the saturation temperature.

b. The temperature of exhaust gases increases

c. Steam temperature does not vary so much.

d. Energy absorption by steam decreases due to the increase of the exhaust gases temperature.

(ii) HRSG performance is affected by the ambient temperature as in the case of gas turbine. Because steam temperature and mass flow rate generated are affected by the gas flow rate and gas temperature from gas turbine.

(iii) A prevention of performance at part load of steam turbine between 40% and 100% which prevent steam generation inside the economizer. Accordingly, the mass flow should not be lower than a certain value which allows such generation in economizer.

(iv) Steam mass flow rate must meet compatibility through each component in the HRSG.

(v) Matching HRSG components to satisfy the duty of heat recovery.

Optimizing the steam turbine engine easing steam turbine designs it narrows matching cases between the steam turbine and plant other components, Wright [89].

Taking all the points listed in the above into consideration a computer model for predicting the performance the CCPP was developed. The flow chart of the developed model is shown in

Fig 5.17. The model was subsequently used to generate the modelling results shown and discussed in Section 5.5.

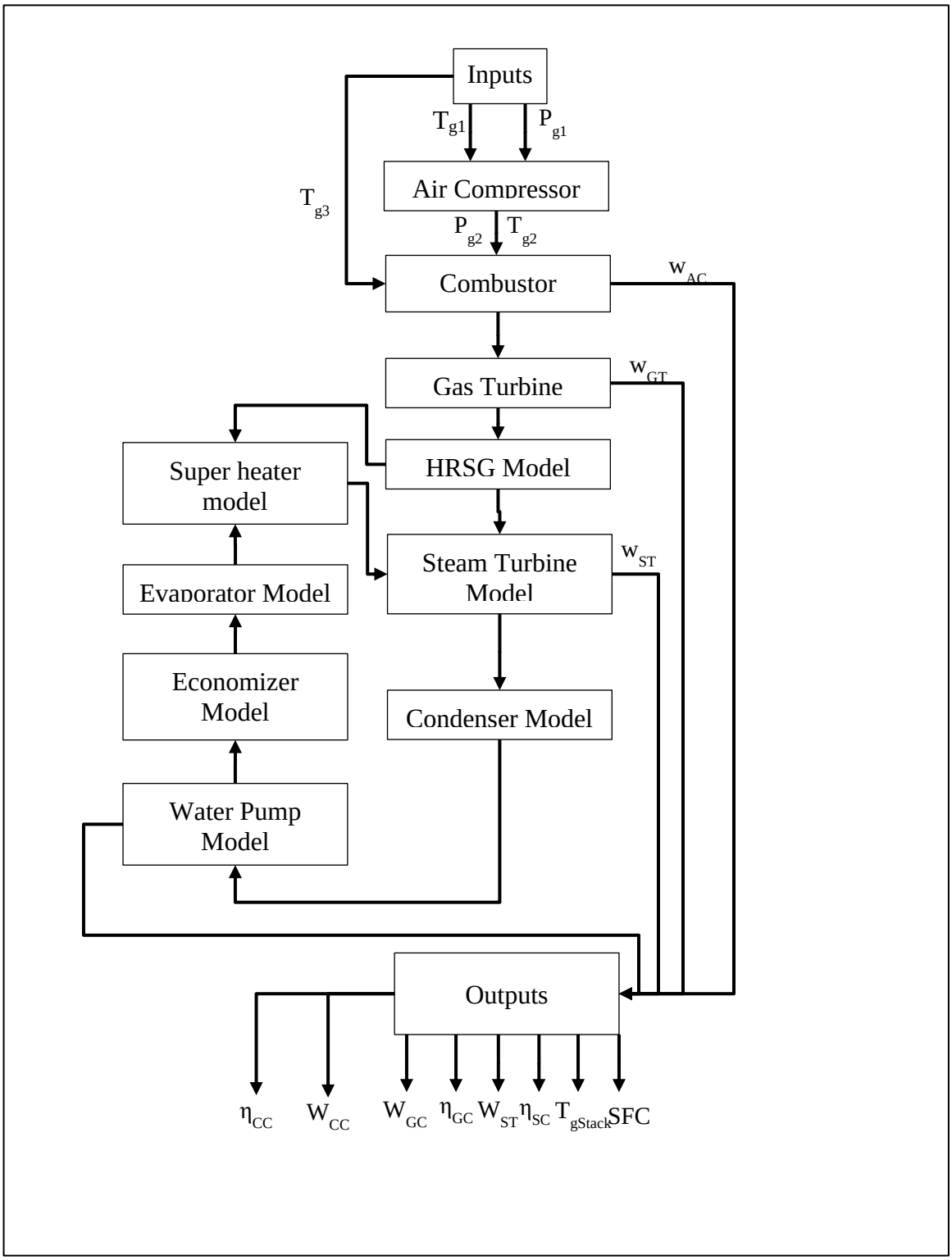

Figure 5.18 Overall model (solution program) flow chart for the SGSSCCPP

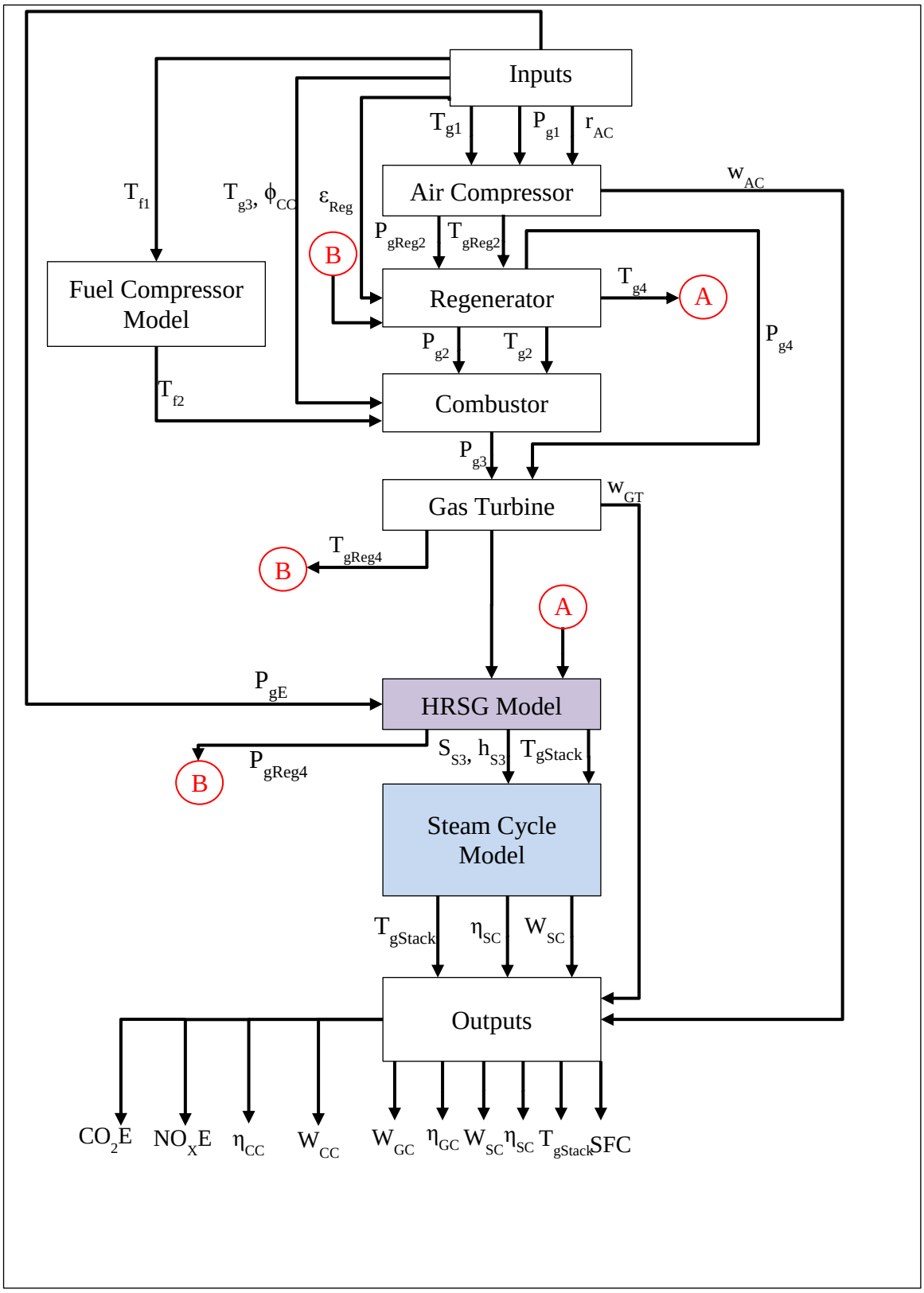

Figure 5.19 Flow chart of regenerative gas turbine cycle model in CCPP model

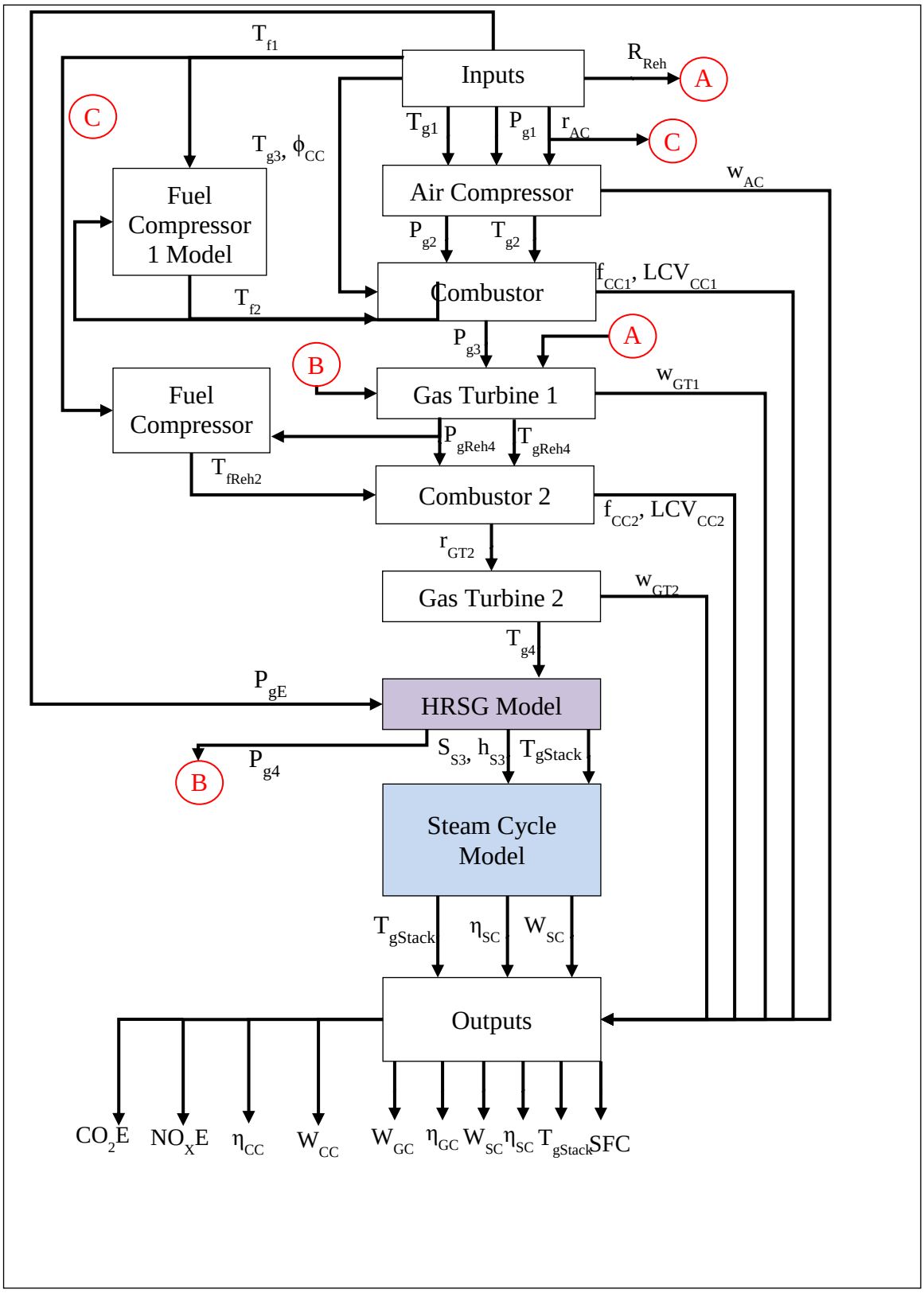

Figure 5.20 Flow chart of reheated gas turbine cycle in CCPP model

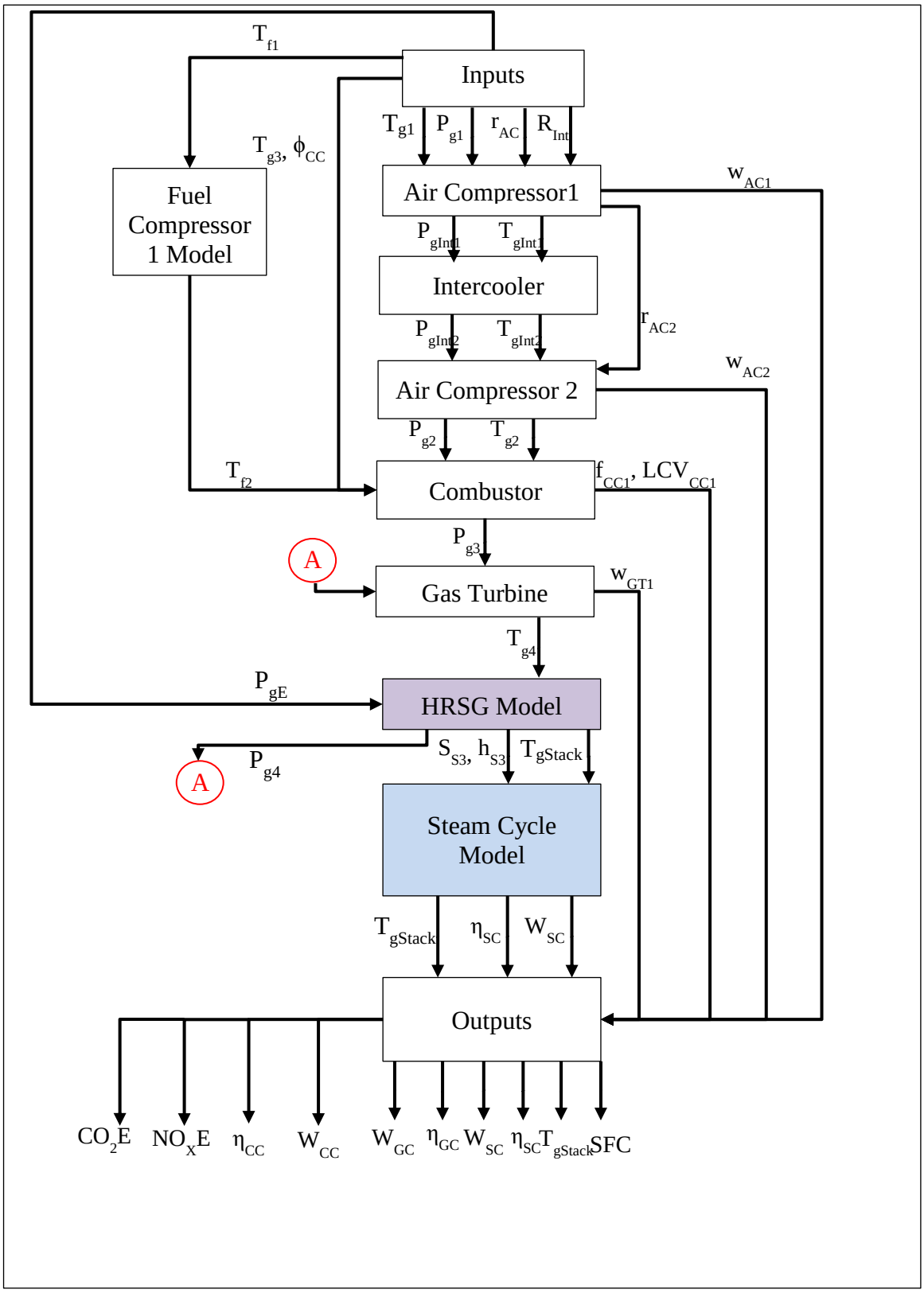

Figure 5.21 Flow chart of inter-cooled gas turbine cycle in CCPP model

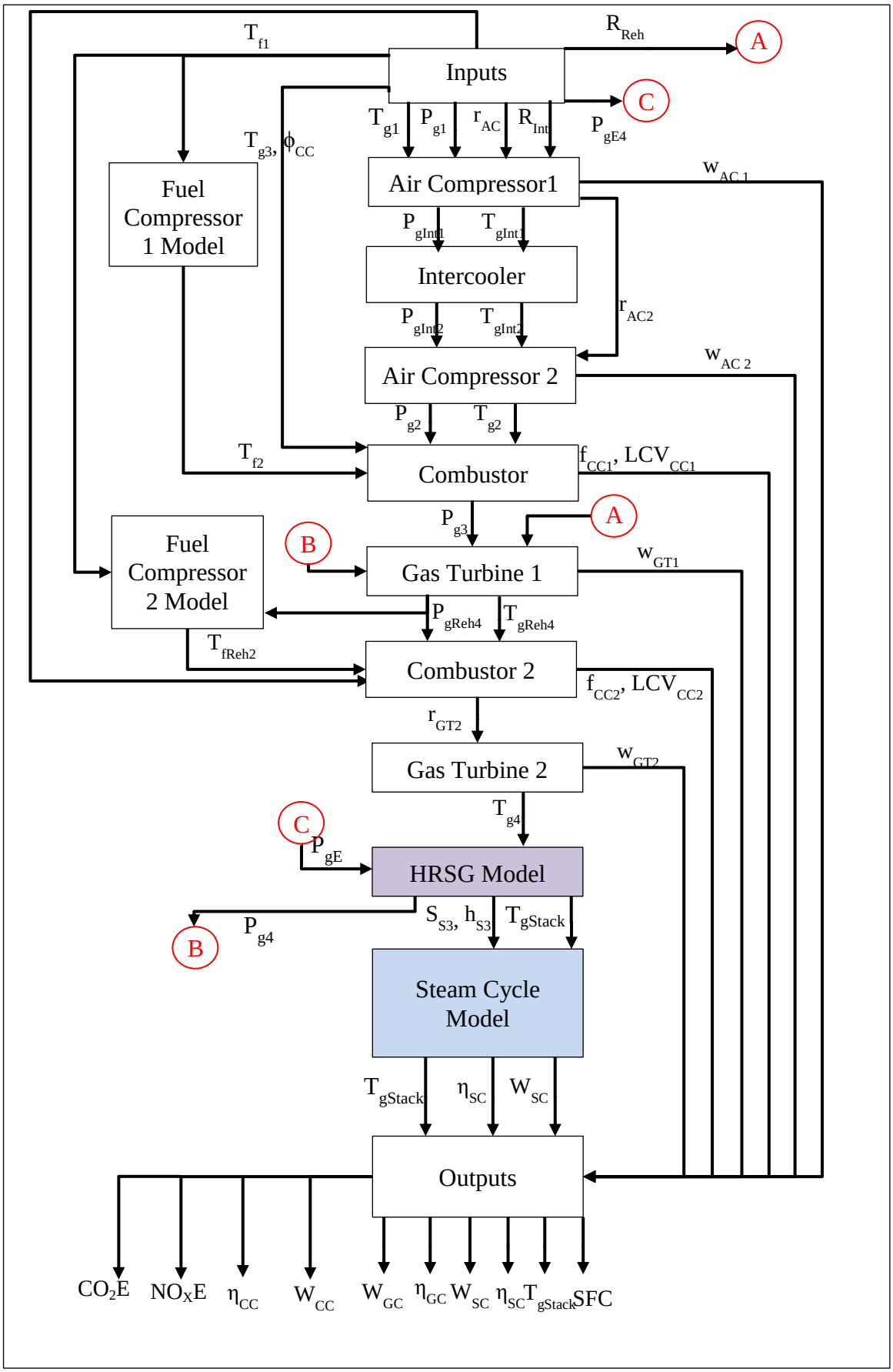

Figure 5.22 Flow chart of intercooled reheated gas turbine cycle in CCPP model

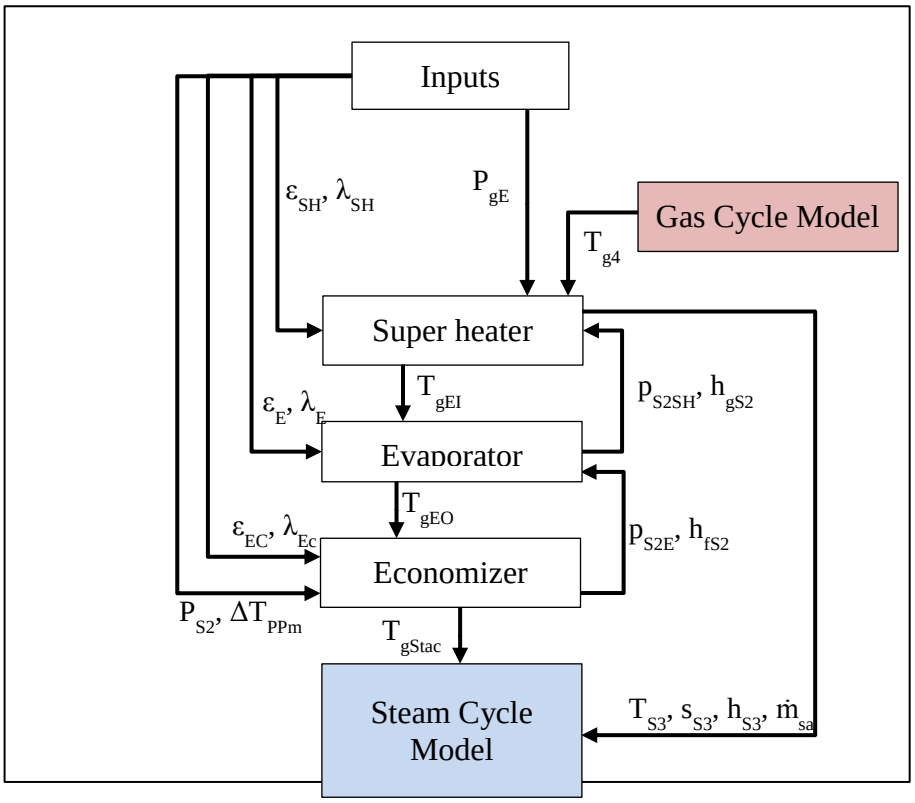

Figure 5.23 Simple and regenerated Steam cycle HRSG model

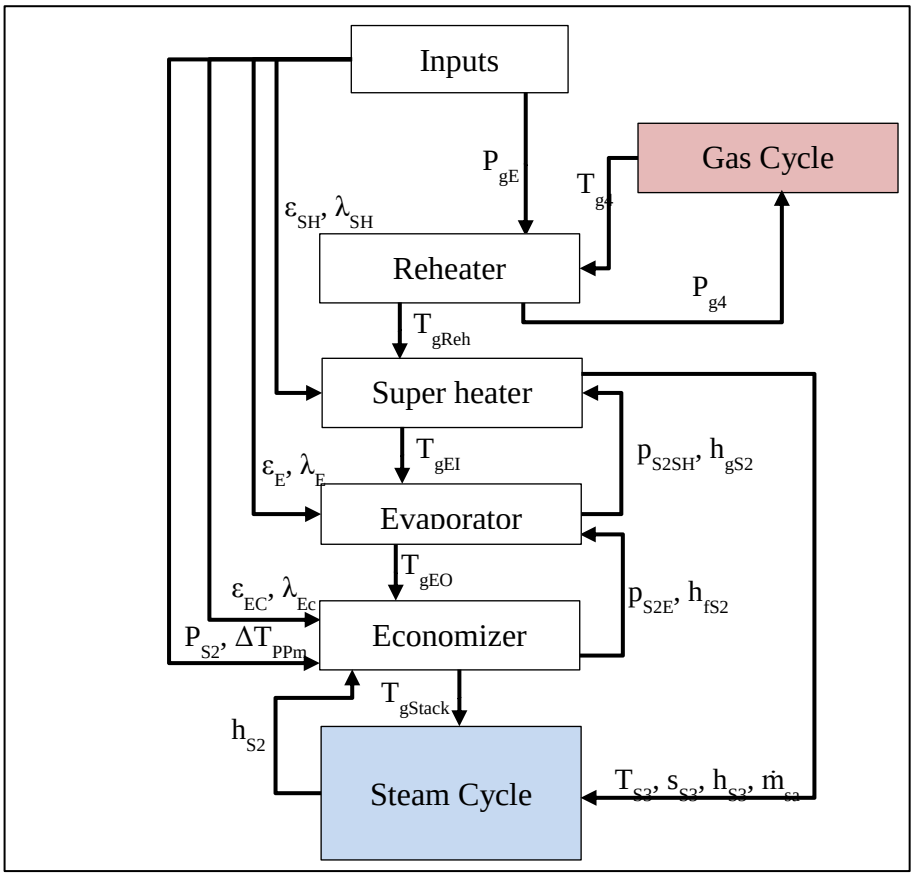

Figure 5.24 Reheated HRSG model flow chart

5.4 Emissions

The exhaust form a gas turbine is a mixture of: CO, CO_2, H_2O, UHC, Particulate matter (mainly Carbon compounds), NO_X and $SO_{x,}$ Lefebvre and Ballal, [86]. Here, CO_2 and H_2O are not always considered as pollutants because both are the natural result of a complete combustion of a hydrocarbon fuel. These two components, however, contribute to and accelerate the global warming effect. They are reduced only by utilizing less fuel, which is combined with improving the efficiency and reducing the operating costs. For gas turbine power plant working on natural gas fuel, the values of UHC, the particular matter and SOx generated from the combustion process are negligibly small. Accordingly, in what follows, only the emission of CO_2 and that generated by NO_X are discussed in this section.

In line with the general expectations, power plants operating on hydrocarbon fuels are expected to increase both in numbers and generating capacity in the future. As a result, emissions of the above components represent an important parameter in the design of future power plants, particularly the combined cycle power plants.

5.4.1 Emissions of carbon dioxide

The atomic ratio of carbon-hydrogen of a fuel is x/y, therefore, for one mole of methane CH_4 x=1, and y =4. Hence, the chemical reaction equation is set as follows:

$$C_x H_y + n (O_2) = a CO_2 + b H_2O \quad \ldots (5.72)$$

The burn of one mole of methane with n mole of O_2 produces a (or x) mole of CO_2 and b (or 0.5y) mole of H_2O. In the balanced equation, the number of O_2 moles n = (x+y/2).

One mole of fuel will weigh =x×M(C) +y×M (H) kg, M (CO_2) = 44 kg

Where, M=the molecular mass, hence

1mole $C_xH_y \rightarrow$ x mole of CO_2

(x × 12 + y × 1) kg of fuel produces $\rightarrow$ 44x kg CO_2 , or

x × 12 + y × 1 kg of fuel = x 44 kg CO_2, therefore,

1 kg C_xH_y = x 44 /(12x + y) kg CO_2 or 1 kg C_xH_y = 44 /(12 + y/x) kg CO_2

Hence, 1kg of methane (CH_4) fuel produces = 44/(12+4) = 2.75 kg of CO_2

For methane reaction:

$$CH_4+2(O_2+3.762N_2) \rightarrow CO_2+2H_2O+2(3.762)N_2 \quad \ldots (5.73)$$

For a complete combustion of 1 mole of CH_4, 44 kg of CO_2 is produced. In the current model, the properties of air were taken the form (Moran and Shapiro, 1999). It is clear that, such air contains a trace of Argon (Ar) and this is taken into consideration in the chemical equation below. Practically, the trace of this inert gas (Ar) is very small and do not make any detectable change in the equations for methane reaction. For an air rich mixture combustion process of an equivalence ratio of φ_1, where $\varphi_1<1$, the reaction equation transfers to:

$$CH_4 + \frac{2}{\phi_l}\left(O_2 + 3.714N_2 + 0.04762\ Ar\right) \rightarrow CO_2 + 2H_2O + \frac{2}{\phi_l}(3.714)N_2 + \frac{2}{\phi_l}(0.04762)Ar + \frac{2(1-\phi_l)}{\phi_l}O_2 \quad \ldots (5.74)$$

From this equation, the total number of moles (n_t) of the products is:

$$n_t = 1 + 2 + \frac{2(3.714)}{\phi_l} + \frac{2(0.04762)}{\phi_l} + \frac{2(1-\phi_l)}{\phi_l} \quad \ldots (5.75)$$

Therefore,

$$n_t = \frac{\phi_l + 9.5233}{\phi_l} \quad \ldots (5.76)$$

It is clear from the above that 1 kg (of hydrocarbon fuel) C_XH_Y = 44x/(12x + y) kg CO_2, 1kg CH_4 = 2.75kg CO_2

For a fuel rich mixture combustion process of an equivalence ratio of ϕ_r, where $\phi_r>1$, the reaction equation transfers to:

$$\phi_r CH_4 + 2\left(O_2 + 3.714N_2 + 0.04762\ Ar\right) \rightarrow \left(\phi_r - 1\right)CO_2 + 2\left(\phi_r - 1\right)H_2O + 7.428\,N_2 + 0.9524/\phi_r Ar + \left(\phi_r - 1\right)CH_4 \quad \ldots (5.77)$$

For one mole of fuel,

$$CH_4 + 2/\phi_r\left(O_2 + 3.714N_2 + 0.04762\ Ar\right) \rightarrow$$
$$\left(\phi_r - 1\right)/\ \phi_r CO_2 + 2\left(\left(\phi_r - 1\right)/\phi_r\right) H_2O + \quad \ldots (5.78)$$
$$\left(7.428/\phi_r\right) N_2 + \left(0.09524\right)Ar + \left(\left(\phi_r - 1\right)/\phi_r\right) CH_4$$

The total number of moles of the products (n_t) can now be calculated as:

$$n_t = \left(3\phi_l + 4.52324\right)/\phi_l \quad \ldots (5.79)$$

For methane CH_4, $x=\phi_l$, $y=4\phi_l$, n_1 (number of moles of the fuel) = ϕ_l, n_2(number of moles of combustion air) = 2, n_3(number of moles of unburned CH_4 = (ϕ_l-1).

ϕ_l mole of CH4 = (16ϕ_l) kg of CH_4 produces 44(ϕ_l-1) kg of CO_2

ϕ_l mole of CH4 = (16ϕ_l) kg of CH_4 produces (16 (ϕ_l-1)) kg of unburned CH_4

The typical relation between thermal efficiency and the load power with CO_2 emissions are depicted by Fig. 5.25 and 5.26. The first is for simple gas turbine cycle while the second is for intercooled reheated regenerated gas turbine.

These figures confirm a certain relation which is quite similar to GC configurations between these two cases and other configurations. In the different cases considered here, the increase in the power generated from the cycle increases the thermal efficiency and reduces the emissions.

For power generation gas turbine cycle's thermal efficiency is expected to operate between 0.3 and 0.4. The operation region of these figures is generated for a certain load required by the generator, which show a high thermal efficiency combined with low CO_2 emissions. If the power load required an increase then, this is combined by a great degradation in thermal efficiency and a significant increase in CO_2 emissions. These results from burning the same fuel mass flow, expansion ratio, (T_{g3}) and (T_{g4}).

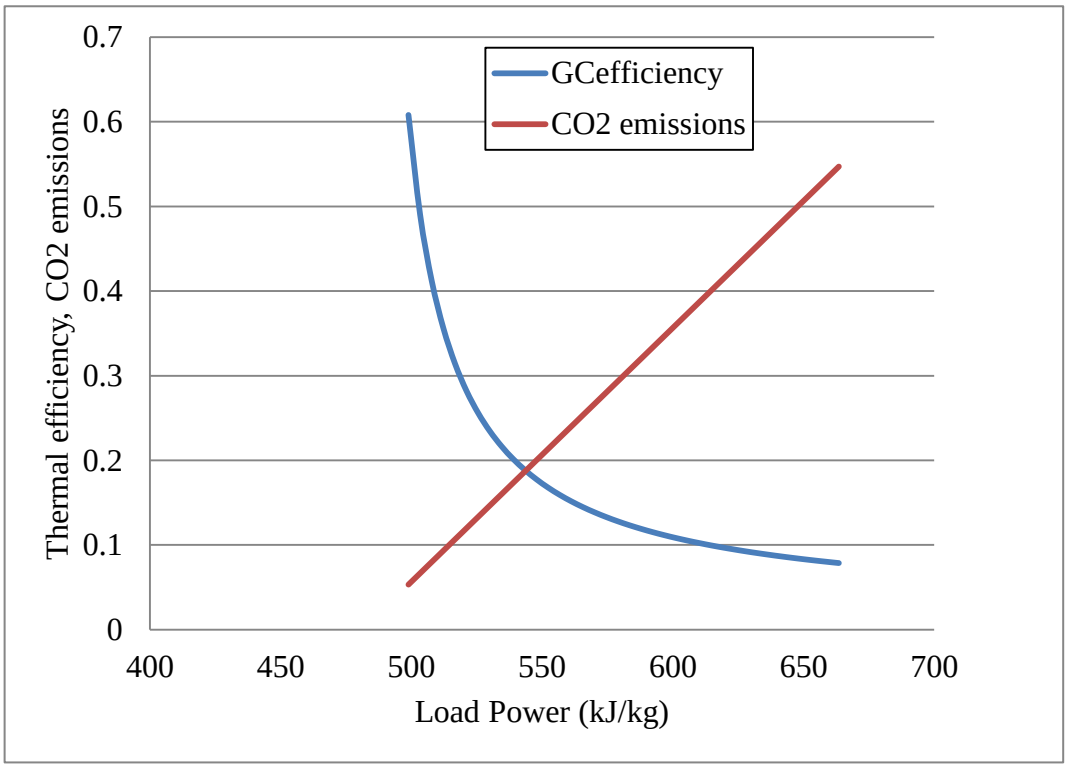

Figure 5.25 The thermal efficiency nad CO_2 emissions versus the load power for one kg of air

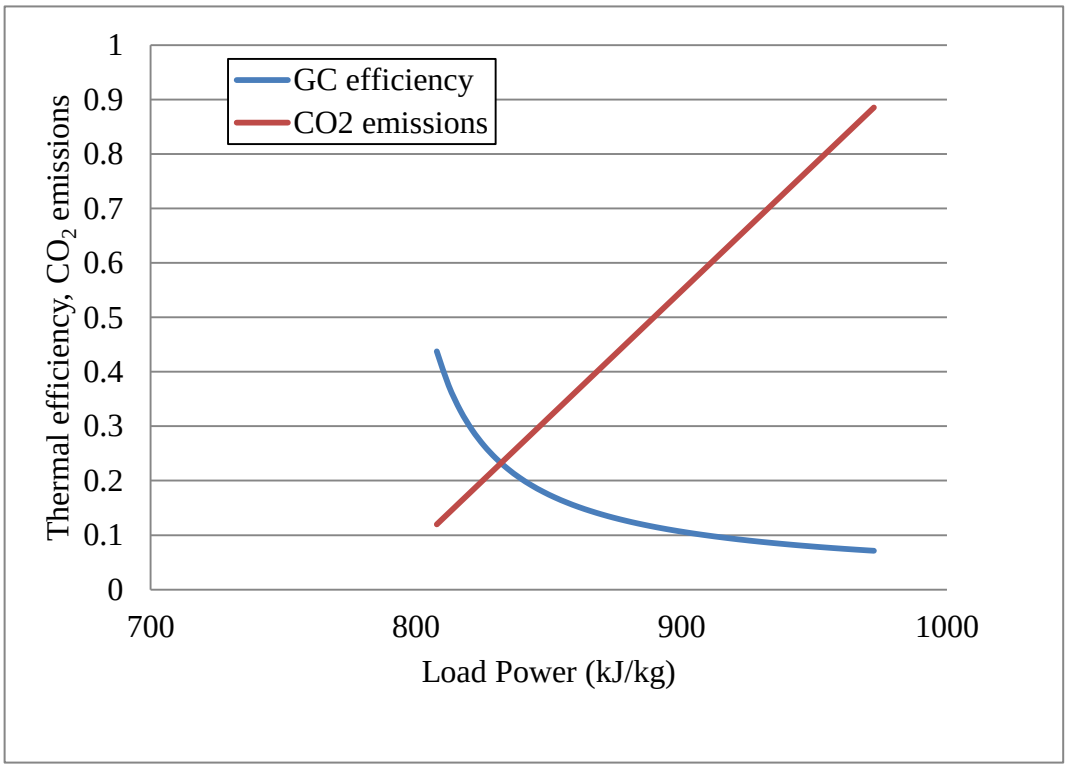

Figure 5.26 The thermal efficiency and CO_2 emissions versus load power for one kg of air

5.4.2 Emission of nitrogen oxide

The formation mechanisms (thermal, chemical, and prompt) of the NO_x are complicated and are not the subject for discussion in the current work. It is well known that NO_x is responsible for producing smog as it reacts with moisture in the presence of sunlight. In addition, NO_x also contributes to acid rain and depletion of the ozone layer.

However, Razak [8] utilized two correlations to predict the NO_x emission level as a result of the combustion of natural gas. In both, NO_X amount is given in (ppmv) at 15% O_2 dry. Razak, transferred the units from (ppmv) to grams NO_x per kg fuel.

The correlation used for obtaining the NO_X emissions based on Rokke et al., [8].

$$e^{NO_x} = 18.1 P^{1.42} \dot{m}_a^{0.3} f^{0.72} \quad \ldots (5.80)$$

Where P is the pressure of combustion in atmosphere, m_a is the combustion air flow (kg/s) and f is the fuel to air ratio. The correlation was presented for natural gas fuel GT and was tested for an output between 1.5 and 35 MW.

Bakken and Skogly [90] developed another correlation to predict the level of NO_x for gas turbine operating on natural gas:

$$e^{NO_x} = 62 \times \left(\frac{P_{g3}}{P_{g1}} \right)^{0.5} f^{1.4} \exp - \left(\frac{T_{g1} 635}{T_{g3}} \right) \quad \ldots (5.81)$$

Where, P_{g3}: is the pressure of combustion (P_a), T_{g3} is the temperature of combustion (°C), f is the fuel to air ratio, the parameters must be corrected to the standard conditions of (T_{g1}=15°C and P_{g1}= 1.013 bar), therefore the NO_X emissions is dependent on (T_{g3}/T_{g1}) and (P_{g3}/P_{g1}) i.e. compressor inlet conditions (T_{g1} and P_{g1}) rather than combustion conditions (T_{g3} and P_{g3}).

In the current work, Bakken and Skogly's correlation was employed in the model to determine the level of NO_x emission from the gas turbine plant of the combined cycle power plant. The predicted level of the NO_x emission is presented in Section 5.6 of this chapter.

5.5 Optimization of conventional combined power cycles

Simplifying the relations between gas turbine and air compressor non-dimensional parameters shows with a considerable accuracy, how the whole gas turbine is working. This is shown in

Fig. 5.27 for Non-dimensional corrected mass flow rate and pressure ratio, which implies the simple gas turbine configuration. It is clear how the gas turbine operating lines even limits the operation of the air compressor.

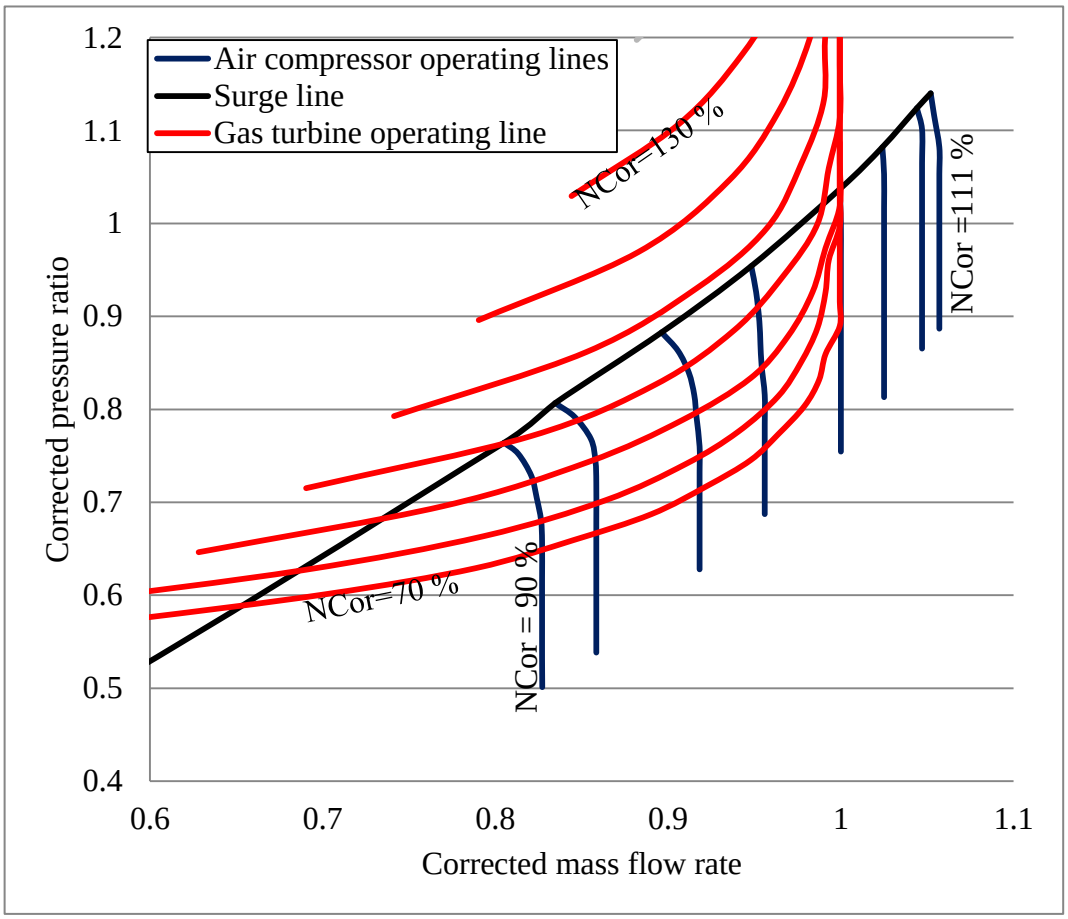

Figure 5.27 Corrected pressure ratio versus corrected mass flow for air compressor running lines imposed on gas turbine running lines

Within the conducted procedure of optimization, running the module of any CCPP was to last from few minutes to several hours. For many cases, running the program for the vast range of parameters required took days. Although and similarly to [24] computer codes was successfully used to optimize reliable heat exchangers arrangements in addition to the engine's main components. The results are different from those predicted by previous studies. This is more due to considered assumption and limitations than the approach, likewise, as reported by Horlock, [12]. However, many other similarities are indicated by:

(1) The input and output parameters limited the entire combination of the CCPP which also reported in [11]. CCPP performance is more sensitive to GC and more governed to its' parameters than SC [35]. However, degradations of both the SC and the GC components linearly addressed its effect on the CCPP performance [35].

(2) The optimization of the HRSG improves the CCPP performance similarly to [26] and [32]. It also confirm GC parameters dominate the unfired HRSG CCPP performance that reported by Horlock [12].

Although the results confirm Topolski [24]contradiction between HRSG units and the CCPP optimum performance, this is not true for the entire operation platform. The optimum efficiency does gather with the optimum HRSG unit's efficiency if these units' outputs are balanced. This indicates that, as long as the gas output from each section satisfies the steam heat requirement of the next unit optimizing HRSG improves the optimum efficiency. However, CCPP has the maximum efficiency with TP HRSG configuration.

The optimization process results confirmed in [31] and [32] indications of the significant effects of X_{s4}, P_{s3} ΔT_{ppm} on CCPP. Many other parameters are investigated in the optimization process but only the most important are reported. The following table 5.2 represent the results from billions of cases for each model with the respect to the limitations and restrictions mentioned previously. Similarly to [34], [36], this study confirms T_{g4}, W_{ST} and W_{GC} are greatly affected by η_{AC} and η_{GT} rather than $\dot{m}g$. This is due to the great mass flow rate to its change in comparison to the change for a running GT engine as can be seen on the AC map. It is important when it is combined with AC and GT performance characteristics (non-dimensional parameters) to bring the total gas turbine close stall limits. In such case, this has a great effect on the steam amount and quality at HRSG components, responsible on deteriorating ST output. In corresponding to [19]reports on T_a effects on T_{g4}, Such effect makes a great determination to the CCPP performance characteristics if Ta influence on T_{g4} is considered. This study agrees with [35] on CCPP performance is more deteriorated by degradation of η_{HRSG} and η_{Con} than η_{ST}. But the parameters of these components are connected in design and during operation. Thus the degradation in a component will have its effect on the successive component as well. This study disagrees on that the degradation in the performance of both cycles' components results in the lowest T_{gstack} [36]. This is more related to components' degradation of GC than the SC. This study refers the low stack temperature to the improvements in HRSG and SC performance. It also shows a better CCPP performance

correspondence to the low T_{gstack}. The results here are when CCPP is optimized for maximum thermal efficiency rather than any other performance parameters.

The optimization results confirm that the maximum efficiency correspondence to the maximum T_{g3} for all CCPP configurations. This agrees with Bassily [31]and [32] results for TP and DP steam engine CCPPs. This model exclude Tg4 of less than 500 from calculations based on the recommendations of [25] and [26] of less than 827 °C for P_{s3} between 30 and 60 bars SGReh and about 590°C for conventional CCPP to optimize the efficiency. For a fixed T_{g4}, these results confirm the increase in the P_{s3} insures steam generation at critical conditions that reported by [30]. However, such increase in P_{s3} requires heat transfer match between T_{g4}, T_{s3} in addition to HRSG components' efficiencies to attain the increase in the efficiency.

This study disagrees to correspond optimum performance characteristics to the maximum Ps3 because in here only unfired, HRSG is considered, but for fired HRSG units, this may be accurate. In other words, there is a match case of maximum heat absorption by the steam from the gases which is confirmed by a set of parameters T_{g4}, P_{s3} and the expected gases' temperature, temperature, .at the inlet of component. It also limited by the performance characteristics of the HRSG units (efficiencies, effectiveness's, and ΔTppm this limitation multiplies for multi pressure steam turbine CCPP similarly as reported by [31]. This opens further debate on (1) new blades' heat resistance to T_{s3}, (2) the kind of HRSG and on what P_{s3}, in this study greater T_{g4} is taken into consideration this pressure and the temperature of the steam at the turbine outlet.

The results here agree with [32] that the optimum CCPP correspondence to maximum rAC except for SGT CCPP. It also agrees to correspond such a condition to minor Ps3 but Ts3 is changed with the parameters set referred above. The optimization results confirmed the minimum ΔT_{ppm} for [32] CCPP's optimum performance. However, this is confirmed for low pressure economizer only as in successful units less heat is required to attain saturation, and the gases' heat content must be kept to enrich vapour content in low pressure.

Although this study agrees on that, the optimization of HRSG and the SC, the ηCCPP can be raised greatly. It disagrees on the figures given in [29] and [30]. These figures of 60 or greater for RegGCCPP, RehRegGCCPP and IntRehRegGCCPP of multi pressure HRSG. Of course, such efficiencies are not attained by the result of the current model. It is however the tendency of the increase in the efficiency by upgrading the GC and the SC of this model. The high efficiencies attained for RehGCCPP, RehRegGCCPP, DPSCCPP by previous studies in [19], [29] and [25]was due to the following:

(1) Voiding the components operation stability limits by considering $X_{s4} < 0.9$, $T_{s3}>1000$ °C and $T_{g3}>1500$°C which requires GT cooling to protect its components.

(2) Using inaccurate simulation to the components to real operation conditions like P_{s4} and ϕ_{CC} effects.

(3) Here the T_{g3} temperature equals the combustion temperature, based on that, the combustor model will consider the heat input as the heat available to the gas and steam rather than the heat already given to the gas and steam excluding the heat losses or cooling prospective.

The results here show that, the optimum conditions are always correspondent to the maximum T_{g3}, ϕ_{CC}, r_{AC}, ε_{EC} and minimum T_{g1}, ΔT_{ppm}. However this study in core is comparative rather than qualitative, and this where if greater T_{g3} are employed, efficiencies of closer to these predicted by others are attained. With respect to industrial operation limits, the most promising solutions among different SC comninations to SG are the DPReh Steam turbine. The most promising CCPP Simple gas turbine configurations based on this study is SGTPReh. In here the results agree with [33]on that RehGTPRehCCPP is the most promising configuration for power generation industry but if the additional fuel heat is efficiently utilized.

CCPP	T_{g1} (°C)	r_{AC}	ϕ_{CC}	T_{g3} (°C)	P_{s2} (bar)	P_{s1} (bar)	ΔT_{PPm} (°C)	ε_{EC}	η_{CCPP} %	w_{CCPP} (kJ/kg)	SFC × 10^4 (kg/kW.h)	e^{NO_X} (PPmV)	e^{CO_2} (Kg fuel)	T_{gstack} (°C)	T_{s4} (°C)
SGSSCC	-10	26.5	0.9	1500	20	0.05	5	0.8	45	566.5	1.6	205.5	69.2	124	32.9
SGRehSCC	-10	36	0.9	1500	31	0.2	14	0.8	48.3	775.3	1.6	226.7	66.5	98.2	203
SGRegSCC	-10	36	0.9	1500	24	0.1	5	0.8	42.5	953.9	1.69	226.7	66.5	200	45.8
SGDPSCC	-10	36	0.9	1500	26	0.1	5	0.8	41.1	709	1. 8	226.7	66.5	127	45.8
SGDPRehCC	-10	27	0.9	1500	26	0.3	5,9	0.6	44	788.1	1.6	206.8	69	224.4	63.5
SGTPSCC	-10	23	0.9	1500	20	0.1	5	0.6	41.6	759.2	1. 7	196	70.3	197.2	45.8
SGTPRehCC	-10	17	0.9	1500	186	0.45	5	0.8	44.2	833	1. 63	176.3	72.64	163	76.9
RegGSSCC	5	36	0.9	1500	20	0.15	5	0.8	44.6	702	1. 6	0.343	57.4	141.4	50.2
RehGSSCC	-10	36	0.9	1500	44	0.05	5	0.8	40.5	1060.5	1.9	161	108.3	123.8	32.9
IntGSSCC	-10	30	0.9	1500	20	0.05	5	0.8	39.1	757	1.8	239.6	74.64	124	32.9
IntRehGSSCC	-10	36	0.4 0.9	900, 1500	44	0.05	5	0.8	30.9	891	1.8	455.5	131.6	132.8	32.9
IntRehRegGSSCC	-10	36	0.9 0.9	1500 1500	25	0.1	5	0.8	30.7	1096	2.7	288.4	157.8	136.8	45.8

Table 5.3 Selected results from a number of the optimized CCPP configurations

5.6 Conclusions

1. Gas turbine operating envelope is greatly affected by the matching between the components in the gas turbine.

2. When practical limitations and restrictions of the gas and steam turbines are employed in the program, the results were significantly filtered.

3. Due to the limitation in the operation ranges of gas and steam turbines further cycles' optimization using operation ranges are linked to advanced configurations like ChGT.

4. Estimating the characteristics of the gas turbine on the characteristics map of gas turbine and air compressor is considered by the long-time iteration processes.

5. Steam turbine operation is limited by satisfying HRSG duty, which is governed by its components performance (efficiency and effectiveness).

6. Emissions of NO_X and CO_2 are of affected by the combustion parameters as well as the combustor inlet air and fuel conditions. Mostly, these affecting parameters are the temperature of combustion, the equivalence ratio and the pressure at which the combustion occurs.

7. The upgrades in HRSG configurations from single pressure to multi pressure add more limits to the operation map of the CCPP. This was featured by the reheated HRSG as well.

8. The optimum CCPP design point for a certain GT configuration is different by integration different STs.

9. The results confirm that, the optimum characteristics of different CCPP corresponding to different states of operation on the performance map.

10. A reliable operation at high Tg3is enabled by the improvement in cooling coating and meatal to preserve GT components, though the top increase in efficiency is limited to a correspondent increase Tg3 to 1500°C.

11. The efficiencies addressed by the results of this chapter are much lower in comparison to those generated by previous researchers. This is due to the difference in the definition of the heat input into cycle to that addressed here. However efficiencies of closer values

to those given by previous investigators were generated if the heat losses due to cooling are neglected.

12. The optimization results show that, by applying advanced GC configurations for CCPP its efficiency does not increase. The opposite is more likely here, which happens because the CCPP here is considered for unfired HRSG only.

13. The change of the ϕ_{CC} is considered here rather than using the conventional ϕ_{CC} of regular CCPP. Therefore the optimization results provide wider range of parametrical study than pervious conventional CCPP investigators.

CHAPTER 6
PARTIAL OXIDATION IN GAS TURBINE

6.1 Introduction and background

As discussed in the previous chapter, increasing the combustion gas temperature prior to its entry to the turbine can improve the gas turbine plant performance and efficiency. Hence, it is expected that gas turbine engine/plant which operates on a turbine inlet temperature of 1500 °C can easily attain an efficiency which exceed 50 %. The use of partial oxidation in the gas turbine engine of a combined cycle power and power plant was, firstly, proposed by Kobayashi et al., [63]. In such systems, the fuel rich combustion chamber products expand in the gas turbines that uses carbon reinforced composites. After expansion, the combustion gases still contain a significant amount of energy as H_2 and CO which are regenerated after mixing the combustion air with the fresh compressed air. This mixture burns with the fuel in the fuel lean combustion chamber and expands through a conventional turbine. Here, conventional turbine is a turbine with alloy steel rotor. As in normal combined cycles, the heat from the gas turbine outlet is used to generate the steam for the steam turbine plant/engine. The combined cycle that uses rich combustion gas turbine is generally called (ChGT), which can operate with a performance better than that of the conventional designs. The efficiency of the ChGT can reach 66% when the equivalence ratio of the rich combustion is 2, Kobayashi, et al., [63].

Air cooling is extensively used in modern gas turbines to attain the high turbine inlet temperature, although it usually generates additional losses (as the air is compressed to a higher pressure prior to its entry to the combustion chamber). However, the rich combustion gas turbine (ChGT) system allows using a greater gases temperature with no such losses. The fuel rich atmosphere is required because carbon composites are sensitive to the presence of oxygen. The optimization of plant performance by increasing the gases temperature at turbine

inlet or by using cooling strategy usually requires advanced materials and complex cooling techniques. Additionally, the work required by the air compressor is greater for such designs than the un-cooled design.

Carbon reinforced carbon composites can withstand gases temperature of up to 1800 °C, but such high temperatures make the materials under oxidation. The fuel rich atmosphere combustion (Sub-stoichiometric conditions) preserves composites' layers and it reduces the formation of NO_X emissions as well. The plant that built based on ChGT designs can reach a thermal efficiency of 65% LHV when turbine inlet temperature and steam cycle parameters are optimized Korobitsyn et al., [64]. At a turbine inlet temperature of 1500 °C without turbine blade internal cooling, it has considered by the previous researcher that the C/C composites is the only promising material for turbine blades.

Blades materials with C/C composites are, however, sensitive to the oxidation at high gases temperatures. Therefore, fuel rich combustion gases of such high temperatures (over 1500 °C) are most suitable to use with C/C blades. Accordingly, turbine blades with C/C composites which are sensitive to oxidation at high gases temperature can resist such high temperature because of the significant reduction in the concentration of the oxygen in the products of rich combustion Yamamoto et al., [62].

A comparative study of Abdel-Rahim and Mohamed [65] showed that the reheated gas turbine has an efficiency that always exceeds the efficiency of POGT, but only for low isentropic temperature ratio. Beyond such limit the partial oxidation configurations were operating more efficiently than (RehGT). The phenomenological designs of turbine cycles had an extensive expansion in the past few years (mainly after 2001). These designs have exposed all the possible contributions of different units of the cycle to improve the cycle's performance. In partial oxidation plant/engine the fuel and the air are mixed and burned into H_2 and CO in the first combustor (1^{st} combustion process).

The advantages from such design are to:

1. Reform the residues of the oil into fuel gas (in turbine operating on liquid fuels).
2. Removes sulphuric components as H_2S
3. Utilizing the remaining gas in the turbine.

The blades of the fuel rich turbines which are made from Carbon reinforced Carbon Composites, suffer from rapid degradation when they exposed to a small amount of oxygen.

Partial oxidation gas turbine (POGT) cycle is a general form under which RehGT cycle is designed. This is because when the whole mass flow expands in both turbines, it becomes a case of reheat only Lior et al., [57].

The power cycle that uses fuel rich combustion with carbon fibre reinforced carbon composites in turbine blades is developed by Kobayashi et al. in 1997 in the University of Nagoya in Japan.

The fuel rich combustion in the first stage creates a reducing atmosphere in the first turbine, which allows operation temperature of high levels up to 1800 °C if C/C composites are in use. It also produces fewer NOX emissions than conventional systems.

The obvious method to increase the thermal efficiency of a power plant cycle is to increase the temperature of the heat source. Such increase reaches 1% for each 100 °C increase as referred by Yamamoto et al., [58]. According to such bases, many studies were undertaken to investigate how to attain such high temperatures, which went in two ways the first through employing new materials, the other was through using cooling techniques. The latter is usually involved with a loss in the efficiency; therefore, it is more important to focus on development of the improved heat resistance materials. The special effort of employing high temperature is promising by using the C/C composites. This is true as there is no current material for turbine blades, which durable enough to withstand a temperature of 1800°C.

The work reported in this chapter investigated the impact of the partial oxidation cycle in gas turbine plant/engine on the overall performance and efficiency of the combined power plants. This was achieved by developing a computer model which as constructed from various sub-models for each of the components involved in the combined power and power plant. In each individual section, details of the sub-models in the form of equations are provided in favour of lengthy description of the sub-model details.

6.2 Combustion of rich and lean fuel mixtures:

Natural gas is the most used fuel consumed in gas turbine used for power generation. Natural gas consists of CH_4=92.6%, C_2H_6=3.6%, C_3H_8=0.8%, C_4H_{10}=0.3%, N_2=2.6%, CO_2=0.1% (Eastop and McConkey, 1993). In this study, methane (CH_4) represents natural gas in its entirety as fuel for gas turbine. The chemical equations involved in the combustion of pure methane are discussed in this hereafter.

The complete combustion of one mole of methane with excess air is represented by Eq. 6.1.

$$CH_4 + 2\left(O_2 + 3.76N_2\right) \rightarrow CO_2 + 2H_2O + 7.52N_2 \quad \ldots (6.1)$$

For the fuel rich or air lean combustion Eq. 61 converts to Eq. 6.2.

$$CH_4 + \frac{2}{\phi_r}\left(O_2 + 3.76N_2\right) \rightarrow \frac{1}{\phi_r}CO_2 + \frac{2}{\phi_r}H_2O + \frac{7.52}{\phi_r}N_2 + \frac{\left(\phi_r - 1\right)}{\phi_r}\ CH_4 \quad \ldots (6.2)$$

For fuel lean or air rich combustion of methane Eq. 6.3 applies.

$$CH_4 + \frac{2}{\phi_l}\left(O_2 + 3.76N_2\right) \rightarrow\ CO_2 + 2H_2O + \frac{7.52}{\phi_l}N_2 + \frac{\left(1 - \phi_l\right)}{\phi_l}O_2 \quad \ldots (6.3)$$

The burning of the residual fuel (the number of moles left from burning one mole of methane of fuel rich/air lean mixture in combustion chamber 1/ CC1 is $[(\phi_r\text{-}1)/\ \phi_r]$), which is the number of moles the methane combustion in combustion chamber 2/CC2 is represented by Eq. 6.4.

$$\left(\frac{(\phi_r\text{-}1)}{\phi_r}\right) CH_4 + \left(\frac{2(\phi_r\text{-}1)}{(\phi_l\phi_r)}\right)(O_2 + 3.76N_2) + \left(\frac{1}{\phi_r}\right)CO_2 + \left(\frac{2}{\phi_r}\right)H_2O + \left(\frac{7.52}{\phi_r}\right)N_2 \rightarrow$$
$$CO_2 + 2H_2O + \left(\frac{7.52}{\phi_r}\right) \times \left(\frac{(\phi_r\text{-}1)}{(\phi_l\phi_r)}\text{-}1\right) N_2 + \left(\frac{2(\phi_r\text{-}1)\ (\phi_l\text{-}1)}{(\phi_l\phi_r)}\right)O_2 \quad \ldots (6.4)$$

In order to estimate the LCV for the lean combustion the chemical equation should be for one mole of the methane fuel.

$$\left(\frac{(\phi_r\text{-}1)}{\phi_r}\right) CH_4 + \left(\frac{2(\phi_r\text{-}1)}{(\phi_l\phi_r)}\right)(O_2 + 3.76N_2) + \left(\frac{1}{\phi_r}\right)CO_2 + \left(\frac{2}{\phi_r}\right)H_2O + \left(\frac{7.52}{\phi_r}\right)N_2 \rightarrow$$
$$\left(\frac{1}{\phi_r}\right)CO_2 + \left(\frac{2}{\phi_r}\right)H_2O + \left(\frac{7.52}{\phi_r}\right)N_2 + \left(\frac{(\phi_r\text{-}1)}{\phi_r}\right) CO_2 + \left(\frac{(\phi_r\text{-}1)}{\phi_r}\right)2H_2O + \left(\frac{7.52(\phi_r\text{-}1)}{(\phi_l\phi_r)}\right) N_2 +$$
$$2\left(\frac{1}{\phi_l} - \frac{(\phi_r\text{-}1)}{\phi_r}\right)O_2 \quad \ldots (6.5)$$

$$CH_4+\left(\frac{2}{\phi_l}\right)(O_2+3.76N_2)+\left(\frac{1}{(\phi_r-1)}\right)CO_2+\left(\frac{2}{(\phi_r-1)}\right)H_2O+\left(\frac{7.52}{(\phi_r-1)}\right)N_2 \rightarrow$$
$$\left(\frac{1}{(\phi_r-1)}\right)CO_2+\left(\frac{2}{(\phi_r-1)}\right)H_2O+\left(\frac{7.52}{(\phi_r-1)}\right)N_2+\ CO_2+2H_2O+\left(\frac{7.52}{\phi_l}\right)N_2+$$
$$2\frac{(\phi_r-\phi_l(\phi_r-1))}{\phi_l(\phi_r-1)}O_2$$

… (6.6)

$$CH_4+\left(\frac{2}{\phi_l}\right)(O_2+3.76N_2)+\left(\frac{1}{(\phi_r-1)}\right)CO_2+\left(\frac{2}{(\phi_r-1)}\right)H_2O+\left(\frac{7.52}{(\phi_r-1)}\right)N_2 \rightarrow$$
$$\left(\frac{\phi_r}{(\phi_r-1)}\right)CO_2+\frac{2\phi_r}{(\phi_r-1)}H_2O+\left(\frac{7.52\left(1-\frac{(\phi_l\phi_r)}{(\phi_r-1)}\right)}{(\phi_l\phi_r)}\right)N_2+\left(\frac{2(1-\phi_l)}{\phi_l}\right)O_2$$

… (6.7)

The enthalpy of reaction is the heat change when reactants (air + fuel) enter and products leave a constant temperature process. For a combustion reaction, this enthalpy is called (enthalpy of combustion). Such enthalpy varies with the change of the temperature and the pressure of the fuel burned. In this study the combustion chamber is modelled assuming steady flow combustion at a constant pressure in order to determine the enthalpy of reaction in each combustor.

6.3 ChGT solution program model

Using Visual Basic Applications (VBA) two functions have been developed to estimate the LCV and the fuel to air ratio in both combustors with reference to the equivalence ratio for each combustor.

In this work and for simplicity, the air is assumed to obey the following assumptions:

1. Air is of a molar ratio of nitrogen to oxygen of 79% to 21%, respectfully.
2. The water vapour content of the air is negligible.
3. No chemical reaction with N_2, although as a part of air components, it undertakes the rise in the temperature.
4. The properties' tables used are for ideal gases.
5. The combustion process occurs based on constant pressure reaction.

6.3.1 Configurations and basic analysis

Two gas turbine cycle's configurations were considered in the current work. In both configurations, the air is mixed initially with extra fuel to form a fuel rich mixture or air lean mixture. This mixture is burned, subsequently, in fuel rich combustion chamber (combustor 1). Combustion products are then allowed to expand in the fuel rich turbine (high temperature turbine). Gases leaving this turbine are then mixed with air to form a fuel lean or air rich mixture. This mixture is burned in the fuel lean or air rich combustion chamber (combustor 2). The combustion products expand in the fuel lean (low temperature) turbine. The two configurations plant design and components are shown schematically in Figs. 6.1 and 6.2.

In this model design/configuration, which is shown schematically in Fig. 6.1, the volume of the air taken by the compressor is assumed constant. Accordingly, the density of the air ρ_a at the compressor intake is calculated using the function DFT at temperature (T_{g1}).

$$M_{g1} = m_a \times \left(\frac{\rho_a}{\rho_{iso}} \right) \quad \ldots (6.8)$$

Where (ρ_{iso}) is the density of the air at ISO conditions, i.e. a temperature of (288 K). The ratio between the mass of the air flowing to the rich fuel combustor to that flowing to the lean combustor is determined by equation (6.9).

$$Y = \frac{1}{\left(1 + \frac{\varphi_{CC1} - 1}{\varphi_{CC2}} \right)} \quad \ldots (6.9)$$

$$w_{GC} = Y\ w_{GT1} + w_{GT2} - w_{AC1} - Y\ w_{AC2} \quad \ldots (6.10)$$

$$\eta_{GC} = \frac{w_{GC}}{\left(\left(Y\ f_{CC1}\ LCV_{CC1} + (1 - Y)\ f_{CC2}\ LCV_{CC2} \right) \times 1000 \right)} \quad \ldots (6.11)$$

$$\dot{m}_{sa} = \dot{m}_{sa1} + \dot{m}_{sa2} \quad \ldots (6.12)$$

The ratio of the mass flow to the first HRSG to the total mass flow of water from the pump is determined using equation (6.13)

$$Ys = \frac{m_{sa1}}{m_{sa}} \quad \ldots (6.13)$$

The performance characteristics of the simple steam turbine bottoming cycle is given by:

$$w_{SC} = m_{sa} \left(w_{ST} - w_{WP} \right) \quad \ldots (6.14)$$

$$\eta_{SC} = \frac{w_{SC}}{\left[(Y + F)\left(h_{g6} - h_{g7}\right) + (1 + F)\left(h_{g011} - h_{g012}\right)\right]} \quad \ldots (6.15)$$

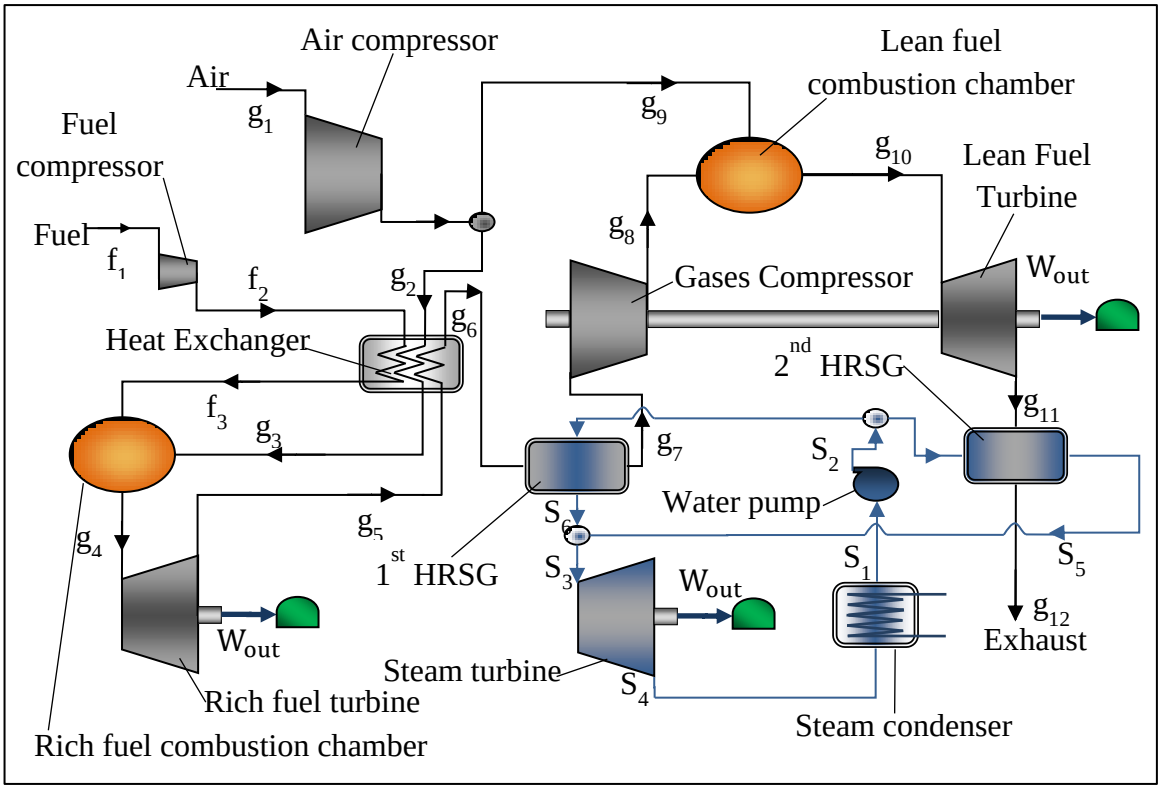

Figure 6.1 Diagram of a combined cycle based on chemical gas turbine

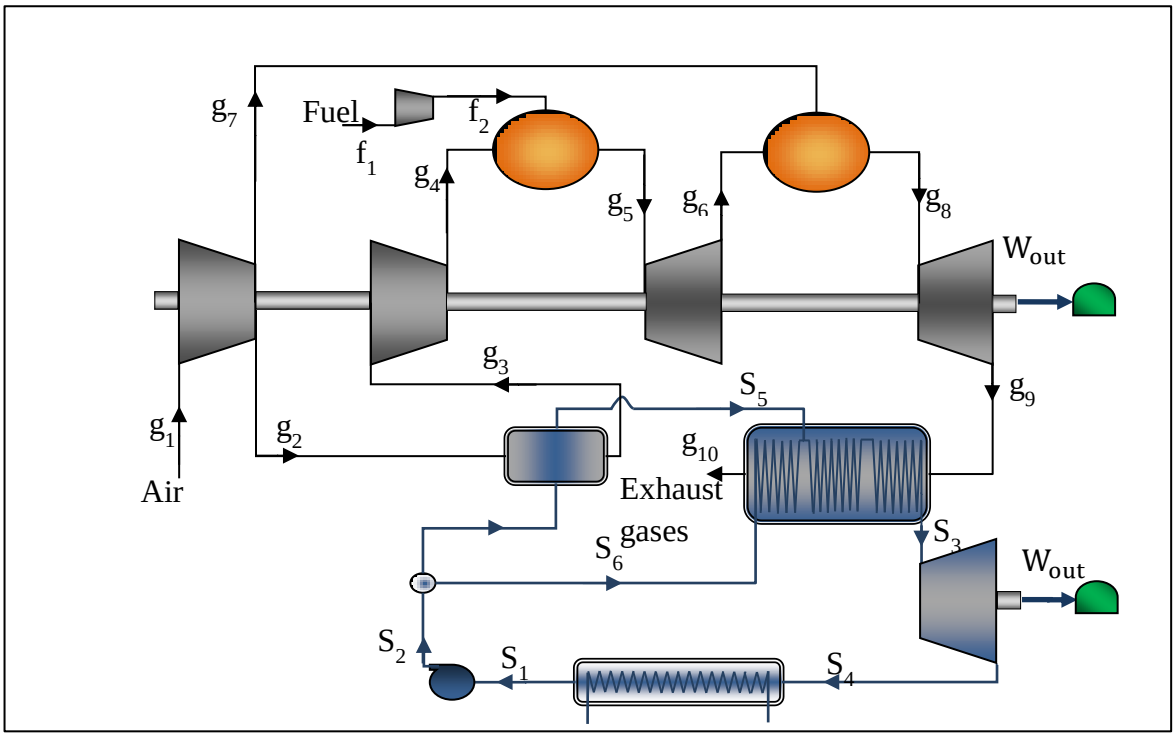

Figure 6.2 Flow diagram of a combined cycle based on chemical gas turbine system, studied

$$\eta_{GC} = \frac{(w_{GT1} + w_{GT2} - w_{AC1} - w_{AC2})}{(Y \times f_{CC1} \times LCV_{CC1} + (1) \times f_{CC2} \times LCV_{CC2}) \times 1000} \quad \ldots (6.16)$$

$$m_{sa} = m_{sa1} + m_{sa2} \quad \ldots (6.17)$$

$$w_{SC} = (w_{ST} - w_{WP}) \quad \ldots (6.18)$$

$$\eta_{SC} = \frac{m_{sa} \times (w_{ST} - w_{WP})}{Y \times (h_{g2} - h_{g3}) + (1 + f_{CC2}) \times (h_{g9} - h_{g10})} \quad \ldots (6.19)$$

$$w_{CC} = w_{SC} + w_{GC} \quad \ldots (6.20)$$

The efficiency of the combined cycle for the first and the second designs are given in equations 6.21 and 6.22 subsequently. The specific work output and the specific fuel consumption are generated using equations 6.23and 6.24. The NO_X and CO_2 emissions are estimated using equations 6.25 and 6.26.

$$\eta_{CC} = \frac{w_{CC}}{\left(Y\, f_{CC1}\, LCV_{CC1} + \left(1 - Y\right) f_{CC2}\, LCV_{CC2}\right) \times 1000} \quad \ldots (6.21)$$

$$\eta_{CC} = \frac{w_{CC}}{\left[Y \times f_{CC1} \times LCV_{CC1} + (1) \times f_{CC2} \times LCV_{CC2}\right] \times 1000} \quad \ldots (6.22)$$

$$W_{CC} = \frac{M_{g1} \times w_{CC}}{1000} \quad \ldots (6.23)$$

$$SFC = \frac{3600 \times \left(f_{CC1} + f_{CC2}\right) \times 1000}{w_{CC}} \quad \ldots (6.24)$$

$$e^{NOx} = e_{CC1}^{\ NOx} + e_{CC2}^{\ NOx} \quad \ldots (6.25)$$

$$e^{CO2} = \dot{m}_f \times 2.75 \quad \ldots (6.26)$$

6.3.2 ChGT program for components' models

The modelling of various components of both chemical gas turbine plants/configurations (ChGT), described above and shown in Figs. 6.1-6.2, are discussed and developed in this

section. Lengthy description of the details of each sub-model is avoided in favour of the model equations employed.

6.3.2.1 Fuel rich compressor model (air compressor)

The compressor is modelled here similarly to air compressor in chapter five; therefore, model functions and equations are similarly used in here. This model is applied for the first compressor of the first design and both compressors of the second design. For the first, the compression ratio as an input is given totally to this model. The compression ratio in Design 2 is given divided between compressors. The distribution of the main air between the first and the second compressors is assumed to be controlled by the parameter (Y) which can be measured by equation (6.9) of Sec. 6.3.1 and as shown below.

The assumptions for the Design 1,

$$T_{g2} = T_{g9} = T_{g1}\left(1 + \frac{r_{AC1}^{K_a} - 1}{\eta_{AC1}}\right) \quad \ldots (6.27)$$

$$P_{g2} = P_{g9} = P_{g1} \times r_{AC1} \quad \ldots (6.28)$$

Similarly for Design 2,

$$T_{g2} = T_{g7} = T_{g1}\left(1 + \frac{r_{AC1}^{K_a} - 1}{\eta_{AC1}}\right) \quad \ldots (6.29)$$

$$P_{g2} = P_{g7} = P_{g1} \times r_{AC1} \quad \ldots (6.30)$$

Furthermore, air enthalpies are functioned to the temperatures. The pressure and temperature at compression's discharge are calculated by equations (5.10 and 5.11) while the specific work output is determined using equation (5.12)

6.3.2.2 Fuel rich combustor

The rich fuel combustion environment significantly reduces the formation of NO_X emissions (Korobitsyn et al., [64]). Accordingly, the amount of the NO_X generated from such combustor is affected by the equivalence ratio of the combustion chamber (ϕ_{CC1}). Kobayashi et al., [63] showed that a stable combustion could be acquired at an equivalence ratio (ϕ_R) of a value as great as (0.7-1.3) at 40 bar. They also reported that the increase of combustion pressure

extends the combustor flammability limit. Although, a high thermal efficiency of 0.66 is calculated when (ϕ_R=2), Kobayashi et al., [63].

$$\dot{m}_f = f_{CC1} \times \dot{m}_{g1} \quad \ldots (6.31)$$

$$P_{g4} = P_{g2} \times \left(1 - \lambda_{CC1}\right) \quad \ldots (6.32)$$

$$LCV_{CC1} = f\left(T_{f3}, T_{g3}, T_{g4}, \phi_{CC1}\right) \quad \ldots (6.33)$$

$$f_{CC1} = f\left(T_{g3}, T_{f3}, T_{g4}, \phi_{CC1}, \eta_{CC1}, LCV_{CC1}\right) \quad \ldots (6.34)$$

Hence, the pressure ratio can be calculated as follows:

$$r_{fc1} = \frac{P_{g4}}{P_{g1}} \quad \ldots (6.35)$$

$$T_{f2} = T_{f1} \times \left(1 + \frac{(r_{fc1}{}^{K_M} - 1)}{\eta_{AC1}}\right) \quad \ldots (6.36)$$

The low calorific value for the lean fuel combustion LCV_{CC1} is calculated using the function (LCVRFTER) in which the LCV_{CC1}=f (T_{f2}, T_{g4}, T_{g5}, ϕ_{CC1}). While the fuel to air ratio (f_{CC1}) for such combustion is estimated by the function (fRFTEREFFLCV) in which f_{CC1} =f (T_{f2}, T_{g4}, T_{g5}, ϕ_{CC1}, η_{CC1}, LCV_{CC1}).

The pressure of the gases through the rich fuel combustor is calculated using the equation of pressure losses (6.37).

$$P_{g5} = P_{g4} \times (1 - \lambda_{CC1}) \quad \ldots (6.37)$$

$$e^{NOx1} = 62 \times \left(\sqrt{\frac{P_{g4}}{P_{g1}}}\right) \times (f_{CC1}{}^{1.4}) \times Exp\left[-635 \times \left(\frac{T_{g1}(°C)}{T_{g4}(°C)}\right)\right] \quad \ldots (6.38)$$

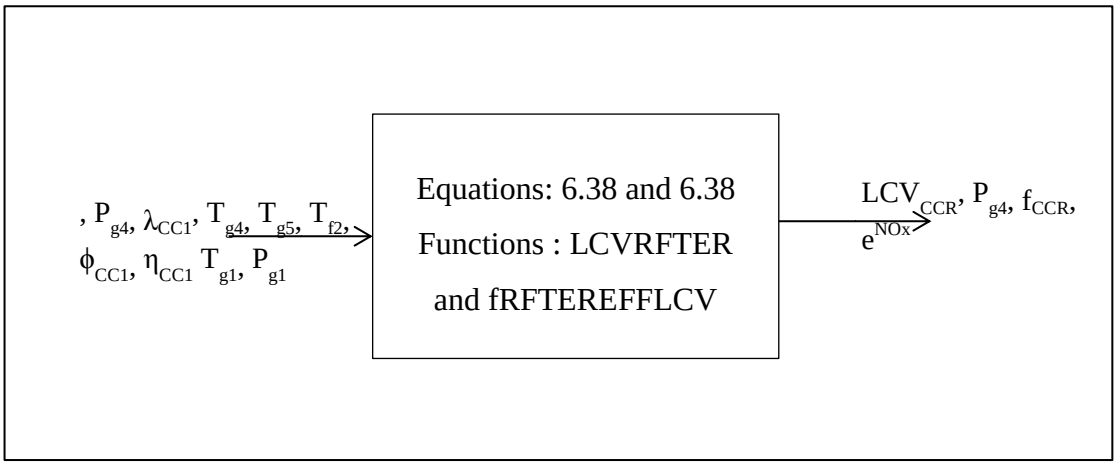

Figure 6.3 Fuel rich combustion chamber model

6.3.2.3 Fuel rich turbine

As discussed in the previous sections, Carbon fibre reinforced Carbon Composites for turbine blades made them withstand gases temperatures of up to 1800 °C. The high temperature gases made these composites a subject to oxidation. Blades oxidation can be prevented when the combustion process is achieved in a fuel rich environment Korobitsyn et al., [64]. In the present work and in order to know how acceptable is this high temperature (T_{g3}) for use in the composites' turbine blade, it was decided that the combustion process can be represented by equation 6.39.

$$\left(\phi_R\right).\, CRCC_{life} = f\left(\phi_R,\, T_{g3}\right) \quad \ldots (6.39)$$

The flow through this turbine must within the flammability limits as indicated by the study made by Kobayashi et al. [63]. The steady flammability limit is reported by Lior and Arai [91] for pressure ranges between 11 and 41 bars. In this model, the expansion ratio, temperature of exhaust gases and specific work output of the first design are calculated by equations 6.40, 6.41 and 6.45 respectively. While for the 2nd design, these parameters are calculated using equations 6.42, 6.43 and 6.46.

$$r_{GT1} = \left(\frac{P_{g4}}{P_{g5}} \right) \quad \ldots (6.40)$$

$$T_{g5} = (T_{g4}) \times (1 - \eta_{GT1} \times (1 - (r_{GT1}{}^{-Kg}))) \quad \ldots (6.41)$$

$$r_{GT1} = r_{AC2} - (1 - \lambda_{CC1}) \quad \ldots (6.42)$$

$$T_{g6} = T_{g5} \times \left(1 - \eta_{GT1} \times \left(1 - r_{GT1}^{-K_g}\right)\right) \quad \ldots (6.43)$$

$$P_{g6} = \frac{P_{g5}}{r_{GT1}} \quad \ldots (6.44)$$

$$w_{GT1} = Y \times (1 + f_{CC1}) \times (h_{g5} - h_{g6}) \times \eta_{GT1} \quad \ldots (6.45)$$

$$w_{GT1} = Y \times (1 + f) \times \left(h_{g4} - h_{g5}\right) \eta_{GT1} \quad \ldots (6.46)$$

$$h_{g5} = f\left(T_{g5}, \phi_{CC1}\right) \quad \ldots (6.47)$$

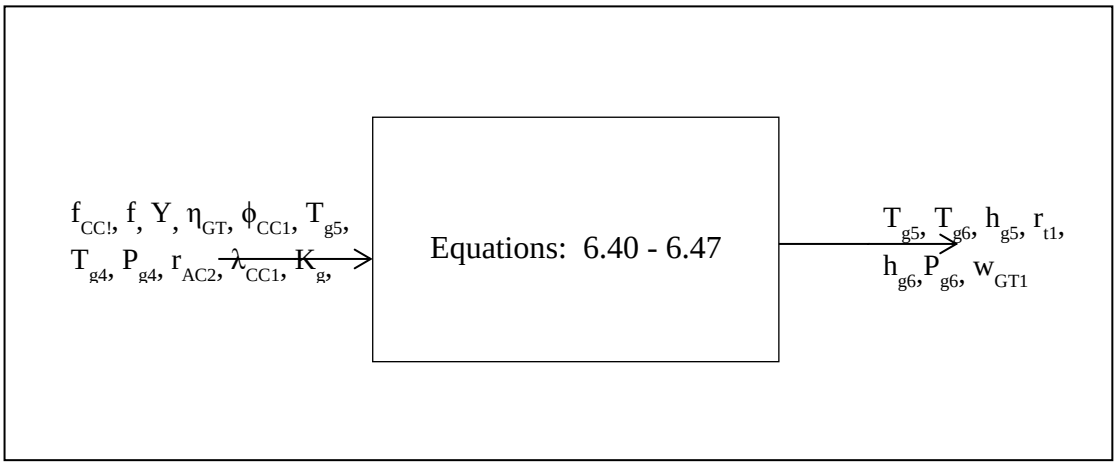

Figure 6.4 Fuel rich turbine model

6.3.2.4 Fuel rich gases HRSG

In this model, the pressure of the gases at the second compressor inlet (P_{g7}) is assumed to be given in which it is ranged around the pressure of the gases at the second HRSG outlet. The pressure of the gases at the first gas turbine discharge is calculated using the pressure losses' equation similar to that considered for the HRSG in chapter five. Similar to conventional CCPP, different HRSG configurations are considered here. The steam to air mass flow rate ratio (m_{sa1}) of the rich fuel gases HRSG simple and regenerated configurations are calculated using equation (6.50). While for reheated HRSG configurations, equations (6.51, 6. 54 and 6. 55) are utilized. For multi pressure fuel – rich gases HRSG, the steam to air mass flow ration at LP and IP streams are considered as a fraction to the HP mass flow rate which was calculated by equations (6.52-55). These fractions are considered with acceptable industrial operating mass flow ratios as in equations (6.48-and 6.49).

$$m_{sa}^{LP} = m_{sa}^{HP} \times m_{R1}^{LP} \quad \ldots (6.48)$$

$$m_{sa}^{IP} = m_{sa}^{HP} \times m_{R1}^{IP} \quad \ldots (6.49)$$

$$m_{sa1} = \frac{\eta_{HRSG1} \times Y \times (1 + f_{CC1}) \times \left(\frac{(h_{g6} - h_{g7})}{1000} \right)}{(h_{s6} - h_{s2})} \quad \ldots (6.50)$$

$$m_{sa1} = \frac{\eta_{HRSG1} \times Y \ (1 + f_{CC1}) \times \left(\frac{h_{Reh1O} - h_{g7}}{1000} \right)}{(h_{s6} - h_{s2})} \quad \ldots (6.51)$$

$$m_{sa1}^{HP} = \frac{\eta_{HRSG1} \times Y \ (1 + f_{CC1}) \times \left(\frac{h_{g6} - h_{g7}}{1000} \right)}{\left(h_{s6}^{HP} - h_{s2}^{HP}\right) + m_R \left(h_{s6}^{LP} - h_{s2}^{LP}\right)} \quad \ldots (6.52)$$

$$m_{sa1}^{HP} = \frac{h_{HRSG1} \times Y \times (1 + f_{CC1}) \times \left(\frac{h_{g6} - h_{g7}}{1000} \right)}{((h_{s6}^{HP} - h_{s2}^{HP}) + m_{R1} \times (h_{s6}^{IP} - h_{s2}^{IP}) + m_{R2} \times (h_{s6}^{LP} - h_{s2}^{LP}))} \quad \ldots (6.53)$$

$$m_{sa1} = \frac{\eta_{HRSG1} \times Y \ (1 + f_{CC1}) \times \left(\frac{h_{gRehO} - h_{g7}}{1000} \right)}{\left(h_{s6}^{HP} - h_{s2}^{HP}\right) + m_R \left(h_{s6}^{HP} - h_{s2}^{LP}\right)} \quad \ldots (6.54)$$

$$m_{sa1}^{HP} = \frac{h_{HRSG1} \times Y \times (1 + f_{CC1}) \times \left(\frac{h_{gRehO1} - h_{g7}}{1000} \right)}{((h_{s6}^{HP} - h_{s2}^{HP}) + m_{R1} \times (h_{s6}^{IP} - h_{s2}^{IP}) + m_{R2} \times (h_{s6}^{LP} - h_{s2}^{LP}))} \quad \ldots (6.55)$$

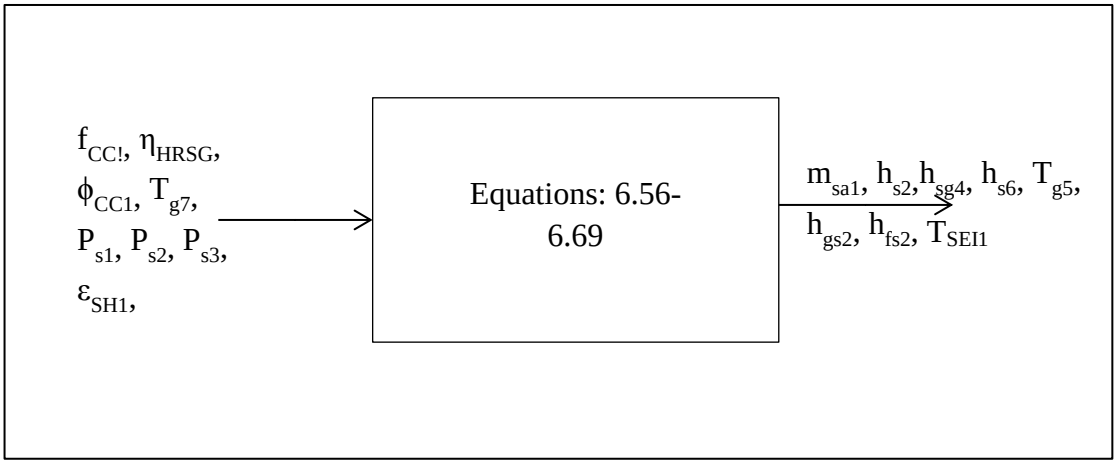

Figure 6.5 Simple fuel rich HRSG model

For simple HRSG model, the following equations are used to calculate models' outputs:

$$h_{fs1} = f\ (Ps1) \quad \ldots (6.56)$$

$h_{gs2} = f(P_{s2})$ … (6.57)

$T_{s2} = f(P_{s1}, P_{s3})$ … (6.58)

$h_{Sg4} = f(T_{g6c}, P_{s3})$ … (6.59)

$$h_{s6} = h_{gs2} + \varepsilon_{SH1} \times \left(h_{Sg4} - h_{gs2}\right) \quad \text{… (6.60)}$$

$h_{g7} = f(T_{g7}, \phi_{CC1})$ … (6.61)

$h_{fs2} = f(P_{s2})$ … (6.62)

$T_{sEI1} = f(P_{s2})$ … (6.63)

$$vs1 = f(P_{s4}) \quad \ldots (6.64)$$

$$T_{gEO1} = T_{sEI1} + \Delta T_{ppm1} \quad \ldots (6.65)$$

$$T_{g7} = T_{gEO1} - \eta_{EC} \times \left(T_{gEO1} - T_{s2}\right) \quad \ldots (6.66)$$

$$\eta_{HRSG1} = \eta_{EC1} \times \eta_{E1} \times \eta_{SH1} \quad \ldots (6.67)$$

$$m_{sa1} = \eta_{HRSG1} \times \left(1 + f_{CC1}\right) \times \left(\frac{h_{g6} - h_{g7}}{h_{s6} - h_{s2}}\right) \quad \ldots (6.68)$$

$$h_{s2} = h_{fs1} + \left(\frac{v_{s1} \times (P_{s2} - P_{s1}) \times 10^5}{(1000 \times \eta_{WP})}\right) \quad \ldots (6.69)$$

6.3.2.5 Fuel lean combustor

In this model, the increase of the ϕ_R and decrease of the ϕ_L increases the efficiency. It controls the air fraction directed to the rich combustor after compression (Y). Kobayashi et al., [63]showed that increasing the pressure of lean combustion kept the flammability limit constant. They also reported for a stable lean combustion for pressure between 11 bar and 41 bar for a lean combustion to a low value of ϕ_L= 0.7. For the lean combustion Kobayashi et al., [63] examined that the effect of the pressure of combustion is almost constant for flammability limit range, by increasing the pressure of the combustion. Fuel lean combustion is well known of its low NO_X emissions Kobayashi et al., [63]. For a certain ϕ_R the difference between the LHV of the Methane and that for syngas generated from the fuel rich combustion can get great as 37%. The low calforic value of the second combustion chamber is estimated using the function (LCVLFTER), which related as $LCV_{CC2} = f(T_{g6}, T_{g7}, T_{g8}, \phi_{CC2}, \phi_{CC1})$.

While the fuel to air ratio for such combustor is estimated using the function (fLFTEREFFLCV) in which $f_{CC2}=f(T_{g6}, T_{g7}, T_{g8}, \phi_{CC1}, \phi_{CC2}, LCV_{CC2})$.The pressure and the temperature of the mixture before combustion occurs is estimated using the function (PmixbyCp) for the pressure and (TmixbyCp) for the temperature. Where, (P_{gmix}) and (T_{gmix}) are functioned to (ϕ_{CC1}, ϕ_{CC2}, P_{g6}, P_{g7}, T_{g6}, T_{g7} and m_a).

$$P_{g8} = P_{gmix} \times (1 - \lambda_{CC2}) \quad \ldots (6.70)$$

This is for the second designs' lean combustion chamber, the first design combustion chamber model is dealt with hereafter.

$$h_{g8} = f\left(T_{g8},\ \phi_{CC2}\right) \times 1000 \quad \ldots (6.71)$$

$$e^{NOx2} = 62 \times \sqrt{\frac{P_{g8}}{P_{g1}}} \times \left(f_{CC2}{}^{4}\right) \times Exp\left(-635 \times \frac{T_{g1}(°C)}{T_{g8}(°C)}\right) \quad \ldots (6.72)$$

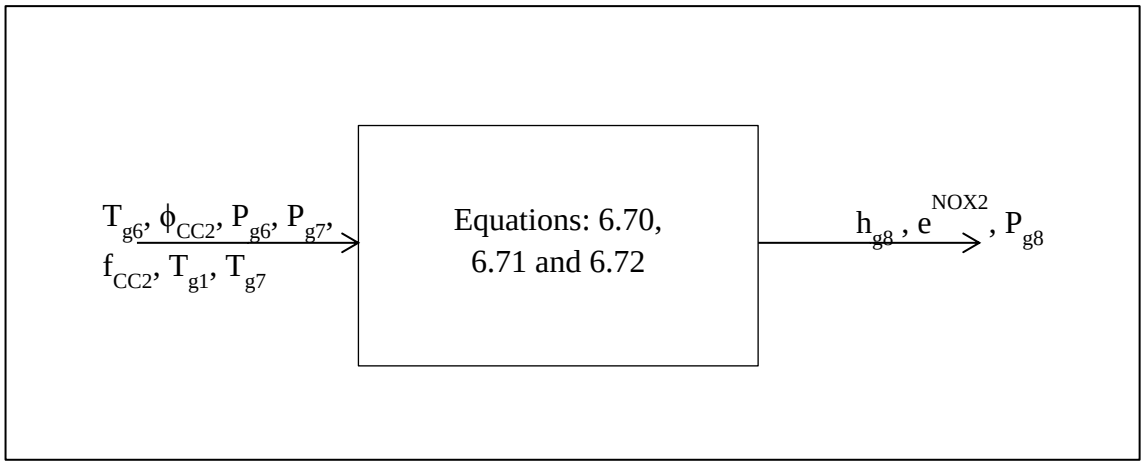

Figure 6.6 Fuel lean combustion chamber model (design 2)

Now for the first design, the inputs are similarly used to compute and predict outputs. Therefore, the following equations and functions represent the same procedure of the pervious configuration. Where, the outputs from the CC_2 model are illustrated in Fig 6.7.

$$h_{g8} = f\left(T_{g8},\ \phi_{CC1}\right) \times 1000 \quad \ldots (6.73)$$

$$P_{gmix} = f\left(\phi_{CC1},\ \phi_{CC2},\ P_{g8},\ P_{g9},\ T_{g8},\ T_{g9},\ \dot{m}_a\right) \quad \ldots (6.74)$$

$$T_{gmix} = f\left(\phi_{CC1},\ \phi_{CC2},\ P_{g8},\ P_{g9},\ T_{g8},\ T_{g9},\ \dot{m}_a\right) \quad \ldots (6.75)$$

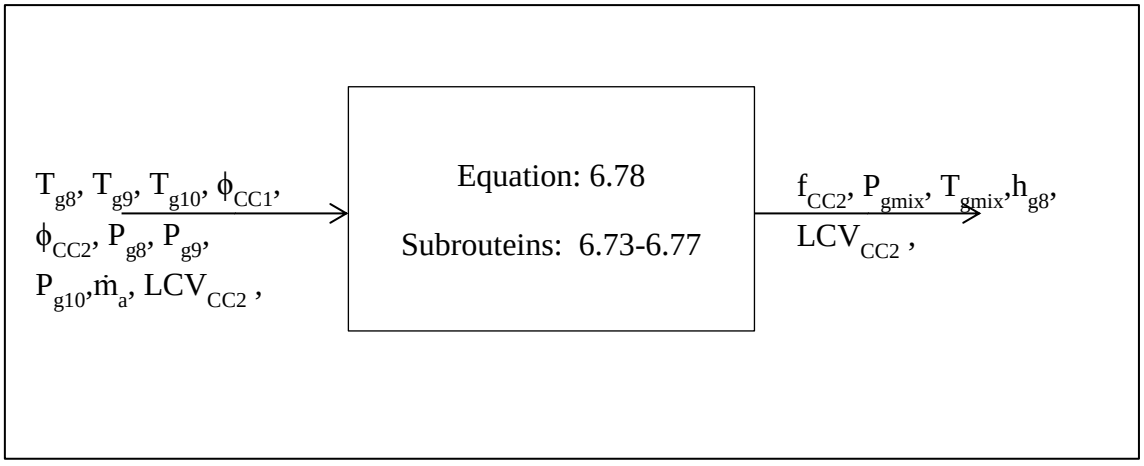

Figure 6.7 Fuel lean combustor model

$$LCV_{CC2} = f\left(T_{g8},\ T_{g9},\ T_{g10},\ \phi_{CC2},\ \phi_{CC1}\right) \quad \ldots (6.76)$$

$$f_{CC2} = f\left(T_{g8},\ T_{g9},\ T_{g10},\ \phi_{CC1},\ \phi_{CC2},\ \eta_{CC2},\ LCV_{CC2}\right) \quad \ldots (6.77)$$

$$P_{g10} = P_{gmix} \times \left(1 - \lambda_{CC2}\right) \quad \ldots (6.78)$$

6.3.2.6 Lean combustor compressor (in design 1)

Reducing the temperature of the gases at this compressor inlet can control any possible corrosive activity. Due to the thermodynamic properties of methane, its' flow through the compressor requires less power input than what air does. Furthermore, the flow is not within flammability limits citing to the study of Kobayashi et al. [63] on the steady flammability limit for pressure ranges between 11 and 41 bar Lior and Arai [91]. Keeping the pressure range within such limits made its operation on the safe side. The equations used to determine air compressors' model outputs used the following equations and function.

$$P_{g8} = P_{g5} \times r_{AC2} \quad \ldots (6.79)$$

$$T_{g8} = T_{g7} \times \left(1 + \left(\frac{(r_{AC2}{}^{K_g}) - 1)}{\eta_{AC2}}\right)\right) \quad \ldots (6.80)$$

$$w_{AC2} = Y \times \left(1 + f\right) \times \frac{\left(h_{g8} - h_{g7}\right)}{\eta_{AC2}} \quad \ldots (6.81)$$

$$h_{g8} = f\left(T_{g7}, \phi_{CC1}\right) \times 1000 \quad \ldots (6.82)$$

6.3.2.7 Lean combustor compressor (design 2)

For the second design, the following equations are applied in this model. This compressor modelled similarly to the low pressure compressor as compress only air.

$$P_{g4} = P_{g3} \times r_{AC2} \quad \ldots (6.83)$$

$$T_{g4} = T_{g3} \times \left(1 + \frac{\left(r_{AC2}{}^{K_a} - 1\right)}{\eta_{AC2}}\right) \quad \ldots (6.84)$$

$$w_{AC2} = \frac{Y \times (h_{g4} - h_{g3})}{\eta_{AC2}} \quad \ldots (6.85)$$

$$h_{g4} = f\left(T_{g4}\right) \times 1000 \quad \ldots (6.86)$$

6.3.2.8 Fuel lean turbine

As indicated by many authors, including Lior and Arai [91], the temperature of the stack gases should not drop below 150 °C to avoid condensation and acids formation. The pressure ratio for the expansion through both turbines for the 2nd design is calculated using equation (6.87) and the fuel lean turbine model is shown in Fig. 6.8.

$$r_{GT2} = \frac{P_{g1} \times r_{AC1} \times r_{AC2} \times (1 - \lambda_{HRSG1}) \times (1 - \lambda_{HRSG2}) \times (1 - \lambda_{CC1})}{P_{gE}} \quad \ldots (6.87)$$

$$r_{GT2} = \frac{P_{g10}}{P_{g011}} \quad \ldots (6.88)$$

$$r_{GT2} = \frac{P_{g8}}{P_{g9}} \quad \ldots (6.89)$$

$$T_{g011} = (T_{g10}) \times (1 - \eta_{GT2} \times (1 - (r_{GT2}{}^{-Kg}))) \quad \ldots (6.90)$$

$$T_{g9} = T_{g8} \times \left(1 - \eta_{GT2} \times \left(1 - r_{GT2}{}^{-K_g}\right)\right) \quad \ldots (6.91)$$

$$w_{GT2} = (1 + f) \times (h_{g10} - h_{g011}) \times \eta_{GT2} \quad \ldots (6.92)$$

$$w_{GT2} = (1 + f_{CC2}) \times (h_{g8} - h_{g9}) \times \eta_{GT2} \quad \ldots (6.93)$$

$$h_{g011} = f\left(T_{g011}, \phi_{CC2}\right) \times 1000 \quad \ldots (6.94)$$

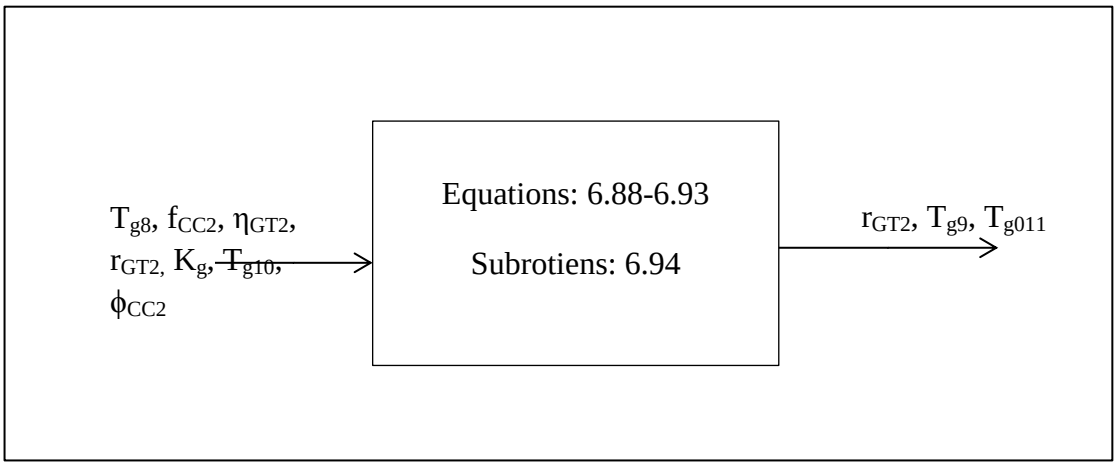

Figure 6.8 Fuel lean turbine model

The pressure ratio of gases expansion in second gas turbine of designs1 and 2 are defined by equations 6.88 and 6.89 respectively. While the temperatures of the gases at turbine discharges are an estimated using equations 6.90 and 6. 91respectively. Whereas the specific work outputs from these turbines are calculated by equations 6.92 and 93 respectively.

6.3.2.9 Fuel lean gases HRSG model

The energy content of the gases leaving the gas turbine is recovered by the water, which turn into steam prior to its entry to the turbine. The previous seven cases are considered for this model with respect to the designs suggested for the current work. To simplify solution, the 1st and the 2nd HRSGs are assumed of the same configuration in the first design. The model and the equations of simple HRSG are hereafter. The developed HRSG models are similar to those discussed in rich fuel HRSG. It also assumed a constant pressure through both HRSGs. The change of other HRSG parameters with respect to assumptions, generate the following:

$$T_{gStack} = (T_{gEO2} - \varepsilon_{EC2} \times (T_{gEO2} - T_{s2})) - 273 \quad \ldots (6.95)$$

$$h_{gstack} = f\left(T_{gstack}, \phi_{CC2}\right) \times 1000 \quad \ldots (6.96)$$

$$P_{g011} = \frac{P_{g012}}{\left(1 - \lambda_{HRSG}\right)} \quad \ldots (6.97)$$

$$h_{Sg011} = f\left(T_{g011c}, P_{s3}\right) \quad \ldots (6.98)$$

$$h_{s5} = h_{gs2} + \varepsilon_{SH1} \times \left(h_{Sg011} - h_{gs2}\right) \quad \ldots (6.99)$$

$$T_{sEI2} = T_{sEI1} \quad \ldots (6.100)$$

$$T_{gEO2} = T_{sEI2} + \Delta T_{ppm2} \quad \ldots (6.101)$$

$$T_{g012} = T_{gEO2} - \varepsilon_{EC2} \times \left(T_{gEO2} - T_{s2}\right) \quad \ldots (6.102)$$

$$m_{sa2} = \frac{\eta_{HRSG2} \times \left(1 + f\right)\left(h_{g011} - h_{g012}\right)}{\left(h_{s5} - h_{s2}\right) \times 1000} \quad \ldots (6.103)$$

$$h_{Sg011} = f\left(T_{g011c}, P_{s3}\right) \quad \ldots (6.104)$$

$$h_{s5} = h_{gs2} + \varepsilon_{SH1} \times \left(h_{Sg011} - h_{gs2}\right) \quad \ldots (6.105)$$

$$T_{sEI2}^{LP} = T_{sEI1}^{LP} \quad \ldots (6.106)$$

$$T_{gEO2} = T_{sEI2} + \Delta T_{ppm2} \quad \ldots (6.107)$$

$$T_{g012} = T_{gEO2} - \varepsilon_{EC2} \times \left(T_{gEO2} - T_{s2}\right) \quad \ldots (6.108)$$

$$h_{g012} = f\left(T_{g012}, \phi_{CC2}\right) \times 1000 \quad \ldots (6.109)$$

$$\eta_{HRSG2} = \eta_{SH2} \times \eta_{EC2} \times \eta_{E2} \quad \ldots (6.110)$$

$$T_{gStack} = T_{gEO2} - \varepsilon_{EC2} \times \left(T_{gEO2} - T_{s2}\right) \quad \ldots (6.111)$$

While for the second design, the following equations are utilized to determine the required outputs,

$$m_{sa2} = \frac{\eta_{HRSG2} \times (1 + F) \times \left(\frac{h_{g9} - h_{g10}}{1000}\right) - m_{sa1} \times (h_{s3} - h_{s5})}{h_{s3} - h_{s2}} \quad \ldots (6.112)$$

$$f = f_{CC1} + f_{CC2} \quad \ldots (6.113)$$

$$h_{s3} = h_{gs2} + \varepsilon_{SH} \times \left(h_{sg9} - h_{gs2}\right) \quad \ldots (6.114)$$

$$\eta_{HRSG2} = \eta_{SH} \times \eta_{E} \times \eta_{EC} \quad \ldots (6.115)$$

$$T_{gEO} = T_{sE} + \Delta T_{ppm} \quad \ldots (6.116)$$

$$T_{g10} = T_{gEO} - \varepsilon_{EC} \times (T_{gEO} - T_{s2}) \quad \ldots (6.117)$$

$$P_{g9} = \frac{P_{gE}}{(1 - \lambda_{HRSG})} \quad \ldots (6.118)$$

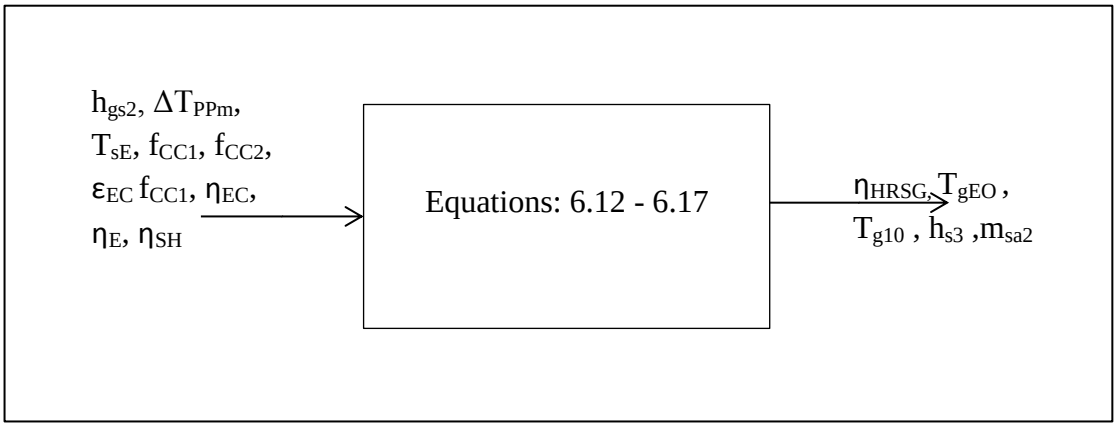

Figure 6.9 Fuel lean HRSG model

6.3.2.10 Steam turbine

The steam turbine was modelled in a similar manner to that described in the chapter 5. The function (hFsP) is used to estimate the enthalpy (h_{s4s}) in terms of (S_{s3}) and (P_{s4}). Furthermore, the entropy (S_{s3}) is estimated using the function (SFhP) in terms of (h_{s3}) and (P_{s3}). The isentropic efficiency is assumed in order to calculate the generated specific work by the turbine as in equation (5. 36) for non-reheated and equation (5.37) for reheated steam turbine. The quality of the steam (dryness fraction) at the turbine outlet is limited in this model as in chapter 5 to X_{s4} = 90%. Applying energy balance on the mixer between the two HRSGs outputs generates equation (6.119).

$$h_{s3} = Ys \times h_{s6} + (1 - Ys) \times h_{s5} \quad \ldots (6.119)$$

$$w_{ST} = \left(\eta_{ST} \times \left(h_{gs2} + \varepsilon_{SH1} \times \left(h_{Sg4} - h_{gs2}\right)\right) - h_{s4s}\right) \times 1000 \quad \ldots (6.120)$$

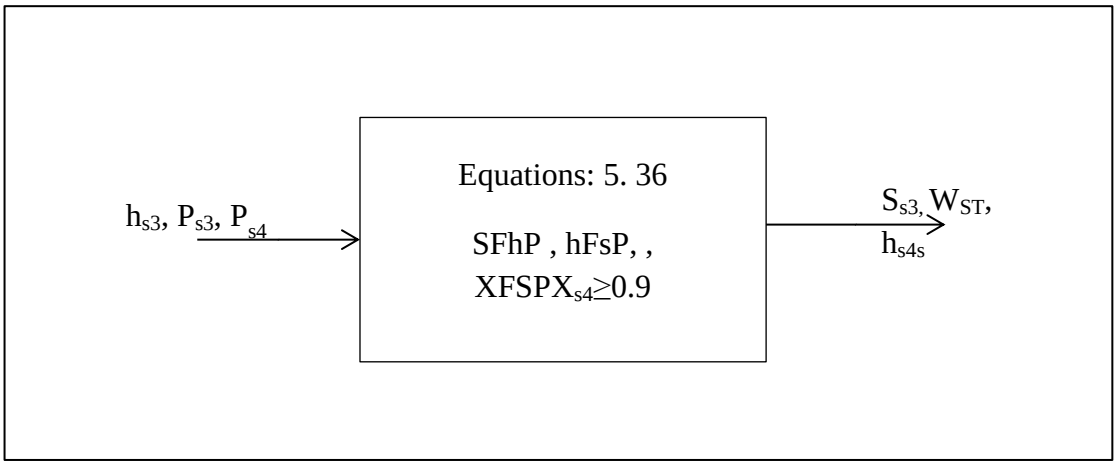

Figure 6.10 Steam turbine model

6.3.2.11 Steam condenser

As for the previous condenser model, the condenser is considered as heat exchanger in which a hot fluid is cooled at constant pressure and temperature (steam is converted to saturated water). Accordingly, the status of the water at condenses' outlet is saturated water at the condenser pressure (steam generator outlet pressure). The function (hfFP) is used to estimate the enthalpy at this point which is related to the pressure of the water at the lower pressure (P_{s1}). In this model, it is assumed that there are no pressure losses through the condenser.

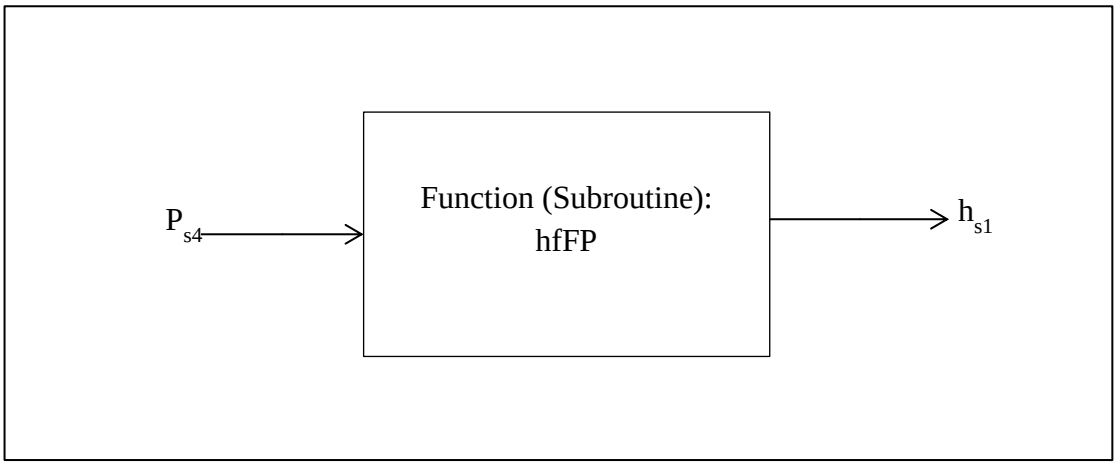

Figure 6.11 Steam condenser model

6.3.2.12 Water pumps model

The water pump is assumed to operate according to the assumptions stated when the conventional combined cycle configurations were considered in the previous chapter. The same equation (5. 44) is used here to determine the specific work consumed by the water pump, whether for single or multi pressure configurations. The enthalpy of the water at the water pump outlet is determined using the equation (5. 45) as in the previous chapter. The temperature of the water at the pump outlet is estimated also using the same function (TFPP) as the $T_{s2} = f(P_{s2}, P_{s1})$ which considers an isentropic compression process in the pump.

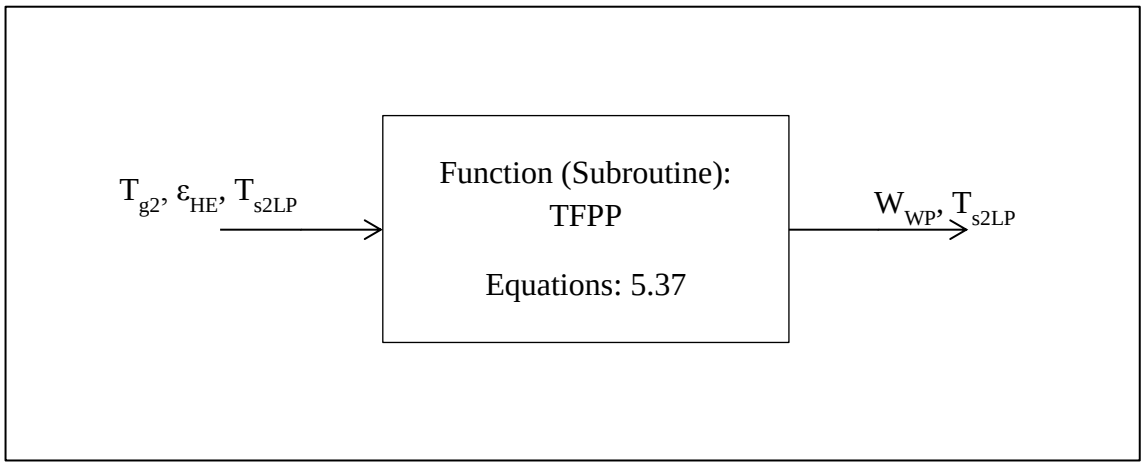

Figure 6.12 Water pump model

6.3.2.13 Compressed air heat exchanger model

This model is developed for the second design in which only part of the water comes from the pump outlet (m_{s1}) to recover the heat of part of the compressed air (m_{g2}). This represented by the ratio (Y) from the air at the compressor s' inlet, which is going to burn in fuel rich atmosphere. It is assumed that this Heat exchanger to work as an economiser, accordingly the status of the water at its outlet is assumed to be saturated water. On the other side of heat exchanger, the temperature of the air at the outlet is calculated using the effectiveness' equation (6.121).

$$T_{g3} = T_{g2} - \varepsilon_{HE} \times (T_{g2} - T_{s2LP}) \quad \ldots (6.121)$$

Where (T_{S2LP}) is the temperature of the liquid water coming from the water pump.

Pressure loss through this heat exchanger is calculated according to the previous assumptions detailed in the previous chapter.

$$P_{g3} = P_{g2} \times (1 - \lambda_{HE}) \quad \ldots (6.122)$$

$$m_{sa1} = \frac{\eta_{HE} \times \left(\frac{h_{g2} - h_{g3}}{1000} \right)}{\left(h_{s5} - h_{s6} \right)} \quad \ldots (6.123)$$

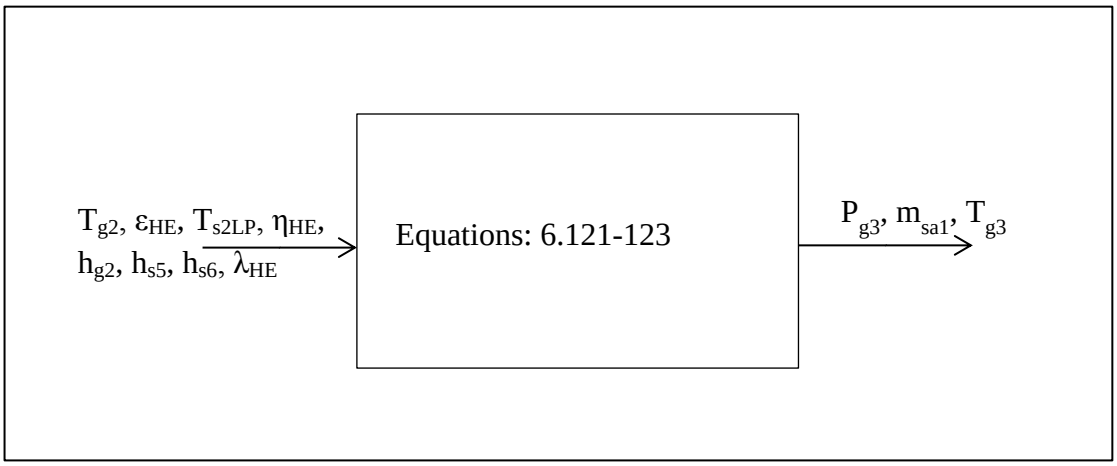

Figure 6.13 Compressed air heat exchanger model

6.3.2.14 Fuel compressor model

In this model, natural gas is considered as the fuel for the plant and the compressor is needed to increase the fuel pressure. This model assumes that the natural gas is mixed with air in the rich fuel mixture combustor (combustor 1) at an identical pressure to that of the compressed air. Initially, the pressure of the fuel (Methane) is assumed to be at the same temperature and pressure of the atmosphere. Hence, the pressure ratio for the fuel compressor is assumed to equate the air compressor ratio. Accordingly, the relations regarded for the air compressor are used here in a similar way to estimate the temperature. Equation (6.124) is generated, where ($T_{f1} = T_{g1}$) and K_M is calculated by equation (6.125), where the specific heat ratio is assumed to be constant (γ_M =1.307).

$$T_{f2} = T_{f1}\left(1 + \frac{r_{AC1}^{K_M} - 1}{\eta_{AC1}}\right) \quad \ldots (6.124)$$

$$K_M = \frac{\gamma_M - 1}{\gamma_M} \quad \ldots (6.125)$$

6.3.2.15 Heat recuperator (design 1)

For the recuperator (design 1), the temperatures of the fluids at the exit from each stream are calculated using the effectiveness equations (6.126) and (6.127) as follows:

$$T_{f3} = T_{f2} + \varepsilon_{Rec}\left(T_{g5} - T_{f2}\right) \quad \ldots (6.126)$$

$$T_{g6} = T_{g5} - \varepsilon_{Rec}\left(T_{g5} - T_{g2}\right) \quad \ldots (6.127)$$

The pressure losses in the gases stream of the recuperator is assumed to be very small and can be neglected, accordingly, ($P_{g5} = P_{g6}$). Here, the function (GCF3) is used to estimate h_{g6} as a function to (T_{g6}, ϕ_{CC1}).

6.3.3 ChGT model specifications

This model was developed for 14 different ChGT gas/steam cycles. This was due to the use of various steam turbine configurations and the connection between the calculations of the gas and the steam turbine/plants.

6.3.3.1 Restrictions to the model

i. The thermodynamic properties of the air are taken from tables given by Moran and Shapiro [5], which were based on tables presented by Keenan and Kaye in [92]. These tables were used to establish the function (GCF2). These tables considered the air as an ideal gas dry air.

ii. In order to narrow the search area a minimum thermal efficiency of 40% is considered to restrict results.

iii. Constant air intake volume or the compressor is operating for a certain volume flow rate which is assumed to be constant for a specific running speed of the compressor.

iv. The ratio between the mass flows of the air that goes to the rich fuel to that left for lean fuel combustor is determined by the equivalence ratios for both combustors (ϕ_{CC1} and ϕ_{CC2} and these values are input parameters).

6.3.3.2 Model limitations

i. As in the previous model, the steam turbine steam outlet must satisfy a minimum steam dryness fraction of 90%.

ii. As it has been preferred by G.E. STAG in the previous model for the combined cycle power and power plants, for non-reheated single and multi-pressure steam bottoming cycles, a temperature of 538 °C or less should be enough. While for reheated configurations this temperature will be limited by 593 °C or greater.

iii. The temperature of the steam at the turbine inlet is restricted by the degree required to satisfy steam utilization to power AWAC system. This will be under further investigation later in chapter 8.

iv. The maximum air flow rate that corresponds to flame blowout are considered as a limit as in chapter 5 but for both fuel rich and lean combustors.

6.3.3.3 Model parameters ranges

Ranges for the operating parameters those undertaken in this study are tabulated in table 6.1.

Parameter	Range
ϕ_{CC2}	0.4 – 1
ϕ_{CC1}	1.05 – 3.3
η_{GT1}, η_{GT2}	0.6 – 0.92
η_{AC1}, η_{AC2}	0.6 – 0.91
η_{ST}	0.7– 0.9
η_{WP}	0.7– 0.92
η_{HRSG}	0.5 – 0.8
η_{EC1}, η_{SH1}, η_{E1}, η_{EC2}, η_{SH2}, η_{E2}	0.5 – 0.8
r_{AC1}, r_{AC2}	4 – 36
T_{g4}	1100 – 1900 °C
T_{g10}	800 – 1800 °C
P_{g4}	20 – 40 bar
P_{g10}	1.1 – 14.2 bar
λ_{CC1},λ_{CC2},λ_{HRSG},λ_{Eco}	0.03 – 0.6
ε_{Rec}, ε_{SH}, ε_{Rec}, ε_{Rec}	0.6 – 0.9
T_{g1}	-10 – 40 °C
P_{g1}	1.013 bar
P_{g5}, P_{g12}	1.1 – 2.1 bar
ΔT_{Pmm1}, ΔT_{Pmm2}	10 – 25 °C
P_{s2},P_{s3}	15 – 350 bar
P_{s1}, P_{s4}	0.05 – 0.55 bar

Table 6.1 Parameters ranges for both configurations models

6.3.3.4 Model performance criteria:

The model must be capable of meeting the following performance criteria:

i. Satisfy the condition of the steam from turbine exhaust is of a temperature not less than 200 °C.

ii. Satisfy that the HRSG heat exchanger is integrated with HRVG.

iii. The mass conservation of exhaust gases through the HRSG.

iv. The mass conservation of steam through the HRSG components

v. Matching gas turbine and steam turbines' components to meet the maximum efficiency greater than 40% with the maximum w_{CC} with the minimum SFC, T_{gstack} and CO_2 and NO_X emissions.

The final model flow diagram for the first design is shown in (Fig.6.14) which indicates the above conducted criteria.

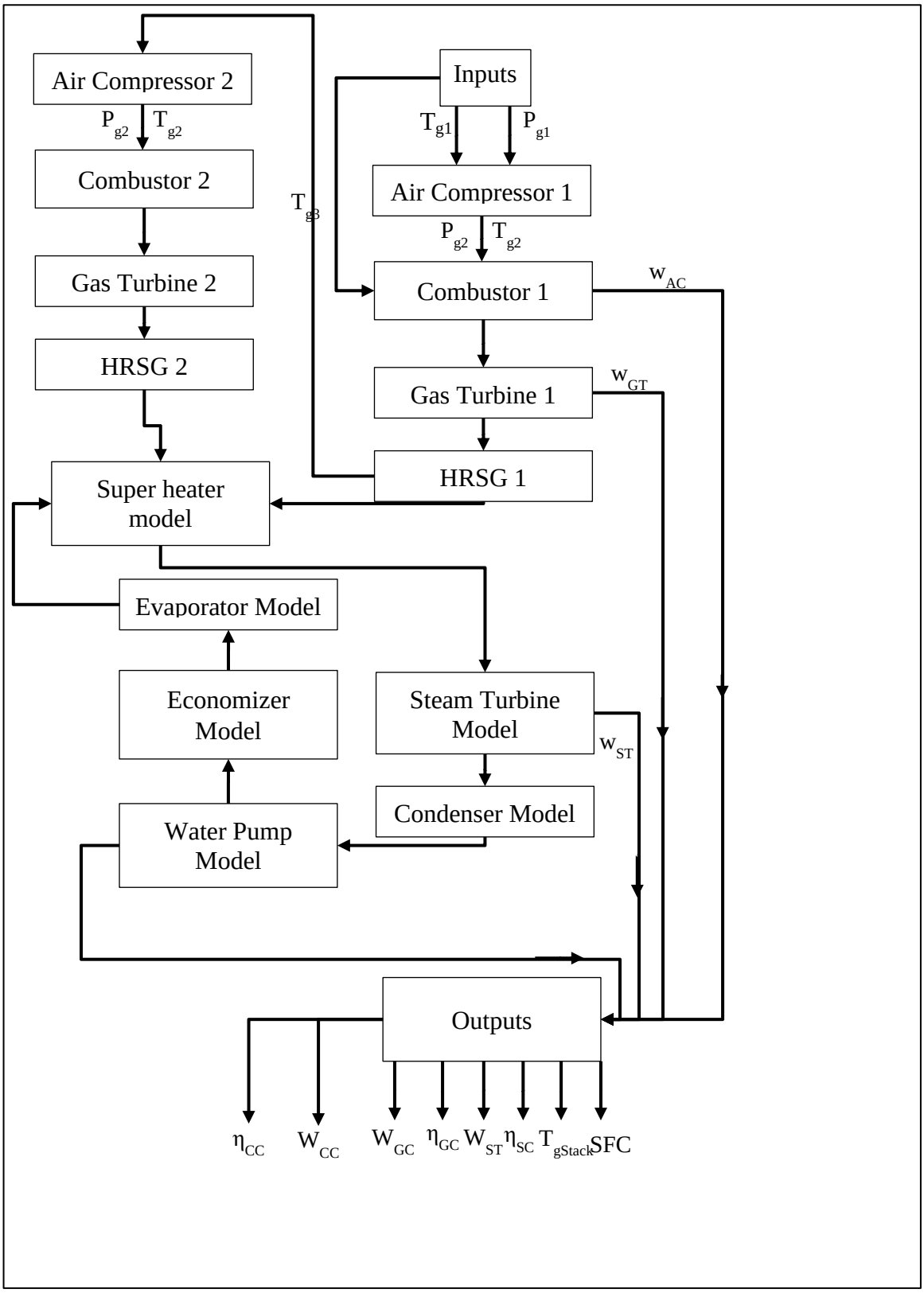

Figure 6.14 Flow chart for the 1st design ChGT solution model

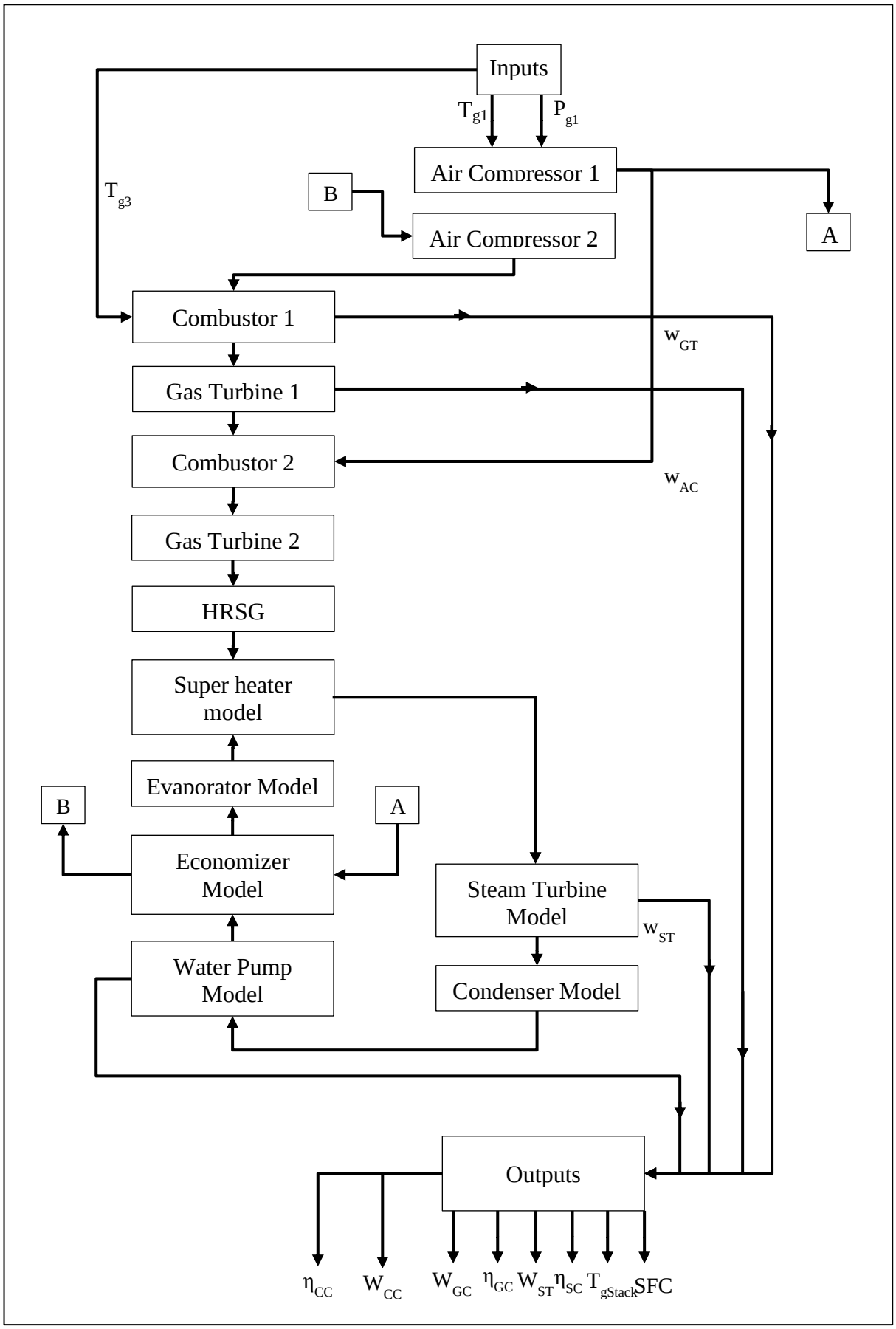

Figure 6.15 Flow chart representing 2nd design ChGT solution model

6.4 Emissions from fuel rich fuel lean combustors in ChGT

As it has been considered and detailed in previous chapter (Section 5.4), CO_2 emission is calculated using the equations of chemical reactions. In this section, there is no need to discuss the details of how to calculate fuel lean combustion process. Therefore, rich fuel combustion is only considered in here.

For the NO_X emissions, the correlations given by Bakken and Skogly [90] those used for the lean combustion NO_X emission predictions are employed here. Although, there is a healthy concern, whether the predicted level of the NO_x is accurate when using these correlations for rich fuel combustion process. This correlation resulted in a very puzzling output when it was applied to the rich combustor when applying P_{ref} and T_{ref} of such equation equal P_{g10} and T_{g10} rather than the ambient conditions at the compressor inlet. Whilst when applying the ambient conditions, P_{ref} and T_{ref}, the output eNO_X gets less than those given by the rich fuel combustor.

6.5 Optimization of the ChGT cycle

The parameters those required to be investigated on the performance of the ChGT are φ_{CC1}, φ_{CC2}, T_{g4}, T_{g10}, r_{AC1}, r_{AC2}, X_{s4}. Other parameters are expected to have a miner effect appears on the efficiency of the CCPP, like the P_{s4}, which its effect is on steam cycles' power generation only and is similar to that for conventional configuration combined cycles. The optimum set of these parameters for maximum efficiency and specific work output and the minimum stack gases temperature and SFC are related to many other design parameters. Further than that, these parameters affects are related to each other.

6.5.1 Fuel rich combustor parameters effect

The effect of the equivalence ratio of the rich fuel combustor is depicted for different compression ratio on the performance characteristics η_{CC}, w_{CC}, and SFC_{CC}. It was discussed regarding the environmental characteristics also, including T_{g12}, eNO_X and eCO_2.

From these figures, it was found that, the fuel rich combustor parameters are: the pressure of the combustion represented by the compression ratio, the equivalence ratio of combustion, and the temperature of the gases at the turbine inlet which assumed to be the same at the combustor outlet. These parameters affect the performance characteristics and the environmental parameters as shown by Fig.6.16 - 6.25.

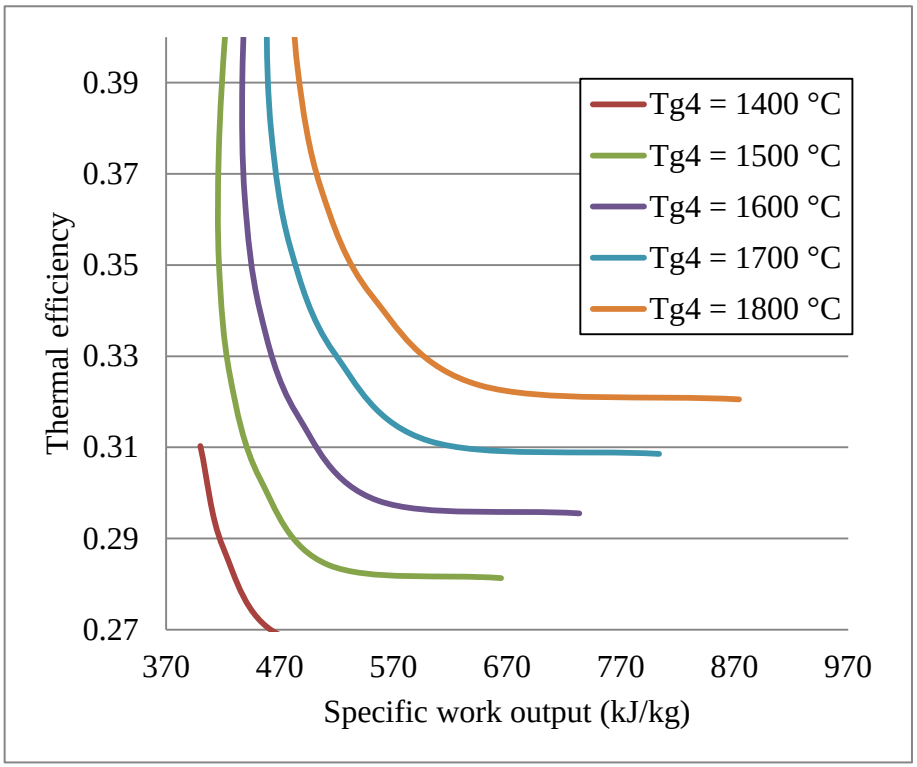

Figure 6.16 GC thermal efficiency versus specific work output affected by T_{g4}

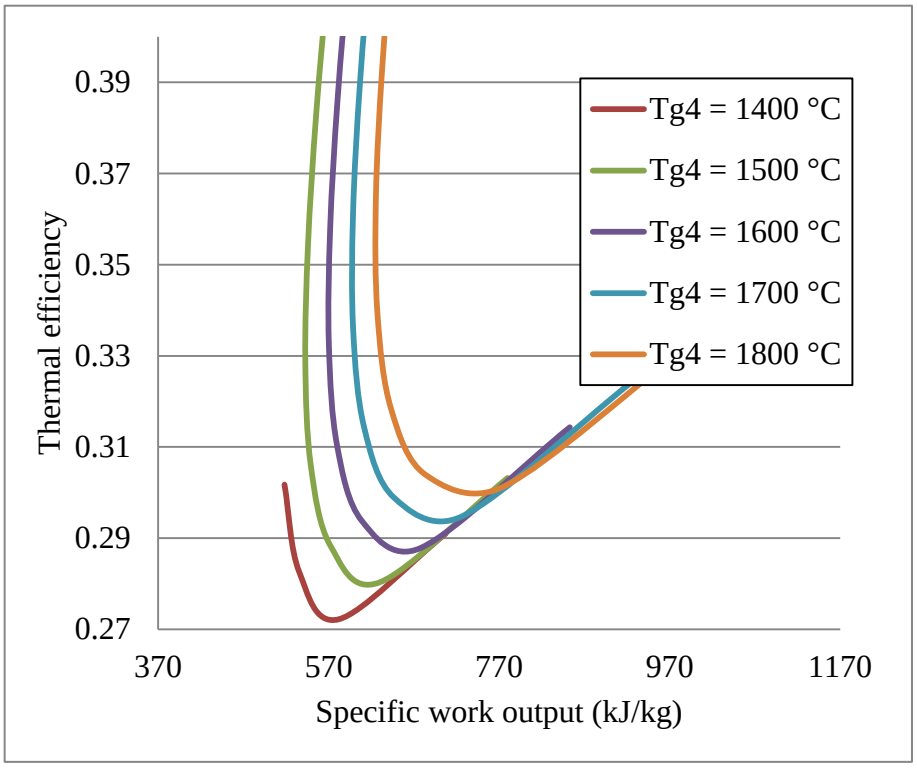

Figure 6.17 ChGT design1 thermal efficiency versus specific work output affected by T_{g4}

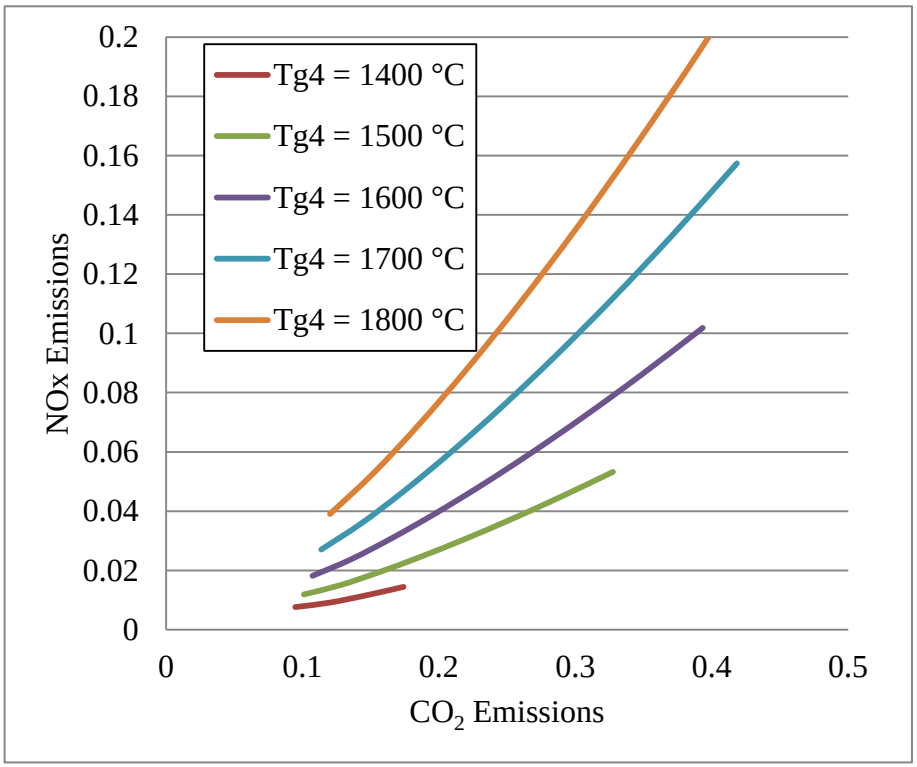

Figure 6.18 Emissions of NO_X versus emissions of CO_2 affected by T_{g4}

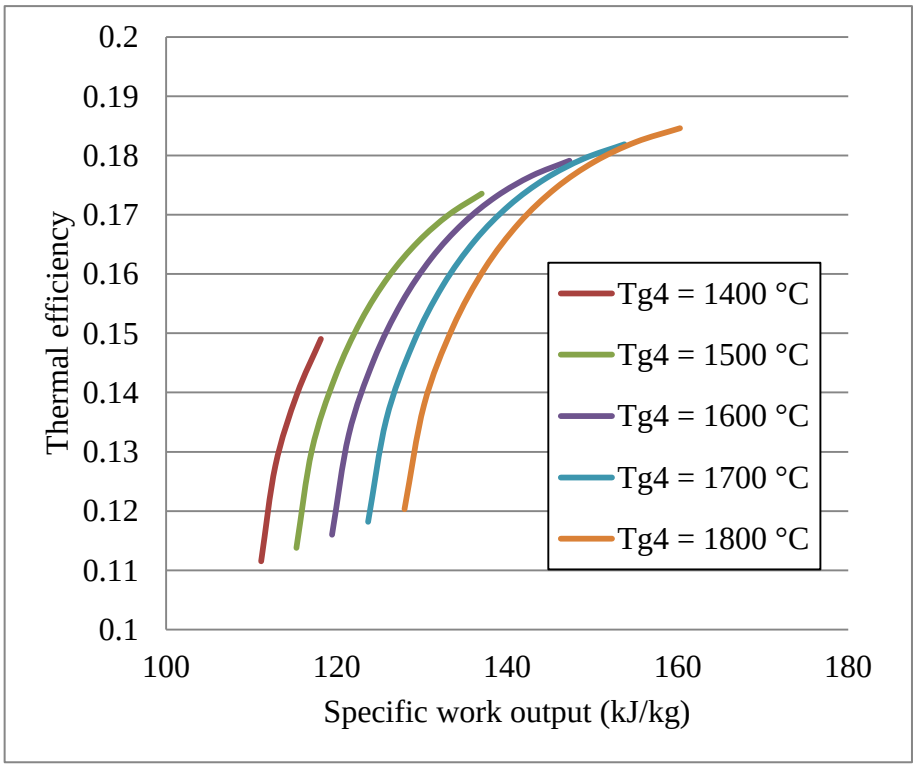

Figure 6.19 SC thermal efficiency versus specific work output affected by T_{g4}

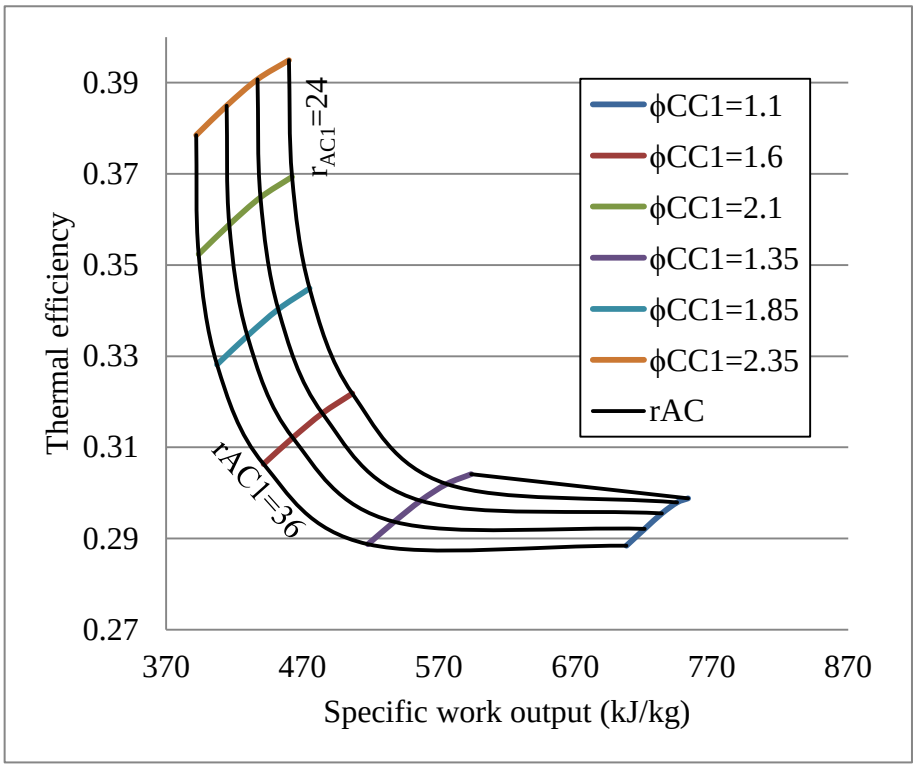

Figure 6.20 Fuel rich combustor equivalence ratio effect on specific work output and the thermal efficiency of ChGT design 1

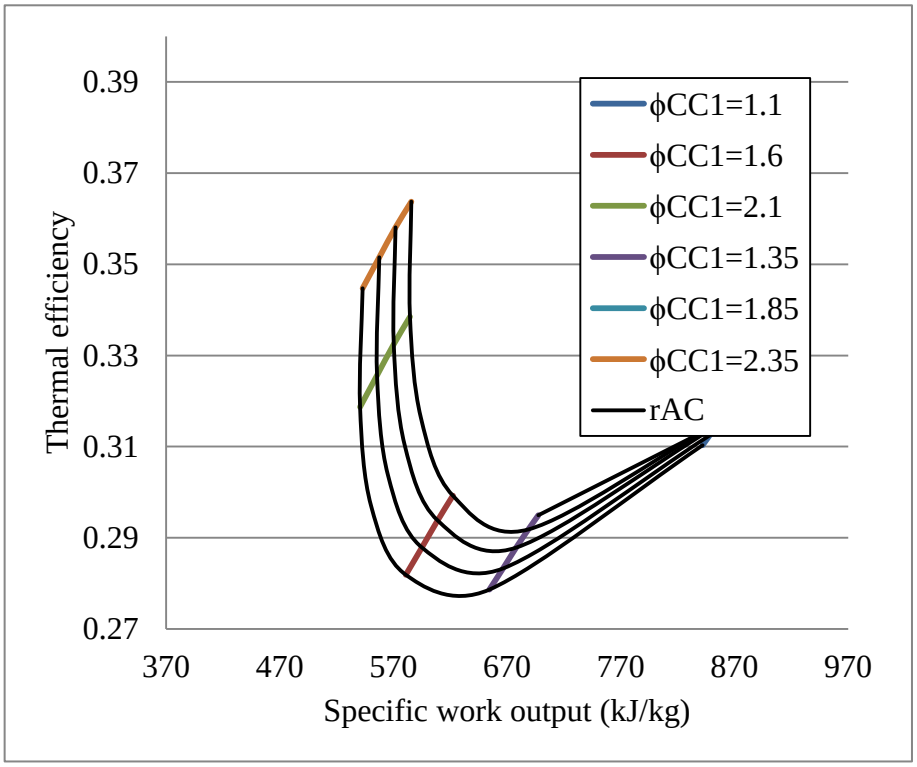

Figure 6.21 Fuel rich combustor equivalence ratio effect on specific work output and the thermal efficiency of GC design 1

The increase in the temperature of the gases at fuel rich turbine inlet does not probably increase the thermal efficiency, although the increase in the specific work output. Similarly, to the conventional CCPP, the effects of the temperature of gases at turbine inlet and the compression ratio at which the gas turbine operates. These parameters are illustrated in Fig.6.22 in which each is functioned to the performance characteristics. For the second design, the increase in T_{g4} increases w_{cc} for the certain r_{AC} on which the gas turbine is designed to operate.

The thermal efficiency of the ChGT increases by such increase, likewise, if GT is designed to operate on high r_{AC}, but if the GT is to operate on low r_{AC} this effect decreases the efficiency, although the increase in the specific work output. Also by increasing T_{g4} the optimum r_{AC} for maximum η_{CC} risen. For the optimum r_{AC}, such increase in T_{g4} can lead to a drop in the thermal efficiency of about 2 percentage points, which is combined by an increase in the w_{CC} by the double.

Accordingly, the CCPP performance characteristics are seriously affected by the change in the temperature of the gases from the fuel rich combustion chamber. However, the most determined parameter here is the r_{AC} in which, for (ChGT of 2nd design), the compressors must be designed to operate on r_{AC} greater than those for Conventional CCPP. Further than in such design, r_{AC} for the low pressure compressor governs the high pressure compressor r_{AC}; such parameter is important to such design.

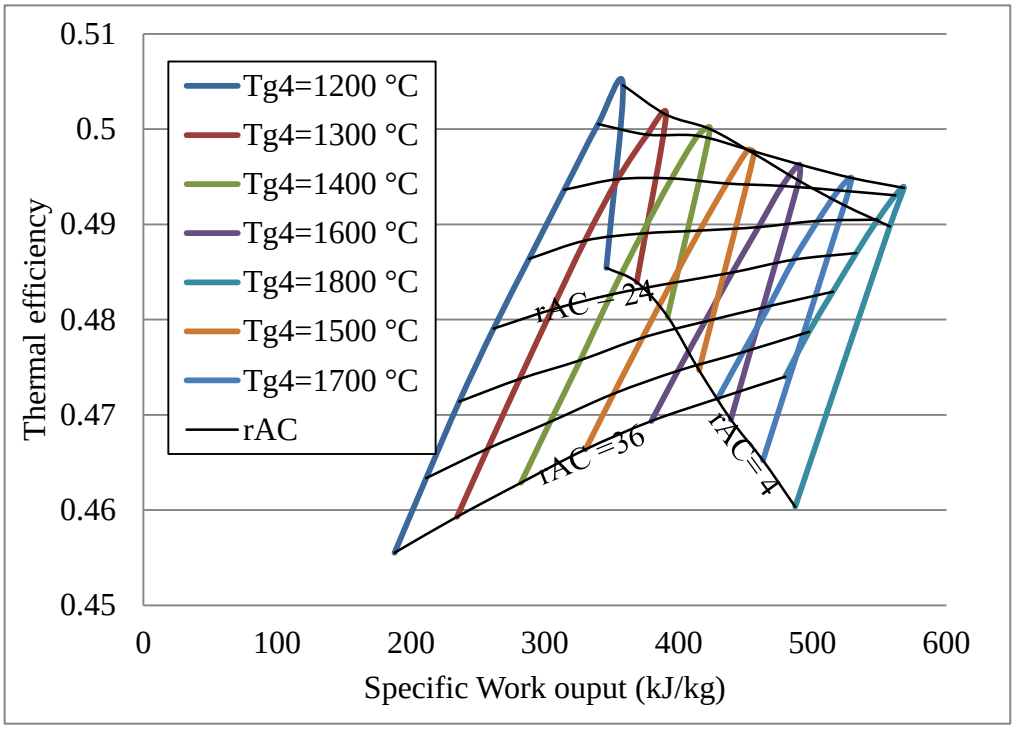

Figure 6.22 The thermal efficiency versus the specific work output of the second design

To complete fuel rich combustor effect on the performance characteristics of a CCPP, its equivalence ratio (ϕ_{CC1}) is depicted in Fig. 6.23. The CCPP performance characteristics compressions ratio profile effect was changed dramatically by such parameter. The increase in ϕ_{CC1} limits the range of the power output from ChGT. This due to its effect on the heat content at turbine inlet, but it is more directed by air mass flow ratio between the combustors. However, the increase in the ϕ_{CC1} increases the efficiency it mostly halves the w_{CC}. The efficiency can be as great as 43% for (ϕ_{CC1}= 3.3). The optimum r_{AC} for maximum w_{CC} is of a low asset value, while the one for the maximum efficiency is of slightly greater value.

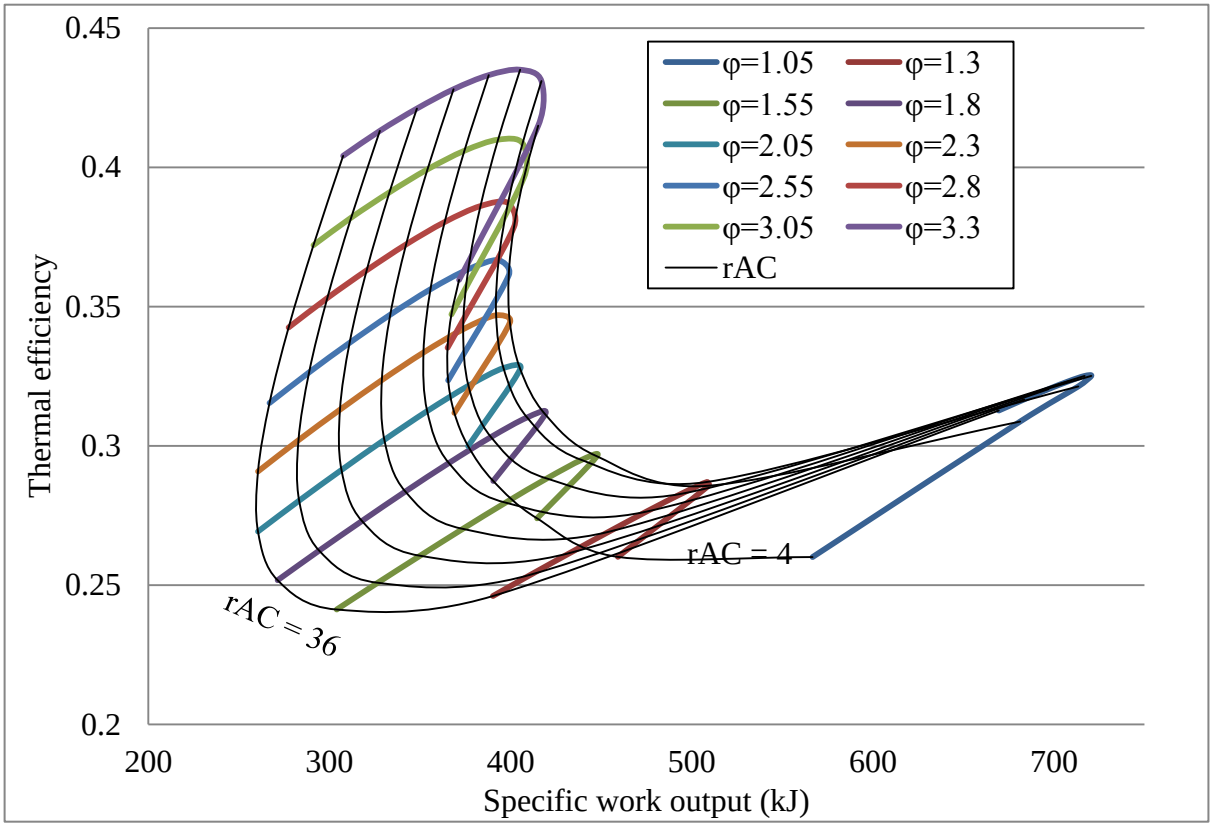

Figure 6.23 The thermal efficiency versus specific work output affected by rich fuel combustion equivalence ratio

The effect of the ϕ_{CC1} on SFC and T_{gStack} is illustrated in Fig.6.24. In such figure, it is clear that the increase in ϕ_{CC1} increases the SFC on the opposite relation to that for conventional CCPP. The temperature of stack gases (T_{gStack}) is greatly affected by the changing ϕ_{CC1}, which was governed by the magnitude of r_{AC} on which the ChGT is designed to operate. For high values of r_{AC} the increase in ϕ_{CC1} reduces T_{gStack}. For modest r_{AC} gas turbines, a similar increase in the ϕ_{CC1} , T_{gStack} is almost independent on such change. While for low r_{AC} gas

turbines, a similar increase in ϕ_{CC1} raises the T_{gStack}. This is due to the high heat content of the gases at combustor outlet corresponding to the low expansion ratio r_{GT}.

Accordingly, in order to satisfy reducing T_{gStack}, the SFC is the same, while η_{CC} is increased. Therefore, to meet such standard, the gas turbine must be designed to operate on high r_{AC}. While the power generated is almost the half. To apply an increase in the w_{CC}, the η_{CC} is assigned to ϕ_{CC1} of less than 2.3, as reducing ϕ_{CC1} from 3.3 to 2.3 is correspondent to deterioration in the efficiency but a limited increase in the w_{CC}.

However, to improve w_{CC} to a modest value this will require a reduction in η_{CC} by not less than 10 percentage points. While, in order to apply w_{CC} maximum such reduction is quite smaller. In general, NO_X emission is increased by the increase in ϕ_{CC1}, which gets minor if the gas turbine is designed to operate on greater r_{AC}. By the increase in ϕ_{CC1}, the emissions of CO_2 are decreased although the increase in NO_X, but for gas turbine of greater r_{AC}, such emissions are increased to regulate to the same amount as in before, as shown by Fig.6.25.

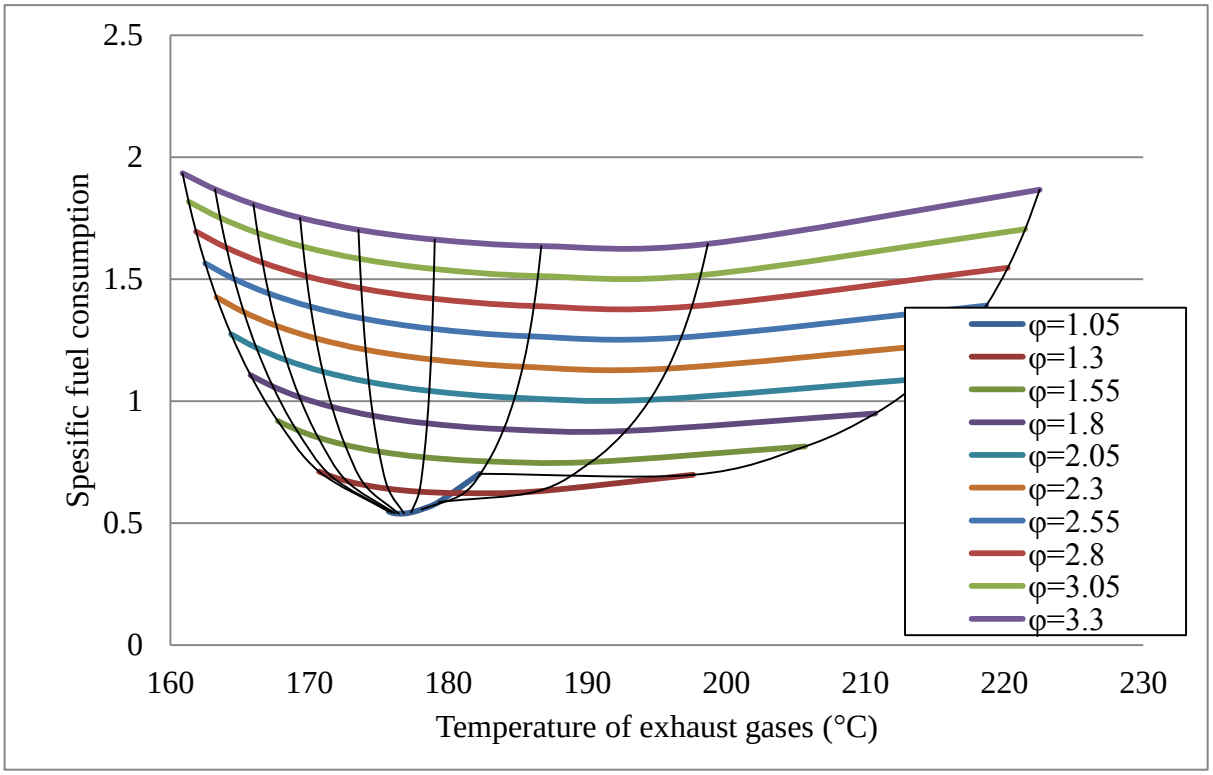

Figure 6.24 The SFC versus exhaust gases temperature affected by equivalence ration of the fuel rich combustor

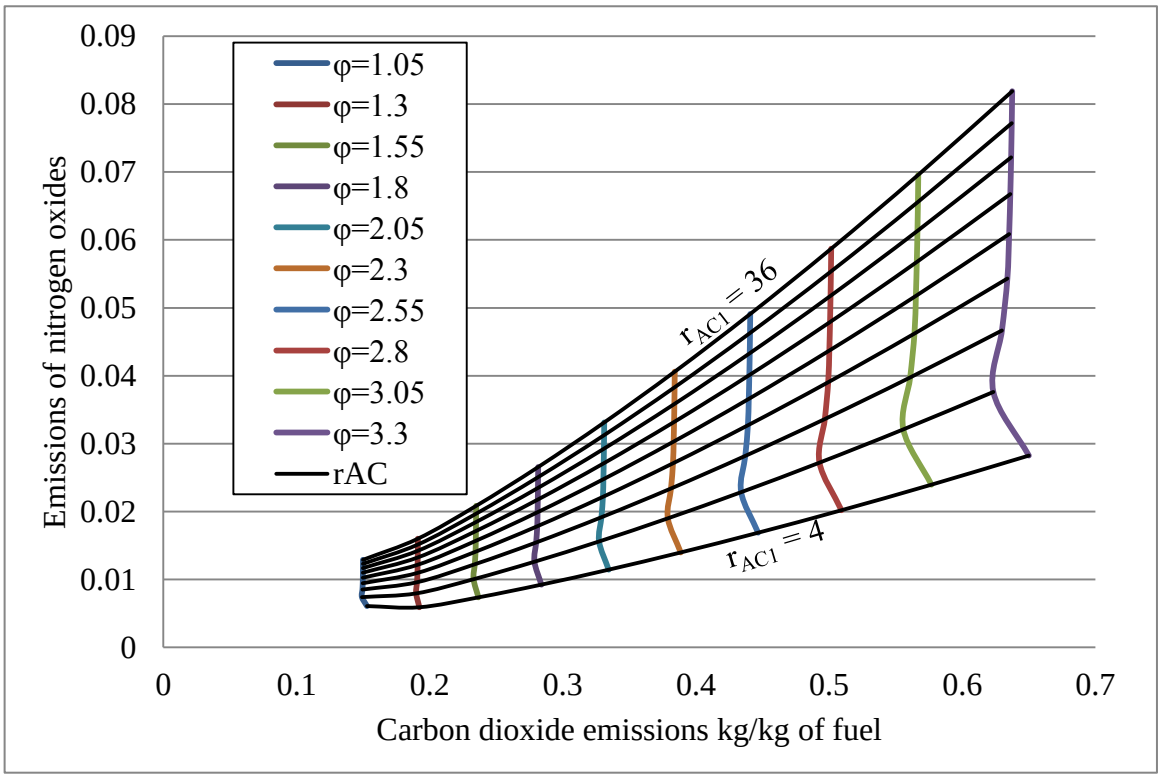

Figure 6.25 The NOx emissions versus CO_2 emissions affected by rich fuel combustion equivalence ratio

6.5.2 Fuel lean combustor parameters effects

For the first design, the ϕ_{CC2} always increases w_{CC} and decreases the η_{CC} if the gas turbine is to operate on modest and high r_{AC2}, while if it operates on low r_{AC2} there will be an increase in the η_{CC}, but such efficiency is already of a low value. The maximum efficiency reduces by 5 percentage points when the ϕ_{CC2} is increased from 0.4 to 0.9. This corresponds to an increase in the w_{CC} of more than 0.25% as shown in Fig. 6.26.

Figure 6.27 shows the effect ϕ_{CC2} on the SFC and the quality of the steam at the steam turbine outlet. It shows that, the SFC is always increased by the increase in ϕ_{CC2}. The effect of ϕ_{CC2} on the steam quality at turbine outlet is governed by r_{AC2}. In which for modest r_{AC2}, the increase in ϕ_{CC2} has no effect on the steam quality. For high r_{AC2}, the steam quality gets towards the vapour end on the saturation diagram. On contrast, the opposite happens when if the gas turbine is designed to operate on low r_{AC2}. However, ϕ_{CC2} has a very slight effect on steam quality at turbine outlet.

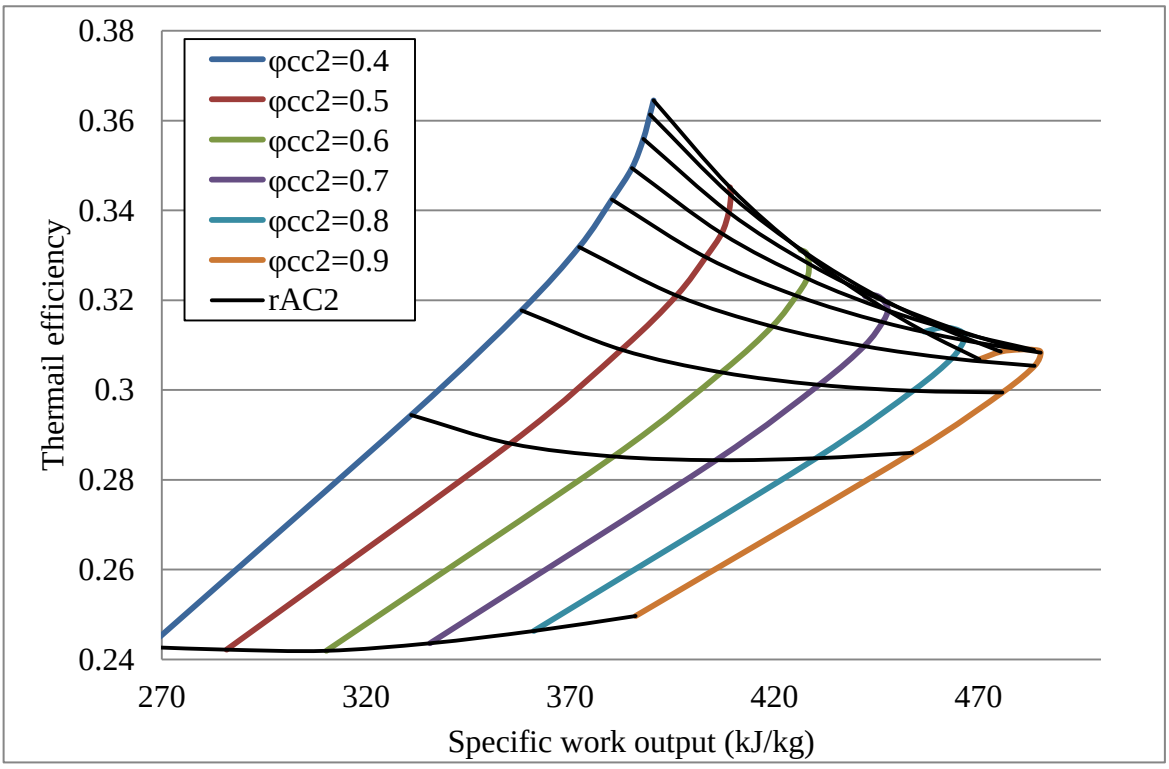

Figure 6.26 The thermal efficiency versus specific work output affected by the equivalence ration of lean fuel combustion in first design

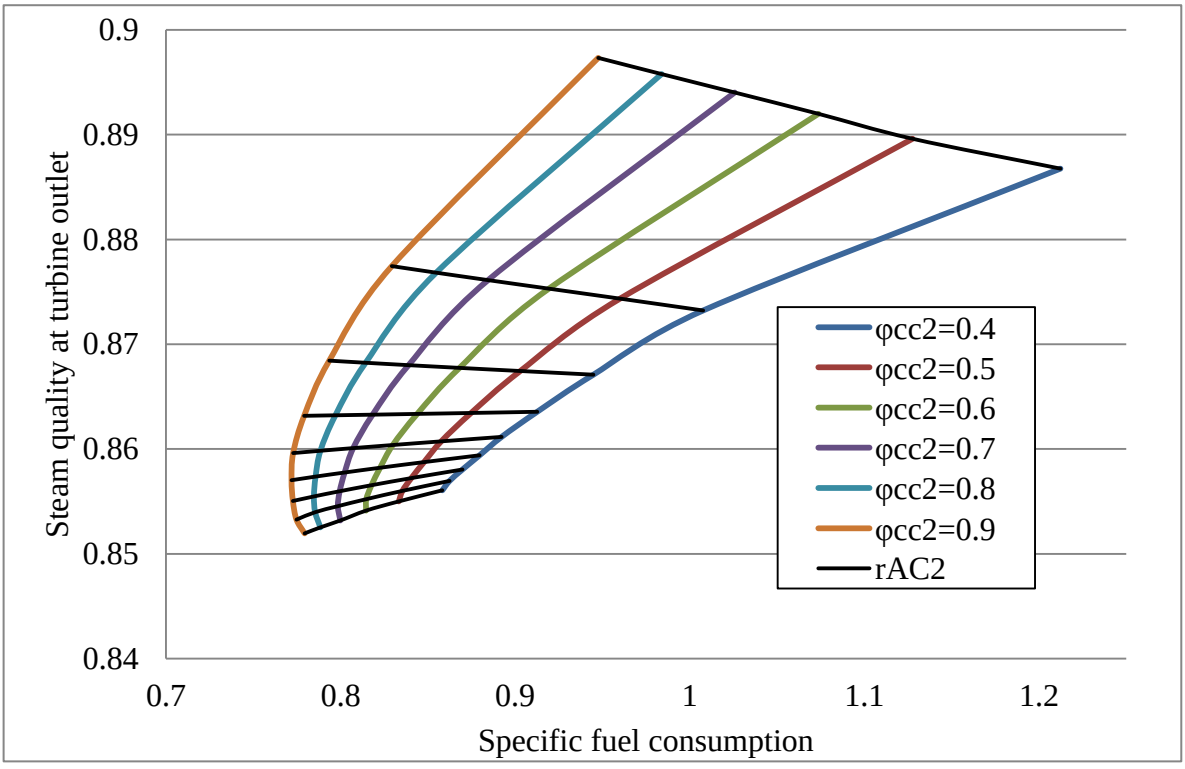

Figure 6.27 The steam quality at turbine outlet versus the specific fuel consumption affected by the lean combustion equivalence ration of the first design

The effects of the second compressor compression ratio (r_{AC}) and the temperature of the gases at the lean turbine outlet T_{g10} on the performance characteristics of the ChGT is depicted in Fig. 6.28. It shows a similar relation between w_{CC} and η_{CC} to that for conventional CCPP. In such figure, the increase in T_{g10} increases η_{CC} but not probably the w_{CC}. Also, the optimum r_{AC} for maximum w_{CC} and η_{CC} gets to greater values by increasing T_{g10}. Figure 6.29 shows r_{AC2} and T_{g10} effects on T_{gStack}, SFC for the ChGT. In such figure, T_{gStack} increases if the gas turbine is to operate on low r_{AC2}. The specific fuel consumption (SFC) increases by the increase of T_{g10}. However, there is a certain r_{AC2} value at which the SFC is the minimum on the r_{AC} profile curve for any T_{g10}.

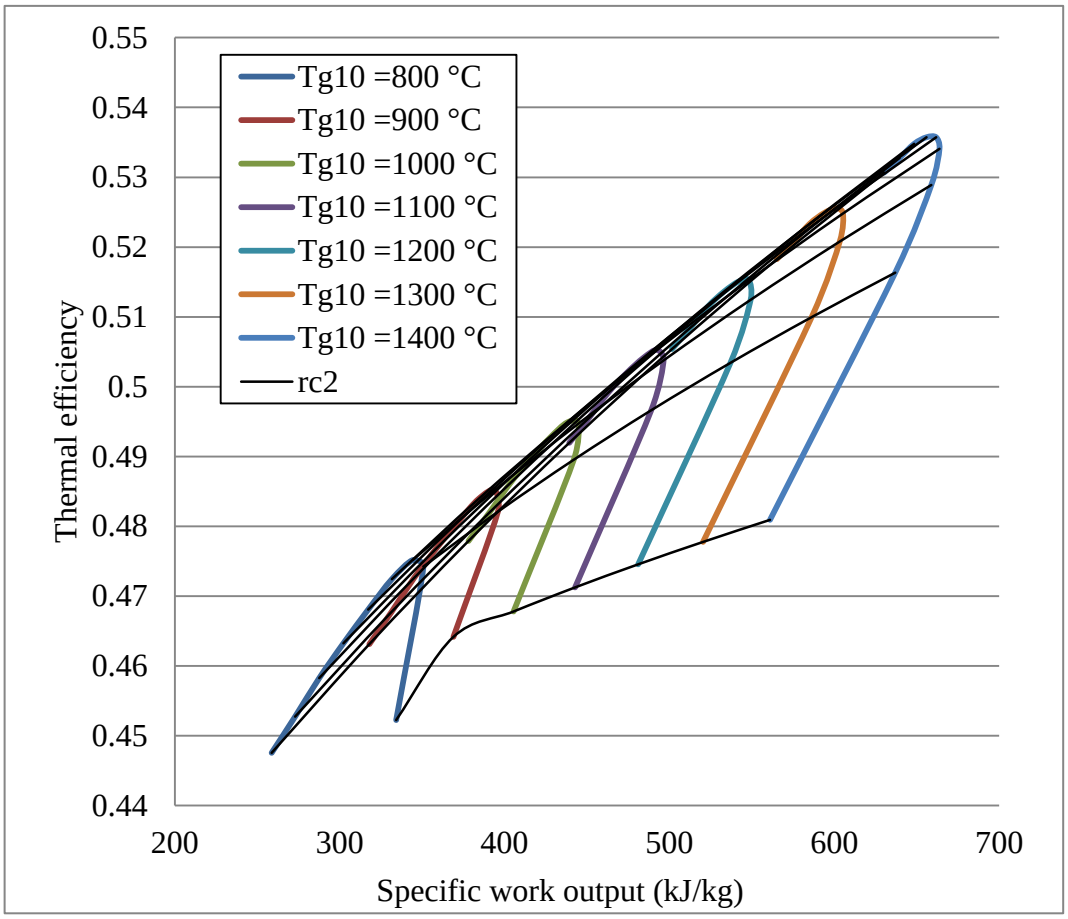

Figure 6.28 Fuel lean combustion temperature effect on thermal efficiency and specific work output for the 2nd design

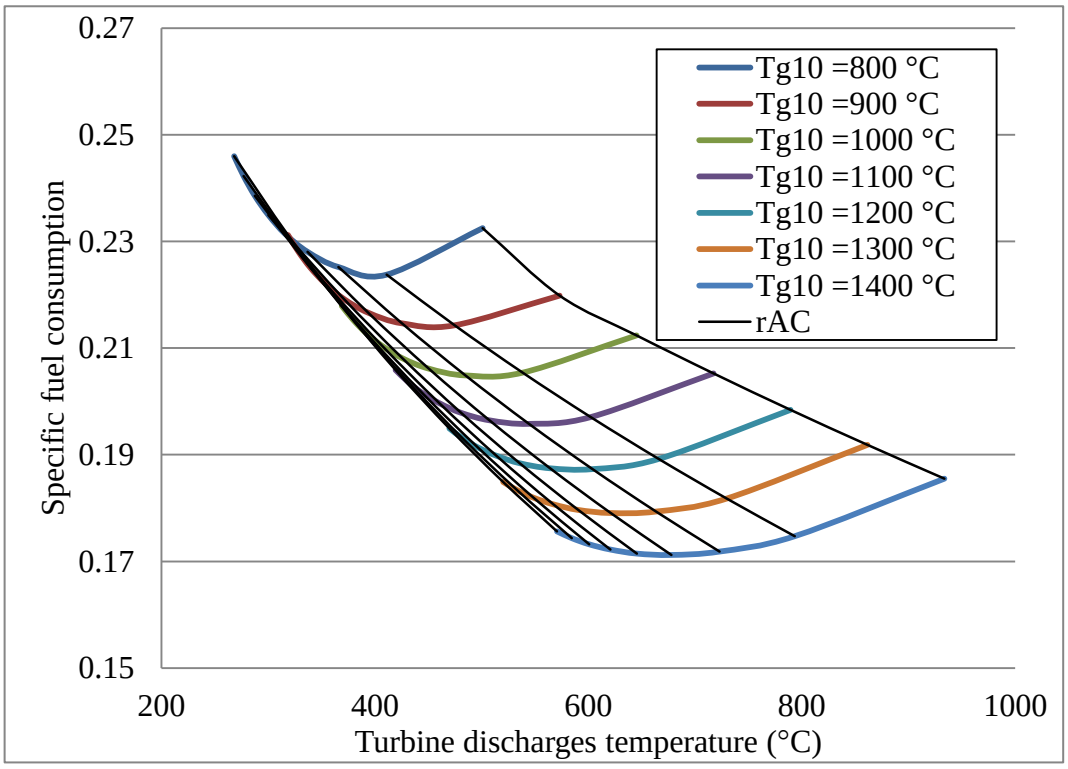

Figure 6.29 The specific fuel consumption versus turbine discharges temperature affected by lean fuel combustion temperature

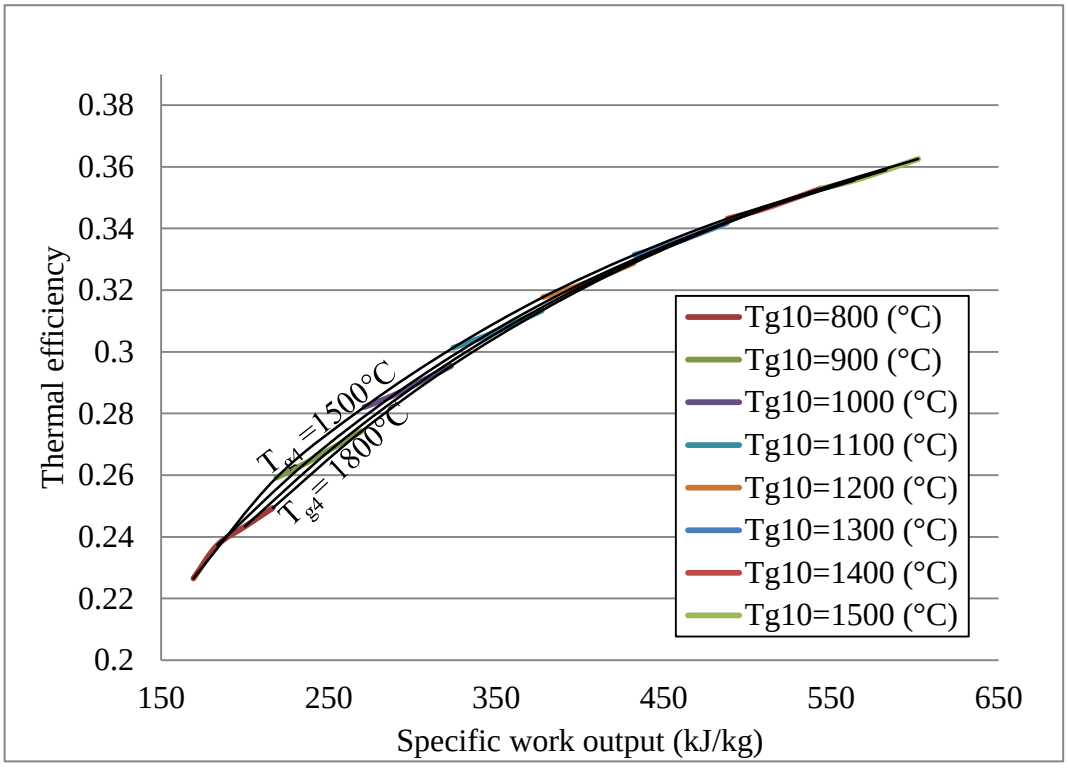

Figure 6.30 The thermal efficiency versus specific work output affected by temperature of lean fuel combustion of first design

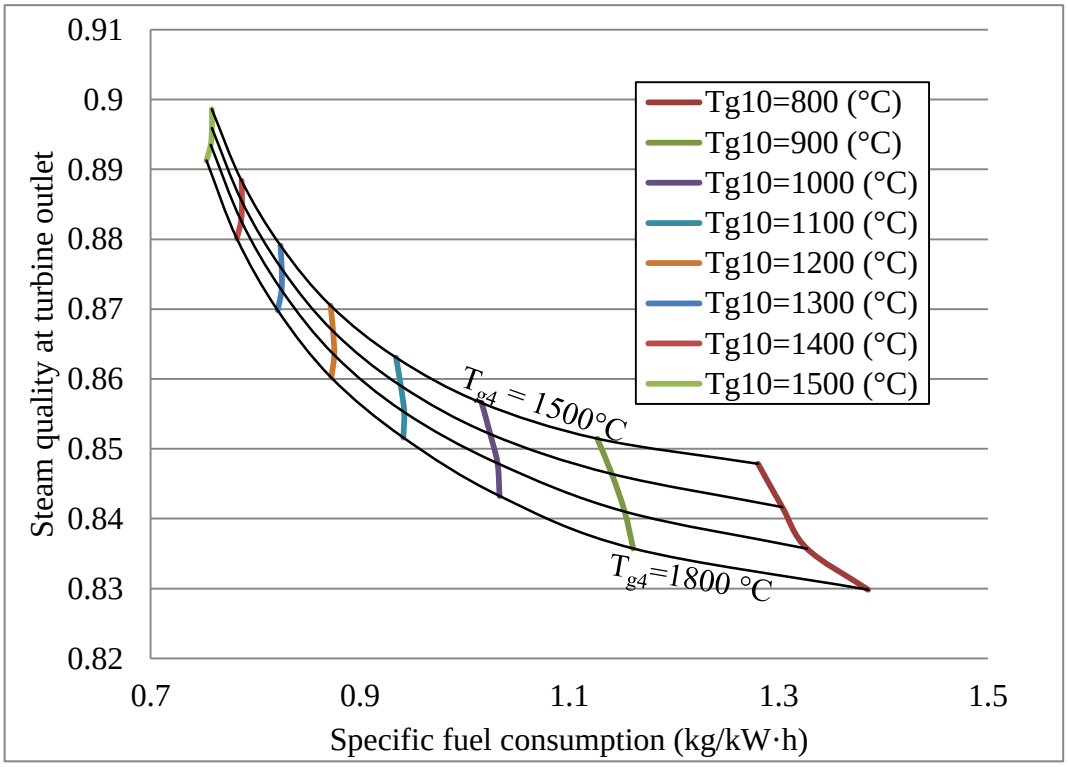

Figure 6.31 Steam quality at turbine outlet versus SFC affected by gases temperature at lean combustion turbine inlet

6.5.3 Combining the effect from both combustors

The sections above discusses the combustors individually, hereafter, their effects are combined in a set of results. These are shown by Figs. 6.32 – 6.36, to illustrate the effects of combining the parameters from the first and the second combustor of the first design.

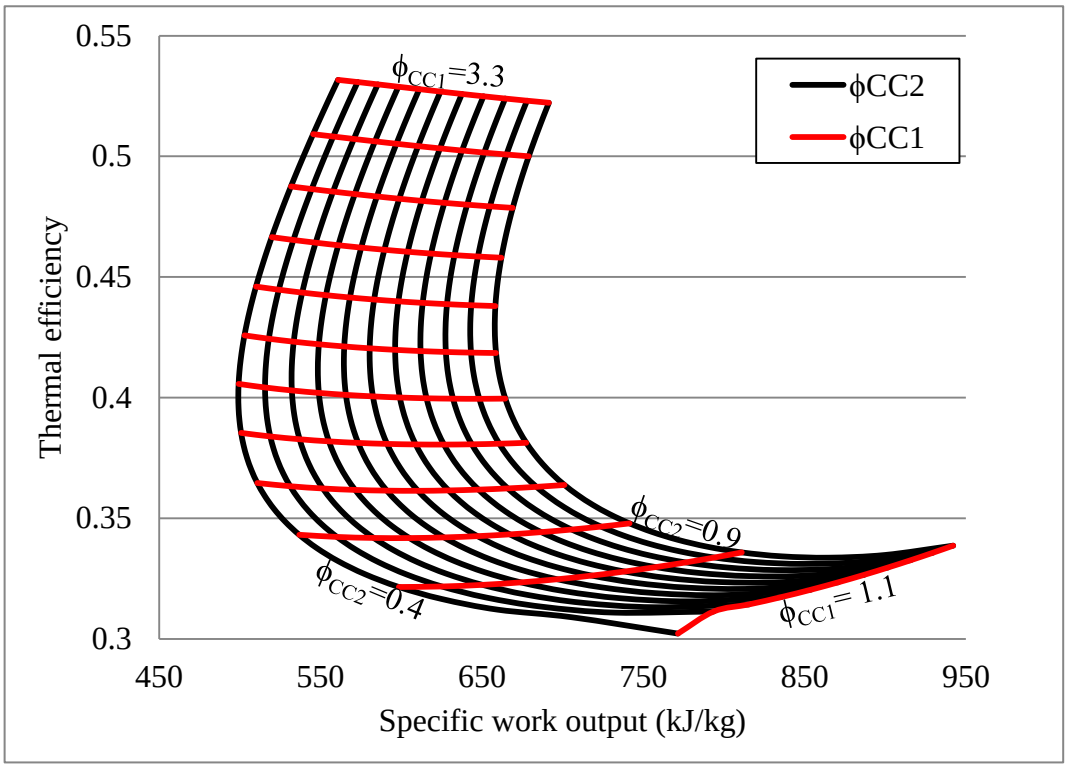

Figure 6.32 GC thermal efficiency versus specific work output affected by the equivalence ratios

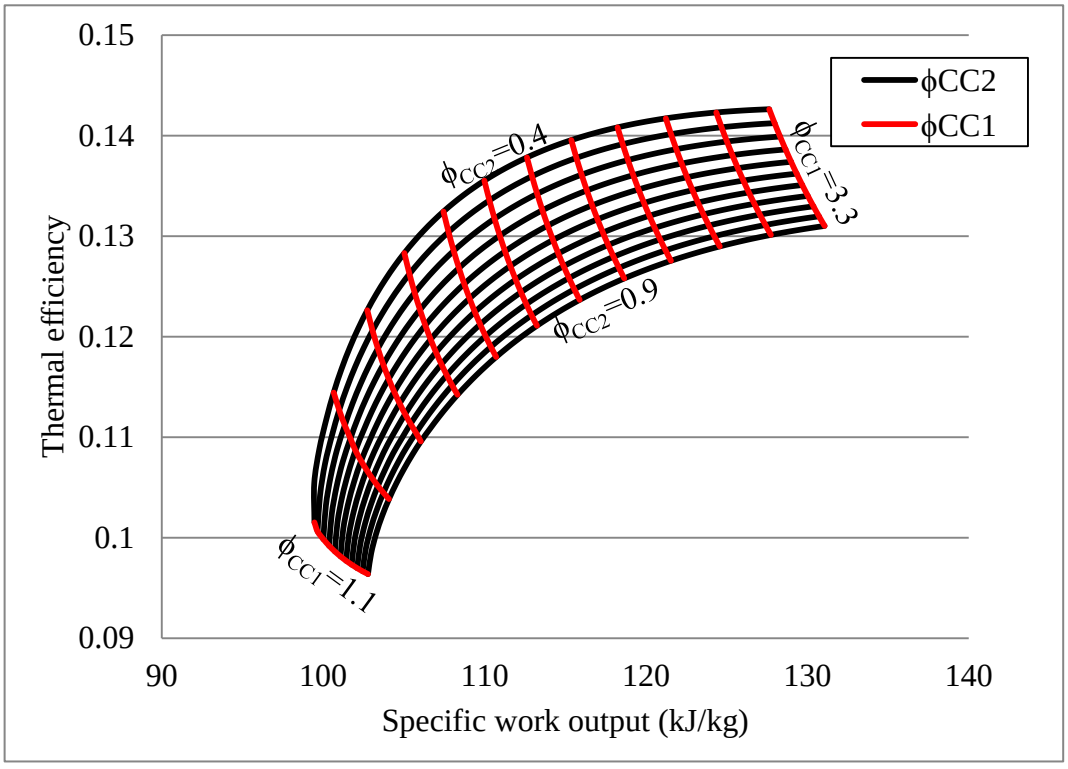

Figure 6.33 SC thermal efficiency versus specific work output affected by the equivalence ratios

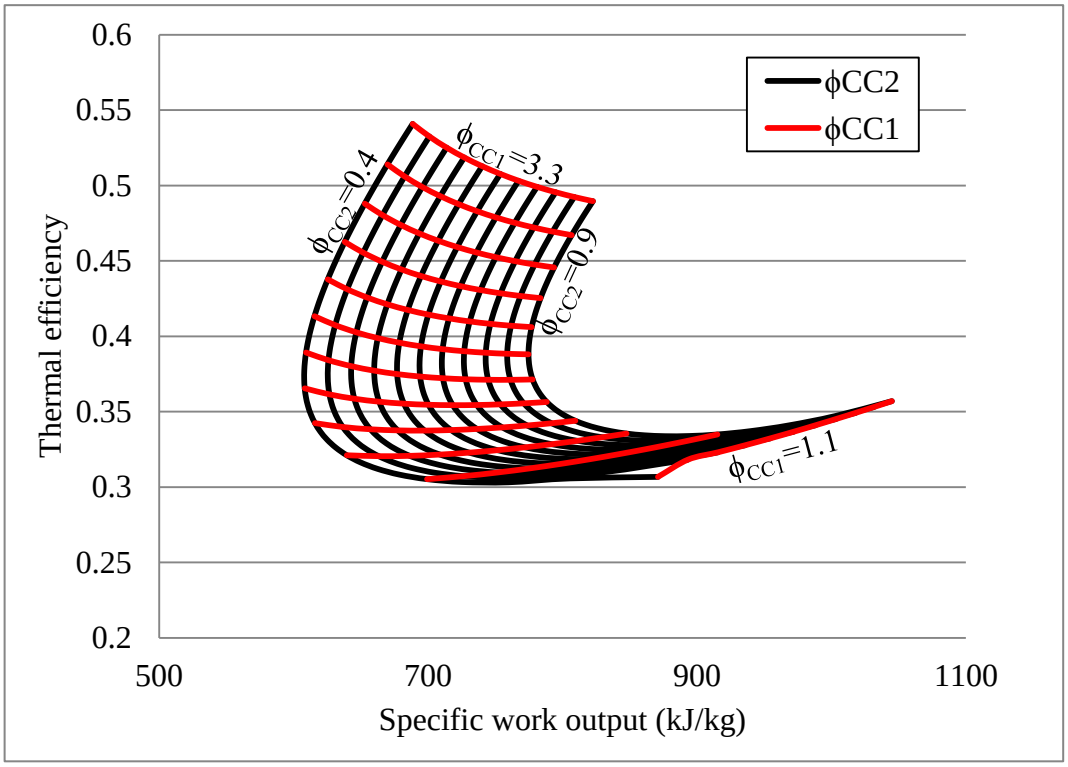

Figure 6.34 CC thermal efficiency versus specific work output affected by the equivalence ratios

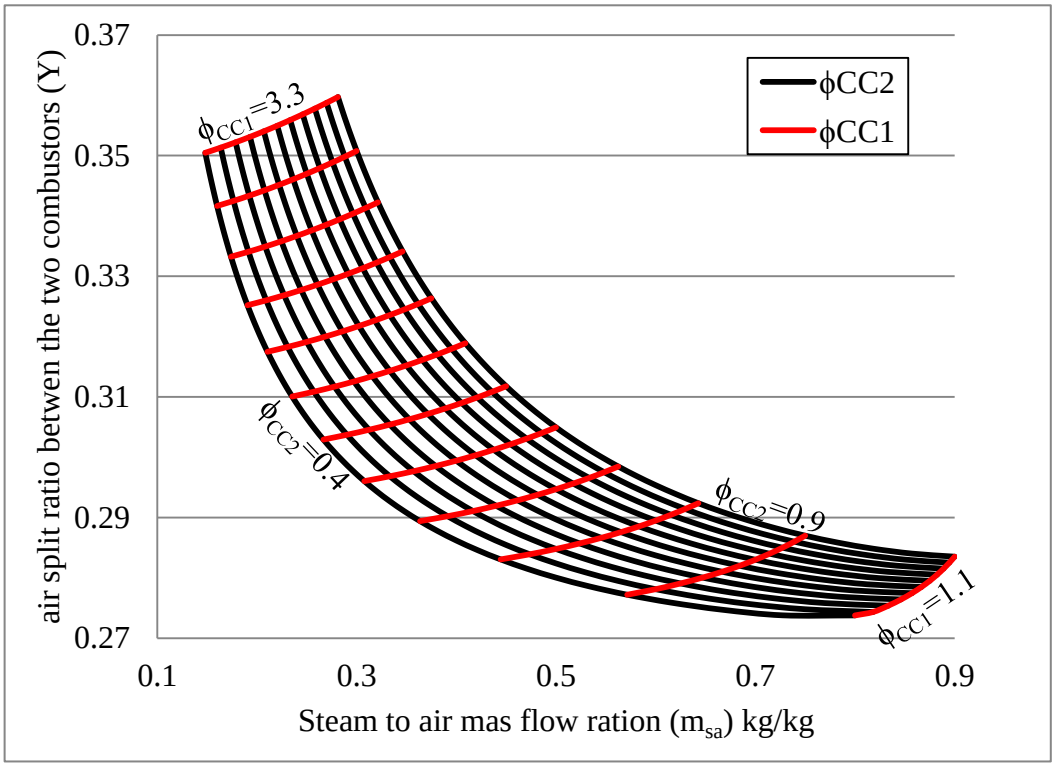

Figure 6.35 Air splits ratio versus steam to air mass flow rate ratio affected by the equivalence ratios

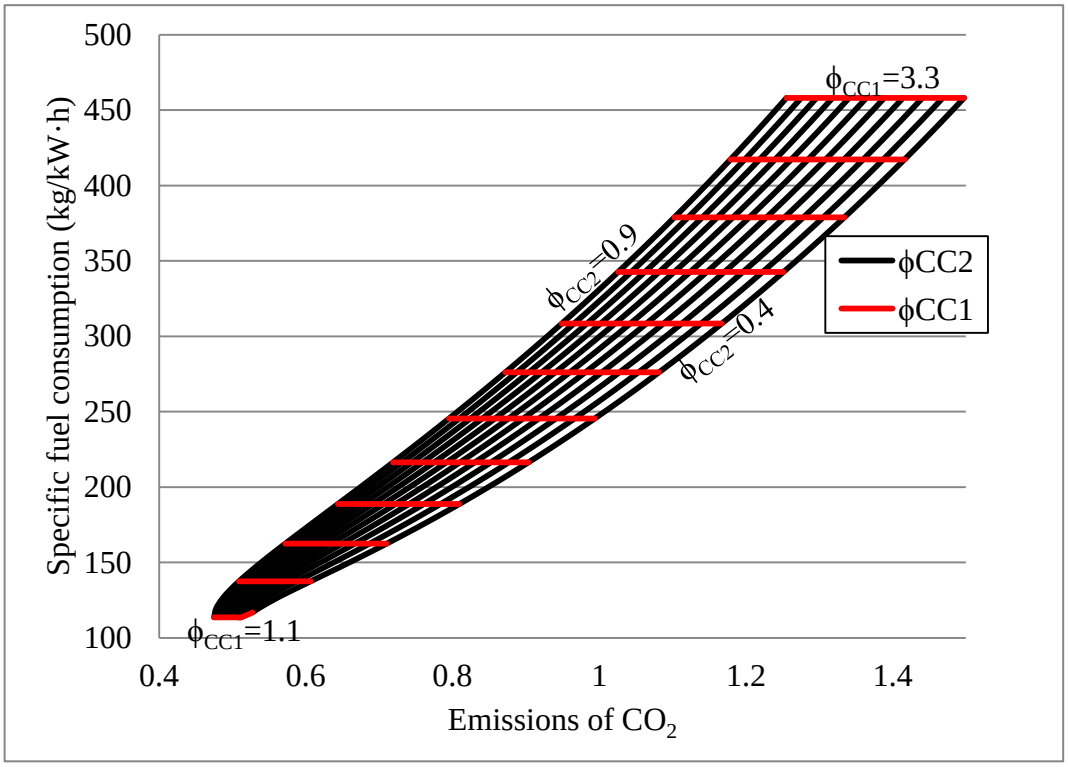

Figure 6.36 Specific fuel consumption versus CO_2 emissions affected by equivalence ratios

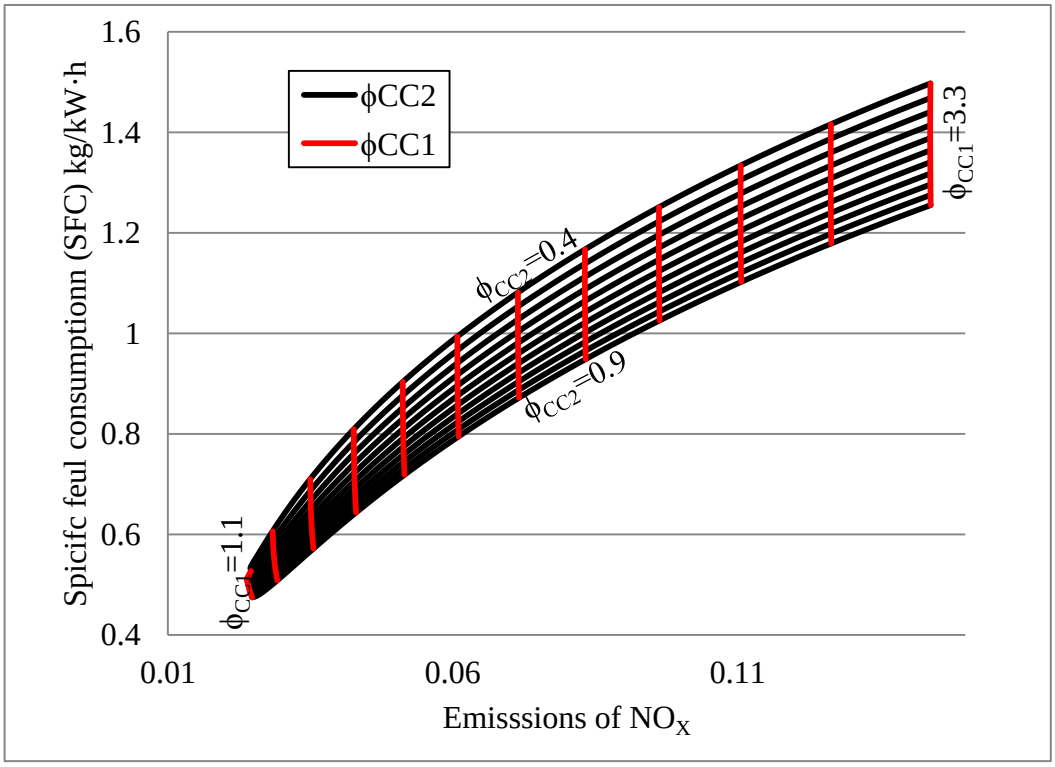

Figure 6.37 Specific fuel consumption versus NO_X emissions affected by equivalence ratios

6.5.4 Condenser and HRSG parameters effects

Condenser and HRSG pressure effects on the thermal efficiency and the specific work output from the ChGT are depicted by Fig.6.38 to Fig.6.41. These figures show how limited is the ChGT operation range as it affected by the steam turbine blade life requirements. Therefore, to satisfy such requirements usually P_{s2} is lowered and P_{s4} is increased. The thermal efficiency of the ChGT is severely affected by reducing P_{s4}. This effect gets minor by increasing P_{s2} as shown by Fig.6.38, 6.40 and 6.41. An acceptable range of η_{CC} is illustrated by Fig. 6. 41. The reduction in η_{CC} by increasing P_{s4} is as great as 3 percentage points when P_{s4} is increased from 0.15 to 0.55 bars.

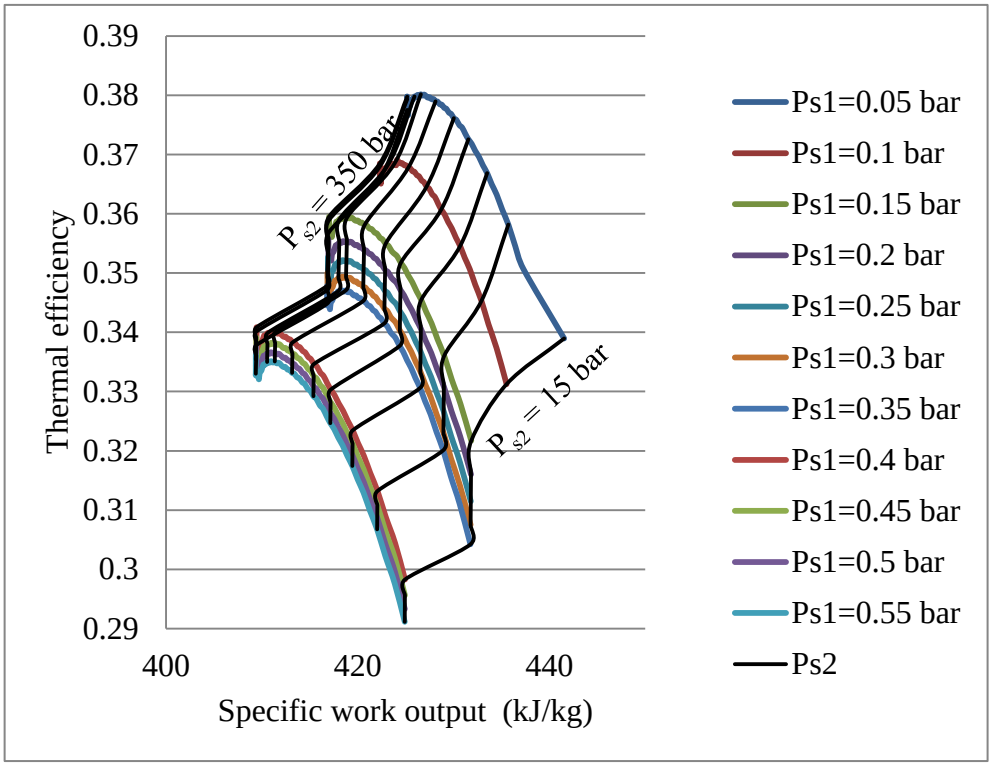

Figure 6.38 The thermal efficiency versus specific work output

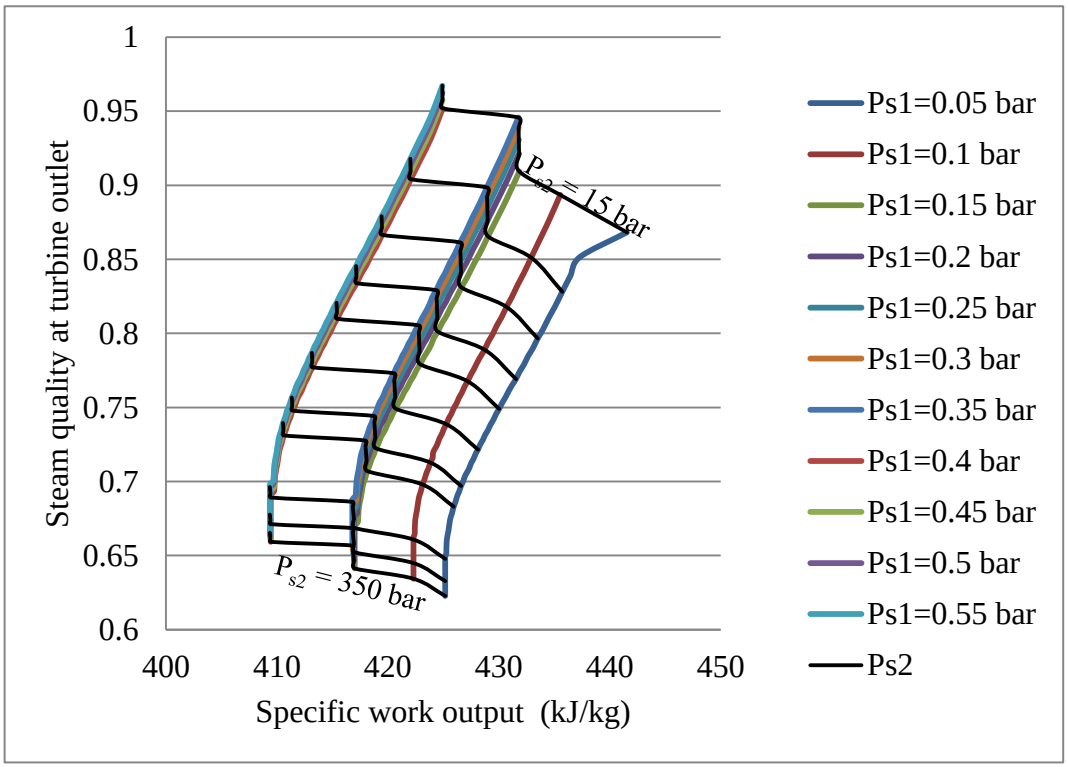

Figure 6.39 Steam quality at turbine outlet versus the specific work output

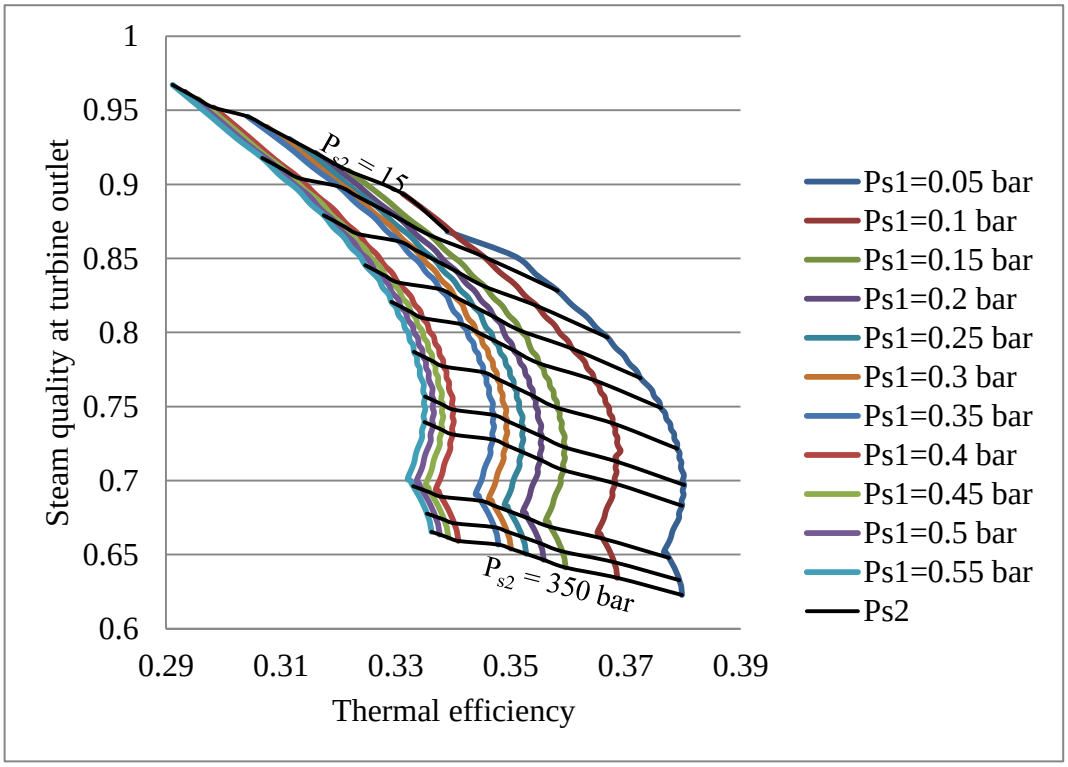

Figure 6.40 Steam quality at turbine outlet versus the thermal efficiency

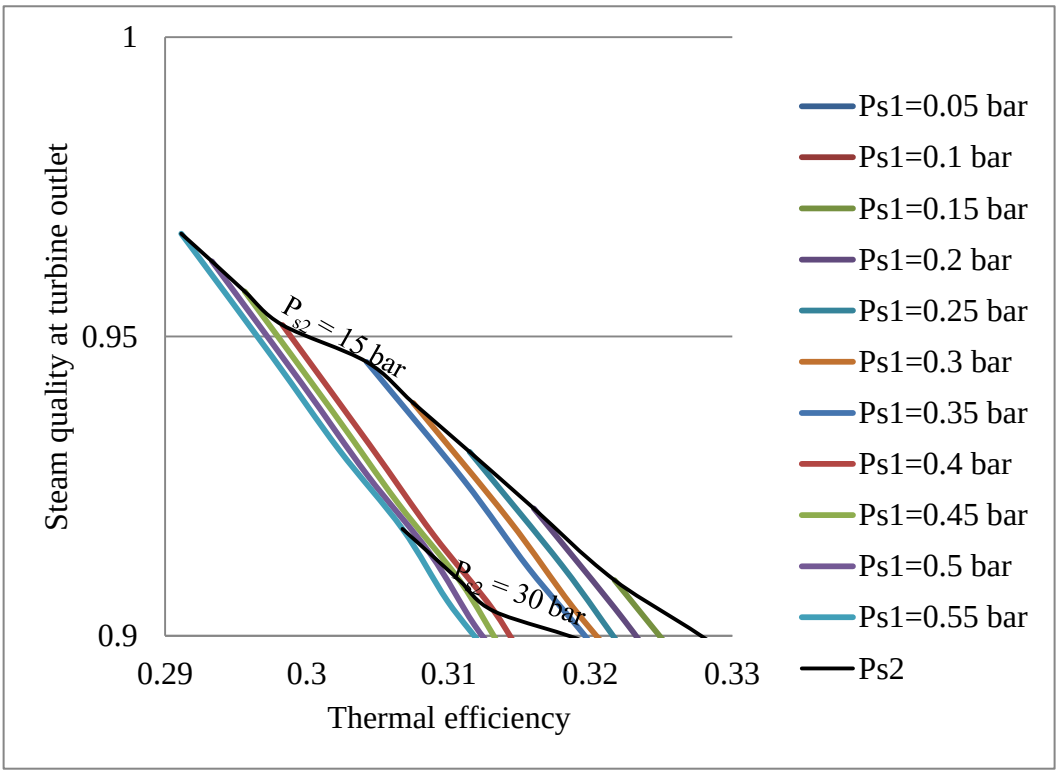

Figure 6.41 Steam quality at turbine outlet versus the thermal efficiency

6.5.5 1st HRSG parameters effects

In this model HRSG, performance is affected by gases enthalpy from fuel rich turbine outlet, water pressure at economizer inlet, and its sections' efficiencies (which depended on its configuration). The influence of the P_{s2} effect on the thermal efficiency and the specific work output generated by ChGT is illustrated in Fig. 6.15. Such effect was undertaken for different fuel rich gas turbine discharges temperatures, which were represented by changing r_{AC}, ϕ_{CC} and T_{g4}. For a certain temperature of discharge, like the one corresponding to a (ϕ_{CC} =1.8, T_{g4}=1400 °C and r_{AC} = 12) the increase in P_{s2} from 20 to 300 bar, it is shown that both η_{CC} and w_{CC} were increased by about 2.5% and 7% respectively. Discharge gases usage to generate steam in the HRSG is strictly governed by P_{s2} magnitude, which was limited by for gas turbines those works on high compression ratio. Figure 6.16 showed that a reduction in the heat content of the rich fuel turbine discharge gases required the steam generation to increase to satisfy HRSG efficiency. While less steam mass flow was required to satisfy such efficiency by T_{g4} increase. Accordingly, ChGT power output and efficiency are increased by the increase in P_{s2}. Although the reduction in the steam generation in the 1st HRSG steam quality at turbine inlet was improved, as a result to the improvement in 2nd HRSG steam quality.

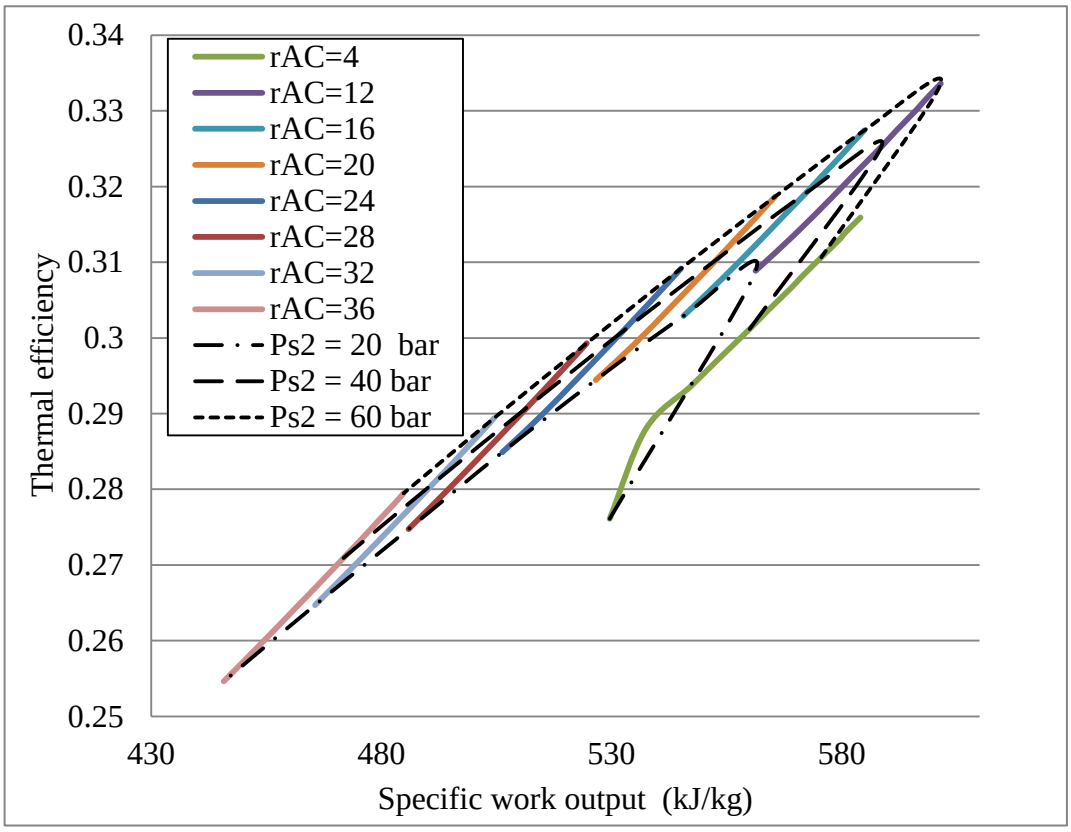

Figure 6.42 Specific work output from the ChGT affected by the P_{s2}, T_{g4} and r_{AC} for the 1st design

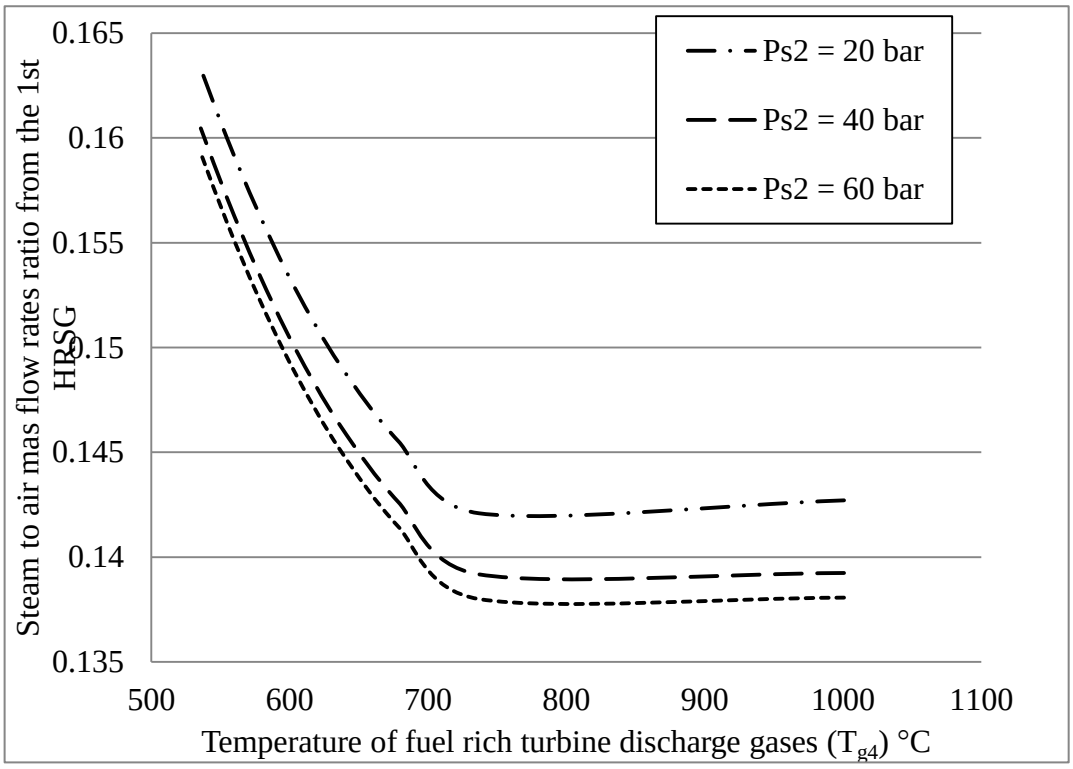

Figure 6.43 Steam pressure effect on steam generation affected by T_{g4}

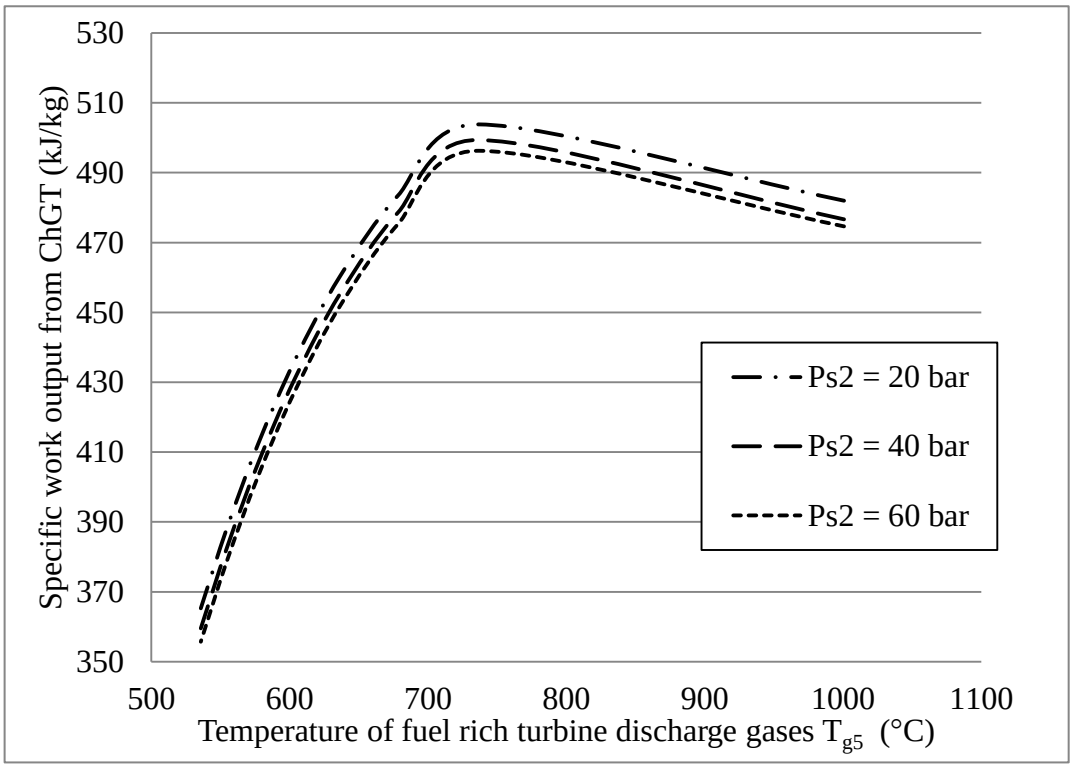

Figure 6.44 Rich fuel turbine gases temperure effect on specifc work output of the ChGT

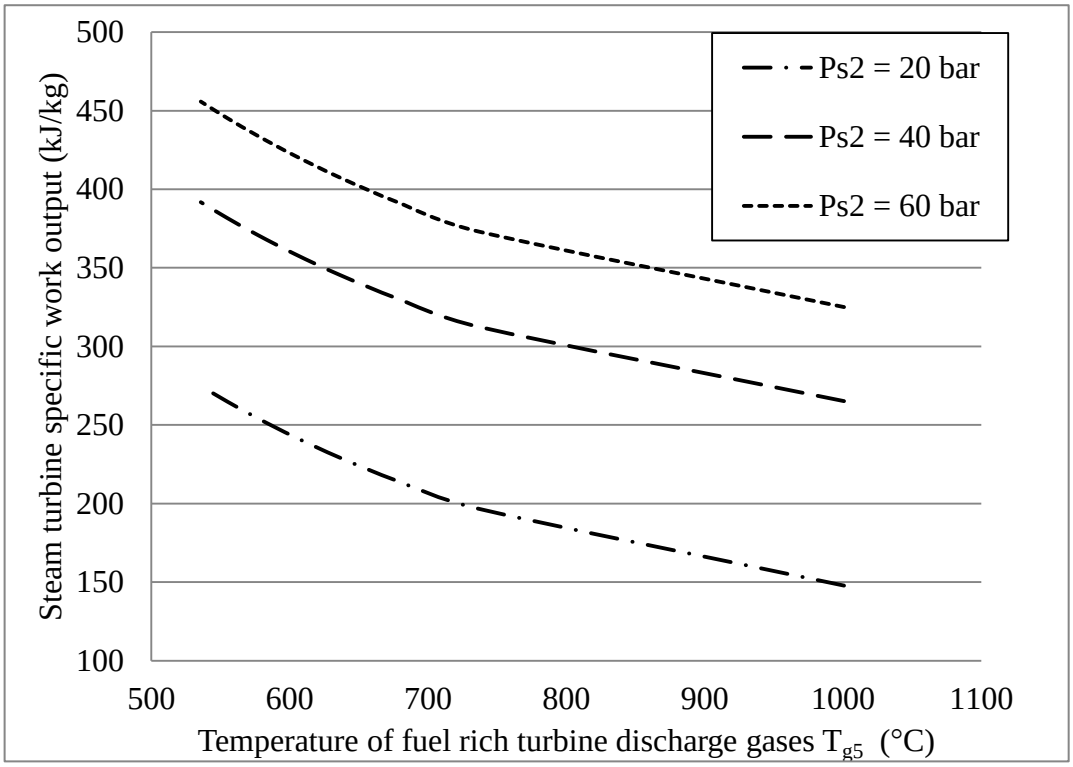

Figure 6.45 Rich fuel turbine gases temperure effect on specifc work output from the steam turbine

6.5.6 Ambient temperature effect

The effects of ambient temperature on the performance and environmental characterizes of the ChGT are discussed here and illustrated by Figs. 6.46 – 6.49. These figure shows ambient temperature's considerable effect on both the efficiency and the SFC of the ChGT, although, its modest effect on its individual cycles. The acceptable range of operation narrows as the temperature approach (0 °C), which appears more for the gas turbines those operating on a low r_{AC}. In general, the increase in Ta deteriorates both the efficiency and the power generation for the ChGT and the GC. The increase in Ta widens the efficiency and specific work output range from the SC for a certain r_{AC} and significantly increases both. The increase in the ambient temperature is combined with an increase in NO_X emissions with a slight reduction in the CO_2 emissions for a certain r_{AC} as shown by Fig.6.49.

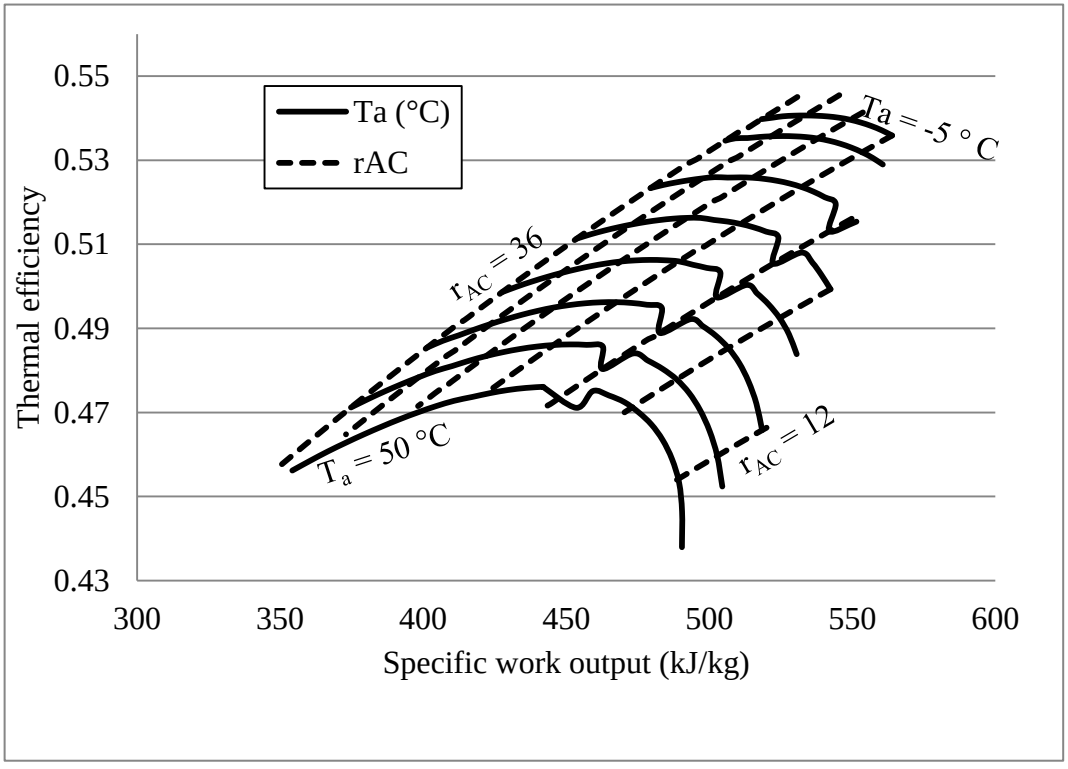

Figure 6.46 Ambient temperature effect on specific work output and the thermal effciiency of the ChGT design 1

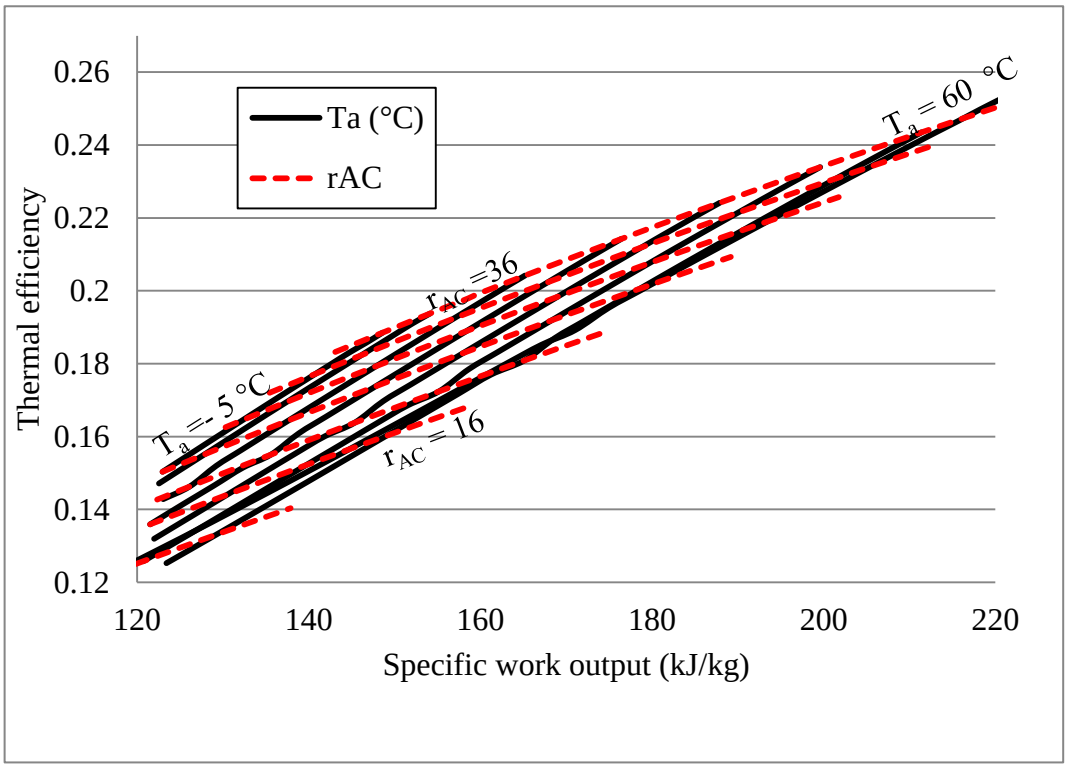

Figure 6.47 Ambient temperature effect on specific work output and the thermal effciiency of the SC in design 1

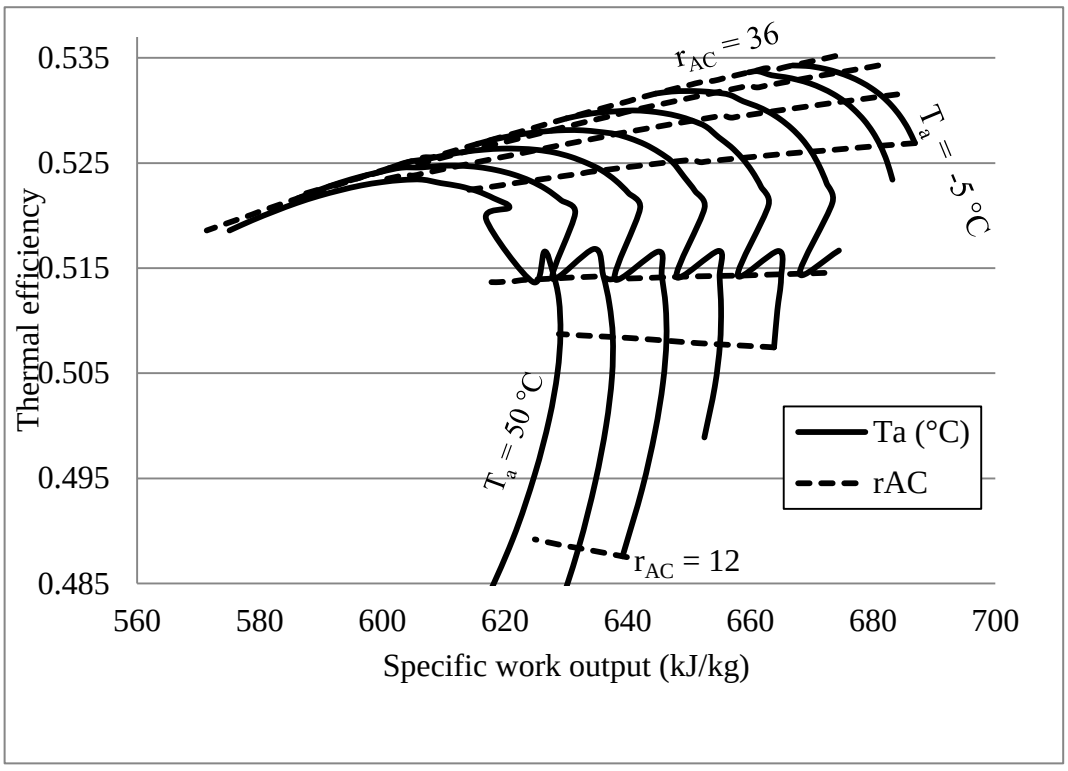

Figure 6.48 Ambient temperature effect on specific work output and the thermal efficiency of the GC in design1

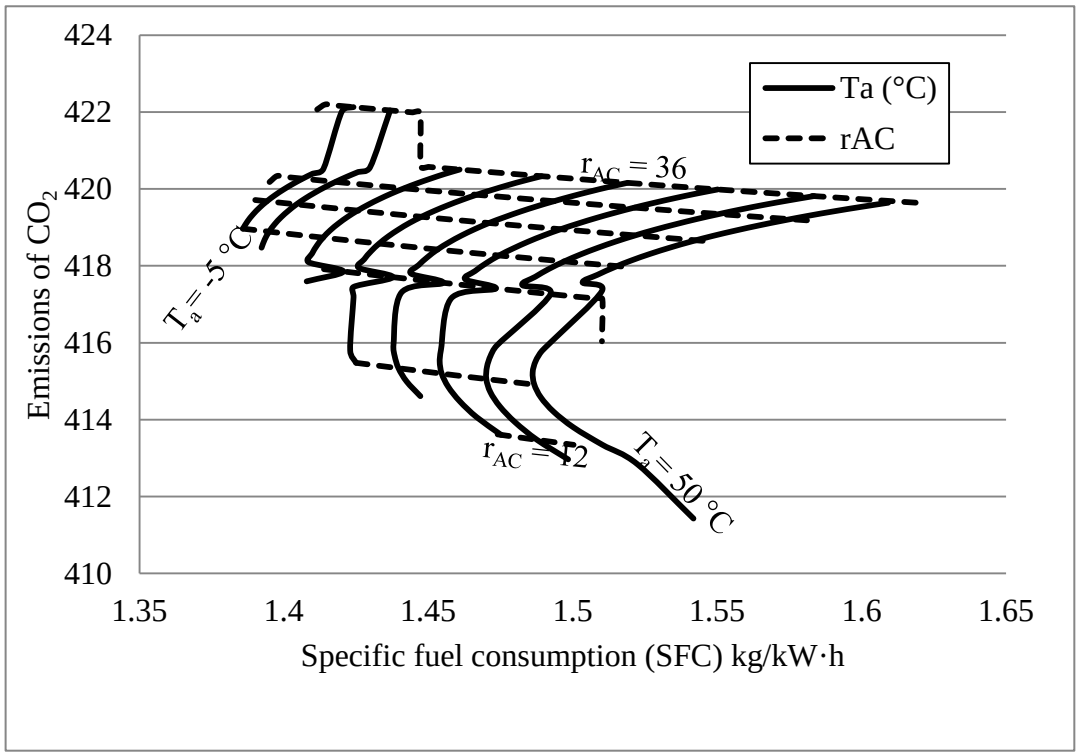

Figure 6.49 Ambient temperature effect on the specific fuel consumption and CO_2 emissions

6.6 Results and discussion from optimization

As a result from the parametric study, optimizing components parameters prove the following points:

(1) The result here confirms that, the partial oxidation by rich fuel combustion and lean fuel combustion competing simple and reheated GC in CC configurations rather than its GC alone, this goes on with the findings from [11], [67], and [10]. The results also confirmed the findings from [65] in which the superiority of the POGT is restricted by a set of parameters and not all over the operating map.

(2) Both the thermal efficiency and the power output from the ChGT are increased by the increase in the temperature of the gases at each turbine inlet, compressions' ratios and the pressure of the steam at turbine inlet and the efficiencies of the components.

(3) Similarly, to the conventional combined cycles the increase in r_{AC} does not probably improve the performance characteristics. The maximizations of these characteristics are restricted by a certain compression ratio, over which the gas turbine cannot be designed

to work on its best performance. This result confirms the findings from [62] about the domination of AC on the performance of the ChGT.

(4) The performance characteristics of ChGT are deteriorated by the increase of: the compression ratios over the optimum values for certain turbine inlet temperature and the pressure of the steam at turbine discharge.

(5) The difference from the conventional CCPP is that, appears by the effect of the combustors' equivalence ratios for a certain turbine inlet temperature and compression ratio. Accordingly, the performance characteristics are boosted by increasing the equivalence ratio of the first combustor and deteriorated by increasing the equivalence ratio of the second combustor.

(6) The main affecting parameters on the 2nd design POGT in a CCPP configuration are (r_{AC}, T_{g4}, ϕ_{CC1}, ϕ_{CC2}, T_{g10}, P_{s1}, P_{s2} and T_a). To optimize the 2nd design configuration using T_{g4}, the optimum r_{AC} is when the gas turbine operates between r_{AC} of 8 and 12. The optimum T_{g4} for maximum specific work output is the highest. The results here agree with [66] findings about the main affecting parameters which are Y and f (determined by ϕ_{CC1},and ϕ_{CC2} in this study) and the effectiveness of the AC, GT and HRSG. Although this is right it misses the effects TITs and r_{AC}, P_{s2} and T_a. The results also confirmed P_{CC1} slightly effect on combustion gases by reducing its NO_X emissions content [63]. By this study, the optimum ϕ_{CC2} is 0.9 and ϕ_{CC1} is 3.3 those are corresponding to the maximum efficiency and its optimum power output. This also corresponds to the highest SFC. It corresponds to the minimum CO_2 conetnt at ϕ_{CC1} and the maximum NO_X content at $\phi_{CC2.}$ It is evident to the results that reducing ϕ_{CC2} reduced the W_{GC} of both designs, although the increase in W_{GT1} and reduction of W_{GT2} that reported by [57]

(7) The optimum ϕ_{CC1} for the maximum efficiency is the greatest, while the optimum for the maximum specific work output is the slightest. Similarly, this value corresponds to the minimum specific fuel consumption (SFC) and the minimum emissions for both NO_X and CO_2. The results also confirmed [64]findings, that NO_X and CC efficiency specific is increased by the increase of the rich gases' TIT. The results her also showed that CO_2 and CC specific work output is increased by the increase of the rich gases' TIT.

(8) The optimum T_{g10} for the minimum SFC is the greatest T_{g10}, while the optimum r_{AC} and T_{g10} to satisfy the maximum the turbine discharge temperature is those corresponding to the maximum T_{g10} and the minimum r_{AC}.

(9) For the 1st design, the optimum ϕ_{CC2} for a certain r_{AC2} to satisfy the maximum efficiency is the minimum, while the one corresponds to the maximum, specific work output is of maximum ϕ_{CC2}. While the minimum SFC is corresponding to an optimum ϕ_{CC2} of a minimum value for a certain r_{AC}. On the other hand, to satisfy steam quality at turbine outlet, i.e. $X_{s4} > 0.9$, the optimum is of highest ϕ_{CC2} if r_{AC} is low and of minimum ϕ_{CC2} if r_{AC} is high.

(10) The maximum efficiency and specific work output correspond to the minimum T_{g10}, while the one to satisfy $X_{s4} > 0.9$ corresponds to the maximum $T_{g1.}$

(11) A maximum efficiency of (0.64) was resulted for the ChGT as shown by the table (6.2), this was corresponding to (r_{AC} = 36, T_{g4} =1800 °C, ϕ_{CC1}=3.1, ϕ_{CC2}=0.4 and w_{ChGT} = 874 MJ).This efficiency was greater than that reported by Yammamotto [67]and Muhammed [66]. It was less than the efficiency reported by Yammamotto [38], Kobayashi, et al., [63], Lior [57] and Korbotsian [64].

(12) The results confirmed a certain range for the operation of Y, this is generated by employing the recommended ranges of ϕ_{CC1} and ϕ_{CC2}. The operating range of Y is between 0.27 and 0.37. This is shown for a certain set of other parameters; however, this is limited this range below the 0.5 value that was used by previous researchers like [57]. However, the results here agree with the findings of [65] about the great effect of Y or the air mass flow ratio between the two combustors on the efficiency and the work output from the ChGT.

rc1	Tg4 (°C)	ϕ_{CC1}	rc2	Tg10 (°C)	ϕ_{CC2}	GC efficiency	SC efficiency	CC efficiency	GC Specific Work Output (kJ/kg)	SC Specific Work Output (kJ/kg)	CS Specific Work Output (kJ/kg)
36	1800	3.1	36	1500	0.4	0.59534	0.1912177	0.641358	693928	180578.07	874505.8
28	1800	3.1	36	1500	0.4	0.58891	0.1662888	0.629249	722568	160721.12	883289.3
36	1700	3.1	36	1500	0.4	0.57947	0.1886706	0.63643	674885	173626.6	848511.7
36	1800	3.1	20	1500	0.4	0.56998	0.1823043	0.578363	667254	181315.24	848569
36	1800	3.1	16	1500	0.4	0.55989	0.178441	0.556769	653287	181444.72	834731.9
28	1800	3.1	20	1400	0.65	0.54999	0.1623597	0.522366	680539	162811.1	843349.9
16	1800	3.1	32	1500	0.65	0.53996	0.1114292	0.547717	828212	121525.97	949738.4

Table 6.2 GC, SC and ChGT performance characteristics results after optimizing turbine inlet temperatures, compression ratios and the equivalence ratios of both combustors

6.7 Conclusions

(1) This chapter developed 14 models of ChGT configurations, including ChGT two designs and the 7 previous designs of the steam turbine cycles.

(2) In the developed model, the steam turbine was integrated with the gas turbine plant in a more interacted manner than the conventional combined cycles.

(3) Likewise, the conventional CCPP, ChGT configurations are affected by the parameters of each of the combined cycles. These effects are significant for the GC rather than the SC. This is because these configurations are ranges of operation are governed by GC parameters.

(4) As in any gas turbine cycle, the increase in the temperature of the gases at any of the turbines inlet improves the performance of the ChGT. While there is a certain value of compressions ratio, which is closer to its high values.

(5) Turbines outlet temperature is of great importance on the performance of the SC therefore, the performance of the total combined cycle. On the other hand, steam cycle parameters are the decisive on limiting these characteristics.

(6) ChGT configurations are affected by the increase of the ambient temperatures; therefore, compressor inlet solutions systems are essential for stabilizing the power and increasing the efficiency, although the reduction in the operation range.

(7) In these configurations, the range of high r_{AC} on which the optimum operating parameters of the GC operate on ranges within those for low ambient temperature. This shows how effective is using the inlet air cooling systems to improve the performance of these CCPPs.

CHAPTER 7
AMMONIA WATER CYCLE TURBINE ENGINE

7.1 Introduction and background

The previous chapter investigated the performance of the CCPP as it enhanced by novel topping cycle strategy. This chapter and the next are focused on the performance of CCPP as it enhanced by novel bottoming cycle strategies. Although SC components are optimized to improve the performance of CCPP, there is a lack of research on optimizing enhanced CCPP, as evident by chapter 3.Which also confirmed CCPP performance optimization by AWMT over conventional CCPP of different GT and ST cycles. However, none combined AWM HRVG within HRSG and non integrated ChGT, AWMT and ST in triple combination. In this chapter, Kalina cycle AWMT is investigated as a bottoming cycle to different GTs with and without different STs.

Even when zero pinch point temperatures difference a satisfactory of matching the temperature profile in heating and cooling processes can't be achieved, due to exergy losses. Such losses are increased at relatively high evaporator and heat source temperatures. Employing multi component mixture as a working fluid can guarantee more efficient heat utilization than the single fluid from the same heat source. The variable boiling temperature of AWM may result in a better heat transfer match with the heat source. The bubble temperature of AWM is lower than that of the steam. Therefore, AWM Kalina cycles can absorb more heat than Rankine cycles from the same source. Additionally, this decreases the heat source exergy losses at exhaust to its lowest magnitude. Furthermore, the condensation of multi component mixture in Rankine cycle increases the efficiency slightly. However, reducing ammonia concentration and increasing pressure of AWM through the condenser gives even better performance as given by Kalina cycle. The flow diagram and the components of a kalina cycle power system that contains one distillation step are shown by Fig. 7.1. The processes go on the fluid in the components are illustrated on AWM T-S diagram in Fig7.2.

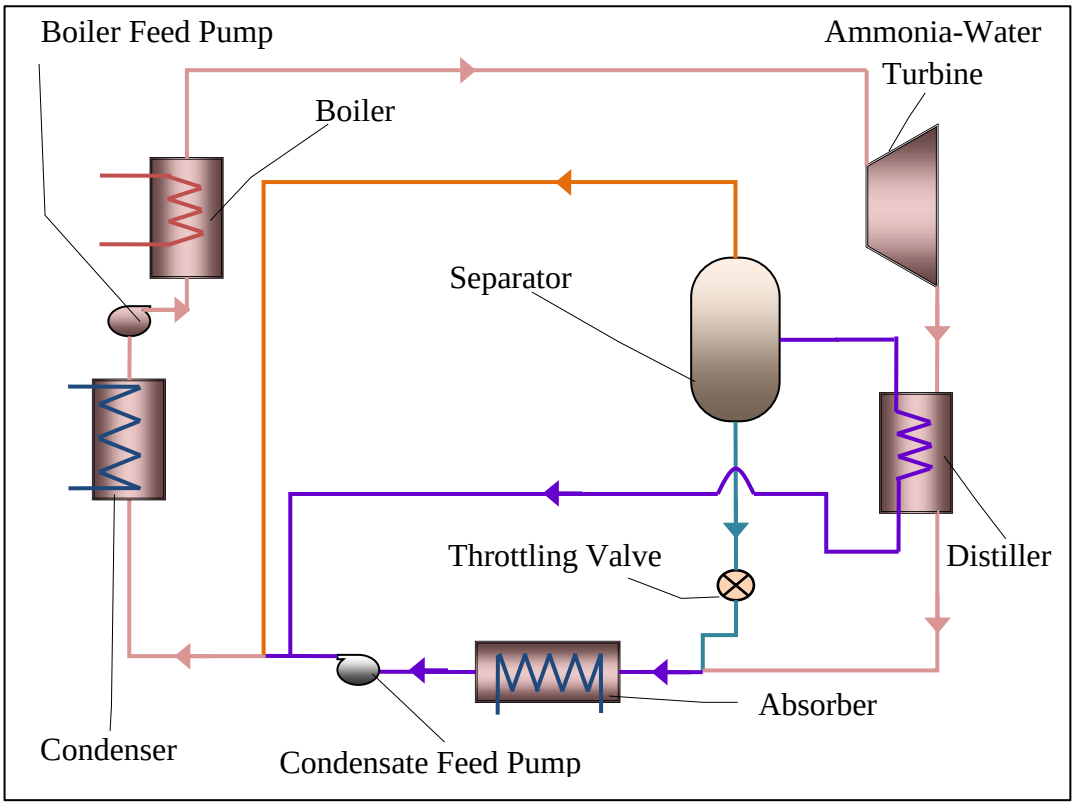

Figure 7.1 Kalina cycle power system one distillation step

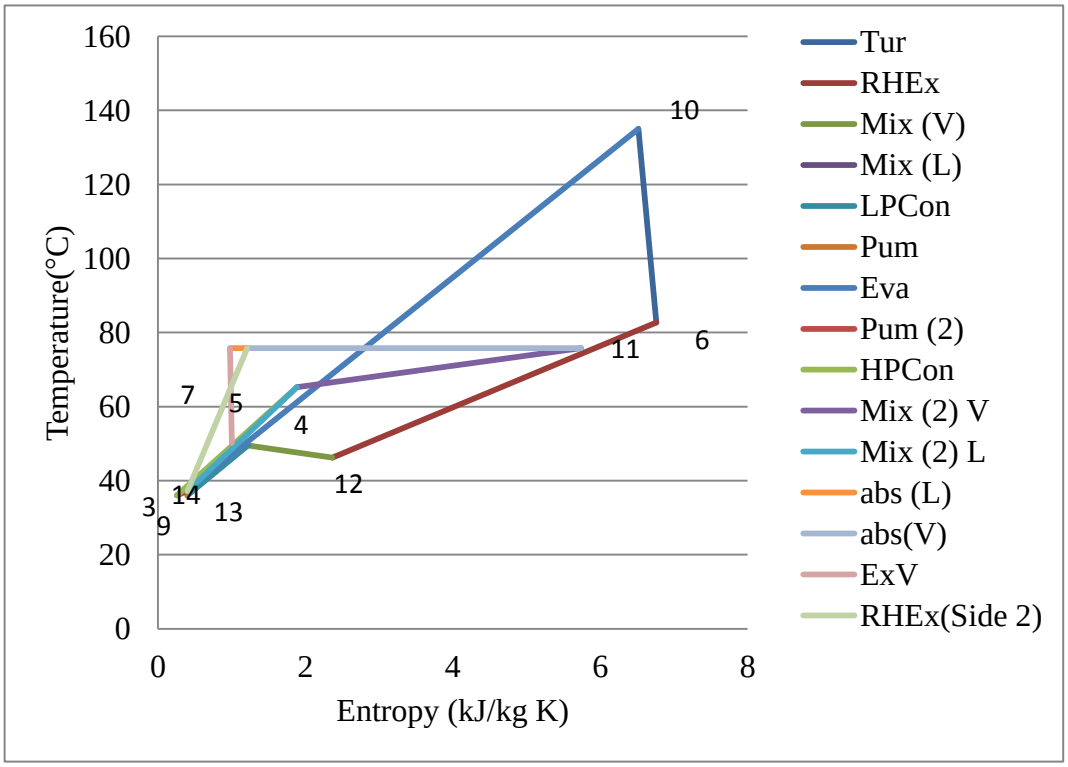

Figure 7.2 kalina cycle processes on temperature entropy diagram

The operation of a kalina cycle under normal conditions requires:

1. A full condensation of the solution through the condenser.

2. The separations of the rich ammonia vapour from the water solution in the flash tank.

3. The heat recovery at the heat exchanger should meet the requirement of the pinch point temperature difference.

The steam engine that works beyond Rankine cycle is the most often used cycle in utilizing the thermal energy of the hot gases to generate mechanical or power output Marston [40]. In practice, Kalina cycle was the principle of many power generation turbine systems. It operates safer and more efficient than nuclear technology. It also requires a low construction cost than other renewables. Applying kalina as a bottoming cycle to gas turbine power plant was analysed by major power companies like GE. It showed a minimum increase of 2.5% in efficiency than conventional two spools gas turbine STAG207FA. The GT /AWMT combined cycle power plant components are depicted in Figure 7.3.

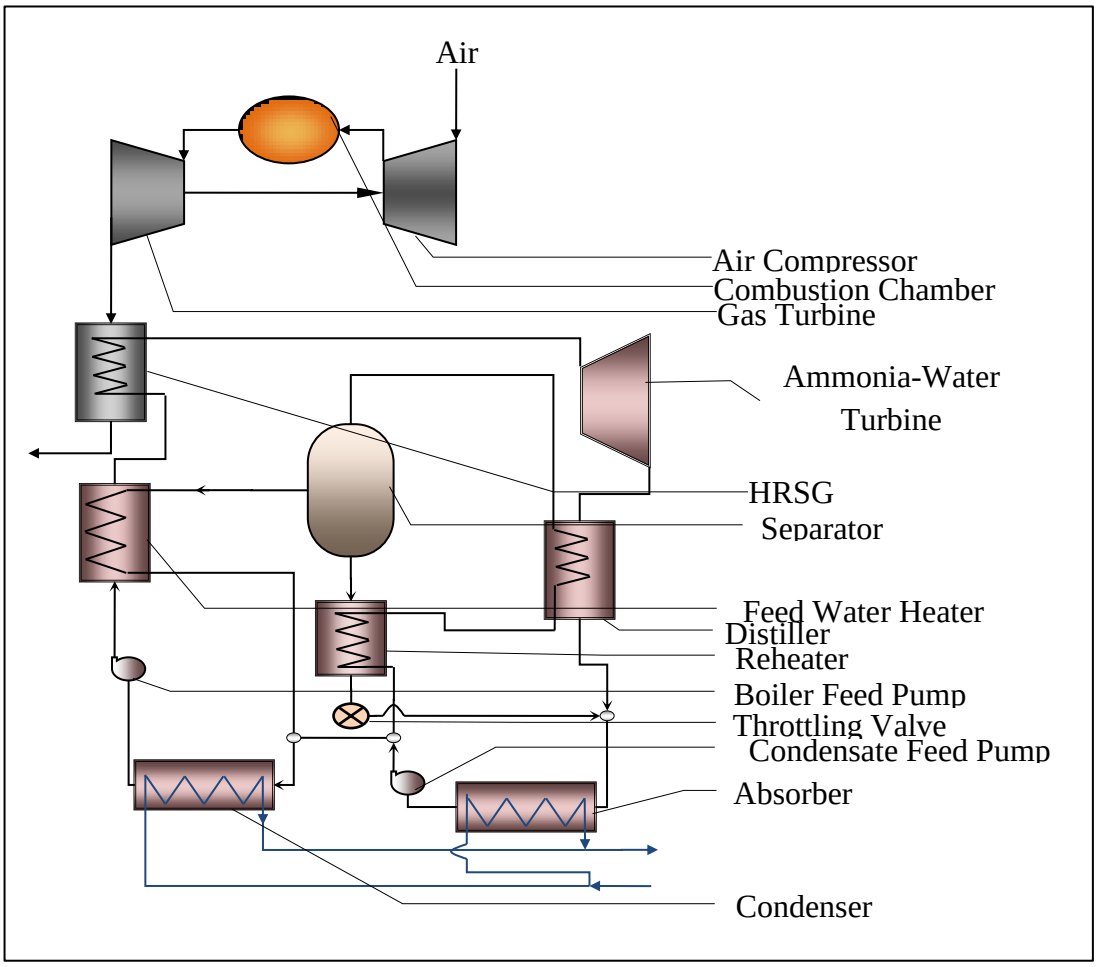

Figure 7.3 Gas turbine / ammonia water turbine combined cycle

7.2 Ammonia water mixture

Although ammonia water mixture was under discussion in chapter three, here, it is (AWM) under further discussion regarding a number of important issues. These undergo: firstly, how safe is to use ammonia water mixture in power plants and how to deal with it as working fluid? Secondly, how to direct the thermodynamic properties into the better performance for the plant? Thirdly, is how to protect the AWM cycle power plant components, when steam turbine components are used and what additional components' changes required for such issue?

7.2.1 Ammonia toxicity

As ammonia is a toxic substance, the safety is number one concern in any facility that contains ammonia as a working fluid. Although the ammonia is highly soluble in water, in some parts of the AWM power plant ammonia concentration gets to high level in the power plant components. Accordingly, these components and the entire plant are required to be fully sealed. While, any ammonia leakage requires immediate procedures to ensure its cut off to maintain its limits beyond fatal limits. In some facilities to get over any uncontrolled ammonia discharge or accidental release, it is collected and discharged to be absorbed by water to eliminate its danger. Accordingly, the need for continuous observation as it is easy to be detected at the levels of safe concentration. The development in the ways of contaminating such leakage is developed. Lately, ammonia has had a great deal of creditability, especially when it has been used to operate a major project for leisure facilities like the UAE Dubai Ski Dum, in addition to its use in power generation like Iceland HRSVIK power plant and recently China new waste power station. However, Canoga Park is the name that always referred to the first kalina cycle power plant powered by gas turbine exhaust gases. Ammonia is important in the HRSGs to reduce the NO_X emissions from the CCPP by the SCR (selective Catalytic Reduction) system.

7.2.2 Ammonia water mixture's thermodynamic properties

The critical conditions as reported from the US NIST for water correspond to a temperature of 373.946 °C and a pressure of 220.640 bars. For ammonia these conditions are 132.25 °C for the temperature and 113.330 bar for the pressure. The properties of AWM used in this study utilize the tables generated by Tellnir-Roth and Friend, [93]. They used Helmholtz free energy equation of state to model AWM's the thermodynamic properties to a range wider than that considered by Tellnir-Roth and Friend, [93]. The mixture is considered as a mixture of two

ideal gases using the properties' tables of ammonia from Haar and Gallagher, [94]. These tables are limited between a pressure of 1 bar to 300 bars and a temperature between -50°C and 350 °C. Mixture' properties off this range, particularly in superheat area, are estimated as a real mixture of two ideal gases using equations (7. 1- 7.4). In these equations, pure steam properties are determined using the functions (hFTP and SFHP), while ammonia properties are estimated from (JANAF tables).

$$\bar{h}_{AWM} = \bar{X}_g \bar{h}_{NH_3} + \left(1 - \bar{X}_g\right)\bar{h}_{H2O} \quad \ldots (7.1)$$

$$\bar{s}_{AWM} = \bar{X}_g \bar{s}_{NH_3} + \left(1 - \bar{X}_g\right)\bar{s}_{H2O} + \bar{s}_{mix} \quad \ldots (7.2)$$

$$\bar{X}_g = \frac{1}{1 + \left(\frac{1}{X_g} - 1\right)\left(\frac{M_{NH_3}}{M_{H2O}}\right)} \quad \ldots (7.3)$$

Where,

$$\bar{s}_{mix} = -\bar{R}\left(\bar{X}_g \ln(\bar{X}_g) + (1 - \bar{X}_g)\ln(1 - \bar{X}_g)\right) \quad \ldots (7.4)$$

Where, R =8.34 (kJ/kmol K) and lookup table functions were used to estimate mixtures' enthalpy, entropy. These functions were developed using Excel VBA of in-house codes to estimate these properties. Additional properties for the state of (X_{aw} = 0, T_{aw} = 0 and P_{aw} =1bar) was employed from IAPWS-IF97 Electronic steam tables to ease calculations.

7.2.3 Material's prohibitions

The suitability of utilizing AWM for power plant components than steam is described by the following points:

i. It requires smaller heat exchangers (due to the high heat capacity)

ii. It has less sensitivity to parasitic load from the working fluid cycle feed pumps (due to the high heat capacity)

iii. It increases the thermodynamic efficiency of evaporation (due to the boil temperature glide instead of the pinch point temperature).

iv. It increases the thermodynamic efficiency of condensation (due to the glide in the temperature of condensation by the change in the concentration instead of the pinch point temperature).

v. It's heat-exchangers designs are more complicated (because it requires the temperature glide).

vi. Conventional steam turbines could be powered by AWM with little modification(due to the very close molecular weight of water to that of ammonia).

Instead of oxidation, the AWC engine high temperature components are exposed to nitridation. Therefore, these components must be selected with more concerns to such issue. Canoga Park plant kalina cycles' materials and equipment were compatible to AWM as working fluid. As it verified no corrosion failures in plant equipment's due to the use of AWM. Oxidation for cycle components is less likely to happen due to the extremely low oxygen content in the working fluid Leibowitz and Mirolli [95]. As illustrated by the following figures, AWM in power generation required more components than those required by regular steam power plants.

For two components mixture, the glide of the temperature increases by the enlargement of the difference between the boiling points of the two pure components. This controls the glide of the temperature of the rich and lean concentrations.

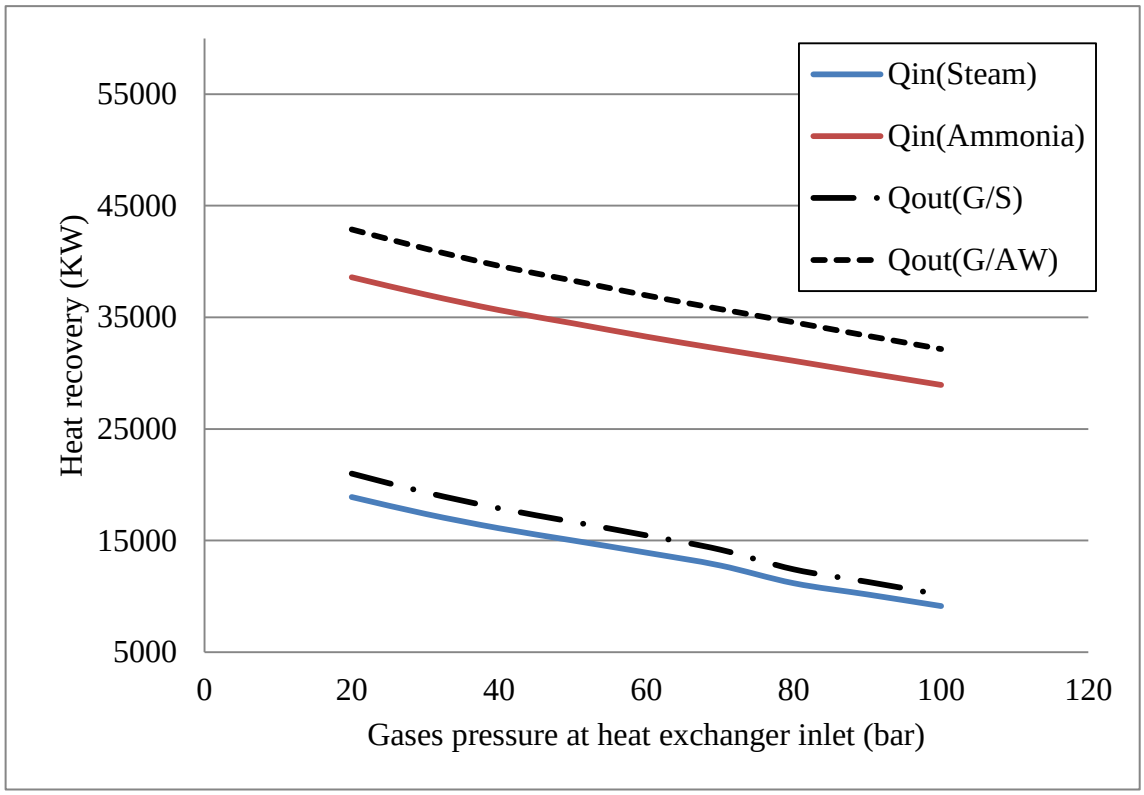

Figure 7.4 Heat transfer between the gas and steam and AWM of the same conditions

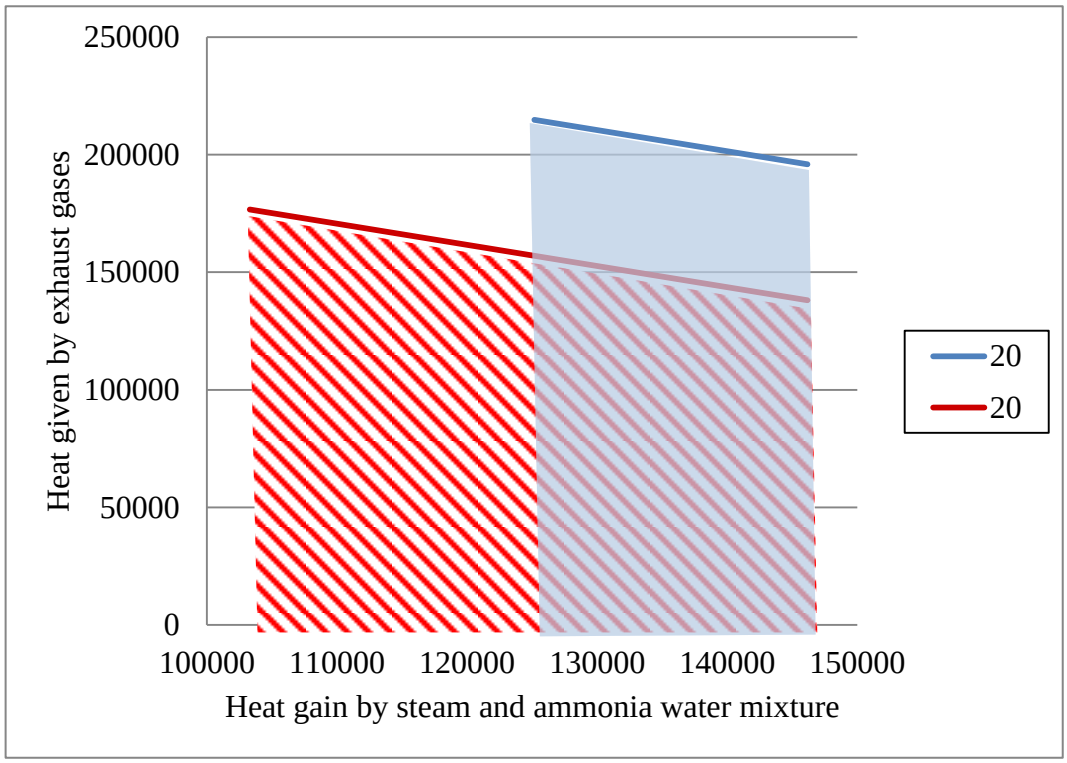

Figure 7.5 Heat extraction from exhaust gases difference between AWM and steam

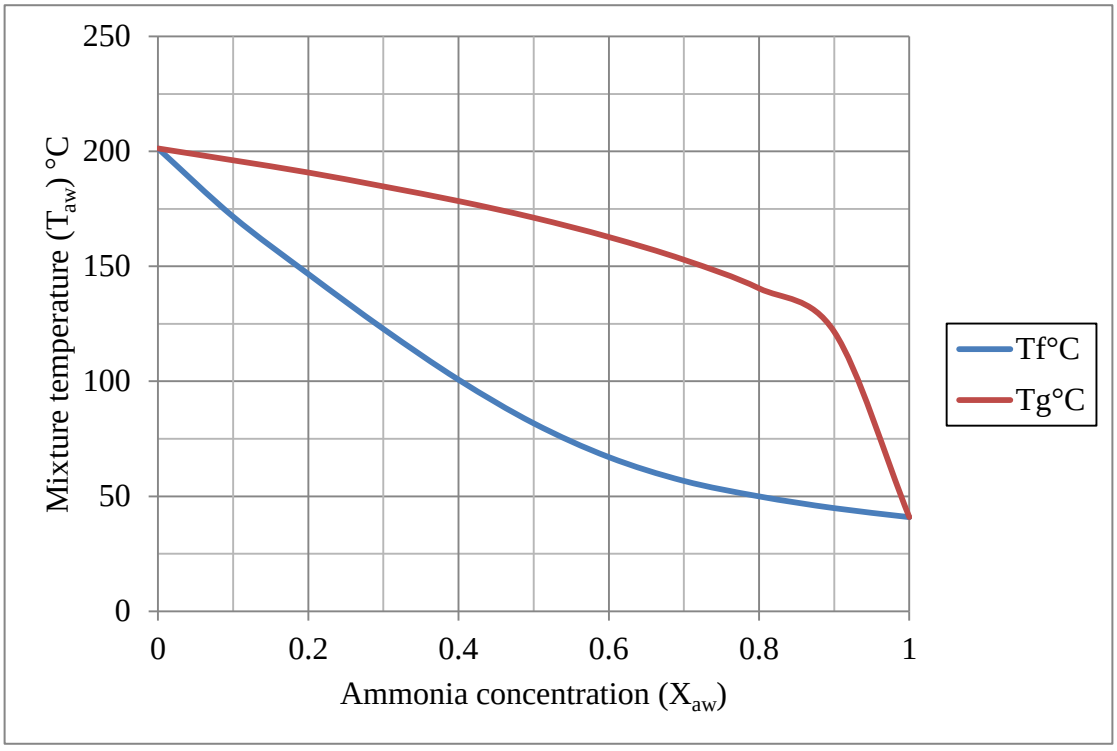

Figure 7.6 Temperature saturated lines distribution for constant pressure

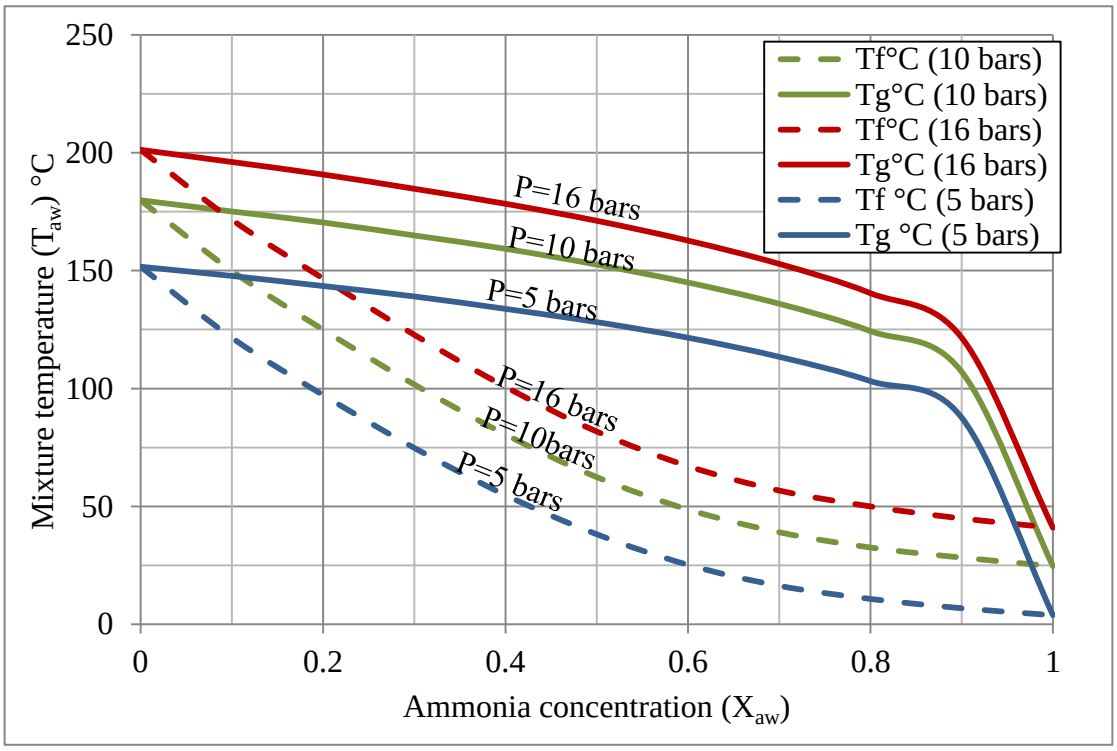

Figure 7.7 Saturation lines alternated by the change in the pressure of the AWM

7.3 AWT engine simulation model

In this model, the way the heat is recovered by AWC is considered to utilize the following:

(1) The HRSG exhaust gases outlet (from economizers' outlet) for the conventional configurations as in Fig.7.2.

(2) For ChGT systems, the gases of the entire discharge rich and lean gas turbines are either directed to the HRSG then HRVG as for conventional configurations as in Fig. 7.8. Alternatively, either one is directed to HRSG while the other to the HRVG as represented by Fig.7.9 and Fig.7.10. The heat recovered by the AWM is taken similarly as that for HRSG in regular ChGT cycle.

(3) The GT discharges gases from the successive HRSG component in an integrated HRVG/HRSG configuration as illustrated by Fig.7.14.

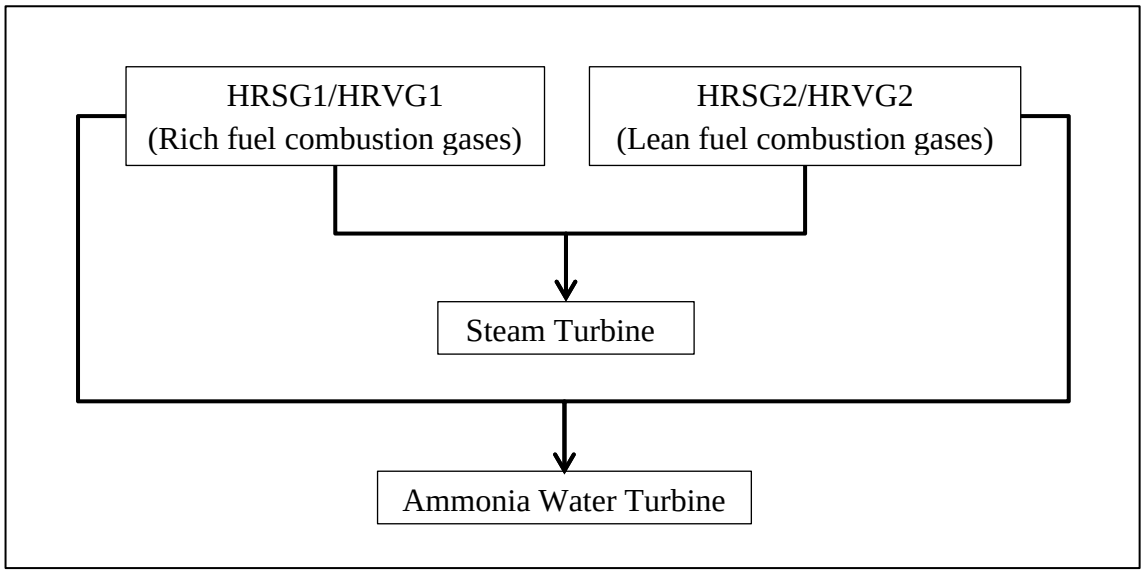

Figure 7.8 The first case of HRSG HRVG integrated to ChGT

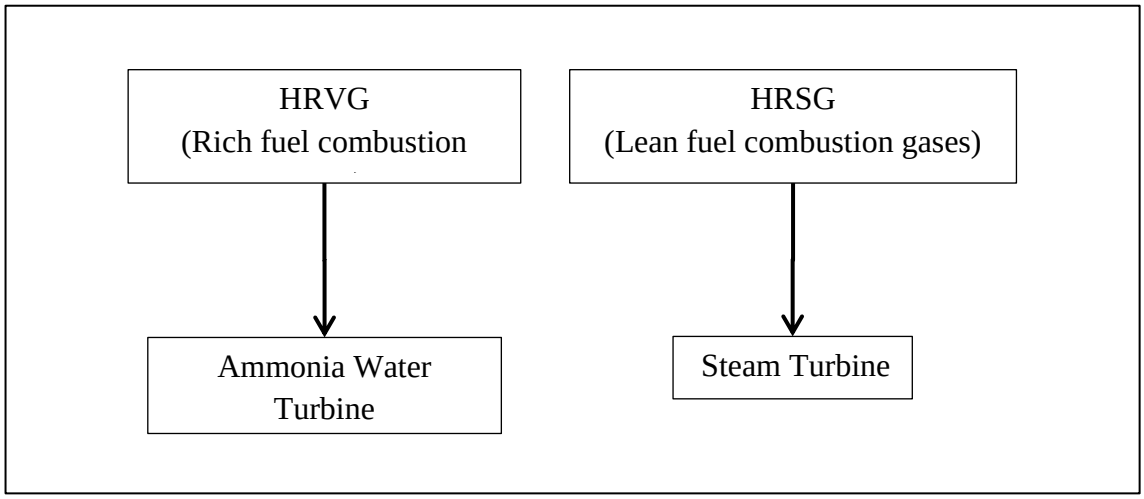

Figure 7.9 The second case of integrating HRSG and HRVG in ChGT

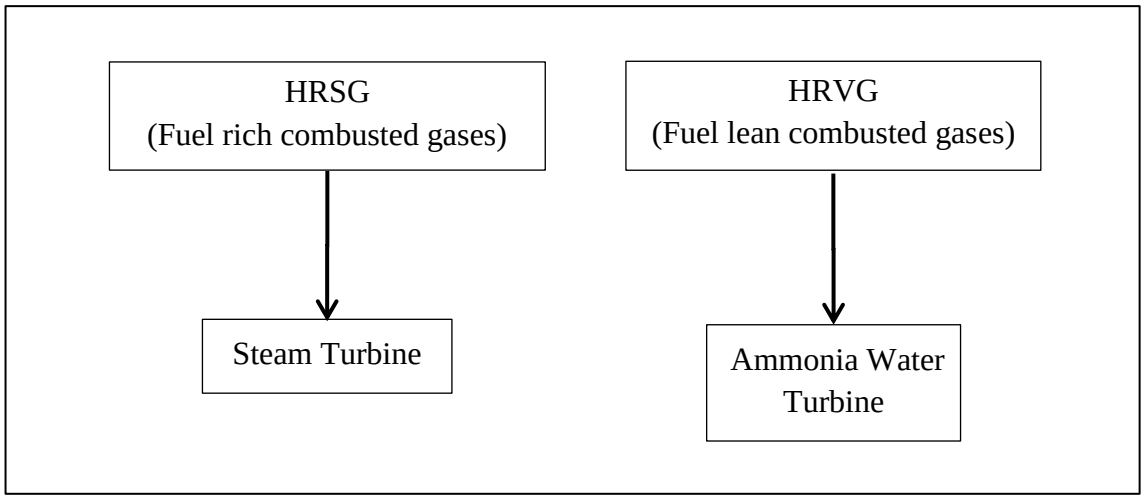

Figure 7.10 The third case of integrating HRSG and HRVG into ChGT

7.3.1 Configurations

In this section, although many configurations were discussed, the configurations on which the parametric study is undertaken are: the simplified Kalina cycle that studied by Marston [40] and the configuration of the Canoga Parck station (in which kalina cycle was firstly used commercially).

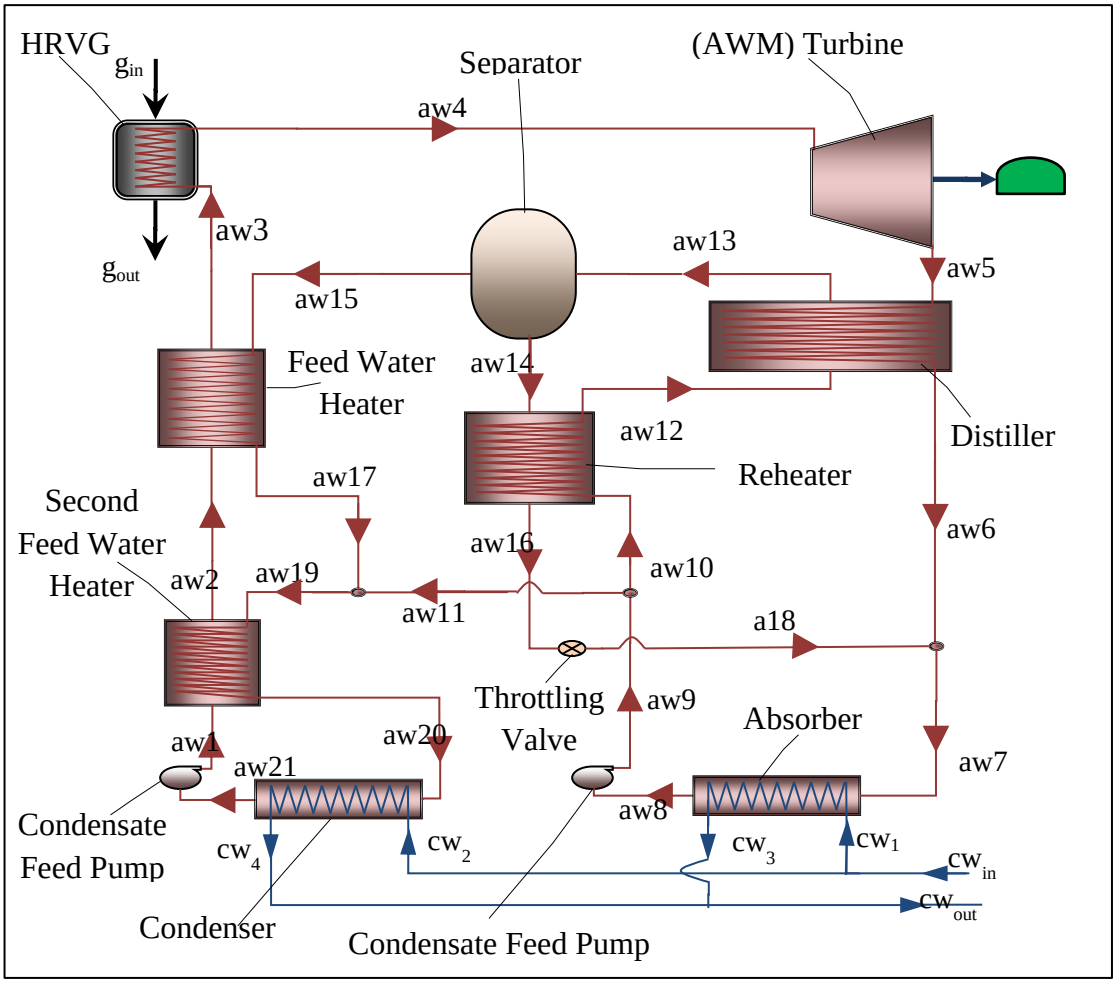

Figure 7.11 The simplified Kalina cycle that studied by Marston [40]

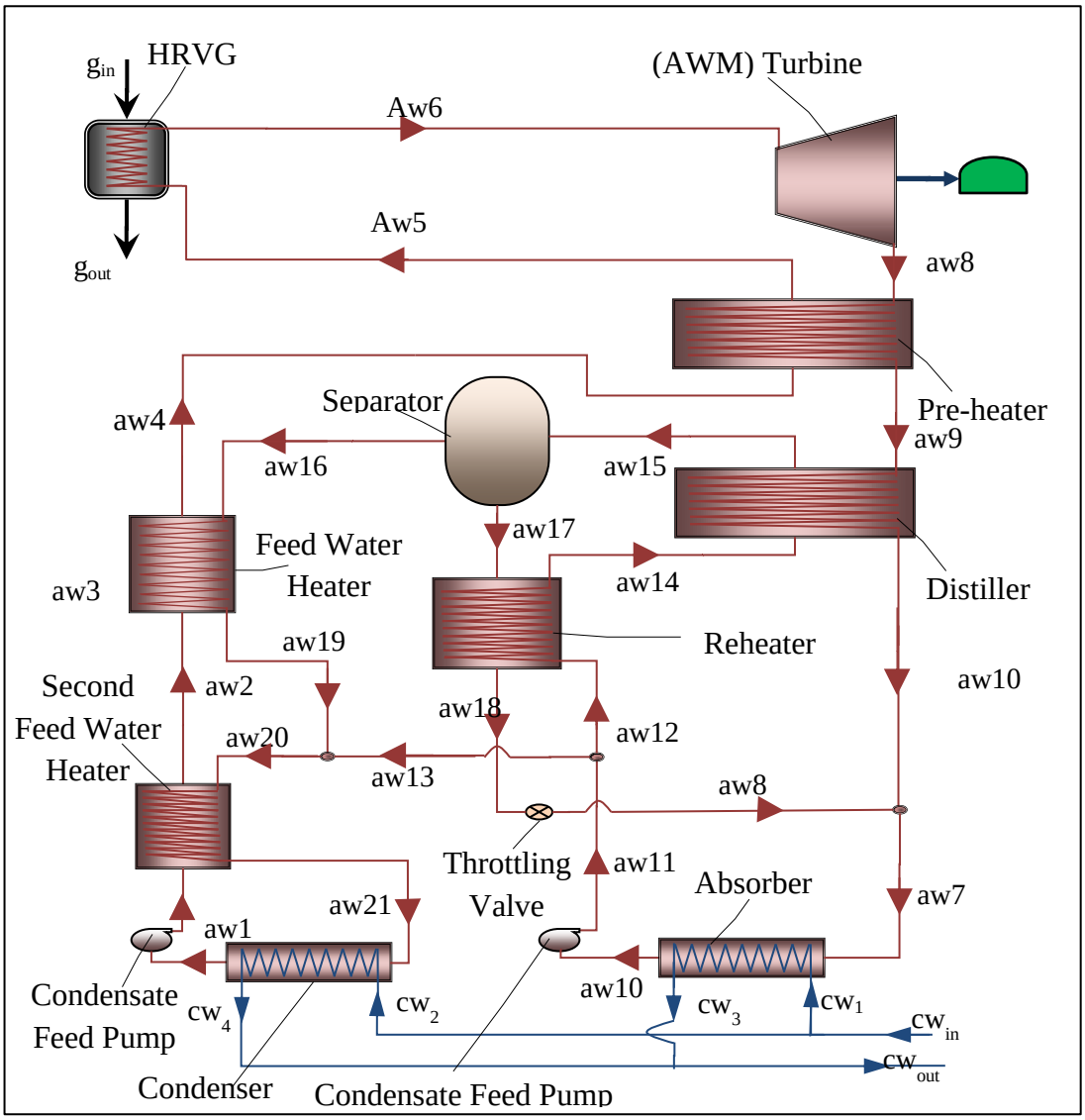

Figure 7.12 Canoga park AWC flow diagram

7.3.2 Ammonia water turbine engine model calculations

The efficiency of the AWC is calculated using the following equation:

$$\eta_{AWC} = \frac{m_{aw1} \times w_{AWC}}{\left(m_a \times (1+F) \times \left(h_{g5} - h_{gstack}\right)\right)} \quad \ldots (7.5)$$

The work generated by the AWT is determined by equation (7.6).

$$w_{AWT} = h_{aw5} - h_{aw6} \quad \ldots (7.6)$$

$$h_{aw6} = h_{aw5} - \eta_{AWT}\left(h_{aw5} - h_{aw6s}\right) \quad \ldots (7.7)$$

Where the enthalpy h_{aw6s} =f (s_{aw6}, P_{aw6}), and the entropies s_{aw6}=$s_{aw\ and}$ s_{aw5}=f (h_{aw5}, P_{aw5})

$$h_{a5} = h_{a4} + \varepsilon_{HRVG}\left(h_{gin} - h_{a4}\right) \quad \ldots (7.8)$$

The function of a separator is to separate an equilibrium state mixture to generate two streams each has a mixture with its own phase (liquid and gas) and mass flow.

$$m_{a15}FG \times \left[x_{aw16} - x_{aw15}\right] = m_{aw5}\left(x_{aw5} - x_{aw15}\right) \quad \ldots (7.9)$$

$$FG = \frac{m_{aw16}}{m_{aw15}} \quad \ldots (7.10)$$

$$m_{aw16}\left(x_{aw16} - x_{aw15}\right) = m_{aw5}\left(x_{aw5} - x_{aw15}\right) \quad \ldots (7.11)$$

$$\frac{m_{a15}}{m_{a5}} = \frac{x_{a5} - x_{a15}}{FG \times \left[x_{a16} - x_{a15}\right]} \quad \ldots (7.12)$$

$$\frac{m_{a13}}{m_{a5}} = \frac{x_{a16} - x_{a5}}{\left[x_{a16} - x_{a15}\right]} \quad \ldots (7.13)$$

Where P_{aw1} is functioned to the temperature and the concentration of ammonia at state 1.

$$P_{a1} = f(x_{a1}, T_{a1}) \quad \ldots (7.14)$$

$$K = \frac{m_{a15}}{m_{a5}} = \frac{m_{a8}}{1 - Z} \quad \ldots (7.15)$$

$$m_{a8} = m_{a17} = m_{a18} = \frac{x_{a9} - x_{a7}}{x_{a8} - x_{a9}} \quad \ldots (7.16)$$

$$m_{a15}\left(h_{a15} - h_{a14}\right) = \left(h_{a6} - h_{a7}\right) \quad \ldots (7.17)$$

$$Z = \frac{x_{a15} - x_{a17}}{x_{a16} - x_{a17}} \quad \ldots (7.18)$$

$$m_{a5} = m_{a6} = m_{a7} \quad \ldots (7.19)$$

$$m_{a15} = m_{a14} = m_{a12} \quad \ldots (7.20)$$

$$x_{a10} = f(P_{a7}, T_{a10}) \quad \ldots (7.21)$$

In the above equations, Z represents the lean solution mass fraction which is ranged between zero and unity (0<Z<1). For the heat recovery steam generator, the temperature of the gases at evaporators' inlet is calculated by equation (7.22). The ammonia enriched vapour and lean solution are calculated by equations (7.23 and 7.26) respectively.

$$T_{gin} = T_{geo} - \left[\frac{\frac{\dot{m}_s}{\dot{m}_a}(h_{fs2} - h_{s2})}{(1+f)Cpg \times \eta_{HRSG}} \right] \quad \ldots (7.22)$$

$$x_{Ev} = X_B + \frac{(X_W - X_B)}{(R_R \times Z)} \quad \ldots (7.23)$$

$$x_{LL} = \frac{(X_B - Z \times X_{Ev})}{(1 - Z)} \quad \ldots (7.24)$$

$$x_{LL} = \frac{\left(X_B (1- Z) - \frac{(X_W - X_B)}{(R_R)} \right)}{(1 - Z)} \quad \ldots (7.25)$$

$$x_{LL} = X_B - \frac{(X_W - X_B)}{(1- Z)(R_R)} \quad \ldots (7.26)$$

7.3.3 Ammonia water turbine engine components modelling

In this section, AWC components are modelled to be used as part of CCPP. Hereafter, it shows how assumptions are made to simplify simulation and what functions are used. Therefore, it shows how deep each model with respect to model specifications.

7.3.3.1 HRVG model

The HRVG utilizes the heat from the gas turbine exhaust. The heat recovery vapour generator performance is satisfied when the components attain the required duty for a certain turbine exhaust temperature and mass flow rate. HRVG components are similar to those in HRSG as in Fig. 7.13 and 7.14.Although its components are more expensive than those by the HRSG.

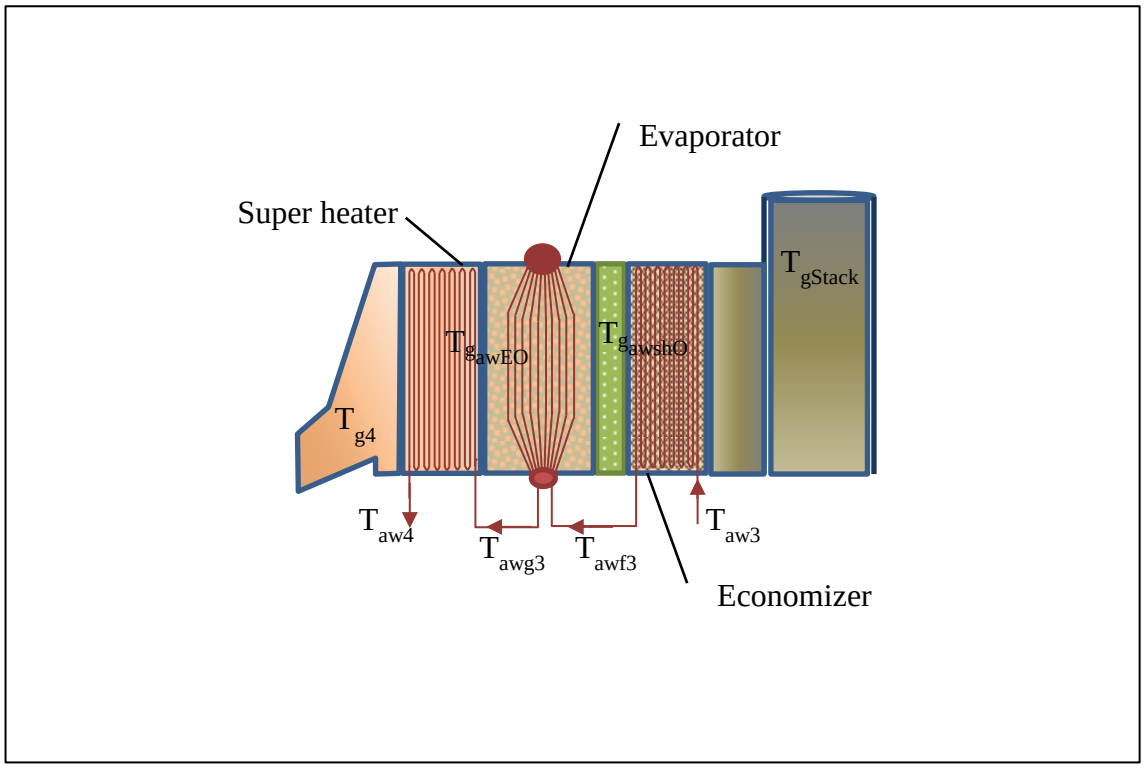

Figure 7.13 HRVG components based in a horizontal flow configuration

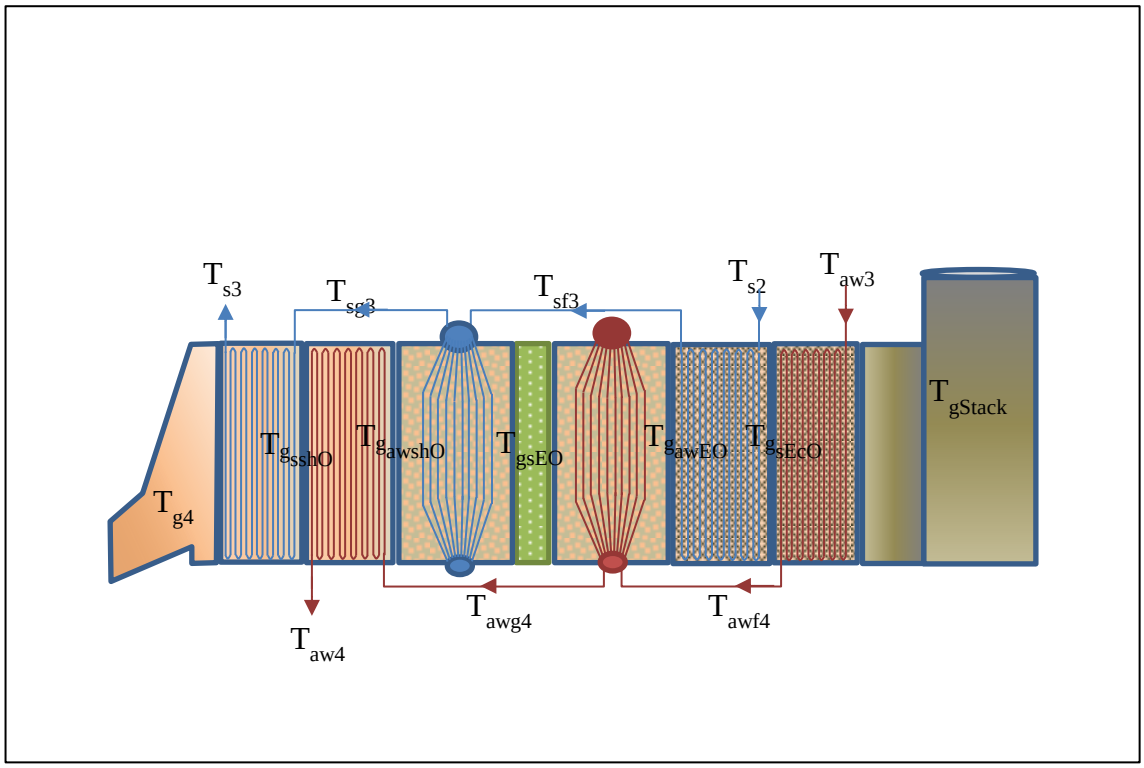

Figure 7.14 Integrated HRVG in a conventional HRSG horizontal configuration

In design, HRVG is also similar to HRSG as shown in Fig. 7.13. In the heat recovery generator, the hydrogen and the vapour water of large amounts increases gases' thermal conductivity and governs the heat transfer. The gases through gas turbine waste heat recover generator usually flue with the pressure of the atmosphere or around its limit and a temperature of (100 to 600 °C). While recovering heat from the gas turbine outlet by AWM is in concept of a temperature range between 200 and 525 °C Srinivas, et al, [43]. Conventional materials like carbon and alloy steel is convenient for HRVG components Ganapathy [88].

For the HRVG model, the mass flow rate of the AWM through the entire HRVG (m_1) is determined using equation (7.27).

$$m_1 = \frac{\eta_{HRVG} \times (1 + f) \times (h_{g5} - h_{gStack})}{(h_{aw4} - h_{aw3})} \quad \ldots (7.27)$$

Where,

$$\eta_{HRVG} = \eta_{EC} \times \eta_E \times \eta_{SH} \quad \ldots (7.28)$$

The enthalpy of the stack gases (h_{gStack}) is determined using the previously made GCF1 as a function to T_{gstack} and $\phi_{CC\ of\ the}$ fuel lean combustion products. While it uses GCF3 if the gases are the fuel rich combustion products.

(A) Economizer

In the economizer as in the steam cycle, the model requires a saturated liquid AWM discharge to full fill economizer duty. Therefore, the enthalpy h_{faw3} is estimated using the function hBFXP at the working concentration and the evaporator pressure. As in the HRSG economizer, the temperature of stack gases is determined using the effectiveness relation of equation (7.29)

$$T_{gstack} = T_{gEO} + \varepsilon_{Ec} \times (T_{gEO} - T_{aw3}) \quad \ldots (7.29)$$

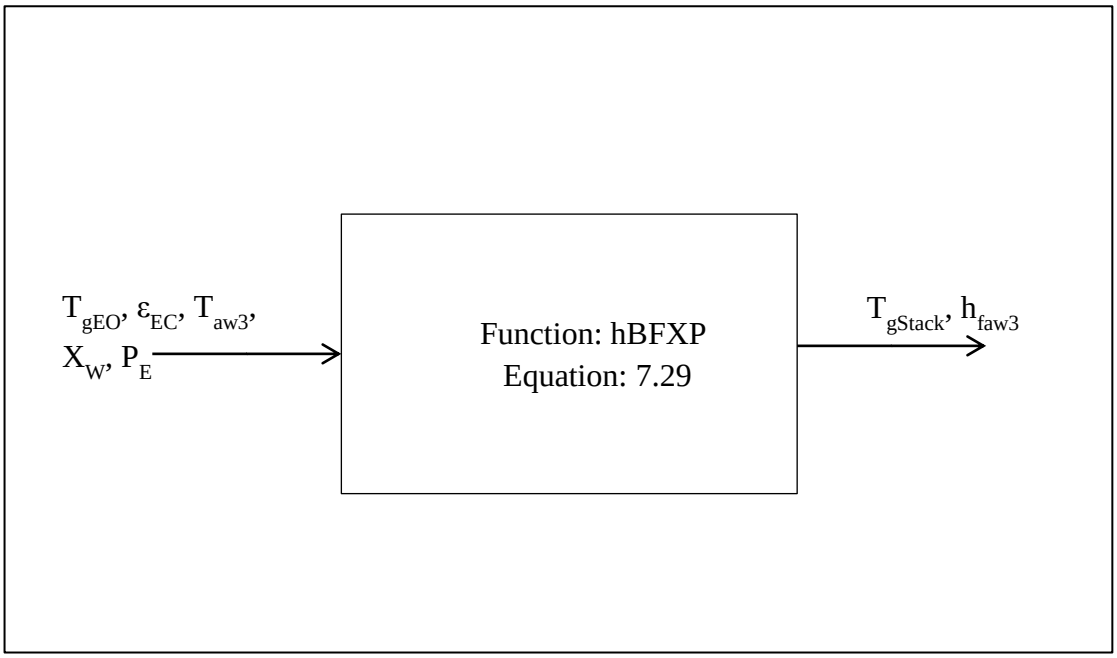

Figure 7.15 Flow diagram of AWC economizer model

(B) Evaporator

At the evaporator, it assumed that, the mixture enters the evaporator as a saturated liquid and discharges as a saturated vapour. Due to the boiling process of the two phase's mixture, on the vapour side the pressure drop is on the order of (6.9 bar) Ganapathy [88]. Therefore, this model neglects such pressure losses.

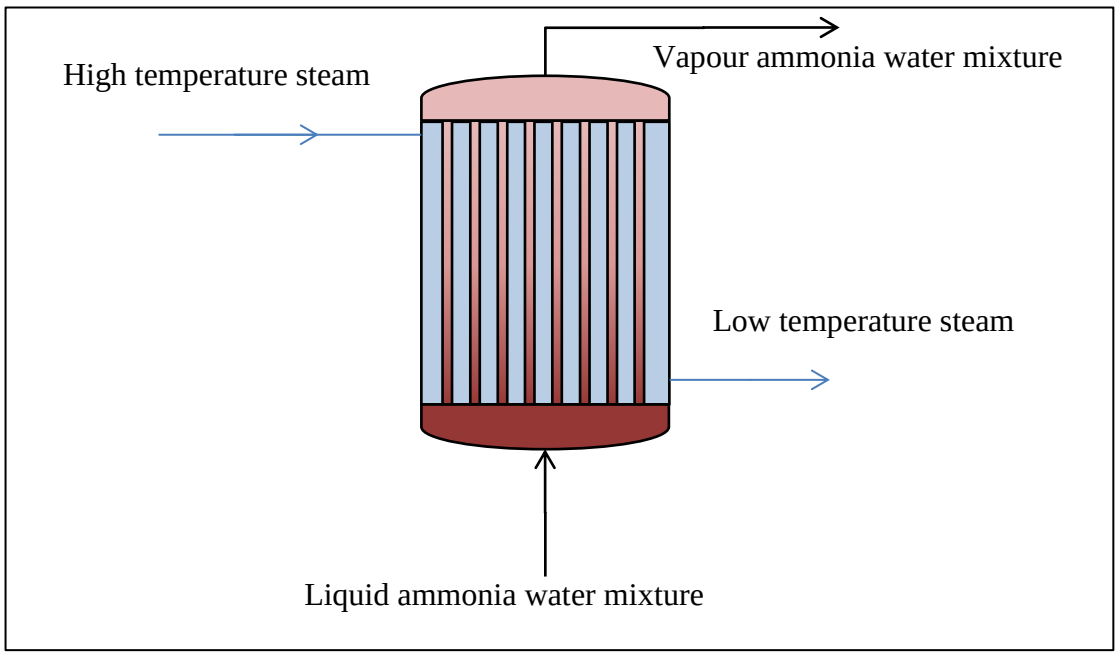

Figure 7.16 Steam/ ammonia water evaporator

Accordingly, the function hDFXP is used to estimate h_{gaw3} for the certain working concentration (X_W) and evaporators pressure (P_E). The temperature of the gases at the evaporator outlet is determined by:

$$T_{gEO} = T_{faw3} + \Delta T_{ppm} \quad \ldots (7.30)$$

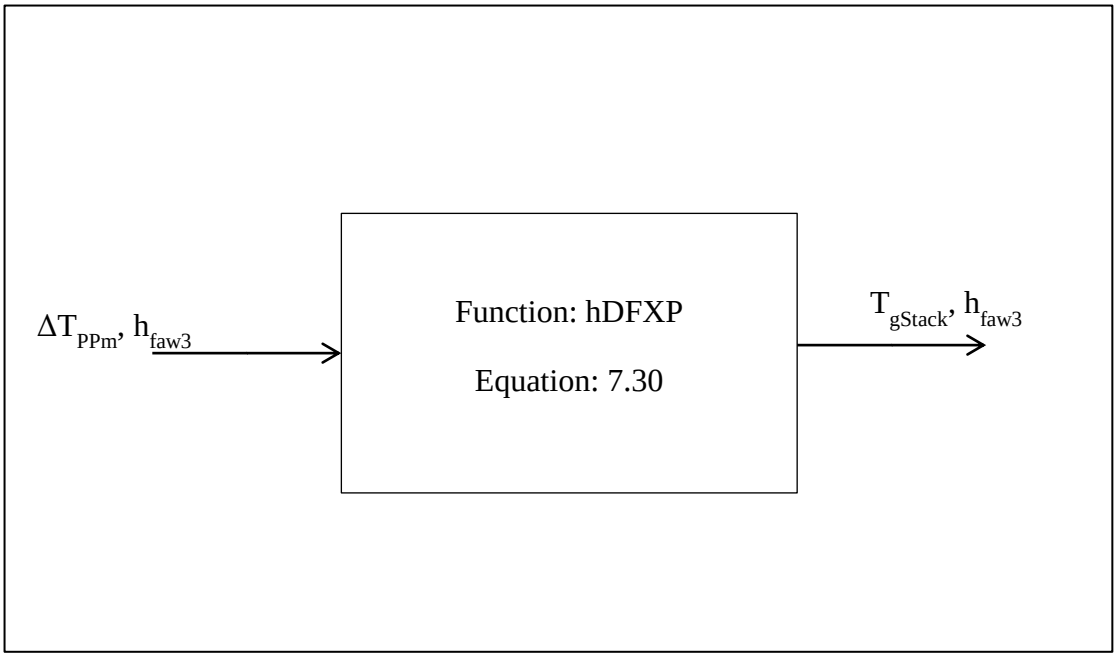

Figure 7.17 Flow diagram of AWC evaporator control model

(C) Super-heater

Super heater model is similar to that for the steam turbine engine in which the input AWM is assumed to be saturated vapour and the exhaust must be superheated to satisfy its duty. In order to use the effectiveness equation for the super heater equation (7.31), the enthalpy of the AWM is estimated using the function hFPTX at the pressure of the evaporator with the working concentration and the temperature of the gases.

$$h_{aw4} = h_{gaw3} + \varepsilon_{SH} \times \left(h_{awTg5} - h_{gaw3} \right) \quad \ldots (7.31)$$

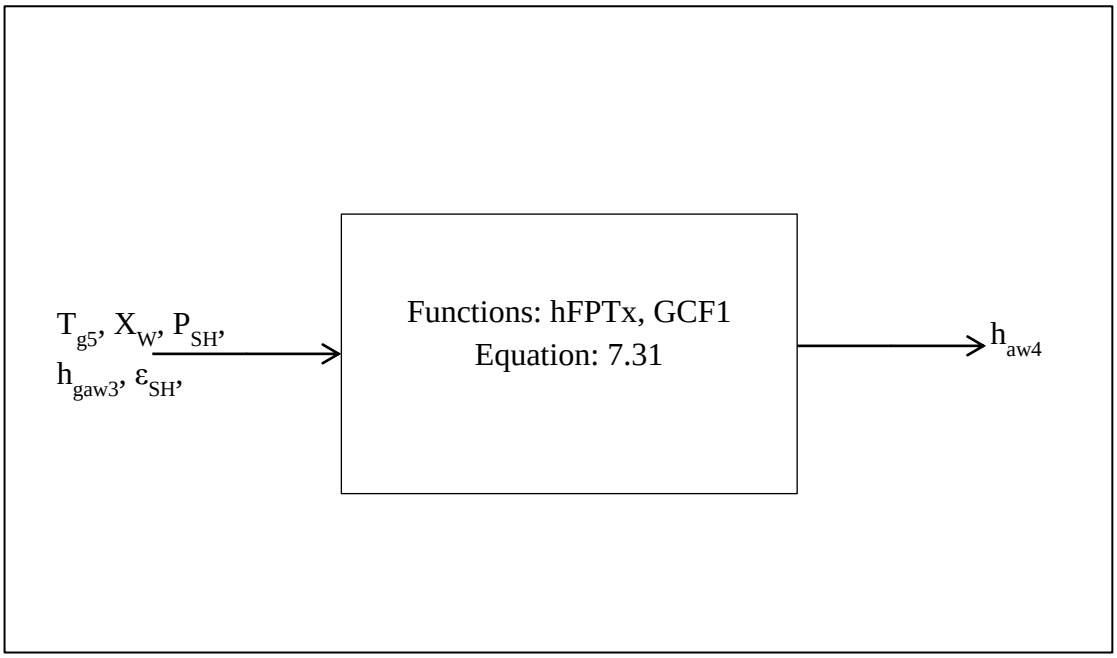

Figure 7.18 Flow control diagram of AWC super-heater model

7.3.3.2 Turbine model

Turbine inlet pressure is considered with regard to the design specification Marston [40]. Therefore, the ranges given by this model are considered with respect to the previous studies and the typical real turbines. In Canoga Park station, the condenser down the turbine was working with an ammonia mass concentration of 42%. Such leaner composition gave the fluid the ability to condensate at lower pressure than that for the same concentration. Therefore, the power output from the turbine itself was boosted. As in the steam turbine work output, as low as the back pressure as greater as the work generated by the AWT. The enthalpy of the AWM at turbine outlet and the specific work output are given by equations 7.32 and 7.33 respectively, which construct the process in the model of Fig. 7.19.

$$h_{aw5} = h_{aw4} - \eta_{AWT} \left(h_{aw4} - h_{aw5s}\right) \quad \ldots (7.32)$$

$$w_{AWT} = m_{awa} \times \left(h_{aw4} - h_{aw5}\right) \quad \ldots (7.33)$$

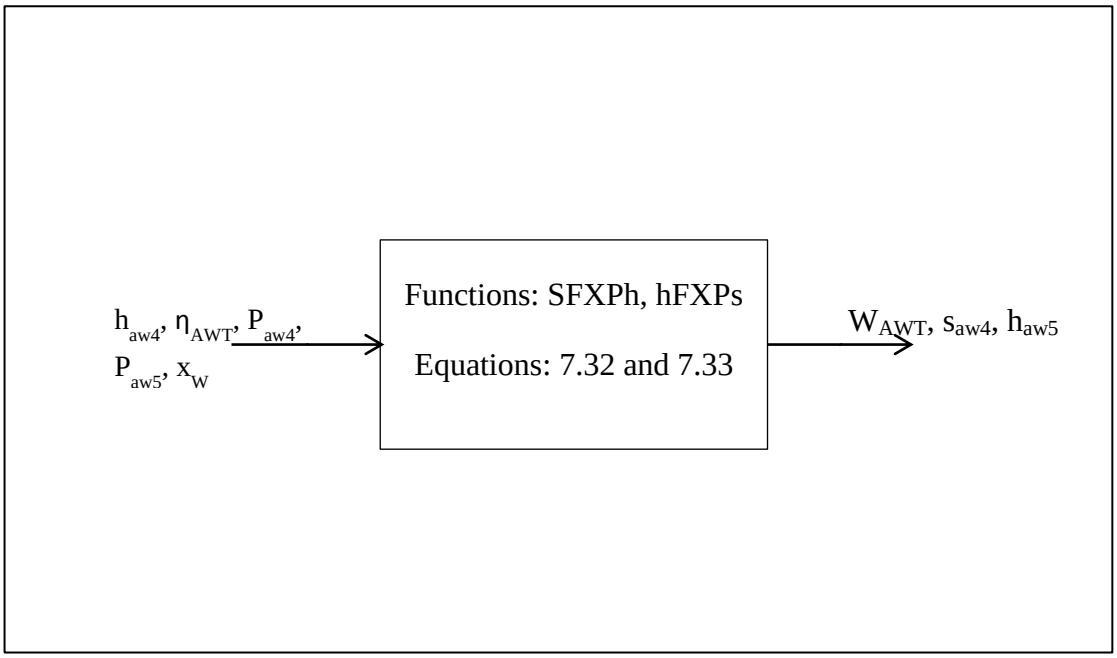

Figure 7.19 Flow chart of AWC turbine model

7.3.3.3 Condenser model

An approximate limit of 120 kW was lost by the Canoga Park station condenser due to its specifications, which were cross flow horizontal. Accordingly, engineers learned that, it should be designed based on vertical counter flow instead Leibowitz and Mirolli [85].

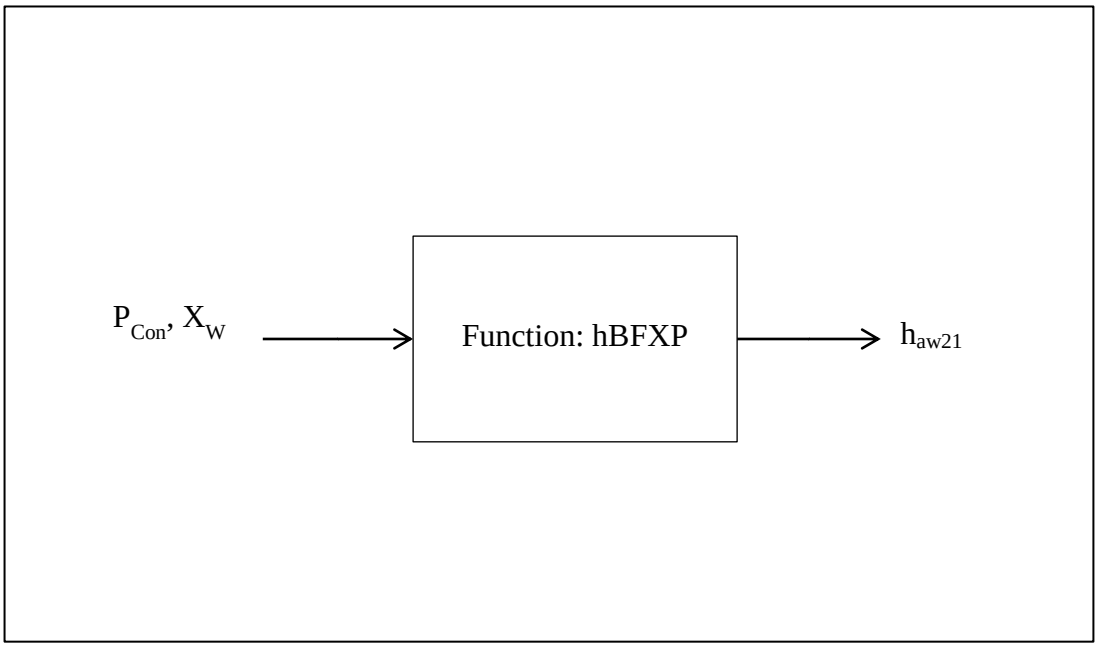

Figure 7.20 Flow chart of AWC condenser model

In this model, the condenser uses cooling water to drop down the temperature of the weak solution before it enters the pump. Here it is assumed, that the mixture is to be cooled to saturation liquid at the condenser outlet. This model is similar to that for the absorber, the same limits are observed here, but with different (x) and (P). Accordingly, the heat required to cool the AWM is different from that for the absorber even when both are operating on the same pressure.

7.3.3.4 Absorber model

Cooling water is not useful to condense the mixture at the turbine outlet due to the high concentration of the ammonia, which requires a very low medium temperature. Therefore, the pressure is increased, and the turbine output is reduced. On the other hand, the mixer reduces the ammonia concentration level to (X_B), therefor the pressure of absorber is decreased and more power is gained than before. The need for dearration is minimized when the back pressure is above the atmospheric pressure. If determined by a temperature of 20°C from cooling water of 15°C and ΔT_w of 5°C. In this model, the mixture leaving the absorber is considered saturated liquid. The mixture at the absorber outlet is assumed saturated liquid. The temperature of the cooling water has to satisfy the above condition. This limits the solution to the minimum heat rejection by which the state of AWM at absorber's outlet is between sub cooled (compressible liquid) and the saturation line at the same concentration and Pressure.

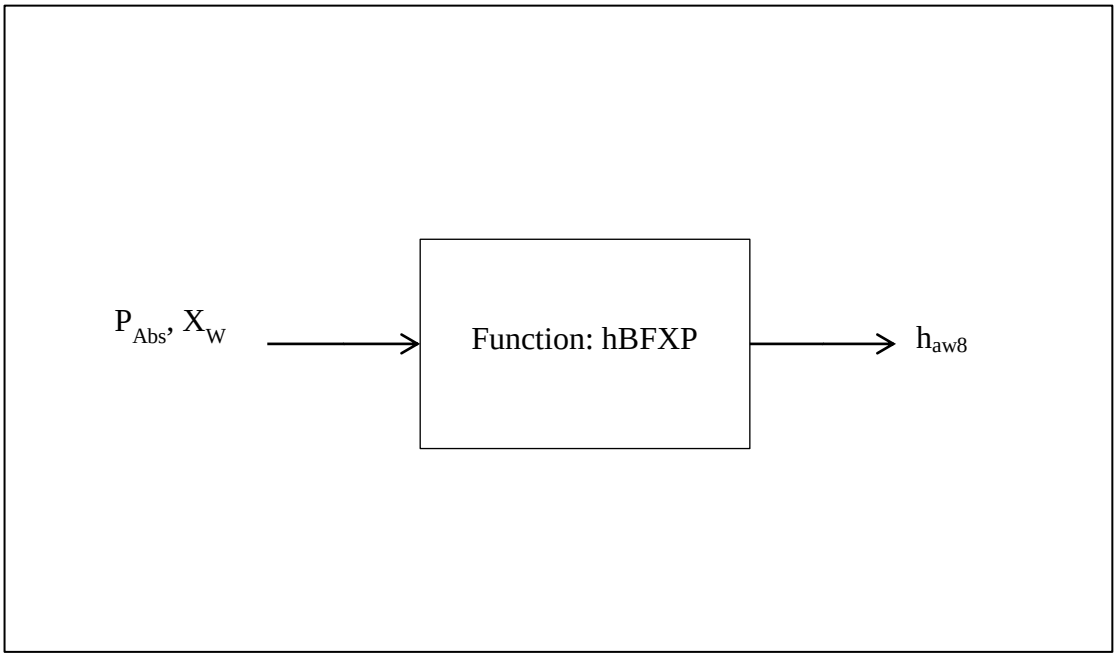

Figure 7.21 Flow chart of AWC absorbers model

7.3.3.5 Distiller (vaporizer) model

It is a counter flow heat exchanger, in which the heat is transferred from the hot AWM vapour from turbine outlet to the basic solution mixture at saturation from the re-heater outlet. Accordingly, the AWM basic solution status must be transferred into the two phase region. Therefore, most of the vapour in this AWM is basically ammonia, while most of the liquid is water content. The mixture from turbine outlet is not expected to experience any change in phase specially before mixing with the liquid lean mixture. The stream which undergoes a change in the phase is the cold stream. Therefore, its heat content is assumed to the minimum here. Its job is to recover the heat from the turbine outlet and use it to vaporize ammonia of the AWM. By this model, the enthalpy of AWM at the distiller outlet is calculated by equation 7.34 using the enthalpies of the saturated mixtures at each end of the separator outlet. However, models' inputs, outputs, functions and equation are illustrated by Fig.7.22.

$$h_{aw13} = h_{aw12} + \varepsilon_{Dis} \ (h_{aw5a} - h_{aw12}) \quad \ldots (7.34)$$

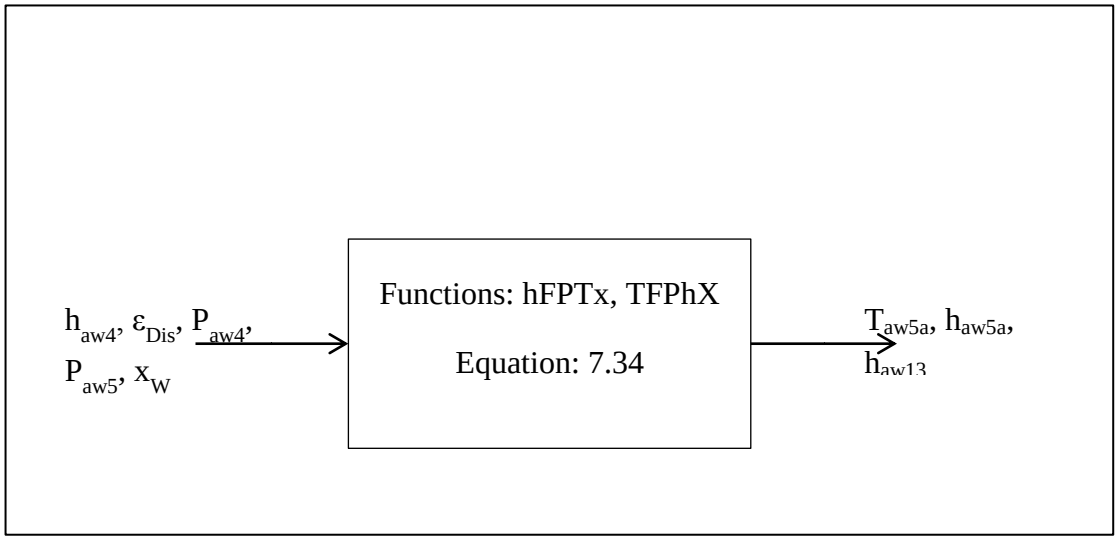

Figure 7.22 Flow chart of AWC distiller model

7.3.3.6 Separator (flash tank) model

Separator is required to remove the remaining liquid in the AWM, which is mostly water. Therefore, it is simulated here to separate the basic solution AWM into two streams. The first is ammonia enriched vapour which heads to the condenser. The second is lean ammonia liquid, which directed to the absorber. This component is modelled to operate on constant

pressure and temperature but to generate mixtures of different concentrations. Accordingly, the properties of AWM at separator outlet as a vapour end is assumed saturated gas, while the property of the other end is assumed saturated liquid. Figure 7.24 shows the operation of this component model on T-X diagram for a certain pressure. The functions hDFXP and hBFXP are used to determine the values of the enthalpies of the AWM at the boiling and the dew point for the same ammonia concentration and pressure, as shown by Fig.7.23.

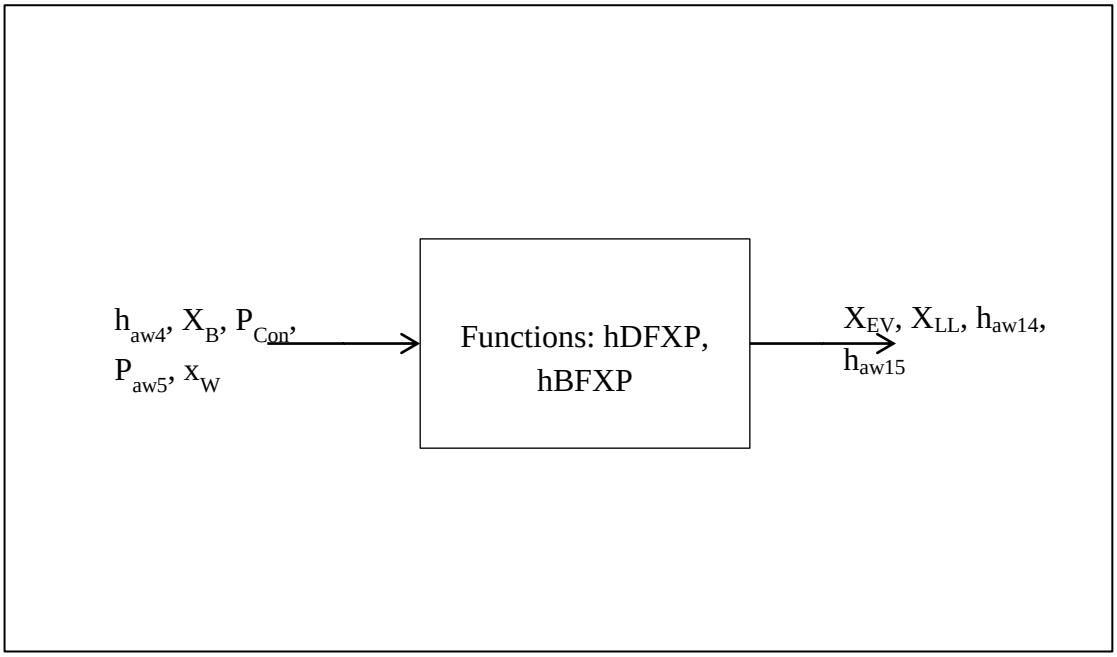

Figure 7.23 Flow chart of AWC separator model

7.3.3.7 Pumps model

The pump is modelled here as it was modelled for the steam turbine engine before. Pumps in this model are assumed to operate while the working fluid concentration remains unchanged.

7.3.3.8 Expansion valves model

In this model, the expansion valve duty is to reduce the pressure of the lean solution from the separator to the pressure of the absorber. As in the expansion valve, the enthalpy is usually constant, h_{aw18} =haw16.

7.3.3.9 Feed heaters model

In this model, the temperature change in the first feed heater is assumed to be fixed; therefore, the change in AWM temperature at feed heater outlet is determined by equation (7.35):

$$T_{aw17} = T_{aw15} - \Delta T_{aw15,17} \quad \ldots (7.35)$$

In order to determine the vapour content in the AWM at the condenser pressure and the working concentration, equations (7.37) and (7.38) are used, after finding T_{gaw17} and h_{gaw17} using the function TDFXP and hDFXP respectively. Furthermore, the magnitudes of T_{faw17} and h_{faw17} are estimated using the functions TBFXP and hBFXP respectively. Figure 7.24 shows such process on T-X diagram for constant pressure.

$$X_{gaw17} = \frac{(T_{aw17} - T_{faw17})}{(T_{gaw17} - T_{faw17})} \quad \ldots (7.36)$$

$$h_{aw17} = h_{faw17} + X_{gaw17} \times (h_{gaw17} - h_{faw17}) \quad \ldots (7.37)$$

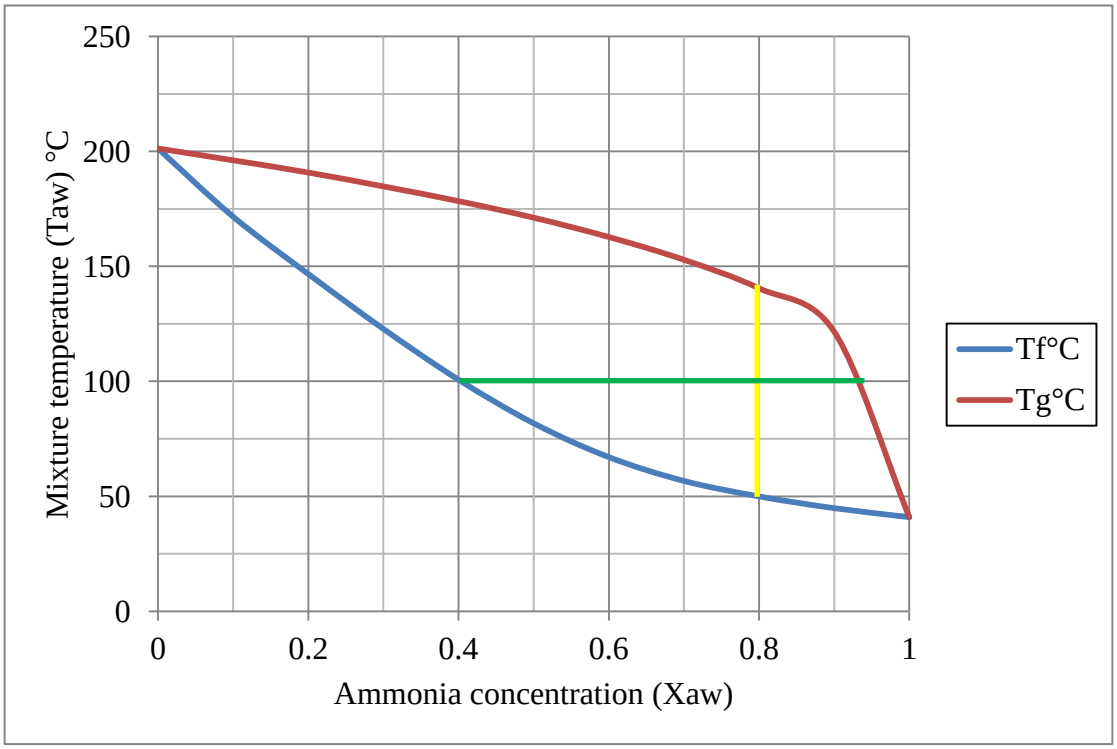

Figure 7.24 Processes of separator and the feed heater for a certain

7.3.3.10 Reheater model

In this model, it is assumed that, the re-heater heats the sup-cooled mixture from the absorber pump outlet to saturation in a constant pressure process.

7.3.4 Ammonia water engine model specifications

As it has been considered for the previous chapter, in here, the points of operation and the restricted areas of operation for this model are discussed.

The final AWC model is illustrated here, in which the parameters, limit loops functions, components models, and out puts are simplified.

7.3.4.1 Model restrictions

i. The heat that is given to the AWC should not affect the power generated from the steam turbine. It won't consider solution even when the summation of the both the AWC and that for the SC are greater than that for the SC if there is a reduction in the SC power output.
ii. As in the HRSG in the HRVG model, the state of the mixture at the inlet of the evaporator is assumed saturated liquid, while that for evaporator exit is assumed saturated vapour.

7.3.4.2 Model limitations

i. The concentration of the basic solution must not get greater than of the working concentration similar to the relation between the lean solution concentration and the basic concentration.

ii. The pressure of the AWM at the turbine outlet is limited by the available properties of AWM to a pressure greater than those of steam turbine cycles.

iii. The temperatures of the AWM vapour at the HRVG economizer inlet.

iv. The temperature of the AWM vapour at first feed heater outlet or the heat transfer through this feed heater.

v. The vapour quality of the AWM at the turbine outlet of not less than 90%.

7.3.4.3 Model operating ranges

The ranges and the certain values of the AWT system parameters are given by the following table, including the type and the controller as introduced by this chapter:

Parameter	Type	Range or Value	Controlled by
T_{g5}	Input	350-750°C	limited by the HRSG output
P_{aw4}	Input	20-165 bar	-
X_W	Input	0.42-0.81	-
R_R	Controlling	$(XW-XB)/((1-XB)*Z) < R_R < (1/Z)$	X_W,X_B,Z and R_R
Z	Controlling	$0 < Z < 1$	-
X_B	Input	0.3-0.6	-
P_{Abs}	Input	0.7- 2 (bar)	-
P_{Con}	Controlling	5 – 10 (bar) $P_{Abs} < P_{Con} < P_{aw4}$	P_{Abs} and P_{Con}
ΔTPH	Input	5-20	-
f	Input	-	gas turbine
η_{AWT}, η_{AWP1},η_{AWP2}	Input	0.6 – 0.92	-
η_{Abs}, η_{Con}	Input	0.6 – 0.8	-
η_{AWC}	Output	-	-
W_{AWC}	Output	-	-

Table 7.1 Parameters ranges for the 1st and 2nd AWC configurations models

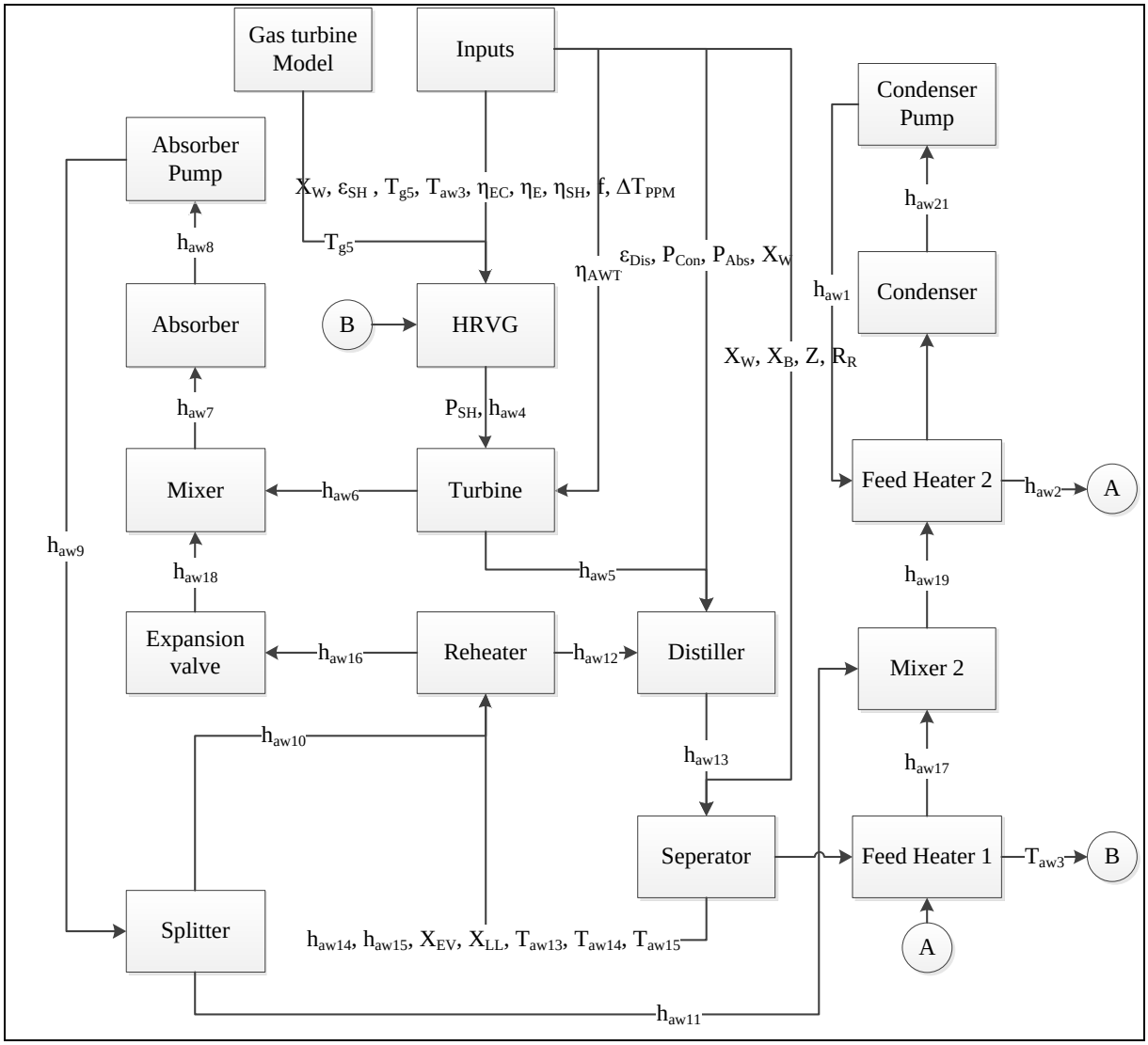

Figure 7.25 Flow chart of AWC simulation model

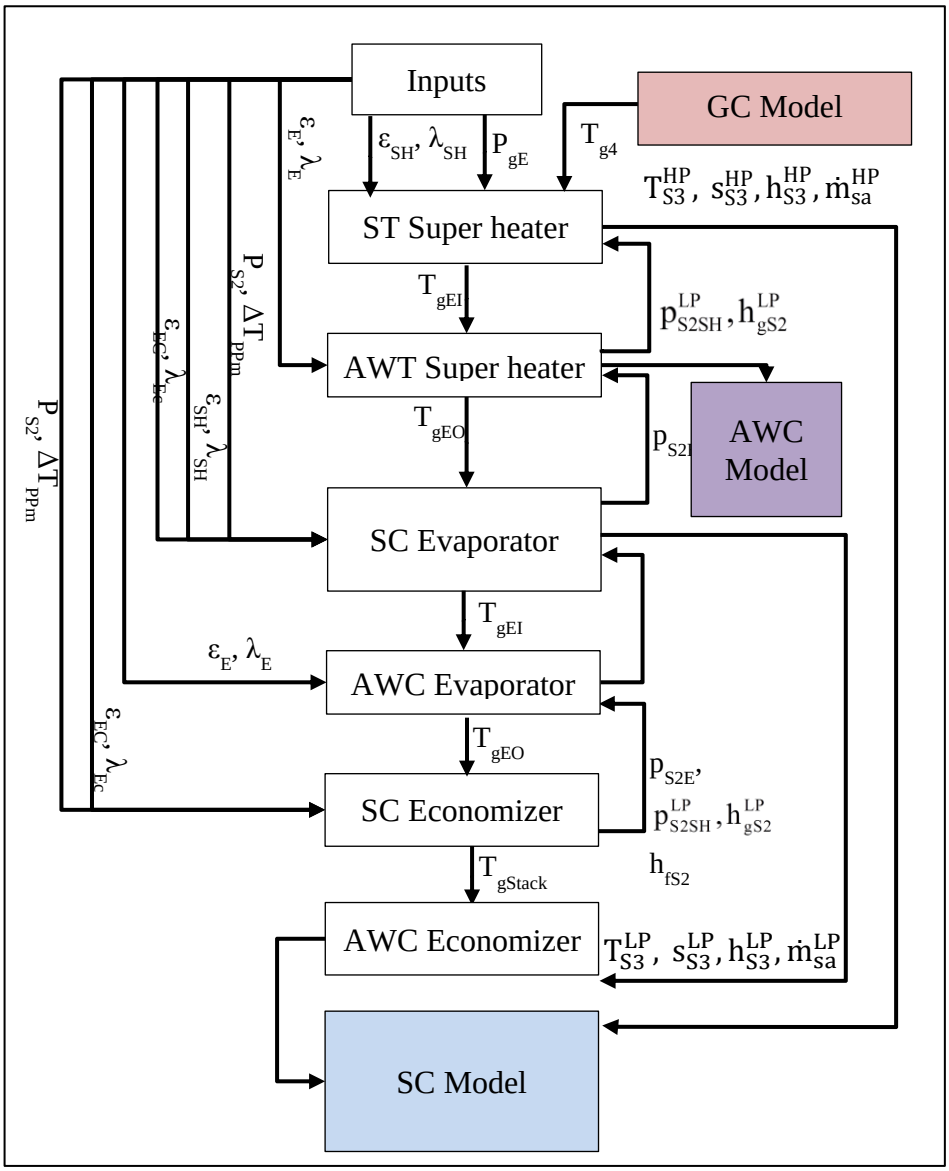

Figure 7.26 Integrated steam\ ammonia HRVG model

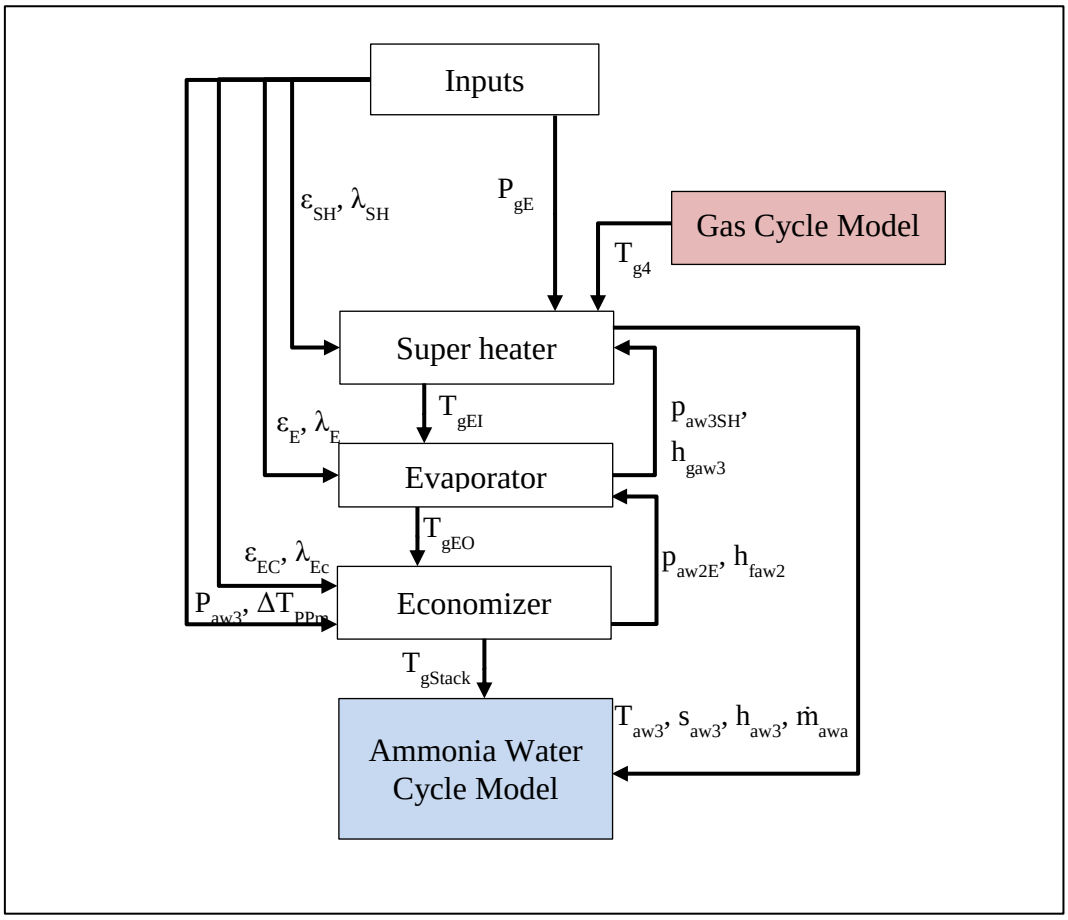

Figure 7.27 Simple AWC HRSG Model

7.3.4.4 Model performance criteria

1. Satisfy an increase in the power generation from the over that for conventional gas /steam CCPP.

2. Satisfy a low temperature of the exhausts.

3. Satisfy better thermal efficiency than conventional gas/steam CCPP when the same temperature form turbine exhaust is utilized.

7.4 Optimizing the ammonia water turbine engine

The following sections discuss the main operating parameters effects on the performance of the AWC, and GC/AWC CCPP. It indicates the parameters those important in optimization and those who have no significant effects on these cycles' performance parameters. The performance parameters of the ammonia-water cycle and gas /ammonia water combined cycle are significantly affected by many parameters. These parameters are X_B, T_{g5}, X_W, T_{aw14}, Z, P_E, P_{abs}, and PCon, which are studied here comprehensively. This was to investigate its effect on

the performance of the CCPP in addition to its effect on the AWC. In this parametric study on the KC the optimization is undertaken regarding the simplicity of the components as reviewed above and the superiority in the performance as shown in what follow as it has been recommended by [40].

7.4.1 Ammonia water cycle parameters effect on Kalina cycle's performance

This section investigates the thermal efficiency and the specific work output of CCPP and AWC regarding the effects of AWC operating parameters.

7.4.1.1 Kalina cycle back pressure (absorber pressure (P_{Abs}))

The effect of AWM pressure at the absorber is great on the performance characteristics of the AWC. Such effect increases Kalina cycle thermal efficiency by 3 percentage points, while it boosts the specific work output to about 15% when P_{Abs} is reduced from 4 to 1.5 bars. Such effect is similar to that occurs by the effect of steam turbine condenser pressure. AWM basic concentration has an insignificant effect on both the efficiency and the specific work output. While the fraction of the mass flow that directed to the 2nd feed heater increases by the increase of X_B. This is to maintain constant X_W, however, this ratio hasn't affected by P_{Abs}.

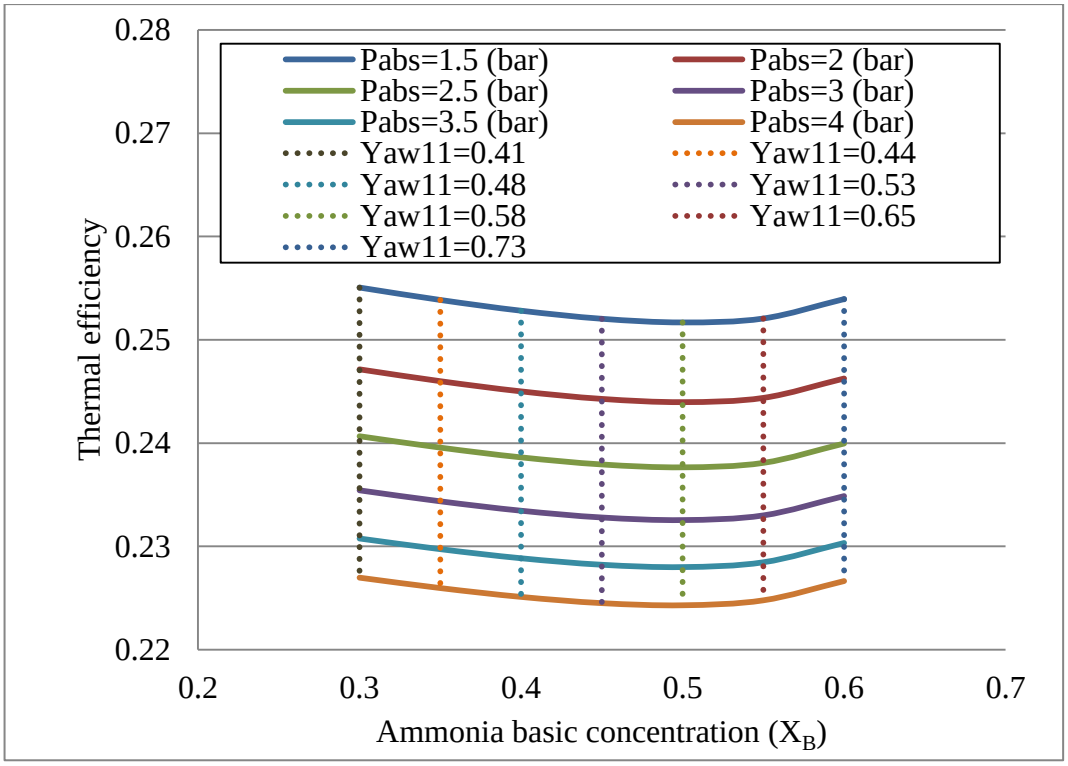

Figure 7.28 KC thermal efficiency versus ammonia basic concentration

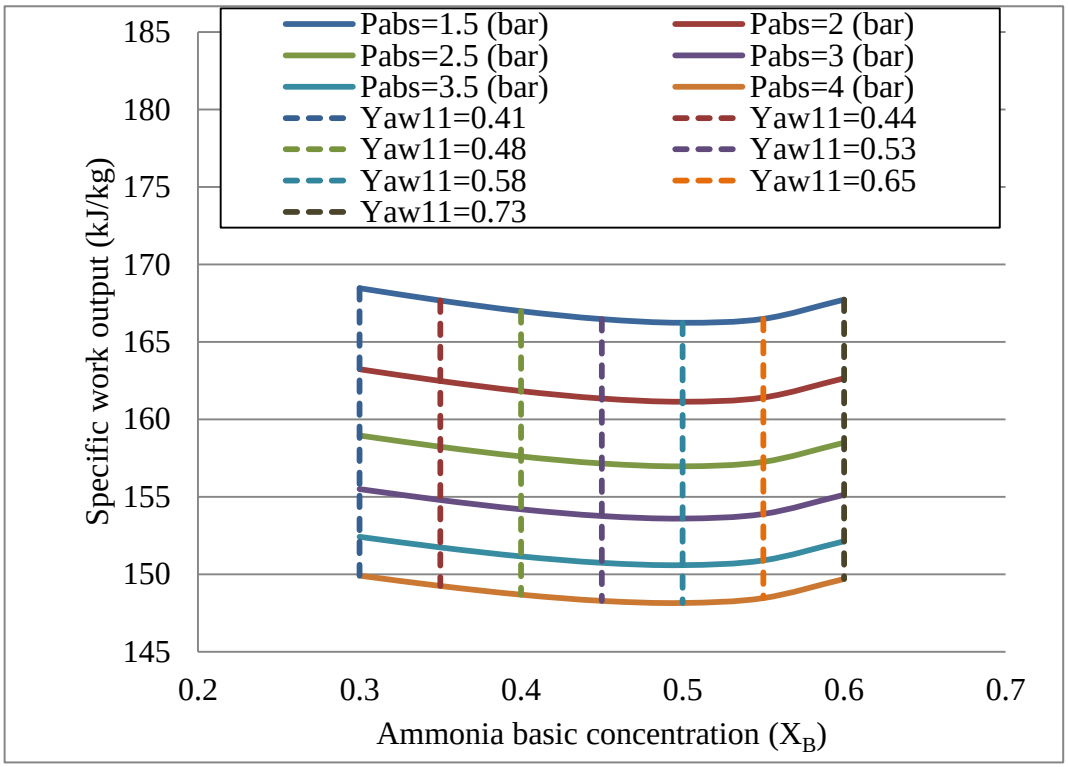

Figure 7.29 KC specific work output versus ammonia basic concentration

7.4.1.2 Kalina cycle turbine inlet pressure and concentration

The effect of AWM pressure through HRVG (P_{Ev}) and the working concentration (X_W) on the performance characteristics of the AWC are illustrated by Figs. 7.30 and Fig.7.31. These figures show the increase of the efficiency (η_{AWC}) and the specific work (w_{AWC}) output of AWC by the reduction of the P_E. While as mentioned before the increase in X_B slightly reduces the both. The decrease in P_E slightly increases η_{AWC} , while it decreases the specific work output which boosted by 7.5% . While a greater increase in the efficiency and specific work output by X_W effect. Such increase can reach 2.5 percentage points of the efficiency and about 7% of the power output. Figure 7.32 shows the effect of gases' temperature from GT discharges (T_{g5}) on the performance characteristics for different X_W. This figure confirms the increase in both characteristics by the increase in T_{g5} for a certain X_W. This effect gets slighter by the increase in X_W. The results here confirm [56] findings of that, the increase of the X_W beyond 0.8455 results in a great increase in the efficiency and the work output of the KC. It also agrees with the findings of [40] about considering the effect of mass flow rate of ammonia at turbine inlet as a performance main parameter. It disagrees by considering separator temperature great effect on w_{KC} but negligible effect on the efficiency of KC.

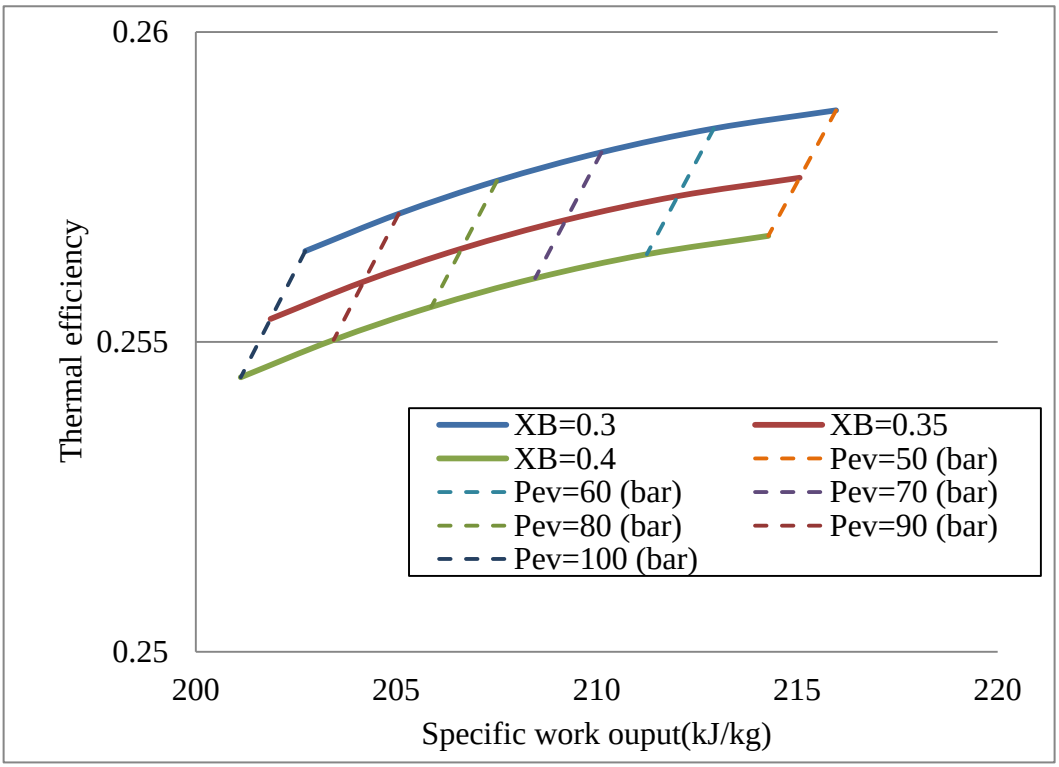

Figure 7.30 The thermal efficiency versus the specific work output for different turbine inlet pressure and ammonia basic concentrations

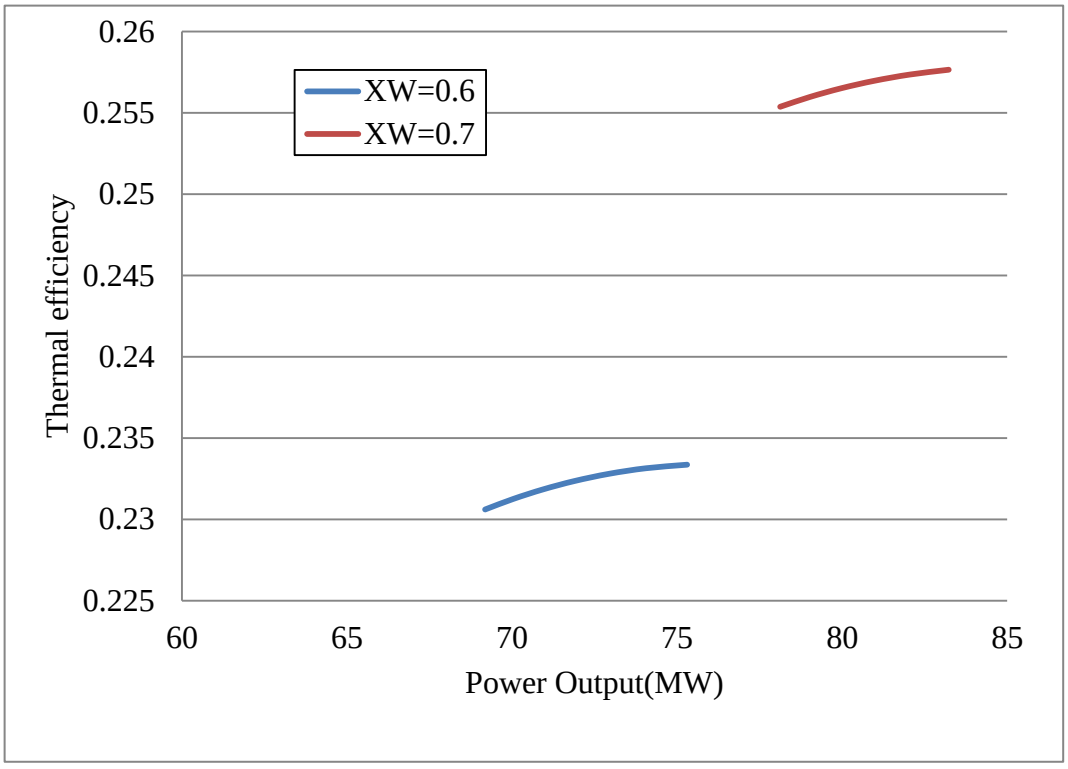

Figure 7.31 The thermal efficiency versus the specific work output for different turbine inlet pressure and ammonia basic concentrations

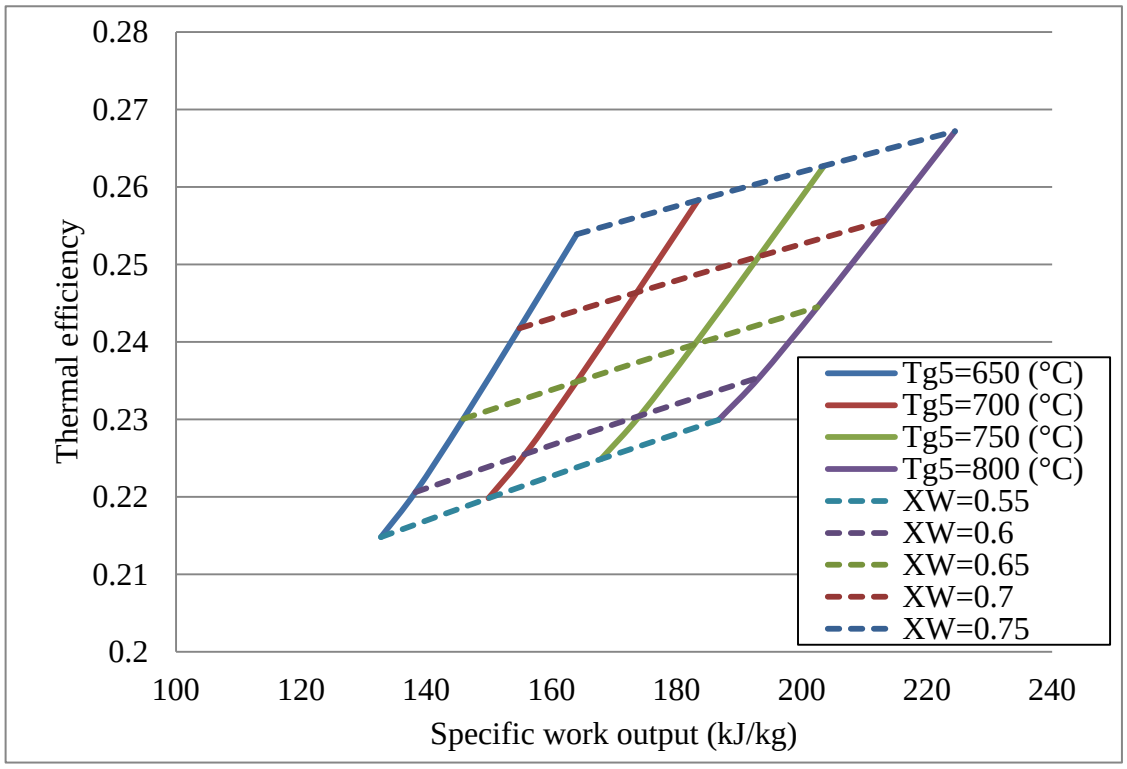

Figure 7.32 The thermal efficiency versus the specific work output affected by gas turbine discharges temperature and turbine inlet ammonia concentration

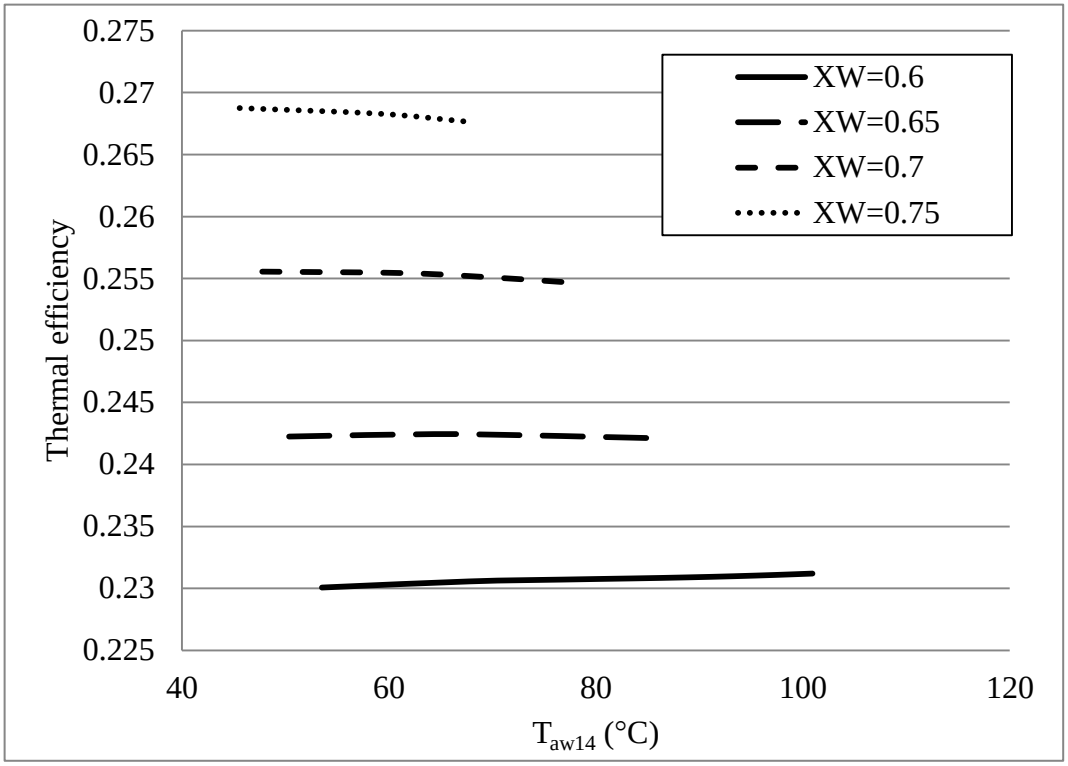

Figure 7.33 The thermal efficiency versus the separator temperature for different ammonia basic and working concentration

Figure 7.33 illustrates the effect of the X_W on the temperature at which the separator is working. It shows that the range of the separator temperature is enlarged by the decrease of the working concentration. By this enlargement, the temperature of the separator can be increased to 20 °C when X_W is decreased from 0.75 to 0.6.

7.4.1.3 Turbine discharge temperature

Figure 7.34 shows the effect of increasing the temperature of the gases from gas turbine outlet on the performance characteristics of the AWC for different P_E. It shows the increase in the thermal efficiency and the specific work output in addition to the enlargement in the power generation range by increasing T_{g5}. The increase in the specific work output was about 0.25% while the increase of the efficiency was about 1.5 percentage points.

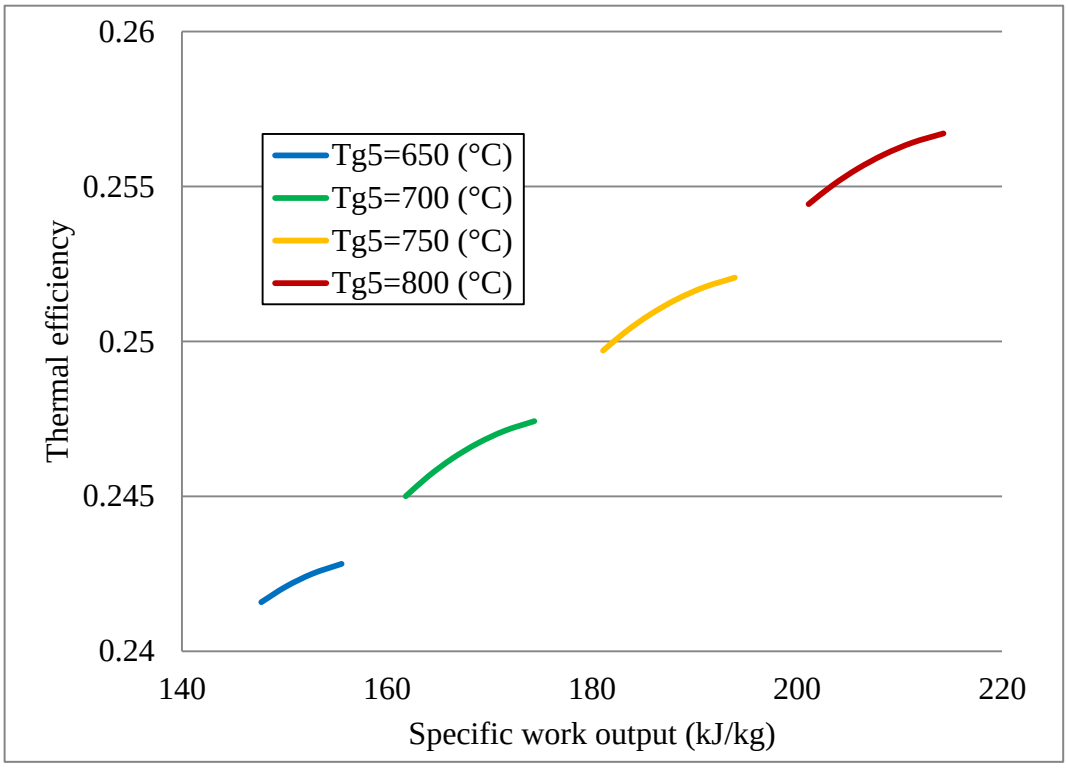

Figure 7.34 The thermal efficiency versus the specific work output affected by HRVG pressure for different gas turbine discharge temperature

7.4.1.4 Lean solution mass fraction (z)

Separator temperature effect on the enriched vapour and the lean solution concentrations are depicted by Fig. 7.35. It shows a slight decrease in the enriched vapour concentration as the separator temperature increase. It also shows a very slight decrease in the lean solution concentration by the same effect.

The effect of the lean mass fraction (Z) on the performance characteristics of the AWC are depicted in Figs. 7.36 and 7.37. The first shows the increase of thermal efficiency of the AWC by increasing the Z, similarly, the second shows the increase in the specific work output by such increase. The increase of the thermal efficiency can get as large as 1.6 percentage points. The increase in the specific work output is boosted by 6 % when z is increased from 0.4 to 0.6.

The effect of Leansolution mass fraction on the AWM mass flow rate for 1 kg of air is illustrated by Fig. 7.38. In this figure, it is also shown how X_B affects this mass ratio for any certain Z value. It confirms X_B effect on the AWM mass flow to the turbine, which has a great effect on the power generated by the AWT and there is a certain value of X_B of the minimum mass ratio. It also confirms the maximum mass ratio for the greatest X_B value. However, the most important was the significant increase of such mass ratio by increasing Z.

By any increase in the pressure of the mixture at the turbine inlet increases the efficiency. While it drops with the increase of the ambient temperature and the temperature of the mixture at turbine inlet. It also decreases by the increase in the concentration of the ammonia at turbine inlet. The temperature of Separator has no effect on such efficiency of the combined cycle. Maintaining the high efficiency for ammonia water kalina cycles are correspondent to an ammonia concentration beyond 70% of the mixture at the turbine inlet.

The results here confirm the slight effect of AWM mass flow rate on improving the performance of KC by indicating the slight increase in AWT output and refer the main parameter on such output to pressure difference between the turbine inlet and PCon. This has been confirmed previously by [54] who place this for the AWT performance only.

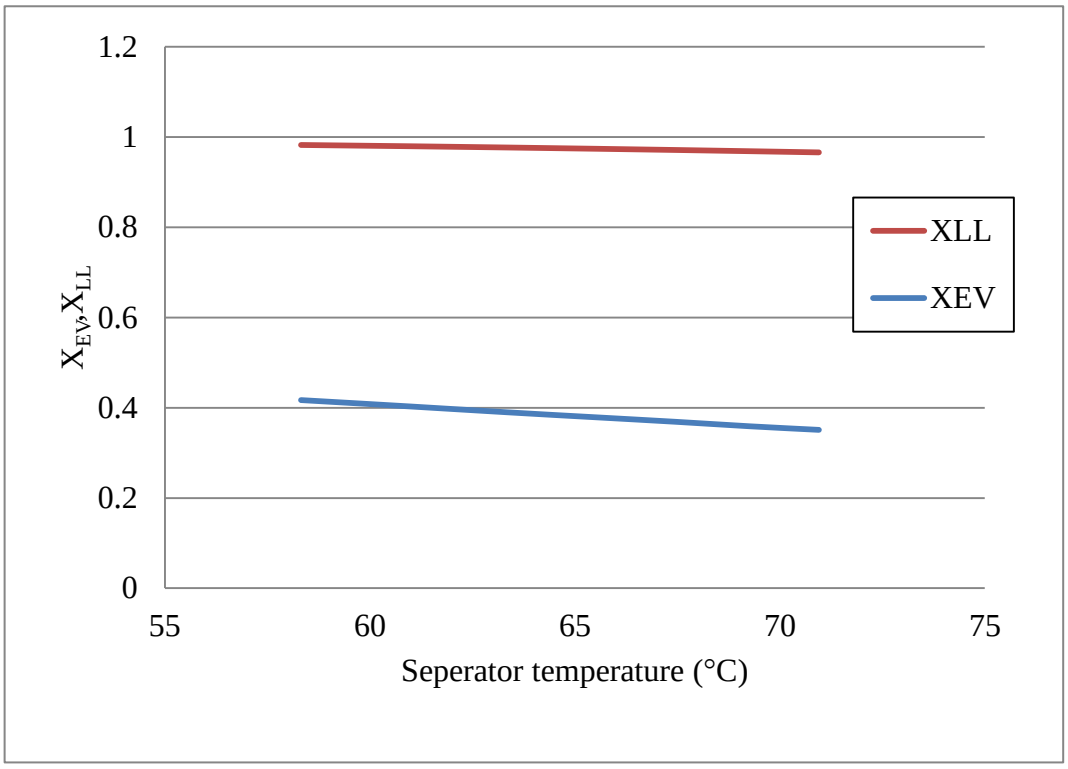

Figure 7.35 Ammonia lean solution and rich vapour concentrations versus separator temperature affected by ammonia lean solution mass fraction

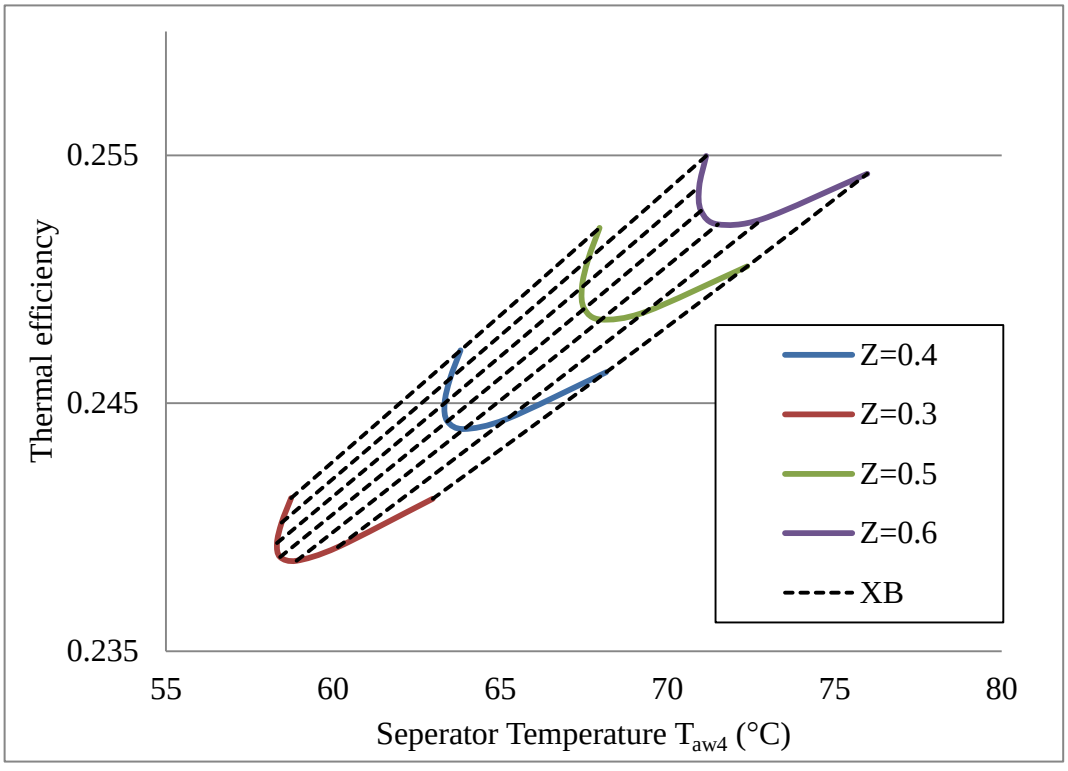

Figure 7.36 The thermal efficiency versus separator temperature affected by ammonia lean solution mass fraction

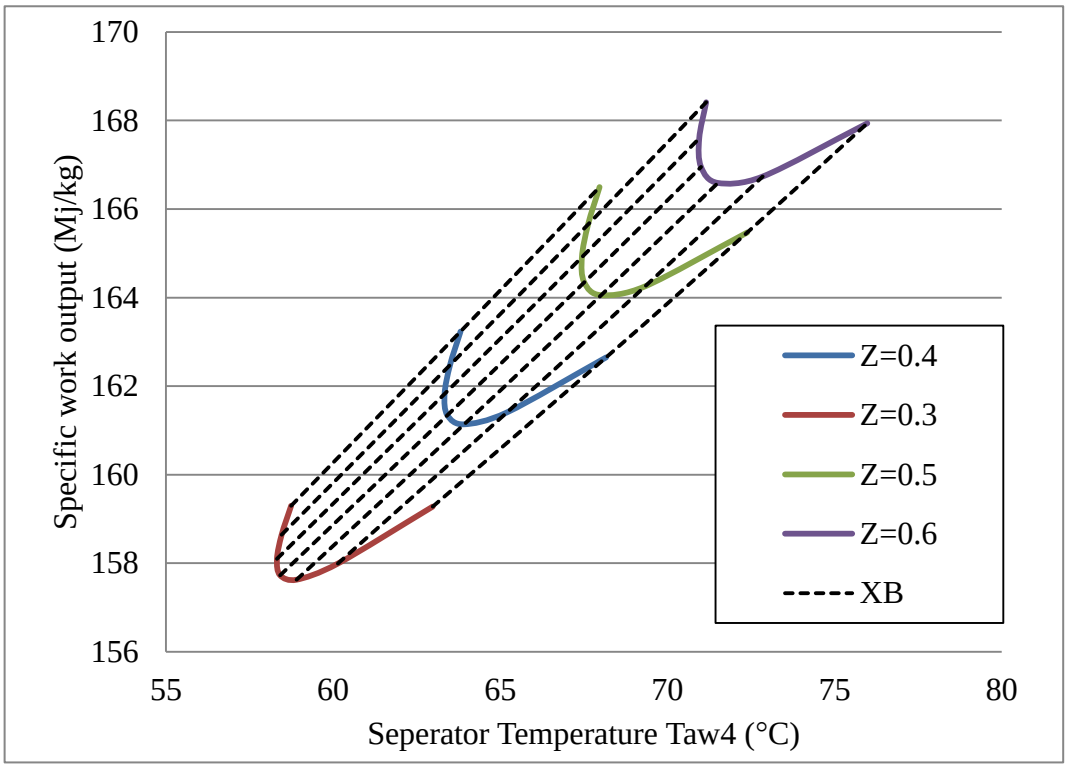

Figure 7.37 Separator temperature effect on specific work output for different Z ratios

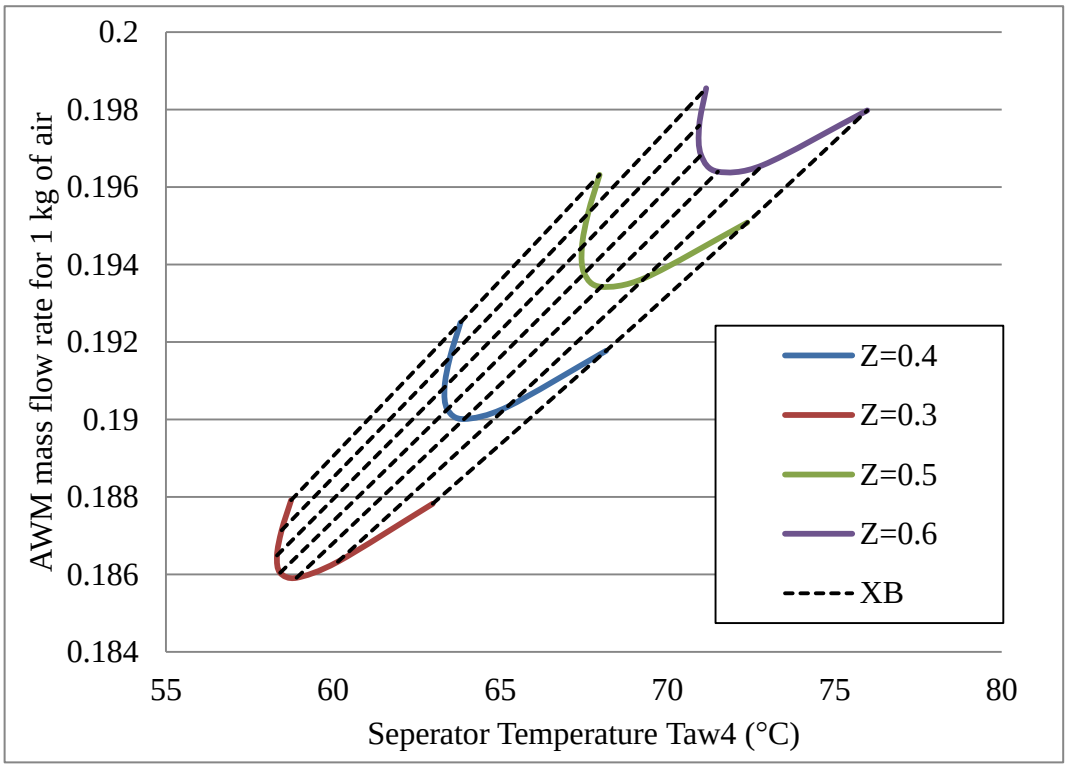

Figure 7.38 Separator temperature effect on AWM mass flow rate for different Z ratios

7.4.2 The results from optimization AWC

The parametric study, optimizing components' parameters results confirm the following:

(1) The efficiency of the AWC was increased by increasing Z, T_{g5}, and X_W. Such efficiency was decreased by the increase of P_E and P_{Abs}. Therefore, to maximize the thermal efficiency, the values of Z Tg5 and X_W are required to be the maximum. While the values of PEv and P_{Abs} must be the minimum. The value of the basic concentration is not of a great importance in maximizing the thermal efficiency of the AWC.

(2) The specific work output from the AWC is maximized by the increasing Z, T_{g5}, X_W XB (after a certain value) and the mass of the AWM at the turbine inlet. It also increases by decreasing P_E and P_{Abs}. Therefore, the optimum of Z, T_{g5} and X_W are the maximum and the optimum from P_E and P_{Abs} are the minimum. Within respect to a mixed fluid, it could be claimed here that, the results were closer to practice by manipulate the P_{Con} than the condensation temperature that was considered by [46].

(3) The mass flow at the turbine inlet is affected by X_B and Z. Therefore, its value is the maximum to maximize AWM turbine power output. Hence, the optimum X_B is the greatest. The maximum XB by the results here is 0.6, which agreed with the findings of Takashita [54] on which XB from experiments and simulation data are to be met. In this study altering XB as an input gave the stronger approach to investigate XB effects on RR and the components where AWM basic solution flows rather than engaging all the results from each component and for a range of RR as reported by [46]. This is more likely to be covered with in experiments.

(4) Lean liquid solution and enriched vapour's concentrations had a very slight effect by the increase in the separator temperature.

(5) The results here agree on dominant parameters on the AWM cycle are Paw4, T_{aw4} and X_W as reported by [46], and the addition of X_B and the multiplication ratio as reported by [38]. In here the results confirm such effect of the above parameters but, not over the temperature of the source whither it was steam or exhaust gases.

7.4.3 AWC parameters' effect on the performance of the gas/ ammonia water CCPP

The performances' characteristics of the gas turbine, the AWC turbine and the Gas/AW CCPP are illustrated in Fig.7.39. This Figure shows the influence of the air compression ratio r_{AC} and the temperature of the gases at a turbine inlet T_{g3} of the conventional gas turbine cycle on the performance of the above power cycles. It shows that it is not just the GC performances are affected by the change in the GC parameters, but AWC turbine performances are under minor influence. It also shows how the CCPP performances are improved by such combination, which was more in efficiency than specific work output.

The thermal efficiency versus the specific work output of AWC, GC and CCPP are illustrated by Fig. 7.40. This figure shows how AWC specific work output (w_{AWC}) is increased more than of CCPP and the GC by the increase of T_{g3} and r_{AC}. On the other hand, the increase of the GC efficiency is greater than that for AWC and the CCPP.

The r_{AC} made a great influence on the AWC performance; the increase of r_{AC} deteriorated both the efficiency and the specific work output of the AWC. This is because the gases lost most of its heat content during the expansion. Therefore, the heat required to optimize the AWC performance characteristics was of low quality. However, this won't affect the performance characteristics of the combined cycle as it efficiency and specific work output increase.

The thermal efficiency of CCPP (η_{CCPP}) is always corresponding to the maximum r_{AC} for a certain T_{g3} and the maximum T_{g3}. The increase of T_{g3} from 1300 °C to 1500 °C reached 2.7 percentage points at high compression ratios. This efficiency corresponded to an increase of η_{GC} and η_{AWC} of 2.1 and 0.7 percentage points respectively. While by the same effect, the w_{CCPP} was corresponded to an increase of about 33%. This was the results from the increase in w_{GC} and the w_{AWC} by 34% and 33% respectively.

Although η_{AWC} did not correspond to the maximum η_{CCPP}, the w_{AWC} was not different from that corresponded to the maximum η_{AWC}. While for a certain T_{g3}, the gas turbines those operated on high r_{AC} had a slightly greater η_{CCPP} than those of low r_{AC}. This reduced the CCPP specific work output by 5%.

Figure 7.40 shows P_E effect on the AWC performance characteristics. These characteristics were degraded by the increase of P_E and for different the r_{AC} and T_{g3}. Such degradation in performance was of a small scale for both the efficiency and the specific work output.

A similar effect was shown for AWC in Fig. 7.41, which shows the effect of the increasing the P_E of the AWC from 50 to 100 bars for different pressure ratios. The uniform of the curve by such effect is the same for all the P_E range considered here. The performance characteristics of the CCPP are both deteriorated by the increase in the PE. However, such decrease was of a minor asset value. The reduction of the w_{CCPP} was about 1.7 %, while the reduction of the η_{CCPP} was about 0.7 percentage point.

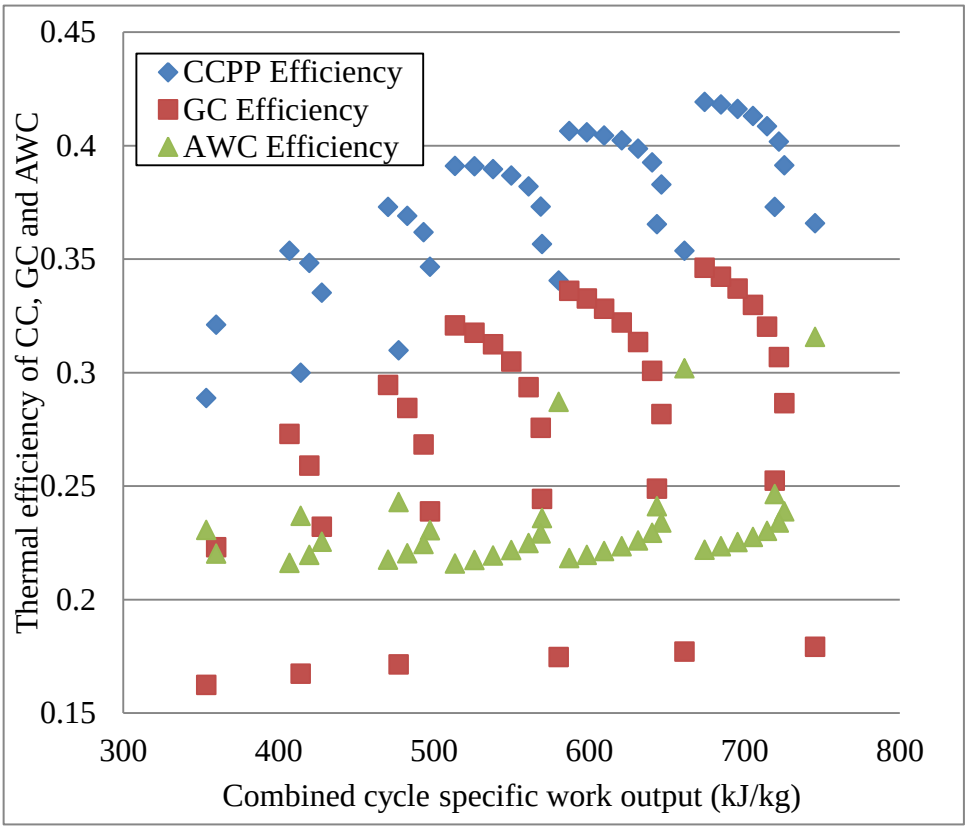

Figure 7.39 The thermal efficiencies of CC, GC and AWC versus their specific work output

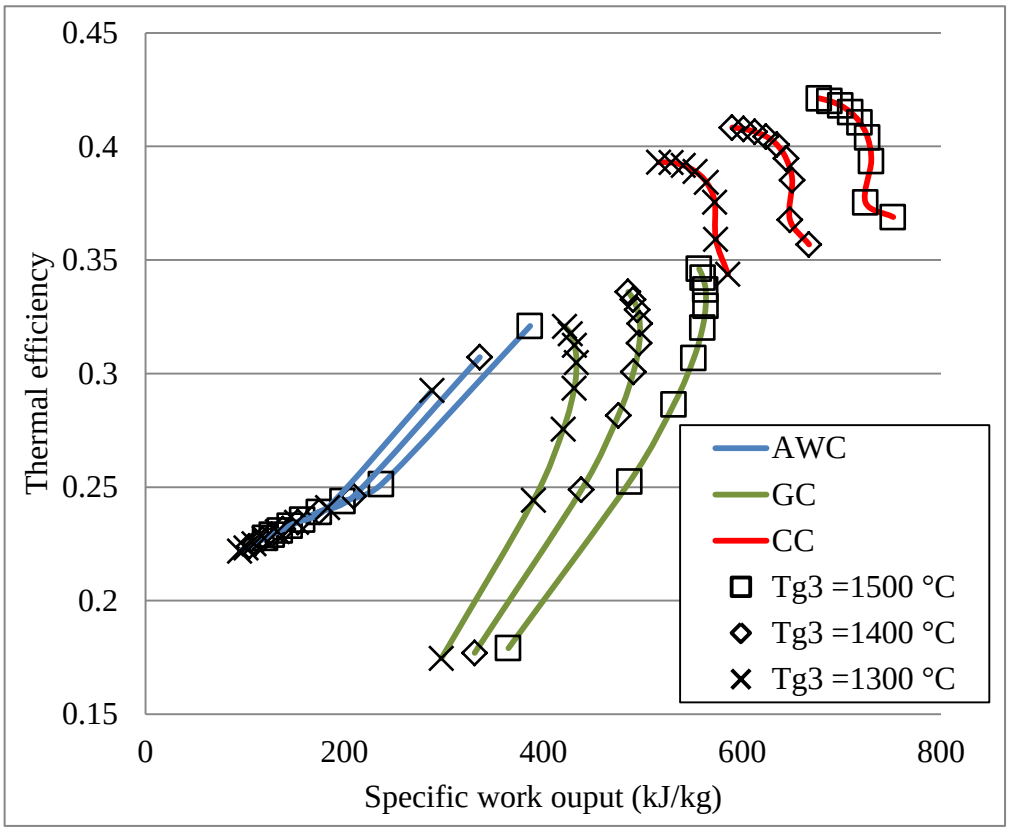

Figure 7.40 The thermal efficiency of AWC GC and CC versus the specific work output

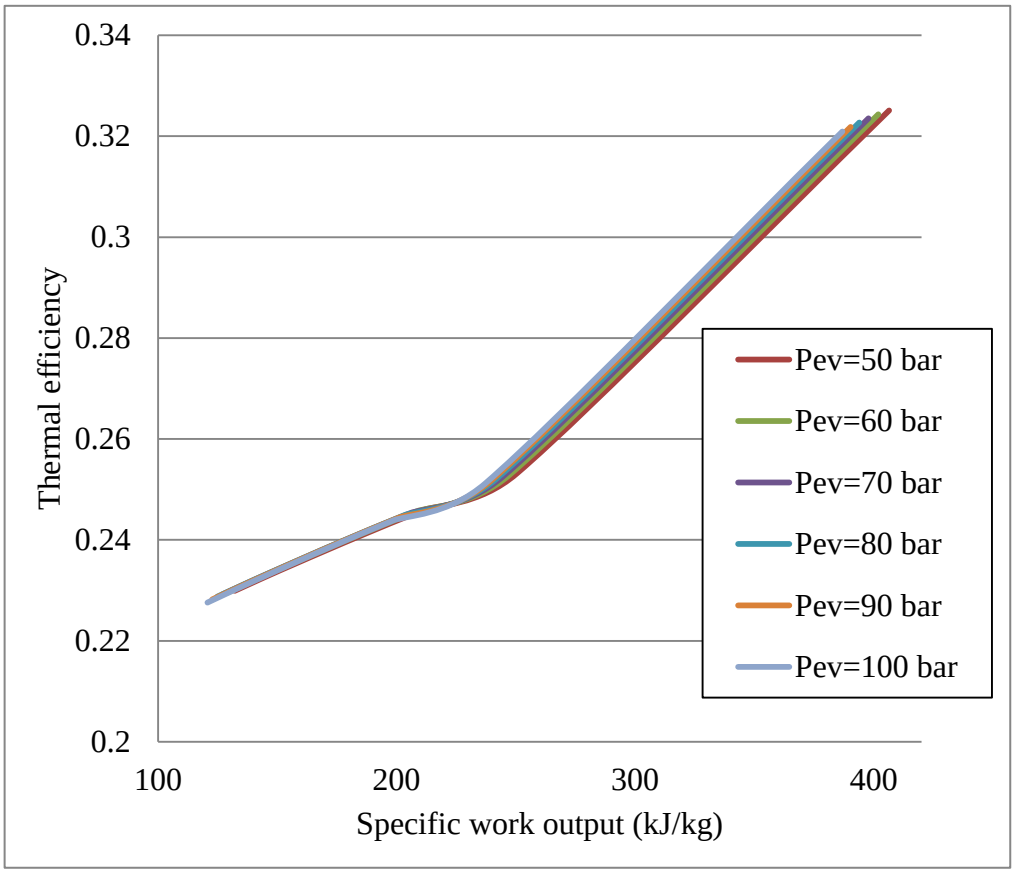

Figure 7.41 The thermal efficiency versus the specific work output of AWC affected by P_E

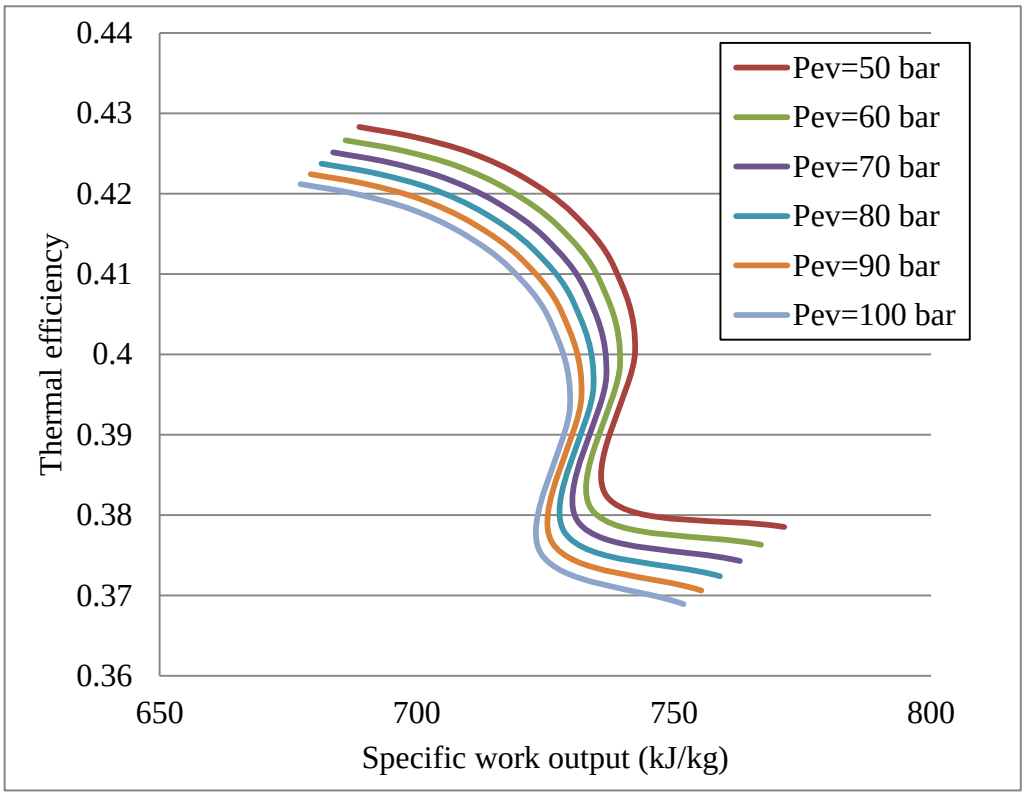

Figure 7.42 The thermal efficiency of CCPP versus the specific work output affected by P_{Ev}

7.4.4 Comparison on ChGT/AWC configurations

The three cases considered previously for ChGT integrated by AWC are under discussion here and discussed by the effect of the P_{Con} and P_{Abs} of the AWC. For the same ChGT parameters, the integration case 3 is more limited than any other case in the range of accepted results.

The efficiency of all ChGT configurations was declined by the increase in the P_{Con} as shown in figure 7.43. By the decrease of the P_{Con} to a certain value of 3 bars, the efficiency stabilized with the increase of the P_{Con}. The results here declared that, the efficiency of the 3rd case has the greatest thermal efficiency and the 2nd has the minimum. The 2nd case was less affected by such parameter than the other two cases. The thermal efficiency of the 1st and the 2nd cases generate identical AWC efficiencies by the effect of the P_{Con}. The thermal efficiency of all cases was increased by the increase of the P_{Con}. For a certain P_{Con}, the efficiency of the 3d case is the lowest. Similarly to the efficiency the specific work output from the ChGT configurations decreased by the increase in the PCon. Such decrease continues by the increase in the P_{Con} till 3 bars over which the specific work output is the same. The 3rd case also has

the greatest specific work output and the 2nd has the minimum for a certain P_{Con}. The 2nd case is the less affected by the variation in such parameter as shown by figure 7.44.

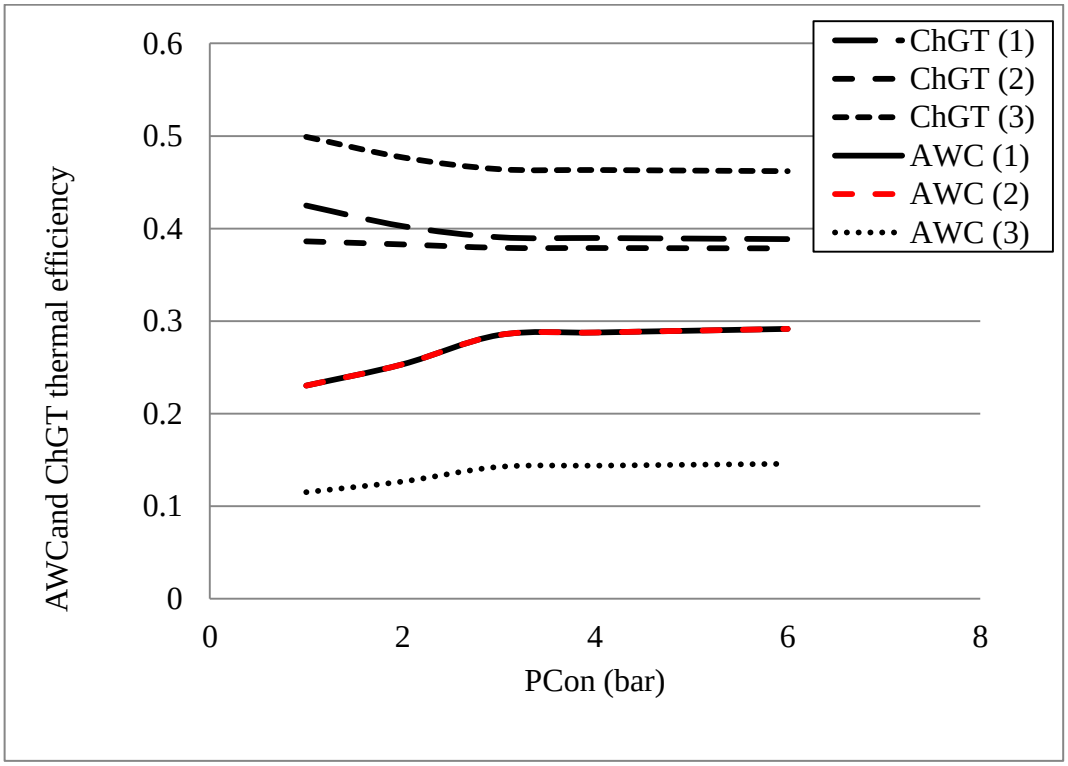

Figure 7.43 AWC and ChGT thermal efficiency functioned to the pressure of condenser

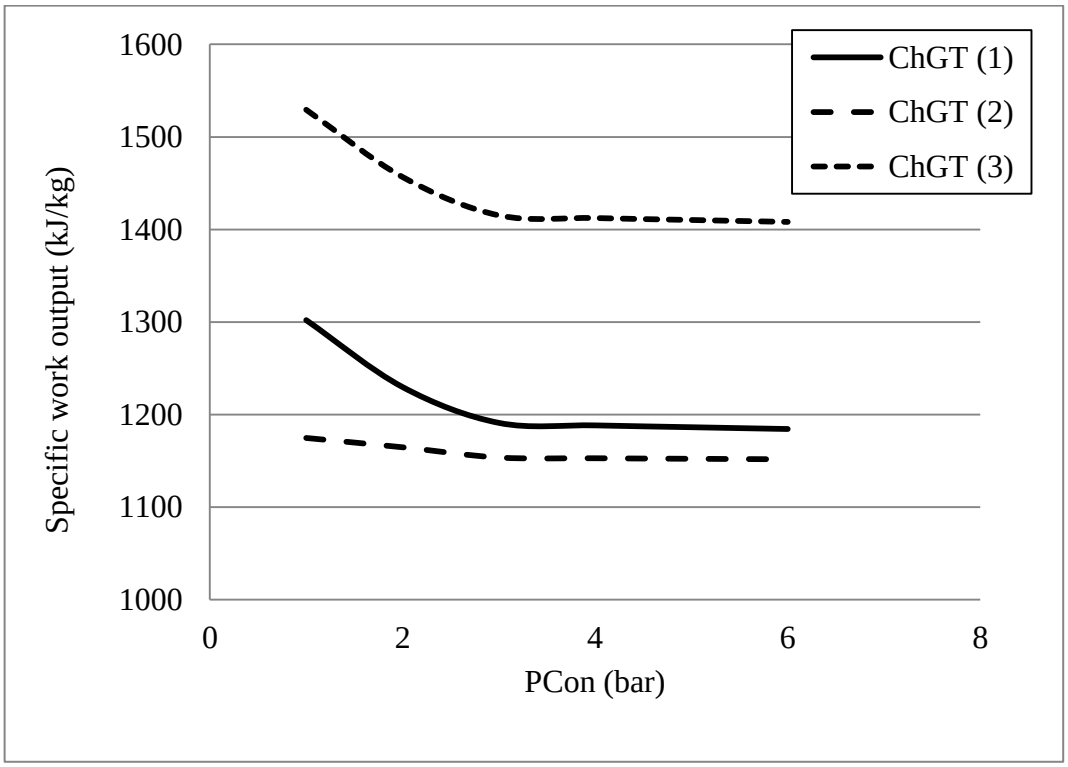

Figure 7.44 ChGT specific work output functioned to the pressure of condenser

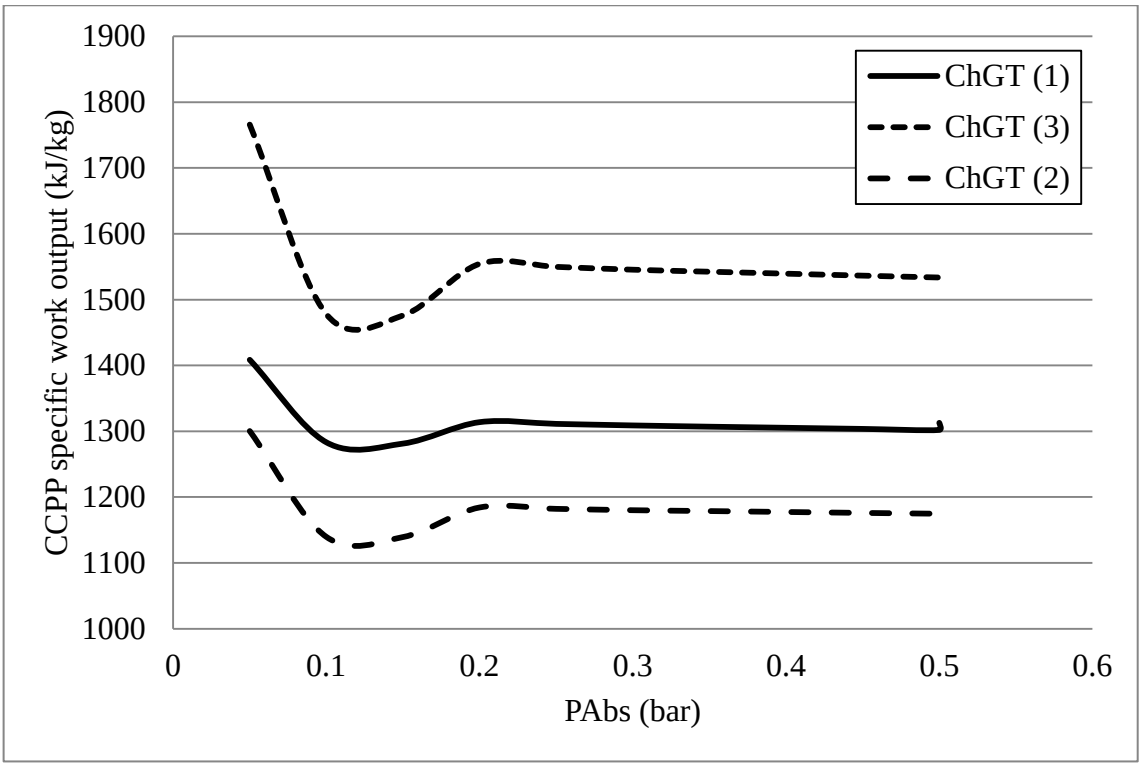

Figure 7.45 ChGT specific work output functioned to the pressure of absorber

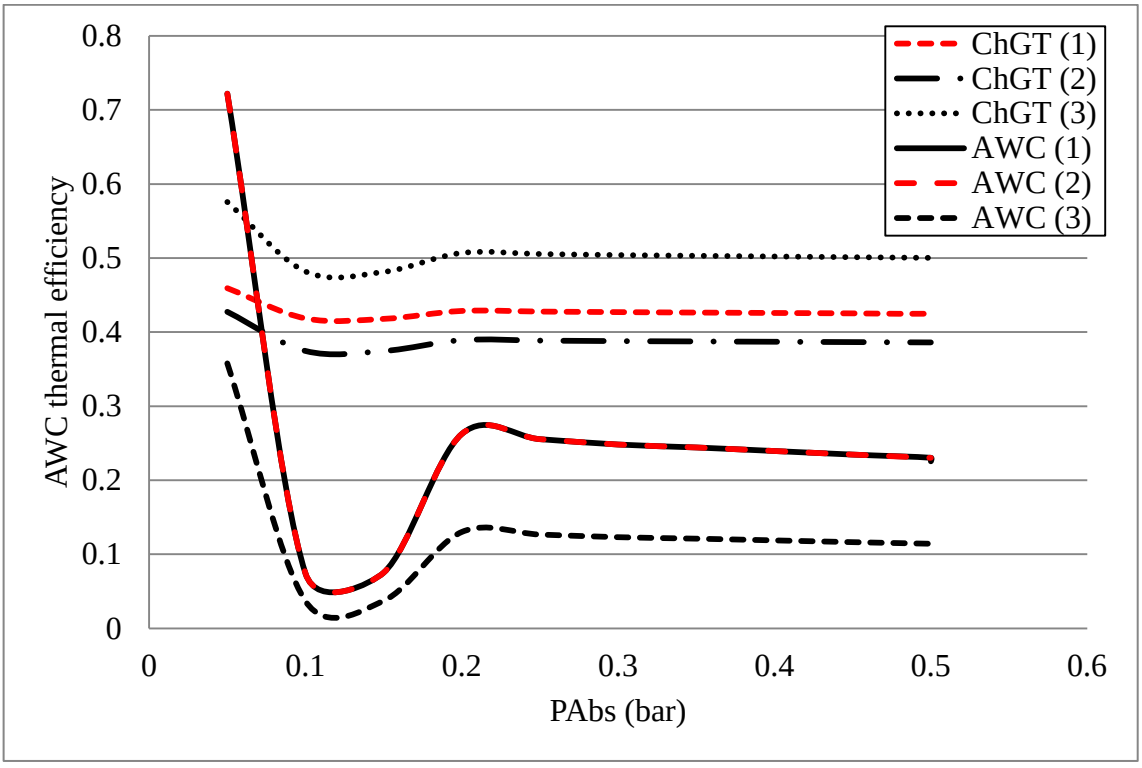

Figure 7.46 AWC and ChGT thermal efficiency functioned to the pressure of absorber

The specific work output from the CHGT decrease s with the increase of the P_{Abs} in all cases. The 3rd cases have the maximum specific work output for a given P_{Abs}. The 2nd case has the minimum specific work output for a given P_{Abs} as shone by figure 7.45. The thermal efficiency of the 2nd and the 1st cases are identical as shown in figure 7.46. For a certain P_{Abs}, the thermal efficiency of the AWC in the 3rd case is lower than the cases above. By the increase in the P_{Abs} in all cases the η_{AWC} drops to its minimum and increases to a moderate value after which it decreases slightly. The behaviour of the ChGT efficiency has a similar tendency with minor effect of the P_{Abs} on its value. The 3rd case efficiency is the maximum for a certain P_{Abs} although the AWC efficiency is the minimum.

7.5 Conclusions

1. HRVG effect on the AWM turbine is similar to that for the HRSG on the steam turbine.

2. The mass flow rate and the temperature of the gases discharged from the gas turbine had a great effect on performance of the AWM turbine.

3. However slight are the effects of the gas turbine parameters on the performance of the AWC these sometimes are of greater effect on AWC performance than its own parameters.

4. Similarly, to the steam turbine cycle, the optimum GC performance parameters are the opposite to those of AW bottoming cycle.

5. On the opposite of the steam cycle, the AWC turbine power output and efficiency deteriorated by the increase in the pressure of the HRVG.

6. The great limit and the inaccuracy of the ammonia water mixture's thermodynamic properties reduced the range of investigation. This is particularly appeared for low pressure with high ammonia concentration. In addition to AWM properties of high pressure and temperature conditions.

7. The increase in GC/AWC combined cycle efficiency is of modest range for the first design. The Performance characteristics of the 3rd case ChGT are the best amongst cases, although, it’s of minor AWC efficiency, it has the major specific work output.

8. ChGT characteristics are more affected by the change in condenser pressure than the absorber pressure.

9. The best ChGT integrated by AWC in comparison to regular ChGT is that for the 3rd case.

10. The performance characteristics are generated for simple steam turbine ChGT, simple AWC. Much better improvements in its performance are expected from an upgraded SC and AWC configurations.

11. Industrially, a combined HRSG HRVG in one component provides better heat distribution between the heat source and the SC and the AWC. The results here show better performance than HRSG and HRVG by itself from the same heat source.

CHAPTER 8
INLET AIR COOLED GAS TURBINE ENGINE

8.1 Introduction

The increase of the ambient temperature will consequently increase the density of the air utilized by the gas turbine. Such increase can severely reduce the mass flow through the engine. Hence, dealing with such high value parameters will get it marks on the performance of the gas turbine i.e. it reduces the power generated by the engine below that usually generated by the same engine during normal weather conditions. Furthermore, the demand for the power normally rise-up at hot weather periods, therefore, a time saver output is required to meet such power demand and to ensure the operation within acceptable performance.

Without a considerable change in the weather, solving such problem is by power augmentation. This will imply either to build new power plants or utilizing inlet –air-cooling strategies to drop the air temperature down. The latter is considered for (1) low costs, (2) less and fast construction and (3) on which an individual facility can perform more efficient. If the right technology is utilized, the gas turbine may operate better than it does even on its typical circumstances. On the other hand and regardless to what cooling system may be used for such prospect, power generation is boosted when the air is cooled below the temperature of the ISO of 15°C at sea level.

The main methods used for gas turbine inlet air cooling are: (1) Thermal energy storage method, (2) Evaporative cooling (or fogging) method and (3) Refrigeration methods. Each of these methods has its own technique by which it operates and a certain range of operation parameters beyond which it limits.

As an example on limits, the temperature of the air after cooling is restricted by a certain degree beyond which crystallize air may be generated if a saturated air is cooled near to its due point. This crystal air flow causes compressor blades' damage bearing in mind that, the airs flow through the compressor is exposed to an increase in the velocity, i.e. a decrease in its temperature Somers, [96].

8.2 Strategies of inlet air cooling

Simply, inlet air cooling devices have been developed to increase the density of the air, thereby increasing the mass flow rate, and consequently, the generated power. While during hot weather, this strategy not just increases the generating capacity, but it reduces heat rate required in the combustion process.

The performance of gas turbine is strongly affected by the environmental conditions, especially ambient temperature. Its output can be increased by 0.36% for each 1°F drop in inlet air temperature. The cost of the inlet air chilling equipment must be paid back by the economic benefits from additional power sales during peak or during operation when the ambient temperature is above the chilled air temperature. For gas turbines in cogeneration or in combined cycle's service, an evaluation for the trade-off of using the exhaust heat might be needed between power augmentation inlet air cooling and the economic benefits of exhaust heat sales.

The diversity of power plants, their configurations and operating modes and periods are the mainly effected parameters in choosing the suitable air cooling system. The importance of inlet air cooling for gas turbines has been increased during last ten years as the demands for attractive peaking power sources are required to maintain electricity utilities.

Power generation is proportional to the mass flow the combustion products. The capacity of a particular unit is subject to ambient site conditions. Adding inlet air technology may results in the air temperature drop below isometric design conditions, thus results in a better performance from gas turbine. This may reach an increase of 20% for warmest sites. It could be considered as another way to increase the temperature ratio of the power cycle. Although refrigeration cooling is, more effective than the evaporative cooling systems, is more expensive than evaporative cooling. However, these costs are it operates more effectively in hot highly humid climate.

8.3 Ammonia-water absorption chillers for gas turbine inlet air cooling

An exhaust heat powered absorption chillers does not require a great deal of power just that needed by its pumps, which is used to be relatively minor from the gas turbine output.

Therefore, such systems are considered to be the state of art for such technology. In this strategy, the waste heat from turbine combustion drives a single-effect ammonia-water absorption chiller, which in turn cools gas turbine inlet air, giving the desired boosted power.

In this integrated cycle, AWAC system can be powered by an exhaust heat of 200°C or lower can be ensured by setting evaporator temperature to 0°C, and 30°C for cooling water, this is concurrent with an ambient temperature of 35°C, and a peak solution temperature is set at 149°C.

The main components of an ammonia-water absorption cycle are condenser, evaporator, absorber, and generator. The extra components consist on throttling valves, pumps, rectifier, and heat exchangers, as illustrated in Fig. 8.1.

Ammonia Water Mixture (AWM) absorption refrigeration machines use low quality thermal energy. Moreover, as the temperature of the heat source does not usually need to be as high as (80-150°C), the wasted heat from many processes can be used to power absorption refrigeration machines. In addition to that it is environmentally friendly, because it's working fluids are natural substances that have no harm on ozone depletion.

The processes of this systems' cycle:

i. Low pressure, high ammonia concentration is pumped from the absorber to a high pressure at the rectifier through heat gaining processes from rectifier and solution heat exchangers and heat recovery vapour generator, in which its splits into high concentration ammonia vapour and ammonia-water solution;
ii. The high pressure high ammonia concentration vapour (almost pure) condensed in condenser, then it passes through condenser evaporator heat exchanger and throttling valve to low pressure strong ammonia solution at evaporator (gas cycle inlet chiller);
iii. In evaporator, ammonia sweeps heat from gas turbine cycle inlet air, thus ammonia vaporizes.
iv. High pressure low ammonia concentration solution goes to the absorber through solution heat exchanger and throttling valve.
v. In the absorber, low ammonia solution (water) absorbs high pressure high concentration ammonia vapour and brings it back into strong ammonia solution.

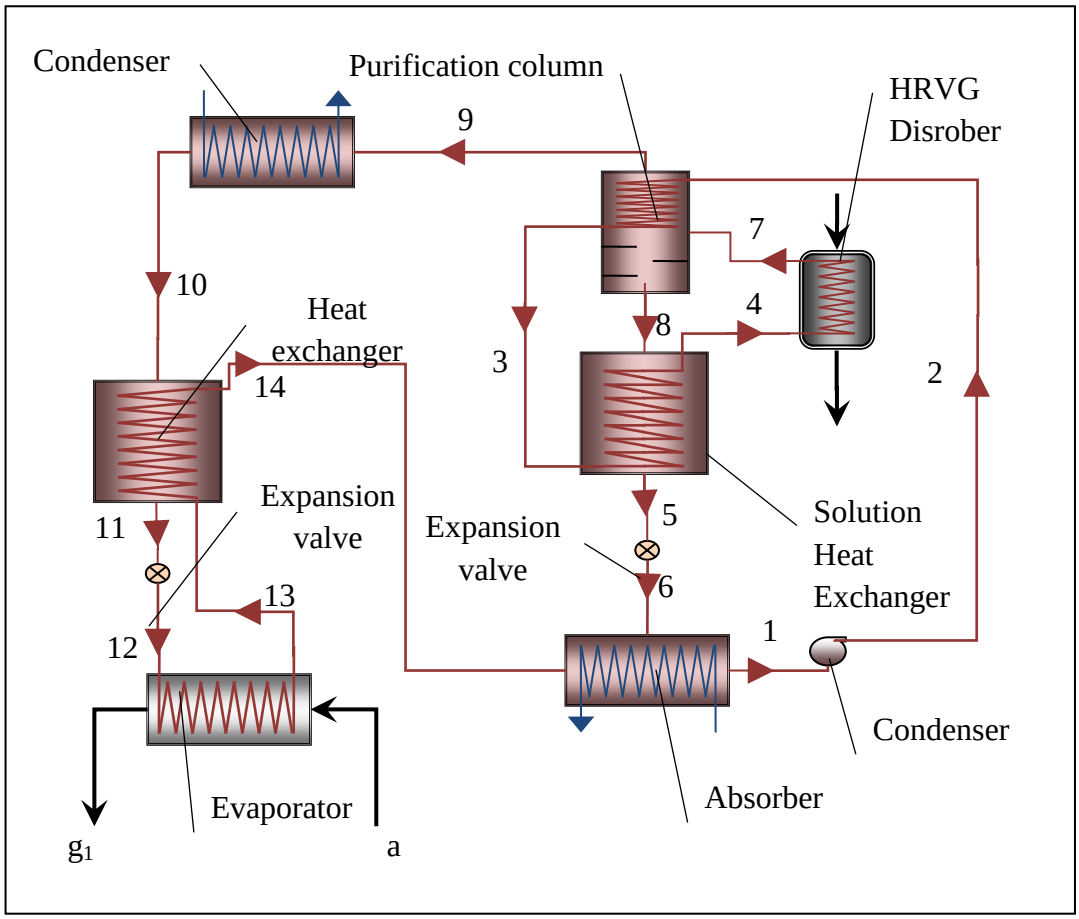

Figure 8.1 AAR for gas turbine inlet air cooling

8.4 Absorption chiller system model program

A model was established from scratch for single and double effect absorption chiller systems. In which the heat from the steam turbine output is to power such systems. Models that dealt with the benefits and the costs of utilizing such strategy relation to atmospheric conditions of different territories had vastly considered in previous studies. These showed such great effect of this strategy in (1) boosting the power output, (2) fuel savings and (3) improving the efficiency, which considered more precious than all benefits for nonstop operation power plants. This program considers the thermodynamic analysis to investigate such effect on the characteristics of different configurations of:

(1) Combined cycle (Gas Turbine/ Steam Turbine).

(2) Triple generation cycles (Gas Turbine/ Steam Turbine/ Ammonia Turbine).

(3) Triple generation cycles (ChGT/ Steam Turbine/ Ammonia Turbine).

The thermodynamic properties of the ammonia water mixture of this model code make use of properties considered for the absorption chillers. These are with narrower ranges than the properties required for the AWC turbine.

8.4.1 The conducted configurations of absorption chiller systems and its basic analysis:

In this study, two configurations of waste heat recovery absorption chillers are investigated. The first is the single effect ammonia water absorption chiller and the double effect ammonia water absorption chiller systems. In both, the heat that powers the system is gained from steam cycle waste heat. The processes to govern AWM conditions through AWAC 1st design system components are described hereafter.

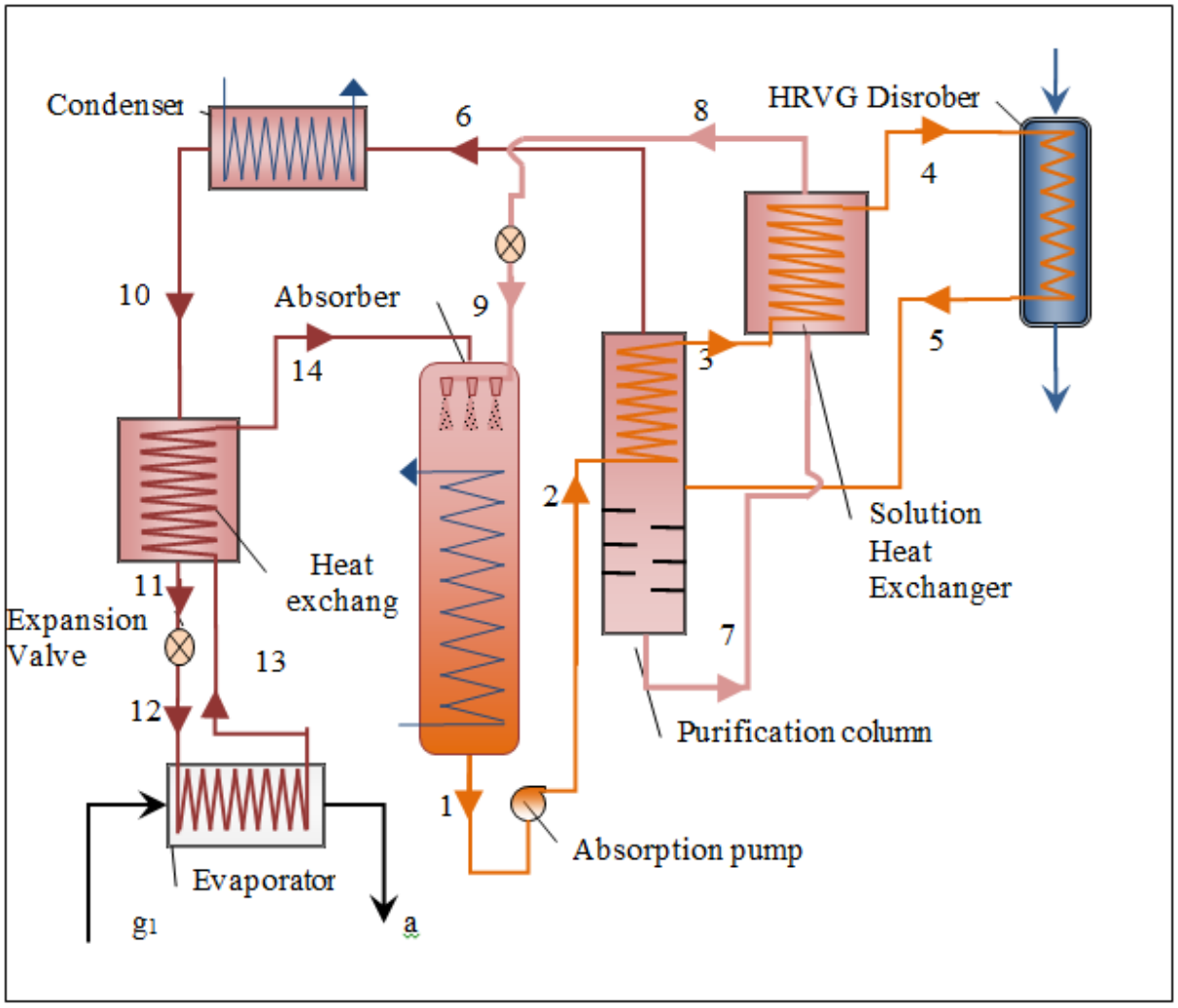

Figure 8.2 Single effect ammonia water

1. The disrober vaporize the basic solution AWM out of the solution heat exchanger using the heat recovered from steam turbine outlet or from HRSG exhaust or HRVG gases.

2. The purification column purifies the refrigerant of the rich solution from that of the lean solution which condensate by the rectifier at the upper end of the column.

3. The rich solution vapour is condensed by the condenser.

4. It expands to lower pressure by the expansion valve.

5. The rich solution evaporates in the evaporator to absorb the heat from the ambient air.

6. At the absorber, the lean and the rich solutions are combined.

7. The basic solution generated by the absorber is then pumped to the rectifiers, the solution heat exchanger and the HRVG disrober.

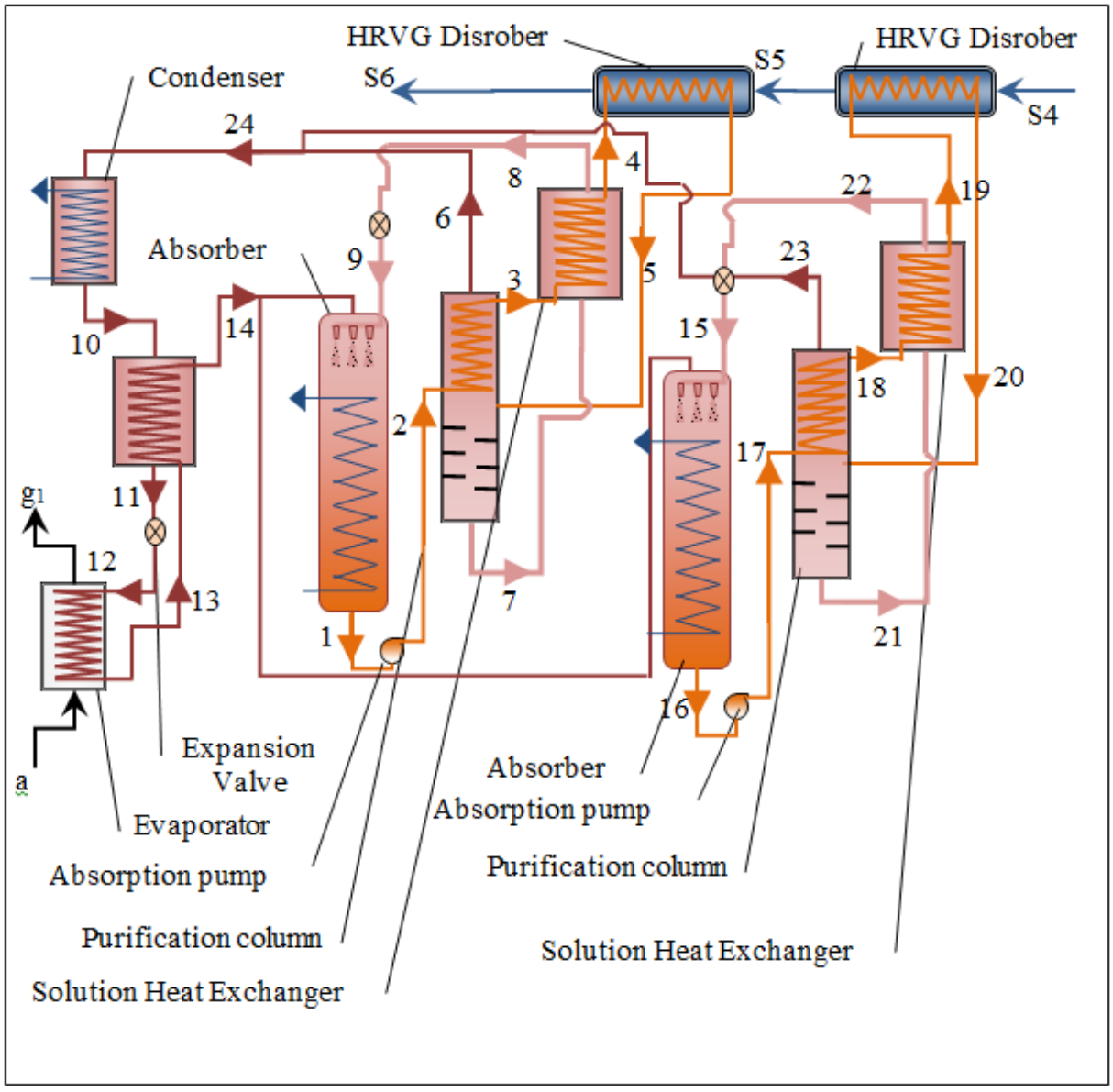

Figure 8.3 Two- stage double effect AWAC

8.4.2 Calculations for AWACS model

As it has been considered previously, the pump is assumed to work isentropically. Accordingly, the enthalpy of the AWM at the pump outlet is expressed by Eq. (8.1). Where $h_{aw1} = f(x_B, P_E)$ and $v_{aw1} = f(x_B, P_E)$.

$$h_{aw2} = \frac{h_{aw1} + v_{aw1} \times (P_{Con} - P_E)}{100} \quad \ldots (8.1)$$

The enthalpy of the AWM at the evaporator outlet is given by equation (8.2). Where $h_{aw12} = h_{aw11}$ and $h_{aw11} = f(x_W, P_{Con})$.

$$h_{aw13} = h_{aw12} + \varepsilon_{Con}(h_{awT_a} - h_{aw12}) \quad \ldots (8.2)$$

In this model, the AWM basic and lean solution's temperatures at heat exchangers inlets are given. The effectiveness equation was used to calculate the enthalpy of the AWM basic solution at the solution heat exchangers outlet as expressed by equation (8.3). Where, $h_{aw3} = f(P_{Ev}, T_{aw3}, x_B)$, $h_{aw7} = f(P_{Con}, T_{aw7}, x_L)$ and $h_{aw71} = f(P_{Con}, T_{aw7}, x_B)$.

$$h_{aw4} = h_{aw3} + \varepsilon_{HE} \times (h_{aw71} - h_{aw3}) \quad \ldots (8.3)$$

Similarly, the enthalpy of the AWM solution at disrober outlet is expressed by equation (8.4), where $h_{awT_{s5}} = f(P_{Con}, T_{s5}, x_B)$. On the other end, the enthalpy of the AWM lean solution at the absorber inlet is given by equation (8.5).

$$h_{aw5} = h_{aw4} + \varepsilon_D \times (h_{awT_{s5}} - h_{aw4}) \quad \ldots (8.4)$$

$$h_{aw8} = h_{aw7} - \varepsilon_{HE} \times (h_{aw7'} - h_{aw3}) \quad \ldots (8.5)$$

Where the enthalpy of the AWM at SHE inlet is determined using the concentration of the basic solution $h_{aw7'} = f(X_B, T_{aw7}, P_{Con})$.

$$y = \frac{(h_{aw4} - h_{aw3})}{((h_{aw7} - h_{aw8}) \times \varepsilon_{HE})} \quad \ldots (8.6)$$

$$F = 1 - y \quad \ldots (8.7)$$

$$\dot{m}_{aw14} + \dot{m}_{aw9} = \dot{m}_{aw1} \quad \ldots (8.8)$$

$$x_W \dot{m}_{aw14} + x_L \dot{m}_{aw9} = x_B \dot{m}_{aw1} \quad \ldots (8.9)$$

$$x_B = x_W \frac{\dot{m}_{aw14}}{\dot{m}_{aw1}} + x_L \frac{\dot{m}_{aw9}}{\dot{m}_{aw1}} \quad \ldots (8.10)$$

$$x_B = x_W \left(1 - \frac{\dot{m}_{aw9}}{\dot{m}_{aw1}}\right) + x_L \left(\frac{\dot{m}_{aw9}}{\dot{m}_{aw1}}\right) \quad \ldots (8.11)$$

$$x_B = x_W (1 - y) + x_L \times y \quad \ldots (8.12)$$

Or

$$x_B = x_W \times f + x_L (1 - f) \quad \ldots (8.13)$$

$$x_W = \frac{x_B - x_L (1 - f)}{f} \quad \ldots (8.14)$$

$$x_W = x_L + \frac{(x_B - x_L)}{F} \quad \ldots (8.15)$$

$$h_{aw6} = h_{aw7} + F \times (h_{aw5} - h_{aw4}) - F \times (h_{aw7} - h_{aw4}) - F \times (h_{aw3} - h_{aw2}) \quad \ldots (8.16)$$

The enthalpy of the AWM at the condenser outlet is estimated using the X_W and the P_{Con} at saturated liquid mixture status.

$$h_{aw11} = f(x_W, P_{Con}) \quad \ldots (8.17)$$

$$T_{aw12} = f(P_E, h_{aw12}, x_W) \quad \ldots (8.18)$$

$$h_{aT_{aw12}} = f(T_{aw12}) \times 1000 \quad \ldots (8.19)$$

$$h_a = f(T_a) \times 1000 \quad \ldots (8.20)$$

$$h_{g1} = h_a - \varepsilon_E \times (h_a - h_{aT_{aw12}}) \quad \ldots (8.21)$$

Where $h_{aT_{aw12}} = f(T_{aw12})$ using the function GCF2 between air temperature and enthalpy.

$$COP_{AWACS} = Q_{Ev} / Q_{Des} \quad \ldots (8.22)$$

8.4.3 Components models

It is easier to depict the equations and the functions that control the inputs and the outputs of AWAC systems' component than to illustrate them in one flow chart. Although some of the components' models considered here are similar to those given for the AWC, these models usually work on different thermodynamic properties.

8.4.3.1 Evaporator model

Manufacturers confirmed a refrigeration temperature of between 5 and -55 °C. Sigler, et al., [76] confirmed that, cooling the air into 0°C is combined with system modifications, therefore recommended 5°C as more advantages for DPCC. The evaporator is modelled as a heat exchanger in which the refrigerant stream at the end of the process is considered at the due point. The pressure losses between evaporators' ends were neglected from the AWM side, while it was taken into consideration from the gas side. In this model, the temperature of the air at AWAC outlet is estimated using the function GCF7 where $T_{g1} = f(h_{g1})$

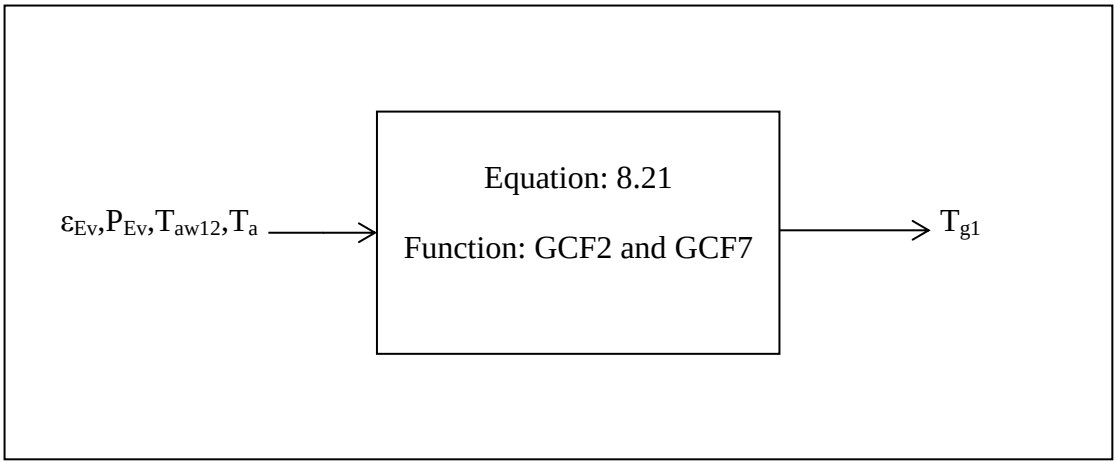

Figure 8.4 Evaporator model

8.4.3.2 Absorber model

The absorber operates similarly as the condenser in regard to the change in the phase of the vapour into liquid. The differences are (1) it works for a binary mixture, (3) the two streams at the inlet are mixed (2) the absorbent stream is already condensed. At the absorber, the ammonia water weak solution absorbs the rich solution mixture. In this model, the basic solution mixture at the absorber outlet is assumed to be saturated liquid at the same pressure of the evaporator. The property of the AWM at the evaporator outlet is assumed to be

saturated vapour. Furthermore, it has been considered that there is zero pressure losses regarded through the process. It has been assumed that, the temperature of the cooling water stream at the absorber inlet is adjustable to maintain saturation states of the primary solution mixture at the absorber outlet. The enthalpy and the temperature of the AWM at the absorber outlet is functioned to the pressure of the evaporator and the basic concentration of the ammonia using the function (hBFXP) where h_{aw1}=f (X_B, P_{Ev}). Applying the energy equation on the absorber generates the following:

$$\Delta Q_{Ab} = \Delta Q_{cw} \quad \ldots (8.23)$$

$$\Delta Q_{Ab} = m_L h_{aw9} + m_W h_{aw14} - m_B h_{aw1} \quad \ldots (8.24)$$

In the above equation h_{aw9} is sub cooled mixture, while h_{aw14} is superheated

$$\Delta Q_{cw} = m_w \left(h_{cw2} - h_{cw1}\right) \quad \ldots (8.25)$$

$$m_W h_{aw14} + m_L h_{aw9} - m_B h_{aw1} = m_{cw} \left(h_{cw2} - h_{cw1}\right) \quad \ldots (8.26)$$

$$\frac{m_W}{m_B} h_{aw14} + \frac{m_L}{m_B} h_{aw9} - h_{aw1} = \frac{m_{cw}}{m_B} \left(h_{cw2} - h_{cw1}\right) \quad \ldots (8.27)$$

$$\frac{m_W}{m_B} + \frac{m_L}{m_B} = 1 \quad \ldots (8.28)$$

$$\frac{m_W}{m_B} h_{aw14} + \left(1 - \frac{m_W}{m_B}\right) h_{aw9} - h_{aw1} = \frac{m_{cw}}{m_B} \left(h_{cw2} - h_{cw1}\right) \quad \ldots (8.29)$$

$$f = \frac{m_W}{m_B} \quad \ldots (8.30)$$

$$f \times h_{aw14} + (1 - f) h_{aw9} - h_{aw1} = \frac{m_{cw}}{m_B} \left(h_{cw2} - h_{cw1}\right) \quad \ldots (8.31)$$

It was reported by Herold [97], that vapour quality of the rich AWM to the absorber is more likely to be superheated. At this certain case, the right hand side of the equation to be null. This happens when assuming that, there is no need for the cooling water, i.e. the cooling is made by the combination between the two mixtures rather than the cooling water. In here a condition appears, which must be satisfied or the model won't meet satisfactory. Accordingly, the equation above changes into the following:

$$h_{aw14} = \frac{h_{aw1} - (1-f)h_{aw9}}{f} \quad \ldots (8.32)$$

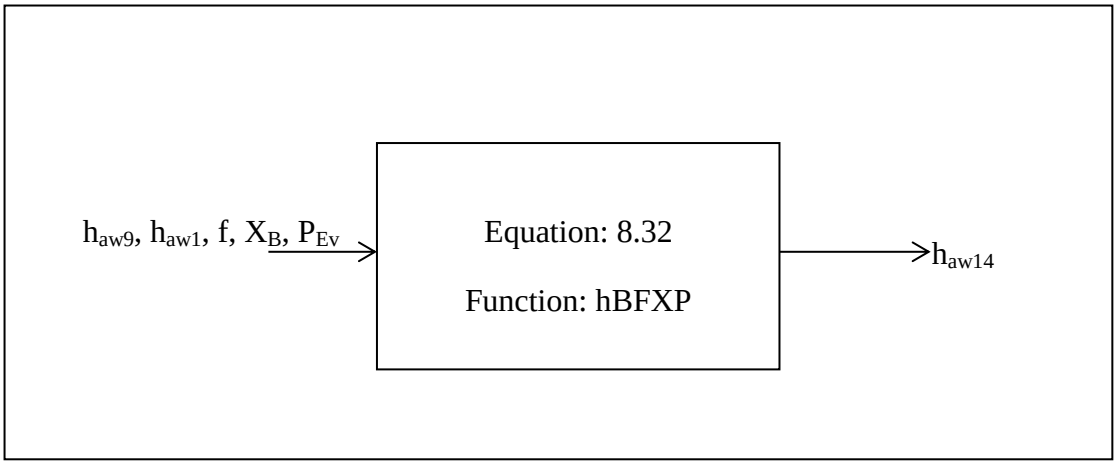

Figure 8.5 Absorber model

8.4.3.3 Pump model:

Pump here is used to keep the circulation of the mixture and to bring the pressure of the basic solution into the condenser pressure level. The saturated liquid mixture at the outlet of the absorber is pumped here to the pressure of the condenser. In this model the same equation used for determining the enthalpy of the at water pump output Eq. (8.1) It has been used here to calculate the enthalpy of the mixture at output. The temperature of the AWM at pump's output at the compressed liquid properties is estimated using the function (CLTFXhP) in which $T_{aw2} = f\left(P_{Con}, h_{aw2}, X_B\right)$. This temperature is estimated, although its magnitude is usually within small change from the temperature of the saturated liquid. Unlike other authors like Somers [96], the work required by the pump is not going to be added to the heat input as an energy given to the system. However, pumps work input is subtracted from the total work given to the whole gas turbine output. Therefore, its magnitude has no effect on the performance of the AWACS.

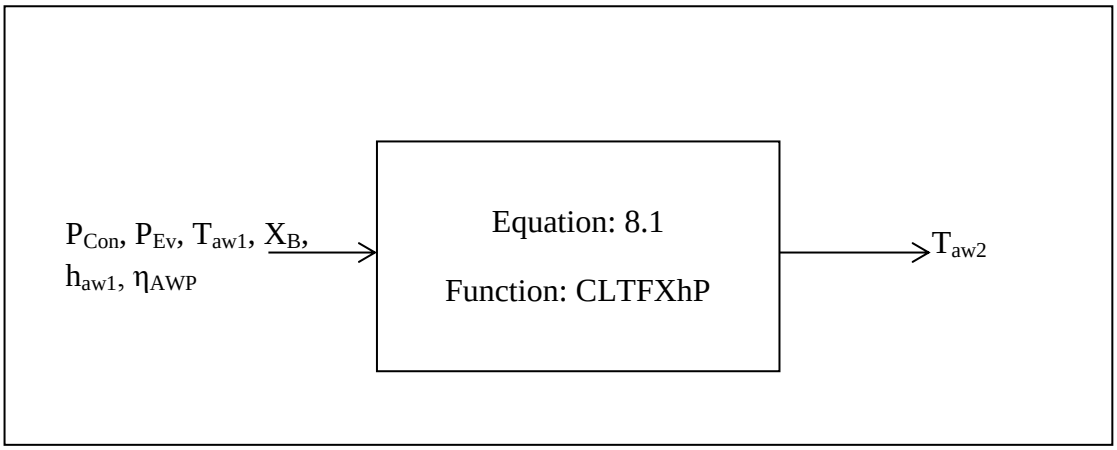

Figure 8.6 Pump model

8.4.3.4 Rectification column model

The temperature difference in the rectifier is assumed by this model to be from 5 to 25 degrees as regarded by previous studies. The rectifier works on: increasing the temperature of the basic solution at solution heat exchanger inlet; But its main job is to condense the low heat vapour mixture. Based on these two objectives, the rectifier is modelled here regarding both its streams. In this model, the solution required to give a relationship between the temperatures of the basic solution at rectifier's two ends. This difference (ΔT_{Rec}) is assumed to be between 5 and 25 °C.

$$T_{aw3} = T_{aw2} + \Delta T_{Rec} \quad \ldots (8.33)$$

The temperature of the basic solution at the rectifier inlet is estimated using the function CLTFXhP in which $T_{aw2} = f(x_B, h_{aw2}, P_{Con})$. This function is built to work on compressed liquid ammonia water mixture. While the enthalpy of the mixture at the rectifier outlet is estimated using the function hFXTP in which $h_{aw3} = (x_B, T_{aw3}, P_{Ev})$.

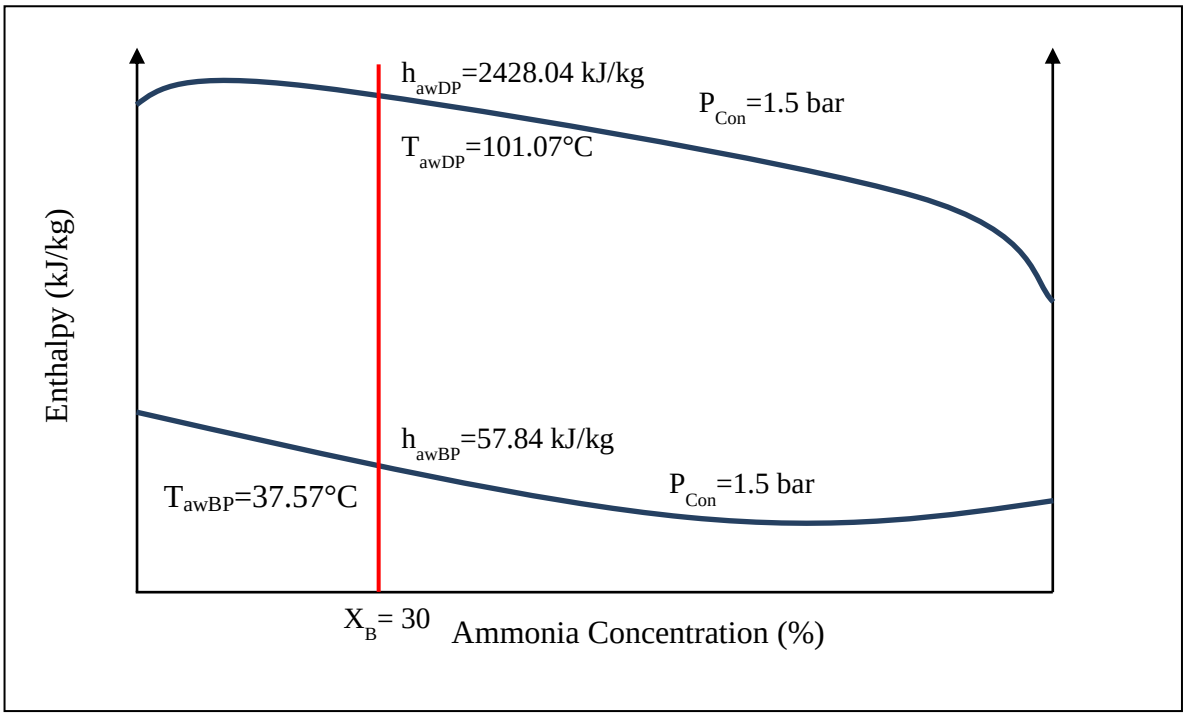

Figure 8.7 Rectification process on enthalpy concentration diagram

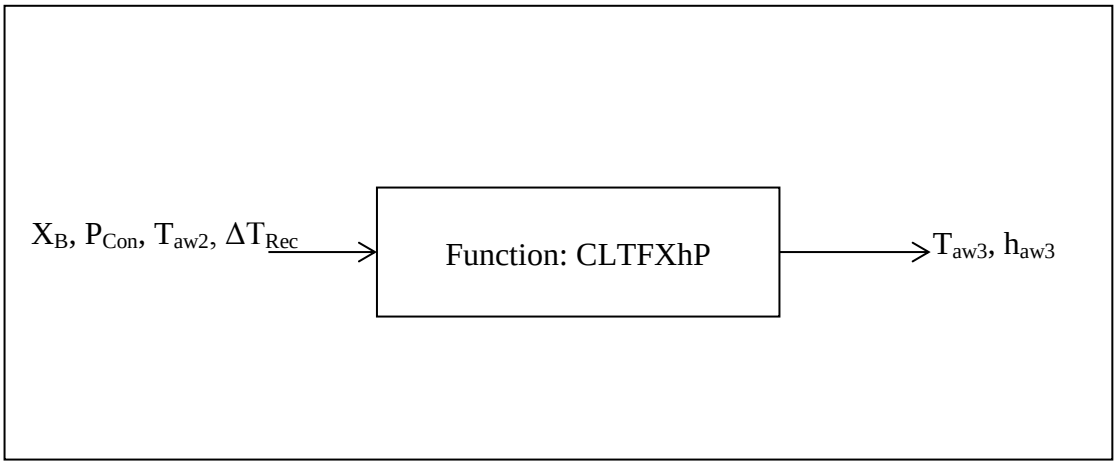

Figure 8.8 Rectification column model

8.4.3.5 Desorber model

Disorber's job is to vaporize a two or more components mixture from condensation. The desorber is modelled to use the heat recovered from the waste heat of turbine exhaust of either the gas turbine or the steam turbine. The assumptions regarded by the work of the desorber are:

1) The minimum acceptable heat recovered must ensure a superheated AWM vapour at the outlet.

2) A constant pressure process.

3) The AWM mass flow though the desorber is totally vaporised through the process.

a. The heat is generated from the HRSG gases output

Authors who considered a minimum limits for the temperature of the gases at desorber inlet and outlet like Sigler who maintain to values of ($T_{g5minimum}$ = 105°C and $T_{E\ minimum}$ =75°C). Others like Khaledi et al identified the minimum required heat source range between 100 and 200 °C. In this study, the temperature of the exhaust gases is limited by economizers' performance and its pressure, which has been greatly affected by the minimum pinch point temperature difference. Which the maximum regarded temperature of the gases at desorber inlet is kept below 350°C.

b. The heat is generated from waste steam

The temperature of the steam is calculated as an output from the steam turbine model. In which the heat source stream is condensed to saturation at the condenser pressure. Manufacturers managed a desorber powered by steam of a temperature between (95- and 180 °C) for single stage system and with a lower temperature range for the double effect system. The enthalpy of the AWM at Desorber outlet is calculated using equation (8.4) where the enthalpy of the AWM at T_{g5} (Or T_{s5}) is estimated using the function (TFPhX).

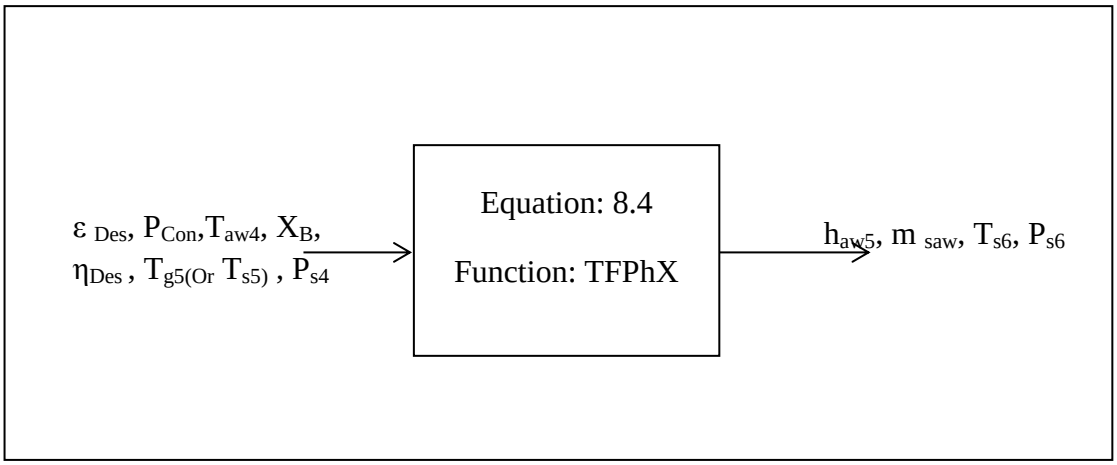

Figure 8.9 Desrober model

8.4.3.6 Condenser model

The condenser works on condensing the rich AWM vapour coming from the purification column into rich liquid AWM to enter the pre-cooler heat exchanger. In this model, this was assumed to be within constant pressure and ammonia fraction. The outlet state is assumed to be at saturated liquid. Therefore, it is assumed that, the temperature of the cooling water at the condenser inlet is altered to keep such limit. According to such consideration, the effect of temperature of the atmosphere on the cooling water has not been regarded in this model. The enthalpy of AWM at the condenser outlet is estimated using the pressure and ammonia concentration at the condenser inlet. Such relation is represented by h_{aw11}= f (P_{Con}, X_W)), using the function (hBFXP). As in the model of the steam turbine condenser, this condenser is assumed to cool the rich solution mixture into saturated liquid.

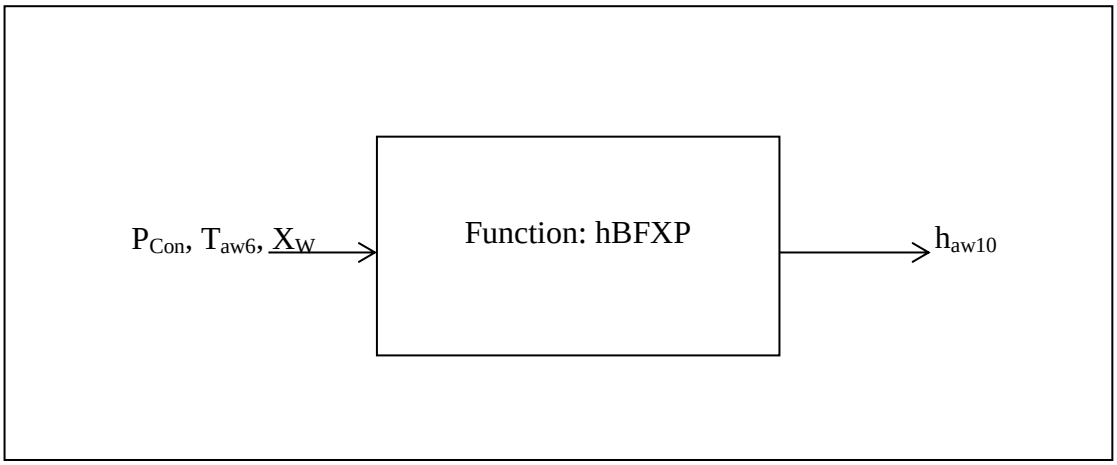

Figure 8.10 Condenser model

8.4.3.7 Solution heat exchanger model

In this model, it has been assumed that there is a specific ratio (θ_{SHE}) between the temperature of the lean solution at the heat exchanger inlet and that for the basic solution stream at the other inlet end.

$$\theta_{SHE} = \frac{T_{aw7}}{T_{aw3}} \quad \ldots (8.34)$$

This is similarly applied on the double effect cycle as well on the second solution heat exchanger to generate (θ_{SHE2}), on the temperatures (T_{aw21} and T_{aw18}). Where:

$$\theta_{SHE2} = \frac{T_{aw21}}{T_{aw18}} \quad \ldots (8.35)$$

$$1 < \theta_{SHE} < \left[\frac{\varepsilon_{Des} T_{s5}}{T_{aw3}} + \frac{\left(1 - \varepsilon_{SHE} - \varepsilon_{Des} - \varepsilon_{Des}\varepsilon_{SHE}\right)}{\left(1 - \varepsilon_{SHE} - \varepsilon_{Des}\varepsilon_{SHE}\right)} \right] \quad \ldots (8.36)$$

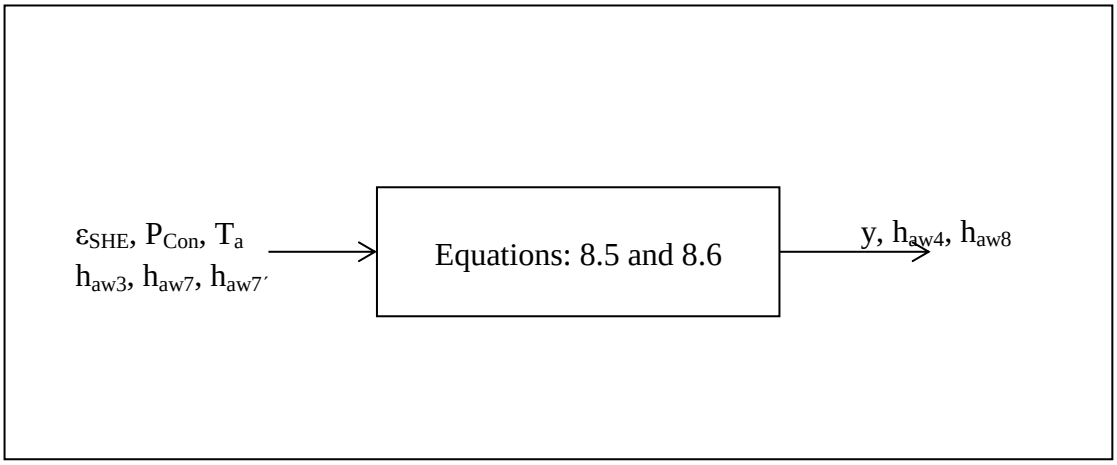

Figure 8.11 Solution heat exchanger model

Iteration is required to estimate the correct (θ_{SHE}) value in which the condition that ends the loop is when X_R is the same for h_{aw11} and h_{aw13} at P_{Con} and P_E respectively. The mass flow rate of the lean solution to that of the basic solution is represented by (y); its value is determined using equation (8.6). It is assumed that, there is no pressure loss throughout this component.

8.4.3.8 Expansion valves model

It has been assumed that the process through the expansion valve is adiabatic. Therefore, this model conducts a constant enthalpy process. Such process is combined with a reduction in the pressure. There is no change in the phase of the liquid AWM stream through the expansion valve. There is also no change in the mass fraction of the ammonia through the expansion valve. Therefore, the change assumed in this model is regarded for the pressure and the temperature which appeared to work oppositely. According to the above, (h_{aw11}=h_{aw12}) and (h_{aw9}=h_{aw8}) for the first and second designs and (h_{aw15}=h_{aw22}) for the second design. Keeping the enthalpy constant and reducing the pressure moves the property of the AWM state at EV outlet towards the two phase area on the properties chart.

8.4.3.9 Pre-cooler model

Using the pre-cooler improves the cooling capacity and the COP of the AWACS. This increase was confirmed by Somers [96], to be about 10%. He considered that such improvement to the basic design as worthy despite the additional initial costs and complexity.

The role of the pre-cooler is to reduce the heat content of AWM before its expansion. This heat is given to the low pressure vapour before it enters the absorber. Precooler effectiveness is used in equation (8.39) to determine h_{aw14}. While precooler efficiency is calculated in equation (8.37), where the vapour stream heat gained from the liquid stream advantaging from the pressure difference. Accordingly, the assumed pre-cooler efficiency must satisfy vapour enthalpy h_{aw14} from equations (8.39) and (8.32).

$$\eta_{PC} = \frac{(h_{aw14} - h_{aw13})}{(h_{aw10} - h_{aw11})} \quad \ldots (8.37)$$

$$h_{aw11} = h_{aw10} - \frac{(h_{aw14} - h_{aw13})}{\eta_{PC}} \quad \ldots (8.38)$$

$$h_{aw14} = h_{aw13} + \varepsilon_{PC} \times (h_{aw13} - h_{aw10}) \quad \ldots (8.39)$$

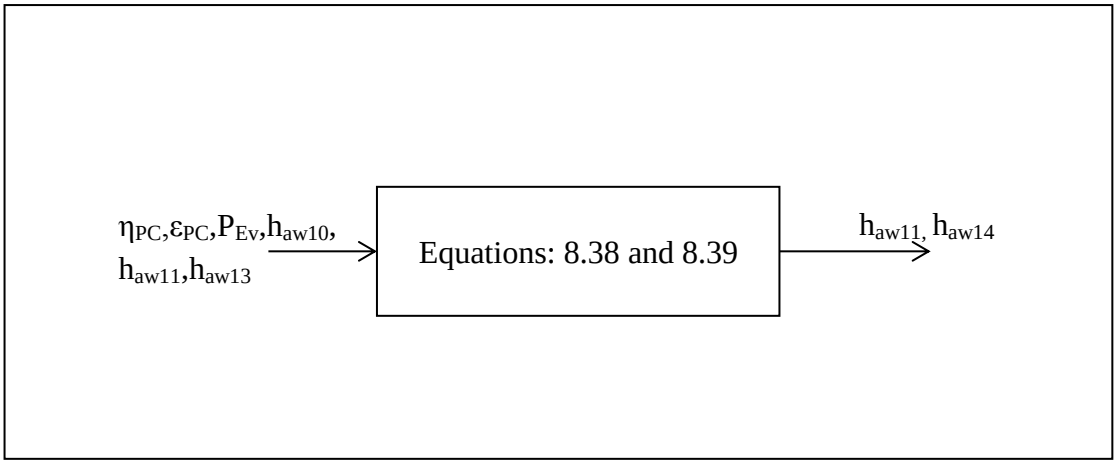

Figure 8.12 Pre-cooler model

8.4.4 AWAC model specifications

There are many factors to consider whether the AWAC is viable for gas turbine inlet air cooling and how efficient is its operation. These factors are included:

(a) Model Restrictions.

(b) Operation limits.

(c) Thermodynamic restrictions.

Many researchers conducted a fixed temperature target for the air at the compressor inlet (or a fixed temperature for the cooling coils of the evaporator). Therefore, the evaporator cooling heat change is already constant. In this study, the temperature of the air at the compressor inlet has a minimum value limit only.

8.4.4.1 Model restrictions

(1) In this model, the heat that powers the chiller system is given to the disrober. To improve CCPP performance with no degradation in any of the combined cycles. The heat is either recuperated from HRSGs' exhaust gases outlet. It can also be supplied by a steam extracted from the right position (after expansion) in steam turbine.

(2) Using the heat from the exhaust gases after steam generation in the HRSG, while using the steam as heat source requires using the steam after expansion. This was to ensure quality of the gases at the heat exchangers' inlet or the steam at the steam turbine outlet.

(3) The powering heat for the AWAC in this study is the steam at the turbine exhaust. This state of steam was restricted by steam turbine performance. It usually restricted by the steam dryness fraction of greater than 90% and the pressure of condensation. In this study previously it has been considered that the pressure of the condenser (P_{S4}) is limited between ($P_{S\ max}$=2 and $P_{S\ min}$=0.55 bars). Using the property tables with regard to these pressures it is clear that the $T_{g\ min}$=32.9°C and $T_{g\ max}$= 120.2°C. This is within the minimum temperature of the steam utilized by manufacturers (95 -180) °C. Otherwise, this steam is not viable to power the inlet cooling system. Therefore, it has to be generated from parts other than the steam turbine output.

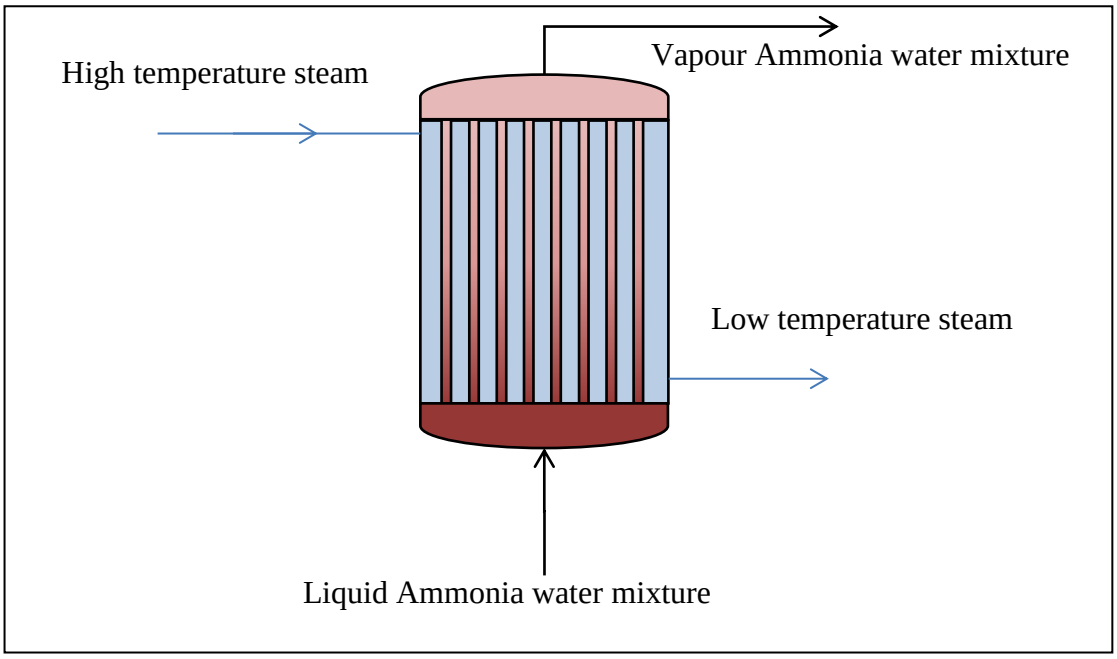

Figure 8.13 Steam/ ammonia water evaporator or desorber

Ranges for the operating parameters those for the absorption chiller systems undertaken by this study are tabulated in table 8.1.

8.4.4.2 Operation limits

The choice for a particular type of absorption chillers is determined by:

(1) The temperature of the heat source.

(2) The fluid streamed steam or exhaust gases.

(3) The mass flow rate of the heat source.

(4) The ambient temperature and the temperature difference required for the compressor inlet.

(5) The single effect AWACS is designed to have a COP of range between 0.7and 0.9. While the double effect system is designed to have a COP of 1.15. In this model, these ranges will be considered.

(6) The temperature of the AWM basic concentration stream T_{aw3} (in simple case) should not be greater than that for the lean stream from the purification column T_{aw7}.

8.4.4.3 Thermodynamic parameters' restrictions

1. This model assumes no heat losses to occur throughout the absorbers and condensers.
2. The pressure losses in absorbers, rectifiers, desorber solution heat exchangers, desorbers and condensers considerably negligible. This is also applied on the pressure losses through the piping systems are neglected too.

Parameter Symbol	Parameter Type	Range
T_{S4}	Input	95-300(°C)
T_a	Input	0-60(°C)
P_{Ev}	Controlling	5-10 bar
P_{Abs}	Controlling	15-35 bar
X_{LL}, X_{LL1}, X_{LL2}	Controlling	0.1-0.5
X_{B}, X_{B1}, X_{B2}	Controlling	X_{LL}+0.1-0.9
ΔT_{Rec}, ΔT_{Rec1}, ΔT_{Rec2}	Controlling	5-25
T_{aw4}	Controlling	$T_{aw3} < T_{aw4} < T_{aw7}$
ε_{SHE}, ε_{SHE1}, ε_{SHE2}	Controlling	0.6-0.8
η_{Des}, η_{Des1}, η_{Des2}	Performance	0.85-0.9

Table 8.1 The range of the parameters

8.4.4.4 Model performance criteria

The control system supports the following to estimate appropriate outputs.

i. The concentration of the ammonia in the working fluid must not be less than 90% to ensure better performance.

ii. The concentration of the lean ammonia fluid must be less than 0.5.

iii. The steam to enter the desorber should not be less than 95°C.

iv. Neither f nor y should be equated to unity.

v. ΔT_{Rec} is ranged between 5 and 25°C.

vi. The temperature of the air guessed for the gas turbine inlet must be compatible to that generated from the AWAC model combined with the air and gases' mass flow compatibility.

The final model flow diagram is shown in (Fig.8.14) which indicates the above conducted criteria.

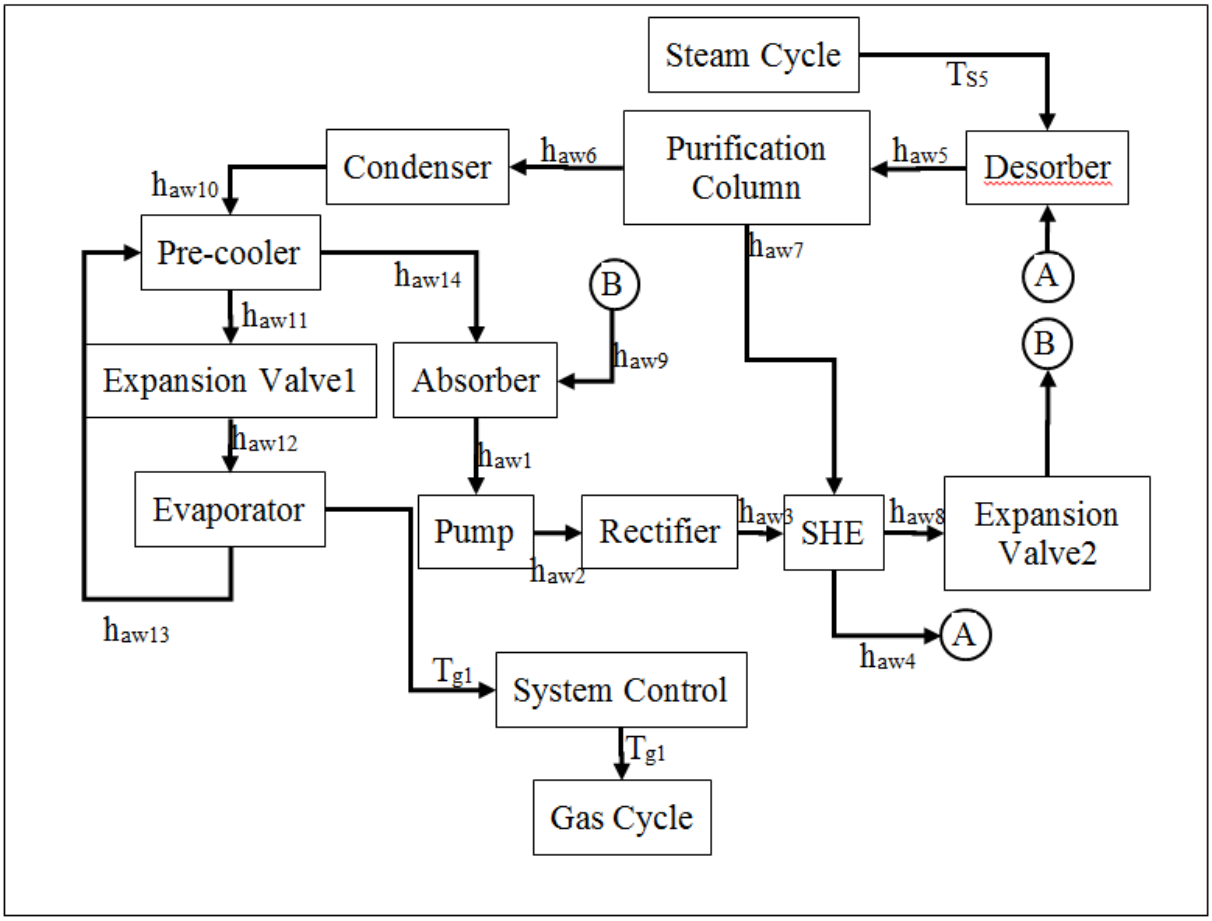

Figure 8.14 AWAC Simulation model program flow chart

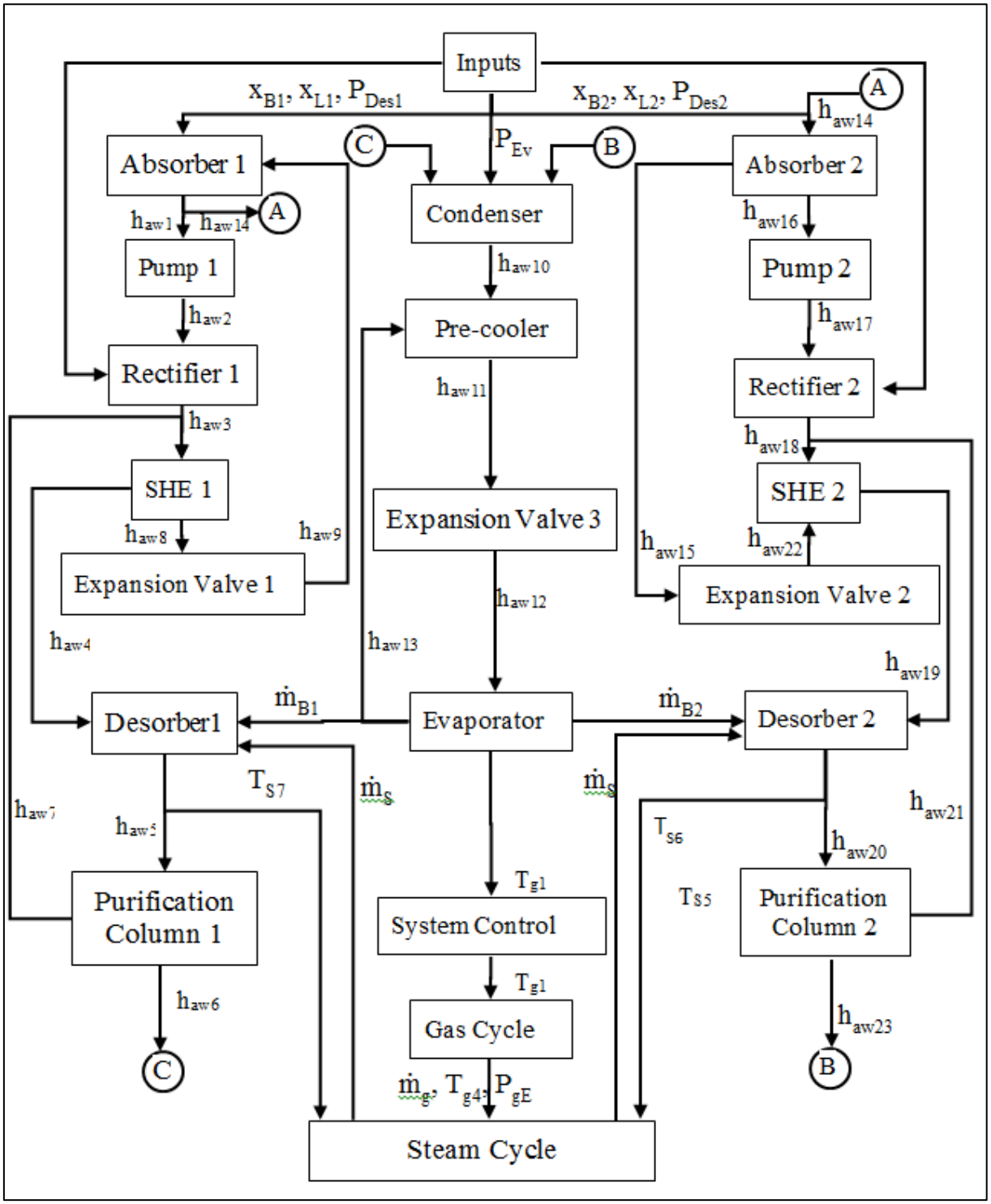

Figure 8.15 AWAC Solution model design two flow chart

8.5 Optimization

The optimization of the AWAC systems is considered here by resolving the solution to a set of components' parameters. Those are with the degrees matched to the required temperature of the air at the compressor inlet. The main parameters given by the ranges above are considered for the optimization. The parameters those affecting the system are: the basic, the working and the lean concentrations of ammonia, the pressure at evaporator, the pressure at condenser, steam to air mass flow ratio, steam to AWM mass flow ratio and components' efficiencies. However complex were the computer codes developed in here, the lack in the accurate thermodynamic properties of the AWM limited system operation radically.

Although it can be said that, the approach of this model made AWM conditions between the condenser, and the evaporator are the dominant on getting the required air temperature. On the other hand, the other parts of systems' cycle decide whether the entire system is to operate or not.

The utilization of the steam to power the inlet air cooling system of a certain CCPP must be taken carefully. The results from the previous chapters and this chapter confirm that, the operation of this system is more governed by the temperature, the mas flow rate and the pressure of the steam side rather than the AWAC system side. Considering the Lucia [79] results of utilizing pressure of 2.5 and 5.5 bars for single and double effects AWAC systems respectively open the debate where this steam is to be extracted from. Here, the steam or gases of much less pressure are investigated. Similarly to Goodheart [69], all components heat exchanging areas are under investigation. Although, this model does not consider the mass flow of the cooling water, which was not affected by the heat source as reported by Goodheart [69].

Here the power generated from the GC is boosted due inlet air cooling at high Ta similarly to Ondryas [74]. The results here confirm the increase in both performances characterises by AWAC rather than the likeliness of power generation reported by Khaledi [77]. An increase in such characteristics is reported here by the drop of the temperature of the air at compressor inlet, which is restricted by Ta itself and the WGC. Most of the previous studies Brown [78], Najjar [75], khaledi [77], confirmed the performance improvement of the CCPP by Inlet air cooling. The results from this study also meet such conclusion. The results of this study also disagree with Khaledi [77]about internal AWAC system influence on optimizing WCC and decrease ηCC. The thermal efficiency is increased if the AWM is heated from the right part in

the steam turbine engine. For the same reason, it also disagrees with Sigler [76], who limited the efficiency improvements to Ta drop from 35 to 5°C.

This study agree with Erickson on that for a certain power output, the increase in thermal efficiency From by Ta drop NOX and CO2 emissions were reduced due to fuel savings. The results here confirm that reducing the temperature below freeze is more viable to obtain better WCC augmentation similarly as Brown [78]. Practically, although the results confirmed a limited increase in the efficiency by inlet air cooling techniques, these results will be of great importance if yearly based calculations are considered as reported by Lucia [79].

8.6 Results and conclusions

1. Points at which the guessed air temperature at the compressor inlet are in match with that generated from the AWAC systems.

2. The AWAC systems performances are greatly affected by the changes in the mass flow of the steam generated by the steam evaporator and the temperature of the steam at turbine discharge.

3. It was convenient for the AWAC systems to predict the required temperature due to the very low temperature form the other end of the cooler where the temperature of the rich ammonia water mixture gets under zero Celsius.

4. In the case of using AWC turbine with the steam turbine, the steam generation from the steam evaporator is significantly affected. Accordingly, the heat required to attain the right temperature at the air cooler outlet is greatly narrowed.

5. AWAC systems show a great influence to the parameters and properties of the AWAC components between the condenser and evaporator than other parts.

6. However, these systems may not be disabled but for a certain regional weather (like cold weather countries), it is a solution for the power plants of these regions during full load operation. It is also suitable to minimize weather changes effects on power generation.

7. Utilization of steam to heat AWM of an AWAC system is restricted by: (a) the viability of the desorber outlet and (b) The usefulness of the steam at ST last bucket. Otherwise, to prevent any power losses from the SC, the steam is better to be extracted from the required pressure with respect to the extracted amount. This provides a great chance for multi pressure SC if steam of reasonable amount is extracted from low pressure or intermediate pressure.

8. The results from chapter seven confirmed the better performance of ChGT3 over other ChGT and CCPP configurations. This system is suitable for extracting AWM from the HRVG directly rather than using the ST outlet. This case provides great deal of optimization which deserves further investigation.

CHAPTER 9
RESEARCH CLOSURE

9.1 Overview on the work done

1. Four different programs were established from scratch to study how CCPPs are influenced by enhancing it with advanced systems. The models for these systems are:

(i) Conventional CCPP, including (6) complex gas turbine cycle systems and (7) steam turbine cycle systems. Those generate (42) CCPP configuration cases.

(ii) POGT integrated to CCPP, including (2) POGT cycle systems and (7) steam turbine cycle systems. Those generate (14) advanced CCPP configuration cases.

(iii) AWC integrated to CCPP, including (2) AWC and (6) complex gas turbine cycle systems and (2) POGT systems. Those generating (14) advanced CCPP configuration cases.

(iv) AWAC integrated to CCPP, including (2) AWAC can be integrated to the (42) CCPP in first point and to the (14) cases in the third point. Those generate (112) different CCPP configuration cases.

2. This research dealt with working fluids, those operating in gas turbines, steam turbines, ammonia water mixture turbines and absorption chillers. Accordingly, the thermodynamic properties of air, water, steam, ammonia, methane is utilized in here. The data of these properties were collected from different sources due to its lack in only one source, whereas if available, it's usually with narrower range or quality. The thermodynamic properties off these data of mixtures are considered as mixtures of ideal gases.

3. In this project visual basic application (VBA) was used to develop the codes, which dealt with the equations of the models. It also was utilized to establish the functions dealt with estimating the properties and performance maps data.

4. In this study ammonia water mixture power turbine cycle is employed as a bottoming cycle to conventional complex and advanced GT designs with and without the steam power turbine.

5. This comprehensive research in its totality was not reported anywhere in literature, which support the claim of originality of the current research. However, some related work reported in the literature were cited and found collectively in section 1.5 and table 3.1.

9.2 Research conclusions

1. Conventional configurations of CCPP have not yet been under full optimization throughout any of the following:

(i) Cycles' parameters optimization.

(ii) Components' performance optimization.

(iii) Matching between cycles' main components

(iv) Optimization by integrating advanced systems.

Accordingly, there is a considerable value of optimization can still be useful to attain better performance from the CCPP.

2. Although the CCPP are designed to operate at design point performance, its components' performances are well affected by the change in the weather conditions. Accordingly gas turbine Inlet air controlling systems are frontally equipped to support CCPP. Thereby, inlet air cooling system is not only supposed to return the inlet conditions to its design point. However, it usually improves the performance of the CCPP components. Based on that, it is required to study the (inlet air cooling systems) as a part of CCPP rather than an individual system. This issue becomes more important when such systems operate using the power and the heat from CCPP outputs.

3. The temperature from the CCPPs' gas turbine discharge is more efficiently used to generate power from AWC rather than the SC turbines. Although, ammonia is

extensively utilized in CCPP at the SCR system, ammonia is not normally utilized to generate power within the CCPP. Furthermore, an ammonia water mixture cycle (AWC) turbines are not used for an output similar to that for heavy duty steam turbines. On the other hand, it has been successfully used in geothermal power plants.

4. Although, commercialy, there are great simulation programs, those can give more detailed description on the components of the conducted configuration, in this research, a number of points are worth to be declared:

(i) There is no certain simulation program that collaborates the considered systems together in one configuration. Therefore, more than one program is required or the whole considered system can be established as it has been done by this research from scratch.

(ii) The thermodynamic properties' data for the fluids utilized by the systems considered in this research are not often available in these programs. Here, the attention is especially on the ammonia water mixture and the rich fuel gases. On the other hand, the properties of other fluids components are available in these programs but for limited ranges. However, these programs are either functioned to given data tables using developed procedures. Here exactly the same is applied using in house made functions, mostly using interpolation.

(iii) The components models considered by these programs are rarely utilizes the components considered by this research or the operating conditions in accordance to the considered configurations. Like the AWM absorber, rectifier, purification column in AWAC system and AWMT and the fuel rich combustor in the ChGT.

(iv) Although some program systems can operate GT or ST systems entirely these lack to recognize CCPP, AWMT (based on Kalina cycle) and ChGT as operating systems further than the complex configurations of GT, ST and HRSG.

5. HRSG performance is entirely affected by the changes in the parameters of the gas turbine. The changes in its performance take a great part on the entire combination and the performance of the steam turbine. Consequently, it has a considerable effect on performance of the CCPP and the temperature of the exhaust gases.

6. Multi pressure HRSG configurations improves CCPP performance, while at the same time, it narrows the range of its operating envelop.

7. There is a lack of sources in modelling and data analyzing for utilizing AWMT as a part of the CCPP instead off replacing the steam turbine.

8. There is a lack of sources these to discuss modelling and data analyzing of the AWAC as a part of the CCPP.

9. The lack in the thermodynamic properties of ammonia water mixture for power generation applications had a considerable effect on the progress of any study that deals with such fluid.

9.3 Recent developments to the CCPP performance

The previous sections listed the conclusions to the development of many approaches to improve, enhance and optimize the thermal power generation systems. It is worth here, to present the recent development in CCPP regarding large companies' new patents. Through which to match the investigation results from this research by its conclusions with the latest inventions in the power generation sector which include similar conductance. Afterwards to attain a list of recommendations that (1) Suits real applications, (2) confirm the conducted results, (3) provide the suggestions for more innovations to the fresh work patent. In here it is enough to undertake only a sample of recent patents.

General electric company development [98] supported CCPP with an exhaust gases recirculation system to preserve minimum NOX with improved flame stability. In such configuration, a portion of the exhaust is recirculated to the AC after mixed with air and a control loop to regulate diffusion fuel using the feedback from the combustion product load pressure, CC firing temperature, recirculated gases rate and CO2 and NOX emissions. In which, it provides lower NOX with DLN but requires a purification unit to preserve GT components from fouling.

TAS Energy company development, [99] a CCPP, where the ST discharges is used to operate an organic fluid power cycle to seize water utilization in these systems. In such invention, the steam condenser is the ORC vaporizer. An air cooled condenser is used for the ORC and the refrigeration cycles. The refrigeration cycle also circulates chilled water is between inlet air cooled system and its evaporator. A thermal energy storage tank may be utilized support GT inlet cooling.

Alstom company development [100], integrated a purification plant into the HRSG of CCPP to absorb CO2 from the exhaust gases and reduce the heat required for SC regeneration. The CCPP connections were optimized to: (1) satisfy the purification plant regeneration section to generate the absorbent weak solution (ammonia or amine) at high temperature using the steam from the HRSG or ST; and (2) the SC performance is improved by utilizing the residual heat, by directing condensed steam from the regeneration section outlet to LP evaporator. It significantly increased CCPP efficiency and slightly deteriorated its performance by such integration. The heat released from the absorbent section can be used to preheat feed water of the steam generator.

Another Alstom company development, [101] integrated a liquefied natural gas regasification system, which absorb heat from the CO2 capture system in a closed circuit to reduce the heat required to for both. Ammonia or amine process is utilized to capture CO2 in the HSRG gases. Additional cooling systems are utilized for rich and lean absorption of the CO2 capture system, or for the cooling the flue gas. The LNG system comprised one or more heat exchanging stages and one or more cooling storage units. The LNG coldness supported the operation of the CO2 capture cooling processes, in which the heat absorbed by the LNG is backup the regasification process. The regasification system is designed to operate on natural gas temperatures between regasification inlet temperature and ambient temperature. From the hot stream side, a chilling temperature medium at the heat exchanger output depending on the required heat for absorption. The CO2 capture can improve the CCPP operating efficiency.

Siemens company development, [102], a CCPP integrated with gasification system and Rankine cycle, which receive the heat from the gasification sub-system, or from the GC. This turbine operates on a mixture of ammonia, CO2, carbon compounds, including halo-carbon refrigerants. The syngas is generated, cooled by generating steam, purified, saturated by steam and filtrated before entering the CC. While O2 depleted air is added to the compressed air to form a diluted compressed air which drops the flame temperature and reduces NOX emissions. A portion of water from the 1st Rankine cycle pump is steamed by gasification auxiliary boiler and supplied to syngas to regulate combustion temperature, combustion temperature profile and gases temperature at CC exit. The hot exhaust from the ST boiler is used to generate low pressure and temperature steam for the 2nd Rankine cycle.

9.4 Observations from the recent patents

- Mainly, the focus of the recent inventions is more about contributing other systems into the CCPP rather than changing its own components. This was made by making use of the waste heat from CCPP parts to operate these systems rather than using externally powered systems.
- Most of the recent upgrades targeted reducing CCPP impact on environment or for fuel savings rather than improving its performance.

9.5 Recommendations

- There are currently little data for pressures and temperature relevant to power generation cycles. Therefore, it is highly recommended to predict accurately the thermodynamic properties of AWM (Ammonia Water Mixture). Particularly, for power generation cycles, especial after the rise in the number of the AWMT power plant in action.
- Within the developments in utilizing ammonia in CCPP and geothermal PP, the power cycles components requires an ammonia and ammonia water mixture thermodynamic properties data of a temperature over 350°C.
- More research is importantly required to provide more shares of ammonia and AWM in CCPPs' conventional components and to study combine its utilizing with other (non-power generation) components.
- Further degree of integration between AWM systems is worth investigating like involve ammonia usage in CCPP components, including ChGT in addition to the components of the HRSG SCR system.
- Using such integrated systems to reduce emissions, improve performance and reduce fuel and water consumption. This included combining (1) gasification systems, (2) CO2 capture system, (3) SCR system, (4) AWT system, (5) inlet air cooling system by AWAC, (6) AWM for steam condensation and ammonia production factory.
- The contribution if applied to the CCPP it may result in enormous results.

- The results from utilizing the ChGT with AWAC and AWC made by this research confirmed that, there is still heat waste between components that may be further utilized to power the previous system, as an example the temperature of the exhaust gases are still of high degrees.

- More studies are required to investigate how to bind the impacts of the power generation from the CCPP and how to enclose the surrounding environment to make zero impacts like one closed system thermally and environmentally.

- It is recommended to study, employing emission's capture or process systems with rich fuel combustion gases HRSG. To investigate how this will affect the emissions for the 2nd stage lean fuel combustion.

- The usual available correlation to predict emissions are invented for lean fuel combustion. Therefore, further research is required to predict the emissions in rich fuel combustion products.

- The current, lack of correlations required to predict natural gas emissions levels do not coop with its huge utilization in power generation. Therefore, further investigation is needed to predict the emission levels resulting from natural gas combustion in turbines.

- It is highly urged to investigate the alternative fluids (AWM, fuel-rich combustion gases) impacts on CCPP components. In Particular, these fluids' influences on the performance of turbines, HRSG and HRVG parts.

REFERENCES

[1] IEA, “key world statistics,” 2012.

[2] IEA, “"World Energy Outlook",” IEA, 2013.

[3] P. Taylor, O. Lavagne d’Ortigue, N. Trudeau and M. Francoeur, “" Energy Efficiency Indicators for Public Electricity Production from Fossil Fuels IEA Information paper In Support of the G8 Plan of Action",” IEA, 2008.

[4] IEA, “CO2 capture at power stations and other major point sources zero emissions technologies for fossil fuels working party on fossil fuels,” OECD/IEA, 2003.

[5] M. Moran and H. Shapiro, Fundamentals of engineering thermodynamics, 4th edition ed., John Wiley, 1999.

[6] A. El-Hadik, “ The Impact of Atmospheric Conditions on Gas Turbine Performance,” *Journal of Engineering for Gas turbine and power,* vol. 112, pp. 590-596, October 1990.

[7] A. Guha, “Effects of internal combustion and non-perfect gas properties on the optimum performance of gas turbines,” *Proceedings of the Institution of Mechanical Engineers, Part C: Journal of Mechanical Engineering Science,* vol. 217, no. 9, pp. 1085-1099, 2003.

[8] A. Razak, Industrial gas turbines: performance and operability, Woodhead Publishing Ltd, 2007.

[9] H. Saravanamuttoo, G. Rogers, H. Cohen and P. Straznicky, Gas Turbine Theory, 6th ed., Pearson, 2008.

[10] J. Horlock, Advanced Gas Turbine Cycles, 1st ed., Pergamon, 2003.

[11] M. Korobitsyn, “New And Advanced Energy Conversion Technologies. Analysis of Cogeneration, Combined and Integrated Cycles,” 1998.

[12] J. Horlock, Combined power plants including Combined Cycle Gas Turbine (CCGT) Plants, perrgamon press, 1992.

[13] J. Horlock, “the optimum pressure ratio for a combined cycle gas turbine plant,” *Proceedings of the Institution of Mechanical Engineers, Part: A, Journal of Power and Energy,* vol. 209, no. A4, pp. 259-264, 1995.

[14] J. Horlock and W. and Woods, “Determination of the optimum performance of gas turbines,” *Proceedings of the Institution of Mechanical Engineers, Part: C Journal of*

Mechanical Engineering Science, vol. 214, no. C1, p. 243–255, 2000.

[15] A. Khaliq and S. Kaushik, "Second-low based thermodynamic analyses of Brayton/Rankine combined power cycle with reheat," *Applied Energy*, vol. 78, pp. 179-197, 2004.

[16] M. Ameri, P. Ahmadi and S. Khanmohammadi, "Exergy analysis of a 420MW combined cycle power plant," *International Journal of Energy Research,* vol. 32, p. 175–183, 2008.

[17] M. Briesch, R. Bannister, I. Diakunchak and D. Huber, "A combined cycle designed to achieve greater than 60 percent efficiency," *Journal of Engineering for Gas Turbines and Power*, vol. 117, pp. 734-741, October 1995.

[18] Q. Z. M. AL-Hamdan, "Design criteria and performance of gas turbine in combined power and power (CPP) plant for electrical power generation," Dept aerospace and mechanical engineering, university of Hertfordshire, 2002.

[19] A. Polyzakis, K. C. and G. Xydis, "Optimum gas turbine cycle for combined cycle Power plant," *Journal of energy conversion and management,* vol. 49, pp. 551-563, 2008.

[20] J. Horlock, "Combined power plants- past, present, and future," *Journal of Engineering for Gas Turbines and Power,* vol. 117, pp. 608-616, October 1995.

[21] O. Bolland, "A Comparative Evaluation of Advanced Combined Cycle Alternatives," *Journal of Engineering for Gas Turbine and Power,* vol. 113, no. 2, pp. 190-197, 1991.

[22] R. Kehlhofer, B. Rukes, F. Hannemann and F. and Stirnimann, Combined-cycle gas \& steam turbine power plants, 3rd ed., Pennwell Books, 2009.

[23] I. Dincer and H. AL-Muslim, "Thermodynamic analysis of reheat cycle system," *international Journal of Energy research,* vol. 25, pp. 727-739, 2001.

[24] j. Topolski and j. Badur, "Comparison of the combined cycle efficiencies with different heat recovery steam generators," *Transactions of The Institute of Fluid-Flow Machinary*, vol. 111, pp. 5-16, 2002.

[25] O. A. S. Al - Qur'an, "Design Criteria and performance of steam turbines in CPP plant for electrical power generation," Department of aerospace and mchanical engineering, University of Hertfordshire, 2002.

[26] W. Xiang and Y. Cheng, "Performance improvement of combined cycle power plant based on the optimization of the bottoming cycle and heat recuperation," *Journal of Thermal Science,* vol. 16, no. 1, pp. 84-89, 2007.

[27] C. Casarosa and A. Franco, "Thermodynamic Optimization of the Operative Parameters

for the Heat Recovery in Combined Power Plants," *International journal of applied thermodynamics,* vol. 4, no. 1, pp. 43-52, 2001.

[28] A. Franco and C. Casarosa, "On some perspectives for increasing the efficiency of combined cycle power plants," *Applied thermal engineering,* vol. 22, pp. 1501-1518, 2002.

[29] A. Franco and A. Russo, "Combined cycle plant efficiency increase based on the optimization of the heat recovery steam generator operating parameters," *International Journal of Thermal Sciences,* vol. 41, pp. 843-859, 2002.

[30] C. Casarosa, F. Donatini and A. Franco, "Thermoeconomic optimization of heat recovery steam generators operating parameters for combined plants," *Journal of energy,* vol. 29, pp. 389-414, 2004.

[31] A. Bassily, "Modelling and numerical optimization of dual- and triple-pressure combined cycles," *Proc. IMechE Journal of Power and Energy,* vol. 218, no. A, pp. 97-109, 2002.

[32] A. Bassily, "Modeling, numerical optimization, and irreversibility reduction of a dual-pressure reheat combined-cycle," *Applied Energy,* vol. 81, no. 2, pp. 127--151, 2005.

[33] A. Bassily, "Enhancing the efficiency and power of the triple pressure reheat combined cycle by means of gas reheat, gas recuperation, and reduction of the irreversibility in the heat recovery steam generator," *Applied Energy,* vol. 85, no. 12, p. 1141—1162, 2008.

[34] A. Zwebek and P. Pilidis, "Degradation Effects on Combined Cycle Power Plant Performance—Part I: Gas Turbine Cycle Component Degradation Effects," *Journal of engineering for gas turbines and power,* vol. 125, no. 3, pp. 651--657, 2003.

[35] A. Zwebek and P. Pilidis, "Degradation Effects on Combined Cycle Power Plant Performance—Part II: Steam Turbine Cycle Component Degradation Effects," *Journal of engineering for gas turbines and power,* vol. 125, no. 3, pp. 658--663, 2003.

[36] A. Zwebek and P. Pilidis, "Degradation Effects on Combined Cycle Power Plant Performance—Part III: Gas and Steam Turbine Component Degradation Effects," *Journal of engineering for gas turbines and power,* vol. 126, no. 2, pp. 306--315, 2004.

[37] H. Micak, "An Introduction to the Kalina Cycle," in *Proceedings of International Joint/ Power Generation*, 1996.

[38] Y. Zhang, M. He, Z. Jia and X. Liu, "A review of research on the Kalina cycle," *Renewable and sustainable energy reviews,* vol. 16, no. 7, pp. 5309--5318, 2012.

[39] C. Marston, ""A Family of Ammonia-Water Adjustable proportion Fluid Mixture Cycles"," *Proceedings of the 25th Intersociety Energy Conversion Engineering*

Conference, vol. 2, pp. 160-165, 1990.

[40] C. Marston, "Parametric Analysis of the Kalina Cycle," *Journal of engineering for gas turbine and power,* vol. 112, no. 1, pp. 107-116, 1990.

[41] O. Ibrahim and S. Klein, "Absorption Power Cycles," *Energy,* vol. 21, no. 1, pp. 21-27, 1996.

[42] C. Marston and M. Hyre, ""Gas Turbine Bottoming Cycles: Triple-Pressure Steam Versus Kalina"," , *Journal of Engineering for Gas Turbines and Power,* vol. 117, no. 1, pp. 10-15, 1995.

[43] T. Srinivas, A. Gupta and B. and Reddy, "Performance simulation of combined cycle with kalina bottoming cycle," *Cogeneration and Distribution Journal,* vol. 23, no. 1, pp. 6-21, 2008.

[44] A. Kalina and M. Tribus, "Advances in Kalina cycle technology (1980–1991): part I development of a practical cycle, energy for the transition age," *Proceedings of the Florence World Energy Research Symposium Florence, Italy,* vol. 97, pp. 97-110, 1990.

[45] A. Kalina and M. Tribus, "Advances in Kalina Cycle Technology (1980-1991): Part II Iterative Improvements," *Proceedings of the Florence World Energy Research Symposium Florence, Italy,* vol. 97, pp. 111-125, 1992.

[46] B. Hanliang, L. Guiyu and L. Xianding, "Optimum Thermodynamic Parameters for The kalina Cycle," *Proceedings of the TAIES,* pp. 415-420, 1989.

[47] Y. M. EL-Sayed and M. Tribus, "a theoretical comparison of the Rankine and Kalina cycle," *ASME advanced energy systems division (AES),* vol. 1, pp. 97-102, 1985.

[48] Y. El-Sayed and M. Tribus, "Thermodynamic properties of water-ammonia mixtures theoretical implementation for use in power cycles analysis," *ASME publication, Advanced energy systems division (AES),* vol. 1, pp. 89--95, 1985.

[49] I. Marrero, A. Lefsaker, A. Razani and K. Kim, "Second law analysis and optimization of a combined triple power cycle," *Energy Conversion and Management,* vol. 43, no. 4, pp. 557--573, 2002.

[50] Y. Amano, T. Suzuki, H. Noguchi, Y. Tanzawa, M. Akiba, A. Usui and T. Hashizume, ""effectiveness of an ammonia-water mixture turbine system to hot water heat source"," *Proc. 1999, IJPGC-ICOPE ASME/JSME PWR,* vol. 34, no. 2, pp. 67-73, 1999.

[51] Y. H. T. Amano, Y. Tanazawa, T. Suzuki, M. Akiba and A. Usui, "A Hybrid Power Generation and Refrigeration cycle with ammonia-Water mixture," *proceedings of 2000 International Joint Power Generation Conference,* pp. 1-6, 2000.

[52] Y. Amano, T. Hashizume, Y. Tanazawa, K. Takeshita, M. Akiba and A. Usui,

"Experimental results of an ammonia-water mixture turbine system," *processdings of JPGC'01 international Joint Power Generation Conference,* pp. 1-7, 2001.

[53] M. Tomizawa, K. Takeshita, K. Tsuri, Y. Amano, M. Akiba and T. Hashizume, "Modeling of the main component of the Bottoming Stage in an advanced Co-Generation system on the operational planning," *JSME international journal. Series B, fluids and thermal engineering, International Conference on Power and Energy System (2001)*, vol. 45, no. 3, pp. 446-450, 2002.

[54] K. Takeshita, Y. Amano and Hashizume, "Experimental results of an ammonia-water mixture turbine system: Part 2—effect of the ammonia mass fraction," *2002 International Joint Power Generation Conference,* pp. 959--964, 2002.

[55] K. Takeshita, Y. Amano and T. and Hashizume, ""experimental study of advanced cogeneration system with ammonia-water mixture cycles at bottoming "," *Energy,* vol. 30, no. 2, pp. 247--260, 2005.

[56] R. Murugan and P. Subbarao, "Effective utilization of low-grade steam in an ammonia-water cycle," *Proceedings of the Institution of Mechanical Engineers, Part A: Journal of Power and Energy,* vol. 222, no. 2, pp. 161-166, 2008.

[57] N. Lior, F. Stenberg and N. Arai, "Development of Novel higher efficiency Lower emissions power cycle Concepts based on Energy and Exergy analysis," *Proceedings of 2001 International Joint Power Generation conference,* pp. 305-310, 2001.

[58] T. Yamamoto, T. Furuhata, N. Arai and N. Lior, "Analysis of a high-efficiency low-emissions " Chemical Gas Turbine" system," *Journal of Propulsion and power,* vol. 18, no. 2, pp. 432-439, 2002.

[59] J. Ribesse, "Gas Turbine with Catalytic Reactor for the Partial Oxidation of Natural Gas and Its Application in Power Stations," *Gas Wärme International, July-August,* 1971.

[60] S. Christianovich, V. Maslennikov and V. Shterenberg, "Steam-gas power stations with multi-stage residual-oil combustion," *Applied energy,* vol. 2, pp. 175-187, 1976.

[61] T. Nurse, "Clean Electric Power Generation Process". USA Patent 4999992, 1991.

[62] T. Yamamoto, T. Furuhata and N. Arai, "Performance of chemical gas turbine system and comparison with other Gas Turbine Based Cycles," *International Journal of Applied Thermodynamics,* vol. 3, no. 4, pp. 155-162, 2000.

[63] N. Kobayashi, T. Yamamoto, N. Arai and T. Tanaka, "Effect of pressure on Fuel-Rich combustion of Methane-Air under high pressure," *Energy Convers. Mgmt,* vol. 38, no. 10, pp. 1093-1100, 1997.

[64] M. Korobitsyn, T. Furuhata and N. Arai, "The Chemical Gas Turbine: Thermodynamic Considerations," *Journal of Nippon Dennetsu Shinpojiumu Koen Ronbunshu,* vol. 36,

no. 3, pp. 683-684, 1999.

[65] Y. Abdel-rahim and H. Mohamed, “optimum performance comparative study of combined gas turbine partial oxidation cycle and reheat cycle,” *IEEE,* pp. 389-400, 2001.

[66] H. Mohamed, “Conceptional Design Modelling of Combined Power Generation cycle for optimum performance,” *Journal of Energy and Fuels,* vol. 17, pp. 1492-1500, 2003.

[67] T. Yamamatoo, N. Lior, T. Furuhata and N. Arai, “A novel high-pressure low NOx fuel-rich/ fuel lean two-stage combustion gas and steam turbine system for power and heat generation,” *Journal of Power and Energy, Part A,* vol. 221, pp. 433-446, 2007.

[68] I. Horuz, “A Comparison between Ammonia-Water and water-Lithium Bromide Solustions in Vapor Absorbtion Refregeration Systems,” *Int. Comm. Heat Mass Transfer,* vol. 25, no. 5, pp. 711-721, 1998.

[69] K. Goodheart, “Low Firing Temperature Absorption Chiller System,” University of Wisconsin, Madison, 2000.

[70] J. Fernandez-Seara and M. Vazquez, “Study and control of the optimal generation temperature in NH3-H2O absorption refrigeration systems,” *Applied Thermal Engineering,* vol. 21, pp. 343-357, 2001.

[71] H. Chua, H. Toh and K. Ng, “Thermodynamic modeling of an ammonia/water absorption chiller,” *International Journal of Refrigeration,* vol. 25, p. 896–906, 2002.

[72] S. Adewusi and M. Zubair, “Second law based thermodynamic analysis of ammonia–water absorption systems,” *Energy Conversion and Management,* vol. 45, p. 2355–2369, 2004.

[73] O. Yang, M. Tsujita and G. Sato, “thermodynamic study on the suction cooling gas turbine cycle combined with absorption-type refrigerating machine using wasted heat,” *The Japan Society of Mechanical Engineers,* vol. 13, no. 63, pp. 1111-1122, 1970.

[74] I. S. Ondryas, D. A. Wilson, M. Kawamoto and G. L. Haub, “Options in Gas Turbine Power Augmentation Using Inlet Air Chilling,” *Journal of Engineering for Gas Turbines and Power,* vol. 113, pp. 203-211, 1991.

[75] Y. Najjar, “Enhancement of Performance of Gas Turbine Engine by Inlet Air Cooling and Cogeneration System,” *Applied Thermal Engineering,* vol. 16, no. 2, pp. 163-173, 1996.

[76] J. Sigler, D. Erickson and H. Perez-blanco, “Gas Turbine Inlet air Cooling Using Absorption Refrigeration: A Comparison Based On Combined Cycle Process,” in *International Gas Turbine & Aeroengine Cogeneration & Exhibition, June,4-7,* New

Orleans, LA, USA, 2001.

[77] H. Khaledi, M. Ghofrani and R. Zomorodian, "Effect of inlet air cooling by absorption chiller on gas turbine and combined cycle performance," *International Mechanical Engineering Congress and Exposition,* vol. 45, pp. 507-516,, 2005.

[78] D. Brown, S. Katipamula and J. Konynenbelt, "A comparative assessment of alternative combustion turbine inlet cooling system," Dept. of Energy, USA, 1996.

[79] M. Lucia, C. Lanfranchi and V. Baggio, "Benefits of Compressor Inlet Air Cooling for Gas Turbine Cogeneration Plants," *Journal of Engineering for Gas turbine and power,* vol. 118, pp. 598-603, 1996.

[80] D. Erickson, I. Kyung, G. Anand and E. Makar, "Aqua Absorption turbine inlet cooler," *International Mechanical Engineering Congress and Exposition,* pp. 49-56, 2003.

[81] B. Dawoud, Y. Zurigat and J. Bortmany, "Thermodynamic assessment of power requirements and impact of different gas-turbine inlet air cooling techniques at two different locations in Oman," *Applied Thermal Engineering,* vol. 25, p. 1579–1598, 2005.

[82] A. Lazzaretto and A. Toffolo, "Analytical and neural network models for gas turbine design and off-design simulation," *International Journal of Thermodynamics,* vol. 4, no. 4, pp. 173-182, 2001.

[83] P. Walsh and P. Fletcher, Gas Turbine Performance, Wiley-Blackwell, 2008.

[84] A. Mirandola and A. Macor, "Full Load and Part Load Operation of Gas Turbine-Steam Turbine Combined Plant," *ISEC,* vol. 8, pp. 8-15, 1986.

[85] A. H. Lefebvre and B. D. R., Gas Turbine Combustion: Alternative Fuels and Emissions, 3rd ed., CRC Press Inc, 2010.

[86] J. Kurzke, "Compressor and turbine maps for gas turbine performance computer programs-Component map collection 2," *Dachau, Germany,* 2004.

[87] N. Srivastava, "Modeling of solid oxide fuel cell/gas turbine hybrid systems," The Florida State University FAMU-FSU College Of Engineering, 2006.

[88] V. Ganapathy, Industrial Boilers and Heat Recovery Steam Generators Design, Applications, and Calculations, Marcel Dekker, Inc., 2003.

[89] J. S. Wright, "Steam Turbine Cycle Optimization, Evaluation, and Performance Testing Considerations," GE Power Generation, 1994.

[90] L. E. Bakken and L. Skogly, "Parametric modeling of exhaust gas emission from natural gas fired gas turbines," *Journal of engineering for gas turbines and power,* vol.

118, no. 3, pp. 553--560, 1996.

[91] N. Lior and N. Arai, “Analysis of the chemical gas turbine system,a novel high-efficiency low-emissions power cycle,” *ASME, International Joint Power Generation Conference,EC,* vol. 5, no. 1, p. 431–437, 1997.

[92] J. Keenan and J. Kaye, “Gas Tables,” John Wiley and Sons, New York, 1945.

[93] R. Tillner-Roth and D. G. Friend, “A Helmholtz free energy formulation of the thermodynamic properties of the mixture { water+ ammonia },” *Journal of Physical and Chemical Reference Data,* vol. 27, no. 1, pp. 63--96, 1998.

[94] L. Haar and J. S. Gallagher, “Thermodynamic properties of ammonia,” *Journal of Physical and Chemical Reference Data,* vol. 7, no. 3, pp. 635--792, 1978.

[95] H. Leibowitz and M. Mirolli, “First Kalina combined-cycle plant tested successfully,” *Power engineering,* vol. 101, no. 5, pp. 44-48, 1997.

[96] C. Somers, “simulation of absorption cycles for integration into refining processes,” University of Maryland, 2009.

[97] H. K. E., R. Radermacher and S. A. Klein, “Absorption chillers and heat pumps,” CRC Press USA, 1996.

[98] A. M. Elkady, “System and method of improving emission performance of a gas turbine”. Patent EP2644998A2, 2nd Oct 2013.

[99] T. L. Pierson and H. Leibowitz, “Process Utilizing High Performance Air-Cooled Combined Cycle Power Plant With Dual Working Fluid Bottoming Cycle and Integrated Capacity Control”. USA Patent US 2013/0298568 A1, 2013.

[100] R. Carroni, A. LIMOA, D. Olsson, J. Dietzmann, C. Pedretti, T. Nugroho, E. Conte and G. L. AGOSTINELLI, “Combined cycle power plant”. Patent WO2013139884 A2,, Sep 2013.

[101] M. Wirsum, C. Ruchti, H. LI, F. Droux, F. Z. Kozak and A. Zagorskiy, “Combined cycle power plant with CO_2 capture plant”. Patent US 2013/0312386 A1, Nov 2013.

[102] J. P. Gutierrez, “Power generation system incorporating multiple rankine cycles”. Patent US 8,371,099 B2, Feb 2013.